

AD-A124 003

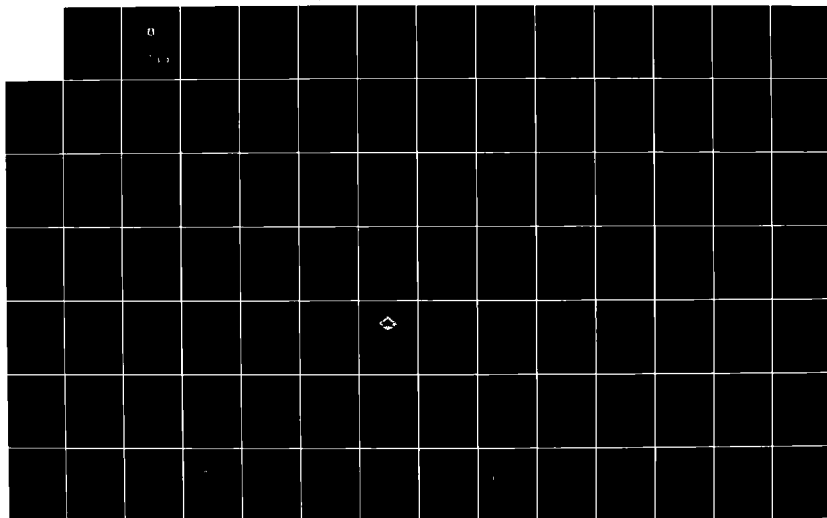
FREQUENCY AGILITY RADAR(U) FOREIGN TECHNOLOGY DIV
WRIGHT-PATTERSON AFB OH 45433-0603
FTD-ID(RS)T-0603-82

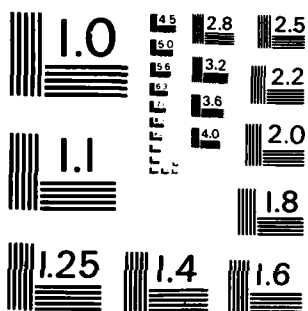
17

UNCLASSIFIED

F/G 17/9

NL





MICROCOPY RESOLUTION TEST CHART
NATIONAL BUREAU OF STANDARDS-1963-A

2

FTD-ID(RS)T-0603-82

ADA 124003

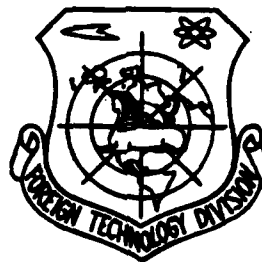
FOREIGN TECHNOLOGY DIVISION



FREQUENCY AGILITY RADAR

by

Mao Yuhai



DTIC
ELECTE
FEB 1 1983
S D D

Approved for public release;
distribution unlimited.

DTIC FILE COPY



83 01 31 169

Accession For	
NTIS GRA&I	<input checked="" type="checkbox"/>
DTIC TAB	<input type="checkbox"/>
Unannounced	<input type="checkbox"/>
Justification	
By	
Distribution/	
Availability Codes	
Dist	Avail and/or Special
A	



FTD-ID(RS)T-0603-82

EDITED TRANSLATION

FTD-ID(RS)T-0603-82

6 December 1982

MICROFICHE NR: FTD-82-C-001648

FREQUENCY AGILITY RADAR

By: Mao Yuhai

English pages: 652

Source: Pinlyu Jiebian Leida, National Defense
Press, October 1981, pp. 1-448

Country of origin: China

Translated by: LEO KANNER ASSOCIATES
F33657-81-D-0264

Requester: FTD/SDER

Approved for public release; distribution unlimited.

THIS TRANSLATION IS A RENDITION OF THE ORIGINAL FOREIGN TEXT WITHOUT ANY ANALYTICAL OR EDITORIAL COMMENT. STATEMENTS OR THEORIES ADVOCATED OR IMPLIED ARE THOSE OF THE SOURCE AND DO NOT NECESSARILY REFLECT THE POSITION OR OPINION OF THE FOREIGN TECHNOLOGY DIVISION.

PREPARED BY:

TRANSLATION DIVISION
FOREIGN TECHNOLOGY DIVISION
WP.AFB, OHIO.

FTD-ID(RS)T-0603-82

Date 6 Dec 19 82

Table of Contents

Graphics Disclaimer	ii
Annotation	iii
Synopsis of Contents	iv
Preface	v
Part One, The Performance of Frequency Agility Radar	1
Chapter I, General Discussion	1
Chapter II, Antijamming Capabilities of Frequency Agile Radar	16
Chapter III, Frequency Agility's Enlargement of Radar's Detection Range	49
Chapter IV, The Increase of the Angle-Measuring Precision of Radar by Frequency Agility	101
Chapter V, The Use of Frequency Agility to Inhibit Sea Clutter Jamming	213
Part Two, The Composition of Frequency Agility Radar	286
Chapter VI, Frequency Agility Magnetrons	286
Chapter VII, The Structure of Noncoherent Frequency Agile Radar	371
Chapter VIII, The Structure of Fully Coherent Frequency Agile Radar	503
Chapter IX, Some Particular Frequency Agile Radar Systems	579

GRAPHICS DISCLAIMER

All figures, graphics, tables, equations, etc. merged into this translation were extracted from the best quality copy available.

Annotation:

This section of the book presents in detail the structure, components, mechanics, and applications of frequency agile radar.

In particular, noncoherent and fully coherent frequency agile radar are discussed, analyzed, and compared. Various types of local oscillators are discussed, such as backward-wave type, electronically tuned, YIG tuned, and varactor tuned. Some automatic frequency control systems are discussed, and comparative analysis is carried out on self-adapting frequency agile radar, moving target indication systems, and frequency scanning radar. Efficiency, frequency range, average and peak power, anti-jamming properties, clutter control, and detectability are considered in light of application to frequency agile radar.

This section of the book is useful for students of radar, as well as technical workers, research personnel, and design engineers in the field of radar. Some basic knowledge of the operational principles of radar in general is helpful. Photographs-1. Tables-10. Illustrations-131. Bibliography-49 references.

Synopsis of Contents

This book is divided into two parts: the first part discusses the performance of frequency agility radar including the strength of antijamming capabilities, the enlargement of the detection range, the raising of detection angle precision and the inhibition of the power of sea clutter. The second part introduces the composition of frequency agility radar focusing on the frequency agility magnetrons, the composition of incoherent and total coherency frequency agility radar and the special frequency agility radar systems.

This book provides scientific personnel references regarding the production and maintenance of radar.

Preface

Up to the present, radar has mainly been used in defensive and offensive weapons systems. As a weapons system it must be able to meet the countermeasures of an enemy. At present, this type of countermeasure is generally called electronic countermeasure. This is because it basically points to measures which use electronics to oppose the countermeasures of electronic weapons.

The methods for jamming radar can be divided into active jamming and passive jamming. Among the two, active jamming is the most effective method especially disturbance type active jamming. This type of jamming method is the transmission of noise jamming signals similar to the operating frequency of the radar. This can cause the echo signal of the radar to be completely drowned out in the jamming signal. If anti-jamming measures are not used then the radar equipment will exist in name only. Thus, there is produced the struggle of countermeasures and anti-countermeasures. This struggle can be considered to begin from not having radar equipment for a long time; the form of the struggle can generally be divided into 3 stages.

The first stage shows the struggle of tuning speed. To avoid the aimed active jamming of an enemy, radar uses mechanical tuning to change the radar's operating frequency to another frequency without jamming. In order to be able to jam this type of mechanically tuned radar, the jammer must be tunable and its tuning speed should be higher than that of the radar. This then makes up the struggle of tuning speed. The apex of the tuning

speed is inertialess electronic tuning. Use of an aiming type jammer with electronic tuning can tune the jammer to the operating frequency of radar in several microseconds to several tens of microseconds after scouting to the transmission frequency of radar. On the surface, this type of jammer seems uncounterable. However, frequency agility radar developed during the beginning of the 1960's is able to cause this type of jammer to have no means of jamming.

Frequency agility radar is a type of radar wherein its carrier frequency energy makes very large jumps in the adjacent pulses. This type of radar is also called jump frequency radar. Because the carrier frequency of each of its pulses is different, before a jammer reconnaissance aircraft receives a radar transmission pulse, it has no way of knowing the frequency of the radar pulse. Thus, there is no way of tuning the jammer to the operating frequency of the radar which then causes the jammer to have no means of jamming the large space from the radar to the jammer. It can, however, reveal the distance of the jammer. Therefore, even if it is an electronically tuned aiming jammer there is still no way of jamming frequency agility radar.

The second stage shows the struggle of the power and the frequency band. In order to be able to effectively jam frequency agility radar, the jammer only need be able to abandon narrow band aiming jamming and use wide band barrage jamming. This type of jammer can transmit fixed power jamming signals in a very wide frequency band. Yet, this will certainly produce the contradiction between power and band width because the wider the band width becomes its power spectral density will necessarily drop. In other words, the frequency agility technique forces the jammer to disperse its power to a very wide frequency band. To keep its power spectral density constant the required total power is enlarged. In the struggle of band width and

power, the jammer is not in an advantageous position. Because jammers are commonly mechanically loaded, their power consumption, volume and weight are limited. However, radar is frequently erected on the ground surface. Moreover, although the operating frequency of a single radar is limited, several sets of radar can be distributed in very wide frequency bands and can even occupy each wave band from P value to Ku. It is virtually impossible for a jammer to transmit a jamming signal with suitable power density in this kind of wide wave band.

The third stage mainly shows the struggle of self adapting capabilities. For the jammer to be most effectively used its power uses self adapting power handling so that although various wave band jammers are installed on aircraft (this occupies a suitable volume and load), yet its primary power is not added to the jammers but self adapts to add different wide wave band jammers based on the danger signal received by the reconnaissance aircraft. At the same time, frequency agility radar, while its self adapting capabilities continually increase, does not blindly and randomly jump but prior to each transmission pulse, carries out full view reconnaissance of its whole operating frequency band. Afterwards, it modulates the carrier frequency of the next pulse to a frequency with the weakest jamming signal. Further, a self adapting antenna array can automatically align the jammer's direction of the zero point in the antenna directivity diagram. It can be considered that up to the present the struggle to raise self adapting capabilities is still being continued.

Tests and theories have both proven that after radar uses the frequency agility system this can not only greatly raise its antijamming capabilities but can also carry a series of advantageous points with it. For example, the frequency agility system can increase the radar's detection distance (when in high detection probability, there is an increase of about 20-30 percent for the slow fluctuating target); it can raise the tracking

precision of angle tracking radar; it can inhibit sea clutter jamming; it can raise the distance resolution and amplitude resolution of the radar; it can eliminate the secondary noise caused by refraction; it can resolve the problem of mutual jamming between similar types of radar, etc. When these situations occur or if there is only one of the advantageous points among these, it is then necessary to use the frequency agility system for newly designed radar. For example, to resolve sea clutter jamming when in a moderate sea situation, even when pulse Doppler radar is detecting a sea target, we can change to use the frequency agility system. Therefore, the commonly used frequency agility system has become a trend of present day radar (especially military radar).

This book is divided into two parts: the first part is divided into five chapters which mainly explain the performances of frequency agility radar by means of theoretical analysis and test results. The second part of the book is divided into four chapters which focus on introducing frequency agility magnetrons and the incoherent frequency agility radar system.

Because the level of the author is limited it was unavoidable that this narration on frequency agility radar have sections which are inadequate. Thus, the reader is invited to point out mistakes so that they may be corrected.

Part One The Performance of Frequency Agility Radar

Chapter I. General Discussion

1.1 What is Frequency Agility Radar?

Frequency agility radar is a type of radar which uses fixed time interval radiation pulse energy. Therefore, it is a type of pulse radar. The carrier wave frequency of its transmitted adjacent pulses quickly change within a fixed range (see fig.1) Its agility form can change in a certain pattern and can also randomly jump.

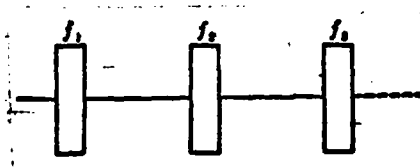


Fig. 1.1 The Agility of the Frequency Agility Radar's Transmitted Carrier Frequency in the Adjacent Pulse

Although the carrier frequencies of the adjacent pulses of most mechanically tuned jump frequency radar also have slight differences yet they cannot be regarded as frequency agility radar. Because the frequency differences between the pulses is very small they do not have the features of frequency agility radar. Only after the frequency differences between pulses increases to a certain value can it have the characteristics of frequency jumps.

This type of special characteristic can be related to the echo between pulses. To cause the echoes between pulses to not be related to the required minimum pulse frequency difference is called the critical frequency difference. The critical frequency difference is different for different quality targets. For example, the critical frequency difference for uniformly distributed clouds and rain and ocean wave targets is approximately the reciprocal of the pulse width. However, the critical frequency difference and radial of targets such as aircraft, guided missiles and satellites with relatively large refraction surfaces or regular shapes form an inverse ratio. Usually, its value is far greater than the reciprocal of the pulse width. From the point of view of the sea clutter interrelation, it is only necessary that the adjacent pulse frequency difference be greater than the reciprocal of the pulse width to be able to be called frequency agility radar. However, from the point of view of antijamming, only when the adjacent pulse frequency difference reaches the entire operating frequency band of the radar (for example, 10 percent band width) can it be called frequency agility radar.

Although frequency diversity radar can also successively transmit pulses with different carrier frequencies, yet because frequency diversity radar is usually composed of two (or several) stationary radar transmitter-receivers, therefore it can usually transmit pulses by two (or several) stationary carrier frequencies. Moreover, these different carrier frequency pulses are transmitted during the same radar operating period, the delay of being separated from one another is very small and afterwards the echoes received from each receiver are integrated. Because each different carrier frequency pulse is transmitted by a different transmitter and received by a different receiver their frequency numbers cannot be very numerous and therefore their antijamming capability cannot compare to frequency agility radar. Yet, in an enlarged detection range, it has similar areas

with frequency agility radar. Moreover, because it is usually double machine operated, its operation reliability is greater than single machine operated frequency agility radar.

Although frequency scanning radar is also a type of pulse carrier frequency jump radar, yet because there is a strict fixed relation between its transmission carrier frequency and beam direction (commonly the angle of elevation), its carrier frequency cannot have random agility but has required changes according to the beam direction. Generally, the carrier frequency of this type of frequency scanning radar has linear changes and cannot randomly jump. The range of its frequency changes must also be much narrower than frequency agility radar.

Although frequency agility radar is a special type of pulse radar system yet it can be compatible with other radar systems, for example, single pulse radar and pulse compression radar. However, when these radar systems are joined with a frequency agility radar system many new problems can arise. For example, in single pulse radar, it is necessary to consider the balance and compensation problems of each phase under frequency agility conditions.

Frequency agility radar must also be compatible with moving target indication radar and pulse Doppler radar to be able to meet certain difficulties which are hard to overcome. Although we have already mentioned several types of flexible methods compatible with moving target indication radar, it is even more difficult for it to be compatible with the pulse Doppler system. It can be considered that to date there is still no ideal plan.

1.2 How Frequency Agility Radar Was Developed

During World War II, in order to avoid enemy jamming and the

mutual jamming of friendly neighboring radar, fixed frequency radar gradually began to change and use variable frequency radar with tunable frequency magnetron. However, the earliest tunable frequency magnetron used a mechanical tuning mechanism for manually tuning. Its tunable range was relatively narrow and its tuning speed was very low. With the continual increase of the tuning speed of the jammer, this type of manually tuned variable frequency radar could not counter an enemy's jamming. During the beginning of the 1950's, a mechanical tuning mechanism with a motor driven cam appeared. The tuning speed of this type of tuning mechanism was increased. Yet, at the time, jammers began to use electronic tuning which caused reconnaissance and tracking speed to be further raised. Afterwards, although the tuning mechanism of the magnetron was changed to hydraulic transmission, the tuning speed could be raised to over 5,000 megahertz/second. Yet because this type of tuning mechanism still had relatively large mechanical inertia its tuning acceleration was still relatively small. Electronically tuned jammers can calculate based on their frequency change tendencies and therefore it can still be effectively jammed. Moreover, it is also very necessary to have a complex hydraulic transmission system and very large tuning power. The appearance of the rotating magnetron greatly increased the tuning speed of the magnetron. Its tuning speed reached to over 1,000 kilomegahertz/second. Thus, it was possible to cause the carrier of frequencies in the adjacent pulses to have large differences (the maximum reached the high and low limiting values of the operating frequency band). The rotating tuning magnetron not only had the greatest tuning speed but also had the greatest tuning acceleration. This is because its tuning mechanism does not make alternating motions but rather rotating motions. Naturally, rotating motion also has mechanical inertia and this type of mechanical inertia caused its tuning curve to become a sine form with frequency which is not easy to change.

However, from the beginning the frequency agility radar

which uses this type of rotating tuning magnetron encountered large technical difficulties. The problem was how to cause local oscillation frequency to be able to track such a fast tuned magnetron transmitted pulse and also to be able to maintain high frequency stability after transmitting the pulse. These problems were successfully resolved in 1963. Afterwards, a series of on-the-spot tests were carried out regarding the performance of frequency agility radar. These results showed that frequency agility radar not only possesses very strong antijamming capabilities but can also enlarge radar detection range and raise radar tracking precision. Therefore, after these on-the-spot test results were made public in 1964, they immediately drew widespread attention. In many nations, not only was old radar refitted into frequency agility radar but there was also widespread use of frequency agility systems in newly designed radar. Frequency agility systems were also used in high precision measuring radar. At the end of the 1960's, it was further discovered that frequency agility systems have excellent effects on inhibiting sea clutter. Thus, this type of system was very quickly expanded to various maritime uses and in surveillance radar. To date, frequency agility radar has become a conventional system in military radar.

1.3 The Advantages of Frequency Agility Radar

Frequency agility radar possesses a series of advantages. To sum up, the main advantages are shown in the following several areas:

(1) Relatively High Antijamming Capabilities

There are many antijamming methods yet they can be summed up as space selection, polarization selection, frequency selection and time selection. Among these, the most important as well as the most effective method is frequency selection. Further,

frequency agility can be considered the most effective frequency selection method. Roughly speaking, it causes the multiple of the increases or radar anti-jamming capabilities to be equivalent to the ratio of the frequency agility range and the radar receiver's band width. Then to further increase its anti-jamming capabilities it is only necessary to increase its frequency agility band width.

(2) Increases the Radar's Detection Range

If the frequency difference of the frequency agility radar's adjacent pulse is larger than the "critical frequency" this can cause the adjacent echo amplitude to be non-interrelated. This can eliminate detection loss owing to the target echo's slow fluctuation. This slow fluctuation of the echo often appears in in fixed frequency radar. Test results show that when relatively high detection probability (over 80 percent) is desired, the detection range of frequency agility radar can increase 20-30 percent more for slow fluctuation targets than fixed frequency radar. It is also equivalent to a 2-3 times enlargement of the transmitter power.

(3) Increases Tracking Precision

This is because the use of frequency agility can increase the frequency of the target's flash movement (angular noise) sighted in the deflection center and this can shift the energy spectrum of the angular noise to outside the angular servo-system band width. This can greatly decrease the angular tracking error caused by angular noise. This type of error is the major source of single pulse radar tracking errors for close range and medium range targets. Test results prove that the flash movement error of an aircraft target echo in over 2-4 hertz noticeably decreases. In the Ku wave band, its tracking error can decrease by one-half and the estimated error of the future point can be decreased by one-third. Use of frequency

agility for large targets such as ships can decrease tracking error by one-half to one-quarter. Frequency agility can also improve the detection angle precision of search radar.

(4) Inhibits Sea Clutter and the Jamming of Other Distributed Noise

When the error of the adjacent pulse carrier frequency is larger than the reciprocal of the pulse width, this can cause the noise of distributed targets such as ocean waves, clouds and rain and chaff to be interrelated. After carrying out video frequency accumulation for these echoes, the target's equivalent reflection surface approaches its mean value and the noise's variance will then decrease. This improved the signal-to-noise ratio. Theoretical computations and test results show that when the pulse number in the radar's beam is $N=15-20$, after using frequency agility, the signal-to-noise ratio can be increased 10-20 decibels. Therefore, this type of system is especially suitable for aircraft and ship radar and can also be used for detecting targets which are at low altitude over the ocean or on the ocean.

(5) Increases Radar's Target Resolution Capabilities

This type of system can decrease the amplitude change of the echo density function \sqrt{N} times. Further, it does not require very many pulses to be able to very precisely detect the mean effective reflection area of the target and thus raise the capability to distinguish targets. This is especially useful in geomorphologic mapping radar.

(6) It Can Eliminate the Jamming in Similar Frequency Bands Close to Radar and Thus Have Better Electromagnetic Compatibility

The reason for this is obvious. Whether the fixed frequency of the friendly radar is operating in the same wave band or operating in frequency agility their probability of meeting is very low. It is approximately equivalent to the ratio of the

radar's band width and agility band width.

(7) Elimination of Quadratic (or Multiple) Surrounding Echoes in Frequency Agility Radar

Because there is atmospheric superrefraction and thus abnormal propagation in a good deal of radar (especially coastal warning radar), the radar can have very far detection range. This can cause distant ground feature noise or ocean wave interference to reflect in the second (or multiple) recurrence period. To a small extent, it can increase the noise background and when serious can even drown out normal target echoes. Yet, in frequency agility radar, because the carrier frequency of the second transmitted pulse is different from the first, during the second period the receiver can then receive the echo of the last period. This also naturally eliminates the quadratic or multiple surrounding echoes. Yet, for this reason, the frequency agility system cannot be directly used in high repetition frequency radar with indistinct distance.

(8) It Can Eliminate the Influence of Beam Splitting Caused by Ground Surface Reflection

Because of the beam splitting caused by ground surface or ocean surface reflection the angular position of the smallest point is related to the operating frequency used by the radar. By changing the operating frequency the position of the smallest point can be changed. Therefore, when the radar operates in frequency agility, this can cause repetition of the split lobe and thus eliminate the influence of lobe splitting. This can greatly decrease the probability of losing targets in radar which records by computer tracking.

Aside from these, it can also eliminate the influence of the radar antenna cover's refraction on detection angle precision; can raise range resolution power; can realize target discrimination; can eliminate blind speed; can eliminate distance blurriness, etc.

Even though frequency agility radar possesses many advantages yet it still has certain problems and shortcomings.

Firstly, when in equipment frequency agility radar is much more complex than most radar. There are added technological difficulties which increase the cost of the equipment and lower operating reliability. For example, the frequency agility magnetron and the automatic frequency control system in incoherent frequency agility radar; the program controlled frequency agility coherent signal source and last stage wide band amplifier in total coherency radar; and the wide band antenna feeder system of the two types of radar are all relatively key technical equipment which require more advanced technical levels and conditions to be able to be solved. At the same time, this also increases the cost of the entire radar.

Secondly, under certain conditions, it is in contradiction with other radar systems and thus they cannot be realized simultaneously. For example, there is some difficulty in joining frequency agility radar and the moving target indication system. At present, only compromise proposals such as component agility or decreased number of frequency channels are able to be used. There are also difficulties in joining it with the high repetition frequency pulse Doppler system. These problems are all topics which are presently being researched.

1.4 How is Frequency Agility Radar Composed?

In composition, it is the same as most pulse radar. It can be divided into two major categories: incoherent frequency agility radar and total coherency frequency agility radar. The transmitter of the former commonly uses frequency agility magnetron. It has no phase relation with the local oscillation. Its simplified block diagram is shown in fig. 1.2.

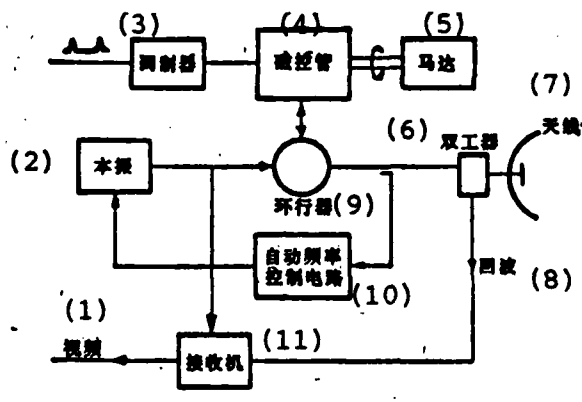


Fig. 1.2 Simplified Block Diagram of Incoherent Frequency Agility Radar

- Key:
1. Video frequency
 2. Local oscillation
 3. Modulator
 4. Magnetron
 5. Motor
 6. Duplexer
 7. Antenna
 8. Echo
 9. Circulator
 10. Automatic frequency control circuit
 11. Receiver

Usually, this type of frequency magnetron is high speed motor-driven. When the motor's rotating speed and action pulse repetition frequency are non-synchronous, a pseudorandom frequency agility signal can be obtained. A noise source can also be used to regulate the motor's rotating speed or action pulse's time position to obtain random jump frequency signals.

The local oscillation of incoherent frequency agility radar must have very high tuning speed so as to be able to keep up with the radio frequency pulse carrier frequency changes

transmitted by the fast speed tuned magnetron. Usually, this type of local oscillation is composed of a backward wave oscillator with voltage tuning. The backward wave tube's local oscillation has a very high tuning speed, a very wide voltage tuning band width and sufficient power output. These features are not possessed by the klystron's local oscillation. In the last several years, completely solidified voltage tuned local oscillation was developed which uses a varactor transistor or bulk effect tube oscillator. When compared with backward wave tube local oscillation, its volume is smaller, weight lighter, power consumption less, life longer and it is more reliable. Therefore, it has already gradually begun to replace backward wave tube local oscillation.

The most important technical factor in incoherent frequency agility radar is the local oscillation's automatic frequency control system. Because the transmitted pulses have agility between the pulses, the local oscillation must keep up with the jumps of the transmitted pulse carrier frequency within a very short time. It must also maintain constancy during the receiving echo time so that after the echo signal passes the mixed frequency it can fall in the intermediate amplification bandwidth. In early developed frequency agility magnetrons there was usually no frequency read-out transducer and it was unable to give frequency presetting information for carrying out rough tuning of the local oscillation frequency. At that time, it was necessary to be able to measure the magnetron cavity's resonance frequency (sometimes called "cold resonance frequency") so that the local oscillation can keep up with the changes of the magnetron cavity's frequency. Usually, the local oscillation itself is used as the test signal source. After a circulator is added in the magnetron's resonance cavity (see fig. 1.2), when the local oscillation frequency is equivalent to the frequency of the magnetron's resonance cavity, the latter can absorb a large portion of the

signal energy and its echo signal takes on a minimum value. Use of this principle with the addition of a suitable control circuit can cause the local oscillation's frequency to keep up with the changes of the magnetron resonance cavity's resonance frequency. In an appended frequency read-out transducer's frequency agility magnetron, the problem is much simpler and at this time the magnetron's frequency read-out signal can be directly used to roughly tune the local oscillation. Yet, because the magnetron's resonance frequency is not completely equivalent to the cold resonance frequency of the resonance cavity the above two methods can only roughly tune the local oscillation. More accurate tuning is needed after magnetron oscillation and a fast single pulse automatic frequency control system is used for regulation. This type of automatic frequency control system must be able to modulate the local oscillation frequency to an exact value within the pulse width of a single transmitted pulse. The control precision of the frequency agility radar's automatic frequency control system is very important because it determines the frequency bandwidth of the received intermediate frequency signal. The lower its control precision the wider the bandwidth occupied by the intermediate frequency signal. The intermediate amplification must be correspondingly increased so as to be able to cause the echo signal to undergo intermediate amplification. This increased the receiver's noise level and lowered the signal-noise ratio.

Incoherent frequency agility radar has relatively low frequency jump flexibility and thus it is quite difficult to join it with other pulse radar systems (for example, pulse compression) and realize even more complex frequency agility radar.

Because the transmitted pulse carrier frequency and the receiver's local oscillation of total coherency frequency agility radar is commonly produced by the same signal source

(usually a highly stable crystal oscillator) and there exists a phase relation between the two. This type of system can possibly realize frequency agility radar with a coherent signal processing system. At the same time because the carrier frequency of its transmitted pulse is produced by a numerically controlled frequency synthesizer it has even greater agility flexibility. For example, it can select any frequency in its operating frequency band an instant before transmission and thus can possibly realize an even more flexible system such as self adapting frequency agility radar.

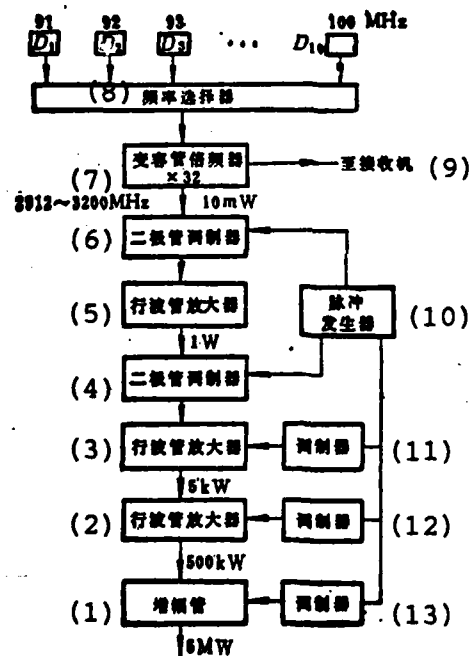


Fig. 1.3 Block Diagram of the Total Coherency Frequency Agility Radar Transmitter

- Key:
1. Amplitron
 2. Traveling-wave tube amplifier
 3. Traveling-wave tube amplifier
 4. Diode modulator
 5. Traveling-wave tube amplifier
 6. Diode modulator
 7. Varactor multiplier
 8. Frequency selector

Key: 9. To receiver
10. Pulse generator
11. Modulator
12. Modulator
13. Modulator

Fig. 1.3 gives the block diagram of a total coherency frequency agility radar transmitter. It includes a low frequency synthesizer and after going through frequency division, frequency multiplication, frequency mixing or a locked system, the 10 phase coherent signals ranging from 91 to 100 megahertz obtained from the crystal resonator is added to a numerically controlled frequency selector. This frequency selector can select any frequency based on the externally added numerical frequency command signals. The selected frequency is added to a varactor multiplier and after 32 frequency multiplications a microwave signal in the 2,912-3,200 megahertz range can be obtained. This microwave signal divides into two lines. One line is sent to the receiver and after 30 megahertz (this can be obtained from the same crystal resonance frequency multiplication) frequency mixing acts as the local oscillation signal. The other line is added to a diode modulator for pulse modulation and afterwards is added to the front amplifier composed of 3 traveling-wave amplifiers for amplification. This causes the power level to be amplified from a milliwatt quantity to 500 kilowatts. It is then added to the end amplifier composed of an amplitron and amplified to a 5 megawatt power level and sent to the antenna for transmission. This type of relatively simple frequency synthesizer can only produce 10 frequencies in the 2,912-3,200 megahertz range. If a more complex microwave frequency synthesizer is used it is possible to attain any frequency in a certain frequency range. In reality, a synthesizer is not needed for accurate frequency for there are usually 10 spectral lines which are sufficient for selection. The entire radar's bandwidth is limited by end power amplification. The antenna feed line system (especially the multilined high powered rotating joint) is also a factor which limits its

bandwidth.

Although this type of total coherency frequency agility radar possesses many advantageous features yet when in equipment its complex level is much higher than that of incoherent radar. Its transmitter system is especially complex. This increases the radar's volume, weight, energy consumption as well as its cost and lowers the system's operating reliability.

Therefore, incoherent frequency agility radar is commonly used in most small sized maneuvering tactical radar (especially ship-based, aircraft-based and missile-based radar). Medium and large size fixed radar or radar with special requirements use total coherency frequency agility radar and specifically select and use the type of radar according to specific tactical and technical requirements.

References

- [1] System properties of jumping-frequency radar. B.C. Gustafson and B-O As. Philips Telecomm.Review. Vol. 25, pp.70-76, 1964.
- [2] Frequency-agile radar jumps ahead. J.B. Brinton, Jr. Microwaves. Sept. 1965.
- [3] Frequency-agile radar, N. Backmark, J.E.V. Krim and F. Sellberg... Philips Tech. Rev. Vol. 28. No.11, 1967, p. 323.
- [4] Radar a radiofrequenza variabile. A. Gilardini. Alta Frequenza. Vol. 38, N. 9. Sett. 1969. pp.657-665.
- [5] Frequency agile radar techniques. A.N. Murthy and J.P. Gupta. J. Inst. Eng. India. Electron and Telecom. Eng. Div. 1971, 52. No. 1, pt. 1. pp. 11-16.
- [6] Multifrequency radar, G. M. Vischin, Voenizdat. 1973.

Chapter II Antijamming Capabilities of Frequency Agile Radar

2.1 Basic Types of Jamming

Generally speaking, the useless signals received by radar receivers can be called jamming signals. So-called useless signals are mainly determined by the special radar use. Therefore, the useless jamming signals for one type of radar can possibly be useful signals for another type of radar. For example, meteorological noise is useless jamming signals for common radar but become useful signals for meteorological radar.

The various types of jamming signals can basically be divided into natural jamming and man-made jamming. "Natural jamming" is the originally existing jamming in the natural world and "man-made jamming" is jamming produced intentionally or unintentionally by man.

Natural jamming mainly includes various ground noise jamming, sea clutter jamming, meteorological noise jamming, bird noise jamming as well as noise jamming from the atmosphere and the common man-made jamming can be divided into intentional and unintentional jamming. The most typical unintentional jamming is the jamming of friendly nearby radar. Aside from this, there are also various types of jamming produced by radio equipment.

Intentional man-made jamming is naturally intentionally produced by an enemy to jam the operation of our radar station. Therefore, it is the most difficult to counter. Although frequency agile radar possesses the ability to counter various natural noises (such as sea clutter), yet it was mainly produced to

counter man-made jamming. The discussion below will focus on intentional man-made jamming.

Intentional man-made jamming can further be divided into passive and active jamming. Passive jamming is sometimes also called negative jamming and active jamming is sometimes called positive jamming. Although some people also consider the absorbing electromagnetic wave coatings applied on a target as negative jamming, this method only reduces the electromagnetic wave energy transmitted by the target but does not produce other jamming signals. Therefore, it cannot be considered as a jamming measure but only a negative anti-radar measure.

In reality, passive jamming is intentionally put in passive reflecting bodies. These reflecting bodies which are the same as real targets can also reflect radio waves. The most effective among them must be considered angular reflecting bodies and semi-wavelength chaff. Angular reflecting bodies have omnidirectional reflection characteristics and the direction of their reflected electromagnetic waves is completely identical with the direction of incidence. Therefore, their equivalent reflection areas are especially large and these can be used to simulate a large warship. During the early period, chaff was made from very thin aluminum foil but now metallized glass fiber is used. Its diameter is only several ten micron and its length is just equivalent to half the operating wavelength of radar. Thus, it can produce resonance in the radar's operating frequency. Although the effective reflection area of each piece of chaff is very small yet it is large in quantity (each time it is put in the number can reach to over several million). Therefore, it can create very strong jamming noise and can also cause attenuation when using useful echo signals. Further, there are also bait rockets and false warheads.

The most outstanding feature of this type of passive jamming

is that the reflected echo signal frequency is the same as the projected frequency of the radar. Therefore, it cannot be eliminated by means of the frequency selection method and frequency agile radar cannot counter it. Yet, like sea clutter, the frequency agile technique has a certain inhibiting effect on distributed passive jamming. Moreover, this type of passive jamming is also limited by various service conditions. Firstly, its length can only cause maximum effect when it equals the semi-wavelength of the radar. Therefore, the radar's operating wavelength must be measured beforehand, or, after using a ferret receiver to detect the radar's operating wavelength, automatically cut off the length of the glass fiber based on the measured length. Secondly, its jamming space has certain limitations and usually requires that beforehand the jamming aircraft of this chaff release be taken in a fighter plane and released along an air corridor. This is also equivalent to knowing the enemy in advance. Thus, military preparation can be done well. Aside from this, even though the weight of these glass fibers are extremely light they are nevertheless limited in air stay time. At present, new materials suitable for distributed jamming such as metallic air suspended bodies and ions are being developed. Furthermore, no matter what direction radar this type of passive jamming is for it is necessary that its operating wavelength be the same and its jamming effects be identical.

Man-made jamming is the most effective and active jamming is the most difficult to counter. This type of active jamming is produced by a jamming transmitter because the effective jamming power produced in the area of the radar receiving antenna forms an inverse ratio with the square of the distance. Thus, it is very easy to attain power which is stronger than useful signal echoes. Further, it is the type of jamming with the greatest danger to radar. Below we will discuss this type of jamming.

Active jamming can be divided into three categories: pressure controlling, disturbing and deceiving. Pressure control jamming mainly uses the above mentioned jammer advantages in power to produce very strong jamming signals and thus drown out the useful signals. This type of jamming can also be divided into continuous wave jamming frequency modulated continuous wave jamming and noise jamming. Among these, noise jamming with frequency spectrums which approach white noise are most effective. This type of noise jamming can also be divided into the sighting, separation blocking and blocking types according to their frequency spectrum width and the position of the relative radar signal frequency spectrum. Disturbing type jamming does not necessarily completely drown out the useful signals but can produce a very large jamming effect on the radar observer or automatic registering equipment so that they have no way of operating normally. Most of this type of jamming possesses the pulse modulation form and it can be multiple synchronous pulse jamming or disturbing pulse jamming. The former has repetition frequency synchronized with the radar pulse and the latter has random repetition frequency, pulse width and amplitude. Deceiving type jamming does not have the operating strength or quantity of pressure controlling radar but employs the method of "using the false to disturb the real" to deceive radar observers or automatic tracking systems. The signals of this type of jamming not only possess operating frequency identical to the radar but its pulse parameters are also the same as those of radar. Only its movement pattern is different. For example, the simulated pulse jamming used to counter search radar can produce a false target with a fixed movement speed and because the power of the jammer is relatively great it can use the effect of the antenna side lobe and form a series of false targets on a luminescent screen. Further, deceiving type jamming for counter- ing range gate automatic tracking radar has a signal with similar delay time as the echo signal when it is first produced but its

strength is greater than that of the echo signal. After this signal uses the variable delayed time circuit it gradually changes the delay time which causes the radar's range tracking gate to erroneously follow this false target. After delay time reaches a certain distance the signal is suddenly lost or returns to its original location. This swings the tracking gate open. To counter the angular tracking of radar another method of deceiving jamming is used. Phase inversion jamming is used for the most typical conical scanning radar. After the jamming receiver receives the radar signals it detects its angular error signal and following phase inversion amplification it is then added to the limited amplification radar signal. This causes the error signal and actual error signal of the signal received by the radar to be completely reversed so that the radar antenna is caused to "spring open" and have no way of tracking the target.

In order for the so-called deceiving jamming to simulate real radar echoes most use reply type jamming. So-called reply type jamming indicates that the jamming receiver and transmitter are an amplification chain formed from a low energy level to high energy level amplifier. Thus, the frequency of the transmitted signal is totally identical to the frequency of the radar signals. This type of jamming cannot be eliminated by use of the frequency selection method and furthermore it cannot be countered by frequency agile radar.

Aside from this, there are also various radar jamming methods and measures for different uses and different systems. These will not be individually enumerated in this book.

Some people consider anti-radar missiles as a type of positive jamming. This type of missile can trace radar (usually tracking radar) beams and thus can accurately shoot and hit radar and destroy it. Actually, because it does not produce jamming signals

and thus cannot act as a type of positive jamming, it can only be considered a type of positive anti-radar measure.

To sum up, the basic jamming types are listed in table 2.1.

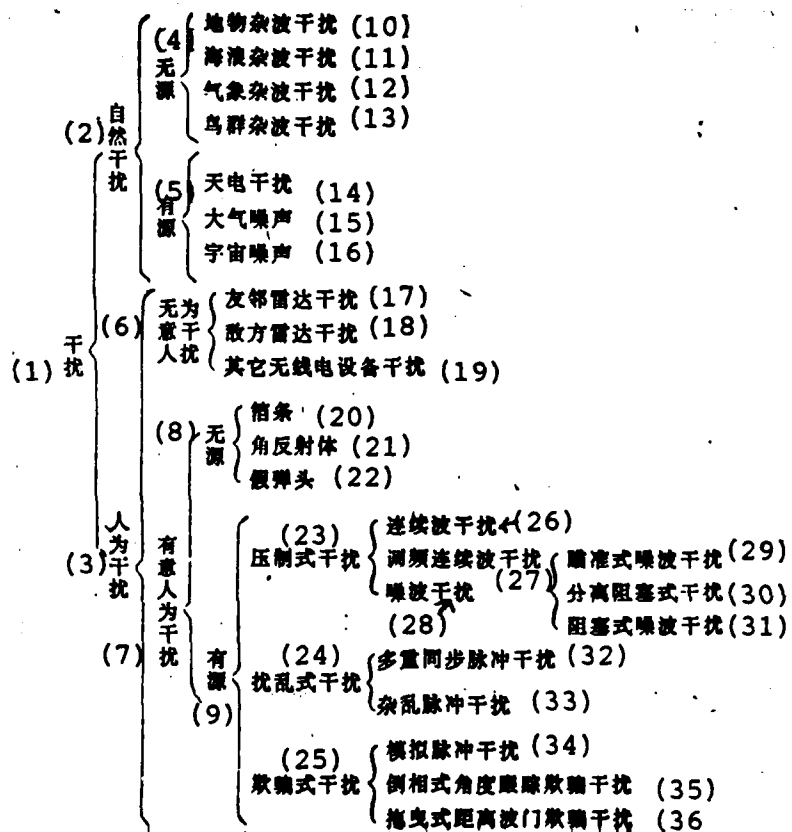


Table 2.1 Basic Types of Jamming

- Key:
1. Jamming
 2. Natural jamming
 3. Man-made jamming
 4. Passive
 5. Active
 6. Unintentional man-made jamming
 7. Intentional man-made jamming
 8. Passive
 9. Active
 10. Ground noise jamming

- Key:
11. Sea clutter jamming
 12. Meteorological noise jamming
 13. Bird noise jamming
 14. Static jamming
 15. Atmospheric jamming
 16. Cosmic jamming
 17. Friendly nearby radar jamming
 18. Enemy radar jamming
 19. Other radio equipment jamming
 20. Chaff
 21. Angular reflecting body
 22. False warhead
 23. Pressure control jamming
 24. Disturbing jamming
 25. Deceiving jamming
 26. Continuous wave jamming
 27. Frequency modulated continuous wave jamming
 28. Noise jamming
 29. Aimed noise jamming
 30. Separated block jamming
 31. Block noise jamming
 32. Multiple synchronous pulse jamming
 33. Disturbed pulse jamming
 34. Simulated pulse jamming
 35. Phase inversion type angular tracking and deceiving jamming
 36. Drag type distance gate deceiving jamming

2.2 The Danger of Active Noise Jamming to Radar

Active noise jamming poses the greatest danger to radar. Below we will focus our discussion on this type of jamming.

The effect of jamming signals on radar operations is mainly manifested in the loss of useful information received by the radar. The specific form of this type of loss is that useful signals are drowned out and the receiver is saturated so that signal input is cut off which produces ranging and angle measuring errors.

Usually, this type of information loss can be indicated by

the pressure control coefficient [1]. Pressure control coefficient K_s is defined as the ratio of jamming signal power P_j in the receiver's input terminal and pulse power P_s of the useful signal. It is indicated as

$$K_s = \left(\frac{P_j}{P_s} \right) \quad (2.1)$$

Yet, the useful signal power of the receiver's input terminal is not constant but is related to the distance of the target and effective reflection area. Therefore, we first researched the ratio of jamming signal power P_j and noise power P_n at the front terminal of the receiver to show the danger of a jammer to radar.

Jamming signal power P_j received in the front terminal of the radar receiver can be computed by the following formula

$$P_j = \frac{P_j G_j (B_R / B_j)}{4\pi R^2} \cdot A \cdot \frac{1}{L_R} \quad (2.2)$$

In the formula

P_j	is the mean power transmitted by the receiver;
G_j	is the jammer's antenna gain of the radar direction;
B_R	is the radar's bandwidth;
B_j	is the jammer's bandwidth (usually $B_j > B_R$);
L_R	is the loss of the radar's receiving system up to the front terminal;
A	is the effective reflecting area of the radar antenna — $G_R \lambda^2 / 4\pi$;
G_R	is the receiving gain of the radar antenna;
λ	is the wavelength;
R_j	is the distance of the jammer from the radar station.

Noise power P_n in the front terminal of the radar can be computed by the following formula

$$P_n = KTB_R \cdot N_r \quad (2.3)$$

In the formula K is the wave Boltzmann constant;
 T is the absolute temperature (indicated by K);
 N_r is the receiver's noise coefficient.

Therefore, the ratio of the jamming signal power and receiver's front terminal noise power is

$$\left(\frac{P_j}{P_n} \right) = \left[\frac{P_j G_j}{B_j} \right] \cdot \frac{A}{4\pi R^2 \cdot L_r} \cdot \frac{1}{KT \cdot N_r} \quad (2.4)$$

It should be noticed that this formula is not related to the radar receiver's bandwidth B_R .

The values inside the square brackets on the right side of the formula represent the jamming power density of the jammer. We know from the formula that this power density forms a direct ratio with transmitted power P_j of the jamming transmitter and the product of jammer antenna gain G_j and forms an inverse ratio with jamming signal frequency spectrum width B_j . The former is basically determined by the delivery means of the jammer and the latter is determined by the type of jammer.

The delivery means of jammers can be divided into tactical aircraft (this aircraft is responsible for tactical fighting), interference aircraft (aircraft responsible for interference), strategic aircraft (including strategic bombers and reconnaissance aircraft), ships as well as throw type small jammers. Because of the differences of delivery means their ability to

provide space and power volume varies.

The operating frequency range of jammers can be made identical to the operating frequency range of radar but the frequency bandwidths of each jammer are limited. Because the power energy level is lower than that of radar it can very easily be the width of an octave. Yet, the wider the bandwidth the lower its power density and the more wanting the jamming effects. Aimed type noise jamming aims the frequency spectrum of the jamming signal on the radar's signal frequency spectrum and its bandwidth is about twice as large as the radar's bandwidth. Its power density is relatively large and its jamming effects are good. Yet, radar can avoid this type of jamming.

(1) 干扰运载手段	(8) 干扰机性能	(22) 年代	年代 (24)
	(9) 有效干扰功率 P_j	100~400W	
	(10) 干扰机天线增益 G_j	10	
(2) 战术飞机	(11) $P_j G_j$ 乘积	1~4KW	~10KW
	(12) 频率范围	500MHz~20GHz	500MHz~40GHz
	(13) 波数	3 (例如-71为L. S. C)	
(3) 干扰飞机	(14) 干扰机天线增益 G_j	(23) 100	
(4) 战略轰炸机	(15) $P_j G_j$ 乘积	100~200KW	1MW
(5) 战略侦察机	(16) 频率范围	100MHz~20GHz	100MHz~60GHz
(6) 舰 船	(17) 有效干扰功率 P_j	1~2KW	
	(18) 有效干扰功率 P_j	5~10W	
	(19) 干扰机天线增益 G_j	10	
(7) 便携式	(20) $P_j G_j$ 乘积	50~100W	1KW
	(21) 波数	1	2~3

Table 2.2 Performances of Various Noise Jammers and Their Estimated Performance

Key: 1. Jamming delivery means
 2. Tactical aircraft
 3. Interference aircraft
 4. Strategic bomber

- Key:
5. Strategic reconnaissance aircraft
 6. Ship
 7. Throw type
 8. Jammer performance
 9. Effective jamming power P_J
 10. Jammer antenna gain G_J
 11. $P_J G_J$ product
 12. Frequency range
 13. Number of wavebands
 14. Jammer antenna gain G_J
 15. $P_J G_J$ product
 16. Frequency range
 17. Effective jamming power P_J
 18. Effective jamming power P_J
 19. Jammer antenna gain G_J
 20. $P_J G_J$ product
 21. Number of wavebands
 22. 1970's
 23. For example
 24. 1980's

Table 2.2 lists the performances of various noise jammers which can be delivered by various delivery means as well as their estimated performances for the 1980's. Although the power energy level of the throw type is lowest yet its quantity is high and therefore it can still present a formidable danger. If a jammer's transmitted noise power is 500 watts, bandwidth is 200 megahertz and antenna gain is 6 decibels, then

$$\left[\frac{P_J G_J}{B_J} \right] = 10 \pi / \lambda^2 (1)$$

Key: 1. Watts/megahertz

Below we will use data for a typical L waveband search radar as an example. If the parameters of this radar are $N_F \times L_T = 8$ decibels, and $A = 10$ decibels (taking 1 meter² as 0 decibels), then when the jammer's range is 200 nautical miles, its (P_J/P_n) value can be computed by the following formula

$(P_j/P_n)=50$ decibels (taking 1 watt/hertz as 0 decibels)

+10 decibels (A takes 1 meter² as 0 decibels)-11 decibels (4π)
 -2x55.7 decibels (taking 1 meter² as 0 decibels) +204 decibels
 (KT)-8 decibels ($N_F \times L$)=33.6 decibels.

These results show that even when the jammer range is 200 nautical miles, the ratio of the radar receiver's front terminal input jammer power and the receiver's noise power is also completely objective. However, this ratio forms an inverse ratio with the square of the jammer range. When the range is 100 nautical miles, this ratio will be greater than 40 decibels. The relation of the inverse ratio formed by this type and the square of the range is shown in fig. 2.1. The receiver's front terminal noise power is indicated by the thick vertical line.

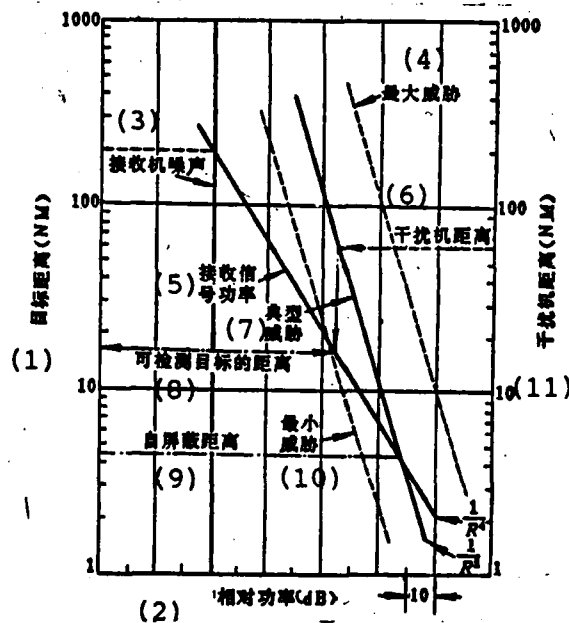


Fig. 2.1 Relation of the Active Jamming Source's Range and Relative Power

- Key:
1. Target's range (NM)
 2. Relative power (dB)
 3. Receiver's noise
 4. Maximum danger
 5. Received signal power
 6. Jammer's range
 7. Typical danger
 8. Range of detectable target
 9. Self-shield range
 10. Minimum danger
 11. Jammer's range (NM)

In order to make comparisons, besides the above examples of typical danger, the figure also draws the minimum and maximum dangers indicated separately by the dotted lines. The hypothetical parameters of these three types of dangers are shown in the following table [2]:

(1) 威胁类型	(6) 最 小	(7) 典 型	(8) 最 大
(2) 干扰机功率 P_J	5W/MHz	10W/MHz	100W/MHz
(3) 波长 λ	10cm	23cm	63cm
(4) 天线增益 G_R	37dB	35dB	31dB
(5) 噪声 + 损耗 $N_F + L_r$	13dB	3dB	3dB

Table 2.3 Typical Parameters of Various Dangers

- Key:
1. Type of danger
 2. Jammer power P_J
 3. Wavelength λ
 4. Antenna gain G_R
 5. Noise + loss $N_F + L_r$
 6. Minimum
 7. Typical
 8. Maximum

It can be seen from the table that because the wavelength is relatively long, the absolute bandwidth of the radar is relatively narrow. Thus, the jammer easily creates relatively

large power density and its formed danger is also relatively large.

The above narration only discussed the relation of the jamming signal power and receiver's front terminal noise power. To study the influence of jamming on signal detection, it is also necessary to study the signal power received by the radar. The echo signal power P_s received by the radar from the target reflection can be shown by the following formula

$$P_s = \frac{P_R G_R^2 \sigma \lambda^4}{(4\pi)^3 R_T^4 L_R^2} \quad (2.5)$$

In the formula P_R is the transmitting power of the radar;
 σ is the target's equivalent reflection area;
 R_T is the target's range.

It can be seen from the formula that echo signal power P_s forms an inverse ratio with the quartic direction of the target's range.

To simplify, we can assume that in the radar's maximum detection range, received echo signal power P_s is equivalent to the radar receiver's front terminal noise power P_n .

Assuming that this radar is in normal condition, we can detect targets for 200 nautical miles which is also the $P_s = P_n$ in the 200 nautical mile area. In this way, it begins from this point in fig. 2.1 and an oblique line is made based on the pattern of $1/R^4$. This oblique line represents the echo signal power transmitted by this target in accordance with the patterns of the target range changes.

Now, two situations exist. One situation is that target range R_T is not equivalent to jammer range R_J . This type of situation

is called separated (or distantly separated) jamming. It is also discharging jamming in a far place by means of a special aircraft loaded with a jammer so as to shield the operational aircraft. Another situation is $R_T = R_J$ and this situation is called self-prepared jamming. The operational aircraft itself carries the jammer or the aircraft itself which is carrying the jammer is the target detected by the radar.

We will first look at the situation of the separated jamming. If the jammer's range is 60 nautical miles we can then find the relative jamming power in fig. 2.1. If the minimum detectable signal power is equivalent to it then the corresponding radar detection range can be found under jamming conditions. In this example, at 16 nautical miles, we can see that its danger level is very grave.

When $R_T = R_J$ under self-prepared jamming conditions the radar detection range is the intersection point of the $1/R^2$ thick solid oblique line and $1/R^4$ thick solid oblique line in fig. 2.1. This range is also called the self-shielded range. It is about 5 nautical miles in this example. This is also to say that only when the range of the radar from the jammer's target is less than the self-shielded range can the radar detect this target. Actually, within 5 nautical miles, the detection of a target has no significance.

Yet, it should be noticed that the above mentioned discussions assumed that the jammer was located in the same place as the target because only at this time can the jamming signal use the radar antenna's maximum gain point. This is only the case when there is self-prepared jamming. When there is separated jamming, the probability of having the jammer and target aircraft in the exact same location is very low because in most circumstances they are not in the same location. At this time, when the echo

signal of the target reflection uses the antenna's maximum gain point, the jamming signal enters from the antenna's side lobe. In this type of situation, the effects of the jammer are not only related to the above mentioned factors but to a very large degree are determined by the radar antenna's side lobe energy level.

The effects of the radar antenna's side lobe energy level on jamming can be seen in fig. 2.2.

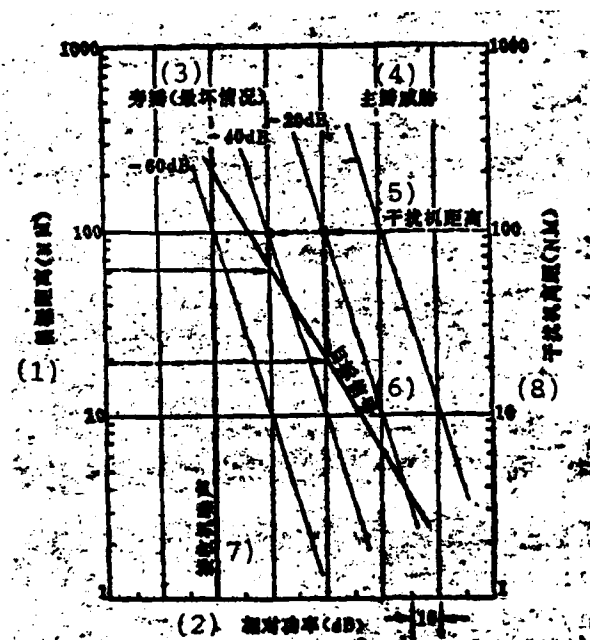


Fig. 2.2 The Influence of the Radar Antenna's Side Lobe Energy Level on the Jamming Effects of Separated Jammers

- Key: 1. Target's range (NM)
 2. Relative power (dB)
 3. Side lobe (worst conditions)
 4. Main lobe danger
 5. Jammer's range
 6. Target signal
 7. Receiver sounds
 8. Jammer's range (NM)

The jamming for the main lobe in the figure is drawn based on the maximum danger conditions in fig. 2.1. For the side lobe energy levels of -20, -40 and -60 decibels, this oblique line shifts left using 20 decibels as the interval. The figure also delineates the minimum detectable target signal (equivalent to the receiver's front terminal noise) in the 200 nautical mile area. Assuming that the jammer is located 100 nautical miles from the radar, when the jamming signal enters from the -20 decibel side lobe, the maximum detectable target range still does not reach 20 nautical miles. If the side lobe energy is lowered to -40 decibels, the maximum range at which the target is detectable can reach 60 nautical miles. If the side lobe power level can be reduced to -60 decibels then it can be considered that the jamming signal entering from the side lobe does not produce any effect on target detection. We can see from this that lowering the side lobe energy level is also very effective in countering the separated type jammer. The difficulty is that this lowered side lobe energy level is very hard to realize technologically.

2.3 Major Antijamming Methods

Generally speaking, so-called "antijamming" is the selection of useful signals from a large mixture of useless signals created by jamming. Our discussion of antijamming will mainly deal with man-made jamming especially man-made active jamming.

The major method for countering active jamming can be divided into three categories: the airspace selection method, frequency selection method, and time selection method.

Below we will separately discuss the principles and special features of these three categories:

(1) The Airspace Selection Method

The so-called airspace selection method uses the difference between the jamming signal source's (mainly active jamming) space

position and the useful target's space position to select useful signals. The airspace selection method can also be divided into the indirect airspace selection method and direct airspace selection method.

The most typical indirect space selection method is the side lobe blanker [3]. This side lobe blanker has a non-directional auxiliary antenna, and its gain must be higher than the antenna's side lobe gain. If the signals received by the auxiliary antenna and those received by the main antenna coincide in time and its amplitude is greater than that of the latter, it can then determine this signal in the main receiver and enter through the side lobe of the main antenna. Thus, a suitable strobtron circuit is used for suppression.

It is very clear that this type of method can only suppress pulse modulation and after the jamming enters the antenna's side lobe (for example, simulated pulse jamming, multiple synchronous pulse jamming or mixed pulse jamming), it is powerless for noise jamming. This type of video strobtron method also suppresses most of the useful signals.

Most contemporary space selection methods use the direct selection method. The so-called direct selection method is the direct use of the antenna's directivity pattern to select useful targets and suppress the jamming signals. Naturally, this type of space selection method requires that the useful target and jamming source not be in the same direction and not be in the same location for two coordinate radar.

At present, there are two types of direct selection methods used: the adaptive antenna array and the ultralow side lobe antenna.

The adaptive antenna array possesses a movable beam zero

point. This beam zero point can use the weight of changed radiation units for control, can use the signals obtained from the auxiliary antenna for forming in intermediate frequency and the main antenna signal's coherent phase reduction, and can also use the single pulse antenna's difference beam zero point. When it detects the jamming signal, a feedback control system is used to automatically aim at the jamming source which causes the received jamming signals to be minimal. Naturally, the major drawback of this type of method is that it only counters one jamming source. When the space jamming source is distributed to several different places, an adaptive return circuit is required for each jamming source and this causes the equipment to be very complex.

Therefore, an even more effective space selection method is the ultralow side lobe antenna. The side lobe of a common plane antenna can only be as low as -20 to -25 decibels at the most. Nevertheless, this ultralow side lobe antenna can decrease more than -40 to -50 decibels. As mentioned in the last section, the decrease of this type of side lobe's level is especially effective for countering separated noise jamming. Yet, it is very difficult to concretely realize a low side lobe antenna technologically.

Theoretically speaking, only if the plane antenna continually lowers the boundary irradiation level on the hole surface can the side lobe be decreased. For example, the theoretical side lobe of the Hamming weighting can reach -49 decibels. Yet, use of this method to lower the side lobe will cause the hole surface usage to lower and thus cause the antenna's gain to decrease. Moreover, it is also very difficult to realize the feed source of these primary irradiation functions. By adding on to the antenna's surface tolerance and feed source, the covering of the support rod can cause its side lobe level to rise. Therefore, the actual side lobe level of the plane antenna is still not lower than 35 decibels.

A method with each radiation source of equal excitation but with unequal distances can be used for the array antenna to lower the side lobe level. Use of this method can realize a side lobe level lower than 30 decibels. It does not influence the main lobe width but can increase the width.

The most effective method for lowering the side lobe level is the use of a waveguide slot array antenna. It is only necessary to accurately design and process the angle, distance, depth as well as the distance within the waveguide of this type of antenna slot to be able to attain a very low side lobe level. A side lobe level below -50 decibels has already been realized. This is very effective for countering a separated type jammer.

(2) The Frequency Selection Method

The frequency selection method mainly uses the difference in the frequency spectrum between useful signals and jamming signals to select useful signals. Naturally, this method can only be used to counter active jamming.

The superiority of the frequency selection method as compared to the low side lobe technique lies in its being able to counter the separated jammer outside the main lobe direction and also being able to counter the same direction or self-prepared jammer inside the main lobe.

The frequency struggle of the radar and jammer first manifests itself as the fight in waveband. Most early radar was focused in the narrow waveband ranges of 23, 10, 5 and 3.2 centimeters. After its operating frequency was fixed this made it very easy to use an aiming noise jammer for jamming. Modern radar has opened up many new wavebands not commonly used in the past. Moreover, some transmitter-receiver equipment in the same radar has many different frequency bands, for example, the SAM-6 guidance radar

has the four frequency bands of G, H, I and J. Although jammers have certain tuning capabilities their tuning capabilities are still able to be confined within the same frequency band. To counter various types of radar operating in the A to J frequency bands^{F.N.1}, it is necessary for the jammer to carry all of these frequency bands. This is impossible for fighter aircraft to do and is quite difficult for tactical aircraft.

The frequency struggle between the same radar and the jammer is manifested in two areas: one is the accelerated jumping frequency speed, the other is the enlarged tuning width. Frequency agility radar which can jump across the entire tuning bandwidth within adjacent pulses has jumping frequency speed that has reached the limit. The tunable aiming type jammer is already powerless (see next section for details) and can only use the wide band blocking jammer. At this time, the focal point of the struggle is mainly concentrated in the bandwidth. However, the tuning range of frequency agility radar can rarely exceed 10-15 percent. Yet, the power of the radar is totally concentrated on a relatively narrow frequency and the jammer forces its power to disperse to a very wide bandwidth. This has a very great influence on its jamming effect. Furthermore, although the noise jammer strives to produce near ideal white Gauss noise, in reality it is never able to do so and there are often spaces on the frequency spectrum. It is only necessary that the radar possess the ability to analyze the jammer's frequency spectrum and also be able to tune its operating frequency to the spaces on these frequency spectrum. Then, its jamming capability can be raised. The main present and future task of jammers is to produce pure white frequency spectrum as best as possible.

F.N.1 The frequency bands represented by each letter are:
A, 0.1-0.25 GHz; B, 0.25-0.5 GHz; C, 0.5-1 GHz; D, 1-2 GHz;
E, 2-3 GHz; F, 3-4 GHz; G, 4-6 GHz; H, 6-8 GHz; I, 8-10 GHz;
J, 10-20 GHz; K, 20-40 GHz.

3) The Time Selection Method

The method of selecting useful signals in the time domain was a commonly used method during the early period. In the past, this type of method mainly used the difference of the jamming pulse between the repetition frequency and pulse width, and the target echo pulse. Naturally, this method can only be used to counter pulse modulation jamming but has no effect on noise jamming.

To counter noise jamming there are at present the following methods in the area of time selection: one is the pulse accumulation method. This method mainly uses successive echo signals in distance (time) which are correlated and noise jamming then has an uncorrelated principle. In reality, this pulse accumulation method was originally used to counter noise inside a receiver. Radar with automatic detection equipment originally had a video accumulator and under normal conditions the radar's detection range was guaranteed by this type of video accumulation. Thus, it was unable to produce further effects when it encountered additional noise jamming. It could only further use the "burn through" technique when the target's direction was known, that is, to transmit more pulses in this direction and at the same time when correspondingly increasing the accumulated pulse number there are further effects. Yet, this cannot be realized in radar in which the antenna carries out peripheral searching. Another method is the use of various types of constant false alarm rate circuits while preventing receiver saturation. This is because receiver saturation can cause it to not have signal output and thus have tremendous loss. Only by using a receiver with a wide range can the various types of constant false alarm rate circuits be made to operate normally. A constant false alarm rate circuit can automatically regulate the detection threshold so that the signal detector's false alarm is kept constant. This prevents an overload on the data processing computer. Yet, the constant false alarm circuit cannot extract

signals from jamming noise but on the contrary when the detection threshold increases and rises with the jamming signals it loses more relatively weak signals.

By comparing the above three major types of antijamming measures we can draw the following conclusions: it is necessary to, as far as possible, cause the jamming signals to have no means of penetrating into the radar receiver. If they jump to the rear side of the receiver or even become video signals it is even more difficult to carry out selection. The space selection method is the most effective yet it is unable to counter self-prepared jammers. The only effective method for countering self-prepared jammers is still the frequency selection method. On the one hand, it is necessary to develop, produce and deploy various types of radar which occupy all the frequency bands; on the other hand, for single radar, we should use adaptive frequency agility radar which can realize pulse jumping within a very wide frequency band.

2.4 The Ability of Frequency Agility Radar to Counter Narrow Band Aiming Type Jamming

Early hostile active jamming usually employed narrow band aiming type jamming. This also used a reconnaissance plane to measure the operating frequency of the radar station and afterwards tuned the jammer's frequency to this frequency so as to jam the radar. This type of jamming method is very effective for a radar station operating at fixed frequency or a radar station which can only tune at slow speeds. This is because it can greatly limit the jamming power focused on the radar's operating frequency and thus lower the volume and weight of the jammer. This is very important for fighter aircraft. Therefore, to date, this type of narrow band aiming type jammer is still one of the major jamming devices. When it is reliably shown

that the radar is operating at a fixed frequency, it is only necessary for a reconnaissance plane to measure the radar's operating frequency in advance and later effective jamming can be realized by tuning the fixed frequency jammer in the fighter aircraft according to the above mentioned frequency. At this time, it is not necessary to carry a complex complete wave band panoramic receiver. Yet, when the radar can realize low speed tuning use of this method is not satisfactory for jamming. It is then necessary to use a panoramic receiver to measure the radar station's operating frequency whenever necessary and at the same time tune the jammer's frequency to the radar station's frequency whenever necessary. Because the complete wave band panoramic receiver is very complex most fighter aircraft cannot carry it. It is then necessary to send out an aircraft with a complete set of panoramic jamming equipment as a screen at the same time the fighter aircraft is sent out. A nearby ship carrying a panoramic jammer can also carry out jamming. Under these conditions, for the radar to be able to counter the aircraft or ship with complete wave band panoramic jamming equipment it only need be able to increase its tuning speed. When beginning, the panoramic receiver and jammer are both mechanically tuned and at the same time the radar's use of a fast mechanical tuning mechanism with a motor driven cam is relatively effective. Yet, after the totally electronically tuned automatic jammer appears, the mechanically tuned radar then faces great danger. The block diagram of this type of electronically tuned automatic jammer is shown in fig. 2.3.

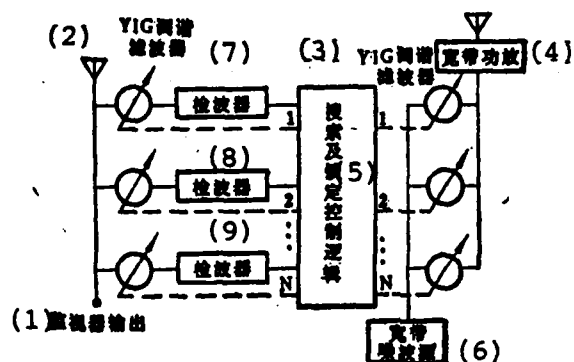


Fig. 2.3 Electronically Tuned Automatic Jammer

- Key: 1. Monitor's output
 2. YIG tuned filter
 3. YIG tuned filter
 4. Power amplification
 5. Search and lock control logic
 6. Wide band noise source
 7. Detector
 8. Detector
 9. Detector

With the use of a YIG tuned filter we can very quickly realize electronic tuning. For example, a WJ-5170 series magnetically tuned filter's response time in a 100 megahertz jump is only 35 microseconds. When beginning, the magnetically tuned filter in the wide band non-directionality antenna input terminal performs sawtooth sweeping to carry out searching. As soon as it intercepts the radar signal pulse it immediately locks-in on the radar's operating frequency and at the same time controls the second magnetically tuned filter causing it to be tuned on

the same frequency. This second magnetically tuned filter is selected by a certain wave band and the noise signals produced from the wide band noise source are added into a wide band power amplifier for power amplification. Afterwards, it is transmitted from the wide band non-directionality antenna. After the first magnetically tuned filter is locked-in on a certain radar station's frequency, the second magnetically tuned filter continues searching and can be locked-in on the newly found radar station frequency. This is done until the N magnetically tuned filter is completely locked-in. After the locked-in signals are lost, it automatically changes into the search position so as to renew the search for the new radar station frequency. This type of automatic tuning jammer easily makes an octave. If several of these automatic tuning systems are used, the microwave band can be easily covered. This automatic jammer is very effective on mechanically jumping frequency radar because the tuning speed of this type of radar is in the zero point several seconds quantity level. Totally electronic jammers can keep up with the jumping frequency speed of this type of radar. Afterwards, although the use of a hydraulically tuned magnetron can increase the radar's tuning speed to 5,000 megahertz/second, it is only necessary to enlarge the bandwidth of the jammer's output noise as well as increase the velocity memory circuit in the logical circuit to be able to carry out effective jamming.

The appearance of frequency agility radar totally changed the circumstances of warfare. This type of radar can tune bandwidths close to 10 percent within pulse repetition periodic intervals. Moreover, it can also realize random jumping without any pattern. This greatly increases the radar's antijamming capabilities.

Firstly, it increases the difficulty of reconnaissance. Frequency agility radar can usually be camouflaged as fixed frequency radar and at the critical moment can use wide band

random jumping frequency. At this time, common panoramic receivers find it very difficult to scout this type of radar. Common complete wave band (or so-called panoramic) receivers operate in the frequency scanning mode and the local oscillation of the superheterodyne panoramic receiver operates in the frequency scanning mode. This is the above mentioned automatically tuned jammer with a magnetically tuned filter which also uses the sawtooth frequency sweeping for searching. Moreover, the higher the frequency resolution of the panoramic receiver (that is the narrower the intermediate amplification bandwidth or filter's bandwidth) the lower the scanning frequency speed. When the radar's transmitted pulse carrier frequency uses random jumping frequency, the probability of being intercepted by the panoramic receiver is very low. Under these conditions, because the panoramic receiver can only occasionally intercept a radar pulse it then becomes difficult to determine the existence of radar stations. Even though the existence of a radar station can be doubted it is also very difficult to determine the position of a radar station and measure its operating parameters. Naturally, this is not to say that frequency agility radar has no way of scouting. If we use a completely open type transient panoramic receiver we can still scout the existence of frequency agility radar and even determine its operating parameters (for example, the jumping frequency bandwidth and pulse width). Yet, at the very least, a large number of presently used scanning frequency panoramic receivers are powerless.

Secondly, even if this open type transient frequency receiver can be used to scout the existence of frequency agility radar, at the same time, it is necessary to measure the transient frequency of each pulse transmitted by the radar. However, to consider using a narrow aiming type for effective jamming also seems impossible. This is because even if the automatically tuned jammer can measure the transient frequency of each pulse transmitted by the frequency agility radar in a very short amount of time

(microseconds) and immediately track the jammer's frequency, it can only carry out jamming after the jammer receives the radar pulse. It is also only able to jam the range interval starting from the range of the jammer to the radar up to the maximum effective range of the radar. When it reaches the following pulse, the radar has already changed its transmitted carrier wave frequency. This new frequency cannot be known before the jammer receives the pulse and thus it also has no way of jamming. In this way, this wide area from the trigger pulse (that is starting from the original point on the display) to the jammer's range cannot be jammed by the jammer. This greatly lowers the jamming effect and because of this the jammer's range can be very easily measured. Just for this reason, it can be considered that frequency agility radar can completely counter a narrow band aiming type jammer with transient frequency scouting and tracking capabilities. Although this type of jammer is not technologically impossible it is quite difficult to realize. Yet, if we change to use the total wave band wide band blocking type jammer, it will be very difficult for frequency agility radar to counter.

2.5 The Ability of Frequency Agility Radar to Counter Wide Band and Noise Jamming

As mentioned previously, only the wide band blocking noise jammer can be used to jam frequency agility radar. This type of jammer can produce white noise jamming in a very wide frequency band. This type of jammer usually uses a voltage tuned magnetron or other orthogonal field device tube which can produce several ten to several hundred watts of jamming power in a several hundred to a several thousand megahertz frequency band. The wider the jamming signal's frequency band the smaller its jamming signal power. For example, a voltage tuned magnetron can give 50-150 watts of power in a 10-20 percent bandwidth but can only give 2-20 watts of power in a wider frequency band (this can reach an octave). The jamming capability of the jammer is usually indicated

by the power (watts/megahertz) in the unit frequency band. Naturally, the wide band jammer's power density must be much lower than the power density of the narrow band aiming type jammer (point jammer). Therefore, although the wide band blocking type jammer can effectively jam frequency agility radar, yet in reality, the frequency agility radar forces the jammer to disperse its power to a very wide frequency band. To attain jamming ability equal to that of the narrow band jammer it is necessary to greatly increase the jammer's total power. This can increase a fighter aircraft's power loss which will occupy a large portion of the electronic equipment's power consumption.

Now we will quantitatively look at the jamming effects of wide band blocking type jammers on frequency agility radar.

As mentioned previously, separated type jamming can use an ultralow side lobe antenna for effective suppression and therefore we will only study the self-prepared type jammer here.

When in self-prepared jamming, the jammer and target lie in the same position and at the same distance. Then, it is only necessary to substitute formulas (2.5) and (2.2) into formula (2.1) to find the pressure control coefficient.

$$K = \left(\frac{P_J}{P_r} \right) = \frac{P_J G_J 4\pi R^4 L_R}{P_r G_r \sigma} \left(\frac{B_R}{B_J} \right) \quad (2.6)$$

It can be known from this formula that this pressure control coefficient forms a direct ratio with the square of the distance, that is, the further its distance the more serious the jamming effect. On the other hand, it forms an inverse ratio with (B_J/B_R) . That is to say, the wider the jammer's frequency spectrum width as compared to the radar's intermediate amplification width the more wanting its jamming effect.

As mentioned previously, when in aiming type jamming, the jammer's bandwidth need only be roughly larger than the radar's bandwidth. Yet, when the radar operates in pulse jumping frequency this forces the jammer to use wide band blocking type jamming. At this time, the jammer's bandwidth must be equal to or exceed the radar's jumping frequency bandwidth. Usually, the absolute value of the radar's intermediate amplification bandwidth is determined by the required range finding precision and range resolution. Further, its relative jumping frequency bandwidth is close to a constant (e.g., 10%). As a result, the shorter the wavelength the larger the value of (B_J/B_R) and the more lacking the jamming effect. Moreover, as previously mentioned the average power of the wide band jamming source can also decrease which will further lower its jamming effect.

As mentioned above, when in self-prepared type jamming its self-shielding range is the range when pressure control coefficient $K_s = 1$. We can derive the expression of self-shielding range R_{ss} from formula (2.6).

$$R_{ss} = \left[\frac{P_R G_R \sigma}{4\pi P_J G_J L_R} \left(\frac{B_J}{B_R} \right) \right]^{1/4} \quad (2.7)$$

It can be seen from this formula that self-shielding range R_{ss} forms a direct ratio with the root extraction of (B_J/B_R) .

Assuming the radar is operating at a fixed frequency, when receiving aiming type jamming, the self-shielding range is 10 kilometers. When it operates at frequency agility it forces the jammer to change and use blocking type jamming whereby its bandwidth increases 100 fold. Then, under other constant conditions, the self-shielding range will increase 10 fold and become 100 kilometers. We can see from this the effects when radar uses frequency agility.

To maintain the original jamming effects, the jammer must maintain its power density the same as the narrow band aiming type jamming when it changes to wide band blocking type jamming. For example, assuming a narrow band aiming type jammer can give 20 watts of power in X wave band with a 10 megahertz bandwidth its power density is then 2 watts/megahertz. Yet, for the wide band blocking type jammer, assuming its bandwidth is 500 megahertz, then to provide the same power density its power must reach 1 kilowatt. Such large jamming power is usually very difficult for fighter aircraft to endure.

It can be seen from formula (2.7) that the self-shielding range forms a direct ratio with the root extraction of the radar receiver's power but is not like the radar detection range which forms a direct ratio with the quartic direction of the radar's transmission power when under non-jamming conditions. Therefore, increasing the radar's transmission power is relatively effective for increasing the radar's detection range when in self-prepared type jamming. For example, assuming the original radar transmission power is 500 kilowatts, if we increase the orthogonal field device power amplification level to a gain of 10 decibels, when its final output power increases to 5 megawatts, this can increase the radar's detection range 3.16 times when in jamming.

We can see from this that an effective method to counter self-prepared type jamming is the use of high powered frequency agility radar. Because the peak power of radar is often limited by transmission systems such as waveguides and rotating joints a pulse compression radar system with high mean power is commonly used. This type of system is completely compatible with frequency agility radar.

2.6 The Ability of Frequency Agility Radar to Counter Common Frequency Nonsynchronous Jamming

Frequency agility radar has very strong antijamming capabilities for countering the common frequency nonsynchronous jamming of friendly nearby radar stations.

Assuming the nearby radar is operating with fixed frequency radar on an identical frequency band, its bandwidth is B_F and the jumping frequency width of the frequency agility radar is B_{FA} . The jumping frequency method is random jumping frequency, that is, the probability of any one point operating in the jumping frequency band is equal. Under these conditions, probability P of the frequency agility radar receiving nearby radar jamming is equal to:

$$P = \frac{B_F}{B_{FA}} \quad (2.8)$$

It is only necessary that the jumping frequency band be sufficiently wide. The probability of this is very small. Usually $P < 0.01$ and this type of jamming is only shown as small light spots on the luminescent screen. Assuming the radar antenna's rotating speed is Ω_A (expressed by rotations/minute) and the repetition frequency is F_P , then the average number N_1 of these jamming light spots on the plane position display is

$$N_1 = \frac{60 \times F_P}{\Omega_A} \cdot P \quad (2.9)$$

If $F_P \cdot P = 4 \cdot \Omega_A = 6$ rotations/minute, the $N_1 = 40$ jamming light spots can be tolerated.

References

- [1] The Basis of Radio Jamming and Radio Techniques in Reconnaissance, Science Press. S. A. Vakin, L. N. Shustov, Moscow, 1968.
Chinese translation: "The Basis of Radio Jamming and Radio Techniques in Reconnaissance," Science Press, 1977.

[2] Noise jamming of long range search radars.
Microwaves, Sep. 1975. pp. 52-60.

[3] ECCM from the radar designer's viewpoint. M.A. Johnson,
D.C. Stoner. Electro'76 Record. 1976.

Chapter III Frequency Agility's Enlargement of Radar's Detection Range

3.1 The Target's Effective Reflection Area Changes With the Viewing Angle

Earlier, when radar was first invented, it was discovered that a target's reflection echo amplitude was not steady but had slow and fast speed fluctuations. It was further discovered that this type of fluctuation was caused by the target's attitude changes opposite the radar. Or perhaps we can say that it was caused by the radar's viewing angle towards the target.

Some have measured real aircraft targets in different viewing angles and found that its transmitted echo signal strength changes are very large. It often only had a several tenths viewing angle change and this could cause a 10-15 dB change in the effective reflection area. Fig. 3.1 shows the results of test measurements on a B-26 aircraft [1].

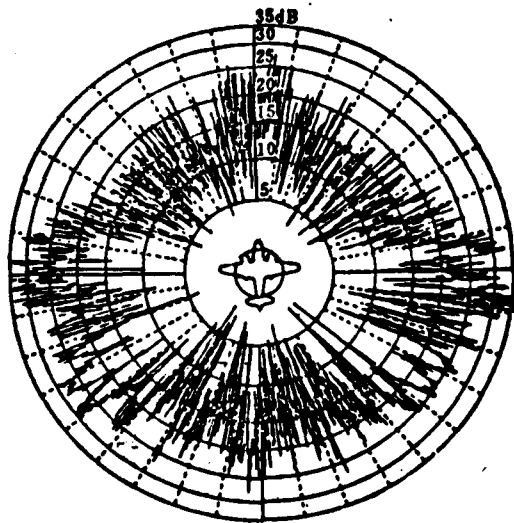


Fig. 3.1 The B-26 Aircraft's Effective Reflection Area Changes With the Viewing Angle

Test measurements on the effective reflection areas of missiles and Telstar satellites gave similar results. Then why is the effective reflection area of radar able to change with the viewing angle and fluctuate? This can be explained by the interference from the different partially reflecting electric waves of the target.

In most situations a radar's target is a complex irregular object (an angular reflecting object is an exception). This irregular object can be seen as a composite of many small scattering objects but the radar's echo is the vector sum of the electromagnetic waves reflected by these scattering objects. Thus, the received echo strength is not only related to the strength of the electromagnetic waves reflected by each scattering object but is also related to their phase. This phase is naturally related to the relative distance of each scattering

object opposite the radar. When the viewing angle changes, the relative distance and phase of each scattering object also changes. The amplitude after synthesis then changes. Because of the two-circuit propagation of the electromagnetic waves the relative distance will change to half a wavelength which will cause the phase to change 360 degrees.

Although the aircraft's target echo amplitude which fluctuates with the viewing angle is very large, we can measure the mean of its effective reflection area in a certain angle range. Table 3.1 lists the mean values of the effective reflection areas [2] of three different model aircraft measured from different viewing angles on each different wave band. Test results show that the effective reflection area measured on the side of the target is largest, the tail is second and the value measured on the nose is smallest. The smaller the model of aircraft the larger the difference. The difference for small aircraft exceeded 40 decibels.

(1) 类 型	(5) 视 角	(3)					
		VHF 0.03~ 0.3 GHz	UHF 0.3~1.0 GHz	L 1~2 GHz	S 2~4 GHz	C 4~8 GHz	X 8~12GHz
(2) 重型轰炸机 或巨型客机 (707, DC-8)	头部 (6)			32	40	10~40	28
	尾部 (7)			15/63	250		25/500
	侧面 (8)			550/500	500		300/300
	平均 (9)		11	24/40	23/40		60
(3) 中型攻击轰炸机 或中型客机 (727, DC-9)	头部 (10)	60/100	1.2/20/30	6/10/20			4
	尾部 (11)	100	6	20	20		
	侧面 (12)	300	200	300	280		800
	平均 (13)			12	12		11
(4) 小型歼击机 或四座客机	头部 (14)	10	6	0.3~7.5	0.2~9.5	0.7~2	1.2
	尾部 (15)	10	3	2	0.6~15		
	侧面 (16)			8~90	35~300		20/30/65
	平均 (17)			0.7/1.8	1.3/2		1.3/5

Table 3.1

Table 3.1 The Mean Values (Using Square Meters as the Unit) of the Radar's Effective Reflection Area For Different Aircraft Measured at Different Wave Bands and Different Viewing Angles

- Key:
1. Model
 2. Heavy bomber or giant passenger plane (707, DC-8)
 3. Medium attack bomber or medium passenger plane (727, DC-9)
 4. Medium fighter or four seater passenger plane
 5. Viewing angle
 6. Nose
 7. Tail
 8. Side
 9. Mean
 10. Nose
 11. Tail
 12. Side
 13. Mean
 14. Nose
 15. Tail
 16. Side
 17. Mean

Fig. 3.2 draws the results of a 1/8 model of a jet fighter measured at 40 kilomegahertz [3]. The data attained has a mean within ± 0.5 degrees (a fluctuation without a mean is even larger).

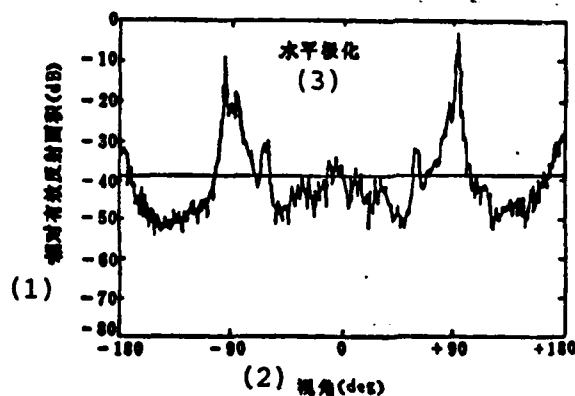


Fig. 3.2

Fig. 3.2 Relationship of Mean Radar's Effective Reflection Area on 1/8 Solid Model of Jet Fighter in 1 Degree and the Position Viewing Angle (Measured Frequency is 40 Kilomegahertz, Equivalent is 5 Kilomegahertz)

Key: 1. Relative effective reflection area (dB)
2. Viewing angle (deg)
3. Horizontal polarization

3.2 Fluctuation of Target Echo Amplitude

We know from the last section that the effective reflection areas of aircraft and other complex targets change rapidly with the viewing angle. Because of this, when the target is opposite the viewing angle of the radar and changes with the time, the echo amplitude received by the radar also fluctuates with the time. In most situations, this type of radar target facing the radar station is in continual motion. This type of motion not only indicates that there are geometric position changes but also shows that there are viewing angle changes (these types of viewing angle changes are also changes of the flight attitude of the target opposite the radar station). There are numerous factors which bring about viewing angle changes. Firstly, a target's geometric position shifts can cause changes in the attitude. Secondly, the influence of the atmospheric turbulence and other factors cause the target to be able to make three axial rotations using the aircraft's center of gravity as the origin, that is, yaw (axial rotation perpendicular to the ground), forward and backward pitch (horizontal axial rotation of revolving and the aircraft is perpendicular in the forward direction), and negative and positive rolling (axial rotation of aircraft in the forward direction). These factors can cause the viewing angle of the aircraft opposite the radar to have rapid and small changes. The viewing angle changes caused by the target movements can cause the target echo received by the radar to fluctuate with the time.

Because of the relative distance change of each scattering object for similar targets, the shorter the wave length the

higher its corresponding phase change rate. This causes relatively high fluctuation frequency. Therefore, we can consider that the echo fluctuation's frequency spectrum is now in direct ratio to the radar's operating frequency (its condition is that the size of the target is at least several times the wave length). The noise modulation density for the X wave band is mainly concentrated below 10 hertz.

On the other hand, test studies show that the amplitude noise frequency spectrums of large targets and small targets are very similar. This is because the relative distance change between each scattering object is the function of the distance between them and the aircraft's center of gravity. It is also the function of the angular yaw. Although large aircraft have relatively large wingspans they have relatively small yaw rates.

When frequency spectrum is used to show this type of echo amplitude, we can have the following empirical formula

$$A^2(f) = \frac{0.12B}{B^2 + f^2} \quad (3.1)$$

In the formula $A^2(f)$ is used to express (modulation percentage)²/hertz;

B is the half power point bandwidth which is indicated by hertz;
f is the frequency which is indicated by hertz

The typical value of X wave band B is between 1 and 2.5 hertz. The bandwidth is even wider for large aircraft because its large reflecting objects are relatively scattered.

We only discussed the low frequency amplitude noise of a target above. Aside from this, target echoes also have high

frequency amplitude noise. There are two types: random noise and periodic modulation. The former is mainly caused by vibration when the aircraft is in flight. It can extend to several hundred hertz and gradually decrease with the increase of the frequency. Its typical value is several modulation degrees per $\sqrt{\text{Hz}}$. Periodic modulation is shown as the spike of the equal intervals on the frequency spectrum. This is mainly caused by the rotation of the propeller blade on propeller aircraft. Its frequency is determined by the number and rotating speed of the blades which is in the range of several tens to several hundred hertz. Its amplitude is then very much related to the radar's viewing angle. It is largest in the forward view direction, the rear view direction is second and the side view is smallest. Its peak value is several times as large as that of random noise.

The fluctuation of radar target echoes can also be indicated by the probability density function of the range.

Theoretical analysis shows that when the radar target is formed from a great many scattered small scattering objects the amplitude distribution of its echo can be expressed by the Rayleigh distribution. Also, the probability density function of its echo voltage v can be indicated as

$$p(v) = \frac{2v}{\sigma^2} e^{-v^2/\sigma^2} \quad (3.2)$$

In this formula, σ is its effective value. This also signifies that the radar's effective reflection area (forms a direct ratio with the received power) is an exponential distribution, or its power signal-noise ratio is an exponential distribution.

$$p(x) = \frac{1}{\bar{x}} \exp\left(-\frac{x}{\bar{x}}\right) \quad (x \geq 0) \quad (3.3)$$

In this formula, \bar{x} is the mean effective reflection area or mean signal-noise ratio.

However, this simple model cannot represent the various complex and real situations. Thus, P. Swerling supposed four situations for the fluctuations of target echoes [4]. These four situations assumed probability density functions for two types of fluctuation. Yet, because the probability density functions did not describe its fluctuation speed level which changes with the time it was also assumed that one type was slow fluctuating and the other fast fluctuating.

The probability density function that he supposed for the first and second types of situations were determined by formula (3.3). The slow fluctuations of type I were mainly correlated in the continuous echo pulse series received when the antenna was scanning the target but were not completely correlated during each sweep of the antenna. The type II situation which is fast fluctuations are not correlated between each continuous echo pulse.

The probability density function of situation types III and IV are determined by the following formula

$$p(x) = \frac{4x}{\bar{x}^2} \exp\left(-\frac{2x}{\bar{x}}\right) \quad \text{for } x \geq 0 \quad (3.4)$$

(1)

Key: When

This probability density function is suitable for targets of this type of model, that is, it is formed from a large steady reflecting object and many small reflecting objects. The sum of the effective reflection area of the large reflecting object and the effective reflection area of the small reflecting objects are equal.

The same is true for the type III situation which is slow fluctuating and type IV situation which is fast fluctuating.

Actually, in the probability theory, formula (3.3) also possesses 2 degrees of freedom chi square distributions; and formula (3.4) has 4 degrees of freedom chi square distributions. In most situations, chi square distributions with $2m$ degree of freedom can be written as

$$p(x) = \frac{m}{(m-1)!} \left[\frac{mx^{m-1}}{x} \right] \exp \left[-\frac{mx}{x} \right] \quad (3.5)$$

However, the above mentioned four types of situations were assumed for convenience of mathematical analysis. The actual situations are much more complex.

To obtain the actual situation of radar echo fluctuation, many people have done tests on various different model aircraft in different wave bands (P, L, S and X). Yet, the obtained results were relatively complex and it was not easy to find regularity within them.

Generally speaking, in the microwave wave band, the probability density distribution of radar target echo fluctuations are quite close to a Rayleigh distribution. When the viewing angle change for a large multiengine aircraft is only 1° or 2° it can very well be expressed by the Rayleigh distribution.

Yet for small aircraft, even if the viewing angle change reaches 8° - 9° it can still not be indicated by the Rayleigh distribution. In the majority of exceptions, a high order chi square distribution can be used for approximation.

For example, the results of measuring a small bimotor jet aircraft in C wave band showed that 1-37 order chi square distribution can be used for indication. Among these, about one-half of the measurement results fell in the 1.4 to 2.7 degree of freedom range. It can be seen from this that the actual situations are much more complex and thus we cannot use a simple mathematical model to express it. This is even more the case for small aircraft.

Furthermore, the test results for jet and propeller aircraft also showed very large differences. Fig. 3.3 gives the test results for large jet and propeller passenger aircraft [5].

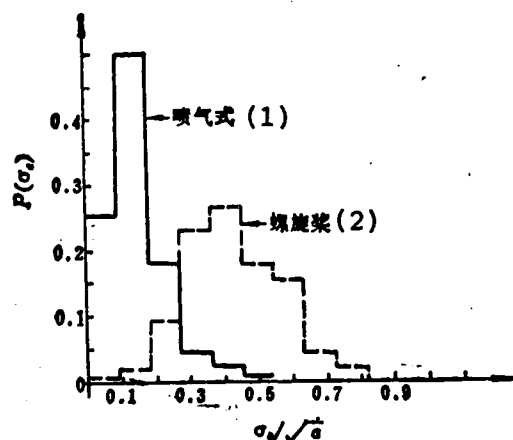


Fig. 3.3

Fig. 3.3 The Probability Density Functions of the Radar Echo Range Standard Difference σ_a for Two Different Types of Aircraft

Key: 1. Jet model
2. Propeller

We can see from the figure that the standard difference of a jet aircraft's range fluctuation is relative small and the range fluctuation for a propeller aircraft is relatively large (the side is an exception). As a result, it is possible to use this characteristic to differentiate these two different types of aircraft.

Aside from this, as regards the fluctuation of the two different speeds supposed by Swerling, a large jet aircraft basically belongs to the uncorrelated slow speed fluctuations in the scanning; when the antenna is scanning the target the echoes of a propeller aircraft are partially related and lie between the two types of fluctuation speeds. Later we will see that only when there is frequency agility radar can they be truly uncorrelated and belong in the adjacent pulses.

The effective reflection areas of guided missiles and satellites lie between a regular geometric shape and complex form. The effective reflection area of a spherical object is completely uncorrelated to the viewing angle. At the same time, the effective reflection area of a rotating ellipsoid is also uncorrelated to the viewing angle and is always equivalent to $\pi r_1 r_2$ (r_1 and r_2 are the two curvature radii of the section perpendicular to the line of sight). Yet, the forms of modern guided missiles and satellites are becoming increasingly complex so that it is difficult to consider them simple geometric figures. In the same way, the effective reflection areas of these types of targets have a strong relation with the viewing angle.

After actual tests were carried out on these types of targets, the results showed that the probability density function of its effective reflection area is close to a logarithmic normal distribution. The following formula can be used to express it

$$p(x) = \frac{1}{x s \sqrt{2\pi}} \exp \left[-\frac{(\ln x - \ln \bar{x})^2}{2s^2} \right], \quad x > 0 \quad (3.6)$$

In the formula, s is the standard deviation of $\ln x$. The special feature of this type of distribution is that it has a relatively long "tail" which has a fixed probability for a relatively large amplitude.

Actually, when the aircraft target is laterally observed, we can also use the above formula to express it. Further, the logarithmic-normal distribution can very well be used for approximation of most ships (all have reflecting objects with relatively large areas).

3.3 Echo Fluctuation When the Radar is Operating in Frequency Agility

The study of the effective reflection area of targets when in different wave bands and different viewing angles began very early. Yet, research on effective reflection areas with even finer different frequencies only began recently.

Up until 1965 people studied effective reflection areas when the target was in 1 kilomegahertz to 10 kilomegahertz. They came to the conclusion that the mean change of the target's effective reflection area in such a wide frequency band was not large. This is mainly because they only studied its mean value but not its fine changes.

However, after precisely measuring the relation of the radar's effective reflection area and frequency we discovered that the radar section is very sensitive to the frequency and viewing angle. The extremely small changes of the frequency can cause large changes in the effective reflection area (see fig. 3.4).

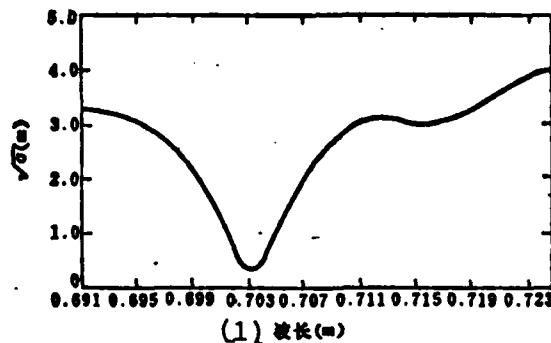


Fig. 3.4 The Relation of the Front End Effective Reflection Area σ and Wave Length λ of a Large Jet Aircraft

Key: 1. Wave length

Because complex radar targets are composed of small scattering objects of many distributed sizes with immense differences, the echoes received by the radar antenna are the vector sum of the electric waves transmitted by these scattering particles. When the frequency transmitted by the radar changes, the phase difference caused by the difference of the propagation path differs with it. Thus, the vortex sum of the electric waves transmitted by each scattering object also changes with it.

Given the dependent relationship of the radar's effective reflection area and frequency, when the radar operates in a jumping frequency, owing to the fact that the carrier

frequencies of each pulse are all different the amplitude of each of its echoes can change greatly. When the radar is operating in a jumping frequency state the echoes received are possibly uncorrelated between the pulses and they quickly jump around its mean value.

To further understand echo fluctuation when there is frequency agility, some people actually tested the echo fluctuations of frequency agility radar [6]. The radar's operation frequency was 5.35-5.85 kilomegahertz and to simplify they used jumping frequency with two types of frequency intervals. That is, the first, third, fifth, seventh...pulses used one carrier frequency and the second, fourth, sixth, eighth... pulses used another carrier frequency. The difference of the two carrier frequencies is changeable and can range from zero change to 192 megahertz. Afterwards, each pulse's echo amplitude is recorded and the mean square value of the adjacent pulse's echo amplitude is found. Test results show that this mean square value is related to the frequency difference of the adjacent pulse's carrier frequency. Fig. 3.5 gives the results of tests on the Sea Hawk aircraft. This is a small model aircraft and its wing span is only 12 meters.

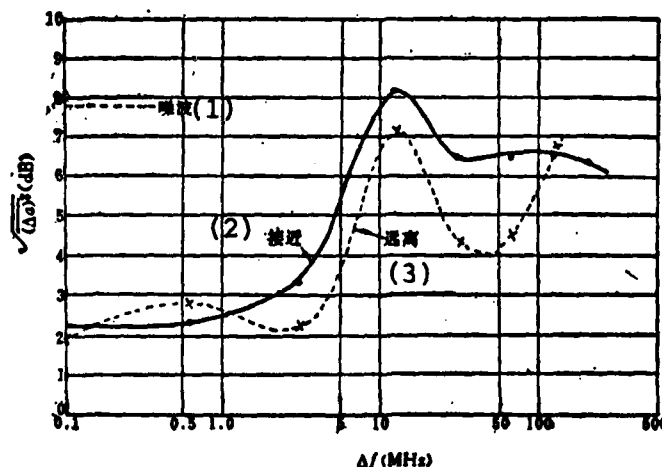


Fig. 3.5

Fig. 3.5 Mean Square Value of Sea Hawk Aircrafts Pulse-Pulse Range Changes

Key: 1. Noise
2. Close
3. Distant

It can be seen from the figure that when the frequency difference value between the pulses gradually increases the mean square value of the adjacent echo's range difference also enlarges. When it reaches a frequency difference of 13 megahertz an extremely large value appears and afterwards there is slight fluctuation. Therefore, it can be considered that when the jumping frequency interval of the adjacent pulse has a critical value (13 megahertz in this case) smaller than this critical value, the adjacent echo range is still correlated. When larger than this critical value it can be considered uncorrelated.

The frequency coefficient of correlation can also be derived from these test results. When the so-called frequency coefficient of correlation $\rho(f)$ is also in a different frequency difference the level of the adjacent echo amplitude is correlated. The coefficient of correlation can be obtained from the measured recording of the echo amplitude:

$$\rho = 1 - \frac{(\overline{\Delta a})^2}{2\overline{a^2}} \quad (3.7)$$

In the formula $\overline{a^2}$ is the mean square value of the echo amplitude;
 $(\overline{\Delta a})^2$ is the mean square value of the adjacent echo amplitude difference

Because of the repeating frequency of the radar used during the tests (196 hertz), there was also possible time decorrelation $\rho(\tau)$. Therefore, it is assumed

$$\rho = \rho(\tau) \cdot \rho(f) \quad (3.8)$$

After the obtained data removes the time decorrelation the relation between the frequency coefficient of correlation $\rho(f)$ and frequency difference Δf can be obtained. The results are shown in fig. 3.6.

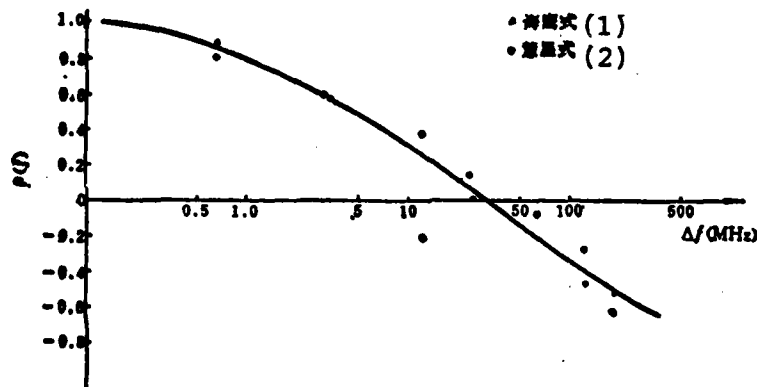


Fig. 3.6 Relation Between the Frequency Coefficient of Correlation and the Frequency Difference Derived From the Test Results

Key: 1. Sea Hawk type
2. Comet type

Among the data used for the two different model aircraft, one type is the small Sea Hawk model and the other is the large Comet model. The wing span of the Comet is 35 meters. However, the results for the two models are almost the same, that is, their frequency coefficients of correlation are zero when the frequency difference is about 20 megahertz. When the frequency difference reaches 20 megahertz this can cause the adjacent echo

amplitude to be completely decorrelated. The first zero point of the frequency coefficient of correlation is also called the critical frequency. It can be seen from the test results above that there is not a large difference between the critical frequencies of the small and large model aircraft. Yet, some theoretical analyses have proven that critical frequency Δf_0 can be expressed by the following formula

$$\Delta f_0 = \frac{C}{2L_0} = \frac{150}{L_0} \text{ MHz/m} \quad (3.9)$$

In the formula, L_0 is the radial measurement of the target.

There are others who think that the frequency coefficient of correlation $\rho(\Delta f)=0.5$ has sufficient decorrelation. At this time, the required critical frequency is 45 (megahertz)/ L_0 (meters) and when $\rho(\Delta f)=0.4$ there is sufficient decorrelation and a critical frequency of 75 (megahertz)/ L_0 (meters) can be obtained. Yet, all of these theories consider that the frequency and radial measurements of the target form an inverse ratio. That is, the more there are large targets the lower the critical frequency needed for decorrelation. As a result, there is still insufficient test data to prove this point.

The results of tests on satellite targets are shown in fig. 3.7.

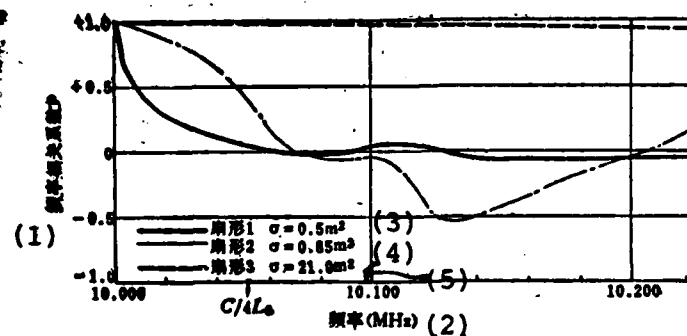


Fig. 3.7 The Relation of the Frequency Coefficient of Correlation and the Frequency of a 54 Inch Satellite (the ρ Value is Calculated From the Correlation of the Single Frequency 10° Fan-Shape Data and Reference Fan-Shape Data)

Key: 1. Frequency coefficient of correlation ρ
 2. Frequency (MHz)
 3. Fan-shape 1
 4. Fan-shape 2
 5. Fan-shape 3

The test was done using radar with X wave band on a satellite with a 54 inch diameter. Three 10 degree viewing angle fan-shapes were selected. The radar equivalent section of the first fan-shape was the smallest, 0.5 square meters. The second fan-shape was a little larger, 0.85 square meters and the third section was largest reaching 21.0 square meters. It can be seen from the figure that the reflections of sections with the largest fan-shape have the strongest frequencies and this does not present any frequency decorrelation. However, the critical frequencies are basically the same in the other two fan-shape areas, about 70 megahertz. When the data of 8 frequencies distributed in a 250 megahertz frequency band takes on the mean value, this can raise the zero point of -25 decibel square meters 17 decibels and raise the zero point of -15 to -25 decibel square meters 10 decibels.

After the radar uses the jumping frequency system this can not only accelerate the echo fluctuation speed so that the adjacent echo amplitude is decorrelated but can also change the probability distribution of the echo amplitude. Fig. 3.8 gives the test results of the probability density function of the equivalent reflection area for a satellite target with a 54 inch diameter in a fixed frequency and staircase jumping frequency.

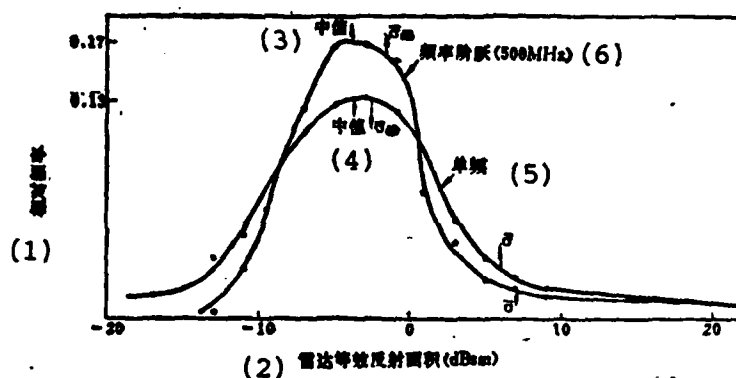


Fig. 3.8 Probability Density Function of the Equivalent Reflection Area For a Satellite With a 54 Inch Diameter

- Key:
1. Relative frequency
 2. Radar's equivalent reflection area (dBsm)
 3. Mid-value
 4. Mid-value
 5. Single frequency
 6. Frequency jump (500 MHz)

We know from the figure that after using jumping frequency the probability of the small section decreases as does that of the large section. This is to say that the jumping frequency causes even more of the echo amplitude measured by the radar to be closer to its mean value.

Tests on guided missile targets can also derive the same type of results. Fig. 3.9 is an example of this.

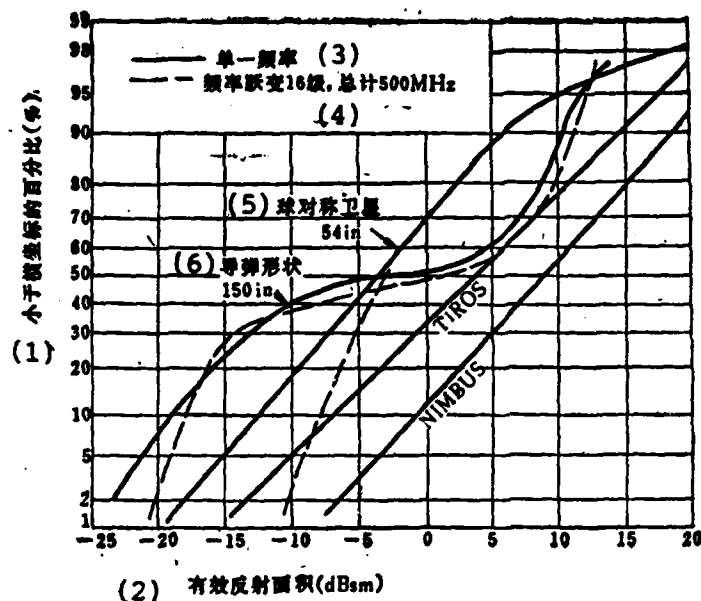


Fig. 3.9 Test Results of the Equivalent Reflection Area Probability Distribution of Satellite Targets and Guided Missiles Using Single Frequency Radar and Jumping Frequency Radar

Key: 1. Percentage (%) smaller than abscissa
 2. Effective Reflection area (dBsm)
 3. Single frequency
 4. Frequency jumping 16 levels, total of 500 MHz
 5. Spherical symmetrical satellite
 6. Guided missile shape

In this figure, the solid line is the test results of the fixed frequency and the broken line is the results of the jumping frequency radar tests which used 16 staircase jumping frequencies (the total bandwidth was 500 megahertz). We know from the figure that use of the staircase jumping frequency decreased the probability of the small reflecting area. Naturally, when the needed detection probability is relatively high, the jumping frequency radar must be much more superior than the fixed frequency radar.

3.4 Influence of Echo Fluctuation on Target Detection

The echo amplitude of an actual radar target is fluctuating, especially for fixed frequency radar. This type of fluctuation is always at a slow speed (this is even truer for far distance targets), its fluctuation frequency is in the several hertz to several tenths hertz and therefore must be able to produce a large effect on the detection of the target echo.

In radar where the antenna carries out circular scanning, the target's slow speed fluctuation can always cause the antenna to have no means of detecting the target in one to several rotations. This can not only cause radar detection probability to decline and the needed signal-noise ratio to enlarge. It can also cause the automatic tracking system to lose the target. This will cause the flight path to be cut off and so require the beginning of renewed tracking.

Because the fluctuation of the target is random, whether we use a theoretical analysis method or test research method it is relatively difficult to quantitatively study the influence of this type of fluctuation on detection.

Now, we will first take a look at the results of a typical theoretical analysis. It is well known that the probability density function $P_n(V)$ of the video noise put out by the radar receiver's detector is a Rayleigh distribution, that is

$$P_n(V) = \frac{V}{\sigma^2} e^{-\frac{V^2}{2\sigma^2}} \quad (3.10)$$

In the formula, σ is the mean square value of the noise discharge. If the mean square value of the video signal discharge opposite

this noise discharge is normalized it is expressed by x . When the obtained threshold level is x_0 the noise quantizing probability P_n is

$$P_n = \int_{x_0}^{\infty} P_n(x) dx = \int_{x_0}^{\infty} x e^{-\frac{x^2}{2}} dx = \exp\left(-\frac{x_0^2}{2}\right) \quad (3.11)$$

The probability density function of constant amplitude sine signals superimposing narrow band Gauss noise is the Rice distribution, that is

$$P_r(x) dx = x \exp\left(-\frac{(x^2 + a^2)}{2}\right) I_0(ax) dx \quad (3.12)$$

In the formula, a is the intermediate frequency signal-noise ratio;

$I_0(ax)$ is the zero order Bessel function

Therefore, the probability P_s of the signal plus the noise exceeding the threshold is

$$P_s = \int_{x_0}^{\infty} P_r(x) dx = \int_{x_0}^{\infty} x \exp\left(-\frac{(x^2 + a^2)}{2}\right) I_0(ax) dx \quad (3.13)$$

If

$$x_0 = \sqrt{-2 \ln P_n} \quad (3.14)$$

is substituted in, we can obtain

$$P_s = \int_{\sqrt{-2 \ln P_n}}^{\infty} x \exp\left(-\frac{(x^2 + a^2)}{2}\right) I_0(ax) dx \quad (3.15)$$

This formula joins together the three parameters of P_s , P_n and a .

If P_n is taken as the parameter we can find the relation of P_s and a . J. I. Marcum has done a good deal of computations [7] and the results are shown in fig. 3.10. This curve indicates the detection of a single pulse and does not consider the accumulation of signals.

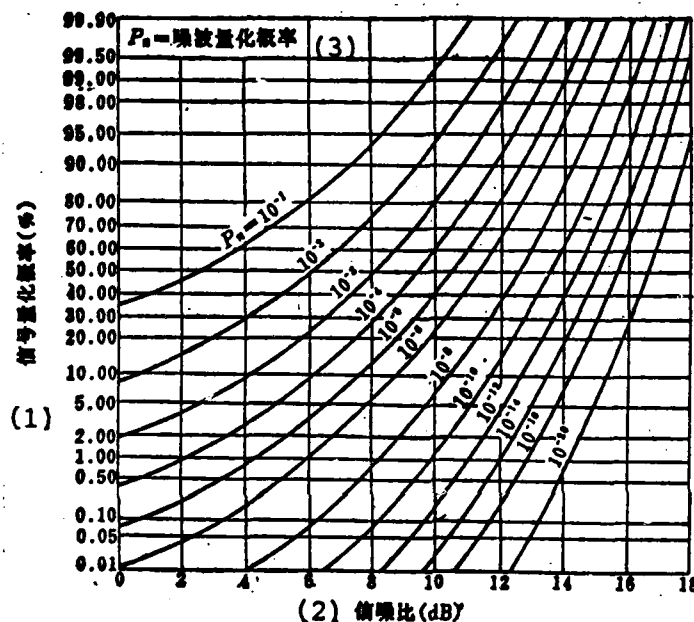


Fig. 3.10 Relationship Between the Noise Quantization Probability, Signal Quantization Probability and the Needed Signal-Noise Ratio

Key: 1. Signal quantization probability (%)
 2. Signal-noise ratio (dB)
 3. P_n = noise quantization probability

When the signal amplitude produces fluctuation, the quantitative relation between these three will change. To simplify, if the signal fluctuates in accordance with Swerling's situation I, its signal-noise ratio is the exponential distribution as was shown in formula (3.3). The results of Swerling's computations in this type of situation are shown in fig. 3.11.

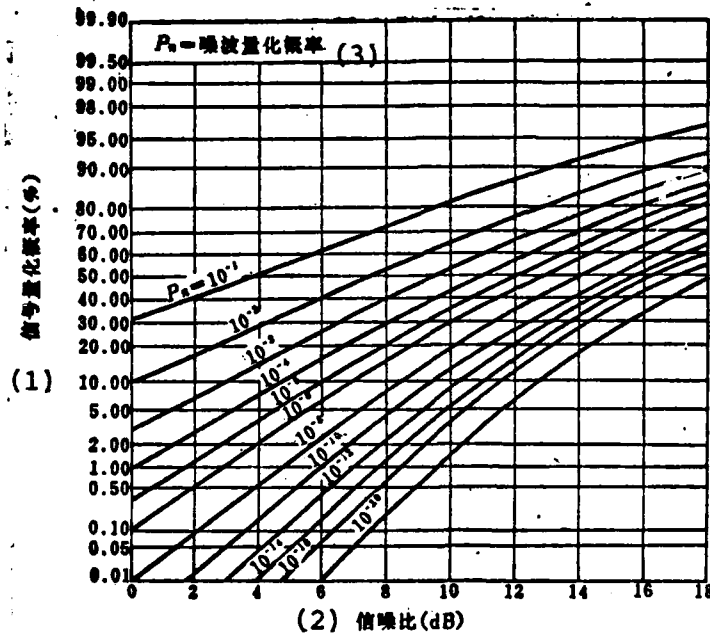


Fig. 3.11 Relationship Between the Noise Quantization Probability, Signal Quantization Probability and the Needed Signal-Noise Ratio When the Signal Creates Exponential Fluctuation

Key: 1. Signal quantization probability (%)
 2. Signal-noise ratio (dB)
 3. P_n = noise quantization probability

By comparing figures 3.10 and 3.11 we can see that when there is identical noise quantization probability and signal quantization probability, the needed signal-noise ratio when the signal creates exponential fluctuation must be much larger than when there is no fluctuation. This is especially the case when in a relatively high signal quantization probability. Fig. 3.12 gives the increased signal-noise ratio needed to obtain the same signal quantization probability when $P_n = 10^{-5}$. It can be seen from the figure that when the required signal quantization probability is 90%, its needed increased signal-noise ratio reaches 4-8 decibels.

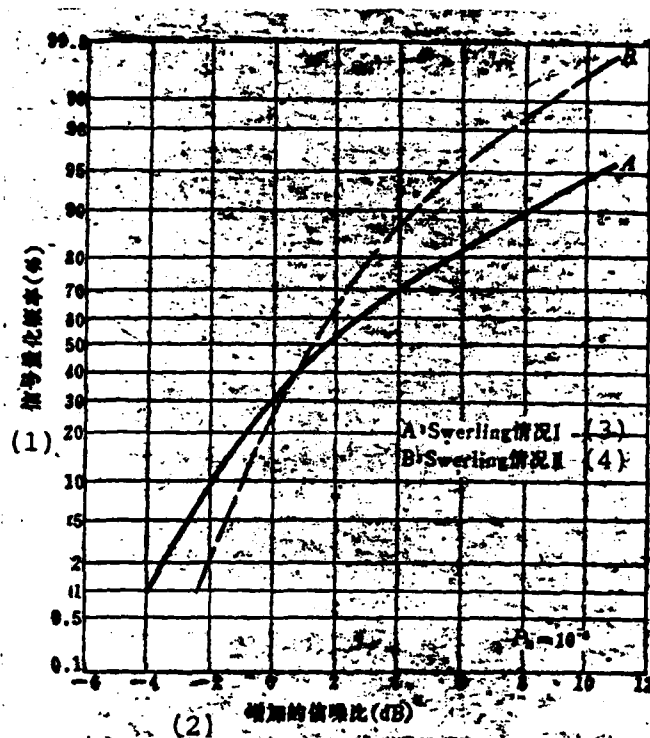


Fig. 3.12 Increased Signal-Noise Ratio Needed For Detecting Fluctuating Target Echoes

Key: 1. Signal quantization probability (%)
 2. Increased signal-noise ratio (dB)
 3. A: Swierling situation I
 4. B: Swierling situation III

At times, this type of additional signal-noise ratio can also be indicated by fluctuation loss L_F . The fluctuation loss is defined as the ratio of the signal-noise ratio needed to detect the fluctuating target and the signal-noise ratio needed to detect the constant amplitude target when the noise probability and signal probability are the same. Fig. 3.13 presents the relationship between the signal probability and fluctuation loss L_F when in different noise probability [9].

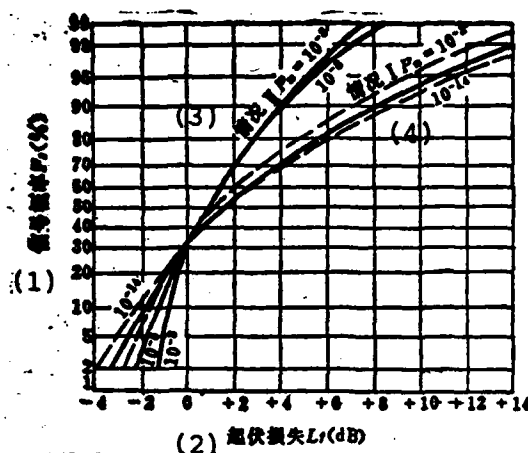


Fig. 3.13 Relationship Between Signal Probability P_s and the Fluctuation Loss When There is Different Noise Probability P_N

- Key: 1. Signal probability P_s (%)
 2. Fluctuation loss L_f (dB)
 3. Situation III
 4. Situation I

We can see from the above figure that this type of loss is mainly produced in a place which requires relatively high signal detection probability. When signal detection probability is lower than 30%, this type of fluctuation loss transforms into "fluctuation gain."

The above discussion focused on the situation with single pulse detection. In actual radar, the number of echoes received from a single target is not limited to one. Thus, use of the video accumulation method can effectively lower the necessary signal-noise ratio. Video accumulation is a method for accumulating the energy of the video pulse series after detection and it appears that it should be able to cause the necessary input electric frequency signal-noise ratio to lower N times (N is the

number of accumulated pulses) when in the same false alarm probability and detection probability. Yet, due to the existing loss of the detector there is no way of realizing this value. The detector's loss is caused by the non-linearity of the detector. It is also the so-called large signals inhibiting the small signals. Detector loss L_d can be expressed by the following empirical formula



In this formula, a_0 is the input signal-noise ratio of the constant amplitude signals. Naturally, the smaller the input signal-noise ratio the larger its loss.

In video accumulation, the greater the number of accumulated pulses the smaller the necessary input signal-noise ratio and the larger the detection loss. If, during accumulation, this type of detection loss is expressed by accumulated loss L_i , it can then be defined as

$$L_i = \frac{Na_0(N)}{a_0(1)} = \frac{N}{G_i(N)} \quad (3.17)$$

In the formula, $a_0(N)$ is the input signal-noise ratio needed when there are N pulses. $G_i(N)$ is the accumulated gain. Obviously the accumulated loss and detection loss have the following relation

$$L_i(N) = \frac{L_d(N)}{L_d(1)} = \frac{(a_0(N) + 2.3)a_0(1)}{(a_0(1) + 2.3)a_0(N)} \quad (3.18)$$

It is only necessary to know that the constant amplitude signal's signal-noise ratio $a_0(N)$ and $a_0(1)$ can compute the corresponding accumulated loss.

In the situation of signal fluctuation, the accumulated effect is similar to the situation of constant amplitude signals. Therefore, formula (3.18) can still be used but it is necessary to replace the $a_0(1)$ and $a_0(N)$ in the formula with corresponding $a_1(1)$ and $a_1(N)$. Fig. 3.14 gives the accumulated loss in the type I signal fluctuation situation.

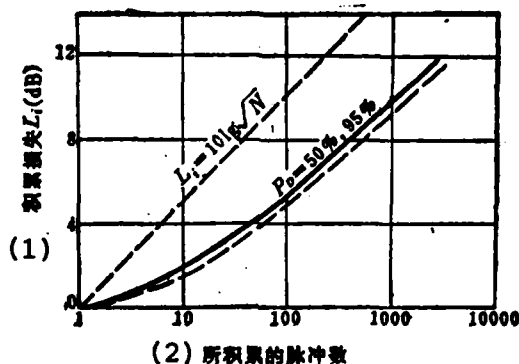


Fig. 3.14 Accumulated Loss When in Type I Fluctuation

Key: 1. Accumulated loss L_1 (dB)

2. Number of accumulated pulses

This loss is accurately computed in a situation wherein the false alarm probability is 10^{-10} and the detection probability is 50% and 95% (results of the two are the same). We used results corresponding to the computation of formula (3.18) as shown in the broken line. It has an error of about 0.5 decibels.

The above discussion concentrated on the situation of slow speed fluctuation. When the target's echo signal quickly

fluctuates from pulse to pulse, their situations are different. When the number of accumulated pulses after envelope detection is greater than two, the effect of fast speed fluctuation is equivalent to the mean value of the target's effective reflection area (or amplitude of the echo). Therefore, when requiring a relatively high detection probability, it is necessary to have a relatively low signal-noise ratio. Fig. 3.15 gives the accumulated loss when in type II fluctuation.

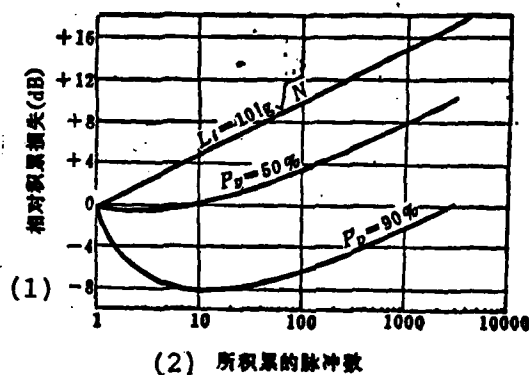


Fig. 3.15 Accumulated Loss When in Type I Fluctuation
($P_D = 10^{-10}$)

Key: 1. Relative accumulated loss (dB)
2. Number of accumulated pulses

It can be seen from the figure that when the desired detection probability is 95% and when the number of accumulated pulses is within 2,000, the decibel number of its accumulated loss is a negative value.

However, the above discussion focused on the results of theoretical analysis. Real situations are more complex. For example, as regards search radar, most often pulse numbers within 3 decibel beams act as the accumulated pulse number. Yet in reality, when the antenna beam searches the target, the

received beam array is modulated by the antenna lobe figure. That is to say, the signal-noise ratio of each echo pulse is different and therefore we cannot use the results of the aforementioned theoretical analysis directly.

Yet, if we consider the lobe modulation effect of the echo pulses its theoretical analysis is extremely difficult. Within this type of situation, an electronic computer is commonly used to carry out simulated test research. The simulated method used is the Monte Carlo method in statistical testing.

Fig. 3.16 gives the results of a series of simulated tests. If the antenna lobe form in these tests is a Gaussian form the number of accumulated pulses is determined by the number of pulses in its 3 decibel beam width. A pair of single signal matched filters are placed in the receiver, the detector uses linear detection and its output uses a sliding window type simulating accumulator to carry out unweighted simulated accumulation (there is no quantized loss). The false alarm probability after single distance unit accumulation is 10^{-6} . It can be seen from fig. 3.16 that when the required detection probability is relatively high, the signal-noise ratio needed for detecting fast speed fluctuating targets is much smaller than the signal-noise ratio needed for detecting slow speed fluctuating targets. Moreover, the greater the number of accumulated pulses the larger their difference.

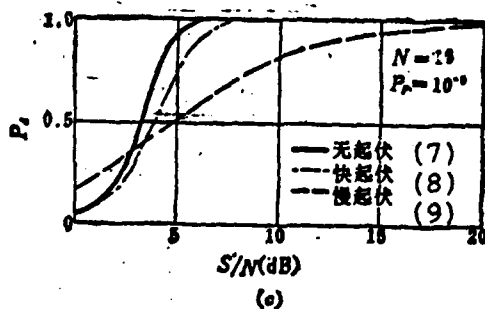
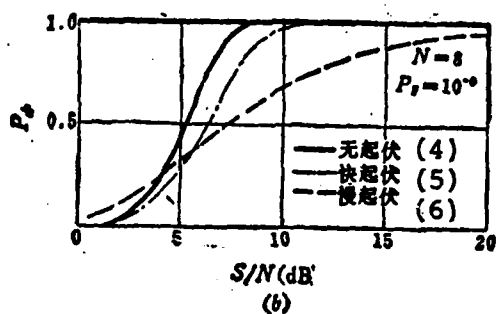
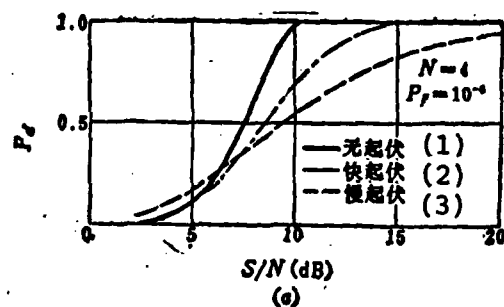


Fig. 3.16 Results of Computer Simulation For the Detection of Three Fluctuating Signals

(a) Pulse number $N=4$, (b) $N=8$, (c) $N=16$

Key: 1. Non-fluctuating
 2. Fast fluctuation
 3. Slow fluctuation
 4. Non-fluctuating
 5. Fast fluctuation
 6. Slow fluctuation
 7. Non-fluctuating
 8. Fast fluctuation
 9. Slow fluctuation

Actual detectors commonly use a binary sliding window detector. After detection, the video signals first pass through the first threshold to carry out amplitude quantization. Afterwards, they then carry out accumulation of the 1 signal in the same distance quantized interval and it is compared with the second threshold. This type of binary sliding window detector has one more quantization loss than the simulated sliding window detector. Fig.3.17 gives the results of computer simulation of the detection performance by this type of numerical detector of different fluctuating signals [1]. This figure also draws a comparison of the rectangular beams and Gauss beams. Their echo number is 15.

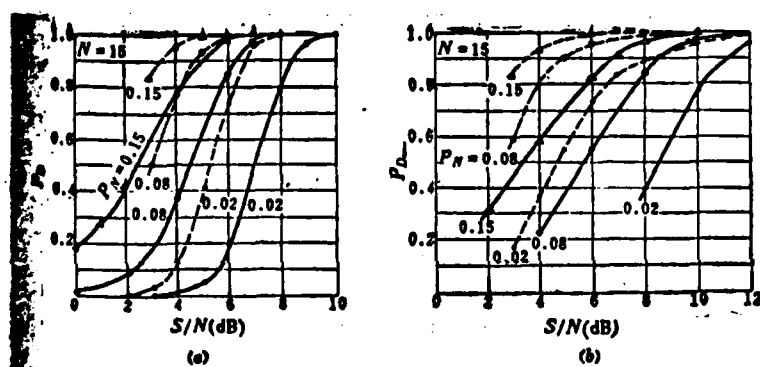


Fig. 3.17 The Numerical Sliding Window Detector For the Detection of Non-Fluctuating Signals (a) and Fast Fluctuating Signals (b). The Broken Line is Rectangular Beams and the Solid Line is Gauss Beams (P_N is the Noise Quantized Probability of the First Threshold)

Fig. 3.18 gives the results of computer simulation of the numerical sliding detector for the detection of three types of fluctuating signals when the false alarm probability is 3×10^{-6} . It can be seen from this figure that when the required detection probability is 90%, the signal-noise ratio necessary for detecting fast speed fluctuating target signals is 6 decibels lower than for the detection of slow fluctuating signals.

It can be seen from this that if we can cause the echo signal to change from slow speed to fast speed fluctuation we can greatly improve detection performance.

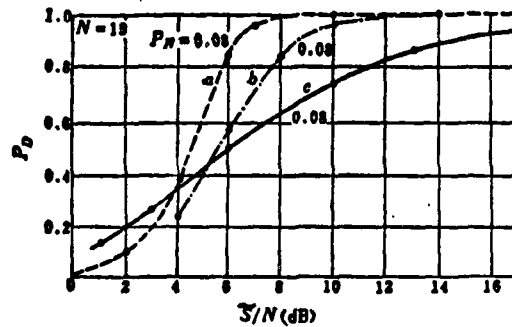


Fig. 3.18 The Detection Performance of the Numerical Sliding Window Detector For Three Different Types of Fluctuating Signals

- a - Non-fluctuating signals;
- b - Fast fluctuating signals;
- c - Slow fluctuating signals.

(The second threshold is 8, when in $P_N = 0.08$ it is equivalent to $P_F = 3 \times 10^{-6}$)

3.5 The Ability of Frequency Agility to Raise Radar Detection

We know from the above discussion that there are two areas of influence of frequency agility on target echo fluctuation. One is accelerating the speed of echo fluctuation which causes it to change from slow speed fluctuation (uncorrelated in antenna scanning) to fast speed fluctuation (uncorrelated from pulse to pulse). The other is changing the probability distribution of the echo amplitude and decreasing the probability of small amplitude echoes. Naturally, these two points are quite beneficial to target detection.

However, because of the decorrelation caused by frequency agility really each pulse cannot be transmitted independently.

Although we can also directly compute the correlation coefficient of its adjacent pulses [12], afterwards its required signal-noise ratio is computed according to its correlation coefficient when they are in different detection probabilities. Yet, for convenience of engineering computations, it would be better to divide this problem into two research steps. Firstly, study the relationship between the frequency agility gain (relative to detecting slow speed fluctuating targets) and the number of independent pulses. Afterwards, study the number of equivalent and independent pulses when there is frequency agility.

When there is frequency agility or frequency diversity, the slow speed fluctuation loss it can eliminate (this is also the frequency agility gain G_{FAT}) is related to the number of independent pulses. Some people have done careful analysis and computations [13] and their results are shown in fig. 3.19.

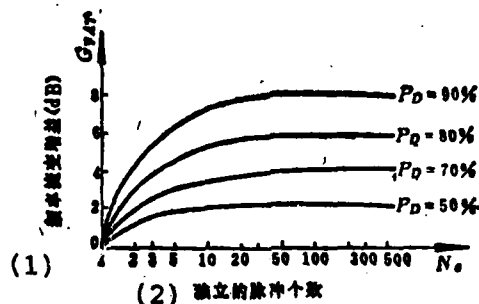


Fig. 3.19 Relationship of Frequency Agility Gain G_{FAT} and the Number of Independent Pulses N_e

Key: 1. Frequency agility gain (dB)
2. Number of independent pulses

We can see from the above figure that G_{FAT} is not only the function of the number of independent pulses but also the function

of the required detection probability. The higher the required detection probability the larger its gain. This is identical to the discussion in the last section. Moreover, when the number of independent pulses exceeds 20 its gain tends towards the limit and does not further enlarge. This relationship can also be very accurately expressed by the following empirical formula [9]:

$$G_{\text{avr}} = \frac{L_f(1)}{L_f(N_s)} = (L_f(1))^{1-1/N_s} \quad (3.19)$$

When expressed by the number of decibels

$$G_{\text{avr}}(\text{dB}) = (1 - 1/N_s) 10 \lg L_f(1) \quad (3.20)$$

In the formula, $L_f(1)$ is the fluctuation loss when there is single pulse. This can be found in fig. 3.13.

Now we will take a further look at the number of pulses, when there is frequency agility, which are determined by these factors [14].

To study this problem, we must first decide the number of frequency communication channels for the frequency agility radar. This number of frequency communication channels is determined by the total frequency agility bandwidth B_{FA} and the required critical frequency Δf_c . Fig. 3.20 draws the relationship of the number of frequency communication channels v with B_{FA} and Δf_c .

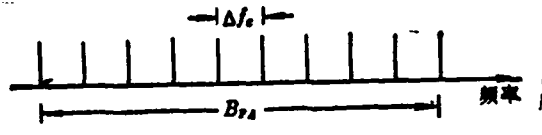


Fig. 3.20 Diagram of Frequency Communication Channels

Key: 1. Frequency

We know from the figure that

$$v = 1 + B_{fa} / \Delta f_c \quad (3.21)$$

and in which Δf_c is determined by expression (3.9).

The present problem is the number of its pulses when the radar's transmission frequency randomly jumps in the B_{FA} range.

If the number of pulses obtained in the T_0 time of the irradiated target is N , then the number of independent pulses N will necessarily be smaller than v . As regards its frequency communication channels the probability of the transmitted N pulses falling in this frequency channel at least once is

$$1 - (1 - 1/v)^N$$

Therefore, the mean value of the number of independent pulses can approximately be the total number of frequency channels multiplied by the probability of each frequency channel, that is

$$E(N_s) = v(1 - (1 - 1/v)^N) \quad (3.22)$$

To more accurately compute the parameters of the non-linear relationships which exist within N_c (for example, detection

probability, it is sometimes also necessary to know the probability distribution of N_c . It is also necessary to know the probability of N pulses having N_c independent pulses. This probability is composed of two items. The first is after transmitting $N-1$ pulses there are N_c independent pulses and then a non-independent pulse is transmitted. The other item is after transmitting $N-1$ pulses there are only N_c-1 independent pulses and then an independent pulse is transmitted. Thus, its probability is

$$P_{N,N} = P_{N,N-1} \cdot N_c/v + P_{N-1,N-1} (1 - (N_c-1)/v) \quad (3.23)$$

For example, when the transmitted pulse number $N=5$ and the frequency communication channel number $v=5$, the mean independent pulse number $E\{N_e\} = 3.4$. Its precise distribution is given in the following table

N_e	1	2	3	4	5
probability	0.0016	0.0960	0.4800	0.3840	0.0384

When $v \gg 1$, formula (3.22) can be approximated by the following formula

$$E(N_e) \approx v(1 - e^{-N/v}) \quad (3.24)$$

Because of this, it is only necessary to be able to compute $E\{N_e\}$ so as to be able to find the gain when there is frequency agility from fig. 3.17 or formula (3.20). This is also the fluctuation loss decreased by frequency agility. For example, when the required detection probability is 90%, the mean number of independent pulses $E\{N_e\} = 6.5$ and we can

AD-A124 003

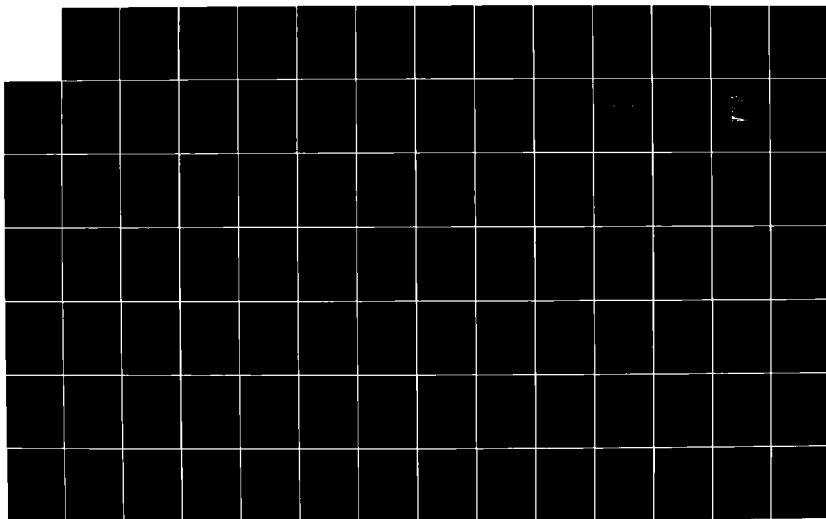
FREQUENCY AGILITY RADAR(U) FOREIGN TECHNOLOGY DIV
WRIGHT-PATTERSON AFB OH 45433-0603
FTD-ID(RS)T-0603-82

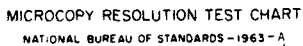
217

UNCLASSIFIED

F/G 17/8

NL





MICROCOPY RESOLUTION TEST CHART
NATIONAL BUREAU OF STANDARDS-1963-A

obtain $G_{FAT}=6.8$ decibels. Even when radar operating under frequency agility conditions has accumulated gain (or accumulated loss) and because of the non-linearity of the detector it faces the noise inside the receiver, its computations are the same as those of fixed frequency radar. That is, it is determined by formula (3.17) or fig. 3.14.

Cumulative detection probability is also sometimes used in the detection of radar targets. The concept of cumulative detection probability is mainly used in search radar where the antenna carries out circular scanning. So-called "cumulative detection probability" points to the probability of the target appearing least once when the antenna rotates j times. If the detection probability of a single antenna scanning is P_D , the probability of the antenna rotating j times and the target still not appearing is $(1-P_D)^j$. Therefore, the cumulative detection probability of the antenna rotating j times and the target appearing at least once is

$$P_c = 1 - (1 - P_D)^j \quad (3.25)$$

Naturally, when the required detection probability is the same, the probability of single detection required for cumulative detection probability is relatively small. Therefore, if the value of j is very large, even if required $P_c=90\%$ the required P_D will also be very low. Given this type of situation, use of frequency agility is not only without advantage but can also be lacking as compared to fixed frequency radar.

To obtain a quantitative concept, fig. 3.21 draws a comparison of the improvement of frequency agility on single detection probability as well as the improvement of cumulative detection probability [15].

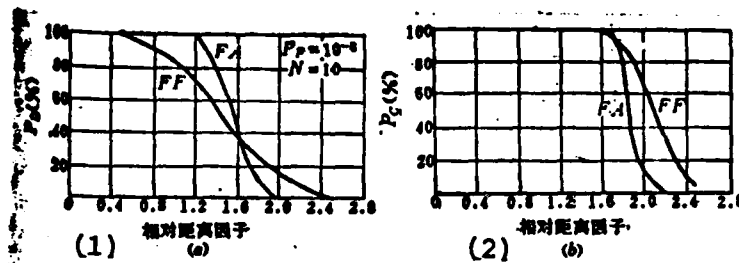


Fig. 3.21 The Improvement of Frequency Agility on Single Detection Probability and Cumulative Detection Probability (In the Fig., FF is the Fixed Frequency and FA is the Frequency Agility)

- (a) Detection probability of a single scanning
- (b) Probability of appearing more than once in 10 scans

Key: 1. Relative distance factor
2. Relative distance factor

The curves in the figure are computed based on when the number of pulses in the antenna beam $N=10$ and the given false alarm probability $P_F=10^{-8}$. The abscissa is the normalized distance of 1 when the fixed frequency radar's single detection probability is 85%.

It can be seen from the curves in figure 3.21 that when single detection probability is 85%, the frequency agility increases the detection range 38%. Above the point of intersection of the two curves the frequency agility always improves the detection probability. However, the situation is different with cumulative detection probability. At this time, only when there is a very high accumulative detection probability required is frequency agility an improvement over fixed frequency. Yet, as in the situation shown in fig. 3.21(b), it does not fit in with the real situation very well. Because with each turn of the antenna

only one time will a light spot be discovered, it is considered that the believability of discovering targets in this way is relatively low. In order for the path tracking computer not to lose the target, it is usually necessary that the antenna make 10 revolutions so that a target will be discovered at least 8 or 9 times. At this time, the required single detection probability is relatively high. Given this type of situation, the cumulative detection probability can be computed by a binomial distribution.

$$P_c = \sum_{k=r}^n \binom{n}{k} P_D^k (1-P_D)^{n-k} \quad (3.26)$$

If it is required that in each rotation of the antenna at least 8 out of 10 times a target is detected and the cumulative detection probability is 90% (which is $n=10, r=8$ in the above formula), then we can use the table examining method to obtain the required single detection probability $P_D=88\%$. Given this type of situation, with the use of frequency agility there will still be tremendous improvement.

Aside from this, what is sometimes quite interesting is the probability of discovering targets outside a certain range. This type of detection probability is not only related to the probability of detection of a single scanning but is also related to the rate of approach of the target. So-called rate of approach of the target δ is the ratio of distance Δ of the target flying near the radar station within the time for one antenna revolution and the distance of the target R_1 .

$$\delta = \Delta / R_1 \quad (3.27)$$

If a target flies at a radial velocity of 1 kilometer per second close to the radar station and the radar antenna revolves once

every 10 seconds, when the target is 100 kilometers from the radar station its rate of approach is 0.1. Naturally, the higher the target's radial velocity, the slower the rotation of the antenna, That is, the larger its rate of approach the closer the radar's detection range. If the radar's single scanning detection probability P_D as well as the target's rate of approach are known, we can then compute and discover the cumulative detection probability of the light spot two or more times.

Based on parameters identical to those of fig. 3.21 (i.e. the number of pulses in the beam is 10 and the false alarm probability is 10^{-8}), fig. 3.22 shows the relationship between the cumulative detection probability computed and discovered two or more times and the relative distance factor when each rate of approach is 0.1. It can be seen from this figure that frequency agility is still far superior to fixed frequency and it is closer to the real situation.

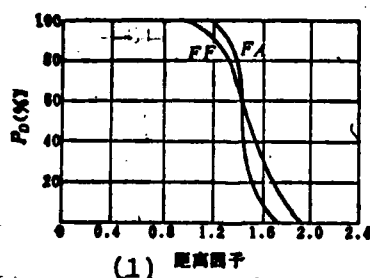


Fig. 3.22 Cumulative Detection Probability When Each Rate of Approach of the Target Flying Near the Radar Station is 0.1 ($N=10$, $P_F=10^{-8}$)

Key: 1. Distance factor

3.6 Results of Actual Test Flights on the Detection Range of Frequency Agility Radar

Although, in theory, it was early found that when radar

operated in jumping frequency this could cause the target's echo to change from fast to slow fluctuation and thus enlarge the radar's detection range, nevertheless, these theoretical analyses all ultimately awaited practical testing so as to prove it.

During the earlier period when frequency agility radar first appeared, some people carried out actual test flights so as to test and verify the enlargement of its detection range [16]. It used 20 pulses in the radar beam which could operate in fixed frequency as well as random jumping frequency. If we only use the two above mentioned Swerling fluctuation models we can then, through theoretical analysis, compute the relationship of its detection probability and signal-noise ratio as shown in fig.3.23.

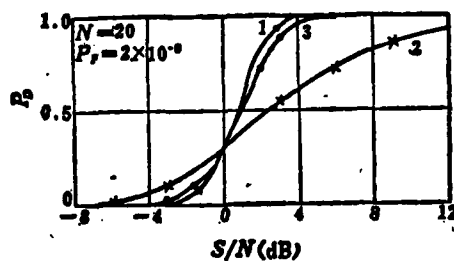


Fig. 3.23 Results of Theoretical Computations of Different Echo Fluctuations for Target Detection

When computing this curve, we take the allowable false alarm rate as 2×10^{-5} . Curve 1 in the figure is the computation results of constant amplitude echoes, curve 2 is the slow speed fluctuation echoes (which are uncorrelated in scanning), and curve 3 is the fast speed fluctuation echoes (which are uncorrelated in the pulses). We know from the figure that when the required detection probability is 90%, the signal-noise ratio required for slow speed fluctuation is 10 decibels

greater than is needed for non-fluctuating echoes; fast speed fluctuation requires about 9 decibels less than slow speed fluctuation.

Three types of aircraft were used for the test flights. The first type was a small jet aircraft, the second type was a small single propeller aircraft and the third was a medium sized double propeller aircraft. The paths of the aircraft were equal velocity straight flights toward the radar and away from the radar. The results are shown in fig. 3.24.

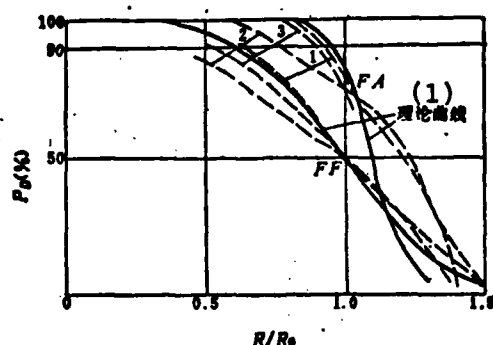


Fig. 3.24 Results of Actual Test Flights on the Enlargement of the Detection Range of Frequency Agility Radar

Key: 1. Theoretical curve

The theoretical curves in the figure are based on the computations of the FA and FF curves in fig. 3.21. Curve 1 in fig. 3.24 corresponds to a small jet fighter, curve 2 corresponds to a small single propeller aircraft and curve 3 corresponds to a medium sized double propeller aircraft. In the figure, the abscissa is the relative distance factor and when using fixed frequency it gives a 50% light spot-scanning ratio distance of R_0 .

It can be seen from the figure that the results of the actual test flights are identical to the theoretical values. When there is a low signal-noise ratio there is a detection probability

higher than the theoretical value. This is because the test flight target has equal velocity straight flight and thus the observer has a certain a priori knowledge concerning the target's position on the screen. There is lower detection probability when in a high signal-noise ratio. The main reason for this is that when in frequency agility all of the pulses cannot be made independent, that is, its effective pulse number is less than 20. The test data also still has measurement errors and statistical errors.

Aside from this, there are others who have carried out actual test flights on the detection range of frequency agility radar. Their results are shown in table 3.2

(1) 检测概率 (%)	(2) 第一组 雷达频率16.5兆赫, 脉冲数=30, 跃频范围 1兆赫/脉冲	(6) 第二组	第三组 (9)
(4) 线性检波器	对数放大器	喷气式 战斗机	小型单螺 旋桨飞机
$P_d \sim 95 \sim 97$	(5) 8.1	(7)	(8)
95	7.8		
90	6.4	6.4	(7)*
80	4.0	4.5	(4)*
70	2.7	2.7	4.7
50	2.1	2.4	7.8
30	1.6	2.0	7.0
10	1.3	1.0	2.5
	1.2	0.7	1.3
			1.2

(11)* 和单频的理论值比较。

Table 3.2 Test Results of the Improvement of Jumping Frequency on Radar Detection Capabilities (Decibels)

- Key: 1. Detection probability (%)
 2. First group
 3. Radar frequency is 16.5 kilomegahertz, number of pulses is 30, the jumping frequency range is 1 megahertz/pulse
 4. Linear detector
 5. Logarithmic amplifier
 6. Second group
 7. Jet fighter

- Key: 8. Small single propeller aircraft
9. Third group
10. Radar frequency is 2.8 kilomegahertz,
the sum of the frequency of the two
intervals is 215 megahertz
11. *As compared to the theoretical value
of the single frequency

In the table, data for the second group are the results of the above mentioned actual test flights. Data for the first group used frequency agility radar with a bandwidth of only 30 megahertz. Moreover, the velocity of the Ku wave band radar target's echo band and radar target's echo fluctuation was originally relatively high yet there was also quite noticeable improvement. Data for the third group was frequency diversity radar with a double frequency. Because of this, the test results should also consider that after detection the two communication channels both increased 1.5-2 decibels.

We know from the results in the table that the improvements caused by use of the logarithmic amplifier were slightly better than those of the linear channels. The improvements on the small single propeller aircraft were better than those on the small jet aircraft. Moreover, when the detection probability was lower than 30% there were still formidable improvements. There are still no satisfactory explanations for these.

Similar results can be obtained in tests on guided missile targets. Fig. 3.25 gives the results of tests on a 150 inch long guided missile target.

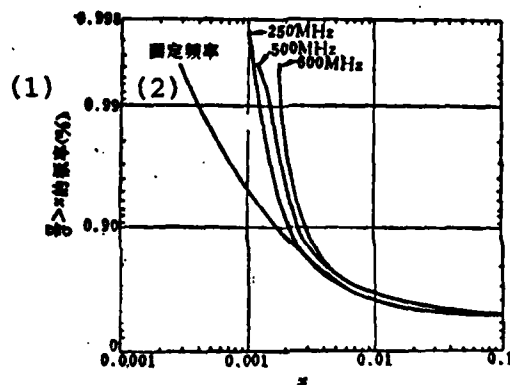


Fig. 3.25 Radar Section Probability Distribution and Jumping Frequency Bandwidth (16 Staircase Jumping Frequency) of a Guided Missile Target (150 Inches Long)

Key: 1. Probability of $\sigma/\bar{\sigma} > x$ (%)
2. Fixed frequency

The radar used can operate in fixed frequency as well as staircase jumping frequency. When operating in staircase jumping frequency, there are altogether 16 frequency increments. Its total jumping frequency bandwidth is shown in fig. 3.25. The ordinate in the figure is the probability wherein the ratio of the equivalent reflection area and the mean equivalent reflection area is larger than a certain value of x . The abscissa is x . The figure gives the fixed frequency as well as the three situation curves of the jumping frequency bandwidth which are separately 250 megahertz, 500 megahertz and 600 megahertz. We know from the figure that after jumping frequency is used for a small x value, the probability of $\sigma/\bar{\sigma} > x$ is far greater than when there is fixed frequency. When the total jumping frequency bandwidth is 250 megahertz, that is, each staircase $\Delta f \approx 16$, although smaller than the critical value of $C/4D$ there is still objective improvement. After the jumping frequency bandwidth is doubled there is only a slight increase.

This is because when the jumping frequency is 250 megahertz this is sufficient to cause its echoes to decorrelate.

When jumping frequency technology is applied to tracking radar, it can, in the same way, raise detection probability. At this time, because of the large number of target echoes more effective video accumulation can be carried out. The video accumulation in common tracking radar is determined by the time constant of the range tracking loop. Yet, if the declining time constant of the target echo is larger than this accumulated time constant, this type of decline can possibly cause the target to be lost.

After using jumping frequency technology, this type of long time decline can be eliminated. This can then enlarge the tracking range.

Researchers have done some 30 odd test flights on various model aircraft targets. After discovering the use of jumping frequency technology, when other parameters were invariant, the range of the first lost target could be made to be about 20% larger than when there was fixed frequency. This is a completely objective increase equivalent to increasing the transmitter's power 3.2 decibels.

3.7 The Influence of Frequency Agility on Lobe Splitting

Early, at the beginning of the Second World War, the influence of ground reflection on radar lobes was discovered. Ground (or sea) reflection can be equivalent to having an image antenna below the ground (or sea) (fig. 3.26).

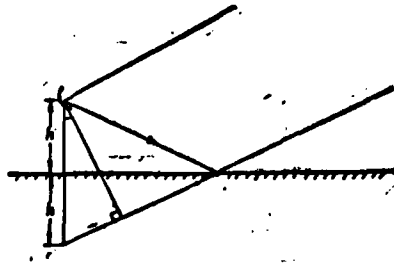


Fig. 3.26 Influence of Ground Reflection on Radar Lobes

This image antenna also radiates electromagnetic waves (in reality, these are ground reflection waves). These electromagnetic waves along with the electromagnetic waves radiating from the original antenna produce an interference effect and form many split interference lobes.

The influence of the path difference of the electromagnetic waves on the phase is knowable. The corresponding angles of the smallest and largest values of these interference lobes are expressed by the following formulas.

$$\theta_{min} = \arcsin \frac{(n-1)\lambda}{2h} \quad (3.28)$$

$$\theta_{max} = \arcsin \frac{(2n-1)\lambda}{4h} \quad (3.29)$$

In the formulas, λ is the radar wavelength, h is the height of the antenna frame and n is the positive integer.

When the radar wave length is 24 centimeters and the height of the frame is 7 meters the first blind spot is 1 degree. Afterwards, there is a blind spot every 1 degree. Following the

increase of the angle of elevation, the radiation of the antenna lobe facing the ground weakens and the reflection of the ground also weakens. Therefore, when there is a high angle of elevation the depth of the blind spots decreases and the intervals of the blind spots become denser.

When a radar frame is on the seashore or on a ship, because the ocean surface's conductivity is very high, the reflectivity of the electric waves is very strong. At this time, the blind spots of the lobe splitting are very deep (see fig. 3.27).

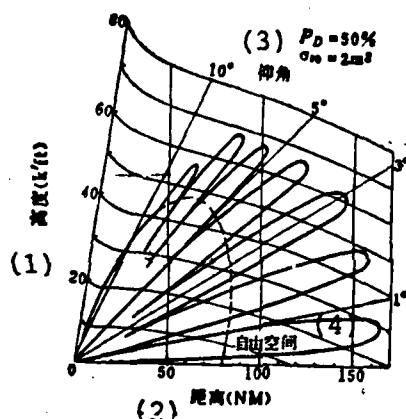


Fig. 3.27 Lobe Figure of AN/UPS-1 Radar on Surface of Water
(Vertical Beam 10° , Upward Warp Angle 2°)

Key: 1. Height (k'ft)
2. Range (NM)
3. Angle of elevation
4. Free space

The effect of the blind spots of this type of lobe splitting (especially blind spots in areas of low angles of elevation) on the detection of far range targets is great. Moreover, it can cause the automatic tracking system to lose the target and even require new acquisition. The method used in the past to resolve

this problem was to cause the antenna to have a small angle of pitch in the direction of the angle of elevation. Yet, this method cannot solve the problem because the speed of the antenna's pitch is very low and can only change in the antenna's rotating period. In this way, when there are many targets, the antenna's pitch cannot simultaneously avoid the blind areas of all of the targets as well as the blind areas of a certain target so as to be able to cause another target to enter the lobe's blind area.

Because the angle of this type of blind spot is the function of the frequency, use of frequency agility can possibly cause the lobe's blind areas of each pulse to completely stagger.

Because the angle of the lobe's blind spot forms a direct ratio with the wave length when there is a low angle of elevation, in order to completely stagger the first blind area it is necessary that the wave length after jumping frequency be 1.5 times that of the original. In this way, the frequency bandwidth of the jumping frequency is still relatively large. For example, when operating in a radar station with a 10 centimeter wave length, in order to totally eliminate the lobe's blind area, it is necessary for it to jump to a 15 centimeter wave length (equivalent to changing from 3,000 megahertz to 2,000 megahertz). If this wide range jumping frequency can be realized, then the blind area of the angle of elevation lobe can be completely staggered. Moreover, this type of lobe jumping is realized between two adjacent pulses (not between two rotations of the antenna). Therefore, when there are multiple targets there is no problem at all.

Yet, due to the limitations of the bandwidths of the high powered components, the actual jumping frequency which can be realized is not this wide. Although this be the case, relatively

narrow jumping frequency is also sufficient to affect the position of the lobe's blind spots. This is because when there is a relatively high angle of elevation the frequency deviation required to compensate for the blind area is relatively small. For example, we know from formulas (3.28) and (3.29) that when $n=6$ it is only necessary to have a 10% jumping frequency range to be able to cause its splitting lobes to attain compensation. This has already been proven in tests.

Early on-the-spot test flights of frequency diversity radar found that its detection range noticeably increased. At the time, it was thought that this mainly caused the results of the mutual compensation of the splitting lobes. In reality, it also included the effects of echo decorrelation. Conversely, the actual tests of jumping frequency radar also included the influence on lobe splitting. Therefore, it is quite difficult to totally distinguish the effects of these two factors.

References

- [1] Radar Handbook, Ed. by M.I. Skolnik, McGraw-Hill Book Co. 1970, chapt. 27.
Chinese translation: "Radar Handbook," Vol. 2, Chapter 8, Defense Industry Publications 1978.
- [2] Radar Design Principles, F.E. Nathanson, McGraw-Hill Book Co. 1969. chapt. 5.
- [3] The jet fighter radar cross section, T.P. Vasserot, IEEE Trans. Vol. AES-11, No. 4, July, 1975. pp.523-533.
- [4] Detection of fluctuating pulses signals in the presence of noise. P. Swerling. IRE Trans. Vol. 1T-3, pp.175-178, Sept. 1957.
- [5] Remarks on target models for the design of radar Systems. K. Von Schlachta, The Record of the IEEE 1975. International Radar Conf. pp. 440-445.

References (continued)

- [6] Some measurements of the effects of frequency agility on aircraft radar returns. W.S. Whitlock, A.M. Shepherd and A.L.C. Quigley. AGARD Conf. Proc. No. 66 on Advanced Radar Systems. AD-715, 485. 1970.
- [7] A statistical Theory of target detection by pulsed radar. J.I. Marcum, IRE Trans. Information Theory, Vol. 1T-6, pp. 59-145. April, 1960.
- [8] Probability of detection of fluctuating targets. P. Swerling. IRE Trans. Vol. 1T-6, pp. 269-308. April, 1960.
- [9] Simple procedures for radar detection calculations. D. K. Barton, IEEE Trans. on AES-5, No. 5. Sept. 1969. pp.837-846.
- [10] A sequential logic for improving signal detectability in frequency-agile search radars. V.G. Hansen. IEEE Trans. on AES-4, No. 5. Sept. 1968. pp. 763-773.
- [11] MeBfehler bei der Azimutbestimmung Von Radarzielen mit dem binären Wanderfenster- Integrator. Kurt. Müller und Walter Röcker. Wiss.Ber. AEG-TELEFUNKEN 44 (1971) Nr. 1, SS.25-33.
- [12] Defection of slowly fading Targets with frequency agility. N.D. Wallace. Proc. IEEE, May, 1969, pp.817-818.
- [13] A unified analysis of diversity radar systems. P.F. Guarguaglini, IEEE Trans. Vol. AES-4, No.2. pp.318-320. Mar. 1968.
- [14] Frequency agility radar range calculation using number of independent pulses. G.Lind. IEEE Trans. Vol. AES-12. No. 6. Nov. 1976. pp.811-815C.
- [15] Improving radar range and angle detection with frequency agility. H.Ray. Microwave J. May, 1966. p. 63.
- [16] System properties of jumping-frequency radar B.C. Gustafson and B.O. As. Philips Telecomm. Review. Vol. 25. pp.70-76.

Chapter IV The Increase of the Angle-Measuring Precision of Radar by Frequency Agility

4.1 The Source of Angle-Measuring Errors For Precision Tracking Radar

Analyses of the angle-measuring precision of precision tracking radar have shown that the source of target angle-measurement errors can be divided into two major categories. One are errors produced by the radar itself and the other type of errors are unrelated to the radar.

The errors produced by the radar itself can be divided into tracking errors and reading errors. Tracking errors include the calibration and drift of the axis of sighting, the effect of wind power and servo noise. Reading errors include horizontal and due north corrections, triaxial orthogonality, mechanical deviations, thermal distortions, gear errors and code errors.

There are two main categories of errors unrelated to radar. One type are caused by electric wave propagation including multipath propagation and atmospheric refraction. The other type are caused by target reflection. This type can be further divided into hysteresis errors caused by target movement and target noisewaves caused by the interference between each of the target scattering object's echoes.

Because the mechanical processing precision of early radar was relatively low, its angular tracking error can be said to be mainly caused by the mechanical parts of the radar. Among these

are included the orthogonality of three axes, the backlash of gears, and errors caused by the data-transmission system. However, following the continual development of manufacturing technology, the errors caused by the radar's mechanical parts decreased to a very small quantity. For example, the errors by single pulse precision tracking radar^(FPS-16) itself are shown in table 4.1 [1].

(1) 误差来源	(5) 以毫弧度表示的均方根角误差	
	(6) 偏置	(7) 随机
(2) 雷达本身的跟踪误差	0.052	0.023
(3) 雷达本身的读数误差	0.025	0.04
(4) 雷达本身的总固定误差	0.057	0.046

Table 4.1 Errors by the Radar Itself

- Key: 1. Source of error
 2. Tracking errors by the radar itself
 3. Reading errors by the radar itself
 4. Total fixed errors by the radar itself
 5. The mean square angular errors expressed in milliradian
 6. Bias
 7. Random

We can see from this table that the errors produced by the radar itself are still quite small and mainly bias errors can try to be eliminated.

The errors caused by electric wave propagation are of two types. One is the errors brought about by troposphere refraction and the other is caused by multipath transmission. The bias value of the first type is about 0.5 milliradian and that of the random type is 0.3 milliradian. The latter type is related to the antenna lobes, radar frame height, ground reflection coefficient and the target's angle of elevation. It is relatively difficult to estimate.

There are three items of error related to the target. The first are the dynamic hysteresis errors created by the target's movements and the servo system's limited bandwidth. On the one hand, these types of errors are related to the movement of the target (e.g. the smallest route from the target to the radar station, the velocity and the height of the target etc.) and on the other hand, they are related to the servo bandwidth. Generally speaking, this type of error is especially serious for close distance and high speed, low altitude targets. Yet, when the target's moving conditions and servo system capabilities are known, an electronic computer can be used to compute the hysteresis error and make corrections.

The other two sources of errors related to the target are errors caused by amplitude blinking and angular noise waves. The first item only exists in tracking radar with conical scanning and the latter exists in all tracking radar. The next section will discuss this problem in detail.

The other sources of errors are relatively complex. They are thermal noise wave errors caused by noise waves inside the receiver as well as from static noise waves. The influence of thermal noise waves on angle-measuring errors are mainly determined by the signal-noise ratio of the target and the bandwidth of the servo system (e.g., when the FPS-16 target signal-noise ratio is 20 decibels and when the servo bandwidth is 2.0 megahertz, the mean square value of the angle-measuring error caused by thermal noise waves is 0.078 milliradian. Because this type of error is related to the target's signal-noise ratio, it is also related to the target's range. In this way, we can draw the relationship of the target's amplitude fluctuation, angular noise waves, servo system noise waves as well as receiver noise waves and the target's relative range (as shown in fig. 4.1)[2].

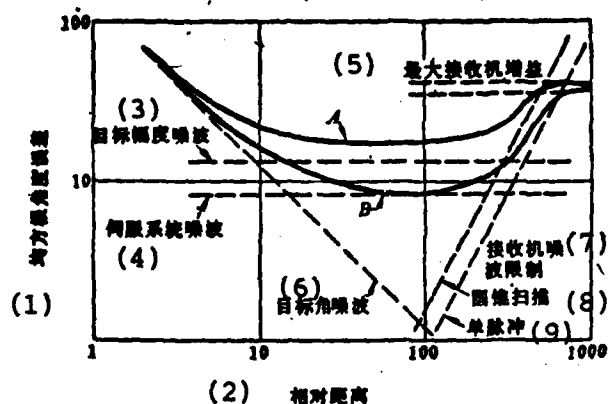


Fig. 4.1 Relationship of Mean Square Value of Relative Angular Error Difference and Relative Range

A - Conical scanning radar;
B - Single pulse radar

- Key:
1. Mean square root of angular error
 2. Relative range
 3. Target's amplitude noise waves
 4. Servo system noise waves
 5. Maximum receiver gain
 6. Target's angular noise wave
 7. Receiver's noise wave limitation
 8. Conical scanning
 9. Single pulse

Curve A in the figure is the total angle-measuring error of conical scanning radar and B is the total angle-measuring error of single pulse radar. It can be seen from these two curves that in a small relative range, the angle-measuring error of conical scanning radar and single pulse radar are nearly identical. Both are caused by the angular noise waves of the target. When in a medium range, because the single pulse radar can eliminate the influence of the amplitude noise waves of the target, there is a noticeable improvement in the angle-measuring error as compared to conical scanning. When in a relatively distant range, the

angle-measuring error is mainly caused by the thermal noise waves of the receiver because the radar's signal-noise ratio decreased. At this time, the angle-measuring errors of the single pulse and conical scanning radar are close. Yet, because of the relatively low sensitivity and relative large equivalent beam width of the conical scanning radar, its receiver noise wave limitation will be produced 5.2 decibels earlier than single pulse radar.

In short, as can be seen from fig. 4.1, use of single pulses can noticeably improve medium range angle-measuring precision. Use of radar beacons can greatly improve the angle-measuring precision of the far range (the beacon increased the signal-noise ratio). However, as for close range, due to the existence of angular noise waves, there is a large limitation on the improvement of the angle-measuring precision whether for conical scanning or single pulse tracking radar. Although the amplitude distribution of the angular noise waves is a Gaussian form (it takes the mean value as zero), yet because its fluctuating frequency is very low there is no way that it can be smoothed away by the servo system of the radar. Therefore, it can produce very large errors in calculating the target's movements. For this reason, effective measures must be employed to decrease the effect of angular noise waves. This is extremely important for close range gun sighting or for ground to air guided missile system radar.

4.2 The Influence of Target Noise Waves on the Angular Tracking Precision of Radar

During the early 1950's it was discovered that the reason tracking radar produces angle-measuring errors lie not only in the radar itself but also in the reflecting characteristics of the target.

The target echoes received by the radar not only fluctuate on the amplitude but the targets observed by the radar viewed in the scattering center are also fluctuating. The former is called the amplitude scintillation (fluctuation) of the target and the latter is called the angular flickering (or angular noise wave) of the target. They are jointly called target noise waves and are differentiated as receiver noise waves, static noise waves, etc.

Then how does this type of target noise wave cause angle measuring errors?

Angle-measuring errors caused by the amplitude scintillation of the target echoes are relatively easy to understand. In the angle-measuring system with sequential lobing (e.g. radar with a beam switch and conical scanning) the determination of the angle is sequentially carried out by relying on the amplitude of the echo signal received from beams in different angle positions. Because this type of amplitude is not simultaneously but sequentially carried out, the fluctuation of the target echo amplitude can cause angle-measuring errors.

The single pulse tracking radar system was developed to eliminate this type of error. This type of radar possesses beams with several different angle positions. Therefore, the amplitude for the target echoes can be simultaneously carried out. In the single pulse system, we can use fast speed automatic gain control to smooth the amplitude fluctuations of the echoes. This basically eliminates the effects of this type of target noise waves.

Another type of target noise wave is so-called angular noise wave (angular flickering). It is the flickering of the target viewed in the reflection phase center. Because most complex

targets are composed of a great many scattering objects, each scattering object reflects part of the echo and its synthesized echo is the vector sum of the small echoes. Because of the movement of the target facing the radar station, the angle of sighting of each of its scattering objects facing the radar change accordingly. After synthesis, the amplitude and phase of the echo also change accordingly. This causes the target echo's phase front (wavefront) received by the radar antenna to be distorted. This type of phase front distortion can cause a disparity between the target angle measured by the radar and the real angle of the target. The angular errors caused by this type of angular noise wave can even be far greater than the angle measurement of the target itself.

As mentioned above, an angular noise wave is formed from the phase front distortion of the target echoes. Therefore, it has an effect on all types of angle-measuring systems. In other words, whether it is a beam switch, conical scanning, amplitude-sensitive single pulse or phase-sensitive single pulse angle-measuring system there is no way to avoid the effect of the angular noise waves.

Because angular noise waves can be expressed by the mean square root value which takes length as the unit, when it transforms into an angular error it is related to the radar tracking range. The target's angular noise waves which are expressed in milliradian can be indicated by the following formula

$$\sigma_a (\text{milliradian}) = \frac{\sigma_a (\text{meters})}{R (\text{kilometers})} \quad (4.1)$$

We can see from this that the angle-measurement error caused by angular noise wave forms an inverse ratio with the target's range. In other words, angular noise waves have an especially serious effect on short range gun sighting radar and

guidance radar.

The use of high precision single pulse radar for the angular automatic tracking of a close range aircraft target mainly has angular tracking errors of the measured target caused by this type of angular noise wave. Its typical time sampling is shown in fig. 4.2 [3].

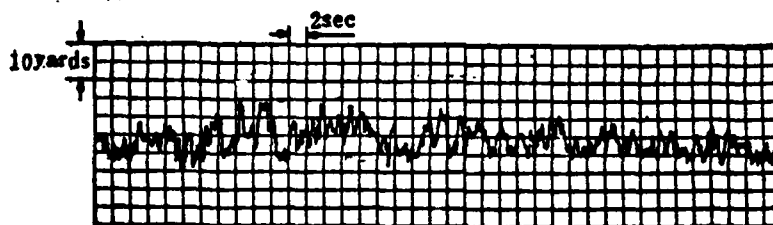


Fig. 4.2 Time Sampling Chart of the Target Angular Noise Waves of a Double Engine Propeller Aircraft

The amplitude distribution of the angular noise waves is a typical Gaussian distribution. The amplitude distribution of the angular flickering of the above mentioned double engine propeller aircraft is shown in fig. 4.3.

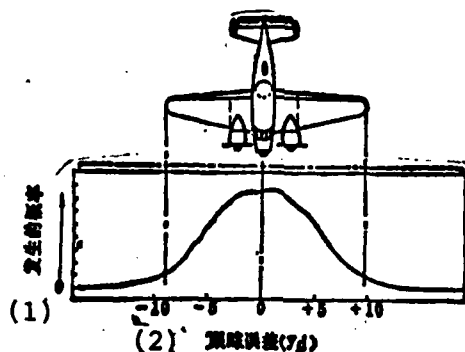


Fig. 4.3

Fig. 4.3 The Angular Vibration Amplitude Probability Distribution Measured For a Double Engine Propeller Aircraft

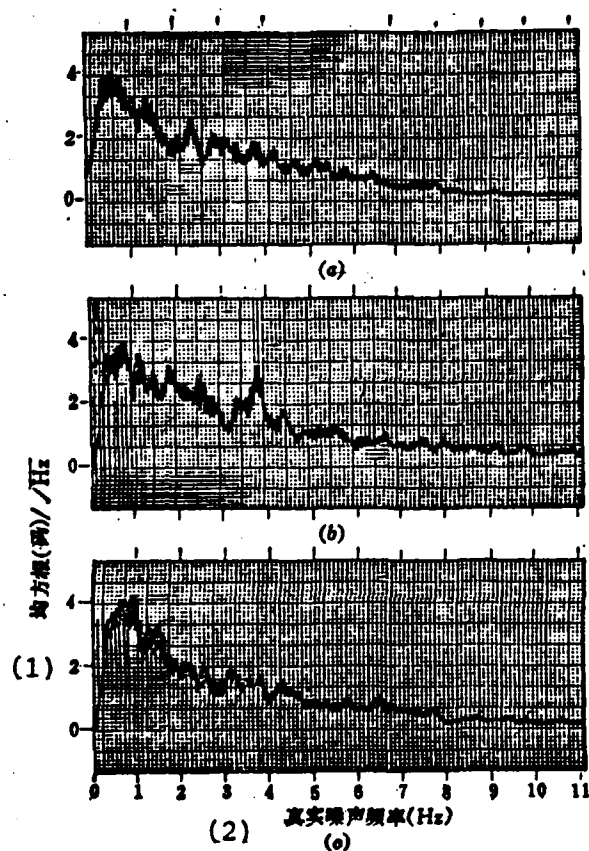
Key: 1. Probability which occurred
2. Tracking errors

A large number of measurements were carried out on various types of aircraft. Measurement results and theoretical analyses showed that if this type of angular noise wave is expressed by the range of the target viewed in the reflection center from the target's center of gravity (its dimension is the length unit), then this type of angular noise wave is unrelated to the target's range (except for very close range). Therefore, the mean square root of angular noise wave σ_a can be expressed in meters. Its results show that σ_a is equal to $r_0 / \sqrt{2}$. In this expression, r is the rotational radius (taken from along the probed angular coordinates) of the target's distribution reflection area. For example, if the target's reflection area has a distribution of a $\cos^2(\pi a/L)$ form (a is a variable, L is its wingspan), then after finding its rotational radius and dividing by $\sqrt{2}$ we can obtain the mean square root of the angular noise wave as $0.19L$. The σ_a value of a real aircraft is between 0.25 and $0.25L$ and is determined by the distribution of its main reflecting objects (e.g., engine, auxiliary fuel tank etc.). The front view angular noise wave of a small single engine aircraft is about $0.1L$, and the σ_a value of a large aircraft (its engine is outside the fuselage and possibly does not have an auxiliary fuel tank) can reach $0.3L$. The lateral viewing angular noise wave of aircraft can also reach $0.3L$.

The σ_a value of complex contoured targets is basically a fixed value. It is unrelated to radio frequency as well as the speed of the target's random movements.

Although σ_a is basically a fixed value, yet the frequency spectrum distribution of the angular noise wave is the function

of radio frequency target movement, atmospheric turbulence and viewing angle. The angular noise wave frequency spectrum of a twin engine propeller aircraft measured from three different viewing angles is shown in fig. 4.4.



Fig, 4.4 The Angular Noise Wave Energy Spectrum Distribution of a Twin Engine Propeller Aircraft From Three Different Viewing Angles

- (a) Front view;
- (b) Lateral view;
- (c) Rear view

Key: 1. Mean square root (yards)/ $\sqrt{\text{Hz}}$
 2. Real noise frequency (Hz)

A typical frequency spectrum form can be written as a Markov type or bandwidth limitation white noise frequency spectrum:

$$W_u(f) = \sigma_a^2 \frac{2f_g}{\pi(f_g^2 + f^2)} \quad (4.2)$$

In the formula $W_u(f)$ is the power spectrum density of the angular noise wave;

σ_a is the mean square root value (meters) of the angular noise wave;

f_g is the half power point frequency (bandwidth (hertz)) of the angular noise wave

f is the frequency (hertz).

Its bandwidth f_g is in direct ratio to the radio frequency and is determined by the effect of the atmospheric turbulence on the target's movements and the target's viewing angle. When in the X wave band and a relatively turbulent atmosphere, the f_g value of a small aircraft is about 1.0 hertz and the f_g of a large aircraft is about 2.5 hertz. When the target's wingspan is at least several wavelengths, its bandwidth is in direct ratio to the radio frequency. Therefore, the f_g value is between 0.3 hertz and 0.8 hertz for the S wave band. This type of narrow wave band signifies that the drift velocity of the target viewed in the reflection center is very low. Therefore, this type of angular noise wave has no means of being smoothed out by the radar's angular servo system but is entered into the data processing system as the real position of the target. This can greatly affect the prediction and measurement of the target's position. Therefore, it is necessary to quantitatively analyze the effect of the target noise waves on the radar's angle-measuring precision.

However, the above discussion only focused on the frequency spectrum of the target noise wave itself. The effects of the target noise waves of this type of frequency spectrum on the radar's angle-measuring precision is not only related to the

characteristics of the radar's angular servo system, but as regards the echo's amplitude fluctuation, it is also related to the characteristics of the automatic gain control. Therefore, it is necessary to carry out further analysis so as to be able to quantitatively understand its effects.

If we can know the frequency spectrum of the target noise waves we can calculate the angle-measuring error caused by the target noise waves based on the characteristics of the servo system and automatic gain control system.

Naturally, the problem is simpler for angular noise waves because angular noise waves are proven by viewing angular flickering in the reflection center. As regards the radar's angular tracking system, it can act as an equal angular input quantity with the target's angle coordinate but is unrelated to the strength of the echo amplitude. Thus, it is also unrelated to the characteristics of the radar's automatic gain control system.

If the angular transmission function of the radar's angular tracking servo system is $Y(f)$, then the variance of the angular tracking error caused by the angular noise waves with a frequency spectrum of $W_u(f)$ is

$$\sigma_e = \int_0^\infty W_u(f) |Y(f)|^2 df \quad (4.3)$$

Assuming the communication band of the servo system is relatively narrow and the angular noise wave assumes a uniform distribution in its range, then it is even simpler and at this time

$$\sigma_a^2 = W_n(0) \int_0^\infty |Y(f)|^2 df = W_n(0) B_n \quad (4.4)$$

In the formula, B_n is the equivalent noise wave communication frequency band of the servo system.

Conversely, if the communication band of the servo system is relatively wide and the angular noise wave assumes a narrow rectangular distribution in the communication band, then the problem can also be simplified and at this time

$$\sigma_a^2 = W_n(0) f_g \quad (4.5)$$

In the formula, f_g is the equivalent bandwidth of the angular noise wave.

When relatively long wavelength (e.g. 10 centimeter wave band) radar is tracking a close range, high speed target, the servo system's bandwidth is relatively wide and closer to the latter type of situation.

No matter what type of situation it is, the angle-measuring variance caused by the angular noise wave is in direct ratio to the zero frequency angular noise wave frequency spectrum density.

The problems of angle errors caused by echo amplitude fluctuation are more complex. This is because although the frequency spectrum of the echo fluctuation is the same as the frequency spectrum of the angular noise wave (because they are all caused by the common mechanism of the interference between each scattering object). However, they are all demonstrated by

the strength of the echo but not expressed by the angle. Therefore, the mechanism of the angle-measuring errors caused by amplitude fluctuation is more complex.

The angle-measuring errors caused at this time can be divided into two categories. The first category only exists in conical search radar and the second category exists in other types of radar.

If the frequency spectrum of the echo amplitude fluctuation is sufficiently wide so that there is sufficiently strong frequency spectrum density $W(f_s)$ in the area of the scanning frequency with conical scanning, then the echo amplitude fluctuation can mistake the error signals caused by the antenna's electric axis not yet being aimed at the target. We have from analysis that the mean square value of the angle tracking error at this time is

$$\sigma_a \cong 0.67 \theta \sqrt{W(f_s) B_n} \quad (4.6)$$

In this formula, θ is the beam width and B_n is the noise band width of the servo system.

If conical scanning frequency f_s is far higher than scintillation frequency spectrum bandwidth B_g , then we can simplify the above formula into

$$\sigma_a = \frac{0.27\theta}{f_s} \sqrt{f_s B_n} \quad (4.7)$$

The second type of angle-measuring error caused by the echo's amplitude fluctuation is directly formed by the low frequency component of the fluctuation. In ordinary circumstances,

the antenna has a fixed biased tracking error ϵ_0 . This is due to the need to overcome the moment created by the wind force or frictional force. When the echo signal is modulated by a low frequency component (in the servo bandwidth), this can cause the bias to produce a counter-modulation and thus bring about an angle tracking error. This error is related to the characteristics of the automatic gain control system. After going through the automatic gain control system the modulation of the echo signal is compressed $|1 + Y_a(f_m)|$ times. In this expression

$Y_a(f_m)$ is the automatic gain control system in the frequency which is the switch voltage gain transmission function of f_m . In this way, the influence of the servo system on the echo scintillation can be expressed by the so-called "scintillation error factor"

$$Y_s = \frac{Y_c}{|1 + Y_a(f_m)|} \quad (4.8)$$

In the formula, Y_c is the closed loop transmission function.

This factor which is relative to the frequency's curve form is not only related to the characteristics of the servo system but is also related to the characteristics of the automatic gain control system.

We know from analysis that when the power spectrum of the scintillation is $W_E(f)$, the power spectrum $W_n(f)$ of the error caused by the scintillation will be

$$W_n(f) = W_E(f) Y_s^2(f) \quad (4.9)$$

Further, the error caused by the scintillation is the integration of the above formula from 0 to ∞ .

In the formula, ϵ_0 is the fixed bias error. When the electric axis of the antenna is aimed totally at the target, ($\epsilon_0=0$), and the error caused by the amplitude scintillation is zero. However, low altitude fast speed targets can often cause bias errors because of the dynamic hysteresis of the servo system. Therefore, this error is one factor which must be considered.

4.3 The Target's Noise Waves When the Radar is Operating in Frequency Agility

As mentioned previously, the angular noise waves of a target are caused by the interference between each scattering object. Thus, it is naturally only related to the movement of the target (viewing angle opposite the radar station) as well as to the frequency of the radar's radio frequency.

When the transmitting frequency of the radar is changed, this will necessarily cause a change of the view in the scattering center. It can be considered that when the radar's operating frequency changes in a very large range, its view in the reflection center will revolve around the real reflection center and form a statistical distribution. When the radar operates in frequency agility and the carrier frequencies of the adjacent pulses are different, its view in the reflection center will revolve around the real reflection center and use very high velocity jumping. In other words, jumping frequency will cause the frequency spectrum of the target's angular noise waves to widen. Because the angle tracking servo system of the radar has a limited bandwidth, it cannot catch up to such fast jumping but can only obtain a mean within a fixed time interval. This time interval is determined by the time constant of the tracking loop. Therefore, it can be anticipated that after radar operates in jumping frequency it can reduce the effect of the angular noise waves on tracking precision.

In reality, when radar operates in frequency agility it not only has an effect on the target's angular noise waves but also affects the amplitude fluctuation (scintillation) of the target echo. It can be imagined that the different pulse to pulse carrier frequencies will cause an acceleration of the scintillation velocity. They will also cause the echo of fluctuation frequency spectrum to widen. Thus, as regards conical scanning radar, because the angle-measuring precision of this type of radar is influenced by echo fluctuation, after using jumping frequency the radar fluctuation frequency spectrum widens. It will then necessarily affect the angle-measuring precision of conical scanning radar.

4.3.1 Relationship of Angular Chatter and Frequency

As mentioned previously, angular chatter is mainly created by the interference in the echoes reflected by each reflecting object which compose the target. It is not only related to the changes of each scattering object's relative position but also to the operating frequency of the radar.

It is assumed that the target is simply composed of two reflecting objects (see fig. 4.5).

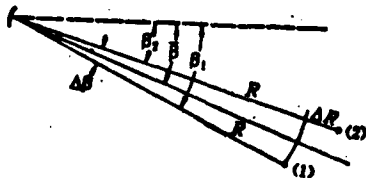


Fig. 4.5 Double Reflecting Object Target Model

If the distance from the target to the radar station is R , its path difference is ΔR (equivalent to the target's radial measurement L_0), the positional angles of the two reflecting objects are separately β_1 and β_2 , and its mean positional angle $\bar{\beta} = (\beta_1 + \beta_2)/2$, the radar's measured angle is

$$\beta = \bar{\beta} + \delta(t)$$

In the formula, $\delta(t)$ is the transient angle error which can be proved [4],

$$\delta(t) = \frac{\Delta\beta}{2} \left[\frac{1-a^2}{1+a^2+2a\cos(\phi(t))} \right] \quad (4.10)$$

In the formula, a is the amplitude ratio of the two signals received by the radar receiver. $0 < a < 1$.

$\phi(t)$ is the relative phase difference of the two reflecting objects observed at the receiving point.

$\phi(t)$ is actually determined by the radar's operating frequency f , path difference $2\Delta R$ and the initial phase relation γ .

$$\phi(t) = \frac{4\pi f \Delta R}{c} + \gamma \quad (4.11)$$

If the path difference $2\Delta R$ is invariant, we can then obtain the relationship of the angle and the frequency error as shown in fig. 4.6.

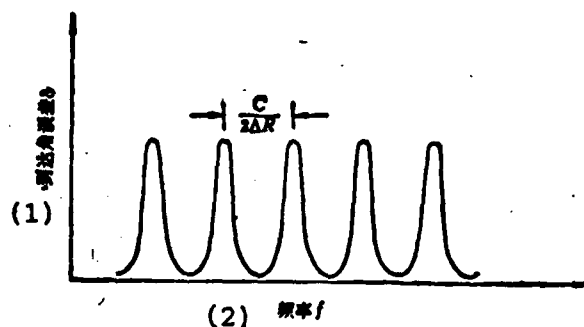


Fig. 4.6 The Angle Error Acting as the Frequency Function

Key: 1. Attained angular error δ
2. Frequency f

It can be seen from the figure that when the frequency changes its angle error changes from the minimum 0 to the maximum (determined by the relative amplitude, path difference, initial phase etc.). It can be proven [5] that when the frequency changes the mean value of the angle error δ_{av} is

$$\delta_{av} = \frac{\Delta\beta}{2}, \text{ when } 0 < a < 1 \quad (4.12)$$

If the radar's carrier frequency has fast speed jumps and its frequency difference is greater than $C/\Delta R$, then the measured target angle will center on its mean value and quickly change. If we can filter out a portion of the fast speed change, we will then obtain a mean value unrelated to the initial phase.

In this way, angular chatter is mainly caused by the viewing angle change (also the change of the path difference) of each of the scattering objects opposite the radar which make up the target. The effect of frequency agility on angular noise waves is mainly the relationship of converting the path difference into the phase difference. Because the angular noise waves are random, in order to further study the effects of frequency agility

on target noise waves it is first necessary to study the effects of frequency agility on the target noise wave's frequency spectrum.

To simplify, we will first consider the frequency spectrum of radio frequency signals. However, we will only study the effects of frequency agility on echo amplitude fluctuation and the angle chatter frequency spectrum. To find the power spectrum of the target noise wave when there is frequency agility, it is first necessary to find the correlation coefficient between its adjacent pulses because the following relation exists between power spectrum ($W(f)$) and relational coefficient $R(\tau)$

$$W(f) = 2 \int_{-\infty}^{\infty} R(\tau) \cos(2\pi f\tau) d\tau \quad (4.13)$$

Thus, it is very difficult to accurately calculate the correlation coefficient between the two adjacent pulses. This is because it is not only related to the frequency difference of the adjacent pulses but is also related to the target's shape and mode of movement.

4.3.2 The Effects of Regular Frequency Modulation on the Target Noise Waves of Simple Target Models

Some people have theorized a type of simple target model, a club-shaped reflecting object with uniform angular velocity rotation [6]. We can obtain an analytic formula of the target noise waves for this type of simple target.

The frequency spectrum of the target echo's amplitude fluctuation $E(t)$ is

$$W_s(f) = \frac{(\overline{E}^2 - (\overline{E})^2)}{f_m} \left(1 - \frac{f}{2f_m}\right) \quad f \leq 2f_m \quad (4.14)$$

In the formula \overline{E}^2 is the mean square value of the echo fluctuation;

$$f_m = \frac{f_0 L \Omega_0}{c}$$

f_0 is the radar's operating frequency;

Ω_0 is the angular speed of rotation;

L is the target's length;

c is the speed of light.

When a 15 meter long target uses 0.1 radian/second uniform rotation, if $f_0 = 10,000$ megahertz then $f_m = 50$ hertz.

The analytic formula of the frequency spectrum of the target echo's angular noise wave is:

$$W_s(f) = \frac{\overline{U}^2}{2f_m} \left(2 - 3 \frac{f}{f_m} + \frac{3f^2}{f_m^2} - \frac{f^3}{f_m^3}\right) \quad f \leq 2f_m \quad (4.15)$$

In the formula, \overline{U}^2 is the mean square value of the target's angular noise wave. Using the Fourier integral inverse transformation, we can find its correlation coefficient from this formula.

The correlation coefficient of the target echo fluctuation is

$$R_s(\tau) = (\overline{E}^2 - (\overline{E})^2) \frac{\sin^2 Y}{Y^2} \quad (4.16)$$

In the formula, $Y = 2\pi f_m \tau$.

The correlation coefficient of the target's angular noise wave is

$$R_s(\tau) = \bar{U}^2 \left[\frac{3\sin^2 Y}{Y^2} + \frac{3\sin^4 Y}{Y^4} - \frac{6\sin^2 Y}{Y^2} \right] \quad (4.17)$$

If the pattern of the jumping frequency can be known we can find the correlation coefficient of the target noise wave when there is jumping frequency as well as find the frequency spectrum of the target noise wave when there is jumping frequency.

Assuming the radar is operating in a regular jumping frequency (frequency modulation) wherein each N pulse of the radar's transmitted carrier frequency is repeated once and at the same time assuming the frequency changes between pulses are larger than Δf_0 (Δf_0 is the critical frequency), we can then consider that the amplitude of each echo is uncorrelated. Given these assumptions, we can obtain the autocorrelation function of the target's angular noise waves when there is regular jumping frequency

$$R'_s(\tau) = \frac{\tau_p}{T_p} R_s(\tau) \sum_{n=-\infty}^{\infty} p(\tau - nNT_p) \quad (4.18)$$

In the formula, τ_p is the pulse width, T_p is the repetition period, $p(\tau)$ is the triangular function of the unit height of $2T_p$.

Therefore, if we know the autocorrelation function $R_u(\tau)$ of the angular noise waves when the radar is operating in

fixed frequency, we can use the above formula to find the autocorrelation function $R'_u(\tau)$ of the angular noise waves when there is regular jumping frequency. By using formula (4.13) we can compute the frequency spectrum of the angular noise wave when there is regular jumping frequency.

In reality, the most interesting is the frequency agility's relative reduction of the angular noise waves. However the variance of the angular noise waves is in direct ratio to the frequency density in its zero frequency area. Therefore, it is only necessary to find ratio Q of the zero frequency spectrum $W_u(0)$ when the radar is operating at a fixed frequency and the zero frequency frequency spectrum $W'_u(0)$ when the radar is operating in frequency agility. Q is called the reduction factor and is defined as

$$Q = \frac{W_u(0)}{W'_u(0)} = \frac{W_u(0)}{2 \int_{-\infty}^{\infty} R'_u(\tau) d\tau} \quad (4.19)$$

It can be calculated with the above mentioned simple target model when the radar is operating in regular jumping frequency

$$W'_u(0) = 2\overline{u}T, \quad (4.20)$$

However, we can calculate $W_u(0) = \overline{u^2}/f_m$ from formula (4.15) and for this reason can find the regular jumping frequency's reduction of the angular noise wave given these conditions

$$Q = \frac{1}{2f_m T} = \frac{\tau_c}{T}, \quad (4.21)$$

In the formula, τ_c is the correlation time when the radar is operating at a fixed frequency. It is defined as

$$\tau_c = \frac{1}{2f_m} = \frac{c}{2f_m L \Omega_0} \quad (4.22)$$

Naturally, when the radar operates in jumping frequency, its uncorrelated pulse number N and product of pulse period T_p should be smaller than correlation time τ_c when the radar operates at a fixed frequency, that is $NT_p \leq \tau_c$. When $NT_p = \tau_c$, we can obtain the maximum Q value.

$$Q_{\max} = N \quad (4.23)$$

If $f_m = 50$ hertz and $T_p = 500$ microseconds, we can calculate correlation time $\tau_c =$ milliseconds. Its maximum reduction factor $Q_{\max} = 20$. The minimum required operating frequency number is also 20.

Similarly, we can also calculate the autocorrelation function of the target echo's amplitude fluctuation when in a simple target model and the radar is operating in jumping frequency

$$R'(\tau) = \frac{\tau_p}{T_p} R_s(\tau) \sum_{n=-\infty}^{\infty} p(\tau - nNT_p) \quad (4.24)$$

By carrying out Fourier transformation we can find the frequency spectrum of the echo's amplitude fluctuation when there is jumping frequency

$$W'_E(f) = \frac{1}{NT_p} \sum_{n=-\infty}^{\infty} W_p\left(\frac{n}{NT_p}\right) \left[W_p\left(f + \frac{n}{NT_p}\right) + W_p\left(f - \frac{n}{NT_p}\right) \right] \quad (4.25)$$

In the formula, $W_p(n/NT_p)$ is the frequency spectrum of unit triangular pulses, the pulse width is equal to $2T_p$ and the center is on n/NT_p .

From this, we can draw the curve of $W'_E(f)$ as shown in fig. 4.7.

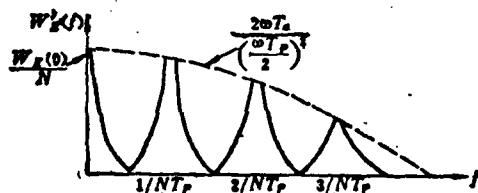


Fig. 4.7 Frequency Spectrum of Echo's Amplitude Fluctuation When There is Jumping Frequency

When there is jumping frequency, the frequency spectrum density of the echo's fluctuation in the zero frequency area also reduces N times. Yet, when $1/NT_p$ approaches conical scanning frequency or its integral number of times, this can produce additional noise in the conical scanning frequency area and thus enlarge the angle-measuring error.

We can calculate the critical frequency of this type of

simple target model as

$$\Delta f_c = \frac{C}{2L \sin \theta} \quad (4.26)$$

In the formula, C is the speed of light and $L \sin \theta$ is the target's wingspan reduced to the range of the line of vision, that is, equal to target depth L_0 .

When the radar's jumping frequency is larger than this critical frequency, it can be considered that there is absolutely no correlation between the two adjacent echoes. When smaller than this value, they are totally correlated. Strictly speaking, the correlation coefficient is the function of the jumping frequency's frequency difference.

We can calculate the correlation coefficient $\rho_E(\Delta f)$ of the echo's amplitude fluctuation for a simple target model as

$$\begin{aligned} \rho_E(\Delta f) &= \frac{\sin^2(2\pi\Delta f(L \sin \theta)/C)}{(2\pi\Delta f(L \sin \theta)/C)^2} \\ &= \frac{\sin^2\left[\pi \frac{\Delta f}{\Delta f_c}\right]}{\left[\pi \frac{\Delta f}{\Delta f_c}\right]^2} \end{aligned} \quad (4.27)$$

The jumping frequency's correlation coefficient $\rho_s(\Delta f)$ of the angular noise waves is

$$\begin{aligned} \rho_s(\Delta f) &= \frac{3 \sin\left[\pi \frac{\Delta f}{\Delta f_c}\right]}{\left[\pi \frac{\Delta f}{\Delta f_c}\right]^2} \left\{ 2\pi \frac{\Delta f}{\Delta f_c} \cos\left(\frac{\pi \Delta f}{\Delta f_c}\right) \right. \\ &\quad \left. + \left[\left(\frac{\pi \Delta f}{\Delta f_c}\right)^2 - 2\right] \sin \pi \frac{\Delta f}{\Delta f_c} \right\} \end{aligned} \quad (4.28)$$

4.3.3 The Effects of Random Jumping Frequency on the Target Noise Waves of Arbitrary Target Models

To find the effects of jumping frequency on the target noise waves of arbitrary target models, we need not first find the analytic formula of the target's noise wave frequency spectrum when there is fixed frequency but only calculate the effects on the original frequency spectrum. This is also sufficient for studying the improvements of jumping frequency on angle tracking precision [1].

If the frequency spectrum of the angular noise wave itself when there is fixed frequency is $W_u(f)$, its autocorrelation function is $R_u(\tau)$. In most situation, $W_u(f)$ and $R_u(\tau)$ have shapes such as those shown in fig. 4.8.

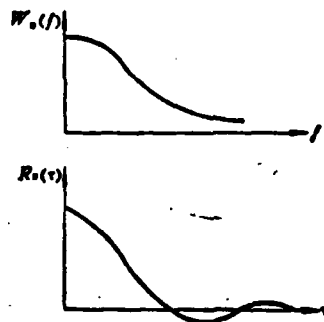


Fig. 4.8 The General Shapes of the Frequency Spectrum of Angular Noise Waves and the Autocorrelation Function (Frontal Approach, X Wave Band, Critical Frequency is 20 MHz)

When we consider the periodic sampling and maintained effect of pulse radar, the correlation function of the angular noise waves is

$$\begin{aligned}
R_{\alpha 1}(\tau) \\
= \sum_{n=-\infty}^{\infty} R_{\alpha}(nT_p) p(\tau - nT_p)
\end{aligned}
\quad (4.29)$$

In the formula, $p(\tau)$ is the trigonometric function of the unit height base width of $2T_p$. T_p is the repetition period. When there was regular frequency modulation in the last section, the autocorrelation function of the angular noise waves was

$$R_{\alpha 1}(\tau) = \sum_{n=-\infty}^{\infty} R_{\alpha}(nNT_p) p(\tau - nNT_p) \quad (4.30)$$

Now it is essential to study the situation with random jumping frequency. When there is random jumping frequency, it is assumed that the maximum range of its jumping frequency is Δf_A and $\Delta f_A \gg \Delta f_c$, Δf_c is its critical frequency. Because the jumping frequency is random, the carrier frequency difference between the two adjacent pulses is possibly smaller than Δf_c and possibly larger than Δf_c . When the possibility of it being smaller than Δf_c is p_c we then consider that the possibility of the adjacent pulses being totally correlated is p_c and the possibility of being uncorrelated is $(1-p_c)$. This thesis has a certain level of approximation yet it can greatly simplify the analysis. When the radar is operating in jumping frequency, the correlation function of the target's angular noise waves is

$$\begin{aligned}
R_{\alpha 2}(\tau) = & (1-p_c) R_{\alpha}(0) p(\tau) \\
& + p_c \sum_{n=-\infty}^{\infty} R_{\alpha}(nT_p) p(\tau - nT_p)
\end{aligned}
\quad (4.31)$$

When $n=0$, the sampling pulse is correlated with itself and the correlation function at this time is equal to the correlation function when there is fixed frequency. When $n \neq 0$, there is correlation between the different samplings and the correlation function at this time is p_c times that of when there is fixed frequency. This is because the definition of the correlation function is the time average. Fig. 4.9 is a schematic of $R_{us}(\tau)$. After the correlation function of the jumping frequency is known, we can use the Fourier transformation to find its corresponding frequency spectrum.

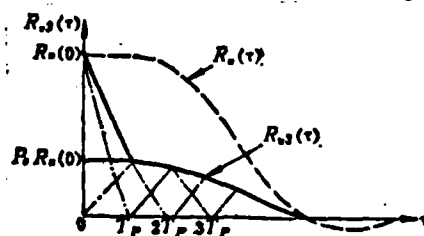


Fig. 4.9 Autocorrelation Function of the Angular Noise Wave When There is Random Jumping Frequency

After $(1-p_c)R_u(0)P(\tau)$ the first item in formula 4.31 undergoes transformation, it gives an energy spectrum item including $(1-p_c)$ times the total angular noise wave power $R_u(0)$ and the pulse repetition frequency $1/T_p$ independent sampling. This portion is "wiped out" to over one-half of the pulse repetition frequency. The second item in formula (4.31) gives an energy spectrum item including angular noise wave power $p_c R_u(0)$. This has a shape similar to the sampled and maintained original frequency spectrum. In actual radar systems, the radar's pulse repetition frequency is far greater than the bandwidth of the angular noise wave. Therefore, the effects of sampling and maintained action on the autocorrelation function and frequency spectrum of angular noise wave is extremely small and can be

overlooked.

In this way, after formula (4.31) undergoes Fourier transformation we can obtain the analytical formula of the angular noise wave's frequency spectrum when there is random jumping frequency

$$W_{\omega}(f) = 2T_p(1 - P_c)R_{\omega}(0) \frac{\sin^2(\pi f T_p)}{(\pi f T_p)^2} + P_c W_{\omega}(f) \quad (4.32)$$

In the formula, $W_{\omega}(f)$ is the angular noise wave's frequency spectrum when the radar is operating in fixed frequency.

To vividly understand the effects of jumping frequency on the angular noise wave's frequency spectrum diagrams of the shape of its frequency spectrum had been drawn in Fig. 4.10. As can be seen in Fig. 4.10b, the frequency spectrum of the angular noise wave when there is a jumping frequency is made up of two components, one of which is the same frequency spectrum shape as the original but has merely been reduced P_c times. The other component has the shape of $\sin^2 x/s^2$, and has been "erased" up to the $f=1/T_p$ points.

Although the only thing calculated above was the effect of jumping frequency on the angular noise wave of the target, it can still be assumed that the effect of jumping frequency on fluctuations in target echo will be the same.

Because the frequency spectrum of echo fluctuation (scintillation) is also of the "low general type" and has an upper frequency



Fig. 4.10 The Effects of Jumping Frequency on Angular Noise Waves

- (a) Radar operating in fixed frequency is the frequency spectrum of an angular noise wave;
- (b) Frequency spectrum of an angular noise wave when there is jumping frequency

limit similar to that of angular noise waves it does not necessarily have the same frequency spectrum shape.

When the radar operates in jumping frequency, the frequency spectrum of the echo fluctuation will also change to be formed from two parts. One part has a shape identical to the original, yet decreases P_c times in amplitude. The other part is also "wiped out" into the shape of $\sin^2 x/x^2$. Its first zero point is in the $1/T_p$ area. The specific shape is similar to that of fig. 4.10.

However, at this time, there is not necessarily any improvement of the angle tracking precision for conical scanning radar. This is because the original echo fluctuation is usually within conical scanning frequency f_s (as shown in fig. 4.11). Jumping frequency actually causes the fluctuation near the conical scanning frequency to enlarge which will possibly increase angle tracking errors.

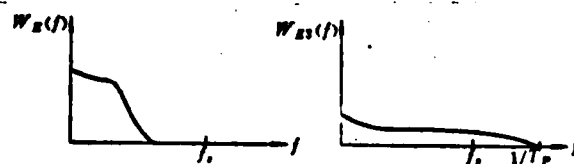


Fig. 4.11 The Effects of Jumping Frequency on the Echo Fluctuation Frequency Spectrum of Conical Scanning Radar

We have already analyzed the effects of jumping frequency on a target's noise wave frequency spectrum above. However, it is not enough to quantitatively estimate the effects of jumping frequency on angle tracking precision. The key lies in the necessity to find the P_c value of the various jumping frequency patterns.

Below we will only study two types of jumping frequency patterns. One type is the random jumping frequency with equal probability distribution. This type is mainly used in frequency agility radar with power amplification. The other type is random jumping frequency with inverse sine distribution. This type of distribution is produced by a random changing pulse repetition frequency carrying out sampling on a sine wave. This type is mainly used in jumping frequency radar with rotary tuning magnetrons. The probability density functions of these two types of jumping frequency patterns are shown in fig. 4.12.

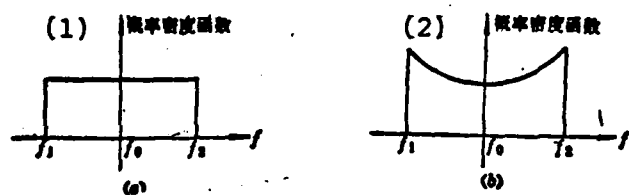


Fig. 4.12 Two Different Types of Jumping Frequency Patterns

- (a) Equal probability random jumping frequency;
- (b) Inverse sine random jumping frequency.

Key: 1. Frequency density function
2. Frequency density function

Assuming x is the carrier frequency of the first pulse, its probability density function is $f(x)$; y is the carrier frequency of the second pulse and its probability density function is

$f(y)$. Functions $f(x)$ and $f(y)$ are totally identical. Letting $z = |x - y|$ be its frequency difference, the z value is always positive. Then, we can find the distribution of z from distributions $f(x)$ and $f(y)$ of x and y

$$F(z) = P(Z \leq z) = \int_{-\infty}^{\infty} \int_{x-z}^{x+z} f(x) f(y) dy dx \quad (4.33)$$

When in random jumping frequency with equal probability, $f(x)$ is a rectangular distribution lying between -1 and +1

$$f(x) = \begin{cases} 0 & x < -1 \\ 0.5 & -1 < x < 1 \\ 0 & 1 < x \end{cases} \quad (4.34)$$

When $f(y)$ is the same function, its result is

$$F(z) = \begin{cases} 0 & z < 0 \\ z - \frac{z^2}{4} & 0 < z < 2 \\ 1 & 2 < z \end{cases} \quad (4.35)$$

The probability density function for z is

$$f(z) = \begin{cases} 0 & z < 0 \\ 1 - \frac{z}{2} & 0 < z < 2 \\ 0 & 2 < z \end{cases} \quad (4.36)$$

z is between 0 and 2.

It is still assumed that the boundary of the distribution for the inverse sine distribution is between -1 and +1. We can know from the definition of the inverse sine distribution that

$$f(x) = \begin{cases} 0 & x < -1 \\ \frac{1}{\pi \sqrt{1-x^2}} & -1 < x < 1 \\ 0 & 1 < x \end{cases} \quad (4.37)$$

$f(y)$ has the same function as this. Thus, the calculation of $F(z)$ is very complex and only by using an electronic computer can we find the numerical values of the approximation solutions as listed in the table below:

z	0.1	0.2	0.3	0.4	0.5	0.6	0.7	0.8	0.9	1.0
$F(z)$	0.1094	0.1905	0.2808	0.3248	0.3837	0.4388	0.4903	0.5398	0.5865	0.6310
z	1.1	1.2	1.3	1.4	1.5	1.6	1.7	1.8	1.9	
$F(z)$	0.6738	0.7149	0.7546	0.7929	0.8300	0.8660	0.9009	0.9348	0.9679	

The probability density function $g(z)$ of $F(z)$ has an approximation expression

$$g(z) = \frac{8}{(2+z)\pi} K\left(\frac{2+z}{2-z}\right) \quad 0 < z < 2 \quad (4.38)$$

In this formula, K is the total elliptic function of the second kind.

The calculation results of the probability distribution $F(z)$ of these two types of random jumping frequency can be expressed by curves (fig. 4.13). The $g(z)$ in the figure is the probability density function of $F(z)$.

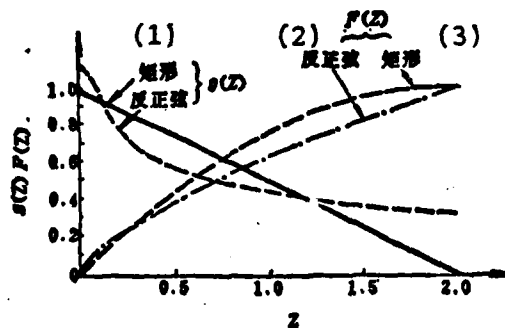


Fig. 4.13 The Probability Density Function and Probability Distribution Function of Two Types of Random Jumping Frequency

Key: 1. Rectangular inverse sine
2. Inverse sine
3. Rectangle

After calculating the probability distribution function of the frequency difference for two types of random jumping frequency, we can calculate the adjacent pulse as correlated probability P_c .

By definition it is obvious that

$$x = \frac{f_2 - \frac{f_1 + f_2}{2}}{\frac{f_1 - f_2}{2}}$$

$$y = \frac{f_1 - \frac{f_1 + f_2}{2}}{\frac{f_1 - f_2}{2}} \quad (4.39)$$

$$z = |x - y| = \frac{2\Delta f}{\Delta f_s}$$

In the formula, Δf_A is the jumping frequency range.

In reality, z is the frequency difference of the Δf_A normalization. $F(z) = P(z \leq Z)$, that is, the probability of the frequency difference is smaller than a certain value. In the above assumption, we assumed that when the carrier frequency difference of the adjacent pulse is larger than a certain critical frequency Δf_c , the echo signal is completely uncorrelated and also smaller than the probability of the critical frequency which is P_c . Therefore, in reality, $P_c = F(\Delta f_c)$. It is only necessary to know critical frequency Δf_c of a certain target to find the corresponding P_c value for this critical frequency based on its jumping frequency pattern. We can calculate the frequency spectrum of the target's angular noise wave when there is jumping frequency from formula (4.32).

As defined in formula (4.19), the frequency agility's reduction factor Q on the angular noise wave variance can be determined by the ratio of the angular noise wave frequency spectrum density in the zero frequency area. Under random jumping frequency conditions

$$Q = \frac{W_{\omega}(0)}{W_{\omega}(0)} = \frac{\sigma_{\omega}^2}{\sigma_{\omega}^2} \quad (4.40)$$

We can calculate its Q value from formula (4.32). Naturally, the Q value is related to jumping frequency bandwidth Δf_A , critical frequency difference Δf_c , pulse repetition frequency F_p and angular noise wave bandwidth B_g .

If we let $k = \Delta f_A / \Delta f_c$ and $\alpha = F_p / f_g$, we can take α as the variant and find the relation between Q and k when in two types of random jumping frequency (as shown in fig. 4.14).

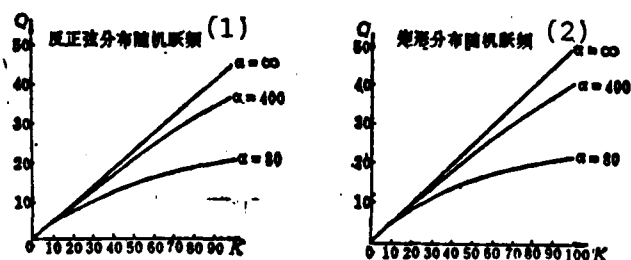


Fig. 4.14 The Relationship Between Angular Noise Wave Difference Improvement and Jumping Frequency Bandwidth When There Are Two Types of Random Jumping Frequency

Key: 1. Inverse sine distribution random jumping frequency
2. Rectangular distribution random jumping frequency

We know from this figure that the wider the jumping frequency bandwidth (relative to the critical frequency difference) the larger the decrease of the angular noise wave variance. When there are identical jumping frequency bandwidths, the higher the repetition frequency (relative to the angular noise wave bandwidth) the larger its decrease.

When jumping frequency bandwidth Δf_A is far greater than critical frequency jumping Δf_c , that is, when the probability P_c of the adjacent pulse's frequency difference being less than the critical frequency jumping is very small, and when rough estimates are made at the same time, the above analysis can then be greatly simplified [8].

When the angular noise wave frequency spectrum density of radar is in a low frequency range, it can be approximated as a rectangular distribution (refer to formula (4.5), that is

$$W_{FF} = \frac{G}{f_g} \quad (4.41)$$

In the formula, W_{FF} is the frequency spectrum density of the angular noise wave;
 G is the probability of the angular noise wave;
 f_g is the equivalent bandwidth of the angular noise wave.

Frequency spectrum density W_{FA} of the angular noise wave for frequency agility type tracking radar changes to

$$W_{FA} = P_s W_{FF} + (1 - P_s) 2G/F, \quad (4.42)$$

Formula (4.42) is derived from formula (4.32).

Assuming we are only interested in the low frequency range, $\sin^2 x/x^2$ can be approximated as 1.

We know from formula (4.40) that the decrease by frequency agility on the angular noise wave is in direct ratio to the ratio of the angular noise wave's frequency spectrum density when there is jumping frequency. Given the above assumptions, it is in direct ratio to the ratio of W_{FF} and W_{FA}

$$Q = W_{FF}/W_{FA} \quad (4.43)$$

Therefore, it is only necessary to substitute formulas (4.41) and (4.42) into formula (4.43) to be able to derive frequency agility's reduction of the angular noise wave. As in the previous analysis, to quantitatively determine the value of Q it is also necessary to find probability P_c of the pulse frequency differences smaller than the critical frequency jumping.

Assuming the total bandwidth of jumping frequency is far greater than the critical frequency jumping and the radar uses equal probability random jumping frequency in the jumping frequency bandwidth, then P_c can be approximated by the following expression

$$P_c = 2\Delta f_c / \Delta f_A \quad (4.44)$$

We know from formula (4.26) that in $\Delta f_c = c/2L_0$, c is the speed of light and L_0 is the radial depth of the target. By substituting in formula (4.44) we can obtain

$$P_c = C/L_0 \Delta f_A = \lambda_{FA}/L_0 \quad (4.45)$$

$$\lambda_{FA} = C/\Delta f_A \quad (4.46)$$

λ_{FA} is the jumping frequency bandwidth's corresponding jumping frequency band length. For example, when $\Delta f_A = 500$ kilohertz, $\lambda_{FA} = 0.6$ meters.

After formula (4.45) is substituted into formula (4.42) and then this together with formula (4.41) is substituted into formula (4.43), we can obtain the decrease of the angular noise wave variance. when the radar is operating in jumping frequency.

$$Q = S_{rr}/S_{ra} = \frac{1}{\frac{1}{L_0/\lambda_{FA}} + \frac{1}{F_c/2f_c}} \quad (4.47)$$

In the formula, it was assumed that $(1-P_c) \approx 1$ because $\Delta f_A \gg \Delta f_c$ which is $P_c \ll 1$.

We know from formula (4.47) that this formula can be approximately written as

$$Q = \begin{cases} F_p/2B_s & (1) \text{ 当 } F_p/2f_s \ll L_o/\lambda_{FA} \\ L_o/\lambda_{FA} = \frac{\Delta f_A}{2\Delta f_s} & \text{ 当 } F_p/2f_s \gg L_o/\lambda_{FA} \end{cases} \quad (4.48)$$

(2)

Key: 1. When
2. When

In other words, decreasing factor Q is equal to the minimum of $F_p/2f_g$ or L_o/λ_{FA} . However, there are two limiting factors here: the ratio of half the pulse repetition frequency and the angular noise wave bandwidth; and the ratio of the target depth and jumping frequency band length. Because the pulse repetition frequency of common radar is far greater than the frequency spectrum width of the target's angular noise wave the latter factor is usually very small. That is, its decreasing factor is usually determined by the ratio of the target depth and jumping frequency wave length. The target's depth is determined by the target's measurements and the viewing angle opposite the radar. Therefore, the decrease of the angular noise wave variant is mainly determined by the jumping frequency wave length which is also the jumping frequency bandwidth, that is

$$Q \approx \Delta f_s \quad (4.49)$$

For example, it is assumed : angular noise wave bandwidth
 $f_g = 2.5 \text{ Hz}$
 pulse repetition frequency
 $F_p = 2,000 \text{ Hz}$
 target depth $L_o = 6\text{m}$
 jumping frequency bandwidth
 $\Delta f_A = 500 \text{ MHz}$
 jumping frequency wave length
 $\lambda_{FA} = 0.6\text{m}$

We can obtain from formula (4.48) the specific value of the first item $F_p/2 f_g = 400$ and the specific value of the second item $L_o/\lambda_{FA} = 10$. That is, the second item is relatively small and is also the determining factor. Therefore

$$Q \approx L_o/\lambda_{FA} = 10$$

The decrease of the angular noise wave's standard difference is \sqrt{Q} . In this case, it is about 3 fold.

None of the above analyses required that we precisely know the formula of the target noise wave. There is also another analytical method [8]. This method assumes that the target's noise wave is a Gaussian form. Its basis is if the target's movements are Gaussian form random yaw movements with a zero mean value we can then find that the target's noise wave frequency spectrum of the echoes of many actually encountered targets are close to the Gaussian form, that is

$$G(\omega) = G_0 \exp\left(-\frac{\omega^2}{\beta^2}\right) \quad (4.50)$$

Thus, its normalized autocorrelation function will possess the following form

$$\rho(\tau) = \exp(-\beta^2 \tau^2 / 4) \quad (4.51)$$

Theoretical research has shown that the statistical characteristics of a complex target's angular noise wave is very close to the statistical characteristics of the phase rate of change of narrow band Gaussian noise waves. The latter has already been thoroughly researched and its autocorrelation function is

$$R_0(\tau) = 1/2(\bar{\rho}/\rho - \bar{\rho}^2/\rho^2)\ln(1 - \rho^2) \quad (4.52)$$

In the formula, $\rho \equiv \rho(\tau)$.

When formula (4.51) is substituted in, we can obtain

$$R_0(\tau) = (\beta^2/4) \sum_{\eta=1}^{\infty} (1/\eta) \exp(-\eta\beta^2\tau^2/2) \quad (4.53)$$

Using the Fourier transformation we can find its power spectrum from the autocorrelation function. We know from the analysis that its power spectrum is in direct ratio to

$$\sum_{\eta=1}^{\infty} (1/\eta^{3/2}) \exp(-\omega^2/2\eta\beta^2)$$

The total sum of this progression in the zero frequency area is 2.612. This shows that the angular noise wave power spectrum is very strong in the zero frequency area when fixed frequency radar detects a complex target.

When the radar operates in frequency agility, the obtained echo frequency spectrum will be widened.

At first, we will not consider the sampling effects of the radar pulses but only study the simplest situation when these are two reflecting object targets. When the frequency changes Δf , the phase change will be

$$\Delta\phi = 2\pi\Delta f(2\Delta R/c) \quad (4.54)$$

In the formula, ΔR is the radial range difference of the two reflecting objects opposite the radar (see fig. 4.5), and c is the speed of light.

If the radar operates in pulsed random jumping frequency, that is, the rectangular equal probability distribution according to the width is Δf_A , then width B_a of its echo frequency spectrum is equal to

$$B_a = \Delta \phi_{\max} / 2\pi T, = 2\Delta f_A \frac{\Delta R}{cT}, \quad (4.55)$$

In simple target models with two reflecting objects, range difference ΔR is actually target depth L_0 . Thus, the above formula can also be written as

$$B_a = 2\Delta f_A \frac{L_0}{cT}, = \frac{\Delta f_A}{\Delta f_c} T, \quad (4.56)$$

In the formula, Δf_A is the critical frequency jump.

We know from the above formula that when the radar operates in frequency agility the bandwidth of the echo's frequency spectrum will widen. Its ratio with the angular noise wave bandwidth when there is fixed frequency is

$$\frac{B_a}{f_s} = \frac{\Delta f_A}{\Delta f_c} \cdot \frac{F_p}{f_g} = k \cdot \alpha \quad (4.57)$$

Most often, $\Delta f_A > \Delta f_c$ and $F_p > f_g$ and therefore $B_a / f_g \gg 1$.
or example, if we substitute the above example in, we can obtain the ratio of the two as 16,000.

In real conditions, it is necessary to consider the sampling effects of the radar pulses. This is because the sample in the radar receiver and the maintained repetition frequency (i.e., the radar's repetition frequency F_p) are smaller than the frequency spectrum bandwidth widened by the frequency agility. Therefore, frequency spectrum folding can occur during the sampling process. In correspondence to the sampling and maintaining $(\sin \pi f T_p / \pi f T_p)$ characteristics, its cut-off frequency will be F_p . At this time, the proportion of its frequency bandwidth is not determined from formula (4.57) but independently determined by F_p / f_g . In the above example, the specific value of $F_p = 2,000$ is between 10^2 and 10^3 .

For example, we can consider that the echo's frequency spectrum width after the radar operates in frequency agility is far greater than the frequency-spectrum width of the target's angular noise wave. This is because the mechanism of the bandwidth and narrow band frequency spectrum produced is completely independent and we can consider that these two exist simultaneously. Thus, when there is frequency agility the problem of estimating the value of the target's angular noise wave is summed up as the problem of estimating the value of the power spectrum of the narrow band signal phase rate when there is a wide band noise wave. It is also the problem of the narrow band signal's phase mean in the accompanying wide band noise wave. Other aspects of this problem have also been thoroughly studied. In this type of situation, the autocorrelation function is

$$R_s(\tau) = -\frac{1}{2} (\beta/\rho - \rho^2/\rho^2) \ln(1 - \rho^2/(1 + a^2)^2) \quad (4.58)$$

In the formula, a^2 is the narrow band's power ratio for the Gaussian random process. When we used it, $a^2 = 1$.

When formula (4.51) was substituted in, we obtained

$$R_{\phi}(\tau) = \beta^2/4 \sum_{\eta=1}^{\infty} (1/\eta 2^{2\eta}) \exp(-\eta \beta^2 \tau^2/2) \quad (4.59)$$

After Fourier transformation, we can find the corresponding phase rate power spectrum when in an accompanying wide band noise wave which is in direct ratio to

$$\sum_{\eta=1}^{\infty} (1/\eta^{3/2}) (1/2^{2\eta}) \exp(-\omega^2/2\eta\beta^2)$$

The zero frequency total of this progression is 0.276 and when compared to the value obtained above it is 1/9.46 (i.e. 9.76 decibels) of the former. This value can also be equivalent to the limiting value of the angular noise wave decrease caused by frequency agility.

By using the relational expression the angular noise wave's autocorrelation function and phase rate we can also derive the expression of the angular noise wave variance when there is frequency agility

$$\sigma_{\phi}^2 = (r_0^2/2) \sum_{\eta=1}^{\infty} 1/\eta 2^{2\eta} = 0.142 r_0^2 \quad (4.60)$$

or

$$\sigma_{\phi} = 0.376 r_0$$

In the formulas, r_0 is the transverse rotating radius of the radar's scattering particle concentration. This value is less than double the aforementioned angular noise wave variance when there is fixed frequency.

When the viewing angle of a twin jet engine aircraft in horizontal flight is near the nose or near the tail, r_0 is equal to one-half the jet engine interval. For the lateral side of a ship's hull, r_0 is about 0.15 times that of the ship's length.

As a result, the above conclusion is made for the following hypothesis. The echo's frequency spectrum width caused by frequency agility is far larger than the echo's frequency spectrum width caused by the target's movements.

When considering the limited bandwidth ratio, the phase rate of the narrow band process which found the mean autocorrelated function in the wide band range can be expressed by the following formula

$$R_0(\tau) = (-\beta^2/4) \ln(1 - \rho_0^2(\tau)) \quad (4.61)$$

In the formula

$$\begin{aligned} \rho_0^2(\tau) &= \{\exp(-\beta^2\tau^2/2)\} \\ &\times \{(\sigma^2 + \exp(-k\beta^2\tau^2/4))/(\sigma^2 + 1)\}^2 \quad (4.62) \\ k &= (\text{帶寬比})^2 - 1 \quad \sigma^2 = 1 \end{aligned}$$

Key: 1. (Bandwidth ratio)²-1

Because the power spectral density of the phase rate is the Fourier transformation of its autocorrelation function, under different k values, the relative amplitude of the zero frequency spectrum density can be found by means of the following integration

$$\int_0^{\infty} R_z(\tau) d\tau$$

The results of this integration calculating the different k values are shown in the following table:

(1)

k	0	10	10^2	10^3	10^4	10^5	∞
减小因子 Q (dB)	0	3.3	6.5	8.5	9.4	9.6	9.8

Table 4.2 Relationship Between the Mean Square of the Bandwidth Ratio and the Reduction Factor

Key: 1. Reduction factor Q (dB)

We can see from this table that when the bandwidth is 10^2 corresponding to $k \approx 10^4$ we can obtain a reduction factor close to the asymptotic value. Afterwards, the k value is again increased while the Q value is not so that it approaches a maximum value of 9.8 decibels.

The results of this analysis are quite dissimilar to the results of the former analysis. We can see from fig. 4.14 that when bandwidth ratio $\alpha = F_p / B_g$ tends towards ∞ , the reduction factor forms a direct ratio with ratio k of the agility bandwidth and critical frequency jumping. It is only necessary that the k value continually increase and the reduction factor Q also continually enlarge. This conclusion does not coincide with the real situation. Test results show that when the jumping frequency bandwidth gradually increases the reduction factor of the angular noise wave variance gradually approaches an asymptotic value equal to about 10 decibels.

To sum up the analysis of the effects of frequency agility on target noise waves carried out in this section, we can make the following conclusions:

(1) In fixed frequency, the spectral line bandwidth of the echo is mainly caused by the angular movement of the target. Its width is about several tenths to several hertz. When there is frequency agility, the spectral line of the echo is mainly determined by the decorrelation effect of the frequency agility. It is determined by the ratio of the agility bandwidth and the critical frequency. After considering the frequency spectrum folding caused by radar pulse sampling, they are mainly determined by the radar's repetition frequency.

(2) In a situation with frequency agility radar, the case will be that the frequency spectrum density of the target noise wave (including amplitude fluctuation and angular flickering) will decrease in the zero frequency area. Its reduction factor is determined by the ratio of the jumping frequency bandwidth and critical frequency difference as well as the ratio of the repetition frequency and target noise wave bandwidth. The larger these ratios the larger the reduction factor. Yet, it will finally reach a limit value of about 10 decibels.

(3) After the radar operates in frequency agility, the frequency spectrum of the echos amplitude fluctuations will be "wiped out" to outside the repetition frequency so that it will enlarge the fluctuation component in the conical scanning frequency area. Thus, it is possible that it will carry additional tracking errors for the conical tracking radar.

4.4 Increasing the Angular Tracking Precision of Radar With Frequency Agility

It can be concluded from the results of theoretical analysis that radar operating in frequency agility can reduce the frequency spectrum density of target noise waves in the zero frequency area. Thus, it can reduce the tracking errors of tracking radar. As a result, radar operating in frequency agility has a quantitative effect on the tracking errors of single pulse and conical scanning radar. This also requires further analysis and study.

The preceding analysis used the concept of critical frequency which considers that when the adjacent pulse's carrier frequency is larger than the critical frequency, the echo signals are completely uncorrelated. However, when less than the critical frequency they are completely correlated. Naturally, this is a rough assumption. From the test results of fig. 3.6 in the last chapter we can also see that the frequency's correlation coefficient is the function of the frequency difference. Therefore, to more precisely estimate the effects of frequency agility on the precision of radar angular tracking, it is also necessary to find the echo's frequency spectrum by taking the correlation coefficient as the parameter [10].

As mentioned previously, the frequency spectrum of the target noise wave can be approximated by the following formula

$$W(f) = \frac{1}{\pi f_c} \cdot \frac{f_c^2}{f^2 + f_c^2} \quad (4.63)$$

Because of the existence of target noise waves there is widening of the echo signal's spectral line (as shown in fig.4.15).

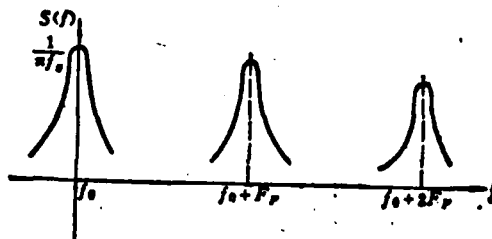


Fig. 4.15 Widening of the Echo's Spectral Line Caused by Target Noise Waves

When the transmitted carrier frequency is not considered but we only take the sampling of the pulse into account, the frequency spectrum of the echo signal can be written as

$$S(f) = \left[\frac{\sin(\pi\tau_p f)}{\pi\tau_p f} \right]^2 \sum_{n=-\infty}^{\infty} W(f - nF_p) \quad (4.64)$$

In the formula, τ_p is the pulse width and F_p is the repetition frequency.

When the radar operates in frequency agility, the radio power spectrum of each echo signal received is different because the carrier frequencies of each pulse are different. If we can calculate the correlation coefficient in the adjacent pulses we can then find the echo signal's frequency spectrum at this time from formula (4.13).

The correlation coefficient ρ_{ij} between the i pulse and j pulse is given by the following formula

$$\rho_{11} = \iint \rho_{11}(f_1, f_1) P(f_1, f_1) df_1 df_1 \quad (4.65)$$

In the formula, $P(f_i, f_j)$ is the probability density function of f_i and f_j , and in most situations we can consider that $P(f_q, f_{q+n}) = P(f_r, f_{r+n})$ (in the formula, $r \neq q$). At this time, formula (4.65) can be written as

$$\rho_n = \iint \rho_n(f_1, f_{1+n}) P(f_1, f_{1+n}) df_1 df_{1+n} \quad (4.66)$$

To calculate the ρ_n value, we must first know the value of $P(f_i, f_{i+n})$. Moreover, $P(f_i, f_{i+n})$ is related to the jumping frequency pattern. If we use random jumping frequency, we can then consider that the frequencies of any two pulses are independent. Therefore, we set up the following formula

$$P(f_1, f_{1+n}) = P(f_1) P(f_{1+n}) \quad (4.67)$$

If the transmitted carrier frequency has equal probability random jumping in the Δf_A range, its probability density function is

$$P(f) = \frac{1}{\Delta f_A} \quad (4.68)$$

It can be proven [11] that the correlation coefficient at this time can be given by the following formula

$$\rho_n = \frac{2}{z} \left\{ \text{Si}(z) + \frac{1}{z} (\cos(z) - 1) \right\} \quad (4.69)$$

In the formula

$$z = 2\pi L_0 \Delta f_A / C = \pi \Delta f_A / \Delta f_0 \quad (4.70)$$

Moreover,

$$\text{Si}(z) = \int_0^z \sin \frac{y}{y} dy \quad (4.71)$$

In the formula

$$y = 2\pi L_0 (f_i - f_{i+n}) / C = \pi (f_i - f_{i+n}) / \Delta f_0 \quad (4.72)$$

Therefore, it is only necessary to know critical frequency difference Δf_c , the carrier frequencies of the two pulses $(f_i - f_{i+n})$ and jumping frequency range Δf_A to be able to calculate correlation coefficient ρ_n . Naturally, when $n=0$, $\rho_n=1$.

If we let $\rho_s(t)$ be the autocorrelation function of the target noise wave itself, then

$$\rho_s(t) = 2 \int_0^\infty W(f) \cos \omega t df \quad (4.73)$$

In this way, when the radar operates in frequency agility, the autocorrelation function of an infinite series of pulses can be written as

$$R_s(t) = \rho_s(t) \left[\sum_{n=-\infty}^{\infty} \rho_n \left(1 - \frac{|t - nT_p|}{\tau_p} \right) \times \text{rect} \left(\frac{t - nT_p}{2\tau_p} \right) \right] \quad (4.74)$$

In the formula

$$\text{rect}(t) = \begin{cases} 1 & \text{当 } |t| \leq \frac{1}{2} \\ 0 & \text{当 } |t| > \frac{1}{2} \end{cases}$$

Key: 1. When

2. When

We can see from formula (4.74) that the existence of ρ_n causes the $R_s(t)$ to decrease even faster than when there is fixed frequency. This signifies the widening of the spectral line. It is only necessary to know the ρ_n value to be able to calculate $R_s(t)$.

Formula (4.74) can also be written as

$$\begin{aligned} R_s(t) &= \rho_s(t) \left\{ \left(1 - \frac{|t|}{\tau} \right) \text{rect} \left(\frac{t}{2\tau} \right) \right. \\ &\quad \left. + \rho_n \sum_{\substack{n=-\infty \\ n \neq 0}}^{\infty} \left(1 - \frac{|t - nT_p|}{\tau_p} \right) \text{rect} \left(\frac{t - nT_p}{2\tau_p} \right) \right\} \\ &= \rho_s(t) \left\{ (1 - \rho_n) \left(1 - \frac{|t|}{\tau_p} \right) \text{rect} \left(\frac{t}{2\tau_p} \right) \right. \\ &\quad \left. + \rho_n \sum_{n=-\infty}^{\infty} \left(1 - \frac{|t - nT_p|}{\tau_p} \right) \text{rect} \left(\frac{t - nT_p}{2\tau_p} \right) \right\} \quad (4.75) \end{aligned}$$

Usually, the transmitted pulse width is much smaller than the target's correlation time. Because of this, we can assume that $\rho_s(\tau_p)=1$ and still does not lose its generality. Therefore, formula (4.75) can be written as

$$\begin{aligned} R_s(t) = & (1 - \rho_n) \left[1 - \frac{|t|}{\tau_p} \right] \text{rect} \left(\frac{t}{2\tau_p} \right) \\ & + \rho_n \rho_s(t) \sum_{n=-\infty}^{\infty} \left(1 - \frac{|t - nT_p|}{\tau_p} \right) \text{rect} \left(\frac{t - nT_p}{2\tau_p} \right) \end{aligned} \quad (4.76)$$

By using formula (4.13) we can find the echo signal's frequency spectrum when there is frequency agility.

$$\begin{aligned} S(f) = & (1 - \rho_n) \left[\frac{\sin(\pi f \tau_p)}{\pi f \tau_p} \right]^2 + \rho_n \left[\frac{\sin(\pi \tau_p f)}{\pi \tau_p f} \right]^2 \\ & \times \sum_{n=-\infty}^{\infty} W(f + nF_p) \end{aligned} \quad (4.77)$$

The above formula shows that after the radar operates in frequency agility, the echo signal's frequency spectrum can be divided into two items. One item is identical to when there was the original fixed frequency yet reduced a factor ρ_n . The other item is a wide band item (not related to n). Its schematic is shown in fig. 4.16.

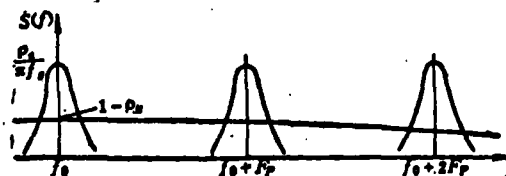


Fig. 4.16

Fig. 4.16 Schematic of Echo Signal's Frequency Spectrum
When the Radar Operates in Frequency Agility

When we compare these results with the results obtained in section 4.3.3, (Fig. 4.10) we can discover that the correlation coefficient ρ_n was used to replace probability P_c which is smaller than the critical frequency.

In single pulse radar, the signal frequency spectrum of the summation and differential channels have similar forms. Therefore, the output signal's frequency spectrum of the phase-sensitive detector is given by the convolution of the intermediate-frequency spectrum and itself. This is similar to being in the square-law detector.

The output terminal's autocorrelation function of the square-law detector is

$$R_s(t) = kR_i^2(t) \quad (4.78)$$

In this formula, $R_s(t)$ is derived from formula (4.76).

After calculations, we can find the output terminal's signal frequency spectrum of the square-law detector

$$S_s(f) = k_1 \left[\rho_s^2 \frac{F_p}{\pi f_s} \sum_{n=-\infty}^{\infty} \frac{f_s^2}{f_s^2 + (f - nF_s)^2} \times \frac{2\pi n F_s \tau_p - \sin(2\pi n F_s \tau_p)}{2\pi n F_s \tau_p} + (1 - \rho_s^2) \frac{2\pi f \tau_p - \sin(2\pi f \tau_p)}{(2\pi f \tau_p)^2} \right] \quad (4.79)$$

In the formula, f_g is the frequency spectrum width of the target noise wave.

Because the servo system and automatic gain control filter are low general models we are only interested in the frequency spectrum near zero frequency. The section is called $S'_e(f)$ and is given by the following formula

$$S'_e(f) = k_1 \left\{ \rho_2^2 \frac{\alpha}{\pi} \cdot \frac{f_g^2}{f_g^2 + f^2} + (1 - \rho_2^2) \right\} \quad (4.80)$$

In the formula, $\alpha = F_p / f_g$.

It is now necessary to study the angle errors produced by this signal frequency spectrum added to the automatic gain control system and the servo system.

We know from formula (4.9) that the frequency spectrum of the errors caused by the target's echo fluctuation is

$$W_e(f) = S'_e(f) |Y_e(f)|^2 \epsilon_0^2 \quad (4.81)$$

When $W_n(f)$ is integrated from $-\infty$ to $+\infty$ and we take the mean square root of this value, we can obtain the value of angle tracking error σ_s

$$\sigma_s = \epsilon_0 \left\{ k_1 \rho_2^2 \frac{\alpha}{\pi} \int_{-\infty}^{+\infty} \frac{f_g^2}{f_g^2 + f^2} |Y_e(f)|^2 df + k_1 (1 - \rho_2^2) \int_{-\infty}^{+\infty} |Y_e(f)|^2 df \right\}^{1/2} \quad (4.82)$$

When the radar operates in fixed frequency, the error of ($\rho_n = 1$) is

$$\sigma_{\epsilon} = \epsilon_0 \left\{ k_1 \frac{\alpha}{\pi} \int_{-\infty}^{+\infty} \frac{f^2}{f_s^2 + f^2} |Y_s(f)|^2 df \right\}^{1/2} \quad (4.83)$$

When this formula is substituted into formula (4.60), we can obtain

$$\sigma_{\epsilon} = \sigma_s \left\{ \rho_s^2 + \frac{\pi(1-\rho_s^2)}{\alpha\sigma_s} B_n |Y_s(0)|^2 \right\}^{1/2} \quad (4.84)$$

In the formula, B_n is the noise wave bandwidth of the servo system.

In this way, we can eliminate the $\epsilon_0 \cdot k_2$ factor and as a result can obtain relative improvement when there is jumping frequency.

Although the above analysis had angle errors caused by echo amplitude fluctuation, the frequency spectrum of angular noise waves is similar to the frequency spectrum of amplitude scintillations. Therefore, the σ_a errors caused by angular noise waves when there is no automatic gain control system can still be expressed by formula (4.62). It is only necessary to replace the $|Y_s(0)|^2$ in the formula with $|Y_c(0)|^2$ (because when there is no automatic gain control system, the Y_s in formula (4.7) changes to Y_c).

The calculation of the angular noise wave error σ_{a1} when there is a fast speed automatic gain control system (single pulse radar commonly possesses it) is very complex. Thus, it is possible to use one for approximation. It has been discovered that because there is correlation between the target's amplitude

and the angle error, the existence of a fast speed automatic gain control system can cause the σ_{a1} to double. Therefore we can still use formula (4.84), only it is necessary to multiply the coefficient by 2.

It must be pointed out that aside from the above mentioned two types of errors in conical scanning radar there is another type of error. This is an additional error caused by the high frequency component of the echo's amplitude fluctuation (in the vicinity of the conical scanning frequency). As mentioned previously, this error can be expressed by formula (4.6) and can be transformed to be written as

$$\sigma_a^2 = 0.458 S'_e(f_s) B_s \quad (4.85)$$

We can obtain frequency spectrum density $S'_e(f_s)$ in the vicinity of conical scanning frequency f_s from formula (2.49) when there is jumping frequency

$$S'_e(f_s) = k_s \left[\frac{\alpha}{\pi} \rho_n^2 \frac{f_s^2}{f_s^2 + f_j^2} + (1 - \rho_n^2) \right] \quad (4.86)$$

Moreover, when there is fixed frequency, letting $\rho_n = 1$ in formula (4.55), we can obtain the energy spectrum density

$$S'_e(f_s) = k_s \frac{\alpha}{\pi} \cdot \frac{f_s^2}{f_s^2 + f_j^2} \quad (4.87)$$

When formula (4.86) and (4.87) are substituted into formula (4.85) we can obtain the expression of this error σ_{a1} when there is frequency agility

$$\sigma_{\theta 1} = \sigma_{\theta} \left[\rho_n^2 + \frac{\pi}{\alpha} (1 - \rho_n^2) \frac{f_s^2 + f_j^2}{f_s^2} \right]^{1/2} \quad (4.88)$$

When the jumping frequency bandwidth is sufficiently wide, the ρ_n value is very small, the ρ_n^2 item can be overlooked and usually $B_g/f_s \ll 1$. At this time, formula (4.88) can be simplified into

$$\sigma_{\theta 1} \approx \sigma_{\theta} \frac{f_s}{f_j} \sqrt{\frac{\pi}{\alpha} (1 - \rho_n^2)} = \sigma_{\theta} \frac{f_s}{f_s F_s} \sqrt{\pi (1 - \rho_n^2)} \quad (4.89)$$

We know from formula (4.89) that it is only necessary when

$$f_j > \frac{f_s F_s}{\pi}$$

that the jumping frequency type conical scanning radar's additional error be larger than the error of the fixed frequency radar.

In this way, we are still unable to conclude whether or not the use of jumping frequency for conical scanning radar improves angle tracking precision. It is also necessary to determine this by the specific radar parameters and target characteristics.

In summing up the above analysis we can draw the following conclusions:

(1) As regards single pulse radar (with fast speed automatic gain control), when there is jumping frequency, the angle tracking errors caused by the echo's amplitude fluctuation changes as shown in formula (4.84). When bias error ϵ_0 is zero,

this error does not exist.

When there is jumping frequency, the angle tracking errors caused by angular noise waves change to

$$\sigma_{\theta_1} = 2\sigma_{\theta_2} \left\{ \rho_{\theta_2}^2 + \frac{\pi(1-\rho_{\theta_2}^2)}{2\sigma_{\theta_2}} B_{\theta_2} |Y_c(0)|^2 \right\}^{1/2} \quad (4.90)$$

When in a non-automatic gain control system, we then remove coefficient 2 and substitute $Y_c(0)$ into $Y_s(0)$.

(2) As regards conical scanning radar, aside from the above two angle tracking errors there is also an error caused by the high frequency component of the echo's amplitude fluctuation. This error occurs when in jumping frequency as shown in formula (4.89).

In order to be able to quantitatively estimate the raising of pulse radar and conical scanning radar angle tracking precision by frequency agility it is also necessary to analyze concrete examples.

Assuming the servo bandwidth of a certain automatic tracking radar system is 5 hertz, the bandwidth of its fast speed automatic gain control system is 90 hertz (used for single pulse) and the bandwidth of its slow speed automatic gain control system (used for conical scanning) is 15 hertz. The characteristics of its $Y_s^2(f)$ are shown in fig. 4.17.

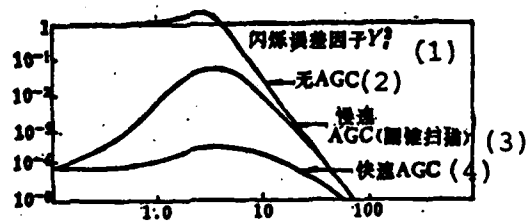


Fig. 4.17 Characteristics of Assumed Radar Angle Tracking System

- Key: 1. Scintillation error factor Y_s^2
 2. Without AGC
 3. Slow speed AGC (conical scanning)
 4. Fast speed AGC

At the same time, assuming the target noise wave's frequency spectrum width f_g is also 5 hertz, then by using graphic integration we can obtain the angle error caused by the target echo's amplitude fluctuation.

When in a system without AGC, it is

$$\sigma_{\theta_1}^2 = \sigma_{\theta}^2 \left[\rho_s^2 + \frac{5.4}{\alpha} (1 - \rho_s^2) \right] \quad (4.91)$$

When in a slow speed automatic gain control system (conical scanning radar), it is

$$\sigma_{\theta_1}^2 = \sigma_{\theta}^2 \left[\rho_s^2 + \frac{6}{\alpha} (1 - \rho_s^2) \right] \quad (4.92)$$

When in a fast speed automatic gain control system (single pulse radar), it is

$$\sigma_{f,1}^2 = \sigma_f^2 \left[\rho_n^2 + \frac{8.8}{\alpha} (1 - \rho_n^2) \right] \quad (4.93)$$

Letting D represent the decrease of the tracking error after jumping frequency, then

$$D = \frac{\sigma_{f,1}^2}{\sigma_f^2} \quad (4.94)$$

We know from formulas (4.91), (4.92) and (4.93) that D is the function of ρ_n and α . We can draw the relational curve of D and ρ_n for different α values. We know from the definition that $\alpha = F_p / f_g$ and now take $\alpha = 50, 100$ and 200 . If $f_g = 5$ hertz then $F_p = 250$ hertz, 500 hertz and $1,000$ hertz. Figures 4.18, 4.19 and 4.20 correspond to the curves obtained from the three different automatic gain control systems above.

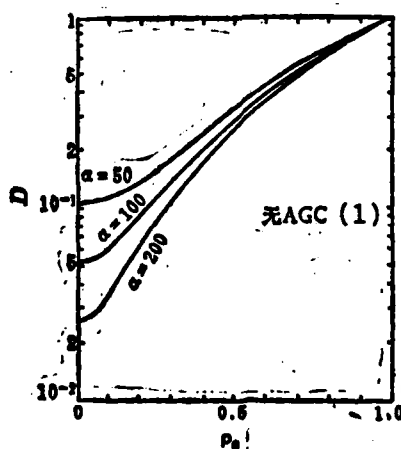


Fig. 4.18 The Decrease of Angle Errors By Jumping Frequency Radar When There is No Automatic Gain Control System

Key: 1. Without AGC

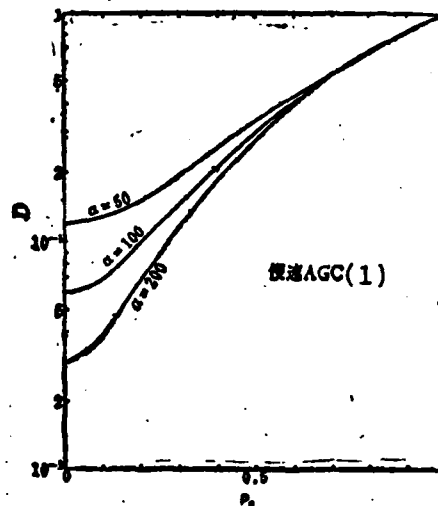


Fig. 4.19 The Decrease of Angle Errors By Jumping Frequency Radar When There is a Slow Speed Automatic Gain Control System

Key: 1. Slow speed AGC

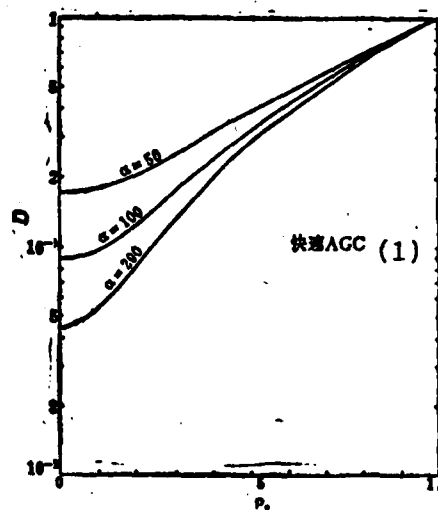


Fig. 4.20 The Decrease of Angle Errors By Jumping Frequency Radar When There is a Fast Speed Automatic Gain Control

Key: 1. Fast speed AGC

We can see from these figures that there is not a great difference between these three situations. Moreover, when $\rho_n = 0$ (i.e., when the adjacent echoes are completely (uncorrelated), D has a limit value D_{\min} . This D_{\min} value forms an inverse ratio with the value of a . In other words, to as best as possible decrease the errors caused by the echo's amplitude fluctuation, the larger the value of a (i.e. pulse repetition frequency) the better.

However, the above discussion only focused on the angle errors caused by the echo's amplitude fluctuation. This type of error is non-existent when bias error ϵ_0 is zero.

The errors caused by angular noise waves can also be determined by formula (4.69). If $\rho_n = 0.1$ and $a = 50$, then the angular noise wave errors after using jumping frequency can also decrease 2.9 times. If bias error ϵ_0 is zero, there will not be any errors caused by amplitude fluctuation. The total angle-measuring errors of a single pulse radar will be determined by the angular noise wave servo system noise wave and receiver noise wave. Aside from the servo system noise waves among the three types of errors, the other two are functions of the operating range. Therefore, we can draw a figure similar to that of fig. 4.1 (see fig. 4.21).

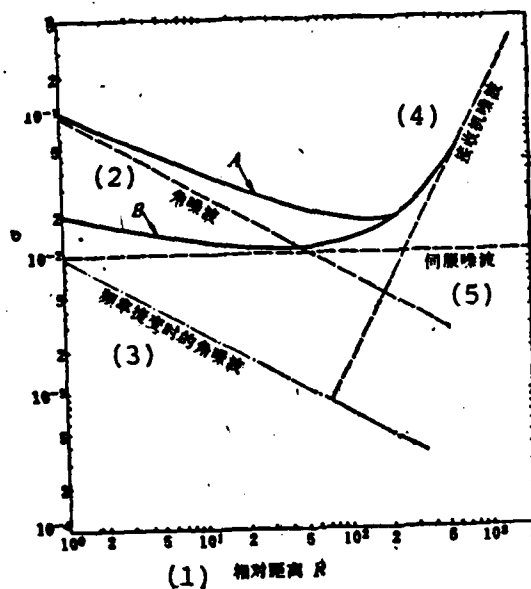


Fig. 4.21 The Relationship of the Single Pulse Radar's Total Angle Error's Relative Range When the Bias Error is Zero

A - Fixed frequency single pulse;
B - Jumping frequency single pulse.

Key: 1. Relative range R
2. Angular noise wave
3. Angular noise wave when there is frequency agility
4. Receiver noise wave
5. Servo noise wave

Curve A in the figure is the total angle error curve of fixed frequency single pulse radar. Assuming bias error ϵ_0 is zero, we can see from the figure that at close range use of jumping frequency can greatly decrease the errors caused by angular noise waves. This is identical to the prediction at the beginning.

To estimate the decrease of conical scanning radar angle tracking precision errors by jumping frequency, $f_s/f_g=6$, then

from formula (4.89) we can obtain

(1) 当 $\alpha = 50$	$\sigma_{a1} = 1.5\sigma_a$
$\alpha = 100$	$\sigma_{a1} = 1.06\sigma_a$
$\alpha = 200$	$\sigma_{a1} = 0.75\sigma_a$

Key: 1. When

When $\alpha=50$, use of jumping frequency can increase the errors caused by amplitude fluctuation. When $\alpha=100$, there is almost no change.

To attain a quantitative concept, use of parameters similar to those of the above example can obtain $\alpha=50$. See fig. 4.22 for the relationship of the conical scanning radar's total angle error and range.

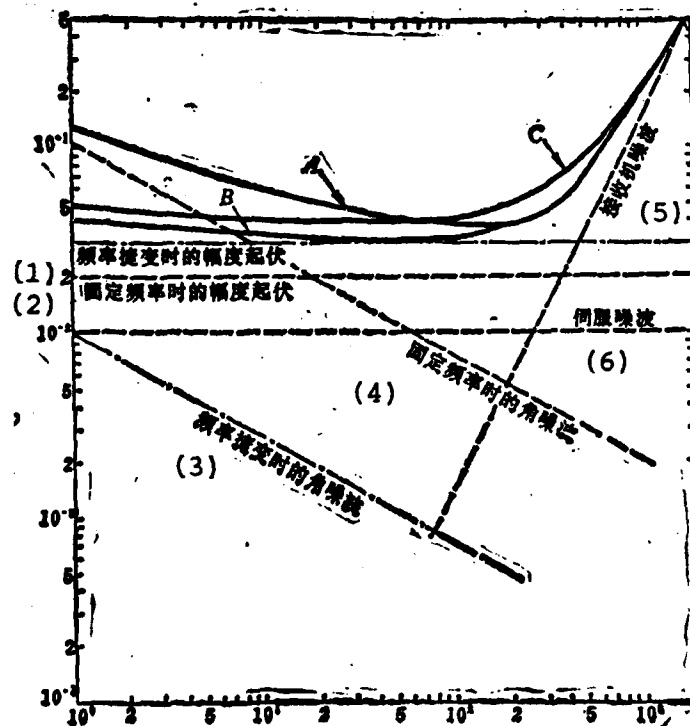


Fig. 4.22

Fig. 4.22 The Effects of Jumping Frequency on Conical Scanning Radar's Angle-Measuring Precision

A - Fixed frequency; B-Jumping frequency, $\alpha = 100$;
C - Jumping frequency, $\alpha = 50$

- Key: 1. Amplitude fluctuation when there is frequency agility
2. Amplitude fluctuation when there is fixed frequency
3. Angular noise wave when there is frequency agility
4. Angular noise wave when there is fixed frequency
5. Receiver noise wave
6. Servo noise wave

It can be seen from the figure that when a relatively high pulse repetition frequency ($\alpha = F_p / f_g = 100$) is used, jumping frequency type conical scanning radar will have a definite improvement over fixed frequency radar (because of the lowering of the angular noise wave). However, if the pulse repetition frequency is exceedingly low ($\alpha = 50$), then the angle-measuring errors in the intermediate and far range will be greater than those of fixed frequency.

4.5 Test Results Raising the Angle Tracking Precision of Conical Scanning Radar With Frequency Agility

Early, in 1964, some people used a conical scanning radar which could operate in frequency agility and fixed frequency to carry out check flight tests on a small jet aircraft [12]. The target had constant velocity rectilinear flight and its shortest navigational path was 1 kilometer from the radar station.

During the check flight, the error voltage obtained from the demodulation circuit area of the range and angle (including position and angle of elevation) tracking loop was recorded. Its waveform is shown in fig. 4.23.

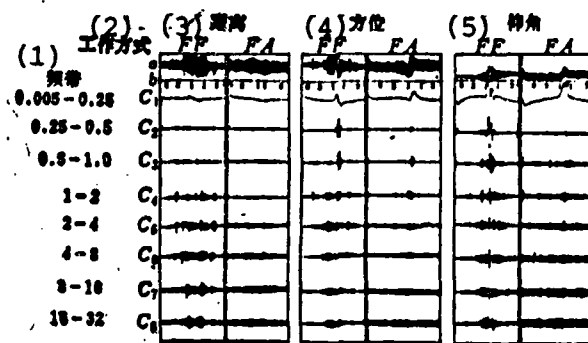


Fig. 4.23 The Decrease of the Tracking Errors of Conical Scanning Radar by Frequency Agility

Key: 1. Frequency band
2. Operating mode
3. Range
4. Position
5. Angle of elevation

The recording in the figure began in the target's 6 kilometer area away from the radar (at this time, the target was flying toward the radar station) and after passing the closest point (1 kilometer) finished in the 4 kilometer area (the target from the radar station). The FF in the figure is the fixed frequency's operating mode and FA is the frequency agility's operating mode. Curve A is the unfiltered original recording and below it is range graduation b expressed in kilometers. To analyze the effects of frequency agility on the error signal frequency spectrum, analysis is carried out on the results obtained by means of the filter. Beginning from 0.005-0.25 hertz, one filter is later arranged for each octave up to 32 hertz. The output waveform of each filter is arranged from C_1 to C_8 .

We can see from the figure that use of frequency agility noticeably reduced the errors of the low frequency area (up to the 2-4 hertz area). This is true of both the range and angle yet in the angle in the close range area this is even more obvious. Because the servo system itself has a certain bandwidth limitation it is often below 4-8 hertz. Therefore, the improvement of the frequency agility on angle tracking errors is very noticeable.

Tests were also carried out on sea targets. The targets were two cargo ships with different tonnage and their range was about 10 kilometers. At this time, a 16 mm camera was fixed on the gun directing radar antenna's sighting telescope and the time of each recording was about 1 minute. Afterwards, analysis of each picture was carried out and the azimuths of the target on the pictures were marked in milliradian. Its results are shown in fig. 4.24. The figure draws the distribution of the azimuth angle errors using 0.5 milliradian on the interval. At the same time, for comparison, the actual form of the observed targets were drawn.

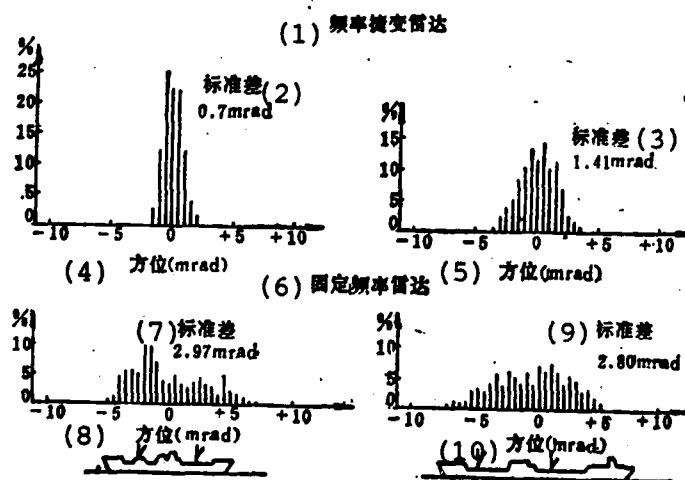


Fig. 4.24

Fig. 4.24 Raising of the Angle Tracking Precision With Frequency Agility for Tracking Sea Target Azimuths

- Key: 1. Frequency agility radar
2. Standard difference
3. Standard difference
4. Azimuth
5. Azimuth
6. Fixed frequency radar
7. Standard difference
8. Azimuth
9. Standard difference
10. Azimuth

It can be seen from the figure that frequency agility noticeably reduced the azimuth angle error. There was a four fold decrease for small targets and two fold decrease for large targets.

These test results can also be compared to the previous analytical analysis. An angular noise wave standard difference of $0.376r_0$ can be obtained from formula (4.60) when in frequency agility. For ships, $r_0 = 0.15L_0$, L_0 being the projection of the hull's length. Therefore the angular noise wave standard difference of the ship target is $0.056L_0$.

In the above example, the field angles of the two ships are 10 milliradian and 15 milliradian. The standard differences of the angular noise waves can be obtained from the above formulas as 0.56 and 0.84 milliradian. The measured standard differences were 0.7 and 1.41 milliradian which are a little larger than the theoretical values. This is possibly the increase of the component in the conical scanning frequency f_s area after the radar operates in frequency agility. This is also a reason for the increase of tracking errors.

4.6 Raising the Angle-Measuring Precision With Step Jumping Frequency Type Single Pulse Tracking Radar

As mentioned previously, frequency agility is mainly used to reduce angular noise waves. This is the principal origin of close range tracking errors by single pulse tracking radar. Therefore, the frequency agility technique has been widely used in homing radar used for proportion guidance on guided missiles.

We will now take a look at single pulse homing guidance radar [13]. The operating frequency range of this radar is 9.2-9.92 kilomegahertz and it can continuously transmit 9 carrier frequencies to produce step jumping pulses (see fig. 4.25).

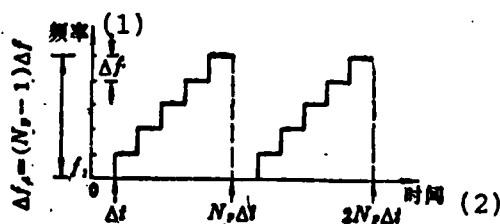


Fig. 4.25 Step Jumping Frequency Signals

Key: 1. Frequency
2. Time

The interval of each of its frequency jumps can be regulated in the 8-80 megahertz range. It can also form and transmit one frequency pulse. Its forming time can be regulated to within 25 microseconds to 51.2 milliseconds (1-2,048 pulses), its transmitting pulse width is 0.15 microseconds and its pulse repetition frequency is 40 kilomegahertz. The radar antenna is a four horn feed parabolic antenna, the beam width is 5° , the gain is 32 decibels, transmitter's peak power is 1 kilowatt, the mean power is 6 watts, the receiver intermediate frequency is 60 MW, and intermediate frequency bandwidth is 25 MW.

To be able to measure the angular noise wave when the radar operates in single frequency and jumping frequency, we used the radar beacon method when carrying out field tests. After a certain delay time (0.5 microseconds), this beacon can transmit relatively strong answering signals. The radar can simultaneously receive skin echo signals and beacon answering signals. Because there is a certain delay time, it can separately measure the angle positions of the skin echoes viewed in the center and the beacon answering signals. Use of the beacon's angle error signals to control the antenna servo system can cause the antenna to be able to accurately track the position of the beacon. Further, the angle difference data between the beacon and skin echo are sent to the data processing system wherein we obtain angular noise wave data. Fig. 4.26 shows the block diagram of the entire test system.

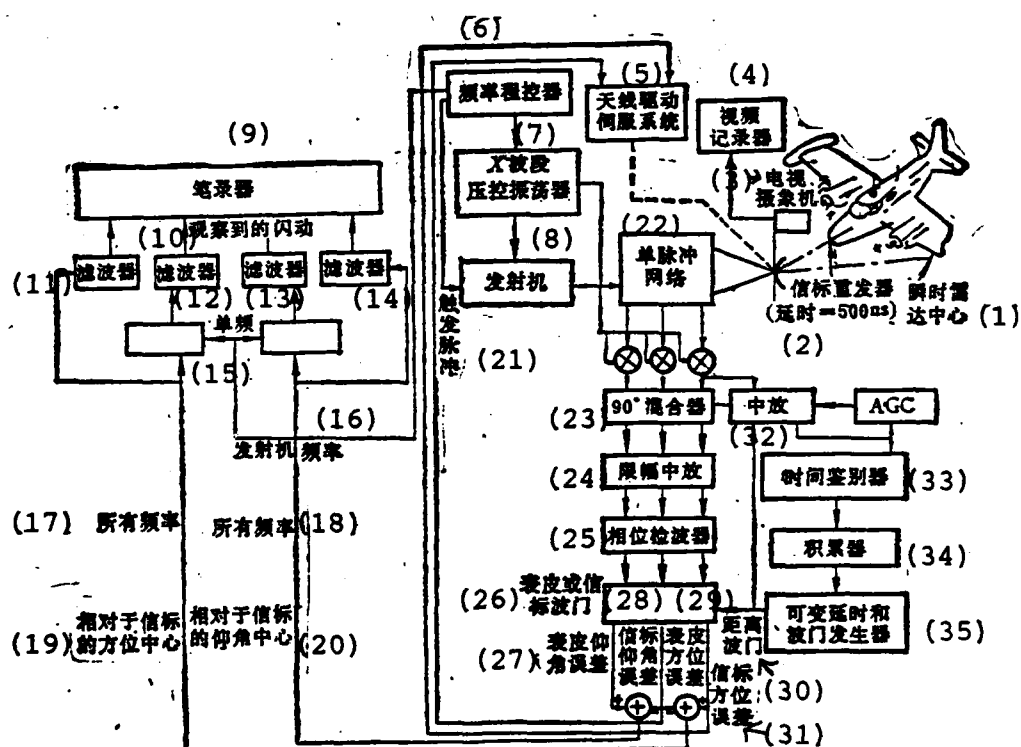


Fig. 4.26

Fig. 4.26 Block Diagram of a Target Angle Flickering Test System For a Step Jumping Frequency Single Pulse Tracking Radar

- Key:
1. Transient radar center
 2. Beacon repeater (delay time=500ns)
 3. Television camera
 4. Video recorder
 5. Antenna drive servo system
 6. Frequency range controller
 7. X wave band pressure control oscillator
 8. Transmitter
 9. Pen recorder
 10. Observed flicker
 11. Filter
 12. Filter
 13. Filter
 14. Filter
 15. Single frequency
 16. Transmitter frequency
 17. All frequencies
 18. All frequencies
 19. Azimuth center opposite the beacon
 20. Angle of the elevator center opposite the beacon
 21. Trigger pulse
 22. Single pulse network
 23. 90° mixer
 24. Limited intermediate amplification
 25. Phase detector
 26. Skin or beacon gate
 27. Skin angle of elevation error
 28. Beacon angle of elevation error
 29. Skin azimuth error
 30. Range gate
 31. Beacon azimuth error
 32. Intermediate amplification
 33. Time discriminator
 34. Accumulator
 35. Changeable delay and gate generator

Tests were done on three different types of targets. Firstly, tests were carried out on double reflecting targets. This type of simplified target is not only worthy of theoretical study but also has certain practical significance. For example, when the radar tracks a target flying low over the sea, the reflections

of the target echo and from the sea surface are the same as double reflecting targets. The difference lies in that it is hoped at this time that it does not track the middle point of the two reflecting objects but that it reflects a relatively strong signal of one (i.e., the real target).

The angle flicker of double reflecting objects is not a random process but is actually totally defined. We know from theoretical analysis that after using frequency agility the reduction factor (see formula (4.10)) of the angular noise wave's standard difference is

$$\sqrt{Q} = \frac{1+a}{1-a} \quad 0 < a < 1 \quad (4.95)$$

In the formula, a is the amplitude ratio of the two reflection signals.

Yet, at this time, its frequency agility bandwidth must be larger than the critical frequency jumping. The measurement results are shown in fig. 4.27.

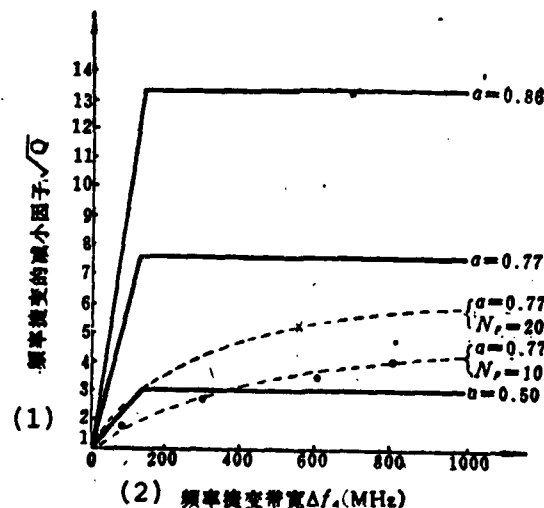


Fig. 4.27

Fig. 4.27 Theoretical and Test Values of the Reduction Factors For Double Reflecting Target Models

The solid lines are theoretical values; the broken lines are test values; the target's range depth = 4 feet; the critical frequency = 125 MHz.

Key: 1. Reduction factor \sqrt{Q} of frequency agility
2. Frequency agility's bandwidth Δf_A (MGz)

We know from the figure that when the total frequency diversity bandwidth is the same, the greater the different frequency number N_F , the greater the improvement factor and the closer it is to the theoretical value. When N_F is 10, it is about 40% of the theoretical value, and when N_F is 20 it is about 60% of the theoretical value. Moreover, very wide bandwidths do not have greater benefits.

Secondly, tests were carried out on aircraft targets. To compare the test and theoretical results, we used the concept of equivalent independent sampling number N_e . That is, after detection, the variance of the accumulated angular noise waves was reduced N_e times as compared to before accumulation.

When the radar operates in fixed frequency, its equivalent independent sampling N_{e1} is only influenced by the time decorrelation. We know from analysis [14] (see chapter V for its proof) that the value of N_{e1} is determined by the following formula

$$N_{e1} = \frac{N}{\left[1 + 2 \sum_{j=1}^{N-1} \frac{N-j}{N} \rho_t(j) \right]} \quad (4.96)$$

In the formula, N is the pulse number and $\rho_t(j)$ is the time correlation coefficient. When $\rho_t(j)=0$, $N_{e1}=N$; when $\rho_t(j)=1$, and when $N \rightarrow \infty$, $N_{e1} \rightarrow 1$.

When the radar operates in frequency agility, the value of its equivalent independent sampling number N_{e2} is not only determined by the time decorrelation but also by the frequency decorrelation.

$$N_{e2} = \frac{N}{\left[1 + 2 \sum_{j=1}^{N-1} \frac{N-j}{N} \rho_f(j) \rho_f(j) \right]} \quad (4.97)$$

In the formula, $\rho_f(j)$ is the frequency correlation coefficient.

After using frequency agility, we can approximately consider that the ratio of the angular flickering (angular noise wave) variance of the receiver's output and variance when (there is) single frequency operation forms an inverse ratio with the equivalent independent sampling numbers in the two types of situations. Further, its reduction factor Q is determined by the following formula

$$Q = \frac{1 + 2 \sum_{j=1}^{N-1} \frac{N-j}{N} \rho_f(j)}{1 + 2 \sum_{j=1}^{N-1} \frac{N-j}{N} \rho_f(j) \rho_f(j)} \quad (4.98)$$

The largest improvement occurred when decorrelation time τ_c with single frequency operation was far greater than repetition period T_p , that is, $\tau_c \gg T_p$. At this time, we can consider that $\rho_t(j) = 1$ and $N_{e1} \approx 1$. Thus

$$Q \approx N_{e2}, \text{ when } \tau_c \gg T_p \quad (4.99)$$

Assuming that each frequency difference of the step jumping frequency is larger than the critical frequency jumping, we can consider that the adjacent pulses are totally decorrelated, that

is, $\rho_f(j) \approx 0$. At this time, the reduction factor is equal to the equivalent independent sampling number when there is jumping frequency and is also equal to the frequency number N_F (see formula (4.23)).

The small single engine Piper Comanche aircraft was used for carrying out tests on aircraft targets. Its wingspan is 11 meters and its length is 7.6 meters. Assuming this target's depth L_0 is 7.5 meters, we can then calculate its critical frequency jump as 20 megahertz. Fig. 4.28 compares the test and theoretical values of the angle flicker reduction factors. During the tests, frequency number $N_F=9$ was used. For the first point, $\Delta f=8$ megahertz (smaller than the critical frequency jump) and the total jumping frequency bandwidth is 64 megahertz; for the second point, $\Delta f=80$ megahertz ($> \Delta f_c$) and the total jumping frequency bandwidth is 640 megahertz. We can see from the figure that when it is larger than the critical frequency jump, reduction factor Q 's root extraction is equal to 3.1, very close to the theoretical value.

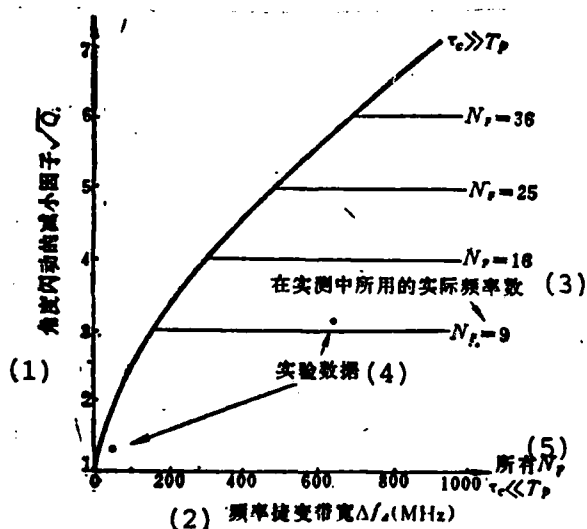


Fig. 4.28

Fig. 4.28 Comparison of the Test and Theoretical Values of the Angle Flicker Reduction Factors For a Small Single Engine Aircraft

- Key: 1. Reduction factor \sqrt{Q} of angle flicker
 2. Frequency agility bandwidth Δf_A (MHz)
 3. The actual frequency number used in testing
 4. Test data
 5. All of the N_F

Tests were carried out on small ship targets in the third type of situation. The background of the small ship targets was sea clutter waves. The existence of this type of clutter can enlarge the angular noise wave output behind the receiver accumulator. Because the additional angular noise waves caused by the sea clutter and the angular noise waves of the target itself are statistically independent, we can therefore consider that the final total variance of the angle error in the accumulator's output is equal to the sum of the variance caused by the target flickers and the variance caused by clutter.

The variance caused by clutter is related to the signal-noise power ratio $(S/C)_0$ [14] in the accumulator's output terminal,

$$\sigma_e^2 = 0.25 \theta_0^2 / (S/C)_0 \quad (4.100)$$

In the formula, θ_0 is the single path half power point noise width of tracking radar. The signal-noise ratio in the accumulator's output terminal is equal to N_e times the signal-noise ratio of its input terminal (see section 5.5 in chapter V),

$$(S/C)_e = N_e (S/C)_i \quad (4.101)$$

Because the actions of the frequency agility causing noise decorrelation and causing target echo decorrelation are different, the N_e in the formula is also different from the former N_e . Letting the equivalent independent sampling number when there is fixed frequency be N_{e3} and the equivalent independent sampling number when there is frequency agility be N_{e4} , then the reduction factor at this time is

$$Q = \frac{\frac{1}{N_{e3}} \left(\sigma_{\theta_T}^2 + \frac{0.250^2}{(S/C)_i} \right)}{\frac{1}{N_{e4}} \left(\sigma_{\theta_T}^2 + \frac{0.250^2}{(S/C)_i} \right)} = N_{e4}/N_{e3} \quad (4.102)$$

In the formula $\sigma_{\theta_T}^2$ is the variance of the angular noise wave prior to accumulation.

If the echoes are totally correlated when there is fixed frequency, then $N_{e3}=1$. At this time

$$Q \approx N_{e4} \quad (4.103)$$

We usually consider $N_{e4} < N_{e2}$, and therefore there is less improvement when there is noise than when there is not.

Fig. 4.29 compares the test results and theoretical values for small ship targets.

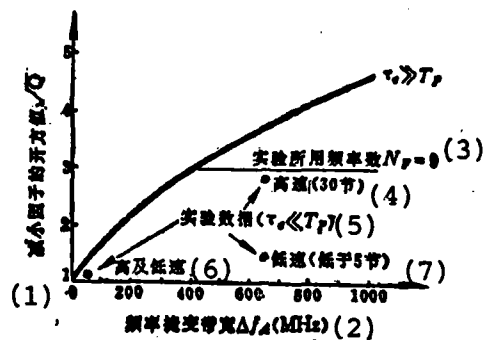


Fig. 4.29 Theoretical and Test Values of the Reduction Factors for Small Ship Targets

- Key: 1. Root extraction value \sqrt{Q} of reduction factor
 2. Frequency agility bandwidth Δf_A (MHz)
 3. Frequency number $N_F=9$ used in test
 4. High speed (30 knots)
 5. Test data
 6. High and low speeds
 7. Low speed (less than 5 knots)

We can see from the figure that for low speed small ship targets, when nine $\Delta f=80$ megahertz step jumping frequency signals are used, the root extraction of its reduction factor is 1.5 times; and for fast speed (30 knots) small ship targets, this value reaches 2.85 times. This is mainly because the spray behind a high speed boat causes the radar antenna to have a very large bias (about 15.6 feet).

By summing up the above test results we know that when step frequency is used in single pulse radar, its tracking precision can improve 1.5-3 times. When the target's angular noise wave is random (in the complex real target), it is necessary that the interval of each frequency jump be larger than the target's

AD-A124 003

FREQUENCY AGILITY RADAR(U) FOREIGN TECHNOLOGY DIV
WRIGHT-PATTERSON AFB OH N YUMA 06 DEC 82
FTD-ID(RS)Y-0803-82

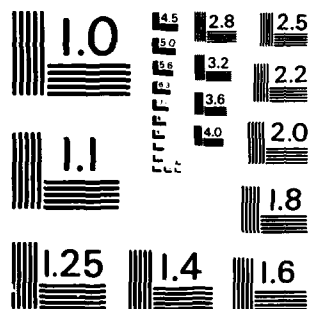
317

UNCLASSIFIED

F/O 17/9

NL

FORM 8-82
PAGE 1
11-82



MICROCOPY RESOLUTION TEST CHART
NATIONAL BUREAU OF STANDARDS-1963-A

critical frequency. At this time, the reduction factor is approximately equal to the frequency interval number. Because the maximum frequency number is limited by certain real conditions, each frequency step should not be selected too large but it is best to have it slightly exceed the critical frequency.

4.7 Signal Processing Technique of Frequency Agility Tracking Radar

4.7.1 Negative Correlation of Angular Noise Waves and Echo Amplitude

Although we studied the influence of frequency agility on the amplitude scintillation and the angular noise waves of echo signals in section 4.3, we have yet to study the relationship between the transient value of echo signal amplitude and the transient value of angular noise waves.

As a result, when actually observing complex target (e.g., aircraft) echoes, it is often discovered that a negative correlation exists between the echo's amplitude fluctuation and the angular flickering. That is, when the echo amplitude is largest the corresponding angular flickering is often smallest.

To further study the relationship between these two, Sims and Graf used an IBM 360/50 electronic computer as well as a Fortran IV program for computational research [15]. The method was as follows: it was assumed that the target's directional diagram was the product of two sine functions, that is, when they used a logarithmic (power) amplitude function for expression it was

$$A = 10 \lg(k \cos(n_1 \phi) \cos(n_2 \phi))^2 \text{ dB} \quad (4.104)$$

In the formula, k is a certain maximum amplitude, n_1 is a certain small integer, and n_2 is a certain large integer. Its latter cosine item represents the fine structure of the lobe and the former cosine item forms a slow changing amplitude envelope. Its phase graph also uses a similar method for forming

$$\alpha = 180 \cos n_1 \phi \quad (4.105)$$

In the formula, n_3 is also a large integer.

Afterwards, it is assumed that there is a target which flies along the following locus similar to the above directional graph

$$\left. \begin{aligned} r &= 4650 - 3.75 t \\ \theta &= 90^\circ + \arctg \left\{ \frac{50 \sin(2\pi(r - 900)/3750)}{r} \right\} \\ \phi &= 45^\circ + \arctg \left\{ \frac{150 \sin(2\pi(r - 900)/3750)}{r} \right\} \end{aligned} \right\} \quad (4.106)$$

In the formula, r is the target's range, θ is the target's azimuth, ϕ is the target's angle of elevation and t is the time.

When this target's flight is similar to that of the above locus, within 0-25 seconds, using 0.025 second intervals for sampling, we can obtain a series of sampling points.

Fig. 4.30 shows the amplitude fluctuation and angular flickering of this target when the frequency is fixed at 10 kilomegahertz. We can discover from this figure that the minimum angular flickering corresponds to the maximum echo amplitude.

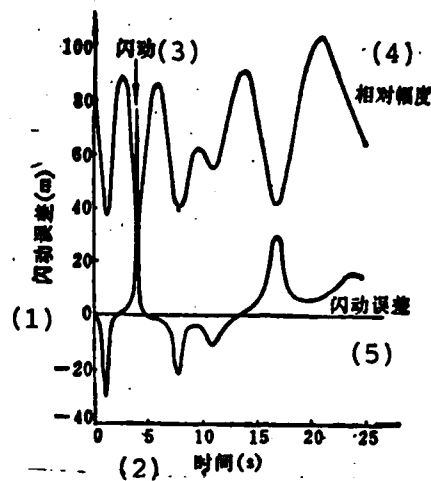


Fig. 4.30 The Relationship of the Simulated Target's Amplitude Fluctuation and Angular Flickering When the Frequency is 10 kilomegahertz

Key: 1. Flickering error (m)
 2. Time (s)
 3. Flickering
 4. Relative amplitude
 5. Flickering error

See table 4.3 for further calculations of the correlation coefficient between the echo's relative amplitude and angular flickering when in different operating frequencies. It can be discovered from this table that a very negative correlation exists between the echo's relative amplitude and the angular flickering.

(1)	频率(GHz)	10.0	9.98	9.96	9.94	9.92	9.90
(2)	相关系数	-0.606	-0.599	-0.621	-0.630	0.622	0.438

Table 4.3

Table 4.3 Correlation Coefficient Between the Relative Amplitude and Angular Flickering of Different Frequencies

Key: 1. Frequency (GHz)
2. Correlation coefficient

Generally speaking, a two dimensional probability density function can be used to express the relationship between the echo's amplitude and angular flickering (see fig. 4.31).

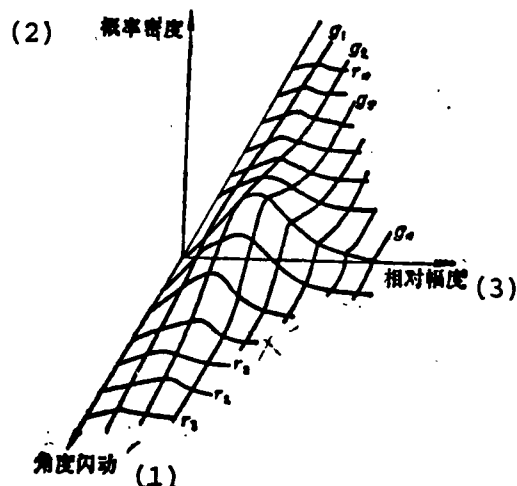


Fig. 4.31 Two Dimensional Probability Density Function of Typical Amplitude and Flickering Errors

Key: 1. Angular flickering
2. Probability density
3. Relative amplitude

In the figure, curves g_1, g_2, \dots, g_n are the angular flickering probability density functions when in different echo amplitudes. It can be assumed that they are Gaussian distributions and have similar mean values. Yet, their variances decrease with the increase of the echo's amplitude,

$$\sigma_1^2 > \sigma_2^2 > \dots > \sigma_n^2$$

(4.107)

4.7.2 Signal Processing Technique of the Method For Selecting the Maximum Amplitude

Based on the above facts there naturally exists the problem of how to carry out signal processing. In most tracking radar in the past, whether or not they worked in frequency agility, all used the simple average method for signal processing. That is, no matter how large the angle tracking system's echo signal amplitude was, they carried out simple average seeking for the echo's angle positions. The angle errors for this type of processing method are naturally quite large. If we were able to use another type of signal processing method, not for seeking the average amplitude of the echo but for selecting the echo's amplitude as the maximum angle signal sent into the angle tracking system, we would certainly then be able to obtain even smaller angle errors. Naturally, this type of signal processing method can only be applied in single pulse tracking radar.

Because the common echo amplitude fluctuation speed is very slow in single pulse tracking radar with fixed frequency, to obtain a relatively large echo amplitude a very long period of time is required. In other words, because the correlation time of the echoes is far larger than the repetition period of the pulses, this type of processing method requires a great number of pulses before seeing results.

However, if we use the frequency diversity or frequency agility technique it is possible to cause this processing method to be even more effective. This is mainly because use of frequency decorrelation increases the number of independent

pulses.

In reality, it is only necessary to select two types of frequencies for diversity reception to be able to obtain distinct improvements. This type of method is sometimes also called the "error selection diversity method."

If two types of frequencies were used for simultaneous transmission in the above mentioned simulated tests [15] and signals with relatively high amplitudes were selected, this would greatly raise its angle-measuring precision. Table 4.4 lists the angle-measuring errors when using this type of signal processing method.

f_1 GHz	f_2 GHz					
	10.0	9.98	9.96	9.94	9.92	9.90
10.0	11.9	7.3	8.0	5.6	7.2	4.8
9.98		10.1	7.7	7.4	6.0	5.8
9.96			9.8	5.5	7.1	5.0
9.94				11.4	5.7	7.5
9.92					12.5	5.9
9.90						19.2

Table 4.4 The Mean Square Root Errors (Meters) Obtained From Using Two Frequency Diversity Methods For Selecting Maximum Amplitude

The data on the diagonal lines in the table represent the errors when there is a single frequency. Naturally, use of this error selection diversity method can greatly reduce the angle-measuring errors.

However, the above results were also obtained through statistics carried out over a long period of time. Relatively few samplings were carried out in a shorter length of time and

although the probability of the echoes of the two frequencies corresponding well to the relatively small echo amplitude were not great still the probability of a certain frequency among them corresponding well to the maximum echo amplitude (i.e., the minimum angular flash) was also not very great.

Therefore, use of a frequency agility technique with many types of transmitting frequencies is relatively ideal. At this time, because the frequency of each transmitted pulse is different, when it is only necessary that the frequency difference of the adjacent pulse be greater than the critical frequency jumping, we can then cause the echo of each pulse to be an independent sample. This does not require the transmission of a great many pulses to be able to obtain close to the maximum value of echo amplitude.

As mentioned previously, there are two types of commonly used frequency agility. One type is random jumping frequency and the other is step jumping frequency. Random jumping frequency is mainly used for countering active jamming. Yet, because its transmitting frequency is completely random, there is a certain probability that the carrier frequency of its adjacent pulse will be smaller than the critical frequency. As regards step jumping frequency, it is only necessary that each step be larger than the critical frequency to be able to guarantee that the adjacent pulse is completely independent. Yet, because the total agility bandwidth has certain limitations, after a certain period it is necessary to go up one step of frequency again only when the frequency of the first step has been staggered. This type of step jumping frequency is sometimes also called systematic jumping frequency. Its drawback is that the frequency jumping has a certain regularity and is therefore unsuitable for anti-jamming. One type of improvement for this jumping frequency method is to randomly select the first frequency and afterwards there will be jumping frequency according to the step pattern.

This method is a compromise between the above two types of methods and is a relatively good method when the agility bandwidth is relatively wide and the number of steps required are few.

When radar operates in frequency agility and it is necessary to select the maximum amplitude, there is the problem of processing the pulse number. That is to say, to select the largest of the amplitudes from among the continuous pulses. The method presently used is as follows: it is assumed that in a certain specific time interval (it can be the staying time of the antenna scanning on the target or the frequency agility period) there are N pulses altogether. If the j pulses among them are processed the largest among the j continuous pulses is selected. At the same time, we use a method similar to the sliding window detector wherein each time the next echo is received the earliest echo is discarded and at the same time we compare this group of j pulses and select the largest one. The target angle information corresponding to this echo is then sent to the angle tracking system. In this way, each transmitted pulse will be compared once until N pulses are reached. Thus, the number of angle errors which can be obtained is $N-j+1$ and the mean square root angle error is defined as

$$\sigma_{rms} = \sqrt{\sum_{i=j}^N \Delta\theta_i^2 / (N-j+1)} \quad (4.108)$$

To quantitatively analyze the influence of various different frequency agility methods and the number of pulses processed, some people have carried out simulated test research using the IBM360/50 computer [16]. The target model used possessed the following radar section

$$\sigma(\Phi) = \{ (50 / (\pi/2)^2) \Phi + 8 \} \cos(k\Phi/2)$$

In the formula, Φ is the azimuth angle calculated from the aircraft nose and $k=2\pi/\lambda$ is the phase constant.

Further, if the depth of this target is at least 7.5 meters, the frequency difference need only be larger than 20 megahertz to be able to cause echo decorrelation. When the radar operates in step jumping frequency (its frequency range is 5.35-5.85 kilomegahertz, its interval is 40 megahertz), the relationship between the mean square root tracking error obtained from computer simulation and the number of processed pulses is as shown in fig. 4.32.

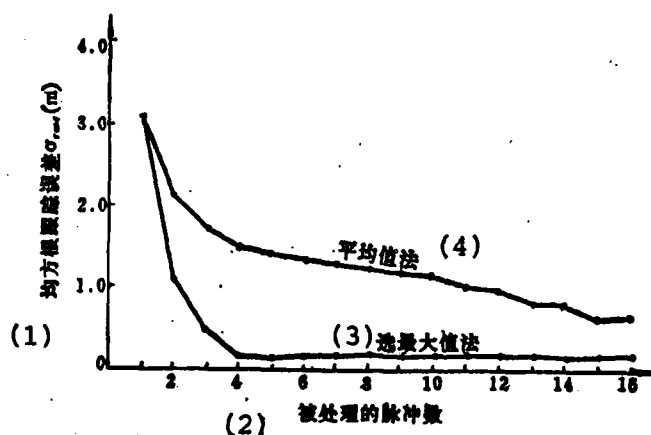


Fig. 4.32 The Relationship Between the Selection of the Maximum Value Method, the Mean Value Method of Tracking Errors and the Number of Processed Pulses (Step Jumping Frequency)

Key: 1. Mean square root tracking errors
 2. Number of processed pulses
 3. Selection of the maximum value method
 4. Mean value method

To make a comparison, the figure draws the tracking errors and uses the common mean value method and maximum value method to carry out signal processing. We can see from the figure that although use of step jumping frequency caused each of the pulses to be uncorrelated, yet when the common mean value method was used, it was still necessary to have a large number of pulses to be able to reduce the tracking errors. However, use of the selection of the maximum value method can cause the tracking errors to quickly converge. This is of great significance in guided missile homing radar which requires fast speed determination of target positions (the tracking loop time constant is short).

Fig. 4.33 gives the relationship of the mean square root angular tracking errors and the number of processed pulses when in different frequency agility methods. For comparison, the figure also gives the angular tracking errors when operating at fixed frequency (5.35 kilomegahertz). The various frequency agility methods all used the selection of the largest value method. Naturally, the convergence must be slower when using the random jumping frequency method. However, the convergence speed of the method of randomly selecting the first operating frequency does not fall very short of that of the systematic step jumping frequency (each step is 20 megahertz).

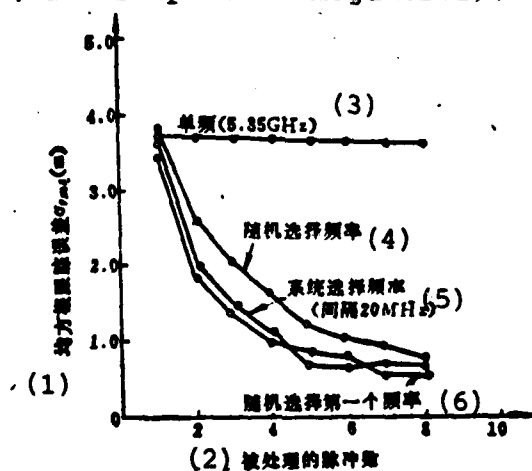


Fig. 4.33

Fig. 4.33 The Influence of Different Frequency Agility Methods on Angular Tracking Errors

- Key:
1. Mean square root tracking errors
 2. Number of pulses processed
 3. Single frequency
 4. Randomly selected frequency
 5. Systematically selected frequency
 6. Random selection of first frequency

To derive a theoretical computation formula for the reduction of angular tracking errors by the signal processing technique of this selection of the maximum value method, we can make the following approximate analysis.

If the echo signal with the maximum amplitude always corresponds to the most precise target position estimated value, then the probability of receiving at least one echo with an error between 0 and e_1 is

$$P(-e_1 < e < e_1) = 1 - \left[1 - \int_{-e_1}^{e_1} p(e) de \right]^N \quad (4.109)$$

In the formula, $p(e)$ is the probability density function of the transient tracking error (if it is a Gaussian distribution) and N is the number of processed echoes. The definition is

$$Q(e_1) = \int_0^{e_1} p(e) de = \int_0^{e_1} \frac{1}{\sqrt{2\pi}\sigma_g} \exp \left[-\frac{e^2}{2\sigma_g^2} \right] de \quad (4.110)$$

In the formula, σ_g is the standard deviation of the original tracking error (i.e., error when there is no frequency agility and selection of the maximum value method) and therefore formula (4.109) can be written as

$$P(e') = P(-e_1 < e < e_1) = 1 - [1 - 2Q(e_1)]^N \quad (4.111)$$

It can be discovered that the probability density function corresponding to distribution function $P(e')$ can approach a Gaussian form. Its standard deviation is

$$\sigma = \sigma_s N^{-0.9} \quad (4.112)$$

The standard deviation of the zero mean value is also equal to its mean square root error and can approximately be considered $N^{-0.9} \approx N^{-1}$. Then, formula (4.112) can approximately be

$$\sigma_{rms} = \sigma_s / N \quad 1 \leq N \leq 4 \quad (4.113)$$

To compare this approximation computation formula with the simulated test results, we used an electronic computer for simulation of the following target: this target possesses Swerling type I fluctuation characteristics, its wingspan is 16 meters, its flight path forms a 14° angle with the radar antenna direction, the initial speed of the target relative to the radar is 300 meters/second, the yaw rate is 5 milliradian/second, tracking begins at 5 kilometers from the radar, the radar's pulse repetition frequency is 500 hertz, and tracking time is 5 seconds. To obtain independent samples, we selected step frequency with an initial frequency of 5.51 kilomegahertz and intervals of 20 megahertz. Results are shown in fig. 4.34.

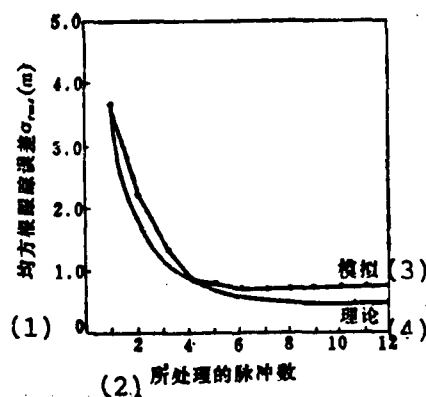


Fig. 4.34

Fig. 4.34 Comparison of an Approximation Formula and Simulation Test Results of Tracking Errors

Key: 1. Mean Square root tracking errors
2. Number of processed pulses
3. Simulation
4. Theoretical

The smooth curve in the figure forms an inverse ratio with N (formula (4.113)). The original tracking error obtained is $\sigma_g = 3.65$ meters which is about 0.23 times the wingspan. When the approximation formula is between $1 < N < 4$ it is the same as the simulation test results. After $N > 4$, the tracking errors obtained from the simulation test do not reduce again. This is also to say that the limit value of its tracking errors is about $\sigma_g/4$. This is perhaps because the maximum amplitude echoes do not correspond to the minimum errors.

4.8 Reduction of Multipath Transmission Errors by Frequency Agility

Multipath transmission is also an important source of errors in tracking radar, especially when tracking low angle of elevation targets. Furthermore, when radar is erected on a damp ground with a very high reflection coefficient on the coast or on ships, very large angle of elevation errors can be caused by the electric waves of multipath propagation. When serious, they can even cause there to be no means of tracking targets.

We will first study the mechanism of multipath propagation [17]. Below we will only study the multipath transmission which are caused by ground (or sea) reflection because this is the most serious. The geometric relation of this situation is shown in fig. 4.35. It is assumed in the figure that the radar antenna is located at point A, the target is located at point T and the ground is a plane.

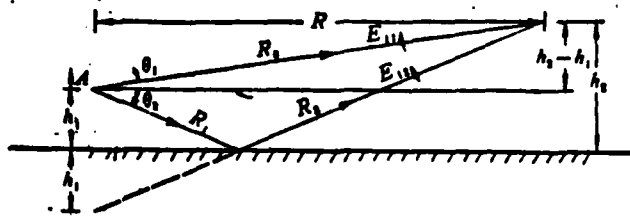


Fig. 4.35 Geometric Relation of Multipath Transmission Caused by Ground (Sea) Reflection

Electric waves are transmitted from the radar antenna and there are two paths which can reach the target. One is the direct waves with a range of R_D . The other is the indirect waves with a range of $R_1 + R_2$. The direct incidence electric field intensity of the target area is E_{i1}

$$E_{i1} = \frac{G_1}{R_D} E_t \quad (4.114)$$

In the formula, G_1 is the antenna's voltage gain and E_t is the electric field intensity of the receiver when it is the point source.

The indirect incidence electric field intensity of the target area is E_{i2} .

$$E_{i2} = \frac{G_2 \rho}{R_1 + R_2} E_t \quad (4.116)$$

In the formula, G_2 is the antenna's voltage gain on the reflection point direction and ρ is the ground surface reflection coefficient.

The direct path range is

$$R_D = [R^2 + (h_2 - h_1)^2]^{1/2} \quad (4.116)$$

The total length of the indirect path range is

$$R_{I_0} = R_1 + R_2 = [R^2 + (h_2 + h_1)^2]^{1/2} \quad (4.117)$$

In the majority of situations with actual multipath transmission $h_1, h_2 \ll R$, and therefore, after formulas (4.116) and (4.117) use binomial expansion, we obtain the first two items and can make good approximations.

$$R_D \approx R + \frac{(h_2 - h_1)^2}{2R} \quad (4.118)$$

$$R_{I_0} \approx R + \frac{(h_2 + h_1)^2}{2R} \quad (4.119)$$

We can obtain the path difference of the indirect and direct waves from the above two formulas

$$\Delta = R_{I_0} - R_D \approx 2h_1 h_2 / R \quad (4.120)$$

From this, we can obtain the phase differences of E_{11} and E_{12}

$$\Delta\phi = \frac{2\pi}{\lambda} \Delta \approx \frac{2\pi}{\lambda} \cdot \frac{2h_1 h_2}{R} = k \frac{2h_1 h_2}{R} \quad (4.121)$$

In the formula, k is the phase constant.

Assuming E_{11} is the 0 phase in the target area, the sum of radiation field intensity E_t is the vector sum of the two

$$E_s = E_{i1}e^{j\phi} + E_{i2}e^{-j\Delta\phi} \quad (4.122)$$

Therefore, the value of the combined field intensity between $E_{i1} - E_{i2}$ and $E_{i1} + E_{i2}$ is decided by $\Delta\phi$.

When $\rho \approx 1$, $G_1 \approx G_2$ and $\Delta\phi \approx 180^\circ$, the combined field intensity tends to be 0. Naturally, this strongly affects tracking performance.

The incident power in the target area is

$$P = \frac{|E_i|^2}{2\eta} \text{ W/m}^2 \quad (4.123)$$

In the formula, η is the inherent impedance of the free space. If the target section is σ , then the scattering power is

$$p_r = \frac{\sigma P}{4\pi} \quad (4.124)$$

In the formula, the unit of p is watts; the unit of p_r is watts/steradian.

The scattering field intensity of the target area is

$$E_s = \frac{1}{R} \sqrt{2\eta p_r} \quad (4.125)$$

The reflection path is identical to the incident path. If the amplitude of the direct wave of the receiving antenna center is E_{r1} , the phase of this point's wave is taken as 0. We can guarantee the far field approximation of a large R and small θ value. The direct field intensity E_{a1} from the receiving aperture center x can be expressed as (see fig. 4.36)

$$E_{a1} = E_{r1} e^{-j\theta \sin \alpha_1} \quad (4.126)$$

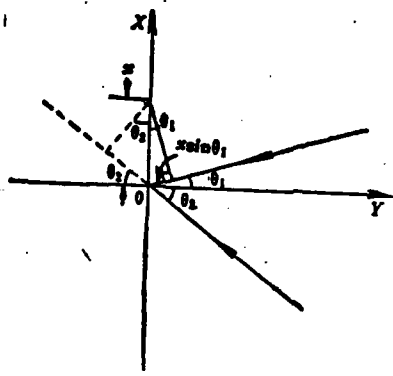


Fig. 4.36 The Path Difference of the Direct and Indirect Waves Opposite the Aperture Center

Further, the indirect scattering wave can be expressed as

$$E_{r2} = E_{r1} e^{-j(kx \sin \theta_2 + \Delta\phi')} \quad (4.127)$$

In the formula, E_{r2} is the indirect echo amplitude in the antenna's aperture center. It is determined by the indirect transmitting wave.

The total electric field is the vector sum of the direct and indirect waves

$$E_r = E_{r1} e^{-j(kx \sin \theta_1)} + E_{r2} e^{-j(kx \sin \theta_2 + \Delta\phi')} \quad (4.128)$$

It is necessary to notice that the $\Delta\phi'$ in the formula is the function of x . Because of the h_1 in formula (4.121), we must now substitute in $(h_1 + x)$, that is

$$\Delta\phi' = -\frac{2kh_1}{R} (h_1 + x) \quad (4.129)$$

We can see from formula (4.128) that although the direct and indirect waves along the aperture are linear phases, their phase

constants are different. This can therefore produce an interference pattern as well as cause them to not again have constant amplitude and linear phase distribution. Because the angle-measuring system of the radar is designed according to uniform waves, non-uniform waves will produce directional errors.

It can be obtained from analysis [1] that the angle of elevation angle-measuring errors caused by multipath transmission can be expressed by the following formula

$$\sigma_e = \frac{\rho \theta_e}{\sqrt{8G_{se}}} \quad (4.130)$$

In the formula, ρ is the reflection coefficient, θ_e is the single path antenna's angle of elevation beam width and G_{se} is the power ratio of the tracking radar antenna and directional diagram peak value, and the error pattern's peak value side lobe level on the direction reached by the indirect waves.

These types of multipath transmission errors can attain to very large numerical values and as a result become a serious problem in high precision tracking radar. Fig. 4.37 gives the test values of the multipath transmission errors for FPS-16 high precision single pulse tracking radar. We can see from this figure that when in a low angle of elevation, the errors caused by multipath transmission can reach 0.1-0.3 mil.

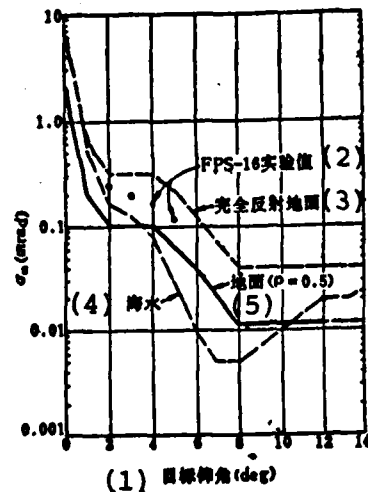


Fig. 4.37 Test Data on the Relationship Between Multipath Transmission Errors and the Target's Angle of Elevation

- Key: 1. Target's angle of elevation (deg)
 2. FPS-16 test values
 3. Total reflection of ground surface
 4. Sea
 5. Ground surface ($\rho = 0.5$)

We know from the former analysis that the k in the phase constant is the function of the frequency. Therefore, the angle-measuring errors caused by the multipath transmission is also the function of the frequency. We can also use computer simulation for verification. Fig. 4.38 gives the computer simulated test results for the angle of elevation errors caused by multipath transmission [17]. The simulated target range is 3 kilometers and the height is 300 meters. It can be clearly seen from the curves that there are different angular positions for different frequencies.

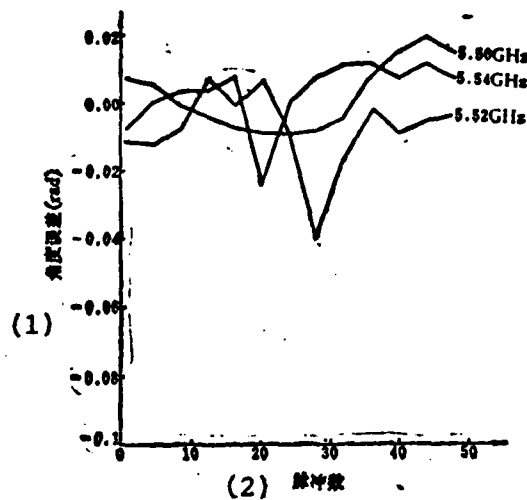


Fig. 4.38 The Relationship of Multipath Transmission Errors and the Frequency

Key: 1. Angle errors (rad)
2. Number of pulses

The results of the computer simulation also show that only when the interval of the frequency is large enough can we guarantee decorrelation between the frequency and angle. Table 4.5 lists the correlation coefficient between multipath transmission errors when there are different frequencies. We can see from this table that its correlation coefficient is extremely small. That is, we can use frequency agility to attain decorrelation.

(1)	頻 率	5.50	5.52	5.54	5.56	5.58
	5.50	1.00	0.07	-0.06	-0.00	-0.31
	5.52		1.00	-0.04	-0.28	0.10
	5.54			1.00	-0.05	0.13
	5.56				1.00	0.05
	5.58					1.00

Table 4.5 Correlation Coefficient Between Multipath Errors When There are Different Frequencies

Key: 1. Frequency

However, we did not find that the simulated computer results of the correlation coefficient between the multipath errors and echo signal amplitude had any similarity to the angular noise waves. Table 4.6 lists the correlation coefficient between the echo signal amplitude and multipath transmission. We can see from the table that there is not a very strong negative correlation between these two. There is also no way of using the maximum value method to reduce the multipath transmission errors. Yet, frequency agility can still certainly reduce multipath transmission errors. We have yet to see the test results in this area.

(1)	頻 率	5.50	5.52	5.54	5.56	5.58
(2)	相关系数	-0.17	-0.08	0.10	-0.20	0.09

Table 4.6 Correlation Coefficient Between the Echo Signal Amplitude and Multipath Transmission Errors

Key: 1. Frequency
2. Correlation coefficient

4.9 Increasing the Angle-Measuring Precision of Search Radar By Frequency Agility

The above discussion focused on the improvements of frequency agility on the angle tracking precision of tracking radar. Actually, frequency agility cannot only raise the angle-measuring precision of tracking radar but can also increase the angle-measuring precision of search radar.

Although the number of echoes received from the target is limited in search radar, because the azimuth rotational speed is not high there is still a certain residence time for the point target. This time is equal to the time that the antenna rotates passed the horizontal beam width. For example, for an antenna which rotates 6 times per minute, when the beam width is 1.5 degrees, the residence time of the beam on the target is 42 milliseconds. When the radar's operating wavelength is relatively short (e.g., in airborne radar) and the scintillation frequency of the radar is relatively high, it is possible that a decaying wave phenomenon of the echo amplitude occur in the beam's residence time. That is to say, at this time the amplitude of the target echo cannot be expressed by Swerling's type I or II (uncorrelated in scanning) as well as type II or IV (uncorrelated in pulses). However, it belongs between the two. That is, the correlation time of the echo amplitude is larger than the pulse repetition cycle but smaller than the antenna's residence time. This type of situation is actually still existent.

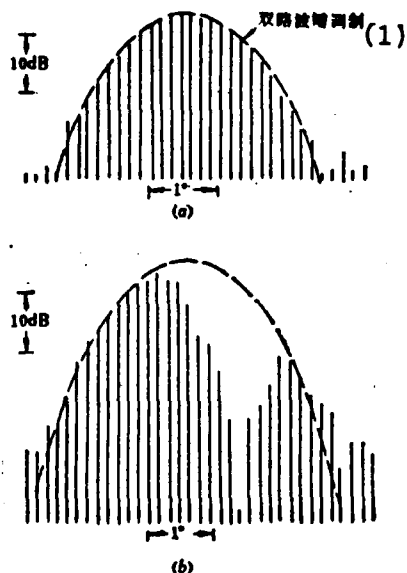


Fig. 4.39 Test Results of Amplitude Envelope Shape Distortion
Created by Echo Amplitude Fluctuation (Pulse
Repetition Frequency=196 Hz, $\Delta f=0$)

(a) Without fading;

(b) With fading.

Key: 1. Two path lobe modulation

Fig. 4.39 are the results of actual tests of a flying target [18]. The radar frequency used was 5.35–5.85 kilomegahertz, the antenna rotation was 6 rotations/minute, the beam width was 1.5 degrees and the pulse repetition frequency was 196 hertz. Fig. (a) is the situation when there is no fading. This type of situation is seldom seen. More common is the situation of fig. (b) because the echo amplitude fluctuation causes a very large distortion of the echo amplitude's envelope.

Modern search radar commonly has a digital type automatic detector. This type of automatic detector uses an amplitude discriminator to carry out binary quantization of the echo

amplitude. The 1,0 signal attained after quantization is later added to the target detector. Usually, this type of target detector uses a digital type sliding window detector. The length of the sliding window is equivalent to the number of pulses in a 3 decibel beam width. The 1,0 signals obtained from the quantization in the same range quantization interval is added to the same sliding window detector. When the density of 1 in the window reaches a certain initial standard, it can then be determined that a target exists and the azimuthal angle θ_1 is recorded when the target starts. Following the antenna's scanning of the target, the density of 1 in the sliding window changes from a gradual increase to a gradual decrease. When its density of 1 is smaller than a certain final standard, it is then determined that the target is ended. At the same time, the azimuthal angle is recorded when it is ended. It can be considered that the real azimuthal angle of the target is determined by the following formula.

$$\theta = \frac{\theta_1 + \theta_2}{2} - \frac{w}{2} \Delta\theta \quad (4.131)$$

In the formula, w is the length of the sliding window (usually equal to the number of pulses N) and $\Delta\theta$ is the angle the antenna rotates in the pulse repetition cycle. When the echo amplitude does not fluctuate, the angle-measuring errors which can be obtained from this type of method are about $(2-3) \Delta\theta$.

We can see from fig. 4.40 that when the echo amplitude fluctuates in the antenna's residence period, this will necessarily produce a great effect on satisfying the azimuth value when there are starting and final standards. Thus, this can create very large angle-measuring errors. These errors will far exceed the angle interval of the transmitting pulse on beam splitting. To quantitatively estimate the angle-measuring errors caused by the target's echo fluctuation, we will analyze

a simple target model below [19].

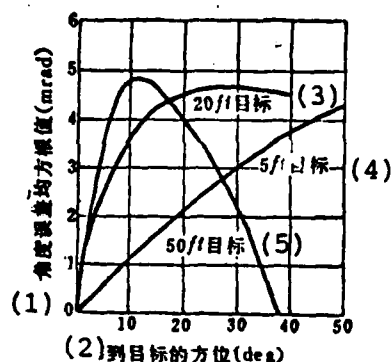


Fig. 4.40 The Angle-Measuring Errors Caused by the Target's Echo Fluctuation on Search Radar

Key: 1. Angle error mean square root value (mrad)
 2. Azimuth reaching the target (deg)
 3. 20 ft target
 4. 5 ft target
 5. 50 ft target

If the target is composed of two scattering objects with a separation of D , it is more or less perpendicular to the direction of the line of sight. At this time, the echo is composed of two components and among them the phase difference is $\frac{2\pi 2D}{\lambda} \phi$. The ϕ in this expression is the azimuthal angle of the target. The combined echo amplitude is

$$\cos\left[\frac{1}{2}\left(\frac{2\pi 2D \phi}{\lambda}\right)\right] = \cos\left[\frac{2\pi D \phi}{\lambda}\right] \quad (4.132)$$

If the range of the target is not an integral number of times the wavelength, at this time there will be a starting phase and the echo amplitude will change to

$$A_r = \cos\left[\frac{2\pi D \phi}{\lambda} + k\right] \quad (4.133)$$

The value of k is between $0-2\pi$.

If the target uses velocity v for uniform velocity linear flight, the tangential component of this velocity is $v \sin \phi_0$. ϕ_0 is the starting azimuthal angle of the target (with the due north included angle). Therefore, the target's azimuthal angle is the function of the tangential velocity, range and time.

$$\phi = \frac{Tv \sin \phi_0}{R} \quad (4.134)$$

If this formula is substituted into formula (4.133), we can obtain the echo's amplitude as

$$A_e = \cos \left[\frac{2\pi DvT \sin \phi_0}{\lambda R} + k \right] \quad (4.135)$$

The beam position of the antenna is also the function of the time and can be expressed by $\Theta = \theta T$. Therefore, $T = \Theta / \theta$. When it is substituted into formula (4.135), we can obtain the echo's amplitude as

$$A_e = \cos \left[\frac{2\pi Dv\Theta \sin \phi_0}{\lambda R\theta} + k \right] \quad (4.136)$$

If the beam width is $1.5^\circ - 2^\circ$, its lobe figure can be expressed by the following formula

$$G = \frac{\cos \pi\theta/25}{1 - \theta^2/156.25} \quad (4.137)$$

In the formula, θ is the angle calculated from the beam center and is expressed in milliradian.

Therefore, the echo's voltage amplitude received by the antenna is $G^2 A_t$ and the received echo signal's power $P(\theta)$ is $G^4 A_t^2$. $P(\theta)$ can be written as

$$P(\theta) = \frac{\cos^4(\pi\theta/25) \cos^2\left(\frac{2\pi Dv\theta \sin \phi_s}{\lambda R\theta} + k\right)}{(1 - \theta^4/156.25)^4} \quad (4.138)$$

This power value is the function of θ .

The "center of gravity" of this signal power will not be the same as the beam's center value ($\theta=0$) and the angle of difference can be calculated by the following formula

$$\delta_c = \frac{\int \theta P(\theta) d\theta}{\int P(\theta) d\theta} \quad (4.139)$$

This formula has different values for different starting phase k values. We can find its standard difference from this

$$\sigma = \sqrt{\frac{\sum \delta_k^2}{N_k}} \quad (4.140)$$

In the formula, N_k is the number of the different k values.

It is only necessary to substitute a typical radar characteristic into it to be able to use a computer to calculate the mean square root value of this angle error. For example, if the radar operates in a Ku wave band, the antenna's beam width is 1.7° , the antenna's rotational speed is 70 degrees/second, the distance of the target from the radar station is 20,000 feet and the velocity is twice the speed of sound. We can then calculate targets with different dimensions (D) and the relational curve between the mean square root value of the angle errors caused by echo fluctuation and the target's azimuthal angle (as shown in fig. 4.40).

It can be seen from this figure that the angle errors caused

by the echo's amplitude fluctuation are not only the function of the target's dimensions but also the function of the azimuthal angle reaching the target. Therefore, this type of error is very difficult to calculate and eliminate in advance.

However, use of the frequency agility technique can greatly reduce these errors. Because frequency spectrum agility can cause the adjacent echoes to be completely uncorrelated, as a result it reduces the low frequency component of the scintillation. However, quick flashing scintillation can be smoothed out by the data processing system. In this way, it can greatly improve the angle-measuring precision of search radar. Besides this, because it removed the low frequency component of the angle errors it can also cause a great reduction of the gate automatic tracking system's loss probability. It is used for normal operation of scanning and tracking systems.

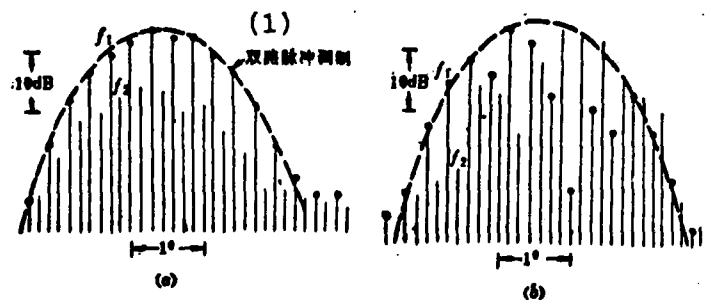


Fig. 4.41 The Echo's Figure in the Beam When the Radar is Operating in Frequency Agility (Pulse Repetition Frequency=196Hz, $\Delta f=64\text{MHz}$)

- (a) Without fading
- (b) With fading

Key: 1. Two path pulse modulation

The effects of frequency agility on the echo fluctuation in beams can be seen in fig. 4.41. This figure draws an echo figure

in the beam when the radar is operating in frequency agility the same as that in fig. 4.39. Fig. (a) is without fading and fig. (b) is when there is fading.

This figure only gives the situation when radar operates in alternating jumping frequency, that is, it only has two frequencies alternately transmitting. Its frequency interval is 64 megahertz which can guarantee its decorrelation. Yet, when there is no fading, we can see that each pulse still has correlation. However, when there is fading, this can eliminate long time fading and when the frequency changes 64 megahertz this can cause the adjacent echo's amplitude to change 25 decibels.

Yet, if the target echoes received by the radar are mainly without fading or are slow fluctuating (this type of situation mainly occurs in meter-wave radar), then the use of frequency agility cannot improve its angle-measuring precision. It can, however, cause its angle-measuring precision to decline. Fig. 4.42 draws the computer simulation results of the relationship between the azimuthal angle errors' mean square root value of the sliding window detector and the signal-noise ratio when in different types of signal fluctuation [20].

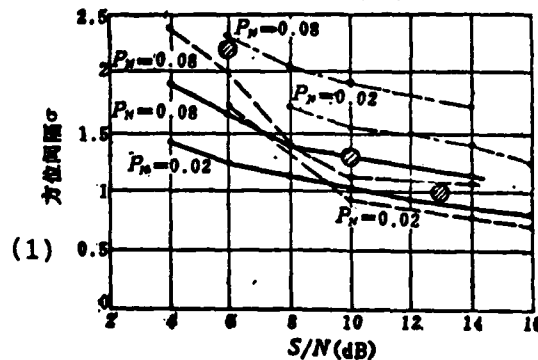


Fig. 4.42

Fig. 4.42 Relationship of the Azimuth Errors of the Sliding Window Detector and the Signal-Noise Ratio When in Different Types of Signal Fluctuation

Key: 1. Azimuthal angle

The number of pulses in the radar's 3 decibel beam is 15, the length of the sliding window is 15 and the signal's detection standard is 8. The broken lines in the figure are non-fluctuating signals, the solid lines are slow fluctuating signals (uncorrelated in scanning), and the dots with the drawn lines are fast speed fluctuating signals (uncorrelated in the pulses). The fast speed fluctuating signals are also equal to when in frequency agility. We can see from the figure that when in the same first threshold noise wave quantization probability P_N , the azimuth angle-measuring errors (expressed by the azimuth interval $\Delta\theta$ number) increase with the signal-noise ratio. When in the same signal-noise ratio wherein non-fluctuating signal angle-measuring errors are minimal, the fast fluctuating signals are then larger.

We can see from this that the effects of frequency agility on the angle-measuring precision of search radar are not invariable. They are mainly determined by the type of echo fluctuation. When the echo fluctuation in fixed frequency is slow fluctuating the use of frequency agility cannot improve it.

References

- [1] Radar System Analysis. D.K. Barfon. Prentice-Hall, Inc. 1964. Chapt. 10.
- [2] Radar Handbook. Ed. by M.I. Skolnik. McGraw-Hill Book Co. 1970. Chapt. 21.
Chinese translation: "Radar Manual," Vol. 8, Chapter 28.
- [3] Chinese translation: "Radar Manual," Vol. 8, Chapter 28, Second Volume of Chinese Translation, Chapter 9.

- [4] Radar target angular scintillation in tracking and guidance systems based on echo signal phase front distortion, Howard, D.D. Proc. NEC. Vol. 15. Oct. 1959.
- [5] The reduction of angle-of-arrival scintillation by a frequency shifting technique. L. H. Kosowsky, S. S. Brody, L. Chanzit, S. Saslovsky. Proc. NEC. Vol. XIX. 1963. p52-71.
- [6] Radar tracking accuracy improvement by means of pulse-to-pulse frequency modulation. Birkemeier, W.P. and N.D. Wallace, AIEE. Trans Commun and Electron. Vol. 81. pp. 571-575. Jan. 1963.
- [7] Reduction of radar tracking errors with frequency agility, G. Lind. IEEE Trans. Vol. AES-4. pp. 410-416, May, 1968.
- [8] A simple approximate formula for glint improvement with frequency agility. G. Lind, IEEE Trans. Vol. AES-8, pp. 854-5, Nov. 1972.
- [9] Reduction of radar glint for complex targets by use of frequency agility. L.A. Nicholls. IEEE Trans. Vol. AES-11, No. 4, 1975. pp. 647-650c.
- [10] Tracking errors in a frequency agility system, P.F. Guarguaglini, AGARD Conf. Proc. No56 on Advanced Radar Systems AD715, 485, 1970.
- [11] Detection of slowly fading targets with frequency agility, N.D. Wallace, Proc. IEEE, May, 1969, pp. 817-818c.
- [12] System properties of jumping frequency radar. B.C. Gustafson and B-O. As. Philips Telecomm. Rev. Vol. 25, pp. 70-76, 1964.
- [13] Homing radar tracking accuracy improvement with frequency diversity. P. Jones, E.A. Mickle, G.D. Swetnam, J. Spacecraft and Rockets, Vol. 8, No. 9, Sept. 1971.
- [14] A quantitative analysis of sea clutter decorrelation with frequency agility, Beasley, E.W. and Ward, H.R. IEEE Trans. on Vol. AES-4, pp. 468-473, May, 1968.
- [15] The reduction of radar glint by diversity techniques. Sins, R.J. and Graf, E.R. IEEE Trans. Vol. AP-19, No. 4, Jul 1971. pp. 462-468, May, 1968.
- [16] Frequency agility processing to reduce radar glint pointing error. J.M. Loomis, E.R. Graf, IEEE Trans. Vol. AES-10, No. 6, Nov., 1974, pp. 811-820.

- [17] Frequency agility and radar pointing errors due to multipath, D.G. Burks, H.V. Poor, Z.L. Burrell, III, and E.R. Graf. AD787, 390, Oct., 1974.
 - [18] Some measurements of the effects of frequency agility on aircraft radar returns. W.S. Whitlook, A.M. Shepherd and A.L.C. Quigley. AGARD Conf. Proc. No. 66 on Advanced Radar Systems, AD715, 485, 1970.
 - [19] Improving radar range and angle detection with frequency agility. H. Ray, Microwave J. May, 1966, p. 63.
 - [20] Measurement errors in determining the azimuth of radar targets with the binary sliding window integrator. K. Muller and W. Rocher. Wiss. Ber. AEG-TELEFUNKEN 44, (1971) Nr. 1. pp. 25-33.
-

Chapter V The Use of Frequency Agility to Inhibit Sea Clutter Jamming

5.1 Characteristics of Sea Clutter

Because sea clutter is not only related to sea conditions (wind velocity, wave height etc.) but also to the radar's operating frequency and polarization there has been no detailed data on sea clutter obtained for a very long time. Up to the end of the 1960's, after a large number of actual tests were done on sea clutter, a large quantity of material was gathered concerning sea clutter. After careful analysis and arrangement there was a more thorough understanding of the characteristics of sea clutter.

The characteristics of sea clutter can mainly be divided into the clutter's intensity, amplitude distribution, mean Doppler frequency shift and frequency spectrum width as well as time and space decorrelation.

5.1.1 The Intensity of Sea Clutter

For convenience of analysis, the intensity of sea clutter will be expressed by the effective reflection area σ .

Because the sea area is far larger than the antenna beam's range of irradiation the sea clutter forms a direct ratio with the radar's irradiation area.

The so-called radar irradiation area is determined by antenna beam width θ_b , operating range R and the radar's transmitting pulse width τ_p . The equivalent reflection area

of sea clutter can be written as

$$\sigma = \sigma_0 R \theta_0 \left(\frac{c \tau_p}{2} \right) \quad (5.1)$$

The proportion constant σ_0 in the formula is called the normalized mean sea wave reverse scattering coefficient, named the normalized reflection coefficient for short. It is expressed in decibels. For example, when $\sigma_0 = -30$ decibels, that is, each square meter of irradiated sea, its scattering noise must be 30 decibels lower than the signal reflected by the target of the 1 square meter radar section. Because the power density received by the irradiated surface is in direct ratio to the sine of grazing angle ψ , it is usually expressed by another reflection coefficient γ . When in a large grazing angle, the following relation exists between γ and σ_0 :

$$\sigma_0 = \gamma \sin \psi \quad (5.2)$$

In the formula, ψ is the grazing angle. F.N.1

The value of σ_0 is related to many factors as shown in fig. 5.1 [1].

F.N. 1 It must be pointed out that the grazing angle is not equal to the angle of depression. When the radar antenna height h and inclined distance R are known, it is determined by the following formula.

$$\psi = \arcsin \left(\frac{h}{R} - \frac{R}{2R_e} \right)$$

In the formula R_e is the equivalent radius of the earth.

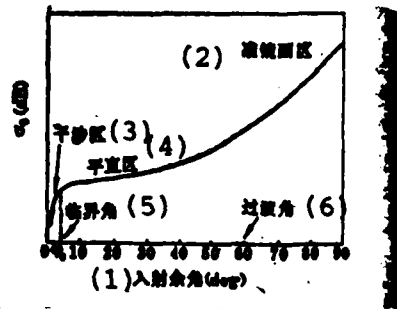


Fig. 5.1 Relationship of σ_0 and the Grazing Angle

- Key: 1. Grazing angle (deg)
 2. Collimating len's surface area
 3. Interference range
 4. Mean value area
 5. Critical angle
 6. Angle of transition

It can basically be divided into three areas: between $60^\circ - 90^\circ$ is the collimating mirror surface area. At this time, the reverse scattering is the same as the mirror's surface, and the σ_0 value increases with the incidence angle and reaches its maximum value. The second area is the mean value area. The σ_0 value changes in this area are not large. The third area is the interference range. There is the mutual interference of direct echoes and echoes reflected on the sea in this area. The common boundary of the interference range and mean value area is the critical angle which is expressed by ϕ_c . The ϕ_c differ with the frequency so that when the frequency is low there is a large change.

Fig. 5.2 gives the relationship of σ_0 and the grazing angle when there are different wave bands and polarization.

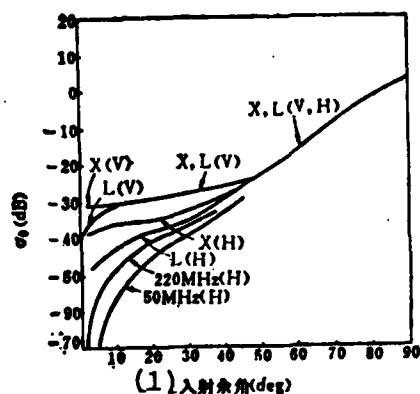


Fig. 5.2 The Relationship of σ_0 and the Grazing Angle When There are Different Wave Bands and Polarization

V: Perpendicular polarization

H: Horizontal polarization

Key: 1. Grazing angle (deg)

We can see from the figure that when in a large grazing angle, the value of σ_0 enlarges with the rising of the frequency and when in the same frequency band, perpendicular polarization is greater than horizontal polarization. The relationship between σ_0 and the sea surface conditions is shown in fig. 5.3. The larger the wind velocity the larger the value of σ_0 .

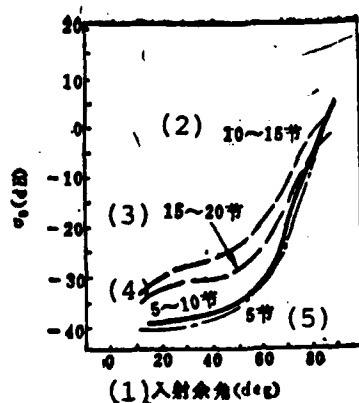


Fig. 5.3

Fig. 5.3 The Relationship Between the Value of σ_0 and the Wind Velocity (X Wave Band, Wavelength=3/2cm)

- Key: 1. Grazing angle (deg)
 2. 10-15 knots
 3. 15-20 knots
 4. 5-10 knots
 5. 5 knots

The curves only give the tendencies of the changes.
 Table 5.1 gives the actual measurement values under various different conditions.

(1) 状态	(8) 极化	(21) 以负分贝值表示的反射系数 (-dB)						
		UHF 0.5GHz	L 1.25GHz	S 3.0GHz	C 5.6GHz	X 9.3GHz	Ku 17GHz	Ka 35GHz
(2) 0 度	垂直 (9)	68°				60°		
	水平 (10)	66°	80°	75	70	66		
(3) 1 度	垂直 (11)	70°	65°	56	53	50	47°	
	水平 (12)	64°	73°	65	56	51	45	40°
(4) 2 度	垂直 (13)	63°	58°	53	47	44	42	38°
	水平 (14)	82°	65°	55	48	46	41	38°
(5) 3 度	垂直 (15)	58°	54°	48	43	39	37	34
	水平 (16)	76°	60°	48	43	40	37	36
(6) 4 度	垂直 (17)	55°	45	42	39	37	34	32
	水平 (18)		52°	42	39	36	34	
(7) 5 度	垂直 (19)		43	38°	35	33	32	31
	水平 (20)	65°	50°	42	35°	33	31°	

(22). 可能有5dB误差, 单基地雷达, 0.5至10微秒脉冲。

Table 5.1 Actual Measurement Values of Normalized Reflection Coefficient σ_0 When the Grazing Angle is 1.0 Degrees

- Key: 1. Sea conditions
 2. 0 degree
 3. 1 degrees
 4. 2 degrees

5. 3 degrees
6. 4 degrees
7. 5 degrees
8. Polarization
9. Perpendicular
10. Horizontal
11. Perpendicular
12. Horizontal
13. Perpendicular
14. Horizontal
15. Perpendicular
16. Horizontal
17. Perpendicular
18. Horizontal
19. Perpendicular
20. Horizontal
21. Reflecting coefficient expressed in negative decibels (-dB)
22. *Possibly a 5dB error for single base radar with 0.5 to 10 microsecond pulses

This table only lists data for when the grazing angle is 1.0 degrees. The reader can refer to reference [2] for data on other grazing angles (0.1° , 0.3° , 3.0° , 10° , 30° , 60°). Low grazing angles are suitable for shipboard or shore radar and large grazing angles are appropriate for use in airborne radar.

The graded definitions of the sea conditions listed in the table are shown in table 5.2.

(1) 級 別	0	1	2	3	4	5
(2) 風速 (节)	0	<7	7~12	12~15	15~19	19~24
(3) 浪高 (英尺)	0	<1	1~3	3~5	5~8	8~12

Table 5.2

Table 5.2 Definitions of Sea Conditions

Key: 1. Grade
2. Wind velocity (knots)
3. Wave height (feet)

In summing up the actual measurement data, we can make the following conclusions:

(1) Reflection coefficient σ_0 enlarges with the rising of the operating frequency. As regards horizontal polarization, it seems to increase with f^m . When the grazing angle is smaller than 1 degree, the frequency is lower than 2 kilomegahertz and when the sea condition is smaller than grade 3, the m value can reach 3. When the grazing angle, frequency and sea condition increase, the value of m tends towards zero.

(2) When the grazing angle is between 0° - 20° , the reflection coefficient enlarges with ψ^n . When in a low angle, low sea condition and low frequency, n reaches 3. When the frequency and sea condition are high, n tends towards zero.

(3) When in a low sea condition and relatively low frequency, the reflection coefficient increases with each 10 decibels of the sea condition. Yet, when in a relatively high sea condition and relatively high frequency, its growth rate reduction can be overlooked.

(4) When in a certain given sea condition, the σ_0 value of the perpendicular polarization is greater than that of horizontal polarization. Furthermore, when in a low sea condition, low grazing angle (< 1 degree) and low frequency, the difference becomes larger.

Even though these conclusions are only qualitative they

were still attained from a large number of actual measurement results. Therefore, they still possess guiding significance for understanding the intensity of sea clutter.

5.1.2 The Statistical Distribution of Sea Clutter Amplitude

Earlier, due to the lack of sufficient test data and for convenience of analysis, it was commonly assumed that the amplitude distribution of sea clutter was a Rayleigh distribution. The probability density function of its amplitude is

$$p(x) = \frac{x}{\sigma^2} \exp\left(-\frac{x^2}{2\sigma^2}\right) \quad (5.3)$$

In the formula, σ^2 is its variance.

This assumption is appropriate for relatively calm sea situations and low resolution radar (the beam width is larger than 2 degrees and the pulse width is larger than 1 microsecond). When in high resolution (the beam width is smaller than 0.1 microseconds) and adverse sea conditions, the sea clutter cannot be approximated by the Rayleigh distribution. According to statistics, about 60% of the time, the seas of the world have wave heights of over 4 feet (equal to the grade 3 sea situation) and thus often deviate from the Rayleigh distribution.

Many actual measurement results show that at this time the amplitude distribution of the sea clutter is closer to a logarithmic-normal distribution.

It is assumed that the probability density function of the normal distribution is

$$p(x) = \frac{1}{\sigma\sqrt{2\pi}} \exp\left[-\frac{(x-a)^2}{2\sigma^2}\right] \quad (5.4)$$

In the formula, a is the mean value and σ is the standard difference.

When $x=a$, $p(x)=1/\sigma\sqrt{2\pi}$, $p(x)$ forms a symmetrical distribution for $x=a$.

It is only necessary to substitute $x=\ln y$ into formula (5.4) to be able to obtain a logarithmic-normal distribution.

$$\begin{aligned} p(y) &= \frac{1}{y\sigma\sqrt{2\pi}} \exp\left[-\frac{1}{2\sigma^2} (\ln y - a)^2\right] \\ &= \frac{1}{y\sigma\sqrt{2\pi}} \exp\left[-\frac{1}{2\sigma^2} (\ln y / y_m)^2\right] \end{aligned} \quad (5.5)$$

In the formula, y is the variable of the logarithmic-normal distribution; y_m is the mid-value of y ; σ is the standard difference of $\ln(y/y_m)$. When the ratio of its mean value and mid-value is equal to 1.065, it is then equal to the Rayleigh distribution.

Fig. 5.4 gives the function figure of the logarithmic-normal distribution. For comparison, the figure also draws the curves of the normal distribution. The major difference between the logarithmic-normal distribution and Rayleigh distribution lies in the "tail" of the former being longer. This is to say that its probability of having large amplitude is greater than that of the latter.

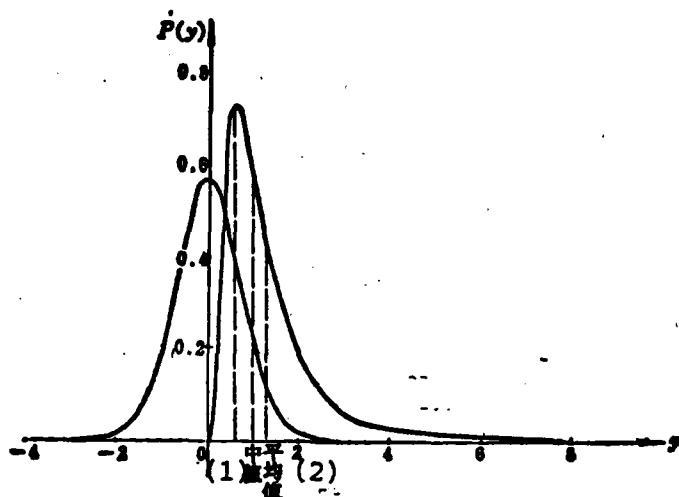


Fig. 5.4 Function Figure of the Logarithmic-Normal Distribution

Key: 1. Mid-value
2. Mean value

Actual measurement results of sea clutter show that when in high resolution radar and relatively diverse sea conditions, the amplitude distribution of its clutter is even closer to a logarithmic-normal distribution [3]. Fig. 5.5 gives actual measurement results. Because the vertical coordinates are drawn according to the logarithmic-normal distribution, the real logarithmic-normal distribution in the chart should appear as a straight line. We can see from the figure that the actual measurement results are even closer to the logarithmic-normal distribution but deviate from the Rayleigh distribution.

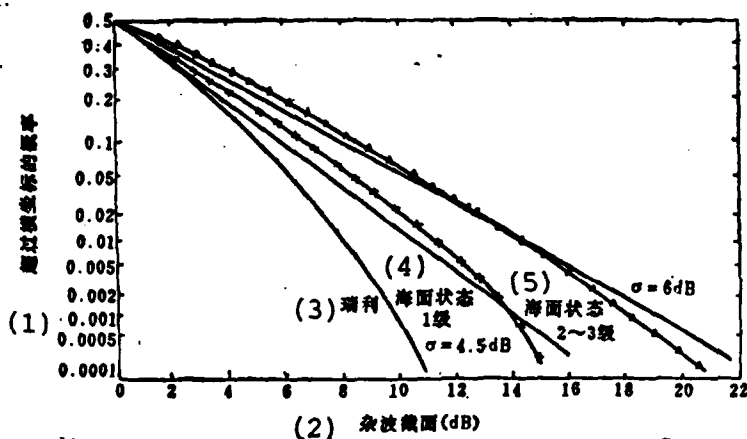


Fig. 5.5 Actual Measurement Results of the Amplitude Distribution of Sea Clutter (X Wave Band of Airborne Radar With Pulse Width of $0.02\mu_s$ and Grazing Angle of 47°)

- Key: 1. Probability exceeding horizontal coordinates
 2. Clutter section
 3. Rayleigh
 4. Sea conditions, first grade
 5. Sea conditions, grades 2-3

Recently, many people have also proposed that the amplitude distribution of sea clutter can be approximated by the Weibull distribution [4]. The so-called Weibull distribution can be expressed by the following formulas

$$\begin{aligned} p(R) &= \alpha \cdot \ln 2 \cdot R^{\alpha-1} \exp(-\ln 2 \cdot R^\alpha) & R > 0 \\ p(R) &= 0 & (1) \text{ 其他值} \end{aligned} \quad (5.8)$$

Key: 1. Other value

In the formulas, R is the detection output voltage value after mid-value normalization and $R=V/V_m$. α is the variant related to

the gradient of this distribution.

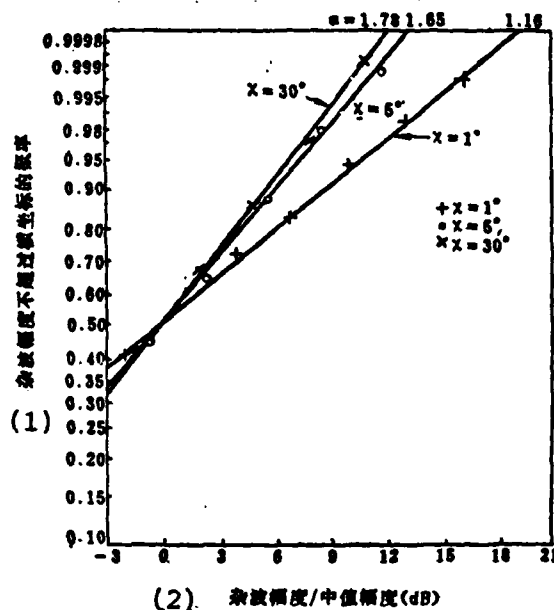


Fig. 5.6 Comparison of the Actual Measurement Results of the Sea Clutter's Amplitude Distribution and the Weibull Distribution (Sea Conditions are Grade 3 with Ku Wave Band, Horizontal Polarization and $0.1 \mu_s$ Pulse Width)

Key: 1. Probability of clutter amplitude not exceeding horizontal coordinates
2. Clutter amplitude/mid-value mid-value amplitude (dB)

We can obtain a very suitable Weibull distribution from the actual measurement results of sea clutter. Fig. 5.6 gives the measurement results on sea clutter. The radar used had Ku wave band, a beam width of 5 degrees, horizontal polarization and a pulse width of 0.1 microseconds. The vertical coordinates in the figure are drawn according to the Weibull distribution. Therefore, the Weibull distribution in the figure should be a straight line. We can see from the figure that the measured results basically lie in a straight line and only when in different grazing angle γ is there different gradient parameter α values. When the beam width of another X wave band

high resolution radar is 0.5 degrees, its pulse width is 0.02 microseconds and its grazing angle is 4.7 degrees, its amplitude distribution is measured to be very close to the Weibull distribution and its gradient parameter $\alpha=1.452$.

5.13 Mean Doppler Frequency Shift and Frequency Spectrum Width of Sea Clutter

Due to the wind force action sustained by the sea, a mean Doppler frequency shift exists in sea clutter. To extend the obtained results to all of the frequency bands, the mean Doppler frequency shifts are commonly expressed by the mean velocity.

Naturally, the mean velocity of sea clutter is directly related to wind velocity and wind direction. However, actual test results show that the mean velocity of sea clutter is not only related to wind velocity and wind direction but to electromagnetic waves and polarization direction as well. Fig. 5.7 shows the actual measurement results [2].

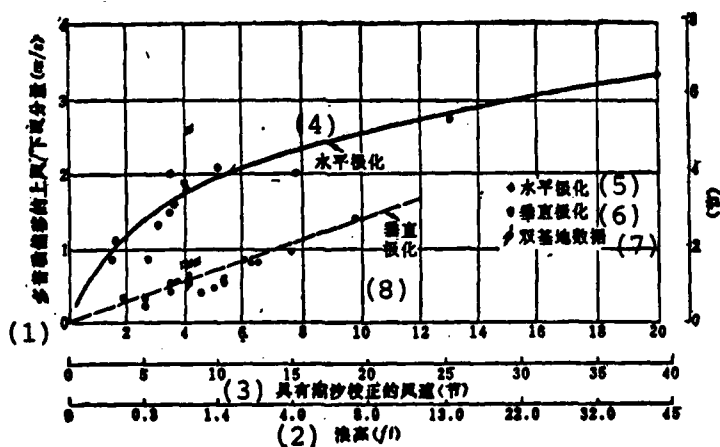


Fig. 5.7

Fig. 5.7 Relationship Between the Mean Velocity of Different Polarization Sea Clutter and Wind Velocity and Wave Height

- Key: 1. Upward wind/anabatic wind component (m/s) of Doppler shift
2. Wave height (ft)
3. Wind velocity with tide corrections (knots)
4. Horizontal polarization
5. Horizontal polarization
6. Vertical polarization
7. Double base data
8. Vertical polarization

We can see from the figure that under the same type of wind velocity, the mean Doppler frequency shift of horizontal polarization electromagnetic waves is two to four times that of vertical polarization. Further, the limit value of the sea clutter's mean velocity is about 7 knots. Although the horizontal coordinates in the figure are wind velocity, yet the mean Doppler frequency shift of the horizontal polarization, the wind velocity and the wave height are all related. The mean Doppler frequency shift of the vertical polarization is primarily related to the wave height and directly related to the orbital velocity of the gravitational waves. These results were measured in a grazing angle range of 0.1 to 10 degrees.

Naturally, the mean Doppler frequency shifts of the sea clutter are also related to wind direction. Fig. 5.8 shows the relationship of the mean velocity and wind direction when in different polarizations [2].

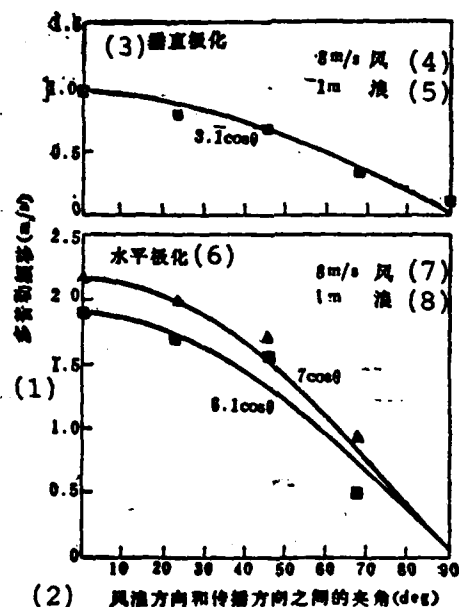


Fig. 5.8 Relationship of the Mean Doppler Frequency Shift of the Sea Clutter and the Wind Direction When There are Different Polarizations

- Key:
1. Doppler frequency shift (m/s)
 2. Included angle between wind-wave direction and transmitting direction (deg)
 3. Vertical polarization
 4. 8 m/s wind
 5. 1 m wave
 6. Horizontal polarization
 7. 8 m/s wind
 8. 1 m wave

We can see from the figure that a cosine relationship exists between the mean Doppler frequency shift of the sea clutter frequency spectrum and the included angle of the wind direction. These test results were carried out at 5.8 kilomegahertz.

Because the radial velocity of each scattering object of the

waves has a certain distribution, this causes the Doppler frequency of the sea clutter to also have a certain distribution. When the sea becomes turbulent, the distribution of its velocity enlarges and the frequency spectrum of the clutter becomes wider. Therefore, the Doppler frequency spectrum width of sea clutter is directly related to the sea surface conditions.

Usually, the Doppler frequency spectrum width σ_f of sea clutter is also expressed by velocity frequency spectrum width σ_v . The following relationship exists between σ_f and σ_v

$$\sigma_f = \frac{\lambda}{2} \sigma_v \quad (5.7)$$

In the formula, λ is the radar's operating wave length. σ_v and σ_f are the standard differences of the velocity and frequency.

The following relationship exists between the standard difference and half power point width for the Gaussian shaped frequency spectrum

$$\left. \begin{aligned} \sigma_v &= 0.42 \Delta v \\ \sigma_f &= 0.42 \Delta f \end{aligned} \right\} \quad (5.8)$$

After analysis of a large number of tests on the envelope detection of sea clutter signals, results as shown in fig. 5.9 can be obtained [2]

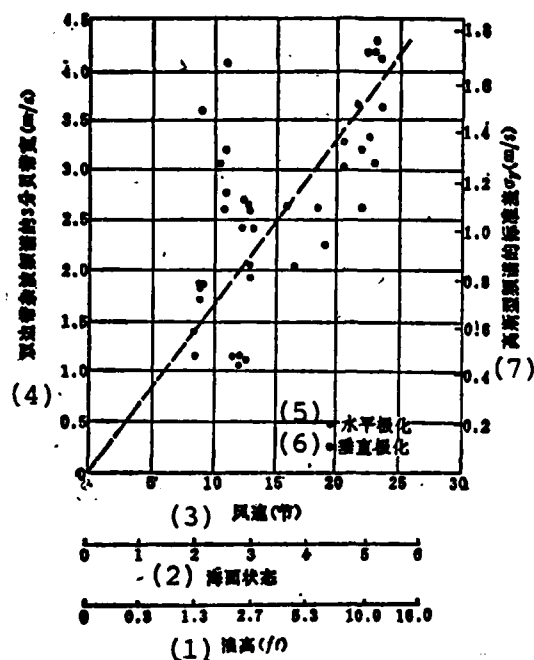


Fig. 5.9 Relationship of the Frequency Spectrum Width of Envelope Detected Sea Clutter Signals, and the Wind Velocity and Sea Conditions

- Key:
1. Wave height (ft)
 2. Sea conditions
 3. Wind velocity (knots)
 4. 3 decibel bandwidth of two sided band clutter frequency spectrum (m/s)
 5. Horizontal polarization
 6. Vertical polarization
 7. Standard difference σ_v of Gaussian frequency spectrum (m/s)

The figure gives the relationship between the frequency spectrum width of the sea clutter, the wind velocity, sea conditions and wave height when there is different polarization. We know from the figure that there is basically a direct relation between these two. The frequency spectrum of seas with waves ranging from calm to typhoon (wave heights from 1 to 6

feet) is in the 1-4 meter/second range.

5.1.4 Time and Space Decorrelation of Sea Clutter

When the Doppler frequency spectrum width is known, it is not difficult to find the decorrelation time of sea clutter.

Naturally, the decorrelation time forms an inverse ratio with the width of the Doppler frequency spectrum. It can be understood in this way: the higher the stormy waves of the sea the wider the sea clutter's Doppler frequency spectrum width and thus the shorter the decorrelation time of the sea clutter.

If the shape of the sea clutter frequency spectrum is a Gaussian shape, then

$$S(f) = S_0 e^{-f^2/\sigma_f^2} \quad (5.9)$$

We know from the analysis that the decorrelation time of the sea clutter is

$$\tau_c = \frac{1}{\sqrt{2\pi}\sigma_f} = \frac{\lambda}{2\sqrt{2\pi}\sigma_v} \quad (5.10)$$

This formula can be expressed by the straight lines in fig. 5.10.

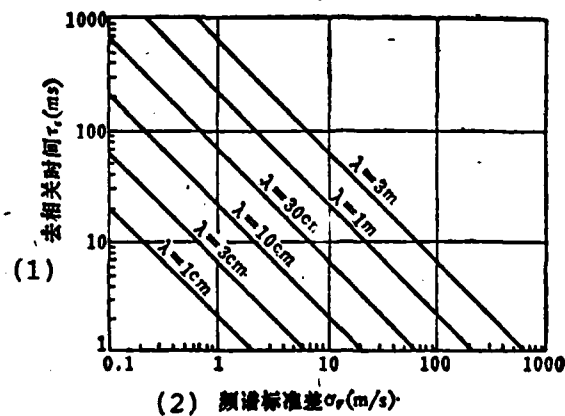


Fig. 5.10 Relationship of the Decorrelation Time of Sea Clutter and the Frequency Spectrum Width

Key: 1. Decorrelation time τ_c (ms)
 2. Frequency spectrum standard difference σ_v (m/s)

As regards certain fixed wind velocity or sea conditions, we can obtain: the Doppler frequency spectrum width (expressed with velocity) σ_v from fig. 5.10 and afterwards obtain its decorrelation time from fig. 5.10 or formula 5.10 based on the radar's operating wave length.

For example, for second grade sea conditions, that is, when equal to a wind velocity of 8 knots, we can obtain σ_v as 0.6 meters/second from fig. 5.9. From fig. 5.10 we can obtain that the decorrelation time of sea clutter for radar with 3 centimeter wave length is about 10 milliseconds and about 30 milliseconds for 10 centimeter wave length radar. We can consider that this is far greater than the pulse repetition frequency of radar. In other words, it can be considered that the sea clutter is correlated in many adjacent echoes.

The space decorrelation of so-called clutter signals is the correlation between the two separated radial sea reflecting signals. Because measurement of the time interval of these two signals is very short, the time decorrelation can be disregarded.

Tests have proven that the interval required to obtain two statistically independent echoes is approximately the range corresponding to one pulse width.

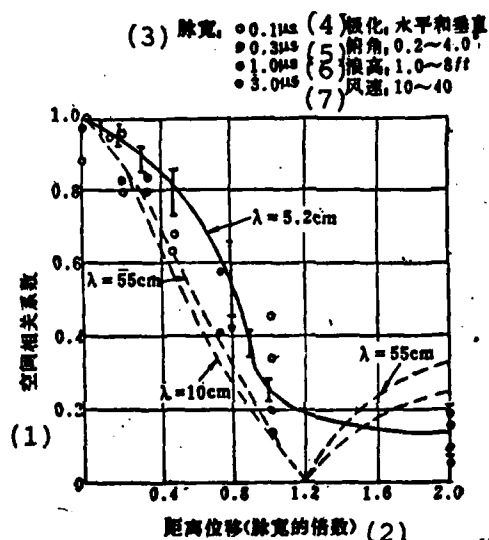


Fig. 5.11 Space Correlation of Radar Sea Clutter

Key: 1. Space correlation coefficient
 2. Range shift (multiple of pulse width)
 3. Pulse width
 4. Polarization: horizontal and vertical
 5. Angle of depression
 6. Wave height
 7. Wind velocity

Fig. 5.11 is the relationship between the space correlation coefficient when the wavelength is measured at 55 centimeters, 10 centimeters and 5.2 centimeters, and the range interval with a reduction of the pulse width [2]. We can see from the figure that whether a very short wave S wave band or C wave band, all

of the pulse width relations are quite evident. Thus, to reduce the space correlation, it is necessary to use very narrow pulse radar.

Furthermore, space correlation also exists in the azimuth direction. This is mainly determined by the antenna's azimuth beam width.

5.2 The Effects of Sea Clutter on Target Detection

Because sea clutter has a relatively large equivalent reflection area, its distribution possibly extends beyond the radar's range of visibility. We know from the last section that the equivalent reflection area of sea clutter is the area determined by the radar pulse unit multiplied by the reflection coefficient [formula (5.1)]. For example, if the horizontal beam width of the radar is 1 degree and the pulse width is 1 microsecond, when the range is 10 nautical miles, the area irradiated by the radar is 48,000 meters². When the reflection coefficient of the sea surface is -30 decibels, its equivalent reflection area is 48 meters². Such a large equivalent reflection area can be compared to a small ship.

When the equivalent reflection area of the sea clutter exceeds a certain limit value, the signal-clutter ratio S/C is equal to a certain minimum value $(S/C)_{\min}$ and it is then considered that there is no way of detecting the target.

We know from the above that

$$(S/C)_{\min} = \frac{\sigma}{\sigma_0 \theta_0 R_{\max}^2 C (\tau/2) \sec \phi} \quad (5.11)$$

or it can be written as

$$R_{\max} = \frac{\sigma}{(S/C)_{\min} \sigma_b \theta_b C(\tau/2) \sec \phi} \quad (5.12)$$

In these formulas, σ is the target's equivalent reflection area; θ_b is the horizontal beam width; τ is the pulse width; and ϕ is the grazing angle.

We can discover from these formulas that when the radar detection of targets is mainly limited by clutter and not by receiver noise waves, its maximum detection range is unrelated to transmitter power. This is because when receiver power is increased; this not only strengthens the echoes from the target but also increases the clutter intensity from sea wave reflection. Yet, this is not equivalent to saying that the power of the transmitter can be fully reduced because if we reduce the transmitter's power the clutter signal intensity can reduce to a level comparable to the receiver's noise waves. At this time, the radar's detection will, similar to common radar, be limited by receiver noise waves. In other words, the above formulas can only be used when the clutter signal intensity is far greater than the receiver's noise waves. Therefore, there is no noise coefficient value in the formulas. For the same reason, antenna gain does not appear in the formulas and it is hoped that the smaller the horizontal beam width θ_b the better. This is only to reduce the range irradiated by one pulse. We can also see from the formulas that to increase the ability to detect targets from the clutter, the narrower the pulse width used the better. This is different from the concept of most radar equations. The narrowing of the transmitted pulses can reduce the mean power of the irradiated target or can increase the bandwidth of the receiver causing the noise waves to enlarge. However, this can only reduce the range of the noise wave limitation. Moreover, this can actually increase the

ability to detect targets in the clutter limitation range.

The $(S/C)_{\min}$ in the formula which is similar to the minimum in a common noise wave limit radar equation can detect the signal-clutter ratio. To determine the minimum signal-clutter ratio in a given detection probability and mean false alarm time, it is only necessary to know the statistical characteristics of the clutter.

As mentioned previously, it is commonly assumed that sea clutter is composed from a large quantity of reflecting objects and therefore its statistical characteristics can be expressed with a Rayleigh distribution (equivalent to narrow band white noise waves). Yet actual measurements show that the statistical characteristics of sea clutter are also related to the transmitted pulse width, beam width and the polarization of the transmitted electromagnetic waves. When the pulse width is over 1 microsecond, the beam width over 2 degrees, the transmission carrier frequency between 3 and 6 kilomegahertz and there is a relatively calm sea, the statistical characteristics of the sea clutter can be approximated by a Rayleigh distribution. Yet, when the transmission carrier frequency is above 6 kilomegahertz, the pulse width smaller than 0.1 microseconds and the beam width smaller than 1 degree, its distribution deviates from a Rayleigh distribution. The deviation of horizontal polarization is more serious and approaches a logarithmic-normal distribution. For example, radar with an X wave band has a pulse width of 8 millimicroseconds and its horizontal beam width is 0.9 degrees. When in vertical polarization, the ratio of its standard difference and mean value is between 1.5 and 2.1 (the specific value of the Rayleigh distribution is 1.0). The ratio of the standard difference and mean value of horizontal polarization is between 6.0 and 13.0. This indicates that even more peaks will appear on the A type display. This is also to say

that when in the same mean value the horizontal polarization will produce more false alarms than the vertical polarization. This can greatly influence the detection of signals.

Aside from this, because the first power (and not fourth power) of the radar's maximum detection range in formula (5.12) directly forms a proportional relationship with all of the parameters, when these parameters change because of inaccurate estimation or for other reasons, this can tremendously affect the maximum detection range in the sea clutter. For example, when the real target's reflection area is 3 decibels smaller than the estimate, in the equation for ordinary, noise limiting radar, it can cause an 84% decrease in maximum detection range, but in the equation for clutter limiting radar it can cause the maximum detection range to decrease by one half. Consequently, radar design personnel must very carefully estimate these parameters to avoid the radar being designed not conforming to requirements.

On the surface, the range equation of the clutter limit forms an inverse ratio with the first power of the range. Yet, in real situations, the echoes of target reflection form an inverse ratio with the fourth power of the range and the sea clutter forms an inverse ratio with the third power of the range (because the equivalent reflection area of the sea waves forms a direct ratio with the first power of the range and eliminates the first power). However, in far distance interference areas, the target echo forms an inverse ratio with the eighth power of the range. The intensity of the sea clutter in the interference area forms an inverse ratio with the seventh power of the range. If the target has a fixed height, then the critical angle of the target is smaller than the critical angle of the clutter. The interference area of the target is even further than the interference area of the clutter. A strange phenomenon can be produced at this time. That is, the target can be detected at close range and when the range enlarges

the target will be drowned out in the clutter. Yet, when the range increases again, the target can be detected up to the maximum area until the target echo and clutter are completely drowned out in the noise waves of the receiver. This can be explained by the schematic in fig. 5.12 [1].

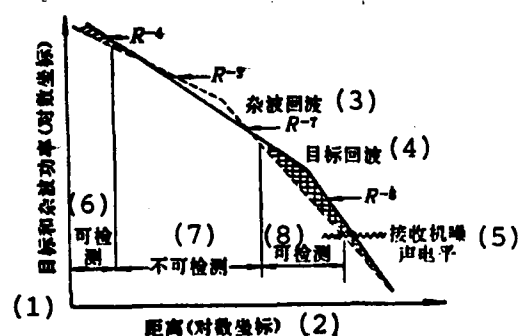


Fig. 5.12 The Target Echoes and Clutter Power Change With the Range (the Shaded Area Indicates That the Target - Clutter Ratio is Detectable)

- Key: 1. Target and clutter power (logarithmic coordinate)
 2. Range (logarithmic coordinate)
 3. Clutter echo
 4. Target echo
 5. Receiver's noise level
 6. Detectable
 7. Non-detectable
 8. Detectable

The solid line in the figure is the target echo power of the logarithmic coordinates which changes with the range. At first, it forms an inverse ratio with the fourth power of the range and later changes to form an inverse ratio with the eighth power of the range. The broken line is the change of the clutter power with the range. At first it forms an inverse ratio with the third power of the range and later forms an inverse ratio with the seventh power of the range. The shaded

area indicates the target echo intensity exceeding the clutter and this can be detected.

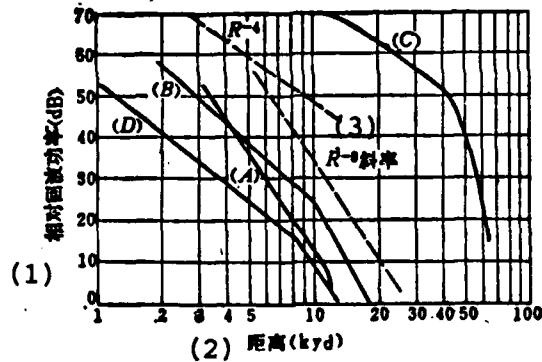


Fig. 5.13 Actual Measurement Results of Different Ship Targets in Different Wave Lengths

- (A) - $\lambda = 150$ centimeters $h_a = 470$ foot small boat;
- (B) - $\lambda = 9.1$ centimeters $h_a = 21$ foot cargo ship;
- (C) - $\lambda = 10$ centimeters $h_a = 470$ foot destroyer;
- (D) - $\lambda = 3.2$ centimeters $h_a = 60$ foot, 40 ton trawler.

Key: 1. Relative echo power (dB)
 2. Range (kyd)
 3. R^{-8} slope

This theory has already been experimentally verified. Fig. 5.13 draws the actual measurement results of different ship targets when there are different wavelengths. Three different wavelengths are used in the figure for the actual measurement of four different types of ships. It can be seen that almost all have noticeable turns from R^{-4} to R^{-8} . Its turning point range occurs in $R = 4h_a h_t / \lambda$ (in this expression h_a is the antenna's height and h_t is the targets height). Only when in a relatively high angle of elevation (curve C) is the turning relatively mild.

The above discussion is only applicable in situations when the grazing angle is relatively small. Yet, when the grazing

angle is very large and is close to vertical (e.g., airborne radar detecting targets on the water), the situation is different. At this time, the irradiated area is mainly determined by the polyhedral angle Ω_b of the radar beam but is unrelated to the radar's transmission pulse width. At this time, the signal-clutter ratio is determined by the following formula.

$$\frac{S}{C} = \frac{\sigma}{\sigma_0 R^4 \Omega_b / \sin \phi} \quad (5.13)$$

At this time, the maximum detectable range is

$$R_{max}^4 = \frac{\sigma G \sin \phi}{\sigma_0 4 \pi (S/C)_{min}} \quad (5.14)$$

In the formula, G is the antenna gain.

This formula forms an inverse ratio with the square of the range of different areas of formula (5.8). It is unrelated to the transmitted pulse width. In reality, when in a grazing angle which is close to vertical, the value of σ_0 is very large, approaching 0 decibels.

Lastly, although formulas (5.12) and (5.14) are for the detection of single pulses, yet when the number of pulses increases these formulas can still be used because with the increase of the target echo, the clutter echo number also increases. In other words, at this time, use of the accumulation technique cannot raise the signal-clutter ratio.

5.3 The Method of Suppressing Sea Clutter and Its Existing Problems

Here, we are not prepared to introduce in detail each of

the various methods of suppressing sea clutter but will only discuss and compare the basic principles and performances.

To reduce the jamming of sea clutter, it is first necessary to, as best as possible, reduce the intensity of the sea clutter. We know from formula (5.1) that to reduce the intensity of sea clutter it is necessary to, as best as possible, increase the resolution of the radar, that is, to reduce the azimuth beam width and reduce the transmitted pulse width. Yet, this can bring about a series of problems. After the azimuth beam becomes narrow, two problems will be produced. One can cause the distribution of the sea clutter to deviate from a Rayleigh distribution and become even closer to a logarithmic-normal distribution. As mentioned previously, this can cause the number of peaking pulses to increase and as a result enlarge the false alarm rate. The other problem is reducing the number of pulses which can provide accumulation. More succinctly, this is reducing the beam's staying time. If this staying time is smaller than the correlation time of the sea clutter (about 10 milliseconds in the X wave band), then none of the obtained clutter pulses are independent. This can reduce the effective accumulated gain of the target in a clutter background.

The narrowing of the transmitted pulse can produce three problems. One is the same as with the narrowing of the beam width. It can cause the statistical distribution of the sea clutter to become even closer to a logarithmic-normal distribution and thus enlarge the false alarm rate. Another problem is the possible reduction of the mean power of the radar transmission which reduces the detection range under a noise wave limitation. Although this problem can be remedied by pulse compression yet it can result in a large increase of the equipment's complex level. The third problem is that extremely narrow pulses can also cause the Doppler frequency spectrum

width of the sea clutter to become narrow because it can already discriminate the single sea waves at this time. For example, some people use narrow beam X wave band radar with a pulse width of only 8 millimicroseconds. When in a wind velocity of 8-15 knots, the measured σ_0 value is in the 0.0001 to 0.0036 meters/second range. This enlarges the clutter's correlation time to 2-60 seconds. Such a long correlation time causes it to be completely impossible to raise the signal-clutter ratio by accumulation. Therefore, the narrowing of the pulse width also has certain limitations.

The other method for reducing the influence of sea clutter is the so-called constant false alarm rate signal processing technique. At present, this technique is mainly carried out in scanning but not between scanning. That is, it mainly considers the problem of the false alarm rate constant of the first threshold (amplitude quantization) output.

The earliest and simplest constant false alarm rate used was the logarithmic amplifier fast time constant circuit (lg-FTC) [5]. We know that the logarithmic amplifier not only has a very large dynamic range but also has the special feature of output variance as the constant. That is, when the input is a Rayleigh distribution, no matter how large the variance of the input, the variance of its output is always constant; equivalent to $a^2 \pi^2 / 24$ (in this expression, a is the slope of the logarithmic characteristics). Only the mean value of the output changes with the mean value of the input. Sea clutter has relatively large variance and mean value at close range. Both of these decrease with the enlargement of the range. After the amplitude distribution of the sea clutter which is close to a Rayleigh distribution is added to a logarithmic amplifier, its output becomes a constant fluctuation which only has a waveform with a mean value which changes with the range (see

fig. 5.14 (b) and (c). This output can only be added to a circuit with a fast time constant which can eliminate its mean component and become completely analogous to the receiver noise wave signals. By adding this type of waveform to a quantized circuit with fixed threshold level, we can obtain a constant false alarm rate.

When the input is a logarithmic-normal distribution, we can use a logarithmic-normal amplifier [6]. This type of amplifier has an even larger suppression effect on the peak pulses with large amplitude.

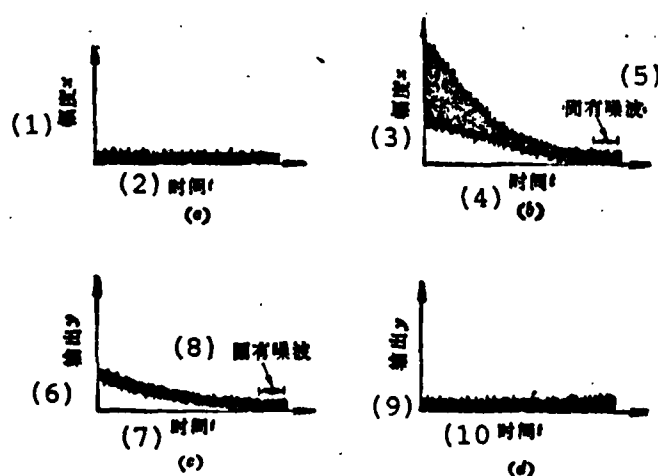


Fig. 5.14 Waveform Changes of Sea Clutter After Using Logarithmic-Fast Time Constant Circuits

- (a) Receiver's internal noise waves;
- (b) Sea clutter;
- (c) Using logarithmic amplifier output;
- (d) Output after using fast time constant circuits

Key: 1. Amplitude x
 2. Time t
 3. Amplitude x
 4. Time t
 5. Intrinsic noise wave
 6. Output y

Key: 7. Time t
 8. Intrinsic noise wave
 9. Output y
 10. Time t

Modern constant false alarm rate circuits widely utilize digital circuits. At present, the most commonly used is the logarithmic unit mean selection of a large false alarm circuit [6]. In reality, this evolves from the digitization of the above mentioned logarithmic fast time constant circuit. Fig. 5.15 is a flow chart of its principle. After the Rayleigh distribution signals pass through the logarithmic detector, we can obtain an output with a constant variant. The unit mean method is used to reduce its mean value, that is, in each $n/2$ unit before and after the detected unit, we use a tap delay line to derive the transient amplitude of each unit. Afterwards, we carry out summation to obtain the mean. To eliminate the boundary effects we use the method of selecting the larger of the mean values of the two sides. When this type of circuit is in 20 decibel step jumping clutter, the increase of the false alarm rate will not reach a parametric level.

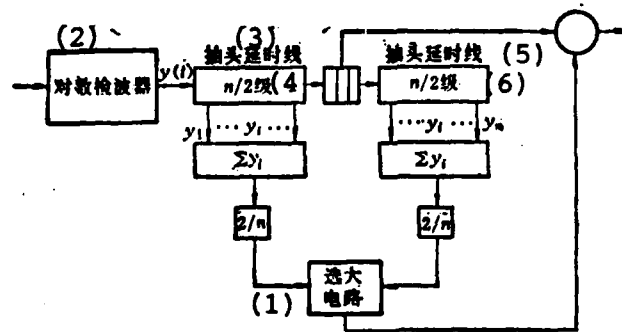


Fig. 5.15 Flow Chart of the Principle of the Logarithmic Two Sided Unit Mean Selection a Large False Alarm Rate

Key: 1. Selected large circuit
 2. Logarithmic detector

Key: 3. Tap delay line
 4. $n/2$ level
 5. Tap delay line
 6. $n/2$ level

When this type of circuit is used to suppress sea clutter, it is still a type of parametric detector. That is, its input signal distribution (Rayleigh) is known and there is only an unknown parameter which requires estimation. As mentioned previously, the distribution of the sea clutter is often not accurately detailed in advance but usually deviates from the Rayleigh distribution. Therefore, at present, the non-parametric detector is commonly used. This type of detector does not require a known clutter distribution to be able to obtain the output of the constant false alarm rate. The simplest non-parametric detector is the "rank value detector." The chart of its principle is shown in fig. 5.16. It compares the amplitudes of the detected unit and each $n/2$ unit; when its amplitude is larger than the latter's, the comparators output is 1 otherwise it is 0. The summation of the comparator's output can obtain a rank value R corresponding to the detected unit. By comparing this rank value and a fixed threshold we can obtain a constant false alarm rate output unrelated to the input distribution.

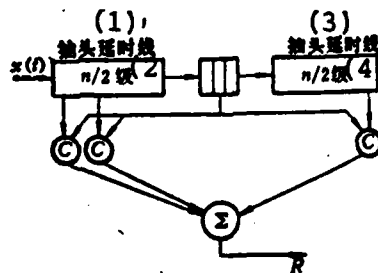


Fig. 5.16

Fig. 5.16 Chart of the Principle of the Rank Value Detector

- Key: 1. Tap delay line
2. $n/2$ level
3. Tap delay line
4. $n/2$ level

The major shortcoming of this type of constant false alarm rate processor is that it only takes the false alarm rate into account in one scanning, that is, the first threshold false alarm. Yet, because sea clutter has very strong correlation, that is in many continuous scanings, its peak positions have very great correlation. Therefore, after spot shaped sea clutter uses this type of constant false alarm rate circuit, there can still form a false alarm rate output in the detector. Moreover, when using the amplitude discrimination method, it is very difficult to obtain a visible angle in the clutter.

The frequency spectrum discrimination method showed relatively good results for suppressing sea clutter. This method uses the difference of the sea clutter and the target echo's Doppler frequency spectrum. For example, the typical moving target display and Doppler system use the target echo's Doppler frequency shift. Yet, because the sea clutter itself has Doppler frequency shifts, when this frequency shift is relatively large, it will also be displayed by the moving target in most moving target display systems.

Improvement factor I of a moving target display system is defined as the specific value of the output signal-clutter ratio and input signal-clutter ratio, that is

$$I = \frac{\bar{S}_o/C_o}{\bar{S}_i/C_i} \quad (5.15)$$

If the clutter attenuation after using a certain system is CA, then

$$CA = \frac{C_i}{C_o} \quad (5.16)$$

Then the improvement factor can be written as

$$I = \frac{\bar{S}_i}{S_i} CA \quad (5.17)$$

We know from analysis that the improvement factor of a primary canceller for a Gaussian frequency spectrum can be written as

$$I_i = \frac{1}{1 - \exp(-2(2\pi\sigma_v/\lambda F_p)^2) \cos 4\pi V_o/\lambda F_p} \quad (5.18)$$

In the formula, σ_v is the standard difference of the clutter frequency spectrum (expressed by meters/second);
 V_o is the mean value of the clutter frequency spectrum (meters/second);
 λ is the wavelength (meters), F_p is the pulse repetition frequency.

For this reason, we can draw the relationship between the improvement factor and clutter frequency spectrum width σ_v (fig. 5.17) [3]. The solid lines in the figure indicate the situation wherein mean Doppler frequency shift V_o is zero and the broken lines are the situation when $V_o \neq 0$.

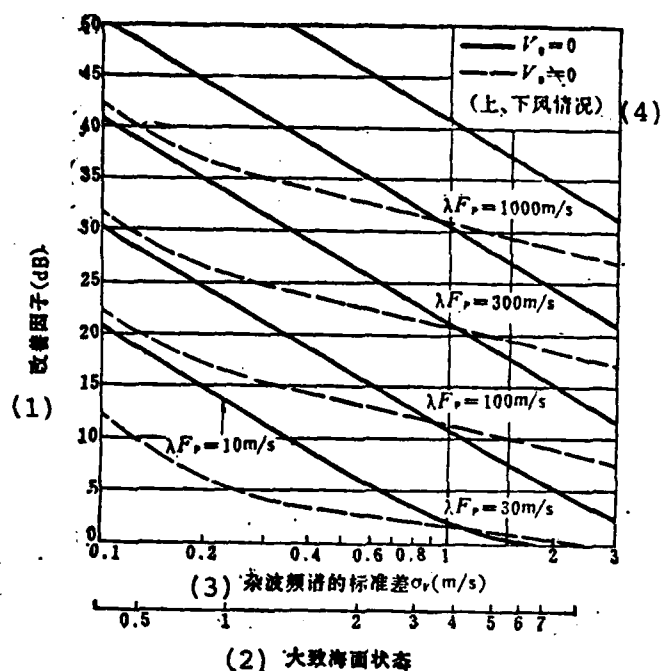


Fig. 5.17 Limitation of the Single Canceller's Improvement Factor on Sea Clutter (Horizontal Polarization)

- Key: 1. Improvement factor (dB)
 2. Approximate sea condition
 3. Standard difference of clutter frequency spectrum
 4. (Up and downward wind situation)

Because σ_v is related to a certain sea condition as shown in fig. 5.9, the abscissa also draws the corresponding sea condition. We know from the figure that the more adverse the sea conditions the smaller its improvement factor. Moreover, when the mean Doppler frequency shift is not equal to zero the situation is even more wanting and when the wave length shrinks or repetition frequency lowers (i.e., λF_p decreases), the improvement factor is more wanting. For example, when radar operates at 3 centimeters, the repetition frequency

F_p is 1,000, the sea condition is level 1 and its improvement factor is only 5 decibels.

In the past, the wind velocity compensation method was used to compensate for the mean Doppler frequency. Yet, because the mean Doppler frequency shift is not only related to the wind velocity but also to the wind direction, when the antenna rotates, it cannot realize total compensation.

There is another relatively effective method for shipborne and airborne radar called the "time average clutter coherent moving target display system" (TACCAR). It is also now called the self adapting moving target display system. This type of system can quickly measure the mean Doppler frequency shift of the clutter and at the same time the notch of the clutter suppression filter will automatically align the clutter frequency spectrums with the Doppler frequency shifts. The drawback of this method is that the equipment is relatively complex and it cannot simultaneously suppress clutter with different Doppler frequency shifts.

The pulsed Doppler system possesses parallel Doppler filter sets. At present, all Doppler filter sets usually use the fast Fourier transformation method for the signals to accomplish equivalent formation. It has excellent suppression power for various types of clutter.

Moreover, at the same time, it can suppress various types of clutter with different Doppler frequency shifts. Yet, its equipment is even more complex, its manufacturing cost is higher and it cannot be fitted on most shipborne radar. At present, it is mainly used in airborne radar to suppress very strong ground clutter. However, when the wind and waves are relatively large and the clutter frequency spectrum widens, the necessary band-suppression filter becomes very wide and

as a result filters out the useful target in the very high velocity range.

5.4 Frequency Correlation of Sea Clutter

Just as frequency agility can cause target echo decorrelation, the jump of the transmitted frequency can cause sea clutter decorrelation. However, because sea clutter can be viewed as a collection of a large number of reflecting objects, its frequency correlation and the target's frequency correlation also have their differences. We will first theoretically calculate the frequency correlation of sea clutter.

We let $R_x(i, j)$ be the standardized correlation coefficient between the i clutter and j clutter. Moreover, we let X and X_j be the voltage received in i times and j times.

We know from the definition of the correlation coefficient that

$$R_x(i, j) = \frac{\overline{X_i X_j}}{\overline{X^2}} \quad (5.19)$$

The clutter signal voltage received can be obtained from the convolution of transmitted waveform $\mu(t)$ and clutter response $c(t)$.

$$X_i = c(t) * \mu_i(t)$$

For the transmitted pulse with a carrier frequency of f_i and a bandwidth of γ_p , $\mu_i(t)$ can be written as

$$\mu_i(t) = \text{rect}\left(\frac{t}{\tau_p}\right) \cos(2\pi f_i t) \quad (5.20)$$

The autocorrelation of X is

$$\begin{aligned} \overline{X_i X_j} &= \overline{(c(t) * \mu_i(t)) (c(t) * \mu_j(t))} \\ &= \mathcal{F} \langle (c(t) * \mu_i(t)) (c(t) * \mu_j(t)) \rangle \\ \overline{X_i X_j} &= \int_{-\infty}^{\infty} c^2(f) \mu_i(f) \mu_j(f) df \quad (5.21) \end{aligned}$$

In the formula, $c(f)$ and $\mu(f)$ are the Fourier transformations of $c(t)$ and $\mu(t)$.

If the clutter echo from a radar's transmitted pulse can be viewed as the collection of a large quantity of randomly distributed scattered points, then $c(t)$ is the sum of the tightly distributed $\delta(t)$ function in time. This also accurately expresses white noise waves. Therefore, its frequency spectrum $c(f)$ can be taken as uniformly distributed and $c^2(f)$ can be replaced by power density c_0 .

For the i transmitted pulse

$$\mu_i(f) = \frac{\tau_p}{2} \text{sinc}(\tau_p(f + f_i)) + \frac{\tau_p}{2} \text{sinc}(\tau_p(f - f_i)) \quad (5.22)$$

In the formula,

$$\text{sinc}(X) = \frac{\sin(\pi X)}{\pi X}$$

When formula (5.22) is substituted into formula (5.21) we can obtain

$$\overline{X_i X_i} = \frac{c_s \tau_p^2}{4} \int_{-\infty}^{\infty} \{(\text{sinc} \tau_p(f + f_i) + \text{sinc} \tau_p(f - f_i)) \cdot (\text{sinc} \tau_p(f + f_i) + \text{sinc} \tau_p(f - f_i))\} df \quad (5.23)$$

Because the product of $\text{sinc} \langle \tau_p(f + f_i, f_j) \rangle$ and $\text{sinc} \langle \tau_p(f - f_i, f_j) \rangle$ is zero, after collation, we can obtain

$$\overline{X_i X_i} = \frac{c_s \tau_p^2}{4} \text{sinc}(\tau_p(f_i - f_i)) \quad (5.24)$$

and

$$\overline{X^2} = \frac{c_s \tau_p^2}{4} \quad (5.25)$$

By substituting formula (5.19) in we can obtain

$$R_x(i, j) = \text{sinc}(\tau_p(f_i - f_j)) \quad (5.26)$$

If received clutter signal x is added to the square-law detector, the output is y . We then know from the special features of the square-law detector that

$$\overline{y^2} / (\overline{y})^2 = 3$$

and

$$R_y(i, j) = \frac{\overline{y_i y_j}}{\overline{y}^2} = \frac{1}{3} + \frac{2}{3} R_x^2(i, j) \quad (5.27)$$

Therefore, we can consider that the normalized frequency correlation coefficient of the square-law detector output terminal's clutter signal is

$$P(\Delta f) = R_x^2(i, f) = \{\text{sinc}(\tau_p(f_i - f_i))\}^2 = \left(\frac{\sin \pi \tau_p \Delta f}{\pi \tau_p \Delta f} \right)^2 \quad (5.28)$$

In the formula, Δf is the change of the transmitted frequency and τ_p is the pulse width.

When $\tau_p \Delta f = 1$, the function of the $\sin^2 x/x^2$ form decreases to zero and when $\tau_p \Delta f > 1$, it decreases to 0.05. In other words, we can consider that when the frequency change is larger than $1/\tau_p$, its echo signals are uncorrelated.

Raindrops can be considered to be formed from a large number of small reflecting objects and are very close to this theoretical model. Thus, their frequency correlation coefficient can very well be expressed by the above formula.

However, the situation is totally different for sea clutter. This is especially the case when the beam width is small and the pulse width is narrow so that a large number of reflecting objects cannot be included in a transmitting pulse. Therefore, the above mentioned theoretical formula cannot describe the real situation very well.

In 1967, some people carried out a large number of tests using 5 centimeter (5.70 kilomegahertz) radar with a beam width of 2.5 degrees and horizontal and vertical polarization in different pulse widths [2]. The results are shown in fig. 5.18.

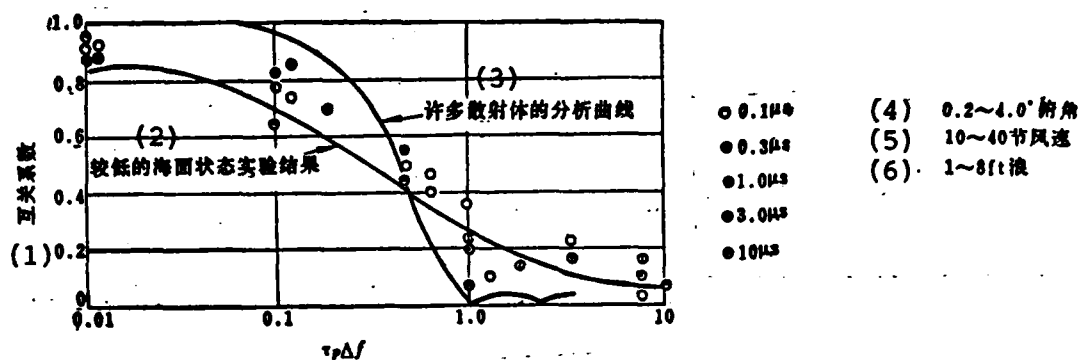


Fig. 5.18 The Product of the Frequency Correlation Coefficient and Pulse Width and the Frequency Difference

- Key:
1. Correlation coefficient
 2. Test results of relatively low sea conditions
 3. Analytical curve of many reflecting objects
 4. $0.2-0.4^\circ$ angle of depression
 5. 10-40 knots wind velocity
 6. 1-8 ft. waves

The top curve in the figure is the theoretical curve of $\sin^2 x/x^2$. The lower curve is the measured results when there are relatively calm sea conditions (wind velocity 3-9 knots, wave height $\frac{1}{2}$ -2 $\frac{1}{2}$ feet, 10° grazing angle). Each separation point represents the results of measurements when in relatively high sea conditions (wind velocity is 10-40 knots, wave height is 1-8 feet).

We know from the figure that the calmer the sea conditions the larger the deviation between the obtained results and the theoretical values. This is also understandable because the larger the wind and waves the more numerous the sea waves split into small scattering objects. Thus, it is relatively closer to assumed conditions during theoretical analysis. On the contrary, when the wind and waves are smaller, the sea

waves mainly combine into one wave.

When $\tau_p \Delta f \ll 1$, the test measured correlation coefficient is slightly smaller than 1. This is a result of the slight time decorrelation when there is a small frequency difference. When $\tau_p \Delta f > 1$ and the pulse width is 0.1, 0.3 and 1.0 microseconds, its correlation coefficient is always smaller than 0.2. If we take into account that the receiver's noise waves and sampling pulse have certain widths, when the correlation coefficient is smaller than 0.2 it can be considered that the echoes are basically decorrelated.

Polarization has a very small effect on the measurement of the frequency correlation coefficient. Fig. 5.19 is the measured frequency correlation coefficient of a C wave band radar with a pulse width of 0.1 microseconds under vertical and horizontal polarization [2].

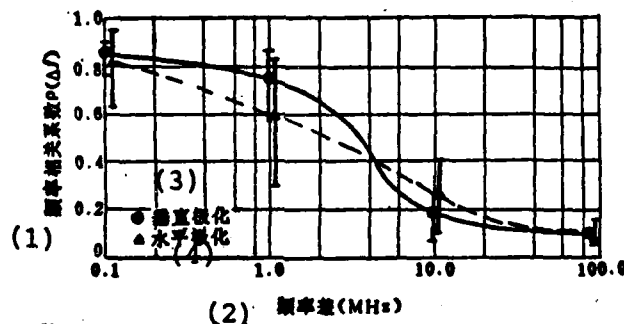


Fig. 5.19 The Frequency Correlation Coefficient When There are Different Polarizations (C Wave Band Radar With Pulse Width of 0.1 Microseconds)

In the figure, line band I indicates the distribution of the data and the point which the curve passes through is its mean value.

- Key: 1. Frequency correlation coefficient
 2. Frequency difference (MHz)
 3. Vertical polarization
 4. Horizontal polarization

The solid line in the figure is vertical polarization and the broken line is horizontal polarization. We can see from the figure that when the frequency difference is very small and very large, the results for the vertical polarization and horizontal polarization are basically the same and, moreover, the data's dispersity is also relatively large. The data dispersity of horizontal polarization is even larger yet the actual dispersity is not that serious. This is because when the data is measured in 5 seconds all of the frequencies are reduced the same average scattering power beforehand. In this way, the invariant data maintained during the entire measuring period is eliminatd.

Similar results were obtained from the tests on raindrop clutter [2]. When the radar operates at a fixed frequency, the measured correlation time of the raindrops is about 1-5 milliseconds (C wave band). If we use jumping frequency between the pulses, to attain very good decorrelation it is only necessary that the product of the jumping frequency difference and pulse width be equal to 1. Fig. 5.20 gives the test results when there are different pulse widths. The radar used in the test operated in the C wave band (5.7 kilomegahertz), the radar's beam diameter in the strobe gate area was 195 meters, the pulse width ranged from 0.4 to 3.2 microseconds and the frequency difference between the pulses was about 500 kilohertz. Thus, there is no $\tau \Delta f < 1$ data for the relatively wide pulse width.

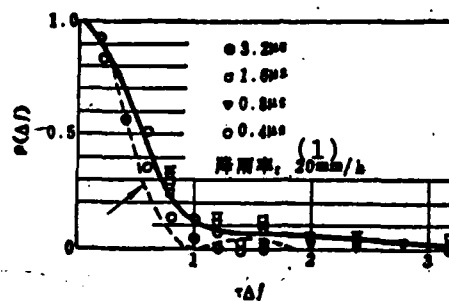


Fig. 5.20 Relationship of the Frequency Correlation Coefficient of Raindrop Clutter and Frequency Deviation (Frequency: 5.7 Kilomegahertz, Beam Diameter: 650 Feet)

Key: 1. Rainfall: 20mm/h

In the figure, each point represents 1,000 samples and are thus the result of a large quantity average. Rainfall during the test was quite high (reaching 20mm/h) and the obtained results matched well the theoretical curve of $\sin^2 x/x^2$. Thus, we know that the use of jumping frequency between pulses can also cause raindrop clutter to decorrelate well. This is also to say that we can use the frequency agility technique to eliminate the jamming of raindrop clutter [8].

Results for tests on ground clutter also showed that frequency correlation was minimum when the frequency difference is $\frac{1}{T}$. Fig. 5.21 draws the measured results of C wave band radar with a pulse width of 2 microseconds on ground clutter.

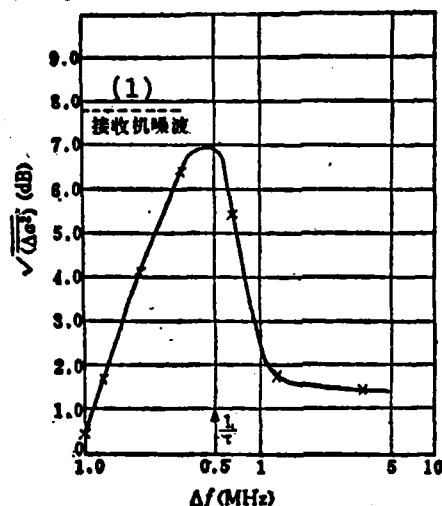


Fig. 5.21 Frequency Decorrelation Test Results of C Wave Band Radar With a Pulse Width of 2 Microseconds on Ground Clutter

Key: 1. Receiver's noise waves

In the figure, the vertical coordinate is the difference of the 2 adjacent carrier frequencies which is the mean square root value (expressed in decibels) of the pulse echo amplitude difference of Δf . The horizontal coordinate is the frequency difference Δf of the adjacent pulse. It can be discovered from the figure that when frequency difference $\Delta f = 1/\tau$, the mean square root value of its adjacent echo amplitude difference is maximum so that at this time the frequency correlation coefficient is minimal. When the frequency difference continuously enlarges, the mean square root value of its echo amplitude difference actually lowers so that its frequency correlation coefficient enlarges.

As mentioned previously, the characteristics of sea clutter frequency decorrelation do not exist in high resolution radar.

This is because when the radar's resolution unit is infinitesimal, it does not have a large number of reflecting objects but can only discriminate single sea waves. Its Doppler frequency spectrum correlation time is very long.

For example, the American Naval Research Laboratory used a high resolution radar with X wave band to carry out actual measurements [10]. This radar's beam width was 0.5° , pulse width was grade 2, short pulses were 20 millimicroseconds, long pulses were 100 millimicroseconds and the pulse repetition frequency was 2,560 hertz. Thus, its time decorrelation can be overlooked.

When radar is fitted on an aircraft, the aircraft's speed is 180 knots, range is 2 nautical miles, grazing angle is 4.7° , there is horizontal or vertical polarization, the flight direction is windward, leeward and cross, then the wind velocity is 25-31 knots, the height of the waves is 2.4 meters and the height of surges is 3.6 meters. Based on calculations of data measured at 12.8 second intervals, its decorrelation time was found in the large range of 12 milliseconds to 193 milliseconds. The total average is 94 milliseconds, the average decorrelation time for short pulses is 124 milliseconds and 64 milliseconds for long pulses. The smaller the resolution unit the longer the decorrelation time. However, they were all much longer than the decorrelation time (10 microseconds) of most low resolution X wave band radar.

We can see from this that frequency decorrelation and high resolution are mutually contradictory. However, to as best as possible reduce the effective reflection area of the sea clutter, it is not advantageous to use very low resolution radar which usually takes no effect on frequency decorrelation as the limit (about 1 degree, 0.1 microseconds).

5.5 Use of the Frequency Agility Technique to Suppress the Jamming of Sea Clutter

As mentioned previously, the best method for suppressing clutter jamming is frequency domain selection which is using the difference between the clutter and target echo on the frequency spectrum. Corresponding techniques are the self adapting moving target display and pulsed Doppler methods. However, their major drawback is that the equipment is too complex so that there are large technical difficulties.

Use of the frequency agility technique can also suppress sea clutter jamming. It basically uses the difference of the target echo and clutter in statistical characteristics when the radar operates in frequency agility. This is a type of time domain selection method.

We know from the last section that frequency agility can cause clutter decorrelation of the adjacent period. This resolves the as yet unsolved problem of most constant false alarm rate signal processors. After frequency decorrelation, the statistical characteristics of the clutter are completely the same as the noise waves. Therefore, the use of common incoherent accumulation can raise the signal-clutter ratio.

Although frequency agility can cause target echo decorrelation to become fast speed fluctuation, yet only after accumulating a certain number of waves does the target's echo amplitude gradually approach its mean value and the variance of the clutter greatly decrease. This can be seen by comparing the clutter of fixed frequency and the probability density function of the target's amplitude when there is frequency agility [11]. Fig. 5.22 delineates the changes of the probability density function of clutter and targets with clutter and targets with clutter under two types of situations.

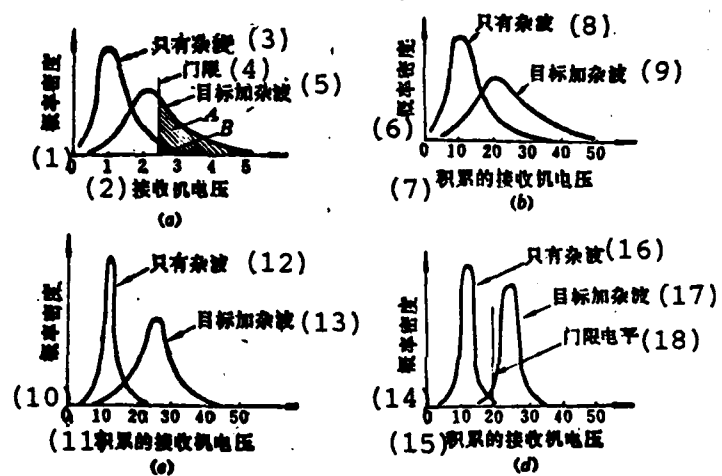


Fig. 5.22

Fig. 5.22 Changes of the Accumulator Output Clutter and Target With Clutter When There is Fixed Frequency and Frequency Agility

- (a) Probability density function when there is single observation with fixed frequency;
- (b) Probability density function after 10 accumulations with fixed frequency;
- (c) Probability density function after 10 accumulations with frequency agility (there is only clutter decorrelation);
- (d) The same as (c) but the clutter and target echo have simultaneous decorrelation.

- Key:
- 1. Probability density
 - 2. Receiver's voltage
 - 3. Only clutter
 - 4. Threshold
 - 5. Target with clutter
 - 6. Probability density
 - 7. Accumulated receiver voltage
 - 8. Only clutter
 - 9. Target with clutter
 - 10. Probability density
 - 11. Accumulated receiver voltage
 - 12. Only clutter
 - 13. Target with clutter
 - 14. Probability density
 - 15. Accumulated receiver voltage
 - 16. Only clutter
 - 17. Target with clutter
 - 18. Threshold level

In the figure, (a) and (b) are the probability density functions of the clutter and signal with clutter after a single observation or the accumulation of 10 observations when the radar operates in fixed frequency; (c) and (d) are the probability density functions of the output after the accumulation of 10 observations when the radar operates in frequency agility. We can see from the figure that when the radar operates in fixed frequency, the clutter distribution of a single observation is similar to the receiver's noise waves. To attain a lower false alarm rate it is necessary to raise the threshold. When the radar operates in fixed frequency, the correlation time

of the clutter is relatively long and therefore the accumulation of 10 observations cannot change its probability density distribution. It is, however, equivalent to a 10 fold increase of the horizontal coordinate and is similar to the situation of a signal with clutter. Thus, we cannot raise its detection probability. If the situations are different when the radar operates in frequency agility, the decorrelation effect of the frequency agility causes its probability density distribution to encircle the area of its mean value. If fig. 5.22 (c) only has clutter decorrelation this will be similar to the detection process when there is noise wave limitation in the receiver. The clutter changes in the same way as the noise wave being uncorrelated from pulse to pulse. After accumulation, we can obtain a more constant mean value because the accumulation in this type of situation is equivalent to adding independent samplings to the statistical distribution of pulses. This can greatly reduce the false alarm probability when there are similar threshold values. If the false alarm probability is maintained invariant, this can lower the threshold level and raise detection probability. In real situations, after the radar operates in frequency agility, the probability density function is as shown in fig. 5.22 (d). The probability density function of a target with clutter is also concentrated in the area of its mean value. At this time, there can be an even lower false alarm probability and even higher detection probability. Naturally, at this time the first determined conditions, the mean value of the sea clutter, must be lower than the mean value of the target with clutter. Therefore, this type of method can only attain visibility under clutter.

It is not satisfactory to use the above mentioned method of only transmitting two types of carrier frequencies to attain frequency decorrelation. This is because after being done in this way, the amplitude of one pulse each interval is still

correlated. Therefore, it is necessary to use the frequency agility method which is random jumping frequency or step jumping frequency.

The decorrelation of sea clutter with frequency agility was proven early through test results. The results of the 1964 tests conducted along Sweden's west coast on sea clutter were published in 1970 [12]. The radar used in the tests had a 700 kilowatt rotary tuned magnetron (YJ1180). Its agility range was 8.9-9.4 kilomegahertz, agility bandwidth was 500 megahertz, and the repetition period was 525 microseconds. This caused random vibration of the repetition period in the 40 microseconds interval and thus the realization of random jumping frequency. The radar used had intermediate resolution, its pulse width was 0.5 microseconds, horizontal beam width was 1.4 degrees and vertical beam width was 30 degrees. The antenna frame was 80 meters and during detection the antenna did not rotate and the beam was aimed at the wave front of the sea waves. At the time of the tests, the wind velocity was roughly 10 meters/second, wave height was 3-5 feet and the sea condition was level 3. Afterwards, a 1 microsecond wide range gate was used to carry out gating on the sea clutter wherein sea clutter at a range of 3 kilometers and 6 kilometers were photographed. The results are shown in fig. 5.23.

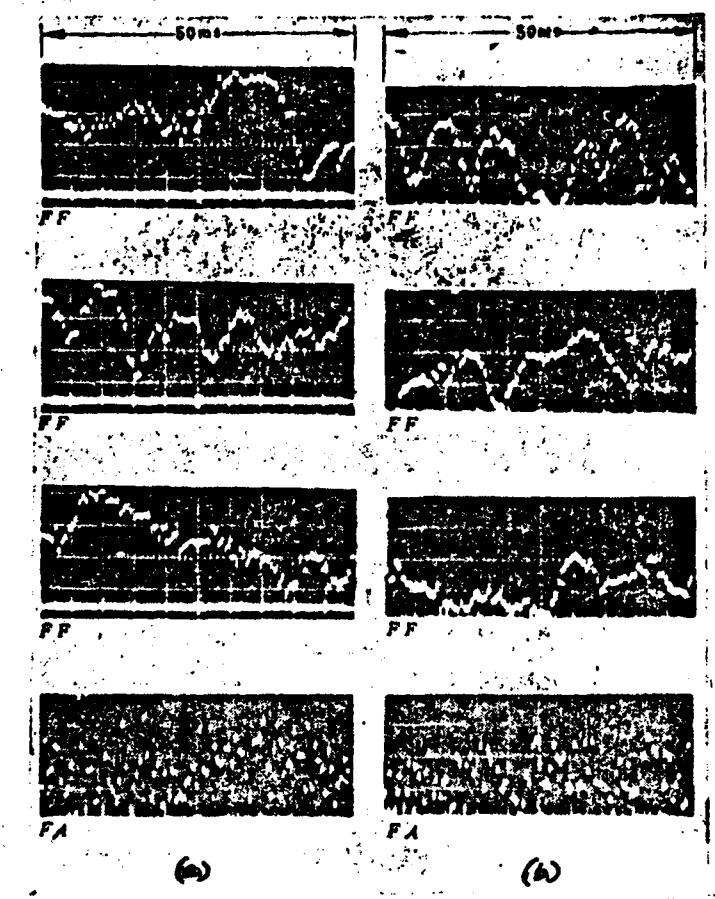


Fig. 5.23 Photographs of Sea Clutter When There is Fixed Frequency (FF) and Frequency Agility (FA)

- (a) Range of 3 kilometers;
- (b) 6 kilometers.

It is clear from the figure that when the radar is operating in fixed frequency (FF), the correlation time of the sea clutter is quite long and when operating in frequency agility (FA), there is basically no correlation between the pulses. We can also carry out statistical analysis of the measured test results to calculate its correlation coefficient. The correlation coefficient $\rho(\tau)$ for an unlimited number of samples is defined as

$$\rho(\tau) = \frac{\overline{X(i)X(i+\tau)} - (\bar{x})^2}{\overline{X^2(i)} - (\bar{x})^2} \quad (5.29)$$

In the formula, $X(t)$ is the signal. When there are a limited number of sample values, its correlation coefficient can be written as

$$\rho(n) = \frac{\frac{1}{N} \sum_{j=1}^N X_j X_{j+n} - \left(\frac{1}{N} \sum_{j=1}^N X_j \right)^2}{\frac{1}{N} \sum_{j=1}^N X_j^2 - \left(\frac{1}{N} \sum_{j=1}^N X_j \right)^2} \quad (5.30)$$

In the formula, $n = \tau/T_p$, and T_p is the pulse repetition period.

The statistically obtained results are shown in fig. 5.24.

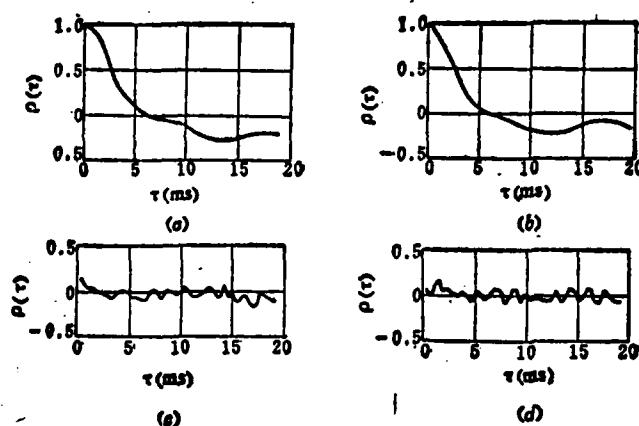


Fig. 5.24 Correlation Function Test Results When There is Fixed Frequency and Frequency Agility

In the figure, (a) and (b) are fixed frequency and (c) and (d) are frequency agility. (a) and (c) are the results at 3 kilometers and (b) and (d) are the results at 6 kilometers. We can see from the figure that when in fixed frequency, the standard difference σ_τ of the correlation time is separately 2.5 and 2.4 milliseconds. The relationship between standard differences

σ_f and σ_v of the frequency spectrum density function is

$$\sigma_f = \frac{1}{2\pi\sigma_v} \quad (5.31)$$

From the standard difference of the velocity shown in figure (5.7) we can obtain the following individual values:

(1) 距离 (公里)	(2) σ_v (毫秒)	(3) σ_f (赫)	(4) σ_v (米/秒)
3	2.5	64	1.06
6	2.4	66	1.10

Key: 1. Range (kilometers)
 2. (Milliseconds)
 3. (Hertz)
 4. (Meters/second)

However, when the radar is operating in frequency agility, its correlation time is very short and we can consider that there is no correlation between the pulses. For this reason, we can obtain

$$R(\tau) = \sum_{i,j=1}^n x_i x_j = 0 \quad (1) \text{ 当 } i \neq j \quad (5.32)$$

Key: 1. When

However, when there is random frequency jumping, it cannot be considered that the frequency difference of each continuous pulse is greater than the critical frequency difference. Therefore, all of the pulses are not necessarily independent.

As regards noise waves, all of the samples in each range interval are statistically independent; their variant is

σ_N^2 . After accumulation N times, the obtained mean variant is σ_N^2 which is $\frac{1}{N}$ times the original.

$$\sigma_N^2 = \frac{\sigma_n^2}{N} \quad (5.33)$$

However, the case is different for correlated clutter. At this time because each sample is not completely independent, after accumulating N pulses, its independent sample number is not equal to N. Here, we can replace it with an equivalent independent sample number N_e . N_e also represents the reduced multiple after the clutter fluctuation passes through the accumulator. If the signal received is x, the output in the square-rule detector is y and the output of the accumulator is z, the N_e is defined as

$$\begin{aligned} N_e &= \frac{[\text{起伏/平均值}]^2 \text{在积累器输入端}}{[\text{起伏/平均值}]^2 \text{在积累器输出端}} \quad (1) \\ &= \frac{\sigma_y^2/\bar{y}^2}{\sigma_z^2/\bar{z}^2} = \frac{\sigma_y^2 \bar{z}^2}{\sigma_z^2 \bar{y}^2} \quad (5.34) \end{aligned}$$

- Key: 1. $[\text{Fluctuation/mean value}]^2$ in the input terminal of the accumulator
 2. $[\text{Fluctuation/mean value}]^2$ in the output terminal of the accumulator

Here, σ_y and σ_z are the standard differences of y and z.

If all of the samples are independent, the $N_e = n$; if the samples are completely correlated, then $N_e = 1$. N_e can act as a measure for the ability of the accumulator in a reduced fluctuation component.

Because

$$z = \sum_{i=1}^N y_i \quad (5.35)$$

and

$$\sigma_y^2 = \overline{y^2} - (\bar{y})^2 \quad (5.36)$$

When formulas (5.35) and (5.36) are substituted into formula (5.34) and we express it with the correlation coefficient R_y of y , we can obtain

$$N_e = \frac{\overline{y^2}/(\bar{y})^2 - 1}{(\overline{y^2}/(\bar{y})^2) \frac{1}{N^2} \sum_{i=1}^N \sum_{j=1}^N R_y(i, j) - 1} \quad (5.37)$$

We can use the correlation coefficient of x from formula (5.27) to express

$$N_e = \frac{N^2}{\sum_{i=1}^N \sum_{j=1}^N R_x^2(i, j)} \quad (5.38)$$

Diagonal symmetry can be used to simplify the double sum in the formula

$$N_e = \frac{N}{1 + \frac{2}{N} \sum_{k=1}^N (N-k) R_x^2(k)} \quad (5.39)$$

If we know the sea clutter's correlation coefficient $R_x(i, j)$, we can find its equivalent independent sample number N_e .

We can obtain the actually measured sea wave correlation coefficient from fig. 5.24. From these measurement results we can obtain the equivalent relationship between independent sample number N_e and pulse number N as shown in fig. 5.25.

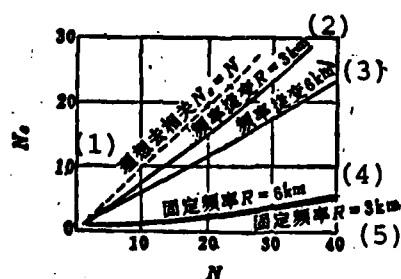


Fig. 5.25 Equivalent Independent Sample Number Obtained From Actual Measurements

- Key: 1. Ideal decorrelation $N_e = N$
 2. Frequency agility $R=3\text{km}$
 3. Frequency agility $R=6\text{km}$
 4. Fixed frequency $R=6\text{km}$
 5. Fixed frequency $R=3\text{km}$

The equivalent independent sample number of fixed frequency when there are 20 transmitted pulses is 2.3 and when there is frequency agility it is 13.4. From the formula deduced by Marcum and Swerling we can calculate a 14 decibel improvement with frequency agility. In this, about 8 decibels were obtained because of target decorrelation (i.e., the reduced fluctuation loss of the fast speed fluctuation as compared to the slow fluctuating signals). The remaining 6 decibels were obtained from clutter decorrelation. However, the improvement of these 6 decibels is very valuable because, as mentioned previously, the echo intensity of sea clutter usually changes with R^{-3} . Therefore, the signal/clutter 6 decibel gain signifies that the clutter limitation range wave increased 4 fold.

The correlation coefficient in formula (5.39) can also be directly calculated. We can obtain the frequency decorrelation

relation of sea clutter from formula (5.26).

Yet, at this time, aside from the frequency decorrelation caused by frequency agility, there is also the commonly existing time decorrelation. If the decorrelation of clutter in time is determined by the Gaussian theorem, then

$$R_r(t_i - t_j) = \exp \left[- \left(\frac{t_i - t_j}{\tau_c} \right)^2 \right] \quad (5.40)$$

In the formula, $t_i - t_j$ is the time between the i pulse and j pulse, and τ_c is $\sqrt{2}$ times the standard difference of the Gaussian curve.

In this way, the total decorrelation of sea clutter should be the product of frequency decorrelation and time decorrelation.

$$R_r(i, j) = \text{sinc}(\tau_r(f_i - f_j)) \exp \left[- \left(\frac{t_i - t_j}{\tau_c} \right)^2 \right] \quad (5.41)$$

Only if we know the law of the jumping frequency and the sea clutter's correlation time τ_c can we find the total correlation coefficient of the total sea clutter from formula (5.41). Afterwards, based on the accumulated pulse number N , in formula (5.39) we can find the suppression effect of the accumulator on sea clutter by finding the equivalent independent sample number N_e .

Below we will take a look at the equivalent independent sample number when in sinusoidal frequency modulation.

A chatter tuned magnetron is commonly used in shipborne radar (see chapter VI) as the source of frequency agility. The tuning frequency of the magnetron is sinusoidal modulated. When its modulated angular frequency is ω_m and initial phase angle is θ , then its tuning frequency can be expressed by

the following formula

$$f = \Delta f_A \sin(\omega_m t + \theta) \quad (5.42)$$

In the formula, Δf_A is the amplitude of the modulation frequency which is also the maximum frequency agility range. If the radar's pulse repetition frequency is fixed and its pulse repetition period is a constant then the radar's transmitted carrier frequency uses the equi-spaced T_p opposite the sinusoidal wave sample. The difference of the carrier frequencies of the i pulse and j pulse is

$$f_i - f_j = \Delta f_A \{ \sin(i\omega_m T_p + \theta) - \sin(j\omega_m T_p + \theta) \} \quad (5.43)$$

When it is substituted into formula (5.41), we can obtain

$$R_s^2(i, j) = \text{sinc}(\tau_p \Delta f_A \{ \sin(i\omega_m T_p + \theta) - \sin(j\omega_m T_p + \theta) \}) \times \exp\left[-2\left(\frac{iT_p - jT_p}{\tau_c}\right)^2\right] \quad (5.44)$$

In this way, for the jumping frequency law with a sinusoidal form (Δf_A , ω_m and θ), we can calculate the equivalent independent sample number N_e , when N pulses are accumulated based on the parameters of the radar (pulse repetition period T_p , pulse width τ_p) and the characteristics of the sea clutter (correlation time τ_c). Then we can know the suppression level of the sea clutter.

Because the modulation frequency law of the sinusoidal form itself is periodic and the sample interval is equi-spaced, when there is a simple integral multiple relation between pulse repetition frequency F_p and modulation frequency f_m , the transmitted carrier frequency can only repeat once after separation for a very small integral multiple period. This can naturally

increase its correlation and cause a reduction of the effective pulse number N_e . When $f_m = (j/i)F_p$ (j and i are integrals), the smaller the number of j and i the stronger its correlation. For example, when $F_R = 2,250$ hertz and $f_m = 2,250/2 = 1,125$ hertz, the transmitted pulse carrier frequency is the same each time. This is equivalent to the situation with fixed frequency. Therefore, if the pulse repetition frequency is fixed the problem of selecting a modulation frequency f_m naturally exists. The selection of a suitable f_m value can cause the number of dissimilar carrier frequency pulses to be maximum. Because the value of N_e is also related to the initial phase angle θ , when necessary a mean is taken for the different initial phase θ in each f_m value. Its calculation is quite complex.

For this reason, some people have used an electronic computer which employs a Fortran program to compute the following specific cases [13]. Assuming $F_R = 2,250$ hertz (i.e. $T_p = 444$ microseconds), and pulse width $\tau_p = 0.1$ microseconds, the accumulated pulse number N_e which can be supplied in the beam equals 30, the maximum frequency modulation range $\Delta f_A = 70$ megahertz, the sea clutter's correlation time is 2.4 milliseconds, and for f_m from 210 to 1,150 hertz in each interval of 10 hertz the mean value of N_e is calculated in the 0° - 90° range. The results have relatively large fluctuation (see fig. 5.26).

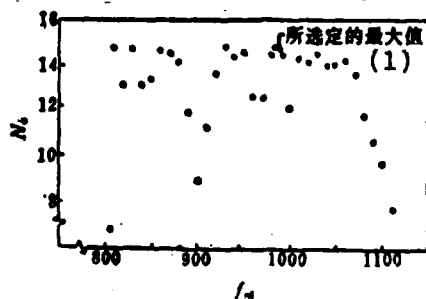


Fig. 5.26

Fig. 5.26 Obtained Value of N_e When in Different f_m
(F_p is Fixed)

$N=30$; $\tau_p=0.1$ microseconds; $\Delta f=30$ megahertz;
 $T_p=444$ microseconds; $\tau_c=3.4$ milliseconds.

Key: 1. Selected maximum value

Because f_m is the rotating frequency of the chatter tuned magnetron motor and its frequency stability has fixed limitations, we should select an area in a certain change range where the N_e change is the most mild. The 988 hertz f_m selected from the figure is the optimal value. The N_e changes in this value area are shown in fig. 5.27.

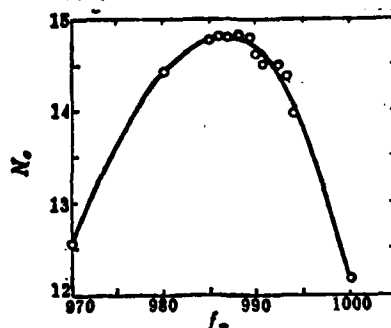


Fig. 5.27 Changes of N_e in the Area of the Optimal Value of Modulation Frequency ($f_m=0.4388F_p$)

With this optimal f_m value, the maximum value of N_e is 14.81. When an f_m change is needed and the change of N_e must be less than $\pm 10\%$, the frequency stability of the f_m must be written $\pm 1.2\%$.

Actually, we can calculate the optimal value of f_m in most situations according to the following formula

$$f_m = 0.4388 F_r$$

(5.45)

At the same time, to attain a more significant general curve, the results of the relational curve of T_p/τ_c and $\Delta f_A/N \frac{1}{\tau_p}$ when calculating to satisfy the required N_e/N value, are shown in fig. 5.28.

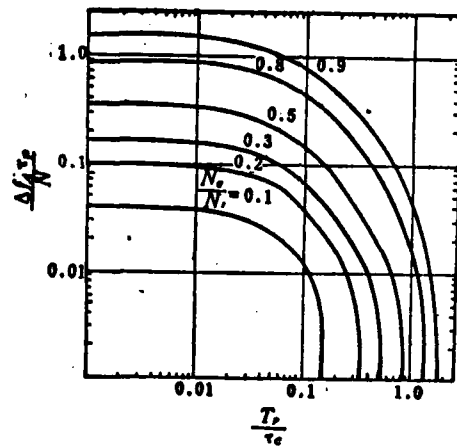


Fig. 5.28 Relational Curve of T_p/τ_c and $\Delta f_A \tau_p/N$

In this figure, N_e/N is the ratio of the equivalent independent sample number and the actually accumulated clutter correlation time, and T_p/τ_c represents the ratio of the radar's pulse period and clutter correlation time. $\Delta f_A/N \frac{1}{\tau_p}$ is the ratio of the jumping frequency range and N fold decorrelation frequency difference (equivalent to the reciprocal of the pulse width). We only calculated the 6 curves of N_e/N in the 0.1 to 0.9 range. We can see from the figure that when T_p is much smaller than τ_c the correlation time is relatively long and the adjacent clutter is not influenced by the decorrelation time. $\Delta f_A \tau_p/N$ is basically unrelated to the T_p/τ_c value.

In other words, at this time the N_e/N value is mainly determined by $\Delta f_A \tau_p/N$. The more the required N_e/N approaches 1, the more necessary it is for the Δf_A to approach the N fold decorrelation frequency difference. However, when in a very small $\Delta f_A \tau_p/N$ (smaller than 0.01 range), the value of N_e/N is mainly determined by the time correlation and when it is required that the N_e/N approach 1 the T_p/τ_c must also approach 1. The repetition period must also be sufficiently long so as to be able to totally rely on the time decorrelation of the clutter to cause the adjacent clutter to be uncorrelated. Although this group of curves was calculated based on $N=30$, it has very good accuracy for $20 < N < 40$.

Assuming the radar's pulse width $\tau_p=0.1$ microseconds, repetition period $T_p=500$ microseconds and $t_c=3.4$ milliseconds then $T_p/\tau_c=0.147$. Then, from formula (5.45), its optimal $f_m=877.6$ hertz. If the required $N_e/N > 0.8$, we can then look up $\Delta f_A \tau_p/N = 0.320$ on the curve or $\Delta f_A > 96$ megahertz. When the required $N_e/N \sim 0.5$ then it is required that $\Delta f_A > 27$ megahertz.

Actually, the maximum possible Δf_A value is determined by the structure of the magnetron. The selection of the clutter tuned magnetron can be based on the maximum possible N_e/N value found on the above curve. Afterwards, we can calculate the suppression level for the sea clutter after using frequency agility.

When using frequency agility radar with random jumping, its equivalent independent sample number can be calculated by formula (3.22) or (3.24) in section 3.5. At this time, after using frequency agility in a clutter environment, we can use the following formula to calculate the gain of target detection [14].

$$G_{FAC} = G_{IFA} - G_{IFF} \quad (5.46)$$

In the formula, G_{IFA} is the accumulated gain with frequency agility and G_{IFF} is the accumulated gain with fixed frequency. Both are expressed in decibels.

When there is incoherent accumulation, gain G_I is determined by the following formula

$$G_I = 10 \lg(N) - L_I(N) \quad (5.47)$$

In the formula, N is the accumulated independent pulse number and $L_I(N)$ is the accumulation loss. When there is incoherent accumulation, the accumulation loss is also a detector loss, that is, the phenomena of large signals suppressing small signals which is determined by formula (3.17) or fig. 3.14. This loss is also the function of the independent pulse number and a more accurate value can be found in fig. 5.29. Therefore, it is only necessary to know the equivalent independent pulse number with fixed frequency and frequency agility from formula (5.47) to be able to find the accumulated gain, when the two types of radar are operating.

AD-A124 003

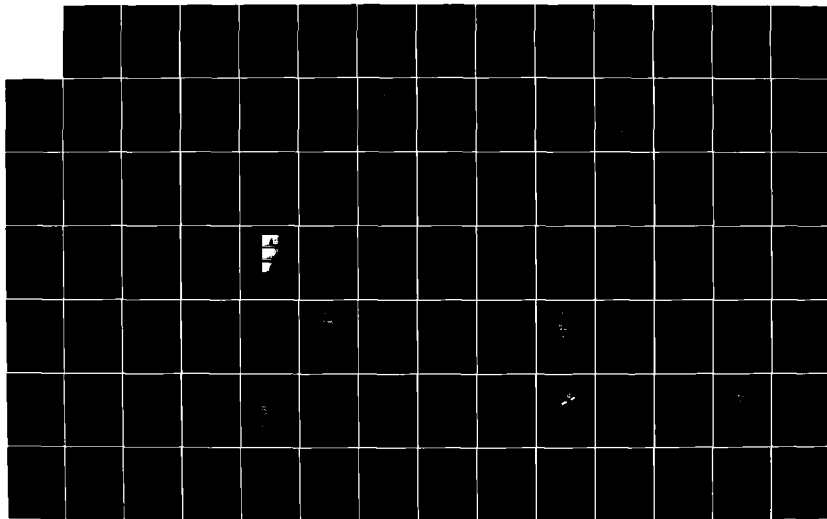
FREQUENCY AGILITY RADAR(U) FOREIGN TECHNOLOGY DIV
WRIGHT-PATTERSON AFB OH M YUMAI 06 DEC 82
FTD-ID(RS)T-0803-82

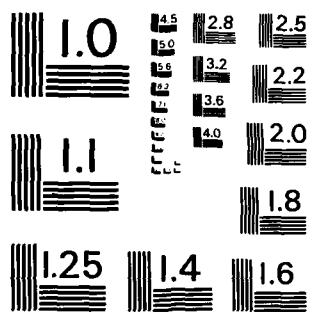
4/7

UNCLASSIFIED

F/G 17/9

NL





MICROCOPY RESOLUTION TEST CHART
NATIONAL BUREAU OF STANDARDS-1963-A

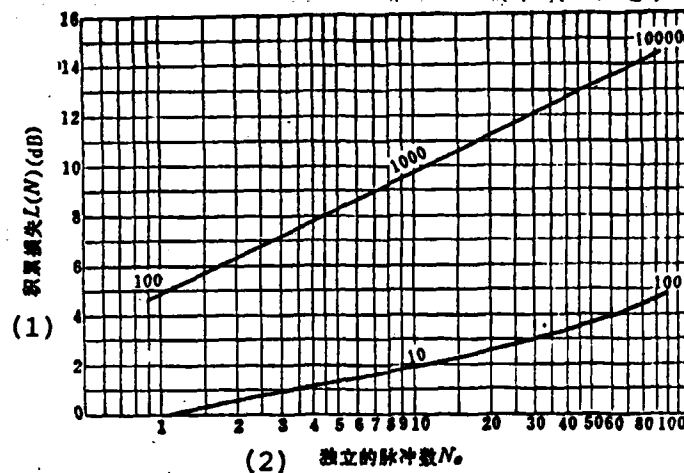


Fig. 5.29 Relationship Between the Accumulation Loss and the Independent Sample Number

Key: 1. Accumulation loss L/N (dB)
2. Independent pulse number N_e

If the radar operates in fixed frequency, because of the time decorrelation of the clutter itself, when accumulation time is relatively long there can also be certain accumulation gain. At this time, the independent sample number N_{eF} can be calculated by the following formula

$$N_{eF} = 1 + T_d / \tau_c \quad (5.48)$$

In the formula, T_d is the target's irradiation time which is also the staying time of the antenna beams.

With the existence of time decorrelation, when the radar operates in frequency agility, the independent sample number cannot be calculated from formula (3.24). Because the mechanisms of time decorrelation and frequency agility decorrelation are totally independent, we can consider that the total pulse number

N divides into N_{eF} pulses. Afterwards, based on formula (3.24), the decorrelation of the frequency agility is added on to these N/N_{eF} pulses. We can then obtain the independent pulse number in each group

$$v \{1 - (1 - N/v)^{N/N_{eF}}\}$$

In the formula, v is the frequency number determined from formula (3.21). The total independent pulse number is

$$E\{N_s\} = N_{eF} v \{1 - (1 - 1/v)^{N/N_{eF}}\} \quad (5.49)$$

When $v \gg 1$, we can attain its approximation as

$$E\{N_s\} \approx N_{eF} v \{1 - e^{-N/N_{eF} v}\} \quad (5.50)$$

After finding N_{eF} and N_e we can calculate the accumulation gain when there is fixed frequency and frequency agility based on formula (5.47).

For example, if a certain radar's pulse repetition frequency $F_p = 2,000$ hertz, the pulse number in the beam $N = 20$. From this, we can find that beam irradiation time $T_d = 10$ milliseconds. It is assumed that the clutter's correlation time $\tau_c = 4.5$ milliseconds (it is equivalent to sea clutter with an X wave band of sea condition level 5; see figures 5.9 and 5.10)

We can find the equivalent independent sample number with fixed frequency from formula (5.48)

$$N_{eF} = 1 + 10/4.5 = 3.2$$

We can find the accumulated gain with fixed frequency from formula (5.47)

$$G_{IFF} = 5.0 - 1.0 = 4.0 \text{ dB}$$

If frequency channel number $v=26$ when there is frequency agility (see formula (3.21)), considering the natural (time) decorrelation, ^{in formula (5.49)} we can find the mean value of the equivalent independent sample number when the radar operates in frequency agility

$$E \{ N_e \} = 18.1$$

By substituting this into formula (5.47), we can find the accumulated gain when there is frequency agility

$$G_{IFA} = 12.6 - 2.5 = 10.1 \text{ dB}$$

Given this type of situation, we can calculate the frequency agility gain in a clutter environment from formula (5.46)

$$G_{FAC} = 10.1 - 4.0 = 6.1 \text{ dB}$$

This can increase the clutter limitation range more than 4 fold.

This data is quite typical and thus we can see that frequency agility is a relatively effective method for suppressing sea clutter of incoherent processing signals in the time domain.

Another commonly used method for causing sea clutter decorrelation is the high rotational antenna. This method actually obtains accumulated gain by using the elongated accumulated time from time decorrelation. When the antenna rotation is raised to only 1 pulse number in the beam its rotating period is not larger than the sea clutter's correlation time. At this time, we can consider that each echo pulse obtained from a certain position is statistically independent. After carrying out accumulation for these pulses, we can obtain the accumulation

gain and reach the goal of suppressing clutter.

This method is regarded as relatively simple because it does not require any refitting of the radar's transmitting parts. It only requires the use of a high speed rotating mechanism and an accumulation tube with long accumulation time. However, its drawbacks are quite obvious because the pulses in the attained adjacent scanning are uncorrelated. For example, if the sea clutter's correlation time is 10 milliseconds, when the antenna rotation is 600 rotations/minute, that is, one rotation each 100 millisecond, there is no correlation in the adjacent scanning. Even higher rotating speeds cannot be tolerated by the mechanical structure but low rotating speeds can increase and lengthen its accumulation time. If the radar's repetition frequency is 5,000 hertz and the beam width is 1.6 degrees, the pulse number inside the beam is about 2. Yet, an antenna rotating speed of 600 rotations/minute cannot be tolerated by most antennas. It can only be endured by an antenna with X wave band and above which have specially designed structures.

Excessively long accumulation time also has many limitations. In the above example, the accumulation of 20 independent pulses only requires 2 seconds. This cannot only be used for detecting low speed moving targets (the range of the target shift in such a long accumulation time should be smaller than the range corresponding to the pulse width) but even more important, because of the movement of the radar installed on ships or aircraft, especially the rocking and swaying, its stable accumulation time is even shorter. Thus, to date, this method has not been widely used.

Although use of high resolution radar can reduce the equivalent reflection area of sea clutter, yet because the reduction of the mean power can bring about a decrease of the noise wave limited detection range, its complex equipment level is

naturally increased. Moreover, high resolution radar can cause its amplitude distribution to be even closer to a logarithmic-normal distribution. Further, the single clutter peak increase causes the false alarm rate to enlarge.

Recent research results show [15] that use of frequency agility (or frequency diversity) cannot only cause the mean sea clutter background to decrease but can also reduce the amplitude of the clutter peak. The peaks of clutter are formed from two types of structures. One type is a huge wave front formed from clutter which seems to be perpendicular to the radar beam. This wave front forms a mirror reflection. Thus, a very strong echo is created yet the probability of forming this type of mirror reflection which is almost perpendicular to the beam is very small. Therefore, clutter peaks are mainly formed by another mechanism. Under the effects of wind power, the sea forms patterned ripples and the intervals of these types of ripples can be compared to the wave lengths of electric waves, like a similar diffraction grating (see fig. 5.30(a)). Because of the interference between each reflected wave, the formed scattering directional diagram is as shown in fig. 5.30(b).

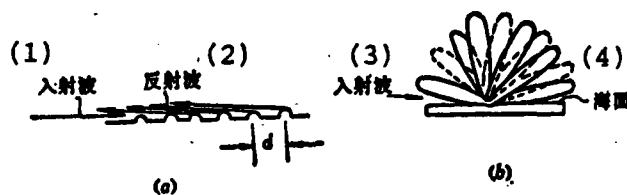


Fig. 5.30 Diffraction Grating Formed By Sea Clutter

- Key: 1. Incident wave
2. Reflected wave
3. Incident wave
4. Sea

When a lobe is aimed in the direction of the incident wave, the radar can receive a peak clutter. Its directional diagram is not only related to each wave's direction d but also to the wave length of the incident wave. For example, when the wave length changes 1%, this possibly causes its directional diagram to change from the solid line in the figure to a broken line. This can cause the peak amplitude received by the radar to produce large changes. We can see from this that a change of the transmitting frequency can cause this type of clutter peak to be decorrelated. Use of this principle can form a multifrequency radar system which can effectively eliminate clutter peaks. Its block diagram is shown in fig. 5.31.

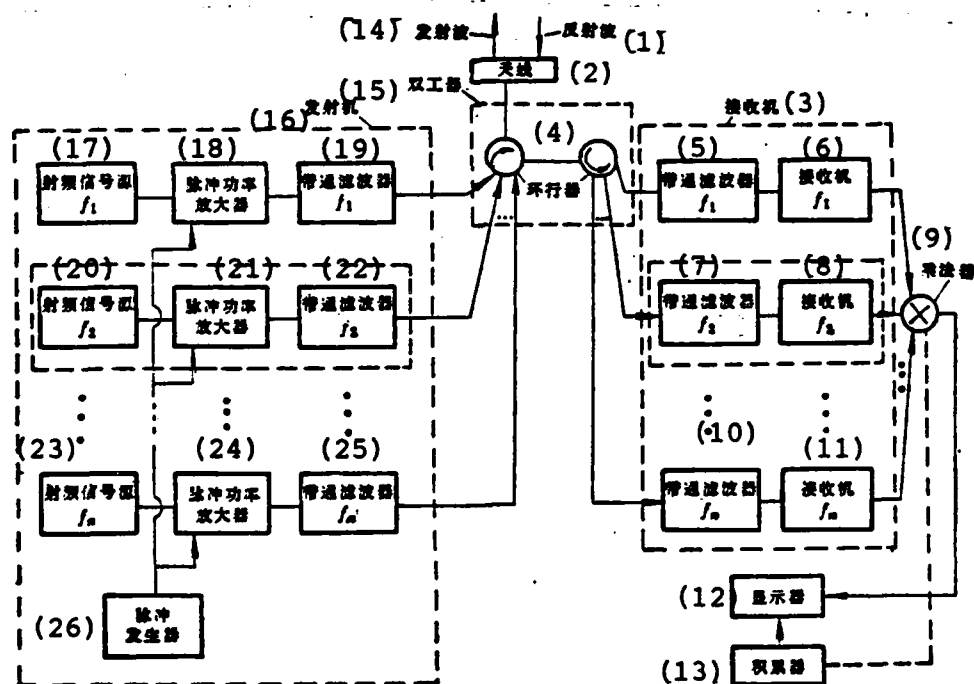


Fig. 5.31

Fig. 5.31 Block Diagram of a Multifrequency Radar System
Which Eliminates Sea Clutter Peaks

- Key:
1. Reflected wave
 2. Antenna
 3. Receiver
 4. Circulator
 5. Band filter f_1
 6. Receiver f_1
 7. Band filter f_2
 8. Receiver f_2
 9. Multiplier²
 10. Band filter f_n
 11. Receiver f_n
 12. Display
 13. Accumulator
 14. Transmitted wave
 15. Duplexer
 16. Transmitter
 17. Radio frequency signal source f_1
 18. Pulse powered amplifier
 19. Band filter f_1
 20. Radio frequency signal source f_2
 21. Pulse powered amplifier
 22. Band filter f_2
 23. Radio frequency signal source f_n
 24. Pulse powered amplifier
 25. Band filter f_n
 26. Pulse generator

This radar can simultaneously transmit frequencies of f_1, f_2, \dots, f_n pulses. After the obtained signals pass through the filter they are received by each frequency's receiver and the obtained signals are added to the multiplier. It is then added to the accumulator or display from the output of the multiplier.

Here, signal processing uses multiplication processing and not averaging processing. This is because multiplication processing can better improve the signal clutter ratio. If the target's echo strength is not related to the frequency (this diverges from the real situation as it is only an assumption for convenience of analysis), the sea peaks then change with the

frequency. If the radar only transmits the two frequencies of f_1 and f_2 , the target echo amplitude of these two frequencies is 1. However, when the frequency is f_1 , the clutter peak's corresponding amplitude is also 1 but when the frequency is f_2 , it is 0.1. If we use the method of finding the average, then the obtained signal-clutter ratio is 1:0.55. This greatly improves the signal-clutter ratio 1:0.1.

In principle, this technique can also be applied to frequency agility radar. At this time, because the pulses of each frequency are continuously transmitted, to carry out multiplication of the continuous echoes obtained in the same range it is necessary to store the echoes of each pulse. This can be realized by using a digital delay line. Actually, to realize a simulated slide window to find the average, it is also necessary to have the same number storages and thus the quantity of equipment is similar. It is only necessary that the summation adder be changed to a multiplier.

To sum up, although the effects of using frequency agility to suppress sea clutter are not ideal, yet because the intensity of common sea clutter is much weaker than ground clutter we can attain certain clutter visibility and thus greatly improve target detection. Of even greater significance is the fact that the difference between frequency agility and other techniques lies in its ability to suppress clutter and even more important having the advantages of being able to counter active jamming, enlarging the effective range and improve angular tracking precision. Thus, on the whole, it is a very worthwhile technique. For this reason, various shipborne, airborne, coastal warning and tracking radar are making wider use of the frequency agility technique.

References

- [1] Radar Handbook, Ed. by M.I. Skolnik. McGraw-Hill Book Co. 1970, chapt. 26. Chinese translation: "Radar Handbook," Vol. 2, Chapter 6, National Defense Publications, 1978.
- [2] Radar Design Principles. F.E. Nathanson McGraw-Hill Book Co. 1959, chapt. 7.
- [3] Detection of targets in non-Gaussian Sea clutter. G.V. Trunk, S.F. George IEEE Trans. Vol. AES-6. No. 5. Sept.1970 pp.620-628.
- [4] Radar detection in Weibull clutter. D.C. Schleher. IEEE Trans. AES-12, No. 6, Nov.1976. pp.736-743.
- [5] Clutter on radar displays. J.Croney. Wireless Engr. p.83-96. April, 1956.
- [6] Further observations on the detection of small targets in sea clutter. J.Croney, A.Woroncow, B.R. Gladman. The Radio and Electronic Engineer Vol. 45.No. 3. Mar. 1975. pp. 105-115.
- [7] Constant false alarm rate processing in search radars. V.G. Hansen. IEE Conf.Publ. No.105. Radar-Dresent and Future. London, Oct.23-25, 1973. pp.325-32.
- [8] Detectability in rain clutter using a pulse to pulse frequency jumping radar. Waters.P.L. Euro-Control Symp. Brussels, 1966.
- [9] Some measurements of the effects of frequency agility on aircraft radar returns. W.S. Whiflook, A.M. Shepherd and A.L.C. Quigley. AGARD Conf. Proc. No. 66 on Advanced Radar-Systems. AD-715, 485, 1970.
- [10] Detection of targets in non-Rayleigh Sea clutter. G.V. Trunk EASCON'71 Record. Washington, D.C.Oct.6-8 1971.
- [11] Clutter and frequency agility. G.Lind. J. Inst.Eng.India Electron and Telecom.Eng.Div. 1971.52.No.1.pt.1.pp.4-6.
- [12] Measurement of sea clutter correlation with frequency agility and Tele-communication Rev.29,No.1, April, 1970,pp.32-38.
- [13] A quantitative analysis of sea clutter decorrelation with frequency agility. E.W.Beasley and H.R.Ward.IEEE Trans. AES-4, No.3. May 68, pp.468-73.

References (continued)

- [14] Frequency agility radar range calculation using number of independent pulses. G.Lind. IEEE Trans. Vol. AES-12, No. 6. Nov. 1976, pp. 811-815c.
- [15] Sea clutter reduction technique. B.L.Lewis. U.S. Pat. No. 4,041,489. Aug. 1977,.

Part Two The Composition of Frequency Agility Radar

Chapter VI Frequency Agility Magnetrons

6.1 General Discussion

The core of incoherent frequency agility radar is the frequency agility magnetron. Because there are many types of frequency agility magnetrons and each of their structural principles is dissimilar, to a great extent their characteristics and parameters determine the characteristics and parameters of frequency agility radar. Therefore, before discussing the composition of incoherent frequency agility radar we must first investigate the types, characteristics and composition of frequency agility magnetrons.

The first microwave radar used high power pulsed magnetrons. Yet, today after over 40 years, the magnetron is still used. This is mainly because the magnetron's volume is small, it is light in weight, has a long life-time and is low in cost. The invention of the coaxial magnetron further developed these advantages. To date, a device with better capabilities than the magnetron has still not been developed among the microwave high power pulsed self excited oscillator devices. This is why magnetron transmitters are still commonly used in modern military and civil radar.

Due to the requirements of electronic countermeasures, early during World War Two, a tunable frequency magnetron was developed. As a result, following the continual increase of the jammer's tuning speed and tuning band width, there was a corresponding

need to raise the magnetron's tuning speed and tuning band width. Early tunable magnetrons used gear or gear-and-worm mechanisms for manual tuning. Afterwards, to raise the tuning speed they changed to use a motor driven cam tuning mechanism. Finally, a hydraulic driven tuning mechanism was used. Although all of these tunable magnetrons can produce radio frequency pulses with frequency differences between pulses yet the frequency differences between pulses which the formerly developed magnetrons could obtain was very small. Although later it was gradually increased they were still only quantitative changes. Only the invention of the frequency agility magnetron caused the frequency differences between pulses to be greater than the critical frequency and thus be able to produce qualitative changes. Naturally, qualitative changes are attained through continuous quantitative changes.

Frequency agility magnetrons can generally be divided into two types. One type is the frequency agility magnetron where the maximum frequency difference between the pulses can reach the entire tuning range. The other type is called the dither-tuned jumping frequency magnetron. Its high speed jumping frequency pulses (called dither-tuning) can only be realized in a relatively narrow frequency range (yet still exceeding the critical frequency differences). The central frequency of its dither-tuning can be tuned within the entire tuning frequency band at relatively low speeds.

Frequently agility magnetrons can be further divided into jumping frequency magnetrons with periodic tuning and jumping frequency magnetrons with random tuning. The tuning mechanism of the former has relatively large mechanical inertia and therefore can only carry out periodic tuning. The mechanical inertia of the latter is relatively small whereas the control power of the tuning system is quite large so that based on the input

frequency command signal we can quickly tune it to a random frequency. Although this be the case, this type of jumping frequency with random tuning still has certain mechanical inertia. Only if we can completely break away from the mechanically and electronically tuned jumping frequency magnetron (including the electronically tuned and magnetically tuned magnetron) is it possible to have inertialess random tuning.

Below, we will first look at frequency agility magnetrons which have actually been used in large numbers.

6.2 Rotary Tuned Magnetrons

In principle, tunable multi-cavity magnetrons are divided into inductance tuning and capacitance tuning. Inductance type tuners have many finger-type tuning wands (sometimes called tuning plungers). When these tuning wands are inserted into the magnetron's cavity, this can change the high frequency magnetic field of the resonant cavity which is equivalent to changing its equivalent inductance. As a result, there is a change in its resonant frequency (i.e., oscillation frequency). Capacitance type tuners have a tuning loop and changing the range between the tuning loop and anode block can change the high frequency electric field of the oscillation frequency. This is equal to changing its equivalent capacitance and as a result we reach the goal of changing its oscillation frequency. Usually, these two methods can realize 10% of the tuning range.

To enlarge the tuning range we can also combine these two types of tuners and attain a 1.5:1 tuning range.

However, these two types of tuners have alternating motion. This can cause difficulty for its vacuum seal and greatly limit its tuning rate.

Earlier, the maximum tuning speed of this type of tunable magnetron was about 5,000 megahertz/second. Although a complex hydraulic servo system is used we can attain a tuning speed of 200 kilomegahertz/second but its tuning acceleration is relatively low. Although it can obtain relatively large transient jumping frequency difference in a single direction, there is no way of continually creating fast speed multiple double direction jumping frequency (i.e., its frequency difference is sometimes positive and sometimes negative). Moreover, it is also necessary to have very large tuning drive power.

In 1960, a type of multi-cavity magnetron with "rotary tuning" was invented [1]. Its structure is very simple yet it can realize fast speed wide band jumping frequency.

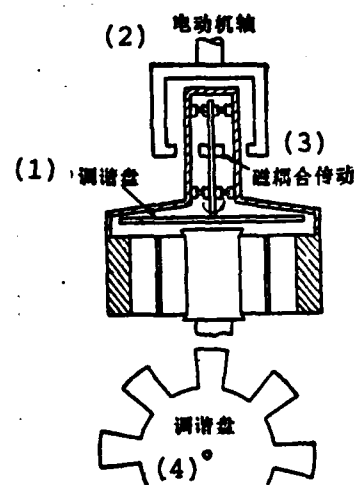


Fig. 6.1 Schematic of the Structure of the Rotary Tuned Magnetron

- Key: 1. Tuning disc
 2. Electric motor axle
 3. Magnetic coupling drive
 4. Tuning disc

Its tuning mechanism is a gear shaped rotating disc and its number of teeth is the same as the number of cavities. This round

disc is fixed on a ball bearing and has magnetic coupling with the outer rotating mechanism. The outer magnet is joined to the rotating axis of the motor. In this way, when the motor rotates, it can cause the rotating disc inside the tube to also rotate. Because the number of teeth of the rotating disc is equal to the number of cavities, the tuned repetition period is equal to the rotation frequency of the motor times the number of teeth. Therefore, we can attain a very high tuning speed.

Fig. 6.2 shows the structure of another type of improved rotary tuned magnetron [2].

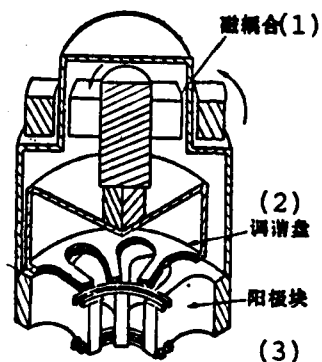


Fig. 6.2 Schematic of the Structure of the Improved Rotary Tuned Magnetron

Key: 1. Magnetic coupling
2. Tuning disc
3. Anode block

The tuning mechanism of this type of tube is a hollow disc with one side open which has a petal shaped crack. When the rotating disc rotates, the cavity of the magnetron is alternately an inductive or capacitive negative carrier. This causes its oscillation frequency to rise or fall. In the same way its rotating disc is supported on the vacuum bearing. There is a

magnetic coupling with the outside surface motor bearing.

Because rotary motion is used to replace alternating motion in the rotary tuned magnetron, when adding the tuning repetition frequency it is necessary to multiply by the number of cavities. As a result, its tuning speed is greatly increased. For example, an early developed YJ1181 X wave band rotary tuned magnetron has 16 resonant cavities and the motor rotates 4,500 times/minute. Its tuning repetition frequency reaches 1,200 times/second. The tuning range of the tube is 8.5-9.6 kilomegahertz and the rotary tuning band width is 450 megahertz. Therefore, its maximum tuning speed reaches 1,080 kilomegahertz; over 10 times faster than the fastest hydraulically tuned magnetron. Such fast tuning speed allows for the possibility of realizing jumping frequency between the pulses.

In order for frequency agility radar to attain the widest possible jumping frequency band width so as to have even higher anti-jamming capabilities, it is hoped that the rotary tuned magnetron will have the widest possible tuning range. When there are similar rotating speeds, larger tuning band widths signify faster tuning speeds.

The tuning band width of a rotary tuned magnetron depends on the crack shape and measurement and the shape of the anode block resonant cavity of the tuning disc as well as the space between the tuning disc and anode block. The closer the space between the rotating disc and anode block, the wider the tuning band width. For example, for an L wave band rotary tuned magnetron, when the distance between the tuning disc and anode block is 0.05 inches, its tuning band width is 100 megahertz; when its distance decreases to 0.03 inches, its tuning band width can increase to 130 megahertz. However, an excessively narrow space can cause high frequency sparks between the anode and tuning disc which can bring about a contradiction between

the tuning band width and the peak value power. At the same time, a tube with a microwave wave band operating at an even shorter wave length has a corresponding shrinkage of the measurement of its tube. When there is high power, the problem of high frequency sparks caused by thermal distribution and thermal expansion is even more important. Thus, it is necessary to first use materials with a small thermal expansion coefficient. It is also necessary to have higher processing precision.

At present, the tuning range of a rotary tuned magnetron with L wave band is about 100 megahertz (i.e., it can reach to about 8% of the band width) and each individual tube can reach 130 megahertz. In the X wave band, it can reach to 500 megahertz and with the Ku wave band it can reach to 670 megahertz which is about 4%.

Table 6.1 lists the major technical indices of the rotary tuned magnetrons produced abroad.

型 (1) 号	(2) 频 段 (兆赫)	(3) 调谐带宽 (兆赫)	(4) 调谐器转速 (转/分)	(5) 调谐速度 (兆赫/秒)	输出峰值功率 (7) (千瓦)	(8) 附 注
QKH1342	UHF	50	2400 (最高3000) (5)	80	2000	连续功率900 (9)
QKH1014	1250~1350	100			1000	
QKH1034	S	150			4000	
QKH1299	X	500	4500	2000	200	(10) 15.5千伏, 15安, 2.0微秒 工作比0.0018
YJ 1180	X	450		1080	200	
YJ 1181	X	450			90	
YJ 1170	8500~9300	800	4000		100	(11) 22.5千伏, 27.5安, 1.5微秒 工作比0.00112, 寿命3000~ 4000小时
YJ 1185	X	450			205	
DX285/YJ1180	8700~9500	800			80	
QKH1168	Ku	500	5000		65	转子控制功率仅12瓦 (12)
YL1320	16000	600				

Table 6.1

Table 6.1 Parameters of the Rotary Tuned Magnetron

- Key:
1. Model
 2. Frequency band (megahertz)
 3. Tuning band width (megahertz)
 4. Tuner's rotating speed (rotations/minute)
 5. (Highest 3,000)
 6. Tuning speed (kilomegahertz/second)
 7. Output peak value power (kilowatts)
 8. Added remarks
 9. Including magnet weight 90 tons
 10. 15.5 kilovolts, 15 amperes, 2.0 microseconds work ratio 0.0016
 11. 22.5 kilovolts, 27.5 amperes, 1.5 microseconds work ratio 0.00112 life-time 3,000-4,000 hours
 12. Rotor control power only 12 watts

Fig. 6.3 draws the development trend of the maximum possible tuning band width for different operating frequency bands.

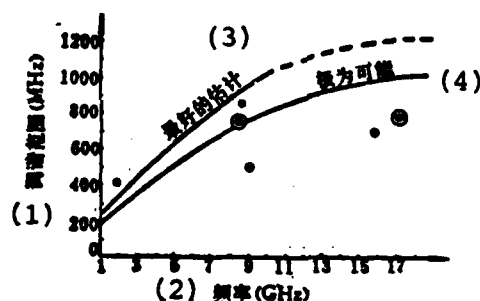


Fig. 6.3 Development Trend of the Maximum Possible Tuning Band Width in Different Operating Frequencies

- Key:
1. Tuning range (MHz)
 2. Frequency (GHz)
 3. Best estimate
 4. Most possible

Fig. 6.4 is a schematic of a section of an L wave band rotary tuned magnetron.

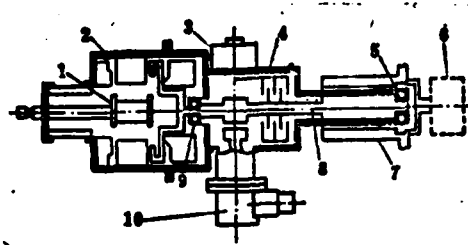


Fig. 6.4 Schematic of an Inner Structural Section of an L Wave Band Rotary Tuned Magnetron

- Key:
- 1. Anode
 - 2. Anode block
 - 3. Transducer output joint
 - 4. Capacitance transducer
 - 5. Ball bearing
 - 6. Outer driving motor
 - 7. Magnetic driver
 - 8. Magnetic follower
 - 9. Ball bearing
 - 10. Electromagnetic trigger locking device

A capacitance transducer is fitted in this tube. This capacitance transducer has a set of fixed pieces and moving pieces, and its capacity is in direct ratio to the magnetron's oscillation frequency. This can provide frequency tracking information for the oscillator. Fig. 6.5 draws the oscillation frequency and the sensing capacitor's capacity change curves of this magnetron when it is in different turning angles of the tuner.

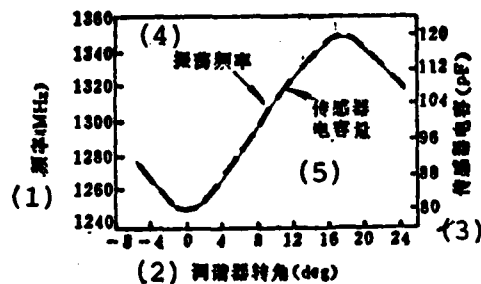


Fig. 6.5 Oscillation Frequency of an L Wave Band Rotary Tuned Magnetron and Change of Sensing Capacitor's Capacity When in Different Turning Angles of the Tuner

Key: 1. Frequency (MHz)
 2. Tuner's turning angle (deg)
 3. Transducer's capacitance (pF)
 4. Oscillation frequency
 5. Transducer's capacity

We can see from the figure that the capacity of the sensing capacitor can use the oscillation frequency of a very high accuracy tracking magnetron. After this capacity undergoes suitable transformation, it can act as preset information to control the oscillator's frequency. This will cause it to be pretuned to the area of an accurate operating frequency. After the magnetron oscillates, it is then locked by the automatic frequency fine tuning system. Problems related to the automatic frequency fine tuning of incoherent frequency agility radar will be discussed in a later section.

The technological key of this type of rotary tuned magnetron is the manufacture of the vacuum bearing. This type of bearing cannot be lubricated with most lubricating oil because the sputtering of the oil can poison the cathode and shorten the operating life of the tube. Formerly, graphite soaked porcelain was used for the ball bearings. This type of bearing must be

able to sustain a temperature of about 500°C during the tube's thermal processing. Recently, nitrogen case hardening stainless steel bearings with a silver-molybdenum bisulphide retainer have been used.

The highest rotating speed of better ball bearings can reach to 10,000 rotations/minute and can continuously operate without breaking down for several thousand hours at 3,000 rotations/minute. This is the major factor for the tube not being limited in life-time.

Rotary tuned magnetron also have certain shortcomings and problems.

(1) Firstly, because it is mainly adapted for use in multi-cavity magnetrons and is not suitable for coaxial magnetrons, the original frequency stability is relatively low. After adding a rotary tuning mechanism, the slack of the mechanical structure and the possible microphonic effect causes the frequency stability of its transmitted pulses when operating in fixed frequency to fall short of most tubes. This causes its visibility under clutter when operating in moving target display radar to be lacking. Usually, an electromagnetic brake is installed in the tube to lock tight the tuned rotating disc when operating in fixed frequency. This reduces the frequency instability caused by mechanical vibrations.

(2) The existence of the rotary tuning mechanism causes difficulties in cooling. Thus, its maximum possible average power must be lower than common magnetrons.

(3) There is a high speed rotating mechanism in the tube's vacuum bubble case. The wear, breakdowns and high frequency sparks of this high speed rotating mechanism can shorten the

life of the tube. Although improvements of the processing technique can partially overcome these shortcomings, yet under the same technical conditions, its average life-time is shorter than common magnetrons.

(4) It can accurately maintain the tuning frequency band boundary value. This is because each tuning period will cover the entire tuning range and the system operating outside the assigned frequency range cannot be allowed. Therefore, it must incorporate the tuning errors into the tuning frequency band. At present, there is still no mechanism to regulate its tuning range. Yet, we can use electronic methods for control which cause synchronization of its pulse repetition frequency and tuning frequency. Afterwards, the proper regulation of its period causes jumping frequency in a certain range.

Even though this be the case, in tuning speed as well as in the maximum frequency difference of the adjacent pulses, the rotary tuned magnetron has no way of matching other types of frequency agility magnetrons.

Aside from this, the proper changing of the shape of its tuned rotating disc can control the shape of its tuning curve. For example, besides the sinusoidal shape, there is also the trapezoid or triangle.

To overcome the above mentioned shortcomings, improvements were made on the structure of this type of rotary tuned magnetron [3]. The first improvement was to enlarge the center hole of the rotor so that it is as big as the outer diameter of the separated area (see fig. 6.6). This can avoid the danger of fires. However, we are still unable to overcome the shortcoming of the sensitivity of the tuning characteristics (center frequency, frequency band) changing the range size from rotating disc to anode. Thus, it is easily influenced by heat and vibrations.

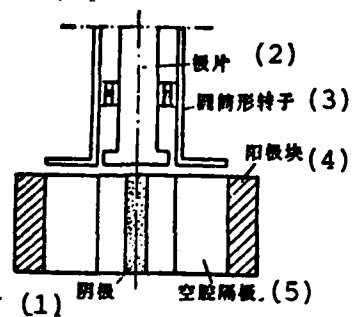


Fig. 6.6 An Improvement of the Structure of the Rotary Tuned Magnetron

- Key: 1. Cathode
2. Pole piece
3. Cylindrical rotor
4. Anode block
5. Cavity separator

As mentioned previously, the induction pin tuning mechanism can avoid the various drawbacks of the disc tuning mechanism. Yet, it requires alternating motion but cannot make rotating motions. To resolve this problem, the induction pin is made cylindrical. It does not extend into the space formed by the cavity blade but extends into the dug out cylindrical notch on the anode block (see fig. 6.7).

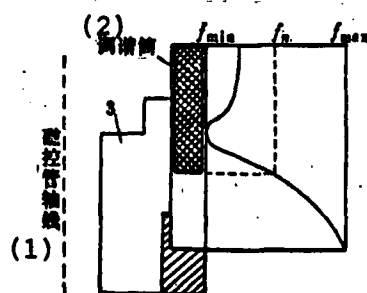


Fig. 6.7

Fig. 6.7 Structure and Tuning Characteristics of the Cylindrical Tuning Plunger

Key: 1. Magnetron's axis
2. Tuning cylinder

To avoid possible parasitic oscillation film, the depth of this cylindrical notch is dug less than half the depth of the anode block. When the tuning cylinder is gradually inserted in, the initial effect is capacitance so that the resonant frequency gradually decreases to minimum value f_{\min} . When the cylinder is put in even deeper, the contour of the cavity tends towards the contour of a typical magnetron. This is because all of the outer parts are sealed and the magnetic field is enclosed from one resonator to another. The path used is the apex of the separated area and is unlike the base of the just passed through opening. As a result, a relatively long path was used and the electric field was gradually lost in the region of the tuning cylinder. The inductance and conductance of each resonator decreased and as a result its resonant frequency gradually increased to f_{\max} (equivalent to the resonant frequency when the notch is not opened). The frequency shift of this tuning method is not as sensitive as the disc tuner on the cylinder's axial shift (caused by temperature and vibration).

- Naturally, in order for the rectilinear motion of the cylinder to change into rotating motion, we must cut many triangular holes on the base of the cylinder according to the number of cavities. In this way, when the cylinder rotates, it is equivalent to alternating motion. These types of triangular holes are replaced by round holes. Although, at this time the entire tuning frequency $f_{\min} - f_{\max}$ cannot be obtained, we can still attain 70% of the tuning frequency band.

The shape of the holes on the cylinder determine that the frequency pattern will change with the time. When the holes are

circular, we can approximately attain a sinusoidal change pattern. By using side holes we can obtain a sawtooth frequency change pattern but its frequency band is narrower.

Fig. 6.8 shows the structure of this type of cylindrical tuning plunger.

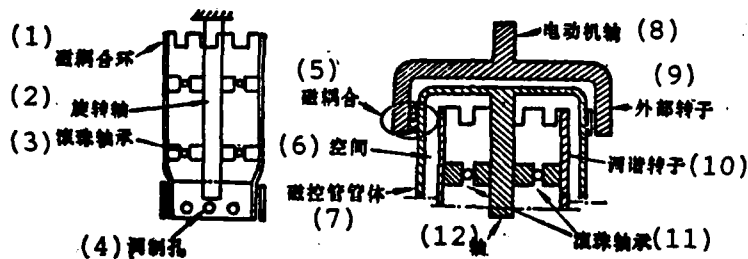


Fig. 6.8 Schematic of the Structure of a Cylindrical Rotor

- Key:
1. Magnetic coupling loop
 2. Rotation axis
 3. Ball bearing
 4. Modulation hole
 5. Magnetic coupling
 6. Space
 7. Magnetron's tube body
 8. Motor axis
 9. Outer rotor
 10. Tuning rotor
 11. Ball bearing
 12. Axis

One end of its rotating axis is fixed on the top casing so as to obtain good heat diffusion. Even though this be the case, the temperature of the bearing can still reach 350°C . Its highest rotating speed can reach 5,000 rotations/minute. The YJ1320 type magnetron in table 6.1 used this type of improved cylindrical tuning plunger structure. Its center frequency is 16,500 megahertz, its peak power is 65 kilowatts and its specified tuning band width is 600 megahertz; it actually

reached 670 megahertz. For example, when the tuning band width was decreased from 670 to 450 megahertz, its peak power could increase from 65 to 95 kilowatts. Maximum frequency pulling is 17 megahertz.

6.3 The Dither-Tuned Jumping Frequency Magnetron

Because of the operating principles of the rotary tuned jumping frequency magnetron discussed in the last section, that magnetron was only suitable for use in multicavity type magnetrons. However, in many areas of performance, the multicavity magnetron does not match up to the coaxial magnetron. For example, in the areas of frequency stability, frequency spectrum purity operating reliability and operating life, the coaxial magnetron is far superior to the multicavity magnetron. The frequency repulsion (electronic frequency shift) of the coaxial magnetron is $1/5$ that of the multicavity magnetron and its frequency pulling caused by the load is $1/3$ that of the multicavity magnetron. Thus, the question of how to realize jumping frequency between the pulses in the coaxial magnetron has become a relatively important subject.

The earliest method for solution was the so-called coaxial magnetron with dither-tuning [4]. The high speed jumping frequency between the pulses of this type of dither-tuned magnetron was only able to be realized in a relatively narrow frequency band (e.g., several ten megahertz). Yet, the center frequency of its dither-tuning can be tuned at low speed by the mechanical tuning method in a relatively wide frequency range. In this way, although the band width of the jumping frequency between the pulses is relatively narrow, its operating frequency range is still wide enough.

Naturally, by using this type of jumping frequency radar with a dither-tuned magnetron we lose a good deal of the superior

performance of jumping frequency radar. Firstly, as regards anti-jamming capabilities, because the frequency band of the high speed jumping frequency is very narrow, the effects of its anti-jamming are naturally lacking. This type of dither jumping frequency radar is easily scouted and at the same time is easily jammed by an electronically tuned wide band noise wave jammer. Secondly, this narrow band dither jumping frequency radar cannot provide the critical jumping frequency band width needed for target echo decorrelation. As a result, we lose the advantages of increasing the detection range and raising tracking precision. However, in any case, in the above mentioned areas this dither jumping frequency radar with a narrow jumping frequency band width is stronger than fixed frequency radar. Furthermore, and most importantly, this relatively narrow dither jumping frequency radar also maintains the capability of jumping frequency radar to inhibit sea or ground clutter. This is because, as we know from the former analysis, the frequency difference required for clutter decorrelation is equal to the reciprocal of the pulse width. If the pulse width is 1 micro-second and the independent sample pulse number N required for each scanning is 20-30, several ten megahertz is sufficient for the dither-tuning band width. At this time, the inhibition of the clutter is approximately \sqrt{N} times. Therefore, this type of dither-tuned magnetron is widely used in airborne and shipborne radar for inhibiting sea clutter.

Because its jumping frequency band width is relatively narrow, the local oscillation's automatic frequency tracking system is greatly simplified and can even be refitted on the original klystron.

Aside from this, because the high speed dither component and low speed tuning component of the majority of dither-tuned magnetrons are completely independent, damage to the high speed

dither-tuning mechanism cannot affect the low speed wide band tuning mechanism. This raises the actual operating life of the tube.

We will now take a look at the structural principles of this type of dither-tuned magnetron.

Fig. 6.9 shows the structural principles of the early dither-tuned magnetron.

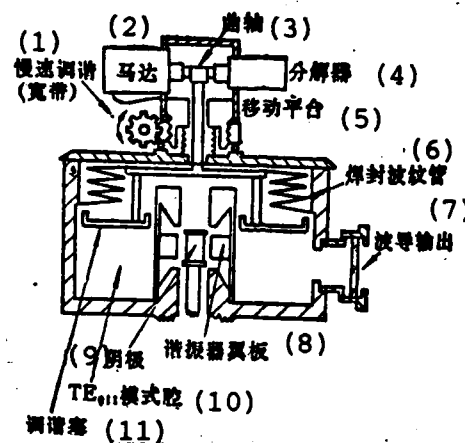


Fig. 6.9 Schematic of the Structure of the Early Dither-Tuned Magnetron

- Key:
1. Slow speed tuning (wide band)
 2. Motor
 3. Crank axle
 4. Resolver
 5. Shifting platform
 6. Welded corrugated tube
 7. Waveguide output
 8. Resonator wing plate
 9. Cathode
 10. TE_{011} type cavity
 11. Tuning plunger

Its detailed structural drawing is shown in fig. 6.10 [5].

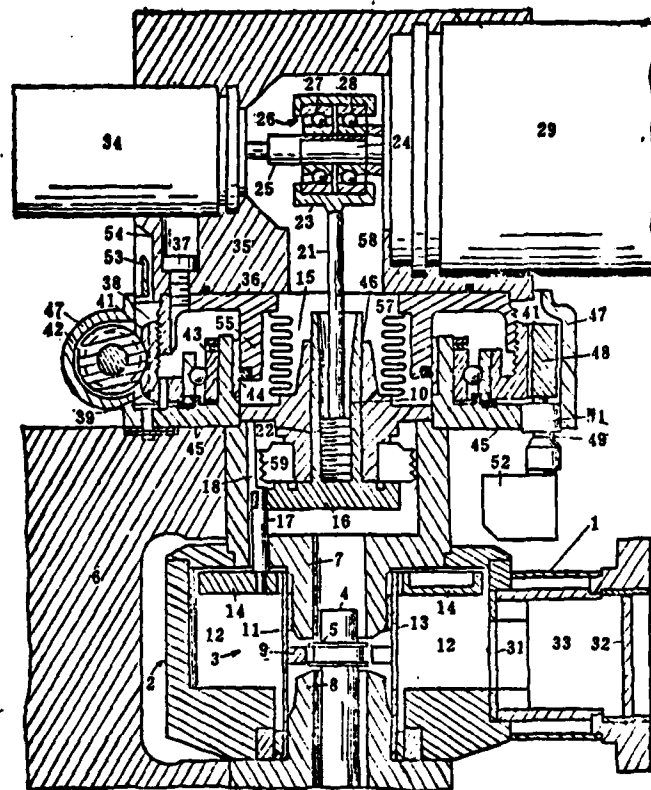


Fig. 6.10 Detailed Structural Drawing of the Early Dither-Tuned Magnetron

The fast speed dither-tuning is realized by drawing support from the cam (24) activator of a high speed motor (34) drive. This cam activator transforms the rotating motion of the high speed motor into the high speed dither alternating motion of a coupling bar. The alternating motion of this coupling bar is transferred by the welded corrugated tube (57) which is vacuum sealed to the tuning plunger (14) in the coaxial resonant cavity. The fast speed dithering of the tuning plunger causes the resonant frequency of the coaxial resonator (the oscillation frequency of

the coaxial magnetron) to have a corresponding fast change. Because the inertia of the mechanical alternating motion is very large, when the motor rotates at a high speed, the range of its alternating motion (dither) cannot be very large. Therefore, the frequency range of its dither tuning is also relatively narrow. In order for the center frequency of its dither to be able to be tuned in a wider range, this type of dither-tuned magnetron often adds a low speed wide band tuning mechanism. Early dither-tuned magnetrons used a worm wheel (41) and a worm to shift the entire tuner platform in order to realize this type of low speed wide band tuning (see fig. 6.9). Although this method is relatively simple mechanically, because the mass of the tuner platform (including the tuning motor, frequency reading resolver etc.) is very large, to prevent tuner slack (this type of slack can produce unwanted frequency modulation when vibrating) it is necessary that the elasticity of the added springs be very strong. Although this elasticity can help to overcome the parasitic frequency modulation, it also increases the moment required when there is low speed wide band tuning. As a result, this causes the speed of the wide band tuning to decrease even more.

Fig. 6.11 draws the relational curve of the moment and parasitic frequency modulation [6] when at different dither speeds. If in 5g oscillation acceleration and the allowable parasitic frequency modulation is 1 megahertz, then its moment must be above 20 ounces-inches (equal to 1,440 grams-centimeters).

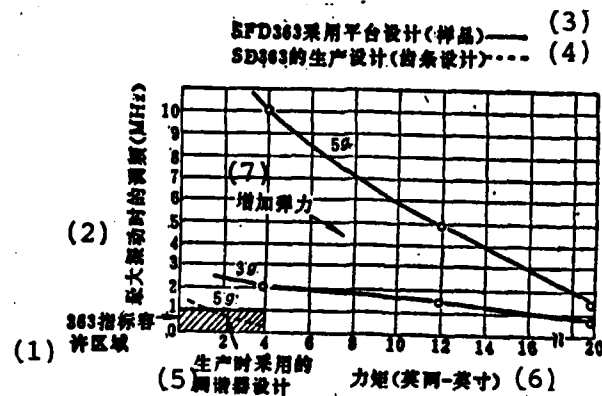


Fig. 6.11 Relationship of the Moment and Parasitic Frequency Modulation When at Different Dither Speeds

- Key:
1. 363 index allowable region
 2. Frequency modulation with maximum oscillation (MHz)
 3. SFD363 uses the platform design (sample) ———
 4. SD363 produced design (rack design) ----
 5. Tuner design used during production
 6. Moment {ounces-inches}
 7. Additional flexibility

Such a large moment of force cannot be permitted and therefore this original dither tuner is very quickly represented by a type of rack vibrator. The structure of this type of rack vibrator is shown in fig. 6.12.

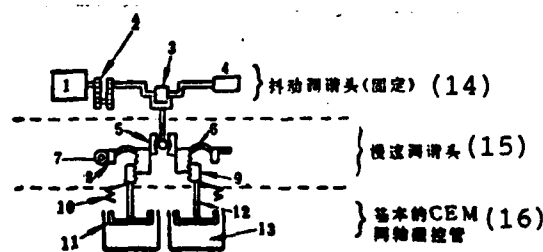


Fig. 6.12 Structural Diagram of Rack Vibrator

- Key:
1. Motor
 2. Geared system
 3. Crank axle

- Key:
4. Reading system
 5. Spherical connection
 6. Elastic disc
 7. Worm
 8. Worm wheel
 9. Thread connector
 10. Vacuum corrugated tube
 11. Tuning plunger
 12. Tuner's connecting rod
 13. TE_{01} cavity
 14. Dither tuning head (fixed)
 15. Slow speed tuning head
 16. Basic CEM coaxial magnetron

Its main feature is that the turning of the low speed tuning mechanism is sent to a corrugated connecting system by the worm wheel worm and is not directly changed into alternating motion. This separates the low speed tuning system and high speed dither system. We can see from fig. 6.12 that the eccentric wheel of the high speed motor drive passes a spherical connection to the screw of the thread connector. The nut of this thread connector is then joined to the tuner's plunger. The low speed wide band tuning system is composed of a worm wheel, worm and a spring disc. This spring disc is connected to the thread connector. When the worm wheel turns, the screw turns with it and the nut attached tuning plunger moves up and down. In this way, the elastic disc is separated from the high speed vibration and the spherical connector is separated from the low speed turning. This type of structure has very good anti-vibration characteristics and does not require a very hard spring to be able to satisfy the requirements of the parasitic frequency modulation. Thus, this greatly reduces the moment of force required for tuning. As shown in the shadowy area of fig. 6.11, when there is 5g vibration acceleration, a tuning moment of 2 ounces-inches (144 grams-centimeters) is needed to satisfy the requirements of 1 megahertz of parasitic frequency modulation. That is, its moment is reduced 10 fold. However, this type of design is naturally more complex in mechanical structure. Many components

are added and there must be excellent coordination between each component so as to avoid unrelated movement.

Fig. 6.13 shows the actual structure of this type of dither-tuned magnetron [7].

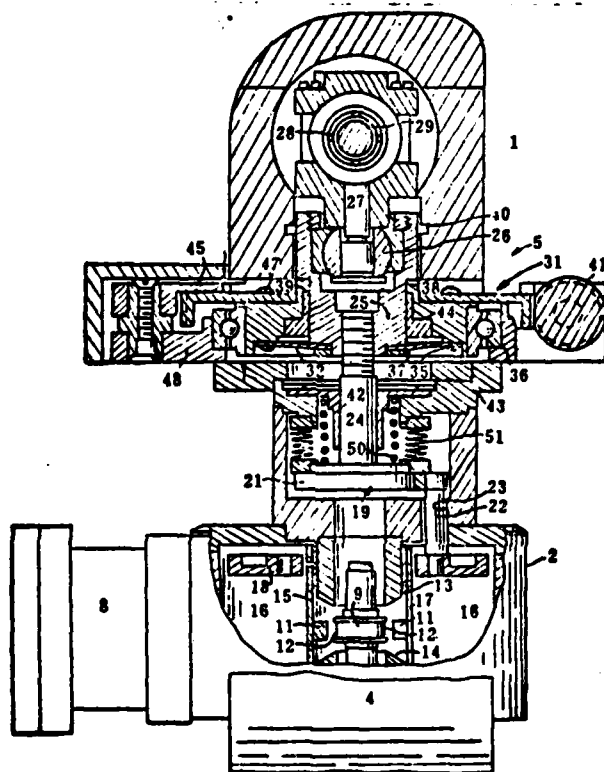


Fig. 6.13 Actual Structural Diagram of Rack Dither-Tuned Magnetron

In the figure, (2) is the common coaxial magnetron and (18) is the tuner's plunger. This tuner plunger is connected by strut (22) and disc (21). These components are all in the vacuum bulb and welded corrugated tube (51) guarantees that the alternating motion is transmitted to those components in the vacuum. The fast speed dither-tuning goes from high speed motor driven eccentric turning axle (29) past spherical connector (26) and is transmitted to the tuning plunger. The rotating speed of the

motor is 12,000 rotations/minute (equal to a dither rate of 200 hertz), its eccentric quantity is 0.0012 inches and the up and down movement of the tuning plunger is about ± 0.0012 inches. Such a large dither quantity is equivalent to dither of ± 10 -15 megahertz for a Ku wave band tube.

Its low speed wide band tuning is realized by the worm (41) and worm wheel (31). Worm wheel (31) is joined by elastic disc (32) and nut (25). Actually, this elastic disc is 3 triangular arranged reeds. It can separate the up and down dither. Nut (25) joins the thread connector and spherical connector. In this way, the rotating motion of the worm wheel can change to the alternating motion of the actuating rod. The quantity of this low speed alternation motion can reach 0.200 inches, and in the Ku wave band, its tuning range can be over 2,000 megahertz.

It is naturally considered that the wider the dither-tuning band width of the dither-tuned magnetron the better. It is of course necessary that the eccentric quantity of the eccentric wheel be enlarged. When in high speed rotation, this type of eccentric wheel can cause very large vibration which will accelerate the wear of the bearing and thus shorten its operating life. If a certain operating life is required, then while enlarging the eccentric quantity we must decrease the rotating speed of the motor. The life-time of the bearing is determined by the alternating tuning power, static load, selection of lubrication as well as by the operating temperature. Improvement of the bearing's lubrication and cooling can prolong the life of the bearing when there is similar dither force. When in relatively high temperature, use of grease lubrication is relatively good while in relatively low temperature oil lubrication is best. Fig. 6.14 gives the relationship between the bearing's static force and life-time when there is oil lubrication and the tuning rate is 200 hertz (the motor rotates 12,000

times/minute) [6]. We can see from the figure that improvement of the bearing's cooling has a very great effect on prolonging the life of the bearing. For example, when the bearing's temperature decreases from 125° to 100°C , its life-time can increase from 200 to 1,000 hours.

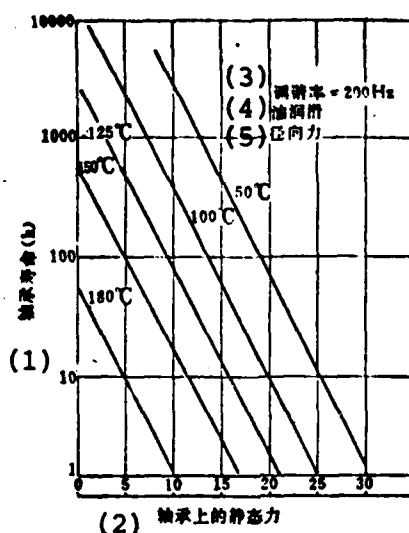


Fig. 6.14 The Effects of Static Force and Temperature on the Life-Time of Dither-Tuned Magnetron Bearings

Key: 1. Bearing's life-time (h)
 2. Static force on bearing
 3. Tuning rate=200 Hz
 4. Oil lubrication
 5. Radial force

However, after using measures to prolong the bearing's life-time, within a certain life-time, the dither band width and dither rate of this type of high speed motor driven, mechanically alternating motion type dither-tuned magnetron approximately form a reverse ratio relation. Table 6.2 gives the basic parameters of dither-tuned magnetrons.

(1) 波数	(2) 型号	(3) 接安 类型	(4) 中心频率 (千赫)	(5) 带宽 (赫)	(6) 调幅率 (%)	(7) 调制频率 (赫)	(8) 峰值功率 (千瓦)	(9) 最大 效率 (%)
C	VMC-1101	A	5.0	220	5	200	600	3.0
	VMC-1001	A	5.7	250	10	200	250	3.0
	VMX-1116	A	8.0	450	25	400	150	3.0
	SFD-354A	T/D	8.5~9.0	60	75		200	2.0
	SFD-367	T/D	8.5~9.0	60	75		200	2.0
	SFD-360	T/D	8.6~9.0	60	95		250	2.5
	SFD-364H	A	9.05			400	200	2.0
	VMX-1008	A	9.05	300	15	300	200	2.0
	VMX-1164	A	9.05	1100	20	1000	250	3.0
	SFD-300A	T/D	9.1~9.5	60	75		75	4.0
	SFD-363	T/D	9.1~9.6	30	200		65	3.5
	VMX-1144	A	9.10	500	25	450	200	2.0
	VMX-1160	D	9.25	100	100		75	2.5
	SFD-354G	A	9.25	500	25	450	200	2.5
	VMX-1175	A	9.25	500	25	400	75	5.5
	VMX-1057	A	9.25	500	25	400	400	0.8
	VMX-1058	A	9.35	500	25	400	200	2.0
	SFD-366 F	D	9.375	150	75		90	4.0
X	VMX-1004	D	9.375	250	30		200	2.0
	VMX-1004A	A	9.375	250	30	(35)	200	2.0
	VMX-1201A	A	9.10	100	(三角波)	1000	200	
	VMU-1117	A	15.025	600	20	450	90	0.5
	BLM-175		16.9~17.0	30	200		35	2.0
	BLM-180		16.9~17.0	30~34	200		45	
	BLM-181		16.9~17.0	30	200		65	2.5
	VMU-1000	T/D	16.9~17.0	30	200		65	2.5
	VMU-1190	D	16.95	300	150		65	1.0
	VMU-1102	D	16.5	200	200		65	2.5
K _a	VMU-1040	D	16.5	200	150		65	2.2
	VMU-1170	A	16.75	550	25	500	20	0.5
	VMU-1042A	D	16.5	250	200		35	2.0
	SFD-345	D	16.5	400	150		35	1.0
	K _a VMA-1043	D	14.5	300	150		45	0.5

(36)注: D—脉冲调制, 中心频率为固定, 在一定范围内以一定频率调制;
 带宽完全由外加调制电压的频率、幅度和调制率决定。

(10) 最大 工作比	(11) 电压 (千伏)	(12) 电流 (安)	(13) 效率 (%)	(14) 最大 频率 (兆赫)	(15) 最大电子 速度 (兆赫/安)	(16) 环境温度 (℃)	(17) 重量 (磅)	(18) 冷却方式
0.0012	35	40						
0.002	25	24						
0.0011	21	24						
0.0011	22	27.5	34	5	0.1	0.2	15.5	风冷(19)
0.0011	23	27.5		5	0.1	0.2	15.5	风冷(20)
0.001	20	25	30	5	0.1	0.2	20	风冷(21)
0.0011	22	27.5						风冷(22)
0.0011	23	27.5		5	0.1	-0.05	15.5	风冷(23)
0.0015	25	27.5						
0.0011	15	15	50	0	0.1	0.2	10.5	风冷(24)
0.0011	16	15		0	0.1	0.2	10.5	风冷(25)
0.0011	22	27.5						风冷(26)
0.0011	15	15						风冷(27)
0.001	22		45					
0.0011	15	15						
0.0012	32	30						
0.0011	23	27.5						
0.0011	15	17.5	6	0.1	-0.2	9.12		风冷(28)
0.0011	22	27.5						
0.0011	23	27.5						
0.002	10	15						
0.0008	13	11		0	0.1	0.4	8.75	风冷(29)
0.0008	125							
0.0011	15	15	35	0	0.1	0.4	9.25	风冷(30)
0.0011	15	15						风冷(31)
0.0012	14	16						
0.0011	14	15	35					
0.0011	14	16		0	0.15	0.4	9.5	风冷(32)
0.0011	13	9.5						
0.0011	13	9.5						
0.001	13	11		15	0.25		5.0	风冷(33)
0.0008	14	15		10	0.5	0.4	9.2	风冷(34)

T/D—可调/脉冲调制, 脉冲调制时的中心频率为可调的; A—脉冲调制, 其他由注

Table 6.2

Table 6.2 Parameters of Dither-Tuned and Precision Tuned Frequency Agility Magnetrons

- Key:
1. Wave band
 2. Model
 3. Agility type
 4. Center frequency (megahertz)
 5. Agility band width (megahertz)
 6. Tuning rate (hertz)
 7. Precision tuning range (megahertz)
 8. Peak power (kilowatts)
 9. Maximum pulse (microseconds)
 10. Maximum operating ratio
 11. Anode voltage (kilovolts)
 12. Anode current (amperes)
 13. Effect (%)
 14. Maximum frequency pulling (megahertz)
 15. Maximum electron frequency shift (megahertz/amperes)
 16. Standard temperature coefficient (megahertz/ $^{\circ}$ C)
 17. Approximate weight (tons)
 18. Cooling means
 19. Wind cooled
 20. Wind cooled
 21. Conduction cooling
 22. Wind cooled
 23. Wind cooled
 24. Wind cooled
 25. Conduction cooling
 26. Wind cooled
 27. Conduction cooling
 28. Conduction cooling
 29. Conduction cooling
 30. Wind cooled
 31. Conduction cooling
 32. Wind cooled
 33. Conduction cooling
 34. Conduction cooling
 35. (Triangular wave)
 36. Note: D-dither-tuned, that is, the center frequency is fixed and there is certain frequency dither-tuning in a certain range; T/D - tunable/dither tuning, that is, the dither-tuned center frequency is tunable; A - precision tuning, its output frequency is totally determined by the wave form with applied tuning voltage, the amplitude and the frequency.

Fig. 6.15 draws the relationship of the tuning ranges and tuning rates of these dither-tuned magnetrons with 1,000 hour life-times [6].

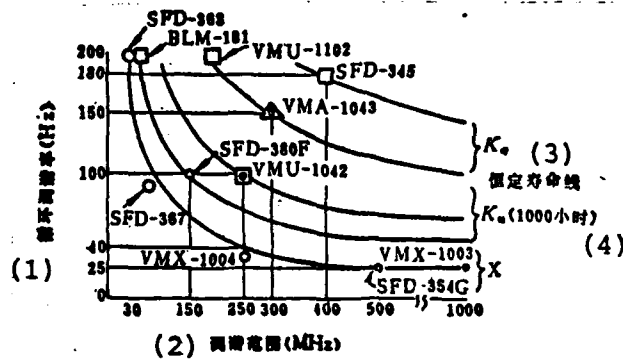


Fig. 6.15 Relationship Between the Tuning Rates of Dither-Tuned Magnetrons With 1,000 Hour Life-Times

Key: 1. Circulating tuning rate (MHz)
 2. Tuning range (MHz)
 3. Constant life-time line
 4. K_u (1,000 hours)

This relationship approaches the relationship of the so-called "G factor." We can see from the figure that a tube with relatively high frequency possesses a large tuning range and high tuning rate when in the same operating life-time. This is because, when the high frequency tube is in the same tuning plunger movement quantity, it possesses a high frequency tuning range. Moreover, the weight of the tuning plunger is lighter than a low frequency tube. Therefore, like the SFD-345 tube, when it operates in the Ku wave band, it can tune a frequency range of 400 megahertz with a 180 hertz tuning rate and still have a 1,000 hour life-time. If fast speed wide band jumping frequency is only used when the enemy discharges jamming, usually, with the use of fixed frequency or narrow band dither-tuning, its life-time can still be greatly lengthened.

6.4 Frequency Reading Resolver of the Dither-Tuned Magnetron

The oscillator in incoherent jumping frequency radar must be able to keep up with the fast speed jumping frequency of the jumping frequency magnetron. If the jumping frequency magnetron is able to give preset information this will greatly simplify the local oscillation of the jumping frequency's automatic frequency fine tuning system.

The dither-tuning mechanism in dither-tuned magnetrons is often driven by a fast speed motor. After the motor's rotating angle passes an eccentric wheel and transforms to alternating motion, this alternating motion forms a direct ratio with the rotating angle. Therefore it is only necessary to have a frequency resolver which can produce a sine wave directly related to the rotating angle. This can be the frequency preset information of the local oscillation. Fig. 6.16 shows the working diagram of the entire system. [8]

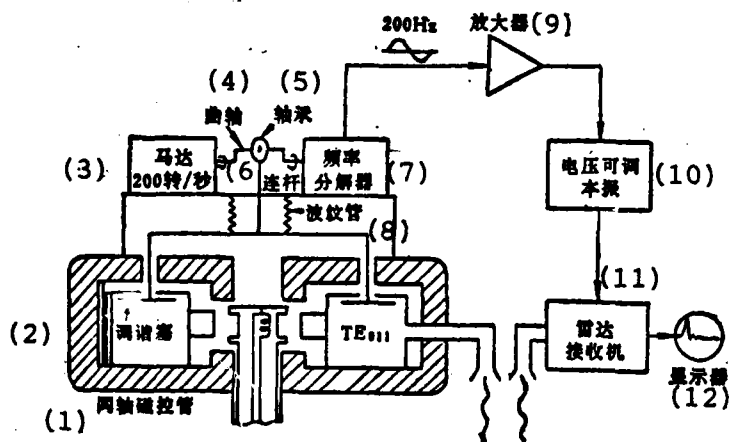


Fig. 6.16 Working Diagram of Frequency Reading Resolver

- Key:
1. Coaxial magnetron
 2. Tuning plunger
 3. Motor, 200 rotation per second
 4. Crankshaft
 5. Bearing

- Key:
- 6. Connecting rod
 - 7. Frequency resolver
 - 8. Corrugated tube
 - 9. Amplifier
 - 10. Voltage tunable local oscillation
 - 11. Radar receiver
 - 12. Display

However, use of a sine wave to represent its tuning frequency has certain conditions. Firstly, it is necessary that the entire crankshaft connecting rod system be very closely coordinated and that there be no spaces. Secondly, the tuning range must be very small ($< 1\%$) and thus can be considered to be operating in the characterisitic curvilinear range of the TE_{011} model resonant cavity's tuning. Thus, at this time, the movement of its tuning plunger forms a rectilinear relationship with the resonant cavity's resonant frequency. If this range is exceeded, it is then necessary to make corresponding corrections.

There are many simulation methods for producing this sine wave. The simplest method is the use of a permanent magnet steel fixed on the turning axle. When the motor's turning axle rotates, this permanent magnet steel induces sine wave voltage in the stator coil (see fig. 6.17) [6]. Although this type of resolver is very simple, it can only be used in a motor with a constant rotating speed. When the motor stops rotating, it has no output and has no way of indicating the real rotating angle position.

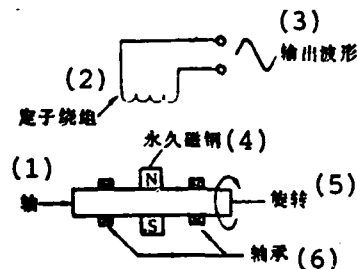


Fig. 6.17

Fig. 6.17 Use of the Frequency Reading Resolver With Permanent Magnet Steel

- Key: 1. Axle
2. Stator winding
3. Output wave form
4. Permanent magnet steel
5. Rotation
6. Bearing

To resolve this problem, we used a high frequency resolver with modulated high frequency carrier waves. Its schematic diagram is shown in fig. 6.18.

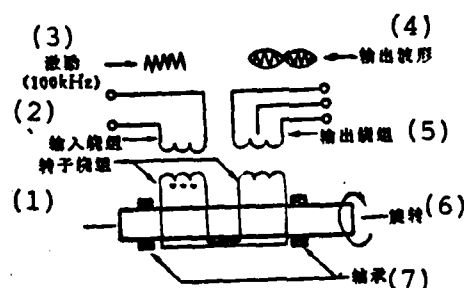


Fig. 6.18 The High Frequency Resolver as the Tuner's Position Reading Component

- Key: 1. Input winding
2. Rotor winding
3. Excitation (100 kHz)
4. Output wave form
5. Output winding
6. Rotation
7. Bearing

The input of the 100 kilohertz excitation signals are from the input winding, and the signals induced from the output winding are related to the rotating angle of the rotor winding. Further, the amplitude of the output carrier wave is modulated by the rotor's rotating angle. This modulated signal is added to the synchronic detector (or phase sensitive detector) for demodulation. The direct current voltage after detection represents the

tuning frequency of the transient magnetron. This type of high frequency resolver is a sensor of the rotating angle position and whether the rotor is stopped or rotating at a uniform speed, it can accurately give the frequency present information. Although this type of resolver presents certain temperature effects, due to the use of the excitation circuit, it is possible to use feedback for compensation.

This frequency reading resolver has very high accuracy reaching over 0.01%. Measurement of the error characteristics of this resolver is a very complex problem. Firstly, we must measure the real frequency of the tuner plunger's magnetron oscillation when in a certain position. Afterwards, by comparing it to the frequency simulated quantity given by the frequency reading resolver we can find the error of the resolver. Two methods can be used to measure this error characteristic. One is the static measurement method and the other is the dynamic measurement method. In the static measurement method the motor is not rotating and is only in several angle positions required for measurement. Afterwards, the frequency meter is used to measure the frequency of the magnetron's oscillation. This is compared with the simulated quantity of the frequency reading and thus we can obtain its static error characteristic. We can find the parabolic error caused by the non-linearity of the TE_{011} model resonant cavity's tuning characteristics from this static error characteristics. Yet, it cannot express the error caused by the entire tuning mechanism and resolver in a dynamic condition. The dynamic measurement method can resolve this problem. In the dynamic measurement method, the motor is rotating at a constant speed which causes the rotation of the motor and the timing pulse of the modulator to be totally synchronized. Yet, it also causes the phase of its synchronizing point to be able to be tuned which is equivalent to the magnetron operating at fixed frequency. The changing of the phase of the

synchronizing point can tune the operating frequency of the tunable magnetron. Because the frequency of the magnetron is fixed, its transmitted frequency can be measured by a spectrometer. By comparing the frequency simulation quantities of this frequency and frequency reading resolver measured by the spectrometer, we can obtain the dynamic error characteristics. Fig. 6.19 shows the dynamic error characteristics of the VMU-1102 dither magnetron measured with this method [6].

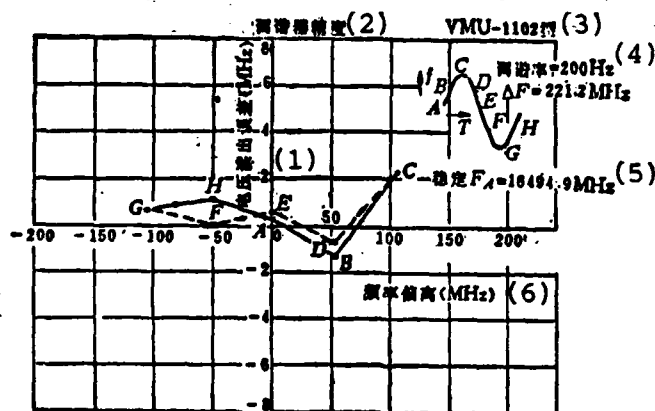


Fig. 6.19 The Accuracy When the Dither-Tuned Magnetron Reading Voltage Sine Wave is Used to Represent the Frequency Time Tuning Characteristics

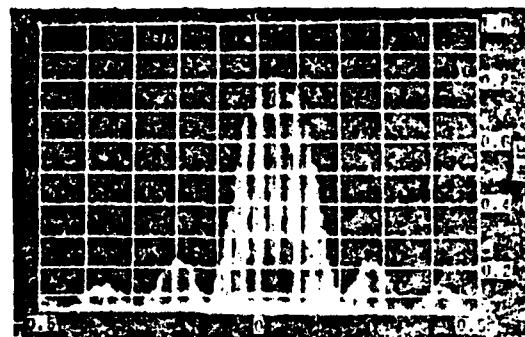
- Key: 1. Voltage reading error (MHz)
 2. Tuner's accuracy
 3. VMU-1102 model
 4. Tuning rate=200 Hz
 5. Steady $F_A = 16,494.9$ MHz
 6. Frequency deviation (MHz)

This magnetron is a dither-tuned magnetron with a Ku wave band. Its maximum jumping frequency range can reach 221.2 megahertz and its highest tuning rate can reach 200 hertz. When we measure the errors of the different points (A-H) during the entire tuning range, these errors were actually the main deviation of much dither circulation. This includes the errors caused by the non-linearity of the tuning characteristics.

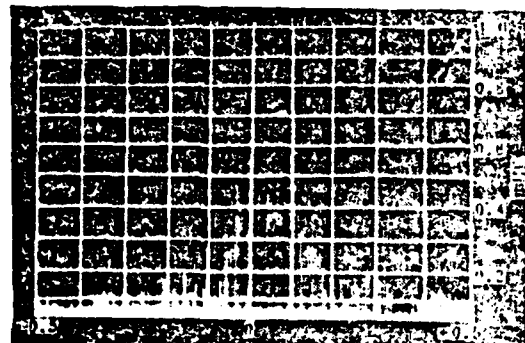
Measurement results on many tubes show that for X and Ku wave band tubes with a dither range of 60 megahertz, its typical accuracy is ± 1 megahertz. For Ku wave band tubes with a dither range of 200 megahertz, its typical accuracy is ± 3 megahertz.

Fig. 6.20 gives spectral photos of the VMU-1102 tube when there is no dithering and when in two different synchronized points [6].

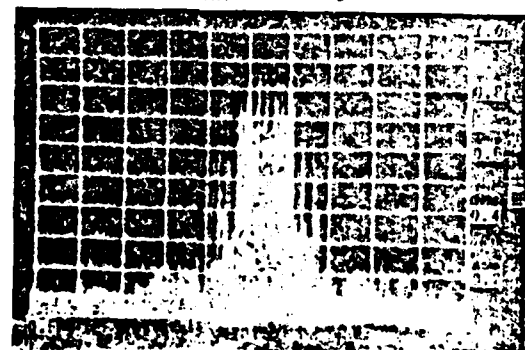
We can see from this figure that when synchronized, the dither frequency spectrum width must be wider than when there is no dithering. This is caused by the parasitic frequency modulation. This parasitic frequency modulation is formed by the minute difference between this period and the next in mechanical position. Its actual change is only ± 5 micrometers.



(a) 不抖动频谱: 脉冲宽度=1.8 μ s 频谱宽度=0.6MHz



(b) 抖动时的同步频谱: $f = 16.6\text{GHz}(\text{max})$ 频谱宽度=0.7MHz
附加调频=0.1MHz (peak)



(c) 抖动时的同步频谱: $f = 16.5\text{GHz}(\text{中})$ (中)
频谱宽度=0.75MHz 附加调频=0.15MHz (peak)

Fig. 6.20 Frequency Spectrum of the Dither-Tuned Magnetron
(Horizontal Staff: 0.3 Megahertz/Square)

Key: (a) Ditherless frequency spectrum: pulse
width=1.8 μ s, frequency spectrum
width=0.6 MHz

- Key: (b) Synchronic frequency spectrum with dithering: $f=16.6$ GHz (max), frequency spectrum width= 0.7 MHz, added frequency modulation= 0.1 MHz (peak)
- (c) Synchronized frequency spectrum with dithering: $f=16.5$ GHz (center frequency), frequency spectrum width= 0.75 MHz, added frequency modulation= 0.15 MHz (peak)

6.5 The Accutuned Jumping Frequency Magnetron

The high speed dither-tuning and low speed band width tuning of common dither-tuned magnetrons is completed by two totally independent tuning mechanisms. The advantage of this type of structure is that the two tuning mechanisms are totally separated, so that when a breakdown occurs in the high speed dither-tuned mechanism the low speed tuning mechanism can be used to tune the magnetron. Yet, it has a very large shortcoming, that is, its tuning flexibility is poor. High speed jumping frequency can only be realized in a narrow wave band and by increasing the band width of high speed tuning, we only lower its tuning speed. Nor can it realize programmed jumping frequency.

To improve its tuning flexibility it is necessary to combine the high speed dithering and low speed tuning mechanism into a tuning mechanism which very quickly responds to the speed. This mechanism can have jumping frequency between the pulses in a relatively narrow range and can also have jumping frequency within the scanning in a relatively wide frequency band. Thus, within each scanning period we can realize fixed frequency moving target display. Naturally, this tuning mechanism is unable to be driven by a motor with a constant rotating speed but must be driven by a fast speed responding position servo system. This type of angular position servo system must have a linear relationship between the command voltage and tuning frequency of the magnetron. Yet, it is well known that a non-linear relationship exists between travel a and tuning

frequency f when using a coaxial magnetron with a TE_{011} model resonant cavity in the tuner (see fig. 6.21) [9]. As mentioned previously, this non-linearity also causes the accuracy of the frequency reading resolver to decline. When the tuning range is increased, the problem of the non-linearity is even more serious. Therefore, the key problem has become how to cause its tuning characteristic to become rectilinear.

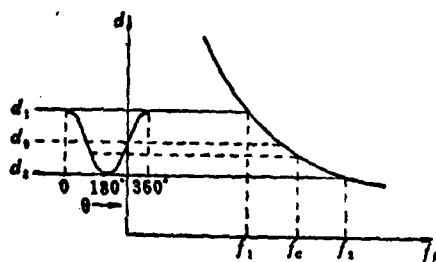


Fig. 6.21 Non-Linearity Timing Characteristics of the TE_{011} Resonant Cavity

By carefully analyzing the relationship between the input voltage, motor's turning angle, tuning frequency and resolver (fig. 6.22) we can discover that there is no sine relationship caused between the output frequency and turning angle by the non-linearity of the tuning characteristics. If we take the tuning plunger's turning angle in the highest point position (d_1 , in fig. 6.21) as 0 degrees, its output frequency lags behind the input voltage (or resolver output voltage) during the first half and when in a turning angle of 90° it reaches the maximum (lag of $2a$ degrees). During the latter half it leads the sine wave of the input voltage and when in 270° it is maximum (lead of $2a$ degrees). On the one hand, this type of lag and lead reduces the accuracy of the resolver's output frequency simulated signals but on the other hand, makes it impossible for the position servo system (the linear relation existing between the frequency and input voltage) to advance.

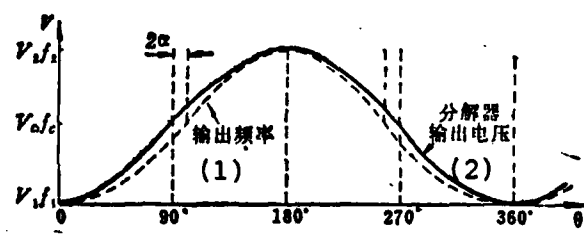


Fig. 6.22 Relationship Between the Input Voltage and Output Frequency and the Resolver's Output Voltage and Motor Turning Angle

Key: 1. Output frequency
2. Resolver's output voltage

It is necessary to make corrections on it in order to resolve this problem.

There are many methods of correction. One method is making corrections on the command voltage of the input based on the tuning characteristics. However, this requires a complex numerical simulated transformation system or function generator. Moreover, this method of correction can only resolve the non-linearity problem between the input voltage and tuning frequency and is unable to resolve the non-linearity relationship between the output frequency simulation and real frequency. It can only produce the same problems when correcting the output frequency. Therefore, it is best to directly correct the non-linearity between the tuner's position and the tuning frequency. Even if there is produced a non-sinusoidal relation between the tuned motor's turning angle and tuning plunger position it is best to compensate for the non-linearity relation between the tuner's position and tuning frequency. A simpler method is the eccentric gear correction method. This eccentric gear pair are two gears with similar eccentric quantities engaged together (see fig. 6.23).

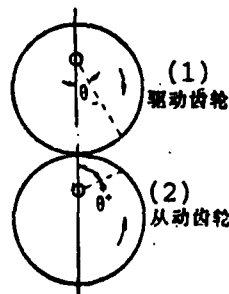


Fig. 6.23 Eccentric Gear Corrector

Key: 1. Driving gear
2. Driven gear

This gear pair has a special feature. If the position is as shown in the figure, when the driving gear rotates a relatively small angle θ , the driven gear rotates a relatively large angle θ^+ , that is, the driven gear leads the driving gear. In a rotation of 180° , the situation is completely opposite. The driving gear must rotate a larger angle θ^+ and the driven gear rotates a θ angle, that is, the driven gear lags behind the driving gear. If the axles of the driving gear and driven gear are joined together, and the axle of the driven gear and eccentric of the tuner's connecting rod are joined together, this can then compensate for the non-linearity of the tuning characteristics. Use of this method can reduce the non-linearity of the tuning characteristics to within 0.5%. Fig. 6.24 is a schematic of this tuning mechanism [6].

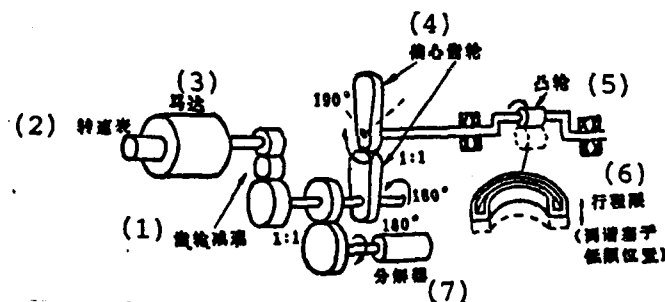


Fig. 6.24 Schematic of the Linearization Correction Mechanism of the Tuning Characteristics

- Key:
1. Gear deceleration
 2. Rotating speed meter
 3. Motor
 4. Eccentric gear
 5. Cam
 6. Travel limit (tuning plunger in low frequency position)
 7. Resolver

After the driving motor undergoes gear reduction, there is a 1:1 engaging by the common gears to the tuner's cam. During the first half period, when the driving axle rotates 180° the resolver also

rotates 180° , yet the cam's turning axle rotates 190° . This leading quantity compensates for the lag quantity of the tuning characteristic. The results of using this corrector have been quite satisfying. Fig. 6.25 draws the error characteristics before and after linearization of the VMX-1003 jumping frequency magnetron [6].

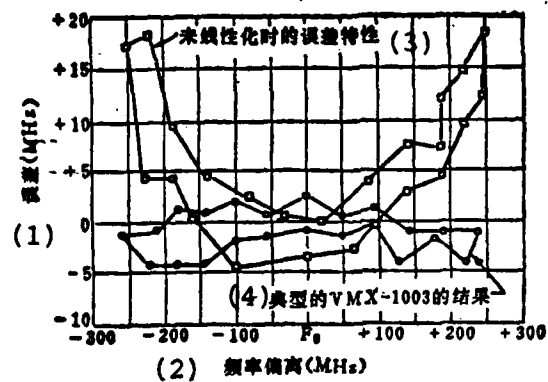


Fig. 6.25 Comparison of Error Characteristics Before and After Linearization

- Key: 1. Error (MHz)
 2. Frequency deviation (MHz)
 3. Error characteristics before linearization
 4. Results with typical VMX-1003

We can see from the figure that the linearization of a tube with a 500 megahertz tuning range can reduce the maximum error from 20 to 5 megahertz.

Fig. 6.26 shows the actual structure of this linearized jumping frequency magnetron [8].

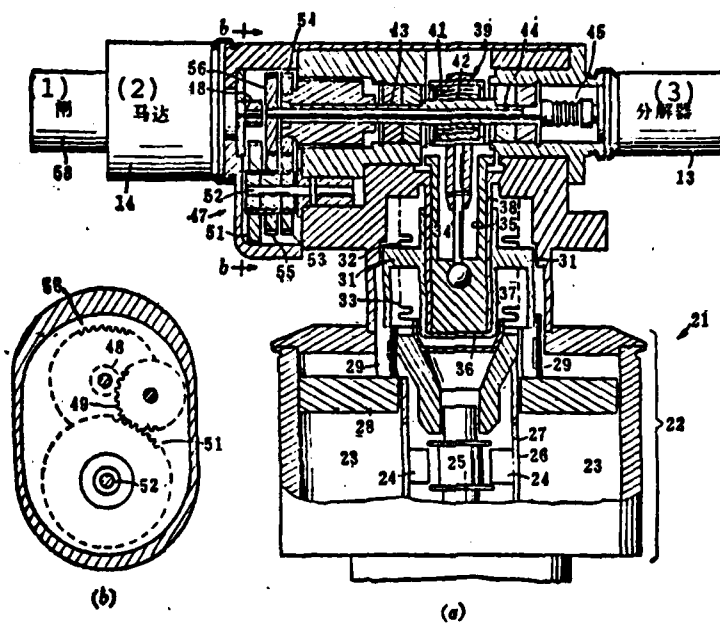


Fig. 6.26 Structural Diagram of a Jumping Frequency Magnetron With a Tuning Characteristic Linearized Structure

Key: 1. Gate
2. Motor
3. Resolver

After the driving motor (14) uses reducing gear system (48), (49) and (51), the rotating speed decreases from 10,000 rotations/minute to 1,500 rotations/minute. A pair of common 1:1 gears will engage the turning of turning axle (52) to turning axle (44) of the resolver. Another pair of eccentric gears, (53) and (54), then engage the turning of turning axle (52) to turning axle (43) of the tuner plunger's eccentric (42). Turning axle (43) is a sleeved axle and the sleeve is outside turning axle (44). This eccentric (42) uses ball bearing (41) to drive plunger rod (34) up and down. Plunger rod (34) is connected by a spherical connector and disc (31). Several protruding struts (29) on disc

(31) are joined with tuning plunger (28). Above and below disc (31) are welded vacuum corrugated tubes so as to guarantee vacuity in the tube. The effect of using the two connected vacuum corrugated tube structure will be discussed in detail below in the section on voice coil magnetrons.

An accutuned jumping frequency magnetron was developed on the basis of the linearized tuning mechanism. The structure of the tuning mechanism of this so-called accutuned jumping frequency magnetron is the same as that shown in fig. 6.26. Its major difference is that a servo motor is used instead of a common high speed motor. Because of its tuning characteristic correction it is rectilinear and thus can possibly use a position servo system (see fig. 6.27) [6]. This greatly increases the flexibility of its jumping frequency.

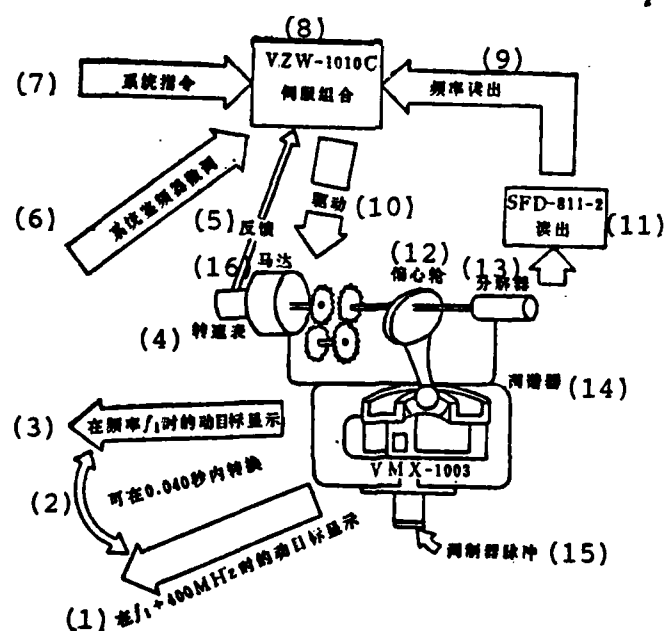


Fig. 6.27

Fig. 6.27 Schematic of the Servo Control System of an Accutuned Frequency Agility Magnetron

- Key:
1. Moving target display when in $f_1 + 400$ MHz
 2. Changeable within 0.040 seconds
 3. Moving target display when in frequency f_1
 4. Rotating speed meter
 5. Feedback
 6. System frequency discriminator's fine tuning
 7. System control
 8. VZW-1010C servo combination
 9. Frequency reading
 10. Driving
 11. SFD-811-2 reading
 12. Eccentric
 13. Resolver
 14. Tuner
 15. Modulator pulse
 16. Motor

The accutuned frequency agility magnetron uses a 400 hertz servo motor. This servo motor is controlled by a VZW-1010C servo combination. There is a 100 kilohertz frequency oscillator in it and the reference oscillation given by this oscillator is added to the frequency read-out resolver on the magnetron. This is added to the synchronized detector (phase detector) and reference signal synchronized detection by the resolver output's 100 kilohertz signal so as to obtain simulated voltage of the frequency read-out. The control command voltage of the supplemented transmission frequency is added to the servo control combination by opposite polarity. Its amplitude range is ± 5 volts. When comparing this voltage and frequency read-out voltage in a servo comparison amplifier, we can obtain an error signal which is added to the servo motor by the power amplification. The output of the power amplification is approximately 100 watts, the servo motor is a single phase (90° phase shift) frequency of 400 hertz and its control voltage is a direct current of 0-35 volts. After the servo motor begins to rotate it

is coupled to the cam by a speed ratio of about 6.5:1 (X wave band tube). Its frequency output signal changes until the comparison amplifier output's error signal is 0. When 0, the tuning frequency of the magnetron is equal to the required command frequency.

To quicken the speed of the frequency jumping, the band width of the entire servo system is made wider. At the same time, to eliminate oscillation wavering during the transient process, the negative feedback of the rotating speed meter is increased in the servo control system. This can further shorten the time needed for attaining a steady condition. The power supply of the rotating speed meter is 400 hertz voltage after a phase shift. Its amplitude is 26 volts (effective value). Fig. 6.28 gives the transient response when there is no negative feedback [6].

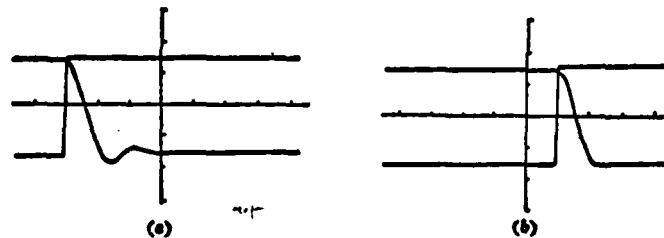


Fig: 6.28 In the Frequency Jumping of an X Wave Band Accutuned Magnetron Without Rotating Speed Meter Feedback and With Feedback, the Fast Speed Jumping Must Include Positive Frequency Peaking. With the Aid of Tuning Speed Negative Feedback We Can Obtain Optimum Tuning

- (a) Top part without feedback: command signal ($\rightarrow +$); bottom part: read-out; vertical: 2V/div; horizontal: 20ms/div; ΔF : 300 MHz; t : 60 ms;
- (b) Top part has feedback: command signal ($\rightarrow +0$); bottom part: read-out; vertical: 2V/div; horizontal: 20 ms/div; ΔF : 300 MGz; t : 31ms

If the frequency jumping of an X wave band accutuned magnetron is 300 megahertz, when there is no feedback, the time

required to reach stability is 60 milliseconds. After using rotating speed meter feedback, this stability time can be shortened to 31 milliseconds; shortened by almost one-half. This servo system can retune the frequency within 0.5 megahertz. Although this is quite accurate as compared to the former system yet this accuracy is not sufficient when operating in a moving target display system. This is because extremely accurate frequency returning is required to coordinate with the highly stable local oscillation. To satisfy this requirement, the following measure is used in this accutuned magnetron. When the magnetron is tuned close to its final frequency the servo system loop is opened and the error signal amplifier receives the output of the frequency discriminator which has high stability local oscillation. This frequency discriminator will transmit the frequency difference of the magnetron's frequency and high stability local oscillation and thus obtain higher retuning precision. Only if the frequency discriminator has sufficiently high output sensitivity will the returning precision of this system be able to reach 0.1 megahertz.

When the accutuned magnetron operates in periodic dither jumping frequency, only if the feedback loop is opened and we add a periodic wave form frequency command to the comparison amplifier can we realize dither jumping frequency. When this periodic wave form is a sine wave, we can obtain a higher tuning range. Naturally, the highs and lows of the tuning rate are related to the tuning band width. When its jumping frequency range is 20 megahertz, the tuning rate can reach 400 hertz and when the jumping frequency range is 500 megahertz, its tuning rate is only 25 hertz. When the input's frequency control command is a triangular wave, its tuning speed declines even more. Fig. 6.29 is a response wave form when a 20 hertz triangular wave is used to control a 150 megahertz frequency [6].

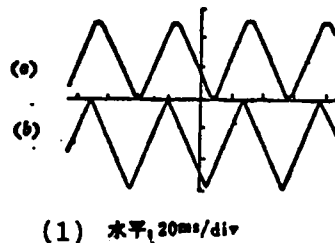


Fig. 6.29 Servo Control Tuning of a SFD-354G Magnetron (200 Kilowatts, 500 Megahertz Dither-Tuning Range). This Accutuned Magnetron Can Reappear Different Tuning Wave Forms In Its Servo Response Characteristic Range

- (a) Magnetron tuner's response: total frequency deviation 150 MHz (X wave band);
- (b) Servo control input wave form: 20 Hz triangular wave

Key: 1. Horizontal

The triangular waves below are servo control input wave forms (i.e. system frequency command). The wave forms on top are the accutuned magnetron tuner's response wave forms. We can see from the figure that there is a phase shift between its response and input wave forms. This is induced by the servo amplifier. At the same time, the responding top end becomes round. This is determined by the limited servo system band width.

The tuning activator of this accutuned magnetron is outside the tube. This possibly improves many other useful tube characteristics. For example, we can add a bimetal compensator to reduce the thermal effects. We can also reduce the temperature coefficient of an X wave band tube with a 500 megahertz jumping frequency range to 0.05 megahertz/ $^{\circ}\text{C}$. The magnetron's heat shift is the function of the mean power. This can improve the heat dispersion of the tube and can be overcome by using a tuner

made of a material with a low expanding coefficient. An X wave band 200 kilowatt accutuned magnetron can reduce the thermal shift to 3 megahertz by using the above measures.

To sum up, the accutuned magnetron possess great tuning flexibility. It can have the following five types of operating modes.

- (1) Fixed frequency
- (2) Manually tuned to any frequency. The tuning method is only to rotate one turn wherein the tuning rate reaches 100 megahertz/second.
- (3) The speed and stability of the jumping frequency between antenna scannings or within certain time intervals can satisfy the requirements of multi-frequency moving target display.
- (4) Programmed tuning. This changes its frequency based on a prearranged program.
- (5) Frequency agility between pulses based on a certain pattern or random jumping frequency.

This causes its operating flexibility to be greatly increased. For example, a certain accutuned jumping frequency magnetron (VMX=1261A) [10] has an operating frequency of 8.6-9.6 kilomegahertz and a peak power of 200 kilowatts. Its tuning rate can reach 40 megahertz/millisecond and its tuning sensitivity is 100 megahertz/volt. When triangular waves are added, the frequency agility range is 100 megahertz and its tuning rate can reach 45 hertz. Moreover, any one of 10 fixed frequencies in the 1,000 megawatt range acts as its center frequency.

This coaxial magnetron possesses relatively high frequency stability. When the load's stationary wave ratio is 1.5, its maximum frequency pull coefficient is 5 megahertz and its maximum electronic frequency shift is 100 kilohertz/ampere. It

can operate very well in a moving target display radar system.

Naturally, this accutuned magnetron also has many shortcomings. Firstly, it requires a very complex servo control system. This increases the cost and reduces its operating reliability. Secondly, because a limited wave band electromechanical servo system is used, there is still a contradiction between maximum tuning rate and maximum jumping frequency band width. Jumping frequency between pulses can only be realized in a relatively narrow band width and a full frequency band jumping frequency requires a relatively long time. Moreover, because it uses a crank shaft connecting rod mechanism, its mechanical inertia is large, its wear is formidable, and its life-time is relatively low.

6.6 Other Types of Dither Tuned Magnetrons

To overcome the problem of excessively large mechanical rotating inertia of the motor's crankshaft connecting rod type dither tuned, various types of dither-tuned magnetrons have appeared. Their main features are that the electronically controlled signals of the frequency command do not go through the motor but use other devices to make changes on the mechanical positions. The principle used is derived from an electroacoustic device (loudspeaker).

6.6.1 The Vibrating-Reed Type Dither-Tuned Magnetron [12]

The vibrating-reed type dither-tuned magnetron uses electro-magnet to attract a magnetically tuned vibrating-reed. This vibrating-reed is inserted into one or many anode cavities or drives the tuning plunger of a coaxial magnetron. Its structure is shown in fig. 6.30.

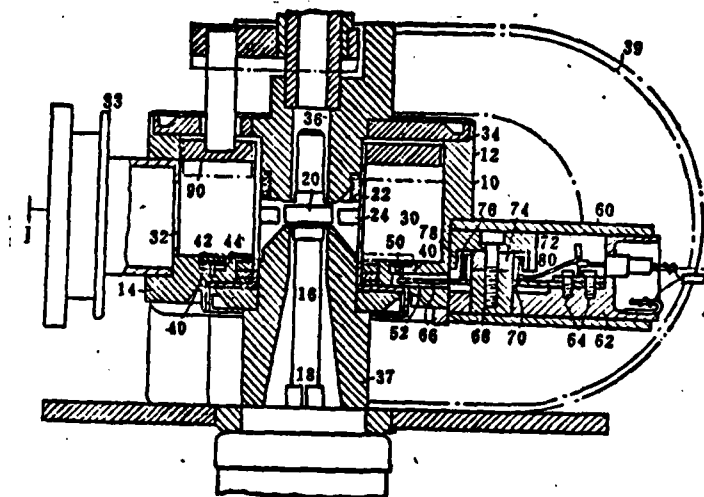


Fig. 6.30 Structural Diagram of the Vibrating-Reed Type Dither-Tuned Magnetron

In the figure, (30) is the coaxial cavity. It is tuned by two mechanisms. One is slow speed wide band mechanical tuning which is realized by the up and down movement of the tuning plunger (90). The other is fast dither-tuning which is realized by the fast up and down dithering of the tuning coil. The tuning coil's thickness is 0.005 inches, its width is 0.200 inches and when its up and down vibration is ± 0.005 inches it can have vibration of ± 15 megahertz in a 16,500 megahertz center frequency. The tuning coil is driven by the vibrating-reed (52). The vibrating-reed is made of copper, its thickness is 0.020 inches, its width is 0.400 inches and it is fixed on an electromagnetic coil (78). This coil is placed in a magnetic field formed by permanent magnet polar blocks (72) and (68). When voice frequency current is used in the coil, it drives the vibrating-reed vibration. Its vibrating-reed operates on a mechanically tuned frequency which carries with it a drawback;

its dither-tuning is fixed. This dither-tuned frequency can be preselected in the 200-1,000 hertz range. Its tuning range is determined by the driving power yet is usually not larger than ± 10 megahertz. The advantage of this tube is that its required tuning power is very small. It only has a load of ampere voice-frequency current input to 0.2 ohm, that is, its driving power is only about 0.2 watts. In order for its tuning speed and range to be stable, its driving signal source must be a stable sine wave oscillator, its frequency stability within 0.1% and its amplitude stability within 10%.

Because the dither-tuning range of this tube is narrow, aside from the dither-tuning mechanism, a low speed wide band tuning mechanism is also often installed.

Below are listed the major parameters of an early made WX-4742 vibrating-reed type dither-tuned magnetron [11]:

Operating frequency	: 8.5 - 9.5 kilomegahertz (mechanically tunable)
Dither band width	: ± 10 megahertz
Dither frequency	: 600 hertz
Peak power	: 200 kilowatts
Average power	: 200 watts (minimum)
Operating ratio	: 0.001
Efficiency	: 38%
Radio frequency band width	: 2/pulse
Pulling coefficient	: 12 megahertz (maximum)
Electronic frequency shift	: 0.3 megahertz/ampere
Stability	: $< 0.5\%$
Pulse width	: 1 microsecond
Pulse repetition rate	: 200-4,000 pulse/second (determined by the dither method)
Peak anode voltage	: 22 kilovolts
Peak anode current	: 27.5 ampere
Weight	: 12 pounds
Cooling	: forced wind cooling
Life-time	: greater than 400 hours
Operating temperature	: -55 to 70 °C

The advantages of this tube are that its dither rate is relatively high (maximum can reach 1,000 hertz) and its required tuning power is small. Its drawback is that the dither tuning range is relatively narrow. Because its structure is quite simple, its area is small, cost low and it is suitable for use in airborne and small shipborne radar.

6.6.2 The Voice Coil Tuned Jumping Frequency Magnetron [13]

Voice coil tuning has the operating principle of using a permanent magnet moving coil type loudspeaker to realize the operating frequency. The tuning device of this type of jumping frequency magnetron is the same as that of the moving coil type loudspeaker. It possesses a circular permanent magnet with a strong magnetic field and there is also a voice coil in the magnetic path's air space. Yet this voice coil is not connected to the paper box but joined to the tube's tuning plunger. When the frequency's command control flow passes the voice coil, this signal is transformed into mechanically alternating movement. This structural principle can be used in coaxial magnetrons as well as in multicavity magnetrons.

Because this type of tuning mechanism does not influence the rotating inertia of the high speed rotating section and the mass of the moving section is small, the mechanical inertia is relatively small and thus it can realize high speed tuning. Its tuning quantity is determined by the tuning power of the input. It is different from the above mentioned dither-tuned magnetron in that it does not require a low speed wide band mechanically tuned mechanism. It is similar to the accutuned jumping frequency magnetron as it can carry out wide band tuning with the same tuning mechanism. However, its tuning rate will decrease when in a wider tuning frequency band.

To quicken the tuning rate it is necessary that the resistance encountered by the tuning be reduced as much as possible. In a coaxial type magnetron's tuning mechanism, its tuning plunger is usually located in the vacuum resonant cavity. To send the tuning movement to the tuning plunger in a vacuum, we must cause the tuning rod to pass through a sealed vacuum film. In early structures, this vacuum film was always perpendicular to the movement direction of the tuning rod. At this time, one side of the vacuum film endures atmospheric pressure and sinks inward. This causes the tuning rod to endure unequal force in two directions of movement. To balance the atmospheric pressure we usually use a spring which pulls in the opposite direction and this increases the resistance during tuning. Moreover, the elasticity of this balanced spring is not the same in different tuning positions. If this type of magnetron is fitted in airborne radar, the atmospheric pressure is unequal at different altitudes so that use of the same spring has no way of completely counteracting this change in pressure. To resolve this problem (most importantly to reduce the resistance during tuning) we use a pair of connected vacuum corrugated tubes in the voice coil tuned jumping frequency magnetron so that the force of its two sides cancel each other and cause the tuning plunger not to be pressured. Fig. 6.31 gives its detailed structural diagram [14].

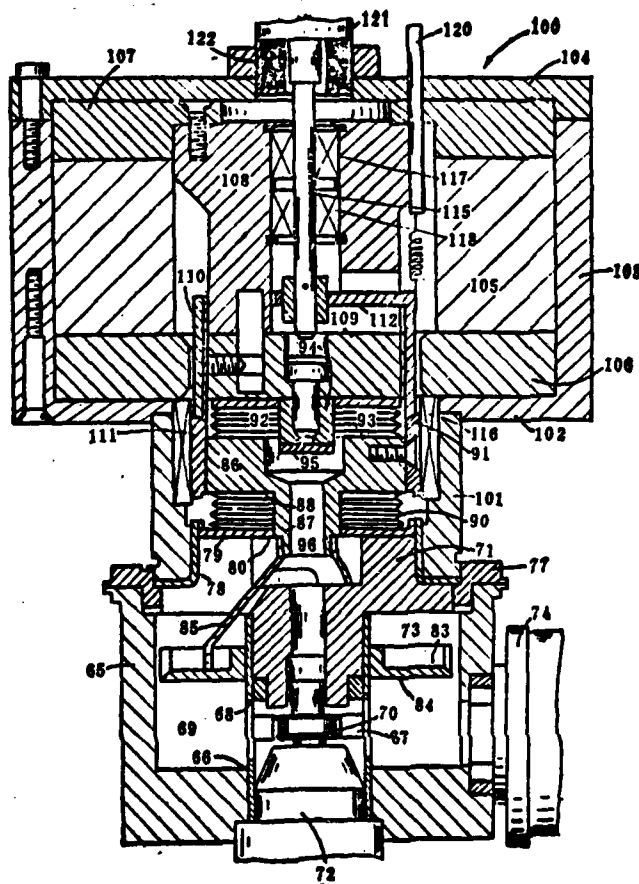


Fig. 6.31 Structural Diagram of the Voice Coil Tuned Jumping Frequency Coaxial Magnetron

In the figure, (65) is the body of the coaxial magnetron and (69) is its resonant cavity. The tuning plunger (84) passes the triple connection claw (85) and is joined to tuning component (86). The sleeve⁽¹¹¹⁾ of tuning component (86) is connected to voice coil (110). (105) is a circular permanent magnet. Its upper part forms an internal magnetic pole by top cover (107) and cylinder (108) while bottom cover (106) forms an external magnetic pole. The voice coil is then placed in the air space formed by the

internal and external magnetic poles. When the voice coil flows past the control flow of the frequency command, because it is located in a strong magnetic field and receives a great deal of force, this causes tuning component (86) to vibrate according to the additional command.

We will now discuss how the tuning mechanism with this structure eliminates the influence of the atmospheric pressure. Two connected vacuum corrugated tubes, (90) and (91), are welded on the two ends, (88) and (92), of tuning component (86). The vacuum corrugated tube (90) below passes through opening (80) and is connected to the vacuum in the resonant cavity. The vacuum corrugated tube (91) on top passes through center opening (96) of the tuning component and is connected to the vacuum in the resonant cavity. The outside of the corrugated tube is joined with the atmosphere. This structure has many good points. Firstly, use of a corrugated tube can cause the direction of the atmospheric pressure to be perpendicular to the direction of the tuning component's direction and thus it will have no affect on the latter. Secondly, after using two joined corrugated tubes, when the tuning component moves up and down, one corrugated tube endures pressure and the other endures pulling force. This can cause the two to be balanced. Lastly, and more important, this structure can keep the total area from changing during tuning. The atmospheric pressure always causes the area of the vacuum to compress. If the tuning component reduces the area of the vacuum section when moving in one direction, when moving in another direction there is an increase in the area of the vacuum section. At this time, it is necessary to block the atmospheric pressure. Therefore, maintaining the area of the vacuum section during tuning can reduce the influence of atmospheric pressure. Because this tuning mechanism is not influenced by atmospheric pressure it is suitable for use at different altitudes above sea level; it is especially suitable for airborne radar.

Because the tuning component of the voice coil tuned jumping frequency magnetron is relatively light and flexible, it can attain a very high tuning rate. It is said that it can reach 1,500 kilomegahertz/second in the X wave band and 5,000 kilomegahertz/second in the Ku wave band. The required driving power is quite small, usually only requiring about 5 watts. However, it is unlike the hydraulic tuning mechanism which requires more than 125 watt tuning power.

To attain an accurate frequency read-out for the local oscillation pretuning, frequency read-out sensors (121) and (122) are mounted on the upper end of the tube. The voice coil's alternating motion is joined to axle (115) by connecting rod (112) and on the top end of axle (115) is installed inner part (122) of the sensor. Actually, this sensor is a transformer. Its outer part (121) has two windings, the input signal is added to its primary level winding and the output signal is taken from its secondary level winding. Inner part (122) is the movable iron core of this transformer. When the iron core is in different positions, the sizes of the output signals derived from the transformer's secondary level are also different. That is, it can obtain a voltage read-out to represent the magnetron's tuning frequency and its accuracy can reach $\pm 0.15\%$.

When actually operating, the bridge type circuit and tuning system are joined. The frequency command control signals are added to an arm of the bridge type circuit and the output signals from the transformer are added to another arm. The output signals of the bridge's other arm are added to the voice coil after amplification. When a frequency command control signal is added the equilibrium of the bridge is destroyed. That is, when an output signal is added to the voice coil, the shift of the voice coil causes a change of the transformer's output signal and its direction of change brings about renewed bridge

equilibrium. At this time, there are no signals added into the voice coil, and the voice coil as well as all of the tuning components remain in the new position. The advantage of this method of tuning is that it can cause the shift of the tuner and input control voltage to form a ratio unlike the moving coil loudspeaker which has a current flow in the voice coil so that its sustained force and additional voltage form a direct ratio.

Because the voice coil tuned tube has no mechanically rotating parts, high speed ball bearings are unnecessary. Thus, its life-time is longer and its operating reliability is higher.

The L-4500 voice coil tuned magnetron is a Ku wave band coaxial magnetron. Its tuning range is 15.5-17.5 kilomegahertz and its tuning band width can reach 2,000 megahertz. When its tuning range covers the entire band width, it is 60 hertz and when in part of the band width (about 600 megahertz), it can reach 200 hertz. The output peak power is 100 kilowatts. When in a standing wave ratio of 1.5:1, the maximum frequency pull is 8.0 megahertz, the electronic frequency shift is 0.15 megahertz/ampere, the maximum lost pulses is 0.25%, the minimum side lobe is 9.0 decibels and it can endure 30g (11 milliseconds) shocks and 15g (5-500 hertz) vibrations.

Because the equivalent pass band of this voice coil tuned mechanism is relatively wide, its tuning speed is fast and its tuning flexibility is relatively high. Thus, it easily realizes random jumping frequency or program controlled jumping frequency.

This voice coil tuned magnetron has been used in many types of radar systems. For example, the MA-1 radar of the Xiusi Company has been refitted as jumping frequency radar which uses a voice-coil tuned magnetron as the high powered jumping frequency pulse generator. Further, when fitted on APQ-113 airborne radar

of an F-111A variable wing attack bomber, the original design used a hydraulically tuned magnetron but later changed to use the voice coil tuned tube of the Lideng Company.

6.6.3 The Piezoelectric Dither-Tuned Magnetron

Its structural principle is as follows. A suspension arm made of sandwich piezoelectric material is used in the magnetron's shell. The two top and bottom pieces of this sandwich material have different polarized voltages. Therefore, the bottom material endures compression and the top material stretching. This causes the suspension arm to bend like the bimetal piece. After this type of mechanical amplification, the tuning plunger fixed on the end point of the suspension arm can move a distance of about 0.01 inches and thus realizes the transformation of the electric signal into a mechanical displacement. Its deflection sensitivity (each deflection) is in direct ratio to L^2/t^2 (L is the length and t is the thickness) and mechanical tuning frequency f_0 is in direct ratio to t/L^2 . Maximum deflection d is in direct ratio to $1/f_0$, and it forms an inverse ratio with its mechanical tuning frequency. The mechanical resonance frequency of the tuner is related to the operating frequency of the magnetron so that the higher the operating frequency, the smaller the size of the cavity and the higher the mechanical resonance frequency. Fig. 6.32 gives the relationship of the tuner's mechanical resonance frequency and radio frequency [15]. This relationship is based on test results from the M5059 magnetron and a proportional model.

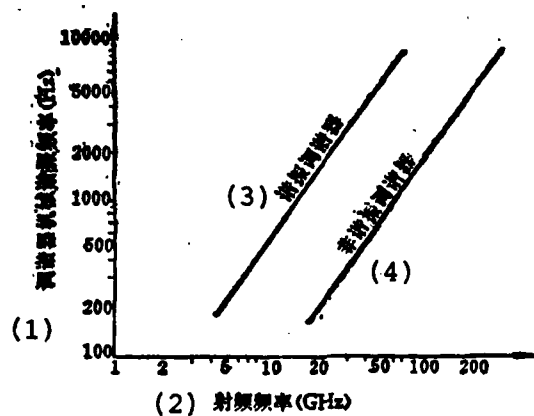


Fig. 6.32 Relationship Between the Piezoelectric Tuner's Mechanical Resonance Frequency and the Magnetron's Radio Frequency

- Key: 1. Tuner's mechanical resonance frequency (Hz)
 2. Radio frequency (GHz)
 3. Resonating tuner
 4. Nonresonating tuner

We can see from the figure that when the radio frequency is lower than 25 kilomegahertz, the mechanical resonance frequency is lower than 350 hertz. This is also the upper limit of this resonator because there is relatively high frequency modulation under resonance conditions. As a result, when the radio frequency is made higher the problem of the resonator's resonance is easier to resolve. Therefore, this type of tuner is suitable for operating in a frequency band of over 8 millimeters. Moreover, in these frequency bands only very small mechanical displacement is needed to be able to attain a relatively large tuning band width. For example, when using a magnetron with an 8 millimeter wave band, the tuner's mechanical resonance frequency $f_0=600$ hertz and maximum mechanical displacement $d=0.014$ inches can provide a 350 megahertz frequency agility range.

Fig. 6.32 also gives the performance of the same piezo-electric tuner when operating in a resonance frequency. When its resonance frequency is used for the drive, the sensitivity of the same tuner can be raised 16 fold. However, this causes its frequency agility to only have a fixed tuning frequency. There is a stagnant ring relationship between this piezoelectric tuner's transient additional voltage and transient frequency deviation (see fig. 6.33). This is mainly caused by the medium loss in the piezoelectric material as well as the phase difference between the additional voltage and tuner's displacement. This phase difference can be corrected by installing a compensation circuit in the tube body. The tuning performances after compensation are shown in fig. 6.33(b).

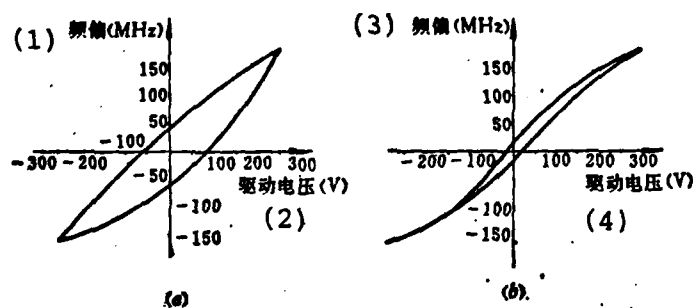


Fig. 6.33 Tuning Performances of a Piezoelectric Tuner

- (a) Tuning performances without compensation
- (b) Tuning performances with compensation

Key: 1. Frequency deviation (MHz)
 2. Driving voltage (V)
 3. Frequency deviation (MHz)
 4. Driving voltage (V)

Because of the non-linearity between the driving voltage and tuning frequency, in order to read-out its resonance frequency there must also be another frequency read-out piezoelectric

sensor. Because the output voltage of this sensor is in direct ratio with its mechanical displacement, the accuracy of this read-out voltage feed to the servo loop follows the non-sinusoidal wave and eliminates the microphonic effects.

During the tuning process, the changes of the tuner's power cause changes in the output power (see fig. 6.34). This is created from the tuning component's radio frequency loss and resonant cavity's external Q value changes caused by the distance change between the anode and tuning coil.

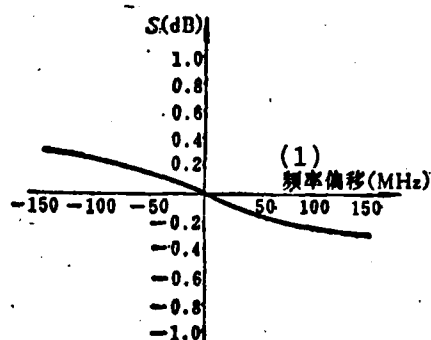


Fig. 6.34 Changes of the Output's Peak Power During the Tuning Process

Key: 1. Frequency deviation (MHz)

The M5059 frequency agility magnetron which uses the piezo-electric tuner principle structure is an 8 millimeter magnetron with 26 wing piece rising sun type anodes. Its peak output power is 40 kilowatts (input power is 210 kilowatts), its maximum agility frequency range is 300 megahertz and its maximum tuning frequency is 1 kilohertz. When the tuner is at 100 hertz the input impedance is 220 kilo-ohm, the tangent value of the loss angle is 0.5 and the pulse is 25-500 millimicroseconds.

The M5124 voltage tuned agility magnetron operates at 80 kilomegahertz. Its peak output power is 4 kilowatts, its agility frequency range can reach 700 megahertz, its mechanical resonance frequency is about 800 hertz and its minimum pulse can reach 3 millimicroseconds.

The tuner with this structure is installed in a vacuum and thus does not require a vacuum sealed corrugated tube or a vacuum bearing. Therefore, its life-time is relatively long. After 1,000 hours of life-time testing there was no decline in performance. Because the input impedance of the tuner is very high, the required tuning power is extremely small and the tuning speed is high (it can reach 600 kilomegahertz/second). However, the drawback is that it can only be used in a relatively high frequency band and the lower the frequency band, the narrower its tuning range.

6.7 The Gyro-Tuned Jumping Frequency Magnetron

All of the above mentioned jumping frequency magnetrons with different tuning methods used the same operating principle to realize resonant cavity tuning. That is, they use the geometric volume method to change the position of one wall of the resonant cavity and thus change the resonant cavity in order to realize resonant cavity tuning. However, the tuning frequency of the tuning cavity not only depends on the size of the geometric volume but also on the dielectric constant of the dielectric material in the resonant cavity or the magnetic conductance coefficient of the magnetic conducting material. If we use controlled voltage or controlled current we can change the dielectric constant of the dielectric material or the magnetic conductance coefficient of the magnetic conducting material (equal to changing the capacitance or inductance of the resonant cavity). Then, we can change the resonant cavity's frequency.

Yet, the medium loss of this type of material is relatively large and as a result it cannot be used under high powered conditions. Further research has shown that even if the dielectric constant of the dielectric material is not changed but we only change its relative position in the resonant cavity we can still change the resonance frequency of the resonant cavity. This is because we change the quantity of the dielectric material facing the direction of the electric field. This so-called gyro-tuned jumping frequency magnetron uses this principle for tuning. Fig. 6.35 is a structural diagram of this gyro-tuned jumping frequency magnetron [16].

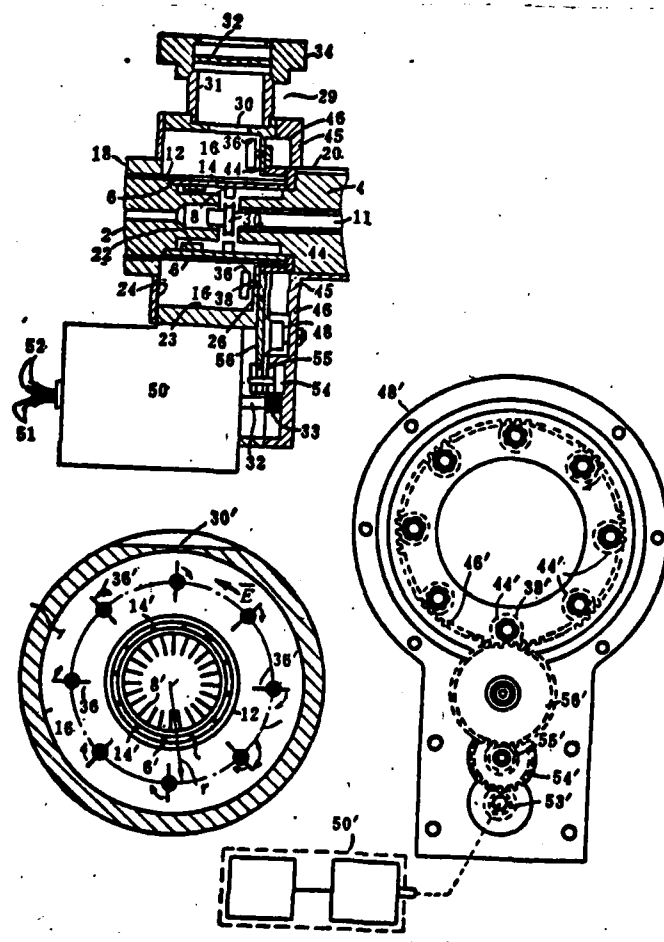


Fig. 6.35

Fig. 6.35 Structural Diagram of the Gyro-Tuned Jumping Frequency Magnetron

The gyro-tuned magnetron is the same as other coaxial magnetrons in that it uses the TE_{011} model resonant cavity. The electric field direction of this model resonant cavity is shown in the figure as vector \vec{E} . Its electric line of force is many concentric circular rings and when many (8 in the figure) are installed in the resonant cavity (16) it can rotate medium wing piece (36). These medium wing pieces go past each of the gears and are driven by the same annular inner gear (44) so that they are in phase rotation. So-called in phase indicates that the included angle α maintained between each wing piece and ring S is consistently equal when rotating. In this way, when α is 90° or 270° (the positions shown in the figure), the quantity of its electric field \vec{E} 's dielectric material is the thickness of the dielectric wing piece. However, when α is equal to 0° or 180° , it is equal to the length of the wing piece with the quantity of the electric field phase direction's dielectric material. When these wing pieces rotate alike, this can cause the resonance frequency of the resonant cavity to change with a sine wave pattern. Then, fast speed modulation is realized for the magnetron's operating frequency.

To be able to have better dielectric performance under microwave high power conditions, the dielectric wing pieces were made of high purity aluminum trioxide ceramic plates. When the dielectric constant of this dielectric material is in a frequency of 8.7 to 9.7 kilomega and the tangent of the loss angle only has 10^{-4} , it can sustain higher power in microwave frequency.

However, in any case, the induced dielectric wing pieces in the resonant cavity can cause the maximum power, which can be sustained by the resonant cavity, to decrease. This is because

of the sparks in the cavity. To raise the maximum power which can be sustained by the resonant cavity, the high pressure insulation gas method is used in the gyro-tuned magnetron. Yet, before doing so we must first separate the mutual effect area of the resonant cavity, high vacuum electrons and field phase. This is easily realized when using a coaxial magnetron with a TE_{011} resonant cavity. Anode wing plate (8) is fitted on a cylinder (6) in this magnetron (see fig. 6.35). Every two wing plates on this cylinder has a long crevice (14) and the energy of the electromagnetic field is coupled by this crevice and the resonant cavity. To separate the resonant cavity and tube we need only make a ceramic sleeve (12) and place it outside the anode cylinder (6). This ceramic cylinder is also made of aluminum oxide. Its two ends are separately vacuum welded on the bottom pole piece and on cylinder (18) (they can also be directly welded on the wall of anode cylinder (6)). This guarantees a continued high vacuum inside the cylinder and then the resonant cavity outside the cylinder maintains high pressure. We can freely use this ceramic cylinder for the microwave energy. The direct welding of many long pieces of ceramic on crevice (14) can also create this separation.

There are many types of gases which can act as insulation gases but they must be able to satisfy the requirements of high dielectric strength inertia (chemically non-reactive), thermal stability, non-toxic, not easily combustible etc. The gas presently used is sulfur hexafluoride (SF_6) and its full pressure reaches 35 pounds/square inch. Yet, a new problem is produced at this time: how to prevent the leaking of this insulation gas (especially the leaking when going past the bearings and other drive components of the mechanical drive system). The method for resolving this problem is to totally seal up the entire mechanical drive section (including the driving motor, reduction gear and frequency reading generator). Only the

lead-in wire (51) (the motor driving signal wire) and lead-out wire (52) (the frequency read-out signal wire) are led-in and led-out by the sealed terminal. At the same time, the wave guide output interface area also adds a welded window (32) made of aluminum oxide ceramic to prevent the leaking of the insulation gas. This guarantees that the insulation gas in the resonant cavity will not leak out under high pressure conditions.

Because there are no components with alternating movement in the gyro-tuned magnetron, the driving motor can operate at a very high rotating speed without shortening its life-time. Therefore, this type of tube can have a relatively high tuning rate. It can use a 200 hertz tuning rate to tune a 300 megahertz band width or use a 400 hertz tuning rate to tune a 260 megahertz band width (in the Ku wave band). The tuning drive power required is small. The added weight of the tuning mechanism is very light; the entire tuning mechanism only adds 1/2 pound to the basic weight of the magnetron.

Although we use a pressurized insulation gas to increase the resonant cavity's power endurance capabilities, yet the maximum output power of this gyro-tuned magnetron is lower than the several above mentioned jumping frequency magnetrons. At present, the output power in the X wave band is 70 kilowatts and only 35 kilowatts in the Ku wave band.

However, the reliability of this simple rotary tuned mechanism is relatively high and the tuning mechanism operating outside the tube's vacuum bulb prolongs the life of the tube itself. Furthermore, because there is no tuning plunger with alternating movement, it can sustain stronger impact and vibration and thus not affect its frequency stability (when operating at fixed frequency).

Therefore, this type of tube is suitable for airborne search, navigation and tracking radar as well as missile homing radar.

6.8 The Magnet Tuned Jumping Frequency Magnetron

All of the above mentioned jumping frequency magnetrons used mechanically tuned mechanisms to realize fast speed jumping frequency. The great majority of coaxial magnetrons (aside from the gyro-tuned) used the movement of a tuning plunger to change the size of the resonant cavity's geometric measurement for its tuning. Although use of various measures can lighten the weight of the tuning plunger as well as the mechanical inertia of the tuning mechanism, in any case, the tuning plunger's weight is at least 100 grams. It is not very possible for such a heavy substance to create alternating movement with a certain amplitude using a 1,000 hertz frequency for the realization of an over 10% tuning range. The flexibility of the tuning is also wanting and this problem is even more outstanding in the low microwave wave band. Therefore, it is necessary to think of a method to quicken the tuning speed and enlarge the tuning band width, that is, not to use mechanical tuning but to use electronic tuning. The magnet tuned jumping frequency coaxial magnetron is one of the more successful among them.

The structure of this magnet tuned jumping frequency magnetron is shown in fig. 6.36.

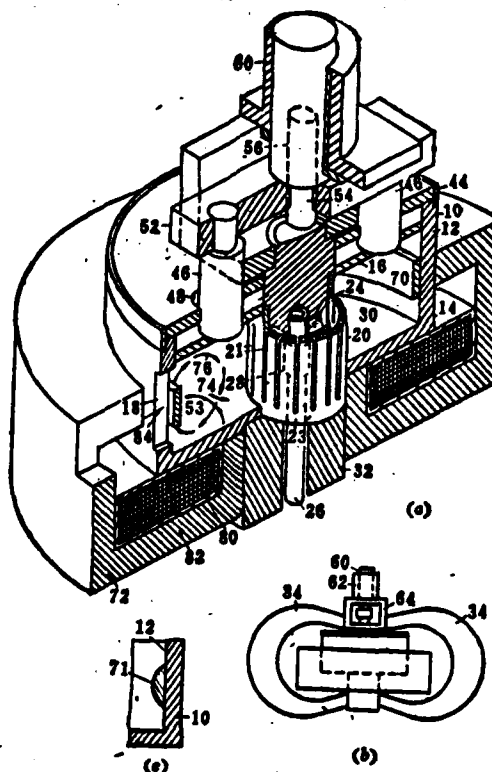


Fig. 6.36 Structural Diagram of Magnet Tuned Jumping Frequency Magnetron

- (a) Sectional diagram;
- (b) External contour diagram;
- (c) Semi-circular magnetic circuit.

Circular ring (70) which is made from yttrium iron garnet (YIG) is the magnetic tuning medium. This material has very small dielectric loss (its $\text{tg}\delta \approx 5 \times 10^{-5}$) and the saturated magnetization is about 400-1,600 gauss. The outer diameter of this circular ring is equal to the inner diameter of the coaxial cavity's outer wall and the section is about 0.050"x0.250" (can also be larger based on the required tuning range). In order for this ring to be able to be securely fixed on the wall

of the cavity, the ring is pressed in using the thermal pressure method. When the cavity is heated to 200°C and the ring is pressed in at room temperature, after the cavity cools to room temperature the ring can be binded. The ring is placed in this part of the cavity to reduce the loss of the magnetic circuit when placed on the outer edge of the TE_{011} electromagnetic field. Electromagnetic coil (80) is placed so as to carry out tuning below the coaxial cavity. The magnetic field direction produced by the electromagnetic coil is shown by arrow (53). The electric field direction of TE_{011} is shown by arrow (74) and its magnetic field direction is shown by arrow (76). The direction of this linear polarized microwave power flow is shown by arrow (84) and the direction of the added direct current tuned magnetic field is the same as its power flow direction. In this way, when we change the size of the added direct current magnetic field which can change the magnetic conduction of the ferrite as well as the distribution of the TE_{011} model's high frequency electric field, we can change the resonance frequency of the resonant cavity. The tuning range is determined by the measurement of the ferrite magnetic circuit and the size of the direct current magnetic field. When we have the above mentioned measurements of the magnetic circuit, the maximum attainable tuning range can reach 1%. If the section area of the magnetic circuit is enlarged to $0.25'' \times 0.25''$ and we use a small coaxial cavity, a 10% tuning range can be realized. However, the specified power is greatly reduced. The tuning speed of this tube is mainly limited by the time constant which is determined by the inductance and direct current resistance of the electromagnetic coil. Use of a suitable design can bring about a tuning frequency of up to 1 kilohertz.

The shape of the magnetic circuit can be semi-circular (as shown in fig. 6.36(c) wherein the central section is relatively thick. This structure can cause the microwave field distribution

in the tuned magnetic circuit to become more uniform and it can also reduce the instability of the self-rotational waves.

The magnetic circuit can also be placed on the bottom of the coaxial cavity and the magnetic field of the TE_{011} model there will be weaker. This can further reduce loss and raise the power limit. Because the ferrite has a high powered saturated critical field, when exceeding this peak power the radio frequency field will be coupled to the self rotational field in the material. This will cause a loss for the microwave signal. The radio frequency is weakest on the corners of the coaxial cavity but because its coupling with the high frequency magnetic field is weakened, when in the same magnetic circuit section, its tuning range becomes even smaller.

The added tuning magnetic field should be as perpendicular with the magnetron's original axial magnetic field as possible so that the mutual effects are minimal. A magnetic shield can also be used to prevent the scattered magnetic field from covering the tuning magnetic field.

To increase its tuning band width, a mechanical tuning device (in the figure, tuning plunger (16) driven by connecting rod (46) is added in the tube.

To raise the power limit of the magnet tuned jumping frequency magnetron we can also use a method similar to gyro-tuning. That is, the use of an aluminum oxide ceramic sleeve outside the anode cavity and the welding of its two ends. This will cause the magnetic circuit to be outside the vacuum and afterwards the coaxial cavity will fill with high pressure insulation gas (e.g. sulfur fluoride).

Another method for realizing magnet tuned frequency jumping

is to cause the transmission directions of the tuning magnetic field and microwave current to be perpendicular to each other. Fig. 6.37 shows the structure of this magnet tuned jumping frequency magnetron.

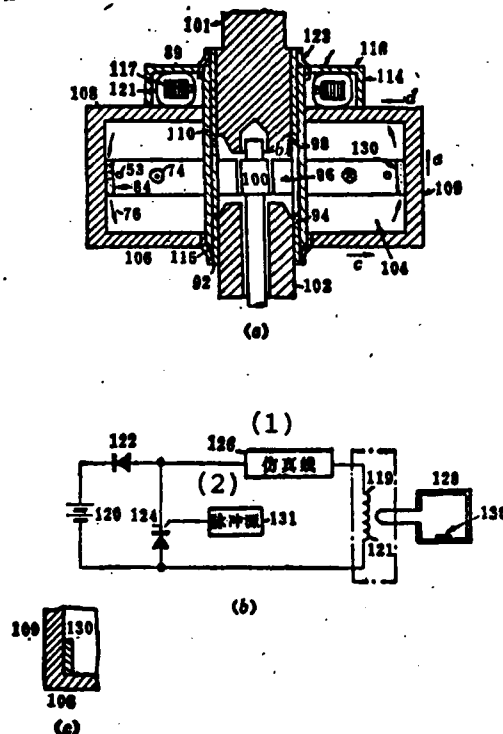


Fig. 6.37 Structure of Magnet Tuned Jumping Frequency Magnetron With Pulse Transformer

- (a) Sectional diagram;
- (b) Exciting circuit;
- (c) Magnetic circuit installed on the bottom of the coaxial cavity.

Key: 1. Artificial line
2. Pulse source

There is no mechanical tuning structure in this tube and therefore its magnet tuning coil is fixed on the upper end of the tube. The structure of its produced magnet tuning magnetic

field is quite ingenious. It is not directly produced from an electromagnetic coil but by a very strong pulsed electric current using the secondary level of the pulsed transformer.

In the figure, (121) is the primary level of this pulsed transformer. It coils on the magnetron's coaxial circular ring (117) made from a belt shaped iron-cored coil. The secondary level of this transformer is a short circuit ring made from the anode cylinder of the coaxial tube and other component structures. This short circuit ring is formed as follows. The outside of the tube's anode cylinder (92) is covered with a sleeve (110) made of a high frequency ceramic so that the anode cylinder will not come into direct contact with the coaxial cavity. The upper end of the anode cylinder and external shield (112) of the magnet tuning coil are welded by (123). The lower end and lower covering plate (106) of the coaxial cavity are welded by (115). In this way, the secondary level short circuit ring is composed of 94-115-106-109-108-114-116-123 and its direction is shown by arrows a, b, c and d. The magnetic field TE_{011} formed from this electric flow is annular and its direction is shown by arrow (76). Its electric field has a coaxial ring shape and its direction is shown by arrow (74). Therefore, the direction of the added tuning magnetic field is perpendicular to the magnetic field of TE_{011} .

When a plane electromagnetic wave passes the ferrite and there is a direct current magnetic field perpendicular to the transmission direction and alternating field, an equivalent magnetic conduction coefficient μ_{ff} is produced which can be determined by the following formula:

$$\frac{\mu_{ff}}{\mu_0} = \frac{\gamma^2 (H_0 + 4\pi M_0)^2 - \omega^2}{\gamma^2 (H_0)(H_0 + 4\pi M_0) - \omega^2}$$

In the formula γ is the gyro-magnetic conductance ratio of an electron. It is equal to 2.8 megahertz/oersted and ω is the angular frequency of the microwave plane wave.

The tuning range of this magnet tuning method can be roughly estimated as: its relative tuning range is equal to the ratio between the area of the ferrite and the electric volume (i.e. inner cavity volume) of the tuning cavity. This is because when in a zero value tuning field, the ferrite is a medium for the cavity field and when the tuning is a critical value the equivalent magnetic conductance coefficient is zero. This inhibits the cavity field causing it to be equal to a shrunken circle of the cavity's volume. Because the equivalent dielectric constant of the yttrium iron garnet is equal to 16, the cavity measurement of the ferrite's section is 1% of the cavity's volume. Then its timing range is 4%. A 10% tuning range can be realized by using this magnet tuning method, yet, at this time, it is necessary that the non-loaded Q value reach to over 1,000 so as to reduce loss. This requires that the ferrite's loss angle tangent be smaller than 1×10^{-3} . Yttrium iron garnet can completely satisfy this requirement. The tuning magnetic field required at this time is about several hundred oersted.

Similarly, the tuning magnetic circuit can be placed on the bottom of the coaxial cavity (as shown in fig. 6.37(c)). This can reduce the strength of the radio frequency field and this can raise the power limit. However, at the same time, this can reduce the tuning range. Therefore, there is a compromise between the peak power and tuning range. If the tuning magnetic circuit is placed in the position of fig. (c), its tuning range will decrease 3 fold and the peak power will increase 10 fold.

To produce a sufficient tuning magnetic field (several hundred oersted), we use a pulsed transformer with controllable

silicon control. Fig. 6.37(b) shows its electronic schematic diagram. When the controllable silicon (124) is triggered by the pulse source (131), primary level (119) passes the 50 ampere peak electric current, the primary level coil has 50 coils on the roll tape shaped iron core and its change ratio is 50:1. Thus, it can produce a 1,000 ampere peak electric current, that is, its magnetic field strength is 1,000 ampere-turns.

The following several problems exist when using ferrite for the magnet tuning of a magnetron:

(1) The ferrite can produce gas and even after long baking there is still an exhaust rate of 0.6 milliliters·torr·grams/hour. Thus it cannot be used in a vacuum.

(2) When ferrite is placed in a strong radio frequency field, it is only necessary that at any time the radio frequency field exceed threshold H_c to be able to bring about high powered unstable quadratic resonance and create power loss and ferrite heat generation. This limits the upper limit of the storage of energy in the ferrite loaded cavity.

(3) The heat conduction capability of the ferrite is lacking so that even if we do not take the effect of the outside temperature into consideration, because there is a radio frequency loss in the ferrite itself, this causes its temperature to gradually rise and its performance to gradually decline. When the component's temperature reaches a curie point, it completely loses effect. To decrease loss and increase efficiency, the ferrite must be located in a place with a weak radio frequency electric field and strong radio frequency magnetic field. Further, we must also use an as thin as possible ferrite strip and copper welding or tin welding to weld it to the cavity wall for good heat conduction. Good cooling is added outside the cavity wall.

(4) In order for the magnetron to operate normally it must

have a very strong magnetic field. Yet, we cannot allow this magnetic field to jam the magnet tuning ferrite and cause false bias and magnetic saturation. The magnetic field direction of the common magnetron is perpendicular to the magnetic field of the magnetron itself. In any case, there can still exist parasitic coupling between the two. Therefore, we must use a magnetic shield between the two. While this shield protects the ferrite, it does not affect the normal operation of the magnetron nor does it cause a bias magnetic field short circuit of the ferrite. Thus, the ferrite cannot be placed too close to the main body of the magnetron.

(5) The speed of magnet tuning is limited by electromagnetic induction and power. To cause the bias magnetic field to be at fast speed, it is necessary to have relatively large power. Moreover, when the frequency is very high, the vortex flow and magnetic hysteresis loss can cause relatively high loss.

To resolve this problem, we will introduce a type of magnet tuned frequency agility magnetron which uses an external ferrite loaded tuned cavity below [18].

This magnet tuned magnetron uses a standard 3 centimeter short circuit wave guide as the loaded cavity and the ferrite used is a magnesium-manganese ferrite to reduce loss and increase power. The ferrite piece must be located in a weak radio frequency electric field and strong radio frequency magnetic field, that is, welded on the narrow wall of the rectangular wave guide (see fig. 6.38).

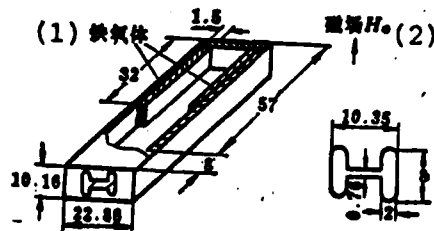


Fig. 6.38 Short Circuit Wave Guide Cavity Welded With Ferrite Pieces

Key: 1. Ferrite
2. Magnetic field H_a

The bias magnetic field H_a added for tuning is parallel to the narrow side of the wave guide. When H_a increases from 0 to 2,000 oersted, the cavity's resonance frequency gradually changes from 8,452 to 9,600 megahertz.

This external ferrite loaded resonant cavity is coupled with the magnetron by the ceramic window of the H shape crevice. A 135° included angle is formed between this output window and the normal output window of the magnetron (see fig. 39(a)).

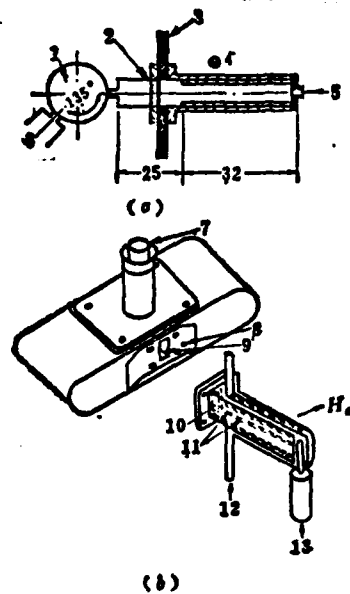


Fig. 6.39 Coupling of the Ferrite Loaded Magnet Tuned Resonant Cavity and the Magnetron

- Key:
1. Magnetron
 2. Ceramic window
 3. Magnetic shield
 4. Ferrite bias magnetic field
 5. Compressed air
 6. Standard Radio frequency output
 7. Standard radio frequency output
 8. Magnetic shield
 9. Ferrite loaded tuning cavity coupling window
 10. Cavity welded with ferrite
 11. Welded on ferrite pieces
 12. Cooling water
 13. Compressed air

To avoid the overheating caused by ferrite loss, a cooling water tube is welded on the outer wall of the short circuit wave guide, compressed air is passed into the wave guide and there is a magnetic shield between the loaded cavity and magnetron to separate the magnetron's magnetic field and the bias magnetic

field (see fig. 6.39(b)). This magnetic shield can reduce the magnetron's leakage of the magnetic field near one end of the magnetron's ferrite by 96% and reduce the magnetic field of the central operating space 4%.

After this ferrite loaded resonant cavity is coupled to the magnetron and the heat is measured, when we measure the change of the bias magnetic field ^{Ha} between 0-2,000 oersted and the mechanical tuning range is 8.5-9.3 kilomegahertz, we can obtain a magnetic tuning range of 65-55 megahertz. Its output power changes from 240 to 185 kilowatts.

Although this magnet tuned frequency agility magnetron can avoid the mechanical tuning components, yet it requires a relatively strong tuning magnetic field which can only be produced by a solenoid coil. Further, because of electromagnetic inductance, there is still no way of attaining a very high tuning rate. Moreover, the higher the required tuning rate, the larger the needed tuning power.

6.9 Voltage Tuning of a High Powered Pulse Magnetron

Although magnet tuned jumping frequency can realize inertialess tuning, yet because it requires an extremely large tuning electric current and because the ferrite in the cavity limits the tube's maximum rated power, it is best to be able to realize voltage tuning for the magnetron.

The problem of voltage tuning for low powered continuous wave magnetrons was resolved earlier. The maximum tuning band width of this voltage tuned magnetron has already exceeded an octave and its maximum output powers has reached several hundred watts. At present, it is widely used in electronically tuned jamming receivers.

However, its use in the voltage tuning of a radar receiver's high power pulsed magnetron is a problem still being researched. Below we will present a plan for the voltage tuning of a large power pulsed magnetron.

Fig. 6.40 shows the structure of an electronically tuned high power pulsed magnetron.

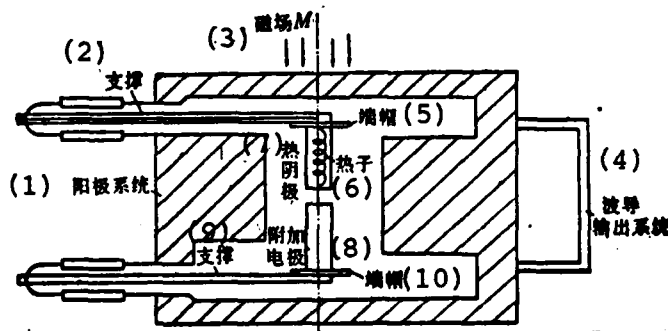


Fig. 6.40 A Plan For an Electronically Tuned High Power Pulsed Magnetron

- Key:
1. Anode system
 2. Support
 3. Magnetic field M
 4. Wave guide output system
 5. End cap
 6. Heater
 7. Thermionic cathode
 8. Added electrode
 9. Support
 10. End cap

This structure is applicable for use in various axial type magnetrons, including various multicavity, rising sun and coaxial magnetrons. The figure does not draw any specific type of magnetron but is expressed by the general name of an anode system.

It is important to place an additional electrode in the tube. This electrode is coaxial with the cathode. The additional electrode is made from a material with a very low

transmission coefficient (e.g., carbon, graphite tungsten carbide, molybdenum and titanium) and thus does not basically transmit electrons. This additional electrode is as close to the cathode as possible so as to affect its space electric charge. It can be the same length as the cathode (but not necessarily) and should be the same thickness as the diameter of the cathode. An end cap is added on to one of its ends.

This additional electrode is connected to the cathode on the circuit as well as with the electric potential of the cathode. At this time, the voltage tuning of this magnetron relies on changing the direct current electric potential of the anode and cathode which is realized by changing its anode current. Although common magnetrons can also rely on changing the anode current to change the frequency, its sensitivity is very low. However, the tuning sensitivity of magnetrons with this structure is very high.

We cannot connect the additional electrode to the cathode and add a negative electric potential facing the cathode on the additional electrode. We can, however, realize electronic tuning by changing the value of this negative electric potential. This can avoid the high voltage tuning system.

Another plan using an electronically tuned medium power magnetron is adding an additional tuning cathode in one or several cavities of a multicavity magnetron. Its structure is shown in fig. 6.41.

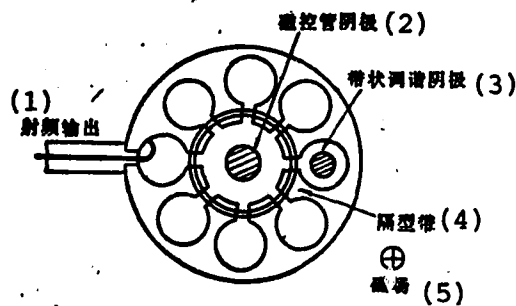


Fig. 6.41 Schematic of the Structure of an Electronically Tuned Magnetron With Tuning Cathode

- Key: 1. Radio frequency output
 2. Magnetron cathode
 3. Banded tuning cathode
 4. Partition band
 5. Magnetic field

A negative voltage is added on this tuning cathode. This negative voltage can change the space electric charge current in the resonant cavity's space. This also changes the resistance of the resonant cavity and thus changes its tuning frequency. When an electronically tuned magnetron with this structure is cold measured at a low signal level (several milliwatts), we can observe the relationship between its tuning sensitivity and magnetic field strength. Fig. 6.42 shows the tuning sensitivity curve measured after being refitted with a CV6035X wave band 14 cavity magnetron. When the added voltage of the diode is 1 kilovolt and the electric current is 200 milliamperes, its frequency deviation can reach 10-15 megahertz.

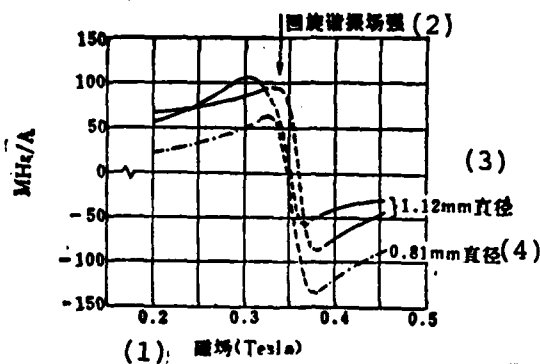


Fig. 6.42 Relationship of the Tuning Sensitivity and Magnetic Field Strength When There is Cold Measuring

- Key: 1. Magnetic field (Tesla)
 2. Gyro tuning field strength
 3. 1.12mm diameter
 4. 0.81mm diameter

However, when the magnetron operates normally, because of the very strong radio frequency electric field strength, the diode current enlarges and the frequency deviation decreases. When heat measuring, the results are summed up as follows:

- (1) The impedance of the diode varies between 500-2000 Ω .
- (2) The frequency deviation increases with diode voltage and current slightly less than linearity, then reaches a maximum value. The optimum ratio of cathode-anode diameter is 0.4.
- (3) Tuning sensitivity changes signs in the vicinity of cyclotron field strength as shown in Fig. 6.43.

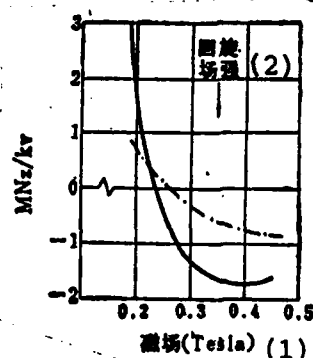


Fig. 6.43 Relationship Between the Voltage Tuning Sensitivity and the Magnetic Field Strength

Key: 1. Magnetic field (Tesla)
2. Gyro field strength

(4) When the magnetron's load mismatch is 1.5:1, its tuning sensitivity is maximum.

(5) Use of a single diode (in a 14 cavity magnetron) can obtain a 2.5 megahertz frequency deviation when in an 80 kilowatt peak output. The power required for tuning is about 1% of the magnetron's output power.

(6) When two tuning cathodes are used, its effect is superposed and when in a 1% tuning power it can obtain a 5 megahertz frequency deviation.

Naturally, such a small frequency deviation cannot satisfy the requirements.

Recently, another new type of electronically tuned magnetron was developed on the basis of this electronically tuned magnetron. This magnetron has an auxiliary resonant cavity coupled with the main magnetron anode. There is an electron multiple bombarder electrode in the auxiliary resonant cavity and a 1-30 kilovolt control voltage is added on this electrode. When a suitable radio frequency voltage is

added to the electrode of this auxiliary cavity, the controlled electron multiple bombardment electrode then discharges. This causes resonant frequency displacement which changes the magnetron's oscillation frequency. The same anode can fit several of these cavities and this can enlarge the total frequency deviation range. At present, a 30 megahertz frequency deviation has been attained in an S wave band 200 kilowatt tube and a 100 megahertz frequency deviation was attained on an X wave band 50 kilowatt tube. This caused the index of this type of electronically tuned magnetron to reach a usable level.

Recently, foreign nations have been developing a digital coded electronically tuned frequency agility magnetron. It uses a coaxial magnetron and PIN diodes are coupled to the outer cavity of the magnetron. The reactance of these diodes are loaded on to this cavity and act as a switchable tuning device of the magnetron's reactance tuning. It is only necessary that the reactance load of each PIN tube form a binary multiple relation for the magnetron's oscillation frequency. We can thus realize digital coding agility of the magnetron's frequency.

Test models of this type of tube operate in the Ku wave band, their center frequency is 16.5 kilomegahertz, their power is 60 kilowatts and their operation ratio is 0.001. The first type has a tuning range of 300 megahertz and a tuning speed of 10 megahertz/millisecond. The second type has a tuning range of 50 megahertz and a tuning speed of 100 megahertz/microsecond. The first is used in common frequency agility radar whereas the second type can realize coded pulse compression in the pulses and thus improve the radar's capabilities.

References

- [1] New magnetron shifts frequency fast. R.E. Edward, Electronics, April 6, 1964. p. 76.
- [2] Radar Handbook, Ed. by M.I. Skolnik. McGraw-Hill Book Co. 1970, Chapt. 7. Chinese translation, "Radar Handbook", Book 4, Chapter 15, National Defense Publication, 1978.
- [3] Les magnetrons modernes a « agilité de fréquence » Toute l'Electronique. No. 382, No. 384, 1975.
- [4] A ditherable frequency, coaxial magnetron having superior frequency tracking capabilities. J. Horrigan and J.R. Martin. Microwave J. March, 1967.
- [5] Ditherable and tunable microwave tube having a dithered tuner actuator of fixed length. R.M. Hynes. U.S. Pat. No. 3, 441, 795. April 29, 1969.
- [6] Frequency-agile coaxial magnetrons. W.A. Gerard. Microwave J. March, 1973. p. 29.
- [7] Dither-tuned tunable microwave tube apparatus. H.H. Chun. U.S. Pat. No. 3441795. Apr. 29, 1969.
- [8] Resolver for dither tuned microwave tubes employing carrier modulation and phase sensitive detection. G.G. Barker, U.S. Pat. no. 3532995. Oct. 6, 1970.
- [9] Dither tuned microwave tube with corrected tuner resolver output. R.C. Stoke, U.S. Pat. No. 3590313. June 29, 1971.
- [10] Cost-effective radar retrofit adds frequency agility. J. Martin. Microwave Systems News, Oct. 1977, Vol. 7, NO. 10, pp. 47-48.
- [11] Dither changes magnetron frequency. Electronics, May, 1965. p. 152.
- [12] A frequency diversity coaxial magnetron. K.D. Powell. U.S. Pat. No. 3414760.
- [13] Loudspeaker tunes Ku-based frequency agile magnetron. Microwaves. Feb. 1965. p. 65.
- [14] Tunable magnetron, K.E. Frerichs. U.S. Pat. No. 3599035. Aug. 10, 1971.

References (continued)

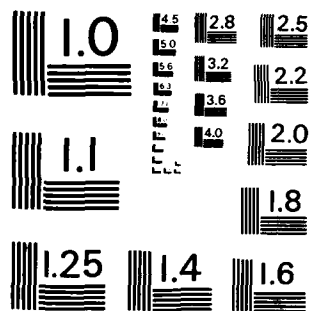
- [15] Frequency-agile magnetrons using piezo-electric tuning elements. B.F. Cooper, D.C. Platts. 1973 European Microwave Conf. Proc. Vol. 2. C-13.
- [16] Tunable coaxial magnetron. D.E. Blank, U.S.Pat. No.3590312. June 29, 1971.
- [17] Ferrite tuned coaxial magnetron. D.C. Buck. U.S.Pat. No. 3333148. July 25, 1967.
- [18] Electronic tuning of high power X-band magnetron with ferrites. J.L. Bahri, Y. Peyrard. Proc. of 4th European Microwave Conf. pp.31-35.

UNCLASSIFIED

517

F/Q 17/9

NL



MICROCOPY RESOLUTION TEST CHART
NATIONAL BUREAU OF STANDARDS-1963-A

CHAPTER VII

THE STRUCTURE OF NONCOHERENT FREQUENCY AGILE RADAR

7.1 GENERAL ACCOUNT

Noncoherent radar is that kind of radar where a fixed phase relationship does not exist between the radio frequency pulse that is transmitted and the continuous vibration of the local oscillator. In actuality, this noncoherent radar is also that kind of radar where the transmitter uses a high-powered self-excited oscillator but is not an amplified chain type. Presently, in the microwave wave band, this kind of high-powered self-excited oscillator still primarily uses a magnetron oscillator. Therefore noncoherent frequency agile radar is also radar that uses a frequency agile magnetron.

Because there is no fixed phase relationship between the radio frequency pulse of the noncoherent radar transmission and the local oscillator, therefore the radar cannot carry out coherent signal processing, for example coherent accumulation, collecting Doppler frequency, etc. Although the method of using a transmitted pulse for coherent oscillation phase locking can also achieve coherence when receiving, and as a result partially resolves these problems, its stability is inferior to that of the fully coherent type. Moreover, it cannot produce the pulse compression and other complicated transmitted signal wave forms. But because the transmitter of the noncoherent radar is far simpler than the coherent radar transmitter of the amplified chain type, and furthermore because its efficiency is high, power consumption is economical, volume is small, weight is light, and cost is low, therefore this magnetron noncoherent radar has obtained extremely wide-spread use in radar of various types of military and civilian radar. It is particularly widely used among the various types of tactical radar requiring high mobility, including various types of mobile antiaircraft surveillance radar, fire-control radar, and airborne and ship-borne radar.

However, the old type magnetron still has a series of weaknesses

among which the most fatal weakness is that it cannot very quickly change its operational frequency, as a result it is very easy for the radar to be subjected to enemy jamming and be put out of operation.

As the preceding explains, in the past a large amount of research work has been carried out in order to increase its tuning speed, until the frequency agile type magnetron was developed to achieve a jump frequency between the pulses, causing the tuning speed to produce a qualitative leap. Since there are abrupt changes in the carrier frequency of adjacent pulses transmitted by frequency agile radar, even if there is a totally electronically tuned jammer, it cannot carry out set-on jamming against it, but can only employ wideband noise blocking jamming. this causes the effects of the jamming to be greatly reduced.

Moreover, the achievement of jump frequency between pulses not only is an improvement in tuning speed, but also causes the whole radar performance to produce qualitative variations. As described in Part 1 frequency agile radar not only improves anti-jamming properties, but also can increase detection distance of radar, improve angle measurement precision, reduce sea wave clutter, etc.

All these cause frequency agile radar to not only be an improvement in the common pulse radar, but also to become a completely new radar system. Therefore, we can say that the emergence of frequency agile technology is a revolution in classical pulse radar systems.

However, this new system is even more important with regard to the old type magnetron noncoherent radar, because retrofitting the old type magnetron radar to noncoherent frequency agile radar is relatively easy to achieve, this retrofitting can even be carried out on the spot on existing equipment. After retrofitting, however, it can cause a great improvement in various properties of the original equipment. This way we can pay the minimum price and make large quantities of nearly obsolete radar obtain new life.

On the basis of foreign reports, the cost of frequency agile magnetrons is only (5-10)% higher than the cost of fixed frequency

magnetrons. So long as the radar transmitter replaces the magnetron then it basically does not need to be altered. Primary modification requires changing the original klystron local oscillator to a backward-wave tube local oscillator or bulk-effect diode local oscillator, and at the same time it is necessary to install a comparatively complicated automatic frequency precision tuning circuit, while making corresponding retrofits to display and data processing components. This way the final cost will increase approximately (10-15)% over the cost of the original equipment. Figure 7.1 thus is a photograph of the additional components that are needed to carry out this retrofitting. Included among them are such components as the precision tuning magnetron, frequency agile local oscillator, automatic frequency precision tuner, and a jamming detection receiver and display.

Because frequency agile radar possesses many advantages, therefore presently many countries not only carry out retrofitting on numerous old type radar that they already have, but also are designing many new models of frequency agile radar; even on radar that already has completed development, the original design has been revised, to change it to frequency agile type radar.

We can estimate that in the near future, frequency agile radar will replace fixed frequency radar in very many applications, and will become the standard pulse radar system.

The differences between the noncoherent frequency agile radar that uses frequency agile magnetrons and common pulse radar primarily are the radio frequency components in the transmitter and receiver (TR). Concretely speaking, these are the three components of the frequency agile magnetron, the frequency agile local oscillator, and the high speed (monopulse) automatic frequency control. The block diagram of the frequency agile radar radio frequency parts that are included in these three components are as Fig. 7.2 shows. The high power radio frequency pulse that the frequency agile magnetron outputs goes to the high powered circulator, it later goes through the TR switch to the antenna, and on the other hand, an extremely small signal is extracted

by the decibel directional coupler and is sent to the self-excited frequency control mixer. The tuning of the frequency agile local oscillator is divided into the two components of coarse tuning and precision tuning; coarse tuning is presetting the local oscillator close to the transmitting frequency before each transmission; precision tuning is conducting high-speed frequency precision tuning at the time of pulse transmission, and the local oscillator frequency is quickly tuned to the correct position. The coarse tuning of agile local oscillator has two methods: One is open loop presetting, primarily used for frequency agile magnetrons that possess a frequency readout device. The other is closed loop cold measurement tracking, that is, during the radar recovery time the signal put out by the local oscillator, after going through the isolator and circulator, goes to the magnetron, and a test is carried out on the cold resonance frequency of the magnetron. After the signal reflected by the magnetron goes through the TR switch and the variable attenuator to the detector, the signal obtained after detection is used to control the operations of the automatic frequency control system. So long as the additional frequency modulation signal is added it can make the agile local oscillator frequency follow the magnetron cold frequency changes.

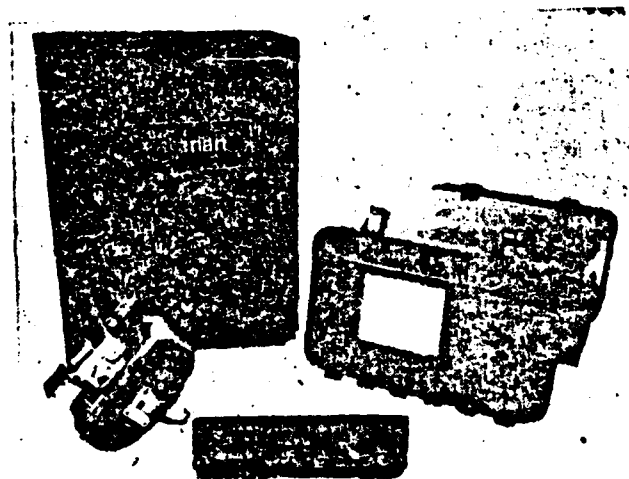


FIG. 7.1 THE SPARE COMPONENTS THAT ARE NEEDED FOR RETROFITTING THE COMMON PULSE RADAR TO FREQUENCY AGILE RADAR THAT USES A PRECISION TUNING MAGNETRON.

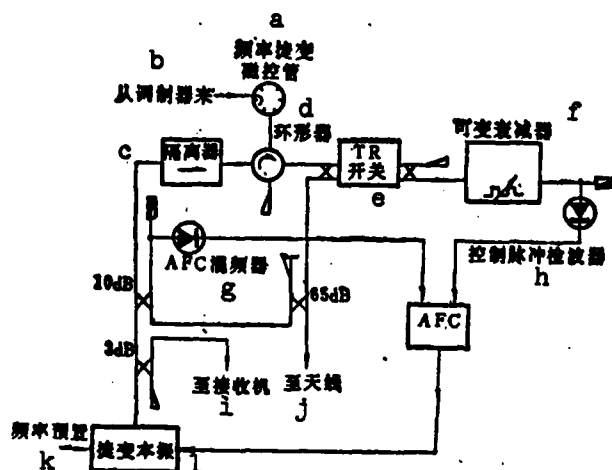


FIG. 7.2 THE RADIO FREQUENCY PARTS OF NONCOHERENT FREQUENCY AGILE RADAR
 KEY: (a) Frequency agile magnetron; (b) Coming from the modulator; (c) Isolator; (d) Circulator; (e) Switch; (f) Variable attenuator; (g) AFC Mixer; (h) Control pulse detector; (i) To the receiver; (j) To the antenna; (k) Presetting frequency; (l) Agile local oscillator

This chapter will emphasize explanation of the frequency agile local oscillator and automatic frequency control systems.

In noncoherent frequency agile radar the operation process of the agile local oscillator is extremely complicated, below we use the frequency agile radar which employs rotational tuning magnetron as an example to explain its operational process⁽¹⁾. Figure 7.3 shows the operational process of this frequency agile radar agile local oscillator. The tuning curves of the magnetron are shown as dashed lines in the figure, at the beginning of the radar recovery period the frequency of the agile local oscillator returns to the lowest initial frequency point 1, then quickly rectilinearly rises to track the cold resonating frequency of the magnetron, and when it is equal to the cold resonating frequency of the magnetron, the signal reflected by the magnetron is minimum, at this moment the automatic frequency control system then causes the frequency of the local oscillator to follow the changes in cold resonance frequency of the frequency agile magnetron.

An instant before the magnetron oscillates, local oscillator frequency steps to a frequency interval, this interval is equal to the intermediate frequency reducing the difference of the magnetron cold and hot frequency, later the high-speed automatic frequency tuning system again carries out accurate precision tuning. In the period of the backward-wave signal of the receiver, the local oscillator frequency must maintain stability without variation, in order for the intermediate frequency signal after the mixer to be able to drop within the center bandwidth. Directly going down to begin a recovery period, the same kind of cycle is again repeated.

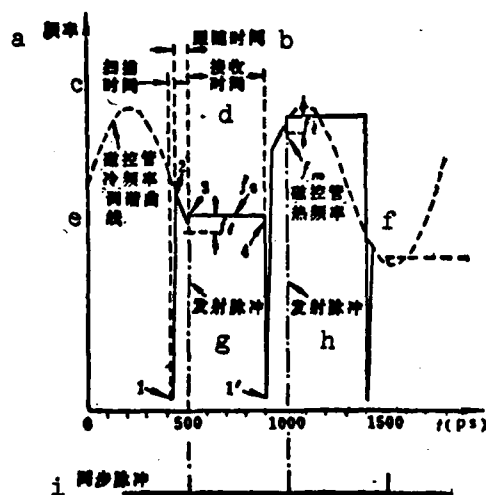


FIG. 7.3 THE OPERATIONAL PROCEDURE OF AGILE LOCAL OSCILLATOR OF FREQUENCY AGILE RADAR THAT USES A ROTATIONAL TUNING MAGNETRON

KEY: (a) Frequency; (b) Tracking duration; (c) Scanning deviation; (d) Receiving duration; (e) Magnetron cold frequency tuning curve; (f) Magnetron hot frequency tuning curve; (g) Transmitting pulse; (h) Transmitting pulse; (i) Synchronous pulse

By the above operational procedure of the agile local oscillator we can see that frequency agile local oscillation must satisfy the following few basic requirements:

(1) It must have the highest tuning speed, generally reaching ± 100 megahertz every microsecond. This is also to say, voltage tuning is necessary.

(2) Its tuning curve not only must be single value, but also must have the best linearity. No matter what operational frequency band it is in, common voltage step variation all correspond to an intermediate frequency.

(3) The instantaneous variation response of its tuning (thus the frequency response on the step voltage) must possess the shortest installed fixed duration (lift duration), the smallest ultra-tuning rate, and the shortest delay time.

(4) Within the duration of the backward-wave of the receiver in the pulse (approximately a millisecond magnitude), it must make its frequency drift minimum, to ensure that the backward-wave signal frequency after the mixer can stably be equal to intermediate frequency. It also requires its "post tuning drift" to be as small as possible.

(5) There must be very good frequency retuning and restabilizing.

(6) It must have ample tuning bandwidth, at least able to match the frequency agile magnetron that is used.

(7) It not only is a broadband oscillator component, but also with the whole tuning bandwidth must have a high enough frequency spectrum purity. Especially when it still requires radar that can operate on moving targets to show the pattern, it must have very good short-period frequency stability.

(8) Within the whole frequency band, it must have powerful enough output (approximately ± 10 milliwatts) and furthermore its power level in the frequency band does not vary greatly.

(9) Other indexes should be able to satisfy basic application requirements. For example, volume, weight, power consumption, life, etc.

The voltage tuning oscillator that can satisfy the above requirements can be divided into the two categories of the electronic vacuum device and the semiconductor device. Earlier, the electronic vacuum device that affected the agile local oscillator source primarily was the backward-wave tube. Recently, with the development of semiconductor devices, they are beginning to use microwave semiconductor oscillators of variable cavity tuning. The following section will respectively discuss these.

7.2 BACKWARD-WAVE TUBE LOCAL OSCILLATOR

The backward-wave tube that is mentioned here refers to a type zero backward-wave tube. It is a linear type electron beam microwave oscillator. It has very wide electron tuning frequency band, and can reach one frequency multiple procedure or match the bandwidth of the wave guide. Typical power output is 50-100 milliwatts. Using the necessary high-speed tuning local oscillator is perfectly suitable. Figure 7.4 is a schematic drawing of its structure⁽²⁾.

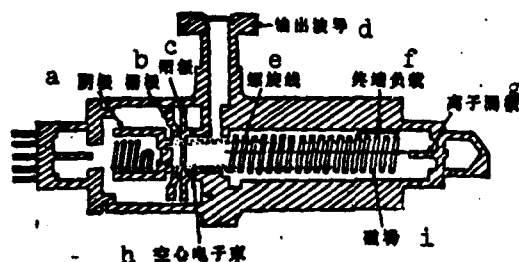


FIG. 7.4 DIAGRAM OF THE STRUCTURE
OF TYPE O BACKWARD-WAVE TUBE
KEY: (a) Cathode; (b) Grid; (c) Anode;
(d) Wave guide output; (e) Helical line;
(f) Terminal load; (g) Ion mixed pole;
(h) Hollow electron beam; (i) Magnetic
field.

Its operational principle is: the electron that is emitted by the circular cathode, after going through grid control and the anode of the belt circular crack, forms a hollow electron beam, the helical line is accelerated, there is an axial directional magnetic

field in the helical line area to make the electron beam focus, the hollow electron beam advances near the inside diameter of the helical line, and gradually is absorbed by the helical line. The speed of the electron beam and the helical line voltage square root form a direct ratio.

The helical line diameter and thread pitch are chosen this way, so that the high frequency electromagnetic wave (it uses the speed near the speed of light and follows helical line propagation) the speed that advances on the edge of the tube axis to near the advancing speed of the electron beam. This way the electron speed will be modulated and produced together. As to the frequency weight that has the same phase as the grouped electron beams, then it produces energy exchange in the electron beam. Because energy is obtained from inside the electron beam, the amplitude of this frequency electromagnetic wave along the helical line gradually enlarges, and finally the output wave guide near the cathode is taken out.

Because the speed of the electron beam is resolved by the helical line voltage, therefore, the backward-wave tube is a very good voltage tuning oscillator device.

The tuning properties of the typical X waveband backward-wave tube are shown in Fig. 7.5⁽²⁾. It can similarly be an index function:

$$\left(\frac{1}{V}\right)^{1/2} = A + \frac{B}{f} + \frac{C}{f^2} \quad (7.1)$$

In which A, B, and C are constant, and are determined by the structure of specific tubes.

Although different tubes possess different tuning properties, if after it uses its restoration then dispersion is within the range of $\pm 2\%$.

When the helical line voltage rises, the electron beam speed increases, and the oscillator frequency then rises. Conversely, the

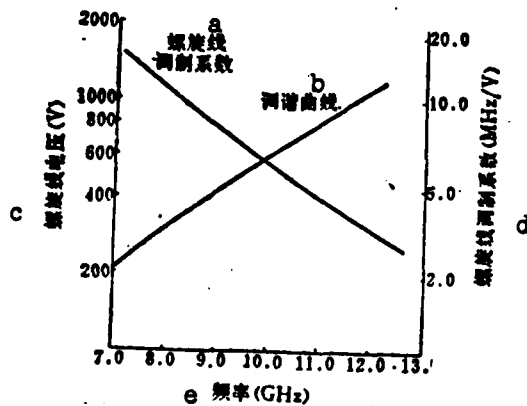


FIG. 7.5 TUNING PROPERTIES OF THE BACKWARD-WAVE TUBE
KEY: (a) Helical line modulation coefficient; (b) Tuning curve; (c) Helical line voltage (V); (d) Helical line modulation coefficient (MHz/V); (e) Frequency (GHz).

frequency decreases. Its modulation system (thus the slope of the tuning curve, expressed with each volt megahertz number) then decreases with increase in voltage.

But when the helical line voltage varies, its oscillator power can also follow the variations, its variations within 1-10 decibels, depending upon operational bandwidth. Its typical power output characteristics are as Fig. 7.6 shows. By the figure we can see that its output power within the range of operational frequency varies one fold or more.

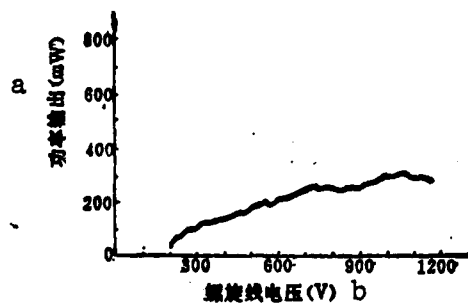


FIG. 7.6 OUTPUT POWER PROPERTIES OF A BACKWARD-WAVE TUBE
KEY: (a) Power output; (b) Helical line voltage.

In many applications (including those regarded as local), its desired output power can stay invariant within the range of a whole operational frequency. Generally there are 3 methods that can be chosen. One is using the common automatic gain control system, first inspecting the radio frequency power level, and later the grid or anode of the feedback control backward-wave tube, in order to keep its output power invariant. But the variation of the grid pressure or anode voltage can raise to the additional frequency variations, and therefore is not desirable to use. The second method is using an attenuator that possesses specific frequency characteristics, its attenuated frequency characteristics are exactly opposite from the output characteristics of the backward-wave tube. The weakness of this method is it causes the design of the attenuator to produce very large difficulties. Moreover the replaced requirements of the backward-wave tube simultaneously replace the attenuator that possesses corresponding attenuated frequency characteristics. Therefore this method also is not ideal enough. The third also is a relatively ideal method, it is an electronic control attenuator that uses a PIN diode (Fig. 7.7)⁽³⁾. The output end of the attenuator carries out sampling on radio frequency power output, with the sample results and continuous flow power level comparisons, the output after differentiating uses a partial flow that controls the diode, thus changing its attenuation rate and achieving its goal of balanced output power. This electronic control attenuator plugs into the output wave guide of the backward-wave tube, its plug-in loss is approximately 1 decibel, and requirement on the backward-wave tube appearance is the load of a very small standing wave ratio, therefore when the output power level is revised it will not extend the lift frequency traction. When standing wave ratio is 1.5:1.0, its frequency traction is less than (1-2)%. The load of exceedingly high standing wave ratio is not desirable, because it can cause the production of tiny wave cracks on the tuning curve of the helical line and the power output curve. Using this method on the tube of frequency multiple procedure we can tune to within $\pm \frac{1}{2}$ decibel with its output power level.

The grid operations of the backward-wave, when there are continuous wave condition operations, are lower than the cathode electric potential.

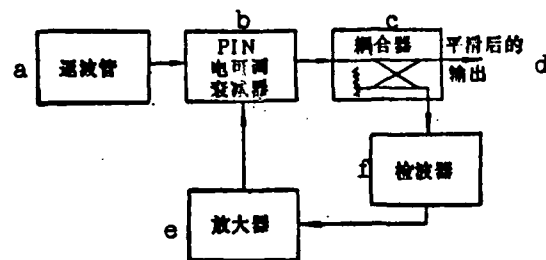


FIG. 7.7 FEEDBACK SYSTEM THAT MAKES THE BACKWARD-WAVE TUBE POWER OUTPUT SMOOTH

KEY: (a) Backward-wave tube; (b) PIN electronic adjustable attenuator; (c) Coupler; (d) Output after being smoothed; (e) Amplifier; (f) Detector

Because the grid generally has no grid flow, therefore it is able to very conveniently be used to adjust the power output electric level or be used for pulse modulation. But the variations of grid voltage also can raise to the variations of oscillator frequency. Its traction coefficient is -2 to -6 megahertz/volts. It is determined by the specific tubes. Therefore if requirements have fairly high stability, then it is necessary to use a highly stable voltage source that possesses very low noise and veinwaves. The grid power source should be able to be adjusted within the range of 0 - 100 volts. In order to ensure normal operations of the tube, the grid power source should have a corresponding safegaurd circuit, causing it to never be able to be in a direct ratio with the cathode, and also never to surpass -100 volts.

The anode and the grid of the backward-wave tube are the same, they possess negative frequency traction coefficients, and their value is approximately -2 to -6 megahertz/volts. It is determined by the frequency range of the tube. Therefore, in order to satisfy the requirements of frequency stability, it is also necessary to use a stable voltage source of low noise and veinwaves. The anode power source should be able to be adjusted within the range of 20 volts to 100 volts, and be able to give current of 13 milli-amps. At the same time, it also should have a corresponding safegaurd circuit so that it cannot surpass the maximum anode voltage and anode current (its specific value is determined by the specific tube).

When the filament of the backward-wave tube, if using an alternating feedback current, also can make its oscillator frequency produce parasitic frequency modulation, generally peak to peak frequency modulation reaches 100kilohertz. In order to avoid this heat hum, it is necessary to use a continuous flow filament power source, and there must be a very good stable pressure device.

Its filament power source generally is $6.3 \pm 5\%$ volts, the filament current is approximately 0.9-1.5 amps. In order to prolong the life of the tube, it is necessary to restrict the surge current when the filament is put through within 3.0 amps, the filament voltage should be adjusted within the range of $6.3 \pm 1\%$ volts. The cathode must be joined with one end of the filament. If using continuous flow filament power source, the cathode must be linked to the positive end of the power supply to prevent the insulating material that is due to the heat element move towards the cathode and shorten the life. When correctly applied, its filament life can reach 5,000 hours or more. The diagram of the power source linkage of the backward-wave tube is as Fig. 7.8 shows.

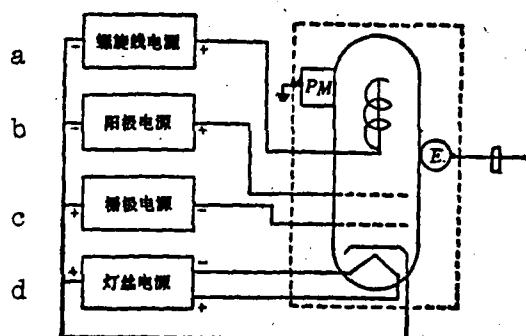


FIG. 7.8 DIAGRAM OF POWER SOURCE
LINKAGE OF BACKWARD-WAVE TUBE
KEY: (a) Helical line power source;
(b) Anode power source; (c) Grid
power source; (d) Filament power source.

When a backward-wave tube is used as the local oscillator of frequency agile radar, it still requires it to be able to have very good frequency readjustments, very fast tuning rate, very high frequency stability, and very pure tuning frequency purity.

So-called frequency readjustment is simply referring to the repeatability of its tuning curve. Also it is the single value between the helical line tuning voltage and its oscillator frequency. This includes readjustment on the same tube and repeatability when the tube is replaced.

Readjustment on the same tube requires all operating conditions to be able to maintain the property of no band rear, it has influential factors of four areas:

(1) The stability of the helical line voltage in itself. Because the helical line voltage possesses a very high tuning sensitivity (its typical value 1-10 mH/amp or 1-10 kH/milli-amp), therefore the instability or the crack wave due to the helical line power source voltage both can raise its oscillator frequency drift or modulation.

(2) The variation of background temperature. Because the variation of background temperature can possibly raise the variation of magnetic field intensity, it therefore produces frequency drift. In the range of -65°C to $+85^{\circ}\text{C}$, the temperature coefficient typical value that has not gone through compensation is approximately $-0.001\%/^{\circ}\text{C}$. The tube after being electrified for 10-15 hours will stabilize unusually close to its balanced frequency. After balancing, its frequency drift generally is less than 0.01% if the operational background temperature of the backward-wave tube has fairly large variation (for example in airborne radar), with the result that when the frequency variation that was raised surpasses the allowed value, then it is necessary to put the tube in a constant temperature.

(3) The "history" of frequency tuning. Because the electron beam power follows the tuning voltage and variations, therefore when the variations of the frequency are within a very wide range, the electron beam power (thus temperature rise of the tube) also can follow the variations. For example, when frequency quickly changes from one end of the frequency band to the other end, the power of the output to the helical line will increase or decrease 7-8 times, to make the tube enter into a

new hot balanced condition it needs a duration of approximately 5 minutes. This frequency error (or called post tuning drift in the typical value of the X wave band) is 1 megahertz.

(4) The variations of the cathode current follows the life. In the application process the cathode emission drops, and therefore causes the frequency and power of the backward-wave tube to vary. In order to promptly discover the aging of the tube, it is necessary to periodically inspect its cathode current and heat emission.. When the cathode flow causes aging and decreases it can use the method of changing the anode voltage to make it return to the original value and be able to prolong the life of the tube. When the cathode emission reduces to near its temperature limitation, it is then necessary to use the method of raising the filament voltage and also raising the cathode temperature to eliminate this effect. Naturally, because this method can shorten the life of the filament it has certain limitations.

As to the frequency tuning repetition when the tube is replaced, it is primarily dependant upon the manufacturing technique of the tube, especially the installed frame of the helical line and the opposite core of the electron gun must be very good. When the manufacturing technique level is comparatively high, the repetition properties of the replaced tube is within $\pm 1\%$. That is once there is a minimum frequency of the minimum voltage fixed rate, its maximum frequency is within 1%.

When the backward-wave tube is used in a frequency agile radar local oscillator, an extremely high tuning rate is required, in order to tune to the frequency that is required within the duration of zero point some to some microseconds.

The tuning rate of the backward-wave tube is dependant upon the tube, especially the structure of the helical line. The time that is required for the electromagnetic wave that is induced from one end of the helical line to turn to the other end is τ . The value of τ is determined by the diameter, the thread pitch, and the length. When the

backward-wave tube operates on the scanner frequency, the signal phase of the other end of the helical line transforms to Δf within this time τ because of frequency variations. If this phase variation exceeds a certain maximum allowed phase deviation, its energy feedback (thus oscillator power) then can reduce to conditions that cannot be allowed, with the result that the oscillator stops.

The similar expression of the backward-wave tube maximum scanning frequency rate (experiential formula)⁽³⁾ is:

$$\left(\frac{df}{dt}\right)_{\max} \leq \frac{1}{\tau^2} \quad (7.2)$$

The typical value of the low frequency end of the helical line of the X waveband backward-wave tube is 400 volts. This corresponds to the worse conditions (longest passing time). At this moment its maximum scanning frequency speed is approximately 40 gigahertz/microsecond. Generally speaking, the tuning speed of the backward-wave tube regarding frequency agile radar local oscillator is ample.

Another requirement regarding the frequency agile radar local oscillator is simply that after the backward-wave tube tunes at high speed to the mutually corresponding correct frequency with the transmitted frequency, it then must keep this frequency within the time interval of the repeated cycle of the pulse with extremely high frequency stability. Because the backward-wave tube in itself is a voltage tuning device with very high sensitivity, therefore in order to ensure its high frequency stability it requires the power source of each electrode (especially the helical line power source) to have a very high voltage stability, and very small vein waves. Aside from this, it also requires the frequency that is raised by the frequency traction to unstably reduce to the minimum. This primarily depends on the reflection coefficient of the inner section terminal of the tube and the standing wave ratio of the load. When the load-standing wave ratio is 1.5:1 (any phase), the frequency traction that it raises $< 1\%$ or 2% , its typical value is ± 1 megahertz.

The backward-wave tube conducts the local oscillator to raise the

klystron, its primary weakness is that the spectrum line purity of its oscillator is fairly inferior, that is, the noise bandwidth of its oscillator is fairly wide. The primary mechanisms that produce the backward-wave tube noise are of the following 3 kinds: (1) In the region of the electron beam there is an ion that is impelled by two emissions of electrons of the helical line or collecting electrode and an equal ion that is produced oscillates. (2) By electrode collision producing ample ions it then reaches the neutralization of the space electric charge and the remittent oscillation that is produced. (3) The longitudinal oscillation that the two emissions of electrons in the helical line or the collecting electrode and anode produce. In it the equal ion system oscillator is primary, the output of its production is within the range of 40 kilohertz to 2 megahertz. Generally, typical conditions are total accumulated frequency modulated noise approximately 1×10^{-6} , then when it is 10 gigahertz it is approximately 10 kilohertz. In an ion carrier wave 100 kilohertz and 1 kilohertz bandwidth, the noise power level decreases to 60-80 decibels or less, in a bandwidth of 2 megahertz of ion carrier wave 30 kilohertz, the noise power level decreases 95-100 decibels or less. Figure 7.9 is a noise frequency spectrum of 50 milliwatts X waveband backward-wave tube, in which the intermediate frequency is 9.4 gigahertz, its second spectrum wave generally is 20-25 decibels lower than the carrier wave. The amplitude modulation noise is extremely small, approximately 90 decibels lower than the carrier wave. This kind of noise output as the noncoherent frequency agile radar local oscillator also can be permitted.

Another fairly large weakness of the backward-wave system is it is necessary to focus the magnetic field. Early backward-wave tubes used an electromagnetic focusing system, this not only causes the volume and weight of the backward-wave tube local oscillator to greatly increase, but also must expend power to a very large focusing power source. Modern backward-wave tubes completely use periodic field constant magnetic focusing systems, this greatly reduces the volume and weight of the backward-wave tube oscillator. In recent years, new rare earth metal constant magnetic materials were discovered, for example, the maximum BH Sum of Samarium Cobalt alloy (SmCo_5) can reach 15-20 megagauss-orst-

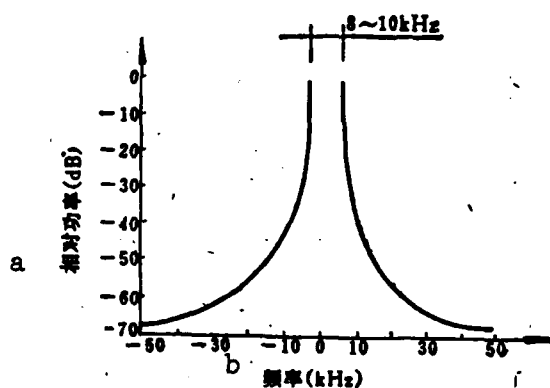


FIG. 7.9 NOISE OSCILLATION FREQUENCY MODULATION OF AN X WAVEBAND BACKWARD-WAVE TUBE

KEY: (a) Corresponding power (dB);
(b) Frequency (kHz)

ed, 25 times as hard as aluminum nickel cobalt 9, and 6 times as hard as platinum cobalt. And, praseodymium Samarium Cobalt Alloy ($\text{Pr}_5\text{Sm}_5\text{Co}_5$) even can reach 20-25 mega gauss-oersted. Using these new constant magnetic materials can even further decrease the volume and weight of the backward-wave tube oscillator.

The magnetic shield on the backward-wave tube local oscillator is also a very important problem. On one hand the backward-wave oscillator with a harmful shield can produce a very strong leaking magnetic field, severely disturbing the operations of other magnetic devices (such as iron oxygen isolator, circulator, the electronic adjustable wave filter of the yttrium iron garnet, and others), on the other hand, the focused magnetic field in itself also can receive the influence of the outer stray magnetic field (such as the power source transformer, etc.), to such an extent as to influence the stability of its oscillator frequency. Therefore it is necessary to use a very good magnetic shield outer cover. Figure 7.10 shows the shield application of the magnetic shield on the magnetic leak.

Aside from the magnetic shield, the backward-wave tube oscillator still must have a very good radio frequency shield. On one hand this

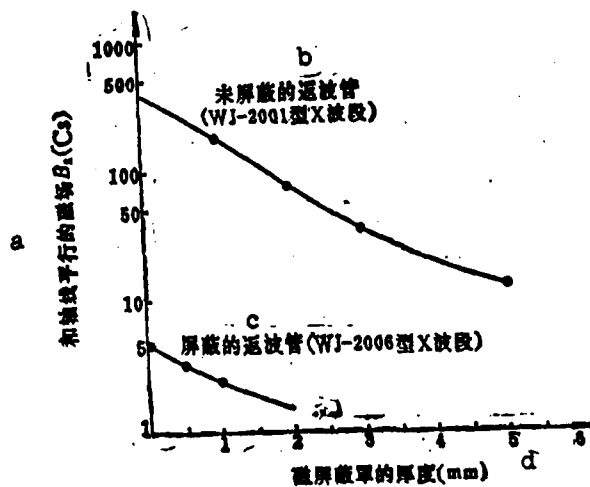


FIG. 7.10 SHIELD APPLICATION OF MAGNETIC SHIELD OUTER COVER ON MAGNETIC LEAK

KEY: (a) Magnetic field B_z (Cs) with parallel axis; (b) Unshielded backward-wave tube (model WJ-2001 X waveband); (c) Shielded backward-wave tube (model WJ-2006 X waveband); (d) Thickness of magnetic shield cover (mm)

shield prevents the oscillator of the backward-wave tube with the output coupler, output electric cable plug seat, and the installed hole of the continuous flow feeder going to the tube; on the other hand it also must prevent the outer radio frequency signal expelling into the tube through the leadwire and plug seat to carry out modulation on its oscillator. This requires its pack through processing and solder sealing, eliminating the continuous flow flight line, and entering each continuous flow feedback through the radio frequency attenuator. Figure 7.11 is a diagram of the packing section of a constant magnetic focusing backward-wave tube.

The backward-wave tube of the cermet type can endure an extremely large shock and vibration, the largest shock that it can endure reaches 50g, and the vibration radio frequency can reach 2 kilohertz. The main problem lies in the frequency modulation weight in the radio frequency spectrum that is raised when the operations are under the environment of shock and vibration. In order to reduce this parasitic frequency

modulation, it is necessary to make the support of the electron gun and helical line be extremely firm, and at the same time make the vacuum housing section and the outer focusing magnetic steel conduct an entire vibration together.

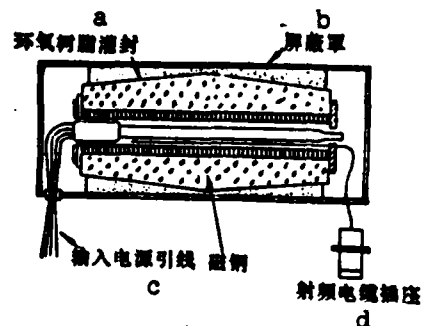


FIG. 7.11 PACKING OF A
BACKWARD-WAVE TUBE
KEY: (a) Epoxy resin; (b)
Shield cover; (c) Input
power source lead, magnetic
steel; (d) Radio frequency
cable plug seat

The dependability and life of the backward-wave tube depends on the material that is used, the structure design, and the manufacturing technique. Under general conditions, the life of the tube is primarily determined by the life of the cathode. And, the life of the cathode primarily depends on its load factor and life. The load factor of the cathode is the current density that is transmitted from the cathode to the electron, generally expressed by amps/square centimeters. In long life tubes, the load factor of the oxidized cathode can use up to 0.4 amps/cm². The environment of the cathode thus depends on the remaining gas pressure in the tube, the poison level of the cathode near the components on the cathode, and ion bombardment. The remaining gas in the tube not only can cause the life of the cathode to shorten, but also can cause the tube output frequency spectrum to be impure and influence the applicable life of the tube by equal ion parasitic oscillation (thus causing at this time the cathode emission to still be fine). The majority of backward-wave tubes can have useful life that guarantee 2500 hours, and in reality many tubes can operate for 5000 hours and even 15000 hours.

The most recently discovered nickel barium magnesium alloy makes the basal material oxidized cathode (containing 0.3% barium), when the temperature of the cathode is 800 degrees, its saturated current value must be 2.5 times higher than nickel tungsten magnesium alloy (containing 4% tungsten), its life (91% of the earlier flow value) can reach 25000 hours, generally 4 times that of the nickel magnesium alloy.

Table 7.1 gives the parameters of some backward-wave tubes.

7.3 ELECTRONICALLY TUNED MICROWAVE SEMICONDUCTOR AGILE LOCAL OSCILLATOR

With the continuous development of microwave semiconductor devices, at present we already can use a complete semiconductor electronically tuned agile local oscillator to replace the backward-wave tube. This electronically tuned microwave semiconductor agile local oscillator possesses the advantages of smaller volume, lighter weight, more economic power consumption, and longer life over the backward-wave tube. Moreover, the frequency of its oscillator is pure and clutter is small. Its primary weaknesses are that the temperature stability is comparatively inferior, the post tuning drift is fairly large, and modulation linearity is fairly inferior, but these problems can all be resolved.

Now we will explain these electronically tunes oscillators that use microwave semiconductors.

The microwave semiconductor oscillators that have practical applications are microwave transistor oscillators, bulk-effect diode oscillators, collision avalanche wave excess duration diode oscillators, and tunnel diode oscillators. In the past, microwave semiconductors could not reach very high operational frequencies, we only had operations on microwave oscillators of L wavebands and S wavebands. In lower than the L waveband, its output power must be higher than any kind of semiconductor device microwave oscillator. Recently, gallium arsenic effect tubes already can operate to Ku wavebands, and possess effective high temperature stability.

TABLE 7.1 The Parameters of Some Backward-wave tubes.

Model #	Frequency (GHz)	Power (MW)	Helical Voltage (V)	Electron Beam Current (mA)	Anode Voltage (V)	Filament Voltage (V)	Filament Current (A)	Weight (pounds)	Volume (inches) ³
WJ-2005	4.0-8.0	20	300-1800	10					3x3x8
SBX-2980	8-12	15	300-1100	8	100	6.3	0.75	0.75	
WJ-2006	8-12.4	50	450-1500	10					
SBX-2981	9-10	50	400- 600	10	130	6.3	0.75	0.75	
WJ-2007	12.4-18	40	550-2000	10					
SBU-4530	15.4-17	20	900-1300	23	40	6.3	0.65	8 oz.	
SBV-4370	34-40	20	1200-2500	20	115	6.3	1.5	7	

The operational stability of gallium arsenic diodes are poor and oscillator noise is great, therefore at present they are not frequently used. Although collision avalanche wave excess duration diodes can obtain fairly large output power, used in semiconductive active phased array radar they are comparatively the most desirable device. But as to the voltage tuning local oscillator, its tuning range is fairly narrow (only approximately 5%), and oscillator noise is also fairly great. But it can operate to extremely high millimeter wave bands.

Because the frequency band of the bulk-effect diode negative resistance properties are very wide, and the reactance weight of its resistance is fairly small, therefore at present high microwave wave bands primarily use bulk-effect diodes to make voltage tuning oscillators.

In summary, in the P waveband to the S waveband (0.5-4.0GHz), basic frequency microwave semiconductor oscillators are primarily used, in S wavebands to X wavebands, multiplefrequency transistor oscillators can be used, and gallium arsenic field effect basic frequency oscillators can be used, in X wavebands to Ka wavebands, bulk-effect diode oscillators are primarily used, in Ka, Q, U, V, E, and W wavebands (26.5-110GHz), collision avalanche wavebands excess duration diodes are primarily used. Because frequency agile radar primarily operates in the microwave band from L waveband to Ku waveband, therefore the following will primarily explain microwave transistors and local oscillators of bulk-effect diodes.

In order to achieve electronic tuning, presently there are two methods that can be used, one method is using yttrium iron garnet (YIG) magnetic tuning, the other method is using varactor tuning. These two methods can both be used in microwave transistor oscillators and bulk-effect diode oscillators. The major advantages of YIG magnetic tuning oscillators are that the tuning range is wide (it can reach a multiple frequency level or higher), tuning linearity is good, oscillator noise is small, and stability is high. Its shortcomings are that tuning speed is low (typical value is 1MHz/microsecond), tuning power is large, and it has the phenomenon of post-tuning stagnation. Moreover, it

still needs to have a magnetic field shield; after adding on the magnet and magnetic tuning coil its volume is great and its weight is heavy.

Varactor tuning is voltage tuning, as a result its tuning rate is high (it can reach 10 GHz/microsecond or higher), moreover its power consumption is economical, weight is light, volume is small and life is long. Its shortcomings are that oscillator noise is great and stability is poor.

Table 7.2 lists property comparisons of these two tuning methods with the backward-wave oscillator⁽⁴⁾. The data in the table is only typical value.

TABLE 7.2 COMPARISON OF PROPERTIES OF THREE ELECTRONIC TUNING MICROWAVE OSCILLATORS

PROPERTY	BACKWARD-WAVE	YIG	VARACTOR
Tuning Range	Multiple Frequency level	Multiple Frequency level	Can reach multiple frequency actually uses 30%
Tuning Curve	$(1/v)^{1/2} = A + \frac{B}{f} + \frac{C}{f^2}$	$f + KI$	$f + KV^n$
Tuning Linearity	Poor	Good	Poor
Tuning Rate	± 10 gigahertz/ microseconds	10 megahertz/ microseconds	± 10 gigahertz/ microseconds
Tuning Drift	Still Good ± 1 megahertz	Still Good ± 1 megahertz	Good ± 0.1 megahertz
Tuning Noise •rms	-320 hertz	-32 hertz	-240 hertz
Output Power NW	100-200	10-30	20-50
Power Variation	3 decibels	2 decibels	2 decibels
Effectiveness	6%	1%	1%
Weight	8 lbs.	1 lb.	3 oz.
Life	3000 hours	10000 hours	100000 hours
Power Source #	3	2	2

•Measurement within bandwidth of 1GHz of 10GHz ion carrier wave

Because these two tuning methods each have particular weaknesses, at present both can be used in frequency agile radar and considered as frequency agile local oscillators, therefore the following will respectively explain these two electron tuning methods, but will emphasize the microwave semiconductor local oscillator with varactor tuning.

7.3.1 YIG TUNING MICROWAVE OSCILLATOR

When YIG or YIG of mixed gallium is placed in the magnetic field, due to its ferromagnetic properties it causes it to produce resonance in the microwave frequency. The reason for this resonance is that when the magnetic field and high frequency field exist, the motion of the magnetic pole raises. The self rotating electron can be seen as a mechanical gyroscope, it can also produce advancement under effects of magnetic moment of a fixed magnetic field. This magnetic moment can be compared with the angular momentum of self rotating matter. If there is an existing emission field that is vertical to the fixed magnetic field, and when its frequency is again exactly equal to the advanced frequency of the YIG sphere, the radio frequency energy then can couple onto the self rotating electron, consequently resonance is produced. Resonance frequency (the frequency of nutation) is in a direct ratio with the constant magnetic field that is added, changing the magnetic field then can change its resonance frequency, its sensitivity is approximately 2.8 megaHz/gaus.

As to the radio frequency field we can say, this YIG sphere can be equivalent to the resonance return circuit of a parallel connection R, L, C , its reactance element (thus its resonance frequency) can use the method of changing the magnetic field strength to change. This way a resonance return circuit so long as it has a suitable negative resistance device parallel connection, it can form a microwave self excited oscillator of an adjustable frequency.

There are many active devices that can be used in this magnetic tuning oscillator, the most common is the bulk-effect diode. Figure

7.12 is a structural diagram of this magnetic tuning bulk-effect diode oscillator.

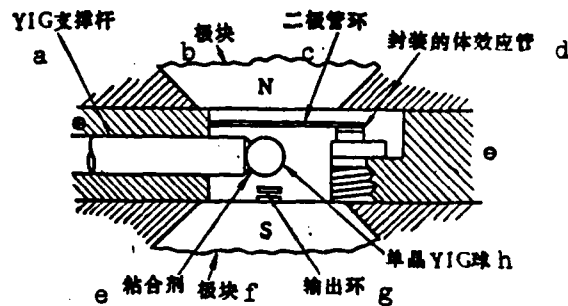


FIG. 7.12 STRUCTURAL DIAGRAM OF MAGNETIC TUNING BULK-EFFECT DIODE OSCILLATOR

KEY: (a) YIG support shaft; (b) Grid piece; (c) Diode loop; (d) Bulk-effect tube -f sealed unit; (e) Binder; (f) Output loop

The primary weakness of the magnetic tuning bulk-effect diode oscillator is that the input power is large and efficiency is low. For example, when the output power of an oscillator with X waveband is 30-50 milliwatts, its operational current reaches 500 milli-amps, its operational voltage is approximately 11-12 volts, and still does not include the inner pressure decrease of the pressure stabilizer and pressure resistance. Therefore, its efficiency is only approximately 1%. Large quantities of power change into heat energy requiring dissipation. This not only is the installation problem of producing a radiator but decreases its operational stability and dependability. Aside from this, the stability of the bulk-effect diode in itself also is fairly poor, this can produce undesirable lateral band signals in the output signal. Therefore, in recent years, the magnetic tuning bulk-effect diode oscillator already gradually is being replaced by a magnetic tuning gallium arsonium field effect oscillator⁽⁵⁾.

The operational current of this kind of gallium arsonium field effect oscillator is only 50 milli-amps, the operational voltage is 7-8 amps, efficiency reaches 10±%. Therefore the power consumption that

is required is fairly small. Furthermore its frequency tuning noise is also very small, for example the frequency modulation noise in a 20 kHz bandwidth ion load frequency placed in a 1 kHz bandwidth of a 10.25 GHz oscillator is approximately -55 to -75 decibels lower than the carrier wave.

The magnetic tuning gallium arsenium field effect oscillator generally uses receiving feedback electric capacity or inductance between the common grid and the ground. The electric capacity feedback can obtain negative resistance in a fairly large bandwidth; the inductance feedback then can show a fairly large negative resistance, therefore causing the easy emergence of slotted circuit coupling. Thus at present the inductance feedback common grid circuit is commonly used (Fig. 7.13a). This feedback inductance actually is a leadwire of a fixed field effect tube core piece, it also provides a continuous flow circuit for the grid. The leadwire inductance of other poles thus should be as small as possible. Inductance resistance X_L of feedback conductance L_G through a phase shift of the field effect tube turns into negative resistance (Fig. 7.13b). After this negative resistance and YIG have a parallel connection (couple), an oscillator can then be constructed.

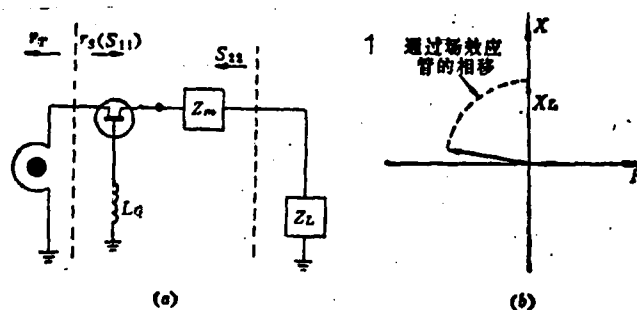
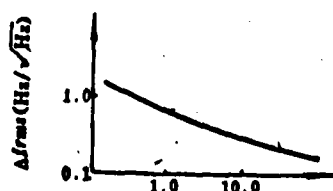


FIG. 7.13
 (a) CIRCUIT OF A COMMON GRID FIELD EFFECT
 TUBE MAGNETIC RESONANCE OSCILLATOR
 (b) FORM OF NEGATIVE RESISTANCE
 KEY: (1) Phase shift through field effect tube

The primary advantages of the oscillator that uses YIG tuning are: tuning range is wide (surpassing a multiple frequency level), tuning linearity is good (as small as $\pm 0.05\%$), and the frequency modulation

noise of the oscillator is small. Among these, the last advantage is especially important, this makes it able to satisfy the requirements of moving target indication systems. Figure 7.14 shows the frequency modulation noise of a typical YIG tuning transistor oscillator.



ion load frequency interval (kHz)

FIG. 7.14 FREQUENCY MODULATION NOISE
OF YIG TUNING TRANSISTOR OSCILLATOR

The primary weakness of the YIG tuning oscillator is that tuning rate is relatively low. As preciously discussed, the tuning of the magnetic tuning oscillator primarily changes the strength and achievement of the magnetic field that is located in the YIG sphere, in order to be able to obtain a variable strength magnetic field, then only an electromagnet can be used. The magnetic field strength that is obtained by the electromagnet forms a direct ratio with the number of rings of the spiral tube coil and the current through the coil. In order to quicken the tuning speed, we must reduce the number of coil rings, this requires an even larger current. This is also simply to say, its tuning speed mutually contradicts tuning sensitivity. Generally, the tuning sensitivity of X bandwave is approximately 20 megaHz/ /milli-amp, to tune to 4gHz then requires a 200 milli-amp current. This coil has approximately 5 ohm continuous flow reactance and 47 milli-henry inductance, its 3 dB bandwidth is approximately 5kHz, that is, its tuning time is approximately ± 100 milliseconds/gHz. This obviously is not sufficient for frequency agile radar. In order to quicken the tuning speed, a small coil is generally added outside the main coil, called the tuning coil. This coil has relatively few rings, therefore it has relatively low tuning sensitivity (generally approximately 310gHz/milli-amps), the continuous flow resistance of the coil is 1 ohm, inductance rate is 1.25 millihenry, its 3 decibel bandwidth can reach 400kHz. This then can cause its tuning speed to reach a maximum

200 megaHz jump change to need 10 milliseconds. This kind of tuning speed still is not suspicious enough for tracking rotational tuning magnetrons, and thus already can be satisfactory for tracking precision tuning magnetrons. Especially because the magnetic resonant oscillator possesses a fairly small oscillator noise, that is, it possesses fairly high short cycle frequency stability, therefore it can be used as a highly stable agile local oscillator or moving target indication radar. This moving target indication radar that possesses frequency agile ability generally uses a same axis magnetron with high stability as a transmitter. In order to be able to achieve the offsetting of the additional pulse, it generally can only form agility, then transmit a series of pulses (2-9) that possesses the same kind of carrier frequency and later have agility until the other frequency again transmits a series, as a result the requirements of speed on local oscillator agility can be decreased. Using the magnetic tuner can satisfy its requirements.

Another shortcoming of the magnetic tuner is that it possesses a magnetic stagnation appearance, this causes the readjustment of its tuning (second time) to be poor, moreover the "history" is related to the tuning, generally its post stagnation is approximately 10GHz, but after a full frequency band jump-change in the same direction the second time of tuning can reduce to 1kHz. When an automatic frequency control circuit is designed, it must consider these characteristics.

The harmonic output of the magnetic tuning gallium arsonium field effect oscillator is approximately -15dBc (second harmonic) to -20dBc (third harmonic), parasitic output is as low as -60dBc, as a result a corresponding output of high purity frequency spectrum can be provided.

In order to improve temperature stability of the oscillator, we use an inner heater, this can make the frequency drift in the range of 0-60°C as low as 5 megaHz.

7.3.2 VARACTOR TUNING MICROWAVE OSCILLATOR

A varactor diode is a voltage control device that uses a semiconductor PN junction to use up capacitance following additional reverse voltage and variations. Its equivalent circuit (shown in Fig. 7.15(a)) can be divided into two parts: one part is the core piece in itself, it can be equivalent to the contact of reactance R_v and variable capacity C_v . The other part is the sealed unit inductance L_{pv} and sealed unit capacity C_{pv} .

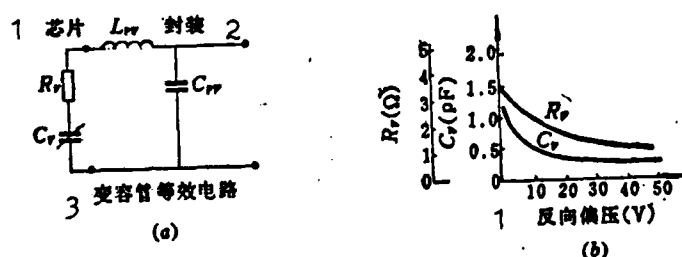


FIG. 7.15 VARACTOR TUNING DIODE OSCILLATOR

(a) Equivalent circuit of varactor

KEY: (1) Core; (2) Sealed unit; (3) Varactor equivalent circuit.

(b) Capacitance voltage properties of varactor

KEY: (1) Reverse bias voltage

The relationship between junction capacity C_v of the varactor and added reverse voltage can be expressed by the following formula:

$$C_v = C_j(0) / \left(1 + \frac{V_R}{\phi} \right)^n \quad (7.3)$$

In which: $C_j(0)$ is junction capacity when there is zero bias voltage;

V_R is added reverse voltage;

ϕ is contact power potential (silicon tube is 0.7 volts);

n is the index that is related to PN junction category (on the gradual change junction is $1/3$, sudden change junction is $1/2$, ultra-sudden change junction is 2).

The relationship between the capacitance of a silicon rapid change junction varactor where a zero bias voltage junction capacitance is 1.5 picofarads and the added voltage is shown in Fig. 7.15(b). Contact

equivalent resistance R_v also is the voltage function (as shown in Fig. 7.15). The definition of the Q value of the varactor is:

$$Q = \frac{1}{\omega C_v R_v} \quad (7.4)$$

for the same purpose, it is stipulated at -4 volts, measured when 50 MHz.

A silicon varactor is a silicon sudden change junction tube, most recently a gallium arsenide ultra-sudden change junction varactor has been developed, this kind of varactor possesses even less reverse current than the silicon varactor, a higher Q value (it can reach 10,000) and a higher reverse voltage and larger variable capacity ratio, consequently it can obtain an even wider frequency band. At this time it can operate to 60GHz or more.

The microwave oscillator of varactor tuning in low microwave bands (L and S wavebands) can use dual pole type transistors as active components, a somewhat higher frequency (C and X wavebands) can use multiple frequency transistor oscillators, even higher frequency bands (X and Ku wavebands) thus can use bulk-effect diodes as active components. Most recently using gallium arsenide field effect tubes we can operate on basic frequency oscillators from a low microwave band directly to a Ku waveband.

When frequency is as low as an S waveband, the transistor diode oscillator that uses varactor tuning can obtain frequency readjustment (second time) and jump frequency local oscillators that have very good frequency stability, moreover its oscillator noise is small and its spectrum is pure. Generally this type of oscillator uses the base ground connection receiving method, the varactor receives in the contact resonance circuit of the collecting electrode, and the oscillator signal uses magnetic coupling (transformer coupling) to output end. Figure 7.16 is a varactor tuning transistor local oscillator circuit and its equivalent circuit⁽⁶⁾. The varactor that is used in it is an arsenium

tube, its parameters are as follows: zero bias voltage capacitance approximately 1.0 picofarad, zero deflection installed carrier frequency is approximately 100GHz, puncture voltage is approximately 20 volts, maximum useage capacitance ratio is 5:1. The entire oscillator uses thin film microband integrated circuits. The tuning range of this oscillator is 1.2-2.0GHz. Its output power is 12-33 milliwatts.

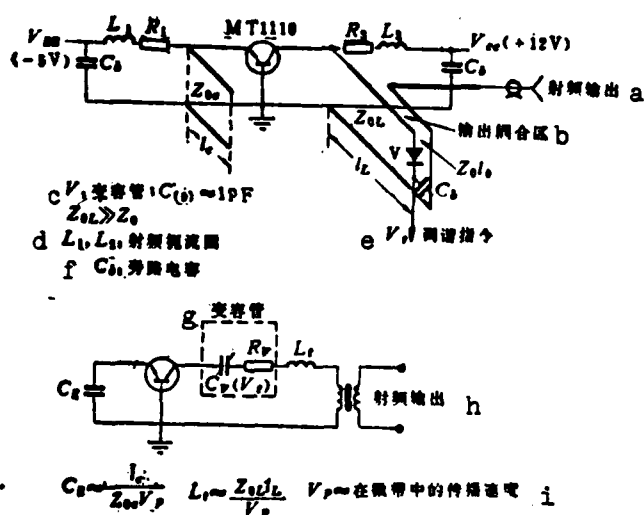


FIG. 7.16 VARACTOR TUNING TRANSISTOR MICRO-WAVE OSCILLATOR

KEY: (a) Radio frequency output; (b) Output coupling area; (c) Varactor; (d) Radio frequency choke; (e) Tuning directive; (f) Lateral circuit capacitance; (g) Varactor; (h) Radio frequency output; (i) Propagation velocity in microband

The transistor that uses the same model number uses the same circuit line form and different element parameters. This oscillator can also operate to S waveband. 2.7GHz can give out 40 milli-watts of power.

In even higher microwave wavebands, we can use the varactor tuning bulk-effect diode oscillators as frequency agile oscillators. The equivalent circuit of a bulk-effect tube is as Fig. 7.17 shows.

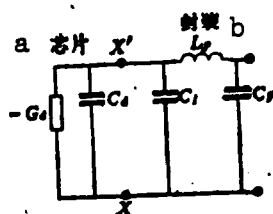


FIG. 7.17 EQUIVALENT
CIRCUIT OF BULK-EFFECT
DIODE

KEY: (a) Core piece;
(b) Sealed unit

Its core can be equivalent to the parallel connection of a negative resistance and capacitance; the sealed unit thus can be equivalent to L and C π type network. This equivalent circuit can be further simplified as the parallel connection or contact of L , C , and $-R$. The bulk-effect oscillator that uses varactor tuning has two circuits, one is a parallel connection tuning oscillator circuit, the other is a contact tuning oscillator circuit, its equivalent circuit is as Fig. 7.18 shows. So long as the absolute value of its negative resistance is as large as the lost resistance that the varactor converted to and the sum of the load resistance, the circuit then enters into an unstable state and produces oscillation. To make its oscillation stable, it then requires the absolute value of the negative resistance to become better as it becomes bigger, the larger the negative resistance, the faster the establishment of the oscillator, the noise of the oscillator is also small, and the possibility of parasitic oscillation production is also small. Aside from this, because the Q value of the thin film micro-band circuit is fairly low, and the bulk-effect diode of the large negative load resistance can operate as low as the Q circuit, therefore it must also choose to use a tube with a large negative resistance.

The contact resistance of the varactor follows the deflection placement and changes, when maximum capacitance, namely when minimum oscillator frequency, it is maximum, this is also the moment when Q value is minimum. Therefore in the tuning frequency band minimum it is easy to produce the problems of low Q value, such as oscillator noise, the incontinuity of model jump-changes, and oscillator frequency, etc.

A low Q value oscillator also increases the sensitivity of the oscillator on circuit parameter variations that are caused by load mismatching and temperature drift. The contact resistance of gallium arsonium varactors is said to be correspondingly more stable than silicon tubes, thus we should as much as possible choose to use gallium arsonium varactors in which contact resistance variations are minimum.

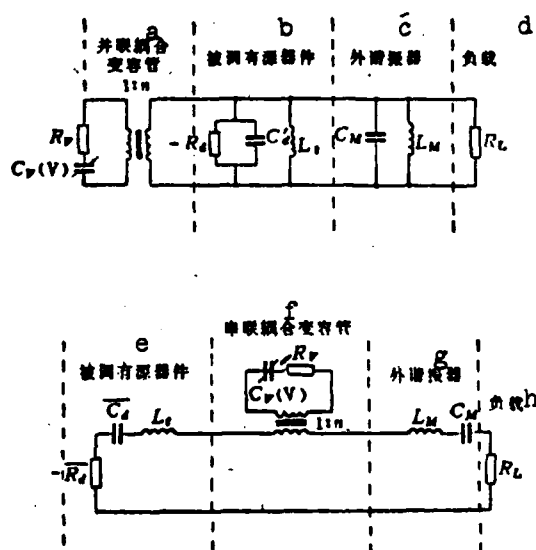


FIG. 7.18 EQUIVALENT CIRCUIT OF A PARALLEL CONNECTION TUNING AND CONTACT TUNING VARACTOR TUNING BULK-EFFECT DIODE OSCILLATOR

KEY: (a) Parallel connection coupling varactor; (b) Tuned active components; (c) Outer resonator; (d) Load; (e) Tuned active components; (f) Contact coupling varactor; (g) Outer resonator; (h) Load

The tuning range of the oscillator is primarily determined by the range of capacity variation of the varactor and the stray parameters. If the varactor capacitance that converts to the oscillator in the return circuit changes from C_{min} to C_{max} , then similarly we can say that the variable range of its oscillator frequency is $f_{max}/f_{min} = \sqrt{C_{max}/C_{min}}$. Due to the existence of stray capacity C_p (for example the tube casing capacity, etc.), it then reduces the frequency variation range, because $f_{max}/f_{min} = \sqrt{(C_{max} + C_p)/(C_{min} + C_p)}$. Therefore, in order to obtain

the widest possible tuning range, it is desirable to reduce the stray capacitance to a minimum. What is most primary in the stray capacitance is the tube casing capacitance. In order to make the tube casing capacitance minimal, the sealed unit of the bulk-effect diode and varactor diode is especially important. In the thin film microband circuit we can use an unsealed unit bulk-effect diode piece and varactor core, this way we can reduce the parasitic capacitance to a minimum, but we can also bring on other problems, such as equipment strength problems and dissipated heat problems. It is necessary to use particular techniques to ensure that it does not damage installation and good radiation.

From the bulk-effect diode we see that the equivalent capacitance of the varactor still depends on extending the mean radio frequency voltage that is on it, the higher the radio frequency voltage, the larger the equivalent capacitance, and the narrower the tuning bandwidth. Therefore it is best to use a varactor piece on the back contact, adding tuning voltage onto the center point, on the one hand doing this, due to its intrinsic rectification effects of radio frequency voltage, can reduce its equivalent capacitance, on the other hand after the two diodes make contact they still can reduce to half with the tube casing capacitance and the junction capacitance.

Figure 17.19 draws out the bulk-effect diode oscillator circuit lines of 2 thin film microband circuits and component linkages⁽⁶⁾. This bulk-effect diode that is used in it is model VSX-9201, its frequency range is 7-11GHz, equivalent parallel connection load $R_d=170$ ohms, $C_d=0.43$ picafarads; equivalent contact negative resistance $R_s=3$ ohms, $L_s=0.5$ nanohenries, tube casing capacitance $C_p=0.1$ picafarads. Converted equivalent $\bar{R}_d=4.5$ ohms, $\bar{C}_d=0.45$ picafarads. The varactor that is used is model GC-1600-00, its parameters are: zero deflection place capacitance $C_v(0) \approx 0.47$ picafarads (contact facing), maximum capacitance $C_v \approx 2.13$ picafarads, the load stop frequency (on the center equal to the bias placed point) $f_{co} \approx 100$ GHz. When parallel connection tuning, the capacitance of the varactor still must have mutual contact with the equivalent circuit of the contact tuning radio frequency ground connection piece. Thus:

$$C_{eff} = \frac{C_v C_r}{C_v + C_r} \quad (7.5)$$

In which $C_r = \frac{2}{\pi^2 f^2 Z_r}$.

For example when $f_r = 10\text{GHz}$ and $Z_r = 20$ ohms, we can compute $C_r = 1$ picafarad. Thus equivalent varactor capacitance $C_{v\text{ eff}} = 1.56$ picafarads, and $C_{veff} = 0.56$ picafarads, its numeric value must be smaller than that of contact tuning. Therefore its tuning range also must be more narrow than that of contact tuning. When we compute using the above parts, the tuning bandwidth when contact tuning is 16%, and when parallel connection tuning is only 11%. But the power output when parallel connection tuning in the whole frequency band is approximately as large as 20 milliwatts, now its alteration is not as large as that of contact tuning. Thus we commonly use a parallel connection on a tuning circuit.

One drawback to using distributed form elements is simply that element parameters and frequency are related. For example, the short pass transmission line with length as l and property resistance as Z_0 , its resistance is $jZ_0 \tan \omega l / c$. To make the dependability of its frequency close to the linear relationship of its pure inductance, we must select l short enough, to make $\tan \omega l / c$ in the operational frequency range it can similarly be $\omega l / c$ very well, at this moment its equivalent inductance is $Z_0 l / c$, we can use changing Z_0 to regulate. Generally its line length should be as small as $1/8$ wavelength. In spite of this, the non-linearity of distributed element resistance and frequency still can influence the bandwidth tuning of the oscillator. Therefore, recently some people used the super small type lumped elements, and constructed a varactor tuning oscillator that had very good properties⁽⁷⁾.

This kind of super small type lumped element possesses very small dimensions, for example the radio frequency choke of the S waveband uses an extremely fine line in a diameter of 80.5mm and winds 7 rings on the glass stick where the length is 1mm and can obtain an inductance rate

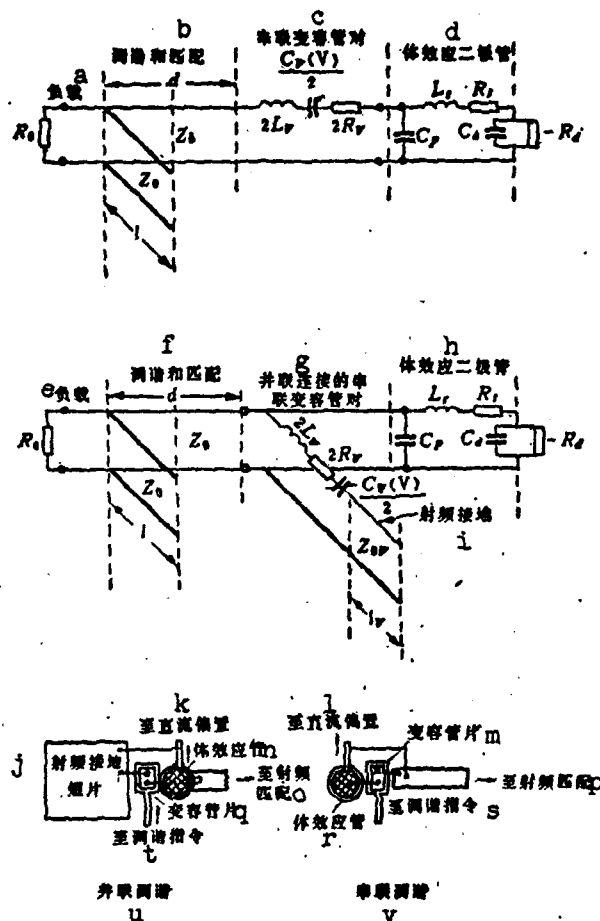


FIG. 7.19 DIAGRAM OF THE CIRCUIT LINE AND LINKAGE OF VARACTOR TUNING BULK-EFFECT DIODE OSCILLATOR

KEY: (a) Load; (b) Tuning and matching; (c) Contact varactor facing; (d) Bulk-effect diode; (e) Load; (f) Tuning and matching; (g) Contact varactor facing parallel connection linkage; (h) Bulk-effect diode; (i) Radio frequency ground connection; (j) Radio frequency ground connection short piece; (k) To continuous flow deflection place; (l) To continuous flow deflection place; (m) Varactor piece; (n) Bulk-effect tube; (o) To radio frequency matching; (p) To radio frequency matching; (q) Varactor piece; (r) Bulk-effect tube; (s) To tuning directive; (t) To tuning directive; (u) Parallel connection tuning; (v) Contact tuning

of 0.2 microhenries. If we use distributed form elements, even if the medium place $\epsilon=9.5$, then the $\lambda/4$ long transmission line length still must be 7.5mm long. The side circuit capacitance where capacity is 10 picafarads is only a small piece that is 0.125mm thick and 1mm^2 . The inductance coil uses a fixed leadwire, the precision tuning capacitance is only 0.75mm^2 . Using these super small type lumped parameter elements we can construct the Olapp circuit line of the S band. Its circuit line is shown in Fig. 7.20. The transistor that the circuit uses is model NE22000 dual model transistor. The varactor that is used is an ultra-sudden change junction silicon varactor. Its tuning voltage alone is 2-10 volts, the tuning frequency range alone is 2.6-3.6 gigavolts, output power is $12\pm 1\text{dB}$ milliwatts. This circuit possesses fairly good tuning linearity (see Fig. 7.21), the maximum value of its deviated straight line is ± 10 megahertz, slight linearity is $\pm 10\%$ specified value, tuning sensitivity is 125 ± 25 megaHz/volt. Because its tuning voltage enters through the critical damped low channel circuit, and this low channel circuit possesses an extremely wide frequency and can go through tuning pulse where the lift time is 2 nanoseconds, therefore its high tuning speed reaches 500 megaHz/nanoseconds. And within 20 nanoseconds we can fix to ± 2 megaHz of the reference frequency at $t_R=1$. The maximum post-tuning drift in 1 microsecond to 10 seconds is ± 500 megaHz.

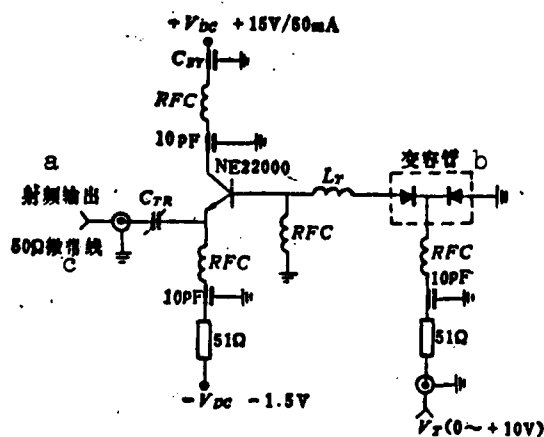


FIG. 7.20 S WAVEBAND VARACTOR TUNING OSCILLATOR THAT USES LUMPED ELEMENTS
KEY: (a) Radio frequency output; (b) Varactor; (c) Microband line

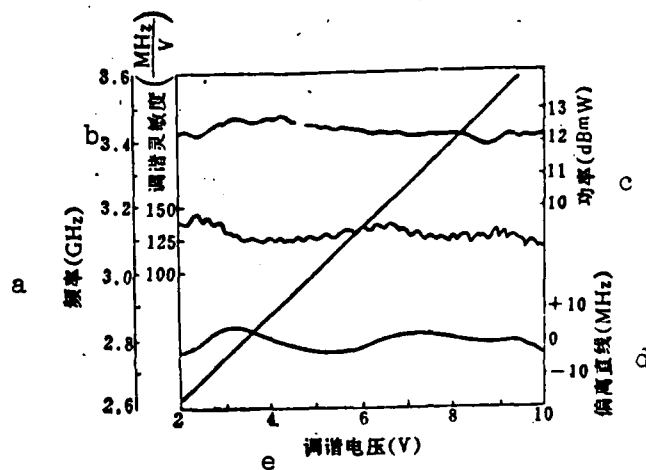


FIG. 7.21 TUNING PROPERTIES OF LUMPED ELEMENT OSCILLATORS
KEY: (a) Frequency; (b) Tuning sensitivity; (c) Power; (d) Deviated straight line; (e) Tuning voltage

7.3.3 VOLTAGE TUNING OSCILLATOR AS AN AGILE LOCAL OSCILLATOR

As discussed above, only the voltage control oscillator of varactor tuning has satisfactory tuning speed and can satisfy the requirements of frequency agile local oscillators. However, as a frequency agile local oscillator there are still other requirements, if we do not pay attention to and adopt different measures, these requirements are relatively difficult to satisfy. In the following section we will respectively discuss them in detail.

(1) The Problem of Tuning Linearity

At present the most commonly used varactor tuning voltage control oscillator uses a contact tuning circuit, its simplified equivalent circuit is shown in Fig. 7.22. In the figure the contact with varactor equivalent as R , L , and C , and the sealed unit capacitance and stray capacitance with varactor and bulk-effect diodes, the total capacitance C_T for equivalence. The tuning frequency of this circuit (also its oscillator frequency) can be expressed by the following formula:

$$f_0 = \frac{1}{2\pi} \left(\frac{C_0 + C_i}{C_0 C_i L} \right)^{-\frac{1}{2}} \quad (7.6)$$

So long as it replaces formula (7.3), we then can obtain the relationship of the oscillator frequency and the additional voltage. Actually, this relationship is somewhat complicated, because the equivalent capacitance of the varactor is related to the mean radio frequency voltage that is extended to it, the higher the radio frequency, the larger the equivalent capacitance.

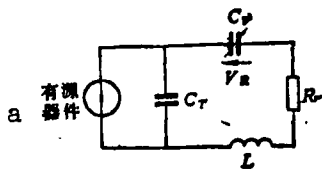


FIG. 7.22 CONTACT TUNING EQUIVALENT CIRCUIT
KEY: (a) Active components

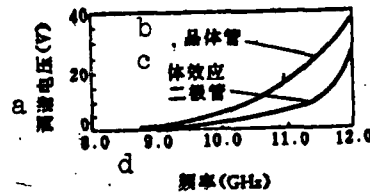


FIG. 7.23 TUNING PROPERTIES OF VARACTOR TUNING TRANSISTOR MULTIPLE FREQUENCY OSCILLATOR AND DIODE OSCILLATOR
KEY: (a) Tuning voltage; (b) Transistor; (c) Bulk-effect diode; (d) Frequency

Figure 7.23 gives the tuning characteristics of varactor tuning transistor multiple frequency oscillator and bulk-effect diode oscillator in 8-12GHz⁽³⁾. By the figure we can see that in order to make the voltage range required by the tuning transistor multiple frequency oscillator it must be somewhat wider, as a result the tuning curve slope variation of the bulk-effect diode oscillator then must be even wider. This is because the typical value of the input capacity of an X waveband transistor is approximately one picafarad, and the bulk-effect diode of the same waveband is 0.3 picafarad. Therefore, in order to tune the same bandwidth, the varactor that the bulk-effect diode oscillator uses must possess minimal capacitance (in high end of the frequency band, its capacity is only approximately 0.1 picafarad), therefore the influence of parasitic capacitance is even somewhat bigger. This is also the reason why the tuning curve slope variations of the bulk-effect diode oscillator are fairly large. The tuning curve variations of the common

wideband transistor oscillator are approximately 5:1 to 7:1 and the tuning curve slope variation of the wideband (as low as multiple frequency level) bulk-effect diode oscillator reaches a high of 20:1.

Aside from the variations of tuning sensitivity, the tuning curve also has slight variations. These variations are due to the influence of load resistance on the oscillator tuning capacitance, and are caused by parasitic oscillation in the radio frequency section. The smooth curve of the deviation theory at the low frequency end of the tuning curve is even more important, this is because the circuit in this frequency range has load Q value due to the reduction and decrease of varactor Q value, as a result it is even more sensitive to the load and parasitic effect.

The amplitude of these variations hinge on the influence of a series of factors, for example, the power output that is needed, the isolation rate of the load, the standing wave ratio of the load, and the percentage of the tuning bandwidth. Operating on the oscillator with a waveband as high as S, within the interval of 200-300 megaHz of the tuning curve, its slope variations can reach 2:1 or 3:1. Figure 7.24(1) gives the curves of the precision tuning sensitivity of the varactor tuning transistor oscillator and bulk-effect diode oscillator. It is relatively easy to achieve the most precise on the narrow band oscillator, consequently only minimal precision tuning variations emerge (as Fig. 7.24(2) shows).

Regarding frequency agile local oscillator, its corresponding bandwidth is not too wide, consequently the slight variations of sensitivity can be overlooked, but its coarse tuning variations are still correspondingly large, and must be revised and corrected. Figure 7.25 gives the tuning sensitivity variation curves of the two varactor tuning voltage control oscillators that act as agile local oscillators⁽¹⁾. By the figure we can see that the tuning sensitivity variations of the varactor tuning transistor oscillator (its later double frequency level) are only approximately 2:1, but the sensitivity variations of

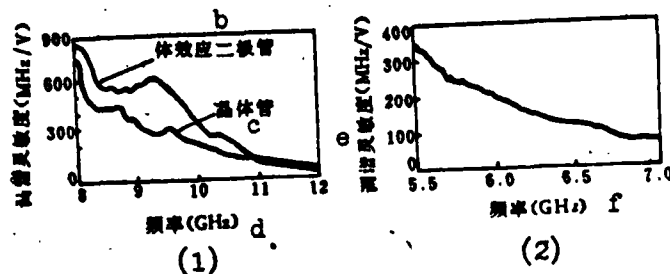


FIG. 7.24 VARIATIONS OF TUNING SENSITIVITY
 (1) Variations of Precision Tuning Sensitivity of Wideband Transistor Oscillator and Bulk-Effect Diode Oscillator (2) Variations of Tuning Sensitivity of Narrowband Transistor Oscillator
 KEY: (a) Tuning sensitivity; (b) Bulk-effect diode; (c) transistor; (d) Frequency; (e) Tuning sensitivity; (f) Frequency.

the varactor tuning bulk-effect diode oscillator still are more than 5:1. Therefore even if under corresponding narrow frequency band conditions its tuning linearity still cannot satisfy the requirements, and must be revised and corrected.

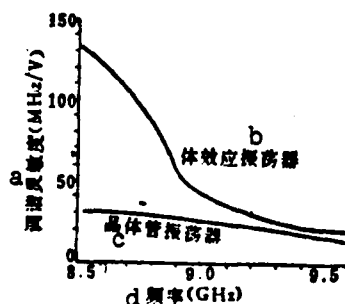


FIG. 7.25 TUNING SENSITIVITY CURVES OF TWO VARACTOR TUNING OSCILLATORS
 KEY: (a) Tuning sensitivity; (b) Bulk-effect oscillator; (c) Transistor oscillator; (d) Frequency

In order to obtain linear tuning properties, we must take a linearized device to the input tuning voltage (a), the linearized device possesses a variable gain amplifier, under different input voltage conditions it possesses different gains (generally restricted gains), making its input voltage exactly right and tuning properties

consistent. Figure 7.26 (a) draws out similar output voltage of the partial broken line. The similar output voltage of this broken line can be obtained by the variable gain amplifier of the TR switch (Fig. 7.26(b)), the control voltage of each transistor is obtained by output voltage feedback, when feedback voltage is equal to its fixed voltage E_{SP1} (thus the corresponding voltage of the first turning point), the first transistor Q_1 leads, with resistance R_3 receiving circuit, to make the gains of the operational amplifier change from the original $(R_1/R_2 + 1)$ into:

$$E_o/E_i = \frac{R_1(R_2 + R_3)}{R_2 R_3} + 1 \quad (7.7)$$

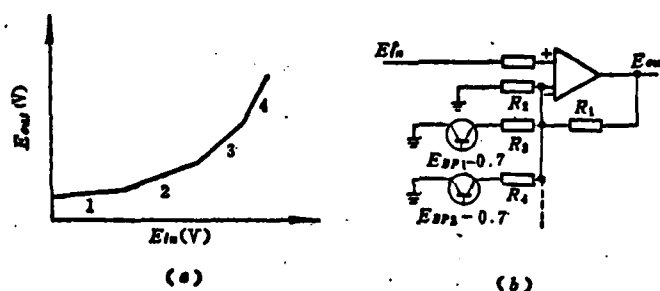


FIG. 7.26 SIMILAR LINEAR TUNING PROPERTIES
(a) BROKEN LINE SIMILAR OUTPUT VOLTAGE
(b) DIAGRAM OF FUNDAMENTALS OF VARIABLE GAIN AMPLIFIER

Following the increase of output voltage, in the feedback circuit of the operational amplifier that has more and more resistance receiving, this obtains the input-output voltage properties that are required.

In order to make the linearized device easy to design, it is desirable to use a high voltage varactor. The requirements of this and the requirements of the bulk-effect oscillator are alike. The non-linearity of the tuning curve of the oscillator must possess repeatability of production, for the convenience of the designing and adjusting of the linearizer. The design of the linearizer can use computer supplementary techniques, entering the original tuning curve data point and the expected rectilinearity into the computer, the computer can compute the required resistance value. Using resistance with precision as 1%, we then can

obtain linearity within (1-2)%, and using precision tuning resistance we can obtain even better linearity. After present varactor tuning oscillators add linearizers with meticulous design, we can obtain tuning linearity that reaches as high as $\pm 0.5\%$. Although they are still a level poorer than YIG tuned oscillators, they already can satisfy the requirements of the frequency agile local oscillator. Figure 7.27 gives the tuning sensitivity curves of the above transistor oscillators after adding a linearizer⁽¹⁾.

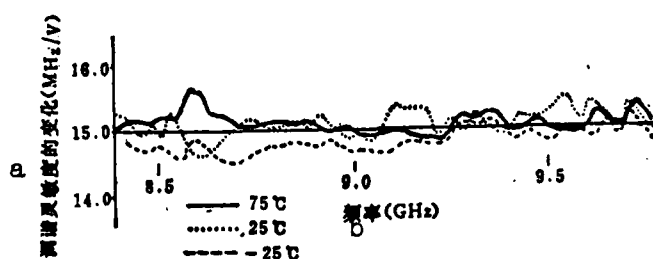


FIG. 7.27 TUNING SENSITIVITY OF TRANSISTOR OSCILLATORS AFTER LINEARIZATION
KEY: (a) Variations of tuning sensitivity;
(b) Frequency

(2) Fixed Time of Tuning

The tuning rate of voltage tuning oscillators is still not too capable of being used to explain its high speed tuning ability, this ability is best expressed by fixed time of tuning. The so-called fixed time of tuning refers to the oscillator jumping the assigned frequency band (generally a full frequency band) and entering into the required time in the range of error of assigned frequency stipulation. This can be illustrated in Fig. 7.28. By the coupling circuit and the influence of the lead wire inductance, when input is a step voltage, the instant change properties of its oscillator frequency possibly are not the monotonic increasing functions of the time, but have small oscillation close to the final frequency. The tuning rate thus generally refers to the largest slope of the instant-change properties. Obviously, this fixed time must be greater than the time that is determined by the tuning rate.

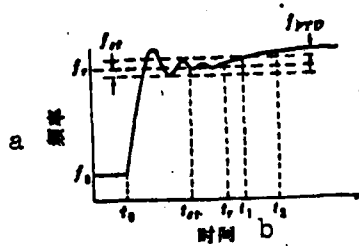


FIG. 7.28 INSTANT CHANGE PROPERTIES
OF VOLTAGE TUNING
KEY: (a) Frequency; (b) Time

Varactor oscillator fixed time primarily receives the limitations of the linearizer and drive circuit bandwidth. For the purpose of simplification, presuming linearizer can be expressed by a simple low pass network, its output voltage will receive index pattern lift:

$$V_t = V(1 - e^{-t/\tau_c}) \quad (7.8)$$

In which τ_c is circuit time constant.

Time $t_{0.01}$ that is required within 0.01% of V_0 reaching its final value is $9.2\tau_c$. From 10% raise to 90% raise time t_r is equal to $2.2\tau_c$. The relationship between circuit lift time t_r and its frequency bandwidth f_s is:

$$t_r = \frac{0.35}{f_s} \quad (7.9)$$

$$\text{or} \quad f_s = 0.16/\tau_c = 1.45/t_r \quad (7.10)$$

If there is a varactor tuning voltage control oscillator, its tuning range is 8-12GHz, required tuning voltage is 50 volts, and requires fixing to within the range of ± 1 megaHz of 12GHz with 1 microsecond. Namely, it requires the output of the linearizer and driver within 1 microsecond to scan within 50 ± 0.005 ($\pm 0.01\%$) volts. We can compute the circuit time constant as 0.11 microseconds. By expression (7.10) we can compute that this circuit should possess a 3 decibel bandwidth of 1.45 megaHz.

The scanning speed of the driver also is a fairly important index, it not only must have sufficiently quick lift time but also it must

have sufficiently large output voltage. Therefore its scanning speed is defined as the ratio of the 10% to 90% output voltage and lift time, thus:

$$S = dv/dt$$

In the above example:

$$S = 40V/0.24\mu s = 166V/\mu s$$

The primary factor of the limited varactor tuning oscillator fixed time is the linearized circuit. The present level is, after full frequency band jump variations, fixed to the time within the 0.02% range of the final value in approximately 1 microsecond. This kind of fixed time already can completely satisfy the requirements of the frequency agile local oscillator.

(3) Post-tuning Drift (PTD)

Another very important property of the voltage tuning oscillator is post-tuning to a newly assigned frequency, stabilizing the ability of this new frequency. In the frequency agile local oscillator, this is generally explained by PTD. It is defined as the largest deviation between the oscillator output frequency and the frequency that time t_1 measures, measuring the time of this frequency deviation ends on t_2 (see Fig. 7.28), actually it also refers to the largest deviation frequency that is measured with the stipulated time intervals $t_1 \sim t_2$. Regarding frequency agile oscillator, obviously in the receiving time (thus within the repetition period of the pulse) its frequency deviation should be as small as the central release bandwidth, when this deviation is equal to or greater than the central release bandwidth, then the sensitivity of the corresponding receiver greatly decreases, when it is severe it goes so far as to have no way to receive the backward-wave signal. Because the frequency agile local oscillator automatic frequency control system adjusts one time for the repeated period of each pulse, therefore there is no influence of the long period PTD on it. The following will emphasize discussion on short period (several microseconds to several milliseconds) PTD.

Actual measurement tests indicate that the post-tuning drift (PTD) of varactor tuning voltage control oscillators not only is related to the type of oscillator, but also is related to the amplitude and direction of frequency jump change. Figure 7.29 gives the actual measurement results of the PTD of varactor tuning transistor oscillators and bulk-effect diode oscillators⁽¹⁾. The varactor that is used is an unpurified silicon varactor. By the figure we can see that within 3-300 microseconds after adding tuning directive, the PTD of the varactor tuning transistor oscillator is within a range of ± 500 kHz, this generally can satisfy the requirements for an agile oscillator: the varactor tuning bulk-effect diode oscillator then possesses approximately ± 1 MHz PTD (if the range of the frequency jump change is the same, it actually still does not stop this value). Although these two oscillators possess PTD of different directions, however when it is the same jump change direction, the PTD of the two reverse signals. By the figure we can see that when the background temperature is fairly low there is a relatively large PTD.

The factors that produce short period PTD are many, the most primary are the heat effect of the radio frequency, the charge of the varactor, and the heat effect of the linearizer.

The so-called heat effect of radio frequency refers to when the operational frequency jump changes, because the efficiency of different frequency times is different, its power consumption is different and the temperature rise that is caused has two different effects. Because heat balance possesses specified time constants, therefore the frequency drift that is caused by the frequency temperature system also has a specified time constant. Although the heat time constants of active components of the microwave are in the 1-100 microsecond magnitude, due to the heat capacitance of the radiator and other factors it can cause the time constant that reaches heat balance to markedly increase.

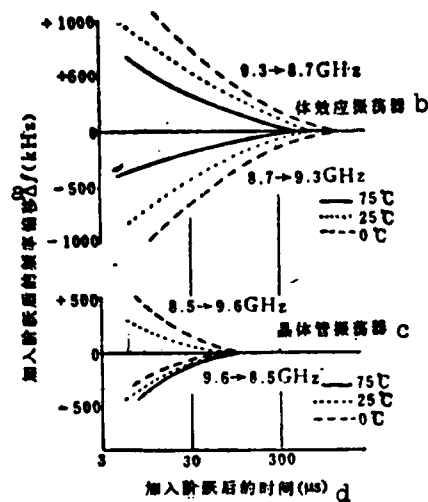


FIG. 7.29 POST-TUNING DRIFT
OF VARACTOR TUNING OSCILLATOR
KEY: (a) Frequency deviation
after adding step; (b) Bulk-
effect oscillator; (c) Transis-
tor oscillator; (d) Time after
adding step

There are many active components that cause oscillator frequency variations by temperature variations, but the most primary one among them is the varactor. If the frequency changes from f_{\max} to f_{\min} , the power consumption of the varactor increases to Δp , and the junction temperature of the active components raises to ΔT_j :

$$\Delta T_j = R_j \cdot \Delta p \quad (7.11)$$

In which R_j is the heat resistance in the junction to the radiator surface, expressed by $^{\circ}\text{C}/\text{W}$. Because the medium power constant of the contact power potential and semiconductor material follows the temperature change, therefore the capacitance of the varactor possesses a specified temperature coefficient. This temperature coefficient is the function that adds reverse voltage (see Fig. 7.30). The capacitance variations that are caused on the given temperature variations depend on the capacitance temperature coefficient on the operational frequency.

If an active component can be equivalent to capacitance C_T and negative resistance contact, then the contact after this active compo-

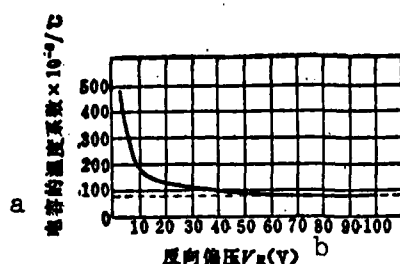


FIG. 7.30 VARACTOR CAPACITANCE
TEMPERATURE COEFFICIENT
KEY: (a) Capacitance temperature
coefficient; (b) Reverse bias voltage

nent and varactor parallel connection is equivalent to the oscillator frequency of the circuit, the frequency sensitivity that is caused by the varactor capacitance variations is:

$$\frac{df}{dC_i(V)} = -\frac{f_0}{2C} \left[\frac{C_i'}{C_i' + C_i(V)} \right]^2 \quad (7.12)$$

In which C is the contact of C_i' and $C_i(V)$.

It is thus evident that we can obtain the frequency drift that is caused by varactor power consumption variations as:

$$f = \frac{df}{dC_i(V)} \cdot \frac{dC_i(V)}{dT} \cdot R_s \cdot \Delta p. \quad (7.13)$$

By this we can see that in order to reduce post-tuning drift (PTD) it is necessary to fully reduce power consumption. Variations in the tuning range reduce the heat resistance between the varactor and active components and the radiator, and reduce the varactor capacitance temperature coefficient and enlarge total capacitance.

When its frequency changes from low to high, varactor power consumption reduces, and its temperature reduces. To make its temperature stable on the original value, we can use a heater. This one-time temperature installation is necessary to make the oscillator operate in a very wide temperature range. The time constant of the constant temperature heater is shorter than the time constant of its natural radiation, therefore the time constant of the drift after jumping from the low end of

the frequency band to the high end of the frequency band must be shorter than the time constant of jumping from the high end to the low end.

There are two types of capacitor variations that are caused by the varactor surface electric charge: one type is short term, the other type is long term. The forms and mechanisms of the two are also different, the former is formed by the charge effect that is caused by exhaustion layer width variations; the latter thus is formed by the removal of impure ions and electrons that are caused by the voltage gradation of the pN junction boundary strength.

We can raise an example to explain the short term charge effect. If varactor voltage jump change is 20 volts, at this moment the exhaustion layer width that is caused increases to 1 micrometer, if the mesodiameter of the varactor junction is 300 micrometers, then the increased cylinder surface area is approximately $1.9 \times 10^{-5} \text{ cm}^2$. Assuming the surface electric charge number of the largest unit area that is allowed on this surface area is $2.3 \times 10^{10} / \text{cm}^2$, we can compute its increased electric charge rate as $7 \cdot 10^{-14}$ coulombs. The corresponding capacitance increase can be computed by $\Delta C = \Delta Q / V$, approximately equal to $1 \cdot 10^{-13}$ picafarads. Assuming total capacitance is 10 picafarads, and the operational frequency is 10GHz, then its corresponding frequency drift is:

$$\Delta f = -\frac{1}{2} \frac{\Delta C}{C} f_0 = -500 \text{ kHz}$$

It is thus evident that the post-tuning drift (PTD) that is caused by the charge effect is considerable, and only by meticulously choosing varactor material, designing its structure, and improving its technique will it then reduce.

Aside from this, poor short term stability by the power source voltage can also cause PTD. Because tuning voltage is the most sensitive, therefore the power source of the linearizer and driver must have fairly high short term stability (fairly small wave veins are primary). The heat effect of the linearizer also is a factor that must be considered.

(4) Frequency Readjustment (Restabilizing)

Frequency readjustment of the oscillator refers to when the original directive voltage is again newly added on after the arbitrary tuning "history", the oscillator has the ability to make this frequency reappear within the appointed error range. The frequency that reappears still must stipulate the directive to reach the last time interval, for example, after the arbitrary jump change returns to the original directive voltage, the frequency of 20 microseconds must be within 0.05 megaHz of the original frequency.

In the mechanically tuned oscillators, tuning restabilizing is primarily caused by mechanical transmission spare components of the tuning machinery and frequency plate. But in the voltage tuning oscillator, the problem of readjustment of the frequency is primarily caused by the heat effect of the varactor in the oscillator. Although the definition of readjustment is stipulated through arbitrary tuning "history", when the frequency jump changes of this different direction that jump from the low end of the frequency band to the medium end and jump from the high end of the frequency band to the medium end, conditions are fairly harsh. This can be seen in Fig. 7.31. The upper part of the figure gives the tuning directive voltage. Because when there are different frequencies the power consumption of the varactor is different, therefore its junction temperature also is different, the low end has fairly large power consumption, resulting in fairly high junction temperature. The high end is opposite. The middle section of the figure gives the junction temperature variations that correspond to the tuning voltage. The lower part of the figure is the influence of the oscillator output frequency. Because now we only consider conditions from low to middle and from high to middle, therefore we can assume that initially the oscillator is already stable in the low end of the frequency band, and after assuming this again there is fairly long term stability in the high end of the frequency band. In the response of the oscillator frequency there is one part primarily caused by the response of the circuit, and the other part caused by heat effect. We can consider that the initial phase is primarily electronic response, later it

is primarily heat response. In the figure t_1-t_2 and t_7-t_8 are the delay times caused by circuit phase shift, while t_2-t_3 and t_8-t_9 are the lift times determined by the circuit bandwidth. We can roughly consider that the varactor junction temperature then begins to vary from t_3 and t_9 , and also brings about post-tuning drift (PTD). If frequency adjustment time is fixed at t_4 and t_{10} , then at this moment corresponding frequency is f_1 and f_2 . The difference of these two frequencies is their readjustment. Obviously frequency readjustment and PTD alike are related to stop time.

(5) Oscillator Noise

Although the noise that is produced by the tuning voltage control oscillator is like that of other semiconductor microwave oscillators, because the Q value of the former is fairly low (generally lower than 10), therefore it has a fairly high noise level.

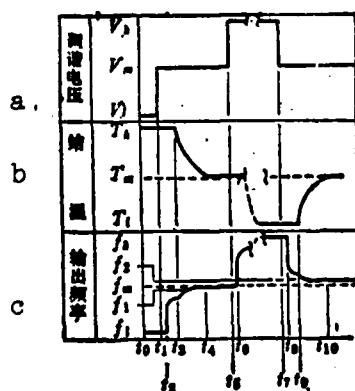


FIG. 7.31 FREQUENCY JUMP CHANGE
GOING DIFFERENT DIRECTIONS
KEY: (a) Tuning voltage; (b)
Junction temperature; (c) Output
frequency

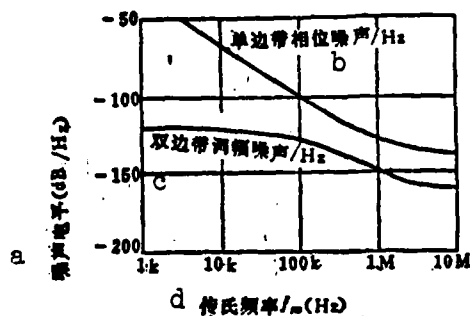


FIG. 7.32 NOISE OF S WAVEBAND
PRESSURE CONTROL OSCILLATOR
KEY: (a) Noise level; (b) Unilateral
band noise phase; (c) Bilateral band
amplitude modulation noise; (d)
Transmitted frequency

Two kinds of voltage control oscillator noise include amplitude modulation and frequency modulation (phase modulation), figure 7.32 gives the amplitude modulation and frequency modulation noise of a typical S waveband varactor oscillator, it is expressed in each hertz bandwidth below the decibel number of the carrier wave. The amplitude modulation noise in ion load frequency 30 megaHz is approximately -170 dB/Hz lower than the carrier wave. This kind of low amplitude modulation noise actually can be overlooked, but the frequency modulation noise in the ion load frequency 30 megaHz will have -140dB/Hz; this must be considered.

There are two areas influenced by the frequency modulation noise that is produced: one area is the increased receiver noise coefficient, the other is the decreased short term frequency stability.

By the oscillator going through leaked signals of the mixer, it will, due to the mismatching of the antenna, be reflected, and the long line will cause its effects such as the same frequency discriminator and will change frequency modulation noise into receiver noise. In order to reduce this effect, we should add an isolator between the antenna and the mixer, and at the same time we should also make the antenna feedline system match as much as possible.

Local oscillator frequency modulation noise in the moving target indication system can bring about the destruction of surplus. The

frequency modulation noise of the varactor tuning voltage control oscillator becomes large, and generally there is no way to satisfy the requirements of a high target moving target indication system.

7.4 LOCAL OSCILLATOR AUTOMATIC FREQUENCY CONTROL SYSTEM OF NON-COHERENT FREQUENCY AGILE RADAR

The automatic frequency control system of the local oscillator of the frequency agile radar receiver can be called one of the primary technological keys of noncoherent frequency agile radar. In this kind of radar, because the carrier frequency of the transmitting pulse is independent (thus is not interrelated with the local oscillator) it jump changes at high speed between the pulses. Therefore, the local oscillator of the receiver must be able to transmit the carrier frequency of the pulse on the track in a very short time to ensure the output in the mixer has a correct intermediate frequency, and later maintain stability in the interval that corresponds to the repetition of the pulse, so that the backward-wave signal is received. This requires the automatic frequency control system to have a very large adjustment range, very fast adjustment speed, very high adjustment precision, and very high post-adjustment stability (this will directly influence post-tuning drift). Final frequency tracking error and stability of the whole automatic frequency control system also determine the central release bandwidth that is needed. Exceedingly large frequency error force must require exceedingly large central release bandwidth, this also can increase receiver noise and decrease message-noise ratio. When severe, it can even go so far as to cause advantageous total loss on the survey distance after using the frequency agile system. By this we can see the importance of the frequency automatic control system.

The automatic frequency control system of frequency agile radar has shared properties with automatic frequency control of common radar, and also has particular properties. Shared properties are that the object of the two is the same, they both ensure a correct intermediate frequency signal frequency to obtain the best receiving conditions.

The operational principles that they use also are similar. But its particular properties lie in the frequency agile radar, frequency jump change between the pulses can be from as high as ± 100 mega to giga hertz, thus the frequency range that is needed is extremely large. Moreover it is very difficult to obtain the next radio frequency information in advance. Even if it can be obtained it is often very rough. The providable tuning time is also very short, it can only be in the recovery period, and accurate error information can only be obtained in the time of pulse transmission. Therefore the providable precision adjusting time is even shorter, corresponding to the transmitting pulsewidth time, at most it can lengthen to the time that corresponds to the shortest effect distance, later it must maintain a high degree of stability. All these particular properties cause the specific achievement of the automatic frequency control system of frequency agile radar to meet with very great difficulties, and becomes one technological key that is comparatively hard to resolve.

7.4.1 MONOPULSE AUTOMATIC FREQUENCY CONTROL SYSTEM

Earlier, in the latter part of the 1950s, when the tuning speed of hydraulic pressure tuning magnetrons exceeded 10GHz/noise (the frequency difference in its adjacent pulse reached 10 megaHz or higher), the problem of monopulse frequency automatic control was already raised.

So-called monopulse automatic frequency control refers to the entire frequency tuning process that must be completed in the monopulse time. That is, it must, in this time, close the loop, measure its frequency error signal, take the control signal to the local oscillator to conduct revision, establish a steady state, and finally break open the adjustment loop. Therefore, the performance of this high speed monopulse automatic frequency control system primarily depends on the reduced degree of total delay time in the whole adjustment and feedback loop. The primary elements included in the whole loop are the local oscillator (backward-wave oscillator or other voltage control oscillator), mixer, amplifier, frequency discriminator, and storage capacitor.

Figure 7.33 is the block diagram of a monopulse automatic frequency control system.

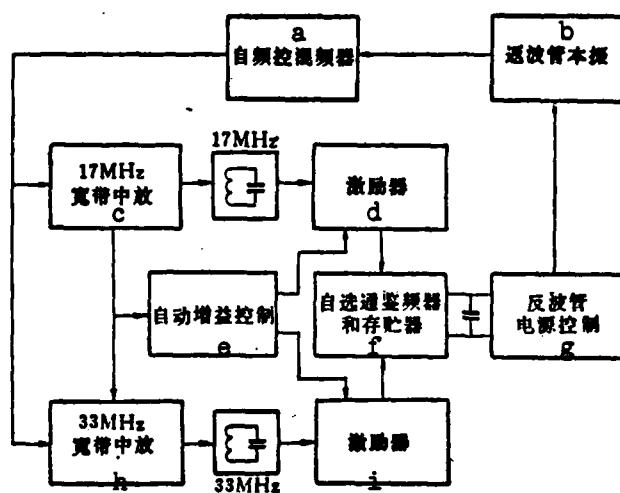


FIG. 7.33 BLOCK DIAGRAM OF HIGH SPEED MONOPULSE AUTOMATIC CONTROL SYSTEM
KEY: (a) Automatic frequency control mixer; (b) Backward-wave local oscillator; (c) Bandwidth central release; (d) Driver; (e) Automatic gain control; (f) Self-gated selection frequency discriminator and storage; (g) Backward-wave tube power source control; (h) Bandwidth central release; (i) Driver

Because the range of frequency error that this system can adjust to primarily depends on the bandwidth of the discriminator, in order to be able to adjust to the range as much as possible it requires sufficient bandwidth of the power release and discriminator. If the two peak intervals of the discriminator are 15MHz, the bandwidth of the central release will hopefully be 20MHz, in order to avoid influencing the symmetry of the frequency discriminator properties. This wide a bandwidth generally can be obtained by using triple parameter difference tuning. Also the intermediate frequency can be divided into two passages. For example, when intermediate frequency is 25MHz, it can tune in 17MHz with a broadband central release, and tune another in 33MHz (see Fig. 7.33). Because the broadband central release has a very low equivalent Q value, therefore its delay time can be made very small.

In this example there is only 0.016 microseconds, and can be overlooked.

The linkage after the broadband amplifier takes the central frequencies respectively as narrow band resonators of 17MHz and 33MHz, the frequency band of this resonator is somewhat narrow in order to form the required frequency discrimination properties, consequently its time constant is rather large. Here there is approximately 0.023 microseconds, and can be overlooked. In a common automatic frequency control system, its delay time is primarily determined by the video frequency detection in the discriminator. In order to fully reduce this delay time, here we use a particular frequency discriminator circuit (See Fig. 7.34), to make its intermediate frequency pulse go directly through the diode to the storage capacitor charge. The drivetube that is used is a beam power pentode 6AN15 (a high frequency high power transistor can also be used instead), it operates on the second type. Because the diode is reverse linked, therefore its pure charge current corresponds to the differences of the response of two intermediate circuits. In order to make the capacitor able to be in a time below 0.1 microsecond it charges to the largest operational voltage of 0.5 volts. The value of the capacitor is chosen as 0.01 microfarads. The diode should also have inner resistance as small as possible (smaller than 10 ohms), at the same time it must have sufficiently large charge current. 6AN5 can give peak charge current of approximately 50 milli-amps mean value, this then ensures the requirement of high speed charging. In order to avoid the discharge of the capacitor in the period between the pulses, several volts reverse bias voltage E_b is added on the diode. The advantages of this self-gated frequency discriminator are that it does not need an additional fixed time pulse to readjust the storage, and the whole sustained time of the feedback return circuit in the transmitting pulse (moreover only in this time) is closed.

The linearity of the frequency discriminator also is a comparatively important problem. Discriminator properties usually use continuous wave determinants. But only when the Q value is extremely low the response of its continuous wave is close to the response on the pulse

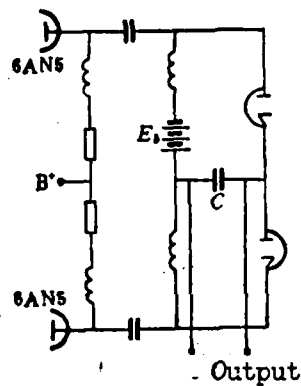


FIG. 7.34 DIAGRAM OF
CIRCUIT OF HIGH SPEED
SELF-GATED DISCRIMINATOR

wave. This can prove that theoretically the continuous wave response within the range of an entire discriminator can reach 2%, within the range of a fairly narrow one (70% bandwidth) can reach 1%. The Q value of a common discriminator tuning circuit is only about 2-3, therefore its continuous wave properties then are close to pulse properties.

Aside from this, the delay time that is created by the distributed capacitance of the wiring of the cable must also be given full attention. Under many conditions this is often overlooked, however this causes very great delay time. So long as we give it full attention, this delay time can then be reduced to a minimum.

Now we can research the entire operational process of the feedback loop of the automatic frequency control system. Its entire operational time can be divided as: closed instant change time, closing in time, setting up time, steady state time, and open instant change time (as Fig. 7.35 shows). If the central frequency of the initial value deviation discriminator of the intermediate frequency is ω_0 , after going through closed instant change time, closing in time, and setting up time after the loop closes it enters into a steady state, this steady state also remains as a fixed safety feature. When the transmitting pulse stops, the loop opens, there is an open instant change process, and finally it reaches its last frequency (the dashed line in Fig. 7.35

shows the influence on the opposite original error of the signal). Its final frequency is slightly different than the central frequency of the discriminator, this is because when the signal of the wideband amplifier stops, the amplifier has an intrinsic frequency attenuated oscillator. Its intrinsic frequency is not equal to the required intermediate frequency. Aside from this, because generally when the magnetron transmitting pulse stops, there is a fairly large frequency partial shift (this is caused by electron frequency shift), it also possibly can produce this final deviation. But because the system is already in a steady state before the pulse stops, therefore the final deviation generally is always in the same direction, consequently it need not be completely eliminated. We also can use the method of adjusting the central frequency of the frequency discriminator to revise and correct it.

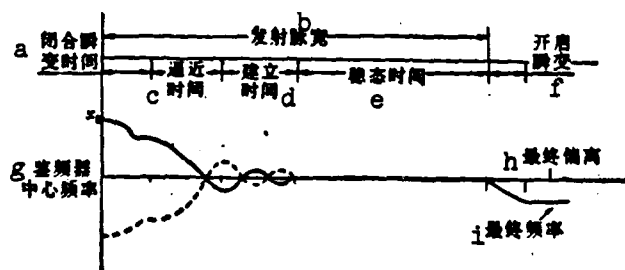


FIG. 7.35 OPERATIONAL PROCESS OF HIGH SPEED
AUTOMATIC FREQUENCY CONTROL SYSTEM
KEY: (a) Closed instant change time; (b)
Radio frequency pulsewidth; (c) Closing in
time; (d) Setting up time; (e) Steady state
time; (f) Open instant change time; (g)
Discriminator central frequency; (h) Final
deviation; (i) Final frequency

We will now first look at the closed instant change process, this instant change process is necessary to establish oscillation in the resonant return circuit. Aside from the oscillation of the additional signal frequency, in the return circuit we also have the attenuation process for free resonant frequency. The duration constant of its attenuation is $2Q/W_0$ (in these examples equal to 0.023 microseconds). The results by the differences of these instant-state sum and steady-state sum (additional signal frequency) make its net-like wrapping have an adjacent undulation. Because the entire loop is closed, therefore

the additional signal frequency actually is variable, and as a result this closed instant change process is very difficult to compute. We generally regard its required time as equal to the time constant of the return circuit of 5 times, approximately 0.113 microseconds.

The frequency modulation-amplitude modulation response of the frequency discriminator also can produce additional delay time, by analysis we can know that with the frequency discriminator equivalent to a low pass wave filter, its time constant can be equal to the time constant of the resonant return circuit (0.023 microseconds). Therefore, its response can be overlooked.

Lastly, what is primary is the closed circuit instant state response after the whole feedback loop closes. This can be analyzed and obtained by open loop transmit function $KG(p)$. We can draw the open loop transmit function in the analogue curve on plane p , and later find the limit of its closed loop transmit function. The attenuation that emerges on $G(p)$ from the latter is equal to the place where gains and phase are $\pm 180^\circ$ or $\pm 540^\circ$. The root influence of its near-original point is comparatively large, by this we can find the instant change process of its attenuated oscillator. When gains are fairly large, the attenuated instant change process is relatively long, moreover it can produce self-excited oscillation. But gains also cannot be too small, because very small gains have no way to obtain the required limit properties. By detailed analysis of the example that was raised, we can know that when gains are 100, they can obtain the approaching time of 0.2 microseconds and the transcending modulation rate of 40%. If we use contact and inner feedback compensation we then can reduce its transcending modulation rate. The setting up time of the whole system depends on the degree of the transcending modulation rate, the largest peak value then can lengthen its setting up time.

The unit that is constructed last can normally operate under conditions of transmitting pulsewidth going to 0.8 microseconds. This corresponds to only having 20 intermediate frequency sine waves. When

frequency deviation of the input reaches $\pm 7\text{MHz}$, we can revise and correct in a range of up to $\pm 50\text{kHz}$. It can then reduce to $1/140$ with frequency error in the time that does not reach 1 microsecond. This satisfies applicable requirements under most conditions.

The primary weakness of this system is that frequency error of the input signal cannot surpass the frequency range of the frequency discriminator, this is not realized on any frequency preset or coarse tuned frequency agile radar.

7.4.2 PULSE CONTROL FREQUENCY LOCKED SYSTEMS THAT DO NOT USE FREQUENCY DISCRIMINATORS

Because even if discussing vibrational tuning step frequency radar, its input frequency errors also can often surpass the frequency discriminating range of the frequency discriminator, therefore it is not sufficient to use only the monopulse high speed automatic frequency control system.

Here we explain a pulse control frequency locked system that does not use a frequency discriminator⁽¹²⁾. In this system, because it does not use a frequency discriminator, therefore its input frequency error range does not receive the limits of frequency discriminator properties. Its operational principle is: on the forward edge of each transmitting pulse, the electronically tunable local oscillator high speed scanning frequency is started, its scanning frequency speed is extremely high, sufficient within the transmitting pulsewidth it then scans the frequency band that occupies the completed transmitted pulse carrier frequency. Once it scans to the correct local oscillator frequency, in the central release a tip pulse is produced, this pulse instantly breaks off the scanning frequency of the local oscillator, and with its frequency locked at this correct value, goes directly to an initial cycle.

The frame drawing of the whole system is shown in Fig. 7.36. The principles of the electronics that correspond to it are shown in Fig.

7.37. Voltage tunable local oscillation K_1 (what is here is the reflection speed modulation tube) by continuous flow current feedback, local oscillator signal through wave guide system 12 couples to mixer 7, jump frequency magnetron (what is used here is a vibrational tuning model) K_2 will transmit a pulse and couple to antenna 6 through coupler 11 to transmit; at the same time part of the energy also goes to mixer 7 and local oscillator signal mixed frequency. The structure of wave guide 13 and coupler 12 makes the transmitting signal able to couple to mixer 7 through the wave guide system; the backward-wave signal has no way to go to mixer 7. The output of the mixer goes to central release 8, central release output thus even goes to the trigger that is formed by V_{42} and V_{52} . This trigger is used to stop halfway at capacity C. The voltage on charge capacity C is mutually contacted through cathode output device V_{22} and power source 5.

When the magnetron transmits a pulse, trigger pulse A that is formed by the forward edge of this pulse divides into two circuits going to this system. One circuit is used to make the trigger reduce, then it makes V_{42} conduct, and as a result it makes V_{32} stop, and consequently does not influence the charge of capacitance C. The other circuit is used to make V_{12} instantaneously conduct, thereby causing capacitance C to discharge at high speed through V_{12} . This way, on the forward edge of each transmitting pulse, the voltage in capacitance C is discharges close with electric potential, at this moment the reflected extreme voltage of the tunable local oscillator is determined by continuous flow power source 5. At this moment the operational frequency that corresponds to the klystron is at the lowest value. After the trigger pulse A that mutually coincides with the transmitted pulse forward edge goes over, capacitor C then goes through R_2 , R_1 , and diode V_5 to charge at high speed by a positive power source, at this moment the local oscillator frequency also frequency scans upward at high speed. Its frequency scanning speed must be sufficiently high to ensure that it scans the possible frequency range of the transmitting pulse carrier frequency within the time of a transmitting pulsewidth. This way, once local oscillator frequency scans to a correct value, and has an intermediate frequency value lower than

this transmitting pulse, the central release after the mixer has a small peak signal to cause the trigger to run. Namely, V_{52} and V_{42} stop. No current circulates on R_6 , the end of R_7 draws near to the electric potential and causes V_{32} to conduct so long as we suitably select the R_2 value, we then can cause capacitor C not to charge again when V_{32} is conducting. Furthermore, due to the reverse bias unit of diode V_5 it causes it to also have no possibility to charge. This keeps the voltage in C to be invariant, thereby causing local oscillator frequency to break off frequency scanning and maintain a correct frequency.

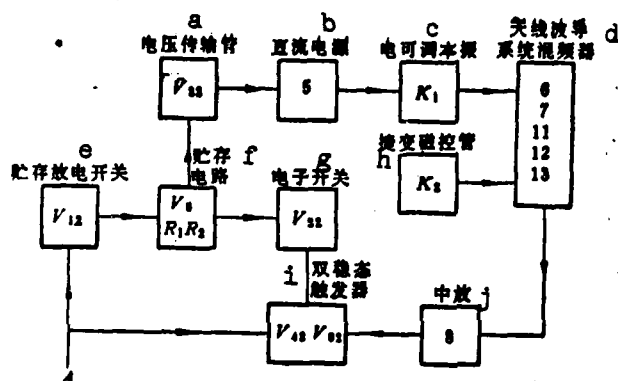


FIG. 7.36 BLOCK DIAGRAM OF PULSE CONTROL FREQUENCY LOCK SYSTEM

KEY: (a) Voltage transmission tube; (b) Continuous flow power source; (c) Electronically tunable local oscillator; (d) Antenna wave guide system mixer; (e) Storage discharge switch; (f) Storage circuit; (g) Electronic switch; (h) Agile magnetron; (i) Dual steady-state trigger; (j) Central release

In this system we use a reflection klystron as a voltage tunable local oscillator. But as everyone knows, the frequency range of the electron tuning of the reflection klystron is very narrow (generally only some 10MHz), moreover its output power also has very large undulation following frequency. If we use the backward-wave tube we then can have very great improvements, not only can the frequency scanning range be wider, but also its output power can be comparatively steady. After changing to using the backward-wave tube to

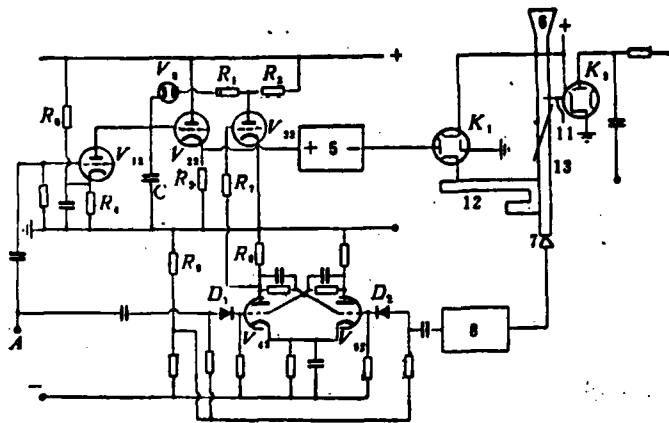


FIG. 7.37 DIAGRAM OF ELECTRONIC PRINCIPLES
OF PULSE CONTROL FREQUENCY LOCK SYSTEM

make a local oscillator, the operational principles of the whole system still are invariant, aside from the power source feedback its remaining parts can basically be invariable.

The primary advantages of this system are that it is simple and does not need to use a complicated trigger, and that its locking range does not receive the limits of the frequency discriminator properties. Moreover, because the local oscillator enters the locked state from the searching state everytime, therefore it can have a fairly wide range of searching and still be unlikely to erroneously lock in a mirror image frequency.

However, its frequency range that can search actually receives the limits of the transmitting pulse. Due to the exceedingly high frequency scanning speed it can cause the tip pulse amplitude of the central release output to reduce and moreover due to the delay time between each trigger level it causes the last locked frequency error to greatly increase. Therefore this system also can only be suitable to the vibrational tuning magnetron, but is not suitable to extremely wide transmitting pulses of step frequency range or the extremely narrow frequency agile radar.

To sum up, the major advantage of this system is its simplicity, and its major weakness is that frequency error is fairly large.

7.4.3 AUTOMATIC FREQUENCY CONTROL SYSTEM OF THE LOCAL OSCILLATOR WITHOUT FREQUENCY PRESET INFORMATION

In noncoherent frequency agile radar that uses rotational tuning, noise coil tuning, and circular tuning wideband jump frequency magnetrons, the frequency differences of the carrier frequency of its adjacent pulse can reach 100MHz. The problem of tracking of the local oscillator at this moment even more markedly stands out. Especially in early rotational frequency modulation (FM) jump frequency magnetrons, they often could not give the frequency readout sensor of local oscillator frequency preset information, this then causes the high speed frequency tracking of the local oscillator to become the primary technological key of jump frequency radar. Below we will explain the local oscillator automatic frequency control system of wideband jump frequency radar.

(1) Local Oscillator Automatic Frequency Tracking Radar of Automatic Detection and Tracking Magnetron Resonance

As accounted above, in early rotational tuning magnetrons, there often was no frequency sensor, and the carrier frequency differences of the adjacent pulse also often reached as high as some 100MHz. The problem of local oscillator frequency automatic tracking at this time then becomes a primary technological key.

By the previous analysis we can know that it must be in the pulsewidth of several microseconds to zero point several microseconds, to revise and correct the differences of some 100MHz frequency of a local oscillator is a completely impossible thing to do. The only method is to measure the "cold tuning frequency" of the magnetron resonance cavity before the radio frequency pulse, and take the frequency as local oscillator preset information. Local oscillator tuning will go up to a frequency that is extremely close to perfect (radio frequency pulse carrier frequency again increases intermediate frequency). Later, after pulse radio frequency, we again carry out high speed frequency automatic control based on actual transmitted pulse. This way it is possible to make the backward-wave signal that

is received fall within the central release bandwidth. Therefore the problem that must be resolved first is the measuring problem of the magnetron resonance cavity cold tuning frequency, and the problem of tracking this frequency in a small phase time interval before local oscillator frequency in the transmitting pulse. Below we will look at the local oscillator frequency automatic tracking system that directly uses a backward-wave tube local oscillator as a cold resonant frequency measuring message source of the magnetron resonant cavity.

The block diagram of the principles of this system is shown in Fig. 7.38⁽¹³⁾. The output of the voltage tunable oscillator that is formed by the backward-wave tube adds onto one arm of an iron oxide circulator, the second arm of the circulator links to the resonant cavity of the rotational tuning (or other type) jump frequency magnetron. The third arm of the circulator links to a microwave diode detector. This way, the output of the backward-wave tube local oscillator then goes to the resonant cavity of the jump frequency magnetron through the circulator. The reflected signal again goes from the resonant cavity through the circulator to the detector. The differences between the energy of its radio frequency and the local oscillator signal frequency and the resonant cavity tuning frequency are related. Assuming the frequency that the resonant cavity tunes to is f_0 and the local oscillator frequency is f_1 , then when the local oscillator frequency varies, amplitude of signal voltage V that is reflected by the resonant cavity will be as Fig. (a) in Fig. 7.39 shows. When the input signal frequency is equal to the resonant frequency of the resonant cavity, the resonant cavity then will "absorb" the energy of the input signal, and its reflected energy then will produce an extremely small value.

At this time, if we use a high frequency signal (for example its frequency is equal to a 4 megahertz wave), to carry out frequency modulation (FM) on the backward-wave tube through the driver, the frequency of the measured local oscillator is f_1 , for the FM of a 4MHz rate in f_1' and f_1'' . Thus the signal that is reflected by the resonant cavity will change into an amplitude frequency signal, the

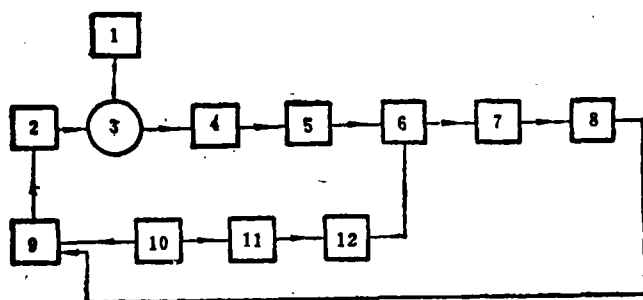


FIG. 7.38 AUTOMATIC FREQUENCY TRACKING SYSTEM THAT USES A BACKWARD-WAVE TUBE LOCAL OSCILLATOR TO DETECT AND TRACK THE RESONANCE FREQUENCY OF A ROTATIONAL TUNING MAGNETRON RESONANT CAVITY
KEY: (1) Rotational tuning magnetron; (2) Voltage tunable local oscillator; (3) Circulator; (4) Dissector; (5) Band pass amplifier; (6) Phase sensitive detector; (7) Integrator; (8) Amplifier; (9) Driver; (10) FM oscillator; (11) Shifter; (12) Amplifier

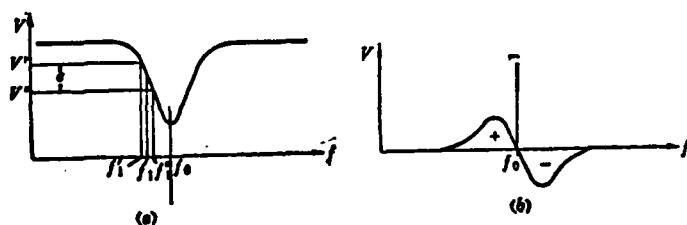


FIG. 7.39 (a) The Relationship Between Signal Voltage V that is Reflected by the Resonant Cavity and Input Signal Frequency (b) The Relationship Between the Amplitude of FM Signal of Detector Input and Its Intermediate Frequency

size of its amplitude frequency is shown in \bullet of Fig. 7.39(a). When the central oscillator of the local oscillator is close to the resonant frequency of the resonant cavity, its amplitude modulation (AM) also gradually reduces to zero. When local oscillator frequency continually rises, the phase shift of its AM turns 180 degrees, later the frequency modulation (FM) continues to increase. This way, the amplitude and phase shift of the exchange signal that the microwave detector puts out areas Fig. 7.39(b) shows. This output signal goes to a standard phase sensitive detector through a tuning after amplified 4MHz by a band pass amplifier. By the 4MHz signal that the FM

oscillator produces after going through a shifter and amplifier goes to a phase sensitive detector as a reference signal. The phase that is shifted by the shifter modulates to the produced phase shift that is equal to the frequency modulation (FM) signal after going through the whole loop (including the driver, local oscillator, circulator, resonator, circulator, amplitude detector, and amplifier). This makes the phase shift of the two signals completely balanced. This way, the output of the phase sensitive detector only reflects the amplitude variations and the phase tuning when the FM signal is reflected by the resonance cavity from this (as Fig. 7.39(b) shows). It takes the output of this phase sensitive detector to an RC integral circuit in order to filter out the alternating weight and guard against self-excitement of the whole system. The signal after the integral is then carried to a continuous flow amplifier, after amplification it returns to the driver circuit. This then constructs a closed loop. This closed loop can cause local oscillator frequency to modulate to equal with frequency f_0 of the resonance cavity. Because only when there is f_0 , the error voltage of the output of the phase sensitive detector can then equal zero. When local oscillator frequency is lower or higher than f_0 , there is error signal output, and furthermore the symbol is opposite. At this time, if resonant frequency of the resonance cavity produces variations due to the movement of the resonant mechanism, so long as the feedback system has ample bandwidth, local oscillator frequency can keep pace with these variations.

But in frequency agile radar, it is not merely required that local oscillator frequency can keep pace with the variations of the resonance frequency of jump frequency magnetrons, but is required to instantaneously keep pace with these variations before the pulse is transmitted, in the period that the pulse is transmitting it adjusts up to the correct frequency, after the pulse transmission ends it then keeps this frequency stable and invariant, so that the received backward-wave pulse directly goes to the beginning of a cycle repetition. Now we will take a look at how this local oscillator frequency tracking system is used in ^{non}coherent jump frequency radar. The block diagram of the principles of its entire system are as Fig. 7.40 shows.

bandwidth that this single steady-state trigger produces corresponds to the farthest backward-wave time, its wave form is shown in Fig. 7.41(a). The rear edge of the pulse that this single steady-state produces (time t_2) is used to trigger another dual steady-state trigger 22- its wave form is shown in Fig. 7.41(c)- and simultaneously causes gate 16 to open. After trigger 22 is turned around by the contact, it causes scanning integrator to begin scanning, the sawtooth wave that is produced (Fig. 7.41(d)) after going through the cathode output device, diodes D_3 and D_1 and gate 16, goes up to capacitor C. This then causes local oscillator to begin scanning from the lowest frequency on up. Its scanning frequency is used for the resonant frequency of the searching magnetron resonance cavity. Its frequency scans f_0 the same as the resonance cavity frequency, and an extremely low value then emerges from the output of the detector. After going through differential amplification, the extremely small value forms a trigger pulse, used to trigger dual steady-state triggers 21 and 22. The turning of the trigger 22 causes scanning differentiator to stop scanning, and also causes the oscillator to break away from the searching state. In order to make the local oscillator revolve into the tracking state to track the variations of the resonance frequency of the resonance cavity of the magnetron (its variations are as f_k in Fig. 7.41(f) shows) and for this trigger signal to make dual steady-state trigger 21 turn around (its wave form is shown in Fig. 7.41(b)), the latter then opens gate 26 and gate 27. The opening of gate 26 causes the 4MHz signal that the frequency modulation (FM) oscillator produces go to the driver, to make the local oscillator begin frequency scanning, and the opening of gate 27 then causes the error signals that are produced by the phase sensitive detector to be able to go through diodes D_2 and D_1 and gate 16 to capacitor C. The closing of this feedback loop then causes the local oscillator to begin tracking the frequency of the resonance cavity of the magnetron. The variation of local oscillator frequency with time is f_{osc} in Fig. 7.41(f). This tracking process directly continues to a trigger pulse until the time. At this moment, the turning of trigger 21 cause gates 26 and 27 to close, and also breaks off the FM signal to go to the driver and the error signal to go to capacitor C. This makes the voltage on capacitor C invariant at this time.

The wave form of point P_1 voltage of the voltage on C is shown by the solid line in Fig. 7.41(e), the wave form of point P_2 is shown by the dotted line, and the wave form of point P_3 is shown by the dot-dash line.. The wave form of P_1 also represents the variation of local oscillator frequency. After the pulse transmission, local oscillator frequency then maintains the frequency of an instantaneous resonance cavity before receiving the trigger in the magnetron. But it is necessary to note that in order to make the receiver able to correctly receive the backward-wave signal, it is necessary to make the difference of local oscillator frequency and transmitting pulse carrier frequency an intermediate frequency. In this system, although local oscillator frequency after the pulse is transmitted stays equal to the frequency of the triggered instantaneous resonance cavity of the magnetron, because the existence of the space electric charge makes the oscillator frequency of the magnetron not equal to the cold resonance frequency of the resonance cavity, therefore, the difference value of this "hot" resonance frequency and "cold" resonance frequency can be regarded as intermediate frequency in the receiver. Generally the "hot" frequency of the magnetron must be $\pm 10\text{MHz}$ lower than the "cold" frequency, its specific value is determined by the specific tube. Of course, even if we consider this frequency difference as an intermediate frequency is not very appropriate, we also can add a fixed voltage on point P_1 after the pulse transmits to revise and correct the local oscillator frequency to a fairly small value, thereby causing the frequency of the intermediate frequency to be equal to the expected value.

Although this system does not use the ordinary automatic frequency precision tuning system, it can also be a normal operation. This system has already been successfully applied in the earliest jump frequency radar of the Phillips Company of Sweden, and from this obtained many valuable results of jump frequency radar spot tests.

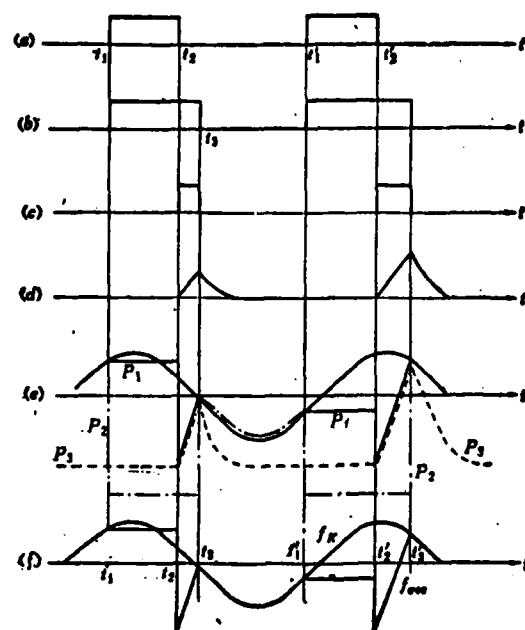


FIG. 7.41 RELATIONSHIP OF WAVE FORM
AND TIME OF EACH POINT IN FIG. 9.40

(2) Frequency Adjustment System of the Revised and Corrected
Magnetron "Cold" and "Hot" Frequency Difference Value
Variations

As is explained above, the intermediate frequency in the receiver that is obtained by using the above method is equal to the difference of the "cold" and "hot" frequency of the magnetron. But this difference value is not invariable. Not only is it related to the model number of the tube, but also makes tubes of the same model number different because of the specific tube, even the same tube is still variable in its operation time. With a fairly long time range it receives the influence of tube ageing, in a medium time it receives the influence and variation of temperature and power source voltage, in an extremely short time it is because the difference position of the operation of the magnetron on the tuning curve can also be different. This variation can cause variation of the intermediate frequency of mixed output, thereby making the signal-clutter ratio suffer loss. Therefore it is necessary to have a facility for revision and correction, to be able to revise and correct the variations of this

"cold" and "hot" frequency difference. The intermediate frequency after causing mixed frequency stays constant from beginning to end, to ensure good receiving properties. Its method is to measure the difference of the transmitting pulse carrier frequency and oscillator frequency, and find the difference of this difference value and predetermined intermediate frequency, using this last difference signal to revise and correct oscillator frequency, so that the frequency that is obtained after mixing is equal to the expected intermediate frequency. Actually, this is also a high speed monopulse control system. As was previously recounted, in this kind of automatic frequency control system where the band has a discriminator, its final frequency error depends on the size of local oscillator frequency error value that requires revising and correcting in a pulsewidth. The error that requires revision becomes large, its final frequency error also then becomes large. Because the magnetron's "cold" and "hot" frequency difference and the standard immediate frequency difference are comparatively large, the amount of revision and correction is comparatively large. Moreover, the speed of the variations of the "cold" and "hot" frequency difference value that is caused by tube ageing and heat effect is correspondingly slow. Therefore we can use a revision system, this revision system has a time constant fairly large low pass wave filter, it can measure and record the frequency that was obtained after many cycles (for example 100 cycles) of local oscillator frequency and transmitting pulse carrier frequency mixing and the mean value of the intermediate frequency difference that was expected. Later using an instantaneous period of this mean value before the transmitting pulse is produced we can conduct further revision and correction on local oscillator frequency to make the amount of revision and correction that needs to be done by the high speed monopulse automatic frequency control system reduce to a minimum. This way, the final error of its local oscillator frequency also then has the possibility to reduce to a minimum. Figure 7.42 is the block diagram of the principles of this automatic frequency adjustment system where the band has frequency correction and revision⁽¹⁴⁾.

The dot-dash line divides this block diagram into two main parts. The top right corner of one part has the radar equipment. It basic-

ally is similar to the block diagram of Fig. 7.40 in a small junction. For the purpose of simplification, we abbreviated the detection and tracking system on the cold resonance frequency of the magnetron (including the frequency modulation (FM) oscillator, phase sensitive detector, etc.) as the frequency tracker. The other top right corner has the automatic frequency adjustor, it is the new automatic frequency control and revision and correction system. Now we will take a look at the operational process of the entire system. Its entire operational process is shown in Fig. 7.43. In Fig. 7.43(a) the solid line sine wave that is marked by f_k is the "cold" resonance frequency of the magnetron, the dashed line sine wave that is marked by f_v is the "hot" resonant frequency of the magnetron, and the graduated jump change that is marked by f_0 is the voltage tunable local oscillator frequency. The instant time of the trigger pulse is noted by t_1 , t_1' , and t_1'' . After time t_1 of pulse transmission local oscillator frequency remains constant and stops at the farthest backward-wave time. Local oscillator frequency jumps to the highest frequency, this highest frequency still must be higher than the highest frequency that can be resonated by the jump frequency magnetron. Later it goes into a rapid rectilinear drop. When its frequency is equal to the "cold" resonance frequency of the magnetron, local oscillator frequency then locks in the cold resonance frequency of the magnetron and tracks its variations, it goes to an instant before the pulse is transmitted, local oscillator frequency then revises to a Δf_1 value by a slow automatic frequency adjusting pulse generator. This Δf_1 value is the mean value of many periods of the difference of local oscillator frequency and transmitting pulse carrier frequency and the expected intermediate frequency difference that are mentioned in the above section. Later, high speed revision and correction is carried out. This revision and correction is as Δf_2 in Fig. 7.43(b) shows, so that the final revision of the local oscillation frequency goes to an intermediate frequency f_m value with actual transmitting pulse carrier frequency differences. Actually, we can estimate that when Δf_1 is the mean value of the difference value of f_d and f_m of many periods, Δf_2 tends to be close to zero.

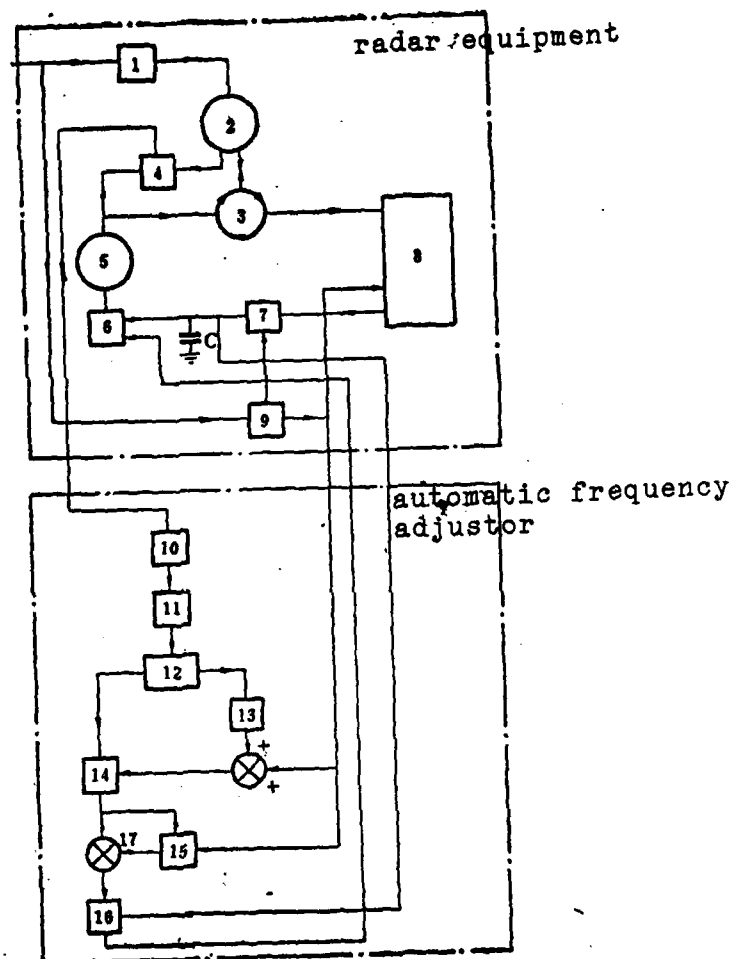


FIG. 7.42 BLOCK DIAGRAM OF AUTOMATIC FREQUENCY ADJUSTMENT SYSTEM WITH BAND FREQUENCY REVISION AND CORRECTION

KEY: (1) Modulator; (2) Frequency agile magnetron; (3) Circulator; (4) Mixer; (5) Tunable voltage local oscillator; (6) Local oscillator frequency control magnetron; (7) Gate; (8) Frequency tracker; (9) Backward-wave time single steady-state; (10) Central Release; (11) Limiter; (12) Discriminator; (13) Gated pulse generator; (14) Locked circuit; (15) Slow automatic frequency adjusting pulse generator; (16) Revision and correction device; (17) Phase increase device

We will now take a look at the operational principle of this automatic frequency adjustor. In Fig. 7.42, the intermediate frequency pulse goes to the central release by the mixer output to conduct amplification and after going through the limiter it is carried to

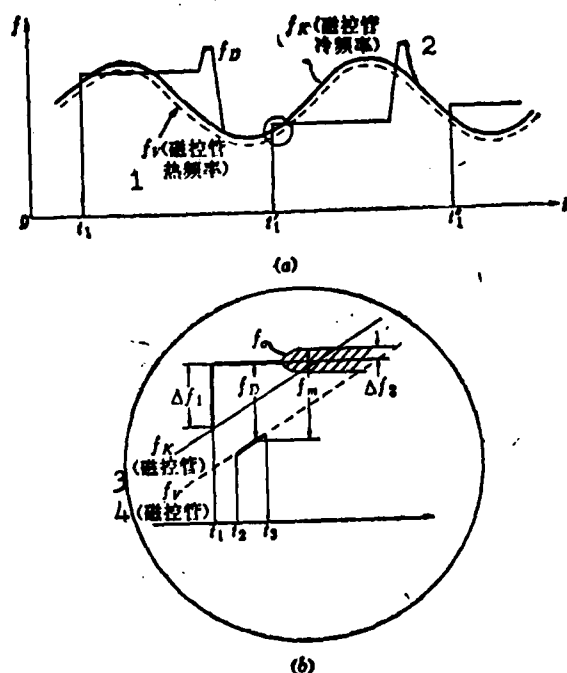


FIG. 7.43 OPERATIONAL PRINCIPLE OF
AUTOMATIC FREQUENCY ADJUSTOR
KEY: (1) Hot frequency of magnetron;
(2) Cold frequency of magnetron; (3)
Magnetron; (4) Magnetron

the discriminator for discrimination. The design of these parts must satisfy the requirements of high speed monopulse automatic frequency control. Due to the magnetron oscillator pulse, in both the beginning and the end there is a frequency traction process. The frequency difference of the central part of its frequency and pulse is a good several megas (as Fig. 7.44 shows). On top of that, in the high speed jump frequency magnetron, its resonance cavity within the pulse transmission period also is already tuned to a specified frequency range, and also can cause variations to occur in the oscillator carrier frequency in the pulse. Therefore, the central part of the discriminator output pulse will hopefully be taken as the standard of error signals. We can eliminate the frequency partial shift at the beginning and end of the pulse. In order to resolve this problem, the system uses a gated pulse generator, a phase adder, and a locked circuit. The amplitude from the output of this locked circuit is

equal to the voltage of the voltage pulse center point of discriminator output, the amplitude is thus equal to the revised voltage pulse of the time of the farthest backward-wave, actually it also is simply high speed revised and corrected voltage. P_{AFR} that corresponds with Δf_2 that was mentioned in the previous section (the detailed operational principles of this partial voltage will be expounded upon below). Two loops are divided out of the locked circuit output, one loop is carried to what is called a slow automatic frequency adjustment pulse generator; the other, after being carried to the phase adder device and the above-mentioned slow adjustment output phase adder is carried to the revision and correction device. In the slow automatic frequency adjusting pulse generator there is a time constant very large low pass detector, it takes the mean value on the large quantity of high speed revised voltage pulse from locked circuit output, and from this controls a width equal to the pulse of the backward-wave time, this voltage pulse actually is the slow revision and correction voltage pulse that corresponds with Δf_1 (the detailed operational principles of this partial voltage will also be discussed below). After this slow revised and corrected voltage pulse and the high speed revised and corrected voltage pulse from the locking device mix in the phase adder then are carried to the revision and correction device. The purpose of this device is to revise and correct the incontinuous linearity of the voltage tunable resonance of the local oscillator. The size of this amount of revision and correction depends on the specific position on the resonance properties, and also the specific frequency of the local oscillator. To this end, in the revision and correction device there is also voltage that comes from the local oscillator driver storage capacitor, to be used as a tolerance in the triggered instant oscillator frequency. This way, after going through the revision and correction device, the output can give the same size frequency jump change on the same input voltage pulsewidth in the resonance of the local oscillator with any frequency.

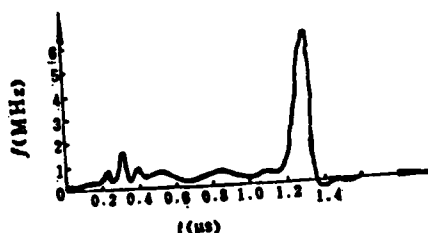


FIG. 7.44 VARIATIONS IN EACH PART OF THE PULSE OF THE CARRIER FREQUENCY OF THE MAGNETRON OSCILLATOR PULSE

Using this slow automatic frequency adjustment system is much better than adding a fixed amount of revision and correction before each trigger. The latter is an open loop control system, the former is a closed loop adjustable system. This closed loop is composed of the slow automatic frequency adjustment pulse generator, revision and correction device, local oscillator frequency control circuit, voltage tunable local oscillator, mixer, central release, limiter, discriminator, and locked circuit. Frequency revision Δf_1 that it produces is to make high speed frequency revision Δf_2 minimal. Actually, after going through many cycles, Δf_2 tends to be close to zero. This can cause local oscillator frequency revision and correction to go extremely close to the correct value (carrier frequency of pulse that was actually transmitted adds on to the intermediate frequency), and also can choose a central release bandwidth that is as narrow as possible to obtain a signal-noise ratio that is as high as possible.

Below we will discuss the specific voltage and operational principles of the locked circuit and the slow automatic frequency adjustment pulse generator. Figure 7.45 gives the principles of these two parts of voltage. The relationship and wave form of the time of each part of it is shown in Fig. 7.46. The voltage pulse that is produced by the discriminator is shown in Fig. 7.46(a). Its pulse-width is equal to the transmitted pulsewidth, in the figure it is 0.5 microseconds, but for the purpose of simplification the forward and rear edge peaks that are caused by the variations in the pulse are not drawn. The pulse from the discriminator output has dual polarity, its polarity hinges on the direction of frequency error. The single polarity you see from the discriminator output (Fig. 7.46(b)) is

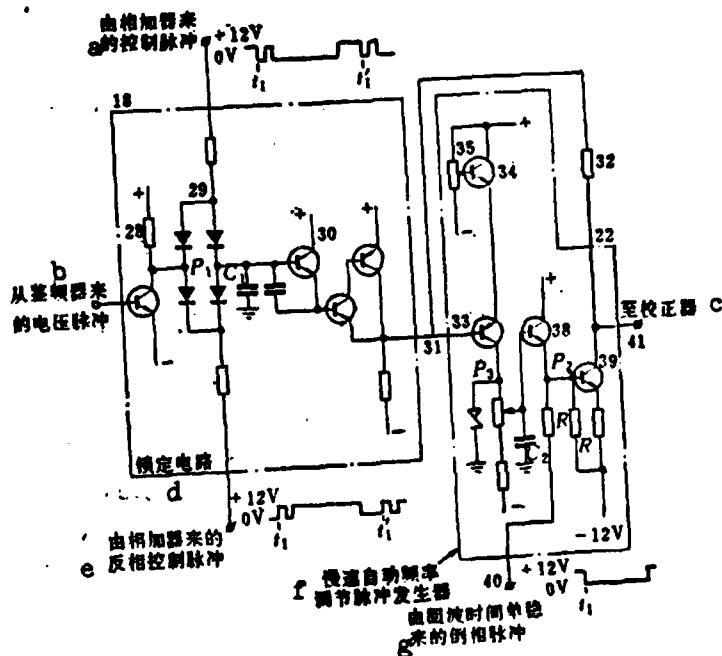


FIG. 7.45 DIAGRAM OF THE ELECTRONIC PRINCIPLES OF THE LOCKED CIRCUIT AND THE SLOW AUTOMATIC ADJUSTMENT PULSE GENERATOR

KEY: (a) Control pulse from phase adder; (b) Voltage pulse from discriminator; (c) to revision and correction device; (d) Locked circuit; (e) Opposite control pulse from phase adder; (f) Slow automatic frequency adjustment pulse generator; (g) Inverted pulse from backward time single steady-state

carried to the gated pulse generator. The width of gated pulse that is produced by the gated pulse generator (Fig. 7.46(c)) must be narrower than that of the discriminator, after the time it also is slightly stagnant, it then corresponds to the center part of the discriminator pulse. This gated pulse goes to the opposite pulse that is produced in the phase adder by the backward-wave time single steady-state (Fig. 7.46(d)) for mixing, and obtains the dual polarity control pulse (Fig. 7.46(e) and (f)) to enter the locked circuit.

The locked circuit includes an amplified stage, a diode gate, a locked capacitor C, and a resistance alternator. The above control pulse goes to this diode gate. Before triggering (thus before t_1),

the whole diode completely conducts, the locked circuit puts out a constant remaining voltage (approximately 5.5 volts), in trigger instant t_1 , the control voltage that goes up to the diode gate suddenly inverts, and the whole diode simultaneously stops. But because it maintains its voltage on capacitor C_1 , therefore the output of the lock circuit still is 5.5 volts. When a fairly narrow gated pulse comes, the whole diode again transmits. Because the gated pulse on the time mutually coincides with the central part of the discriminator output pulse, therefore when the diode gate conducts, the voltage that emerges in the locked circuit input end corresponds to the voltage of the central part of the discriminating pulse, this input voltage makes the voltage of point P_1 produce a variation, and through the diode gate turns on capacitor C_1 , making the voltage on C_1 change to a new value that corresponds with input voltage. After the gated pulse stops, the diode gate closes, and the voltage on capacitor C_1 then continuously keeps this value invariant directly to the backward-wave time end. In order to avoid leakage from capacitor C_1 in the backward-wave time, the output in the locked circuit uses a resistance alternated state that possesses an extremely high input resistance. Therefore, the output voltage of the locked circuit in the interval of the backward-wave time is a constant. When the backward-wave time ends, the diode again newly conducts, but because at this moment there is no input signal, therefore the charge on C_1 very quickly returns to the remaining value, its output voltage also changes back to the 5.5 volt remainder value, going directly to the new trigger beginning. The size of the locked circuit output deviated remainder value is called P_{AFR} (as shown in Fig. 7.46(g)), it also corresponds to the amount of high speed revision and correction Δf_2 .

The output of the locked circuit is divided into two loops: one loop goes to the input amplified stage of the slow automatic frequency adjusting pulse generator, the other loop goes through an added resistance (this also is simply the phase adder in Fig. 7.42) directly to its output end. Its input amplified stage contacts by two transistors, the above base with one transistor has one electric poten-

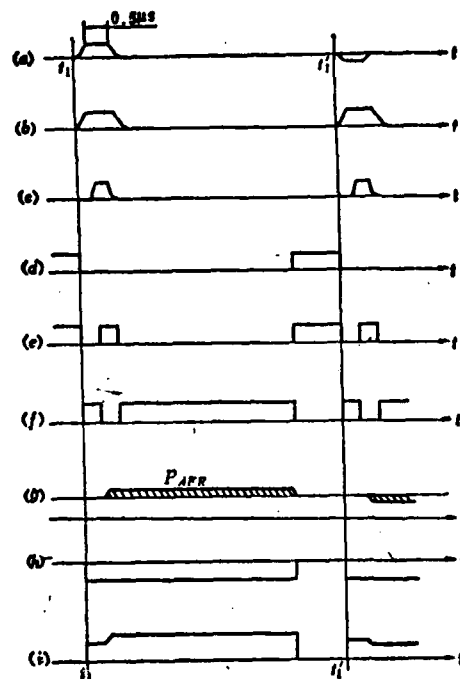


FIG. 7.46 DIAGRAM OF RELATIONSHIP
AND WAVE FORM OF TIME OF EACH
SECTION

tiometer, adjusting this potentiometer can eliminate the 5.5 volt remaining voltage of the input end. The input of this amplifier comes in contact with capacitor C_2 that possesses a very large time constant (this is just the above-mentioned low pass wave filter), and comes into contact with the transistor 38 base. Finally after going through transistor 39 and the original voltage output phase adder, it is put out. Before trigger instant t_1 , point P_2 has a voltage close to zero volts (refer to Fig. 7.46(h)), the locked circuit output at this moment is the remainder voltage, final output (Fig. 7.46(i)) also is zero. At trigger point t_1 , the backward-wave time control pulse that goes to 40 jumps down from +12 volts to 0 volts. This jump change will emerge on point P_2 , its numeric value is determined by transistor 38, the voltage that is charged is determined on C_2 . Therefore on output end 41 there also will emerge a positive jump change, the charge that was charged of its value will be determined by C_2 . This jump change actually corresponds to frequency revision Δf_1 . The output of the locked circuit in instant t_1 still will have remaining voltage and therefore will not have any influence on the final output

voltage. After the radar pulse is transmitted, a P_{AFR} voltage pulse is put out by the locked circuit, after going through phase added resistance 21 goes to the output end, causing the output voltage also to have a corresponding variation (see Fig. 7.46(i)). It also repeatedly goes up to the original jump change. Because the voltage of the locked circuit output and in the backward-wave time on C_2 remains invariable, therefore the final output on 41 in the backward-wave time also remains invariable. Going to the end of the backward-wave time, the control voltage of 40 end returns to +12 volts, the voltage of the output point when the backward-wave ends also returns to zero volts.

Because the circuit that contains capacitor C_2 has a very large time constant, therefore the voltage on capacitor C_2 is dependent on the results of past numerous measurements (thus the output value of numerous locked circuits). The voltage jump change of output end 41 in time t_1 is dependent on the voltage of C_2 , this jump change also is precisely what is used in revision and correction local oscillator frequency (thus revision and correction amount Δf_1), therefore this revision and correction amount is also related to the results of past numerous measurements. Due to the large duration constant of C_2 , therefore its adjustment will be carried out in a closed loop adjustment system. The results of its adjustment will cause the mean value of the locked circuit output to be zero. Capacitor C_1 thus discharges to each pulse, therefore each output voltage P_{AFR} of the locked circuit and that of the above are not related. This high speed automatic frequency adjustment system in the pulse transmission time still can be considered to be a closed loop adjustment system, but after the pulse is transmitted, the loop newly opens and changes into an open loop control system.

In order to ensure capacitor C_2 can initially have a suitable initial voltage (because at this time there is no past measurements that determine the voltage on C_2), in order to make the local oscillator able to revise to near the correct frequency as soon as it opens, and make the frequency after mixing able to fall within the range of the discriminating properties of the discriminator, appropriate measures

are still adopted in this circuit. The collecting electrode of its transistor 33 goes through a steady pressure diode to ground (see Fig. 7.45), therefore the voltage on point P_3 cannot be larger than zero volts. The maximum negative voltage of point P_3 also receives the puncture voltage (for example 3.5 volts) control of this steady pressure diode. Because its output voltage links to C_2 through an electric potentiometer, therefore the appropriately adjusted electric potentiometer also can ensure that there is a minimum negative voltage on capacitor C_2 . This way, on capacitor C_2 there also is a maximum high voltage and a minimum low voltage limit. The selection of these two prescribed limits is to make local oscillator frequency when there is an opener able to revise to the output frequency of the mixer to fall within the discriminating range of the discriminator (actually it also is to make the mean value of its prescribed limit value correspond to the mean value of "cold" and "hot" frequency differences). After entering into the discriminating range of the discriminator, the voltage on C_2 then will make slow variations, and depending on the mean value of frequency differences of previous measurements, finally reaches steady-state to make the high speed revision and correction minimal.

But, actual measurement tests clearly indicate that the amount of revision and correction in its pulse after going through many cycles is not equal to zero. This is because in this system, after using a feedback loop with a large time constant, although it can eliminate extremely slow variation factors that are due to tube ageing, temperature effect, etc., and to high speed alterations of the "cold" and "hot" frequency in the pulse that arise due to operations after different positions of tuning properties, tuning stagnation, and other factors, there still is no way to eliminate them.

(3) Automatic Frequency Adjustment Systems that Simultaneously Possess Slow and High Speed Revision Ability

As is accounted above, after using slow automatic frequency adjusting, although able to eliminate the "cold" and "hot" frequency

difference values of the magnetron that are caused by such factors as replaced tubes, tube ageing, and temperature variations, this system still cannot cause the discrimination output of the frequency error pulse of the transmission instant to be equal to zero. This is because there are still some factors of high speed alterations that exist. These factors have no way to use the method of eliminating by numerous measured mean values. Among these factors are tuning stagnation properties and delay time due to the trigger pulse and transmitting pulse. For example, due to the existence of this delay time it makes the "cold" resonance frequency when actually transmitting and the "cold" resonance frequency of the trigger instant all different. Although the time of this delay is invariable, because the slope of each point on the tuning curve is different it makes these difference values also all different. Therefore, this makes the frequency differences of the transmitting instant that are measured in the discriminator all be different in each pulse. Obviously this difference value forms a direct ratio with the slope of the tuning curve in the trigger instant. Moreover, with different position of the tuning curve different post-tuning stagnation also is related with the slope. Therefore if it can again add a new revision and correction in the trigger instant that forms a direct ratio with the tuning curve slope, it also then can make intermediate frequency after mixing even more close to the expected intermediate frequency, thereby able to select the narrowest possible central release bandwidth.

Below we will discuss the operational principles of this automatic frequency adjustor with an additional high speed revision and correction circuit, the block diagram of the principles of the entire system is shown in Fig. 7.47⁽¹⁵⁾. The relationship between its operational process and time is shown in Fig. 7.48. In it is the "cold" resonance frequency of the magnetron, f_v is the "hot" frequency, f_{osc} is local oscillator frequency. Figure 7.48(b) is an amplified figure of part of (a). By the figure we can know that its operational process is basically the same as the operational process of the previously mentioned automatic frequency adjusting system. Its difference is only in the trigger instant. Aside from revision amount Δf_1 with the

original kind of added frequency, it still simultaneously adds revision amount Δf_2 that forms a direct ratio with the tuning curve slope at this instant. Due to the existence of this new added amount if revision, it causes the reduction of the absolute value of revision amount Δf_3 of the frequency from the discriminator output after the pulse is transmitted. This can cause local oscillator frequency to be even closer to the correct value. Below we will take a look at the relationship between the wave form and the time of each point. Wave form is as Fig. 7.49 shows. In it the wave forms of (a) to (g) are the wave forms when there is no additional high speed revision and correction system. From Fig. 7.49(g) we can begin to explain the operational principles of this high speed adjustment and correction circuit. This wave form can be seen with the linkage of the block diagram of Fig. 7.47. The voltage that is taken from the storage capacitor of the local oscillator frequency controller goes to a differential circuit. The voltage on the capacitor represents the local oscillator frequency, but because the local oscillator, in the phase time before triggering, tracks the "cold" resonance frequency of the magnetron cavity, therefore this voltage also replaces the tuning curve of the magnetron. The wave form that is obtained after the voltage goes through integration is shown in (g) of Fig. 7.49. This voltage after going through amplification in the amplifier goes to a locked circuit. On this locked circuit a control pulse that comes from the backward-wave single steady-state is added. One gate 26 in this pulse control locked circuit makes it open within this time interval before the backward wave time stops at the trigger, and makes the differential wave form that is amplified go through this gate to storage capacitor 27. In the trigger instant, gate 26 closes directly to the end of the backward-wave time. This storage capacitor 27 then keeps a voltage that is equal to the derivative value in the trigger instant (this also is a voltage that forms a direct ratio with the slope of the tuning curve), and goes directly to the end of the backward-wave time. The wave form of the voltage of the locked circuit output is shown by (h) in Fig. 7.49. This voltage again goes to gate 28, and gate 28 also is controlled by the control pulse that the backward-wave time single steady-state gives out. This pulse causes it to

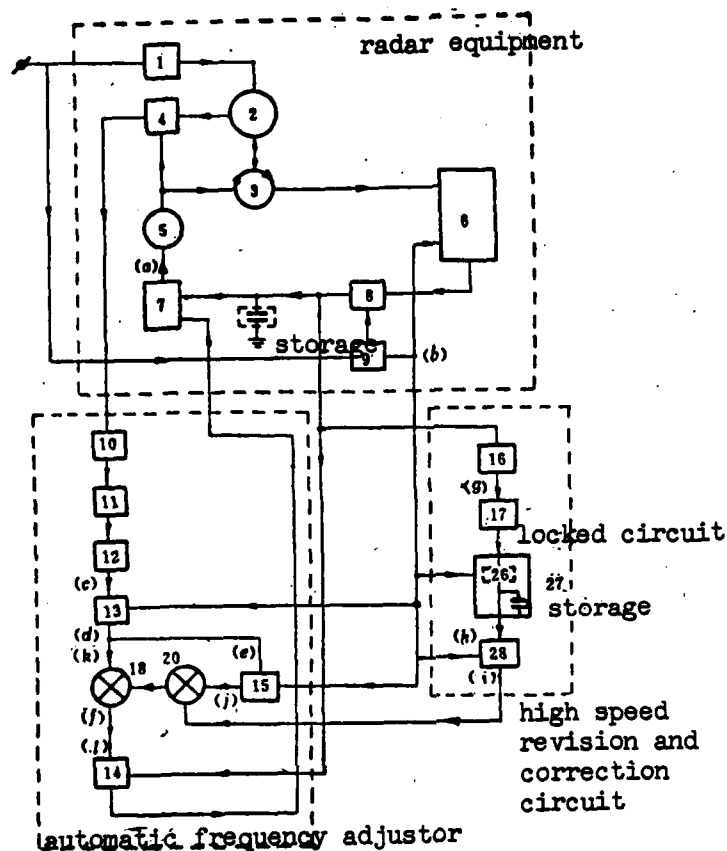
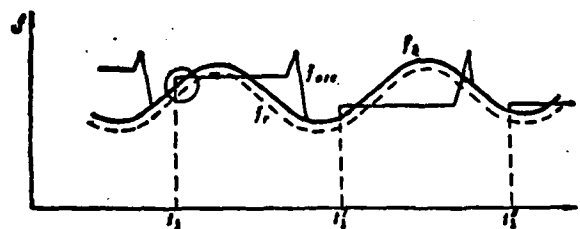


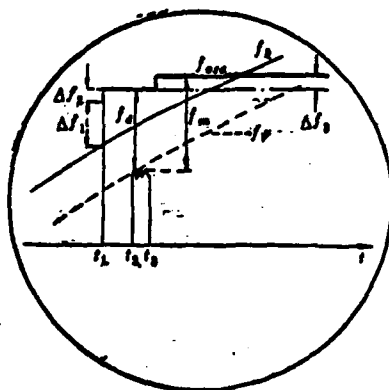
FIG. 7.47 BLOCK DIAGRAM OF PRINCIPLES OF AUTOMATIC FREQUENCY ADJUSTOR WITH ADDITIONAL HIGH SPEED REVISION AND CORRECTION CIRCUIT

KEY: (1) Modulator; (2) Frequency agile magnetron; (3) Circulator; (4) Mixer; (5) Tunable voltage local oscillator; (6) Frequency tracker; (7) Local oscillator frequency control; (8) Gate; (9) Backward-wave time single steady-state; (10) Amplifier; (11) Limiter; (12) Discriminator; (13) Locked circuit; (14) Revision and correction circuit; (15) Integrator; (16) Differential circuit; (18, 20) Phase adder; (28) Gate

only conduct within the backward-wave time. This makes the value of the voltage on storage capacitor 27 able to pass through only after the trigger. The wave form of the voltage that is put out from gate 28 is shown by (i) in Fig. 7.49. The amplitude of this voltage replaces the derivative value of the tuning curve of the trigger instant, its



(a)



(b)

Fig. 7.48 DIAGRAM OF VARIATIONS OF
MAGNETRON FREQUENCY AND LOCAL OSCIL-
LATOR FREQUENCY

bandwidth thus is equal to the backward-wave time. After phase adding of this voltage in phase adder 20 and revising voltage (j) of the original differentiator output, it is then carried to the revised voltage phase adding that is put out by the phase adder 18 and the discriminator. Due to the existence of the high speed revision and correction circuit, it causes the absolute value of the error voltage of the discriminator output to be smaller than in the past, expressed by P_{AFR} (as shown by (k) in Fig. 7.49). The total voltage after phase adding (see Fig. 7.49(1) is again carried to the revision and correction circuit to correct the nonlinearity of the local oscillator tuning sensitivity. The newly entered-into high speed revision varies from pulsewidth to pulsewidth. Moreover it essentially is an open loop adjustment system. The adjustment constant of this open loop adjustment system should adjust to cause minimum discriminator output of revised pulse P_{AFR} . For example it can amplify the amount

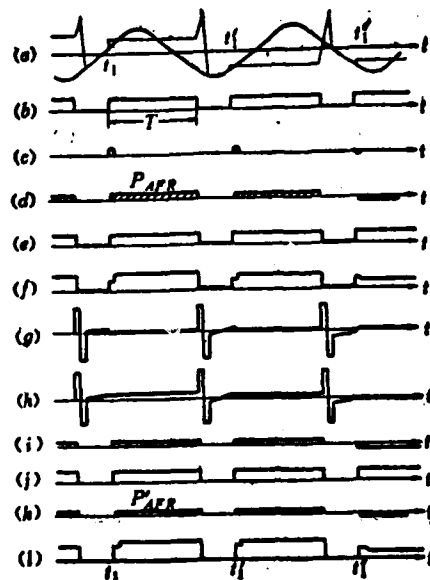


FIG. 7.49 DIAGRAM OF WAVE FORM
OF AUTOMATIC FREQUENCY ADJUSTMENT
SYSTEM THAT POSSESSES HIGH SPEED
REVISION AND CORRECTION

of the amplifier after adjusting the differential circuit, and at the same time detect the voltage pulse of the discriminator output to its amplitude minimum. Later it makes its amplified amount and adjustment constant remain invariant.

As previously discussed, this high speed revision and correction system can correct the deviation related to the position of the trigger on the tuning curve, for example, due to the delay time between the trigger and the transmission, and due to the post-tuning stagnation. This revision is also necessary on systems that have frequency sensors. On jump frequency magnetrons that have frequency readout resolvers, its frequency sensors can replace the frequency tracker in Fig. 7.47, and use its frequency readout data within the phase time interval before the backward-wave time ends at the trigger, to directly control local oscillator frequency, and make it track the magnetron frequency. If the frequency that is read out corresponds to the magnetron's "cold" resonance frequency, the entire frequency automatic adjustment system is no different from the system shown in Fig. 7.47.

Of course, it also can read out the magnetron's "hot" oscillator frequency and increase the expected intermediate frequency; at this moment then we can eliminate the slow automatic frequency adjustment system. But due to the magnetron's "hot" oscillator frequency we also can follow the variations of the replaced tubes, tube ageing, and temperature effect, in order to fully reduce the amount of revision and correction in the discriminator, it is still desirable to use the slow automatic frequency adjustment system. In modern times the majority of jump frequency magnetrons have precise frequency readout devices, at least we can replace the complicated frequency tracking systems that were previously discussed, and greatly simplify the system.

7.4.4 THE MONOPULSE AUTOMATIC FREQUENCY CONTROL SYSTEM THAT HAS FREQUENCY PRESET INFORMATION

The majority of modern frequency agile magnetrons possess frequency readout devices. They can give accurate frequency preset information. Aside from these there are some frequency agile magnetrons (for example precision tuning magnetrons) that in themselves possess accurate closed loop servo systems, their oscillator frequency can be assigned by additional directive voltage. After this directive voltage corresponds to the intermediate frequency voltage, it even more can be regarded as local oscillator frequency preset information. Under this condition, the automatic frequency control system discussed above can be greatly simplified.

(1) Open Loop Frequency Presetting

Open loop frequency presetting carries out sampling on the magnetron frequency readout signal before each pulse transmits, after the voltage that is obtained corresponds to the intermediate frequency voltage, it carries out presetting on local oscillator frequency. The presetting is conducted in the open loop form (Fig. 7.50)⁽¹⁶⁾. Generally it is desirable to use an accurate linear loop, then all the transmitting functions K_1 that go directly from the frequency readout to the voltage control oscillator are linear. But actually the frequency readout and the voltage control oscillator in themselves have nonlinear

errors, these errors are represented respectively by δf_T and δf_L . Aside from this, the magnetron and local oscillator both have a hot drift, respectively expressed as $K_T \Delta T$ and $K_L \Delta T$. If the mean frequency of the transmitter is \bar{f}_T , time variation measure is $\Delta f_T(t)$; the mean frequency of the local oscillator is \bar{f}_L , time variation measure is $\Delta f_L(t)$; thus the accuracy of its open loop presetting can be expressed by:

$$f_T - f_L = (\bar{f}_T - \bar{f}_L) + \Delta f_T(t) \left[1 - \prod_{i=1}^N K_i \left(\pm \sum_{i=1}^N |\delta K_i| \right) \right] + (K_T - K_L) \Delta T \pm \delta f_T \pm \delta f_L \quad (7.14)$$

In which K_i is the typical open loop transmit gain, and δK_i is the gain capacity difference under actual operating conditions. Because in actual applications, the primary concern is high speed tracking on pulse variations $\Delta f_T(t)$, moreover, frequency variations that are caused by slow temperature variations can be compensated by common temperature compensation techniques, therefore $(K_T - K_L) \Delta T$, this sum can be omitted.

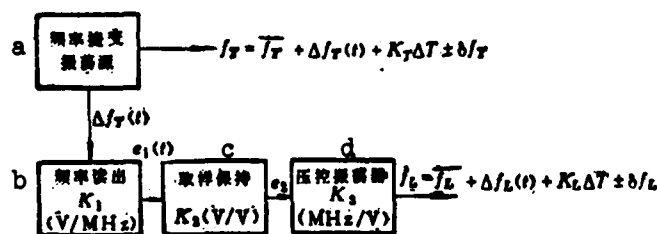


FIG. 7.50 OPEN LOOP FREQUENCY PRESETTING
KEY: (a) Frequency agile oscillator source;
(b) Frequency readout; (c) Sampling maintenance; (d) Voltage control oscillator

Aside from this, in an accurate linear loop, f_L is in a direct ratio to $\Delta f_T(t)$ by ℓ_1 , its loop gain must be 1, thus:

$$\prod_{i=1}^N K_i = 1.0 \quad (7.15)$$

From this we can obtain the expression after simplification:

$$f_T - f_L = (\bar{f}_T - \bar{f}_L) \pm |\Delta f_L|_{max} \quad (7.16)$$

In which sum $(\bar{f}_T - \bar{f}_L)$ is equal to the required intermediate frequency f_1 and $|\Delta f_1|_{\max}$ is open loop preset error:

$$|\Delta f_1|_{\max} = \Delta f_T \sum_{i=1}^N |\delta K_i| + \delta f_T + \delta f_L \quad (7.17)$$

From this we can see that open loop preset error not only changes with the linearity and stability of the prepared transmit function gains, but also still corresponds to agile source frequency, deviation Δf_T of its mean value \bar{f}_T from a direct ratio. Therefore the open loop tracking error depends on the probable distribution of Δf_T revolving around \bar{f}_T . (7.17) represents the numerous preset errors when there are numerous deviations. Figure 7.51 gives the largest preset errors of the function $\sum |\delta K_i|$ that conducts accumulative gain stability when frequency agile bandwidth $2\Delta f_{T(\max)}$ of the transmitter respectively are 100, 200, and 600MHz, for the purpose of simplification we presume the total sum of the tuning nonlinearity is 10MHz. From the figure we can see that when frequency agile bandwidth is 600MHz, and accumulative gain stability is 0.1, its preset error can reach approximately 40MHz.

It is necessary to note that when preset error is larger than intermediate frequency, there will be a possibility that the problem of mirror image frequency will occur. For example the originally designed local oscillator is one intermediate frequency higher than the frequency of the transmitter but when the local oscillator frequency is one intermediate frequency lower than the frequency of the transmitter, after going through mixing it also can obtain the intermediate frequency signal, but at the same time the error signal that is read out from the discriminator is exactly reversed, thereby causing the automatic frequency control system to have no way to operate normally.

There are several methods that can resolve this problem, but the simplest and most effective method among them is using the mixer that restrains the mirror image. The operational principles of this mixer are shown in Fig. 7.52. When $f_L > f_T$, the intermediate frequency signals that are produced on point C by the two mixers are alike, when

$f_L < f_T$, the intermediate frequency signals that are produced are opposite and cancel out. This then resolves this problem.

(2) Open Loop Frequency Precision Tuning

From the above analysis we can know that the presetting errors of open loop frequency are very large, and simply cannot satisfy the requirements to normally receiver signals, and must make further precision tuning after the pulse transmission.

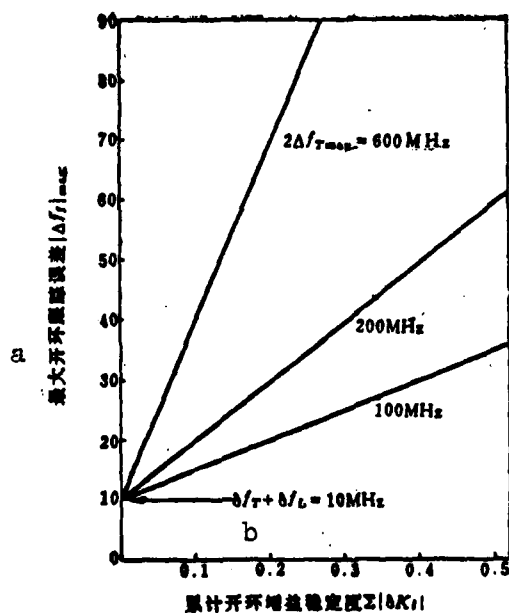


FIG. 7.51 OPEN LOOP PRESET ERRORS
THAT CONDUCT ACCUMULATIVE GAIN
STABILITY FUNCTION

KEY: (a) Numerous open loop tracking errors;
(b) Accumulative open loop gain stability

The most simple method is open loop frequency precision tuning. This is after the pulse is transmitted, we take the even more accurate frequency error signal, and again make further adjustment on the local oscillator frequency. The frame diagram of this open loop precision tuning method is shown in Fig. 7.53⁽¹⁷⁾. Under ideal conditions $K_3 K_4 K_5 = 1$. We can note that the differences of this open loop frequency precision tuning and closed loop precision tuning lie in that

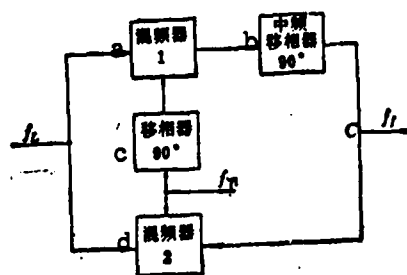


FIG. 7.52 MIXER THAT RESTRAINS
MIRROR IMAGE FREQUENCY
KEY: (a) Mixer; (b) Intermediate
frequency shifter; (c) Shifter;
(d) Mixer

it uses time delay sampling and maintains the circuit, also that the frequency differences that are obtained are not instantly used to control the local oscillator, but delay time at least until after the pulsewidth is transmitted and then controls the local oscillator. Therefore the loop is not closed.

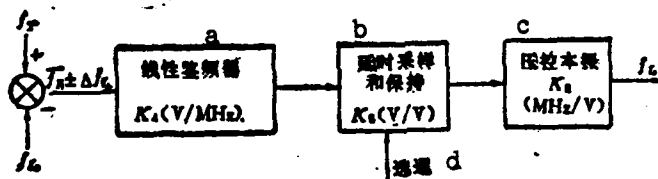


FIG. 7.53 FRAME DIAGRAM OF OPEN LOOP FREQUENCY
PRECISION TUNING
KEY: (a) Linear discriminator; (b) Delay time,
sampling and maintenance; (c) Pressure control
local oscillator; (d) Gate

The numerous error $\Delta f_{I1\max}$ of this open loop precision tuning system can be expressed by the following formula:

$$|\Delta f_{I1}|_{\max} = |\Delta f_I|_{\max} \sum_{i=1}^5 \delta K_i + \delta f_r \left(1 + \sum_{i=1}^5 \delta K_i \right) + \delta f_L \quad (7.18)$$

In which δK_i is gain capacitance difference. δ_{IF} is the capacitance difference of the cross point of the discriminator. If the discriminator is sufficiently stable, then the above expression can be simplified as:

$$|\Delta f_{i+1}|_{\text{max}} = |\Delta f_i|_{\text{max}} \sum_{i=1}^5 \delta K_i + \delta f_i \quad (7.19)$$

If preset error $|\Delta f|_{\text{max}}$ is 40MHz, accumulative gain stability is 0.1, and pressure control oscillator linearity is 5MHz, then we can obtain that the numerous differences of this open loop precision tuning are approximately 9MHz, this obviously cannot satisfy the requirements.

Therefore we can have an entire system where the reason for this kind of large error lies in going directly from the discriminator to the revision and correction on the local oscillator, analogued, if we can use the digital type discriminator to directly obtain the digital form error signal, then not only can we eliminate accumulative gain instability, but also we can use the digital technique to revise and correct the nonlinearity of the pressure control oscillator, thereby reaching very high precision. The following will discuss this digital type open loop system⁽¹⁸⁾.

First we will take a look at the basic operational principles of a digital type discriminator. This digital type discriminator uses vernier techniques to measure the time of intermediate frequency signals of 2 cycles. It uses the oscillator at the instant of intermediate frequency signal positive slope past point zero, making frequency f_1 begin oscillation, after going through 2 cycles, the oscillator begins operation at the instant of its positive slope past the limiter gate again makes two frequencies $f_1 = 1.01f_1$. At the same time a computer begins to carry out calculation on f_2 . When the positive directional edge of these two oscillator signals coincide, the computer stops calculating. At this moment the computer reading is in a direct ratio to the intermediate frequency signal cycle. For example, if $f_1 = 10\text{MHz}$, then its cycle T_1 is 100 nanoseconds; if $f_2 = 10.1\text{MHz}$, then its cycle T_2 is 99 nanoseconds. Because when f_1 shifts to $2T_0$ (in which T_0 is intermediate frequency signal cycle) the oscillator begins, each f_2 catches up to nanoseconds after a cycle. As a result when the two phases are completely alike, the computer reading expresses the nanosecond $2T_0$ value. Using this method we can use a comparatively

low speed computer and a comparatively high speed coinciding gate circuit to accurately measure the cycle of the intermediate frequency signal. If the total error that is caused by the gate circuit is ± 0.5 nanoseconds (this is what actually can be obtained), then the discrimination error that is caused by this will be as Table 7.3 shows.

TABLE 7.3 ERROR OF DIGITAL FORM DISCRIMINATOR

Intermediate Frequency f_0 (megahertz)	20	30	40	50	60	70	80	90	100
Computer Reading $2T_0$ (millimicrosecond)	100	66	50	40	33	28	25	22	20
± 0.5 ns Corresponding Error(%)	± 0.5	± 0.75	± 1.0	± 1.25	± 1.5	± 1.75	± 2.0	± 2.25	± 2.5
Corresponding Discrim- inator Error(megahertz)	± 0.1	± 0.225	± 0.4	± 0.62	± 0.9	± 1.23	± 1.6	± 2.02	± 2.5

From the table we can see that the precision of this digital type discriminator still is very high. For example if the intermediate frequency of the central release is 60MHz and the allowable discrimination range is ± 40 MHz, then from 20MHz to 100MHz its largest error is ± 2.5 MHz. Moreover, because this method only measures the intermediate frequency of 2 cycles, therefore it is especially suitable to extremely narrow pulsewidth frequency agile radar, for example radar where the pulsewidth is 100 nanoseconds.

Now we will take a look at the composition of the whole system (see Fig. 7.54). The forward edge of the transmitting pulse that comes from the transmitter goes to new signal steady-state 12, the delay time of the single steady-state is selected approximately as less than one half of the transmitting pulse, so that the two intermediate frequency signals in the selected pulse carry out measurement, this way they can avoid the influence of frequency traction and electron frequency shift. The pulse that is put out by the single steady-state acts as a reduction pulse to go to JK trigger 18 and 20. When the first negative directional intermediate frequency signal after the termination of single steady-state delay time causes trigger 18 to turn into condition "1", the gate latch circuit that is composed of RS trigger 24 will open, this then causes oscillator 22 with frequency

as 10.0MHz to begin oscillation. After going through the intermediate frequency signals of two cycles, trigger 20 changes into "0" state, causing gatelatch circuit 30 to open, and oscillator 28 with a frequency of 10.1MHz begins oscillation. The signal of oscillator 28, after going through gate 46, goes to 7 binary computers to conduct computations, in which the first three are composed of J-K triggers, and the latter four are composed of a medium scale level four computer. After the output of oscillators 22 and 28 respectively go through and don't go through inversion, they go to gate 42 to carry out coinciding, using the turning of the inverter the delay time can obtain very precise coincidence. When it coincides, gate 46 prohibits, the computer stops calculating, its reading from the digital analogue alternator 50 alters into an analogue rate output, and again going through corresponding alterations goes to the pressure control local oscillator to carry out revision and correction. In order to prove it is open loop precision tuning, the revision and correction signal goes through a gate circuit control, its gate control signal is produced by R-S trigger 54, this trigger also is controlled by the state of the fourth computer only after this computer changes to "1" (corresponding to 0.8 microseconds), can the revision and correction signal go through the gate circuit to go to the pressure control oscillator. In order to prove the accuracy of the measurements, oscillators 22 and 28 must immediately oscillate after the open signal emerges, moreover the first cycle and the later cycle must be completely alike. The relationship between the delay time that extends to the initial oscillator and the temperature coefficient of oscillator frequency is crucial, so long as the properties of the two oscillators are alike.

We can see that this open loop frequency precision tuning not only has fairly high precision but also has fairly simple design, the highest operational frequency of the digital integrated circuit that is used is approximately 125MHz. Based on the highest level of existing integrated circuits, the method can be applied to intermediate frequencies that reach as high as 350MHz.

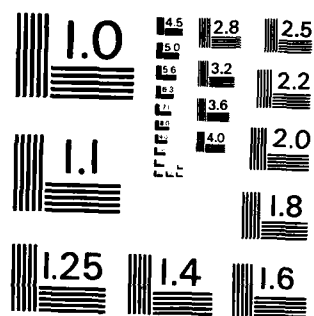
FREQUENCY AGILITY RADAR(U) FOREIGN TECHNOLOGY DIV
WRIGHT-PATTERSON AFB OH N YUMA 06 DEC 82
FTD-ID(RS)T-0803-82

617

F/G 17/9

NL

A 10x10 grid of squares, with the top-left square missing.



MICROCOPY RESOLUTION TEST CHART
NATIONAL BUREAU OF STANDARDS-1963-A

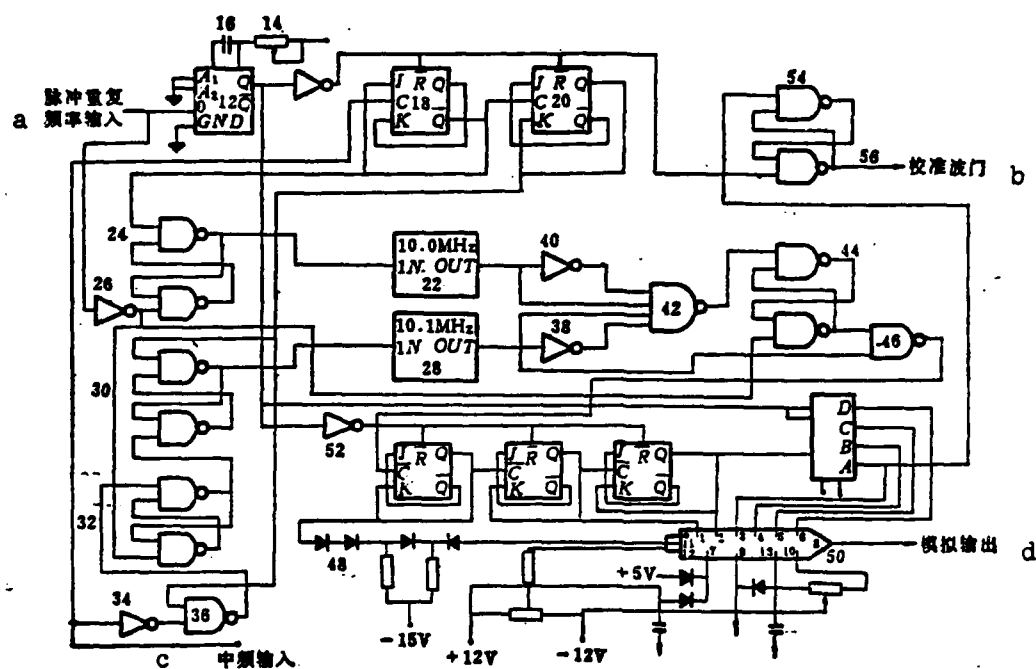


FIG. 7.54 DIGITAL TYPE OPEN LOOP FREQUENCY PRECISION TUNING SYSTEM
KEY: (a) Input of repeated frequency of pulse; (b) Detection;
(c) Intermediate frequency input; (d) Analogue output

(3) Closed Loop Frequency Precision Tuning

Presently what is in fairly common use is closed loop frequency precision tuning, or sometimes called feedback frequency revision and correction. The block diagram of this method is shown in Fig. 7.55⁽¹⁶⁾. The local oscillator before the pulse is transmitted is preset by open loop preset signal $e_2(t)$ to frequency f_L , and after keeping with the transmitted frequency differences obtains an average intermediate frequency and error frequency Δf_I , after this error frequency reduces the mean value to $\overline{\Delta f_I}$ it goes to the discriminator to conduct discrimination, the inverse function of the discriminator is K_d (expressed by volts/MHz). Its output goes to the sampling where inverse function is $F(s)$ to maintain the circuit and later is carried to the voltage control local oscillator. Because the voltage control oscillator signal in the adjustment period again returning to the mixer, can continuously obtain error signals. This closed loop adjustment system is only closed in the pulse transmission period, therefore we must

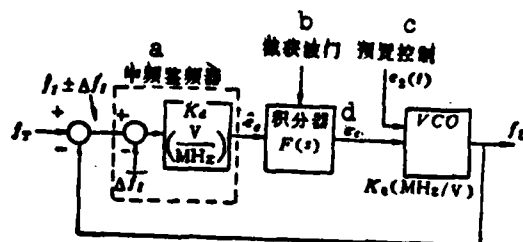


FIG. 7.55 CLOSED LOOP FREQUENCY PRECISION TUNING

KEY: (a) Intermediate frequency discriminator; (b) Intercepted wave gate; (c) Preset control; (d) Differentiator

research its instantaneous change process. The error response of its closed loop can be expressed by the alternate expression:

$$\frac{\Delta f'_I(s)}{\Delta f_I} = -\frac{1}{1 + K_d F(s) K_v} \quad (7.20)$$

In which $\Delta f_I(s)$ is the open loop error alteration, $\Delta f'_I(s)$ is the alteration of the influence on the closed loop error of Δf_I revision. When the transmitting pulse oscillates, the forward edge of the preset intermediate frequency error that is obtained by comparison of f_T and f_0 can initially be expressed by the step where amplitude is Δf_I (see Fig. 7.56(a)). If hopefully this preset error uses time constant T_L to indexly attenuate to 0 (Fig. 7.56(b)), then the device chosen for treatment must be an integrator. At this time, actual closed loop error response (Fig. 7.55(c)) can similarly be expressed by the following expression:

$$\Delta f'_I(t) \approx -\frac{\Delta f_I}{1 + K_L} (1 + K_L \exp(-t/T_L)) \quad (7.21)$$

In which K_L is low frequency open loop gain, T_L is closed loop error revision and correction time constant. In the actual system, it cannot reduce to zero with the open loop preset error, but only can compress to $f_I/(1+K_L)$, then $(1+K_L)^{-1}$ represents closed loop error compression ratio. If closed loop time constant $T_L=50$ nanoseconds, then we can compute the interception time that is required in order for its revision and correction to be within a difference percentage of the

closed loop error steady-state value as the function of the closed loop error compression ratio (See Fig. 7.57).

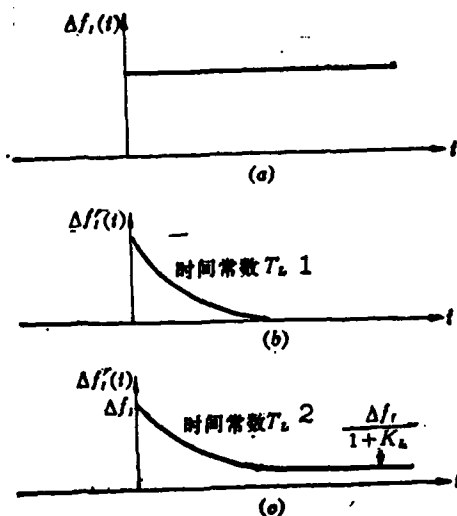


FIG. 7.56 CLOSED LOOP ERROR INSTANT CHANGE RESPONSE

KEY: (1) Time constant; (2) Time constant

Starting out from the point of view of actual applications, naturally the smaller the expected compression ratio and the shorter the interception time the better. From the figure we can see that these two requirements are mutually contradictory. This is also to say that the smaller the compression ratio, the longer the interception time. Generally the open loop gain of the loop is approximately between 50-100, a very small gain can make error compression ratio very large, and a very large gain can make loop operations unstable, and also increase interception time. Test results clearly indicate that this closed loop precision tuning circuit can be within 0.25 microseconds, with the 10MHz open loop error signal reducing to within 600KHz. Obviously, we must apply this closed loop precision tuning circuit to the system where pulse transmission is less than 0.2 microseconds, moreover, it is very difficult to have a correspondingly high precision tuning accuracy.

In Fig. 7.56, presuming the loop time constant is 50 nanoseconds, the time constant actually can possibly surpass its value. Aside from

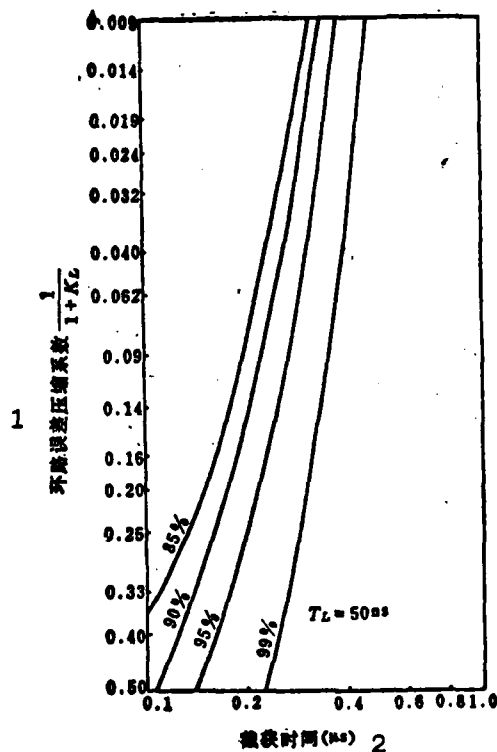


FIG. 7.57 RELATIONSHIP OF LOOP INTERCEPTION TIME AND ERROR-COMPRESSION RATIO
KEY:(1) Loop error-compression coefficient; (2)Interception time

this, the delay time in the loop can also increase the interception time. When its interception time is larger than the pulsewidth, the precision tuning accuracy of this closed loop precision tuning circuit can greatly decrease. Under these conditions, the amount of increased closed loop adjustment can reduce precision tuning error.

Below we will discuss using microwave delay time wires to increase adjustment amount of closed loop precision tuning system.

With the development of supersonic technology, especially the research achievements of molecular acoustics, we now already have the possibility to manufacture and operate in supersonic delay time of microwave wavebands. These delay time wires use vulcanized cadium as a supersonic energy converter and use sapphire monocrystals as

a delay time medium. These supersonic delay time wires use a cylinder sapphire of 1-2cm long, and can obtain a several microseconds delay time. Even together with the energy converter, its inserted consumption loss is very small. This way, after the input end of the microwave delay time wire of a terminal short circuit goes up to a microwave pulse, it can obtain a several microseconds pulse series of amplitude gradually attenuated intervals. Using this method we can increase the adjustment amount, thereby raising the accuracy of precision tuning.

Figure 7.58 is a frame diagram of a repeating automatic frequency precision tuning system that uses microwave delay time wires. The transmitting pulse that comes from the agile magnetron, after going through a fixed directional coupler to take out a small part of energy goes to a low power three point iron oxide system circulator, from the second point of this circulator it goes to a terminal short circuit microwave delay time wire. This way, from the third point of the circulator it can obtain a series of amplitude gradually attenuated pulses, its interval is equal to double the delay time of the delay time wire, this series of pulses goes to a microwave limiter that is made by a PIN diode so that after going through limiting the amplitude of each pulse will be equal. Later it goes to the output phase mixing of a mixer and voltage tunable local oscillator (the one that is drawn in the figure is a backward-wave tube), after mixing the intermediate frequency signal that is obtained immediately goes to a high speed automatic frequency precision tuning system. Because the local oscillator frequency in an instant before transmission uses the agile magnetron frequency readout to carry out preset coarse tuning, therefore the intermediate frequency signal after mixing can be sure to fall within the range of discrimination properties of the discriminator. Even though the frequency error of the first intermediate frequency pulse can be comparatively large, after going through the first closed loop adjustment it further reduces the local oscillator frequency error, thereby causing the carrier frequency of the second intermediate frequency pulse that is obtained after mixing to draw even closer to the expected intermediate frequency, and at the same time carries out the second closed loop adjustment, to further reduce local oscillator

frequency error. If this continues going to the time that corresponds to the closest backward-wave (generally approximately ten some micro-seconds to several ten microseconds, the use and stability of observation radar), the whole system has already gone through at least 3-4 times of adjustment or more, while local oscillator frequency error can shortly reach a degree that can be overlooked. If the wear and tear of the microwave delay time wire is small enough, it can obtain a long series of pulse transmissions with very small amplitude attenuation and very many pulses (this is also a very long continuation time), thus local oscillator frequency can carry out many adjustments. This way not only can preset frequency errors be reduced in the beginning, but also the problem of post-tuning drift of the voltage control local oscillator can be resolved.

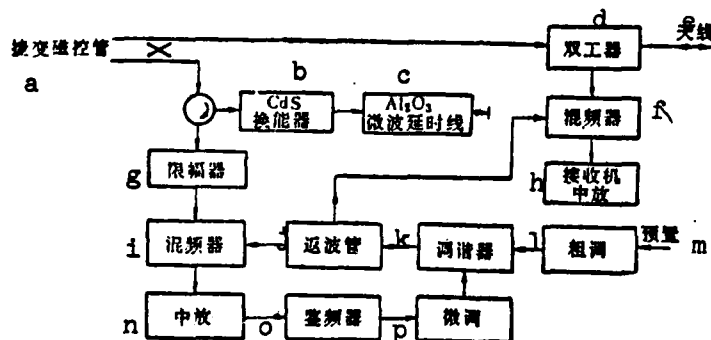
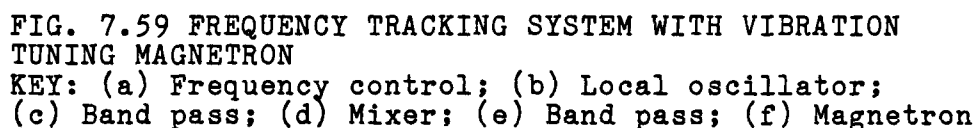


FIG. 7.58 REPEATING AUTOMATIC FREQUENCY PRECISION TUNING SYSTEM THAT USES MICROWAVE DELAY TIME WIRES
 KEY: (a) Agile magnetron; (b) Energy converter; (c) Microwave delay time wires; (d) Dual processor; (e) No wires; (f) Mixer; (g) Limiter; (h) Receiver central release; (i) Mixer; (j) Backward-wave tube; (k) Tuner; (l) Coarse tuning; (m) Presetting; (n) Central release; (o) Discriminator; (p) Precision tuning

(4) Automatic Frequency Precision Tuning System of Open Loop Presetting on Closed Loop Presetting

In vibration tuning magnetrons, because the tuning is carried out according to patterns (usually sine waves), therefore it is possible to also add closed loop adjustments on frequency presetting to



473

but due to the nonlinearity of magnetron tuning, the frequency sensor in itself also can produce a certain error, thus the error of this open loop presetting is appropriately $\pm 1\text{MHz}$.

After the pulse is transmitted, a high speed automatic frequency precision tuning system is used to further revise and correct local oscillator frequency. At this time, after the 0.2 microsecond narrow pulse that is limited by the magnetron mixes with local oscillator frequency, a $30\pm 1\text{MHz}$ intermediate frequency signal is obtained, after going through amplification in the amplifier this intermediate frequency immediately goes to a high speed discriminator. The two tuning return circuits of this discriminator respectively tune to 29 and 31MHz. In order to obtain fairly small delay time and fairly high linearity, the Q value of the return circuit must be fairly low ($Q=4$). The discriminator then can obtain the voltage value of representative frequency error. In order to obtain a fairly good sample of this error, storage capacitor C_5 with a fairly large change time constant ($t=2$ microseconds) is selected. After the pulse transmission ends, the sample value of this error is delivered to integral amplifier A_2 . This is carried out through a gate circuit that is composed of a field effect tube BG_1 . This gate circuit is stopped in the pulse transmission period. Because in the pulse transmission period the mixer puts out on negative directional pulse, this pulse causes the conduction of diode D_4 . Field effect tube negative directional partial placement will cause it to stop. When the pulse transmission ends, partially placed circuit C_4R_5 discharges at very high speed (its time constant is 0.02 microseconds) so that the field effect tube conducts at very high speed, therefore the frequency error signal will be delivered to integral amplifier A_2 . The output of this integral amplifier is carried through a revised resistance R_{12} to phase adder amplifier A_4 . The revised resistance is what the open loop gain in order to revise the whole feedback system. After going through a high speed automatic frequency precision tuning system, it is possible for local oscillator frequency error to revise to an even smaller error range.

But because local oscillator resonance sensitivity is not constant in different frequency ranges, therefore, after going through revision

and correction by the above two methods, local oscillator frequency still has errors. Its manifestation is in the output of integral amplifier A_4 , it still contains 200Hz base frequency weight, in order to eliminate this error a phase sensitive detector that is composed of diodes D_5 and D_6 and resistor R_{10} and R_{11} is added to this system. The output of integral amplifier A through capacitor C_6 and resistor R_9 couples to an arm that is composed of the positive directional diode D_5 of the phase detector. The frequency readout signal that is put out by amplifier A_1 thus respectively goes through resistor R_L and voltage divider R_7 and R_8 to positive directional diode D_5 and reverse diode D_6 . Because this frequency readout signal is symmetrical on the two arms of the phase detector, therefore among them the effects of the positive semicycle and the negative semicycle cancel each other out. The frequency error signal that comes from integral amplifier A_2 only goes to its one arm, therefore so long as there is any 200Hz base frequency weight among them, its positive semicycle then will go through positive directional diode D_5 to A_3 . The size of this positive semicycle also is a magnitude of base frequency weight amplitude that is contained in the frequency error signal that is put out by integral amplifier A_2 . After this signal goes through amplification in another amplifier A_3 , it is carried to light bulb Z_1 that is installed in a cassette, the brightness of the bulb follows the variations, at this time the resistance value of the phototube in the cassette also follows the variations. This changes the passage gain, and also changes the strength of the 200Hz frequency readout signal transported from amplifier A_1 to phase adding amplifier A_4 . It is used to compensate the variations of the local oscillator frequency tuning sensitivity. Actually it also corresponds to a closed loop control system that is added on by the open loop control system of the frequency readout of the frequency sensor. This even further reduces frequency error of the local oscillator.

This system can be applied to mechanical jamming devices of collision prevention radar, this radar uses the principles of phase jamming to measure the angle of elevation of the surface features (or pitching angle), and altitude of the automatically controlled aircraft to pre-

vent collision (the so-called collision prevention radar is topography tracking radar). We have already discovered that using vibrational tuning jump frequency techniques in this kind of radar can reduce the influence of undesirable input clutter on its performance. But after using vibrational tuning, due to the imperfections of the automatic frequency control system it is possible to make the frequency of the intermediate frequency of the clutter output diverge from standard value. But, in this radar, the angle of elevation of surface features depends on measuring the phase angles of backward-waves that are obtained in different signal passages. In order to avoid the different phase shift properties that each intermediate frequency signal passage possesses, it is necessary to use the standard intermediate frequency signal of a transistor controller to carry out revision and correction, after revision and correction we can consider the completely identical phase properties that each signal passage possesses on this specially designated intermediate frequency. But if the intermediate frequency deviates, then it can produce phase error. We already know that each 1MHz deviation of a frequency can produce 10 degrees phase shift, this corresponds to 1 degree space angle of elevation error. In order to make the angle of elevation error less than 1/10 degree (the electronic phase angle error is less than 1 degree), then the intermediate frequency error must be less than 0.1MHz, considering that Doppler frequency can raise to 20KHz error, then we only can allow automatic precision tuning systems to have 50KHz error.

The vibrational tuning magnetron that the above-mentioned system uses can use a 200Hz tuning frequency to tune to ± 25 MHz frequency range, pulsewidth is 0.2 microseconds, repeated frequency is approximately 4KHz, thus the maximum frequency difference in the adjacent pulse is approximately 5MHz, open loop preset error is ± 1 MHz. Final error in closed loop adjustment is less than 50KHz. This can satisfy the requirements of the indexes for the above-mentioned entire system. Therefore it makes frequency agile technology able to successfully be applied to collision prevention radar with a mechanical phase jamming device.

7.5 SEVERAL FREQUENCY AGILE FORMS OF NONCOHERENT FREQUENCY AGILE RADAR

Frequency agile radar hopefully can be operated on many agile forms, each different agile form is for satisfying different requirements. Comprehensively, it hopefully can operate in the following several forms:

(1) Arbitrary Fixed Frequency

Frequency agile radar hopefully can operate on a fixed frequency that has an arbitrary tuning frequency range. Its goal has the following few aspects:

(a) Camouflage as fixed frequency radar. After retrofitting fixed frequency radar as frequency agile radar, this is even more necessary. At this time radar ordinarily operates on original fixed frequency.

(b) Making moving target indication systems able to operate normally. Because in noncoherent frequency agile radar it is very difficult to use dual pulse or grouped agile moving target indication systems, when no active jamming or clutter jamming have primary contradictions it generally still can only operate on fixed frequency moving target systems.

(2) High Speed Agility in a Small Scope

Its primary goal is to restrain clutter. Generally the vibration tuning magnetron is used, so long as the frequency differences between the pulse are enough to make clutter effected then it is fine to use that. This form also can be used to avoid narrow band sighting from jamming aircraft and reduce the detection and interception probability.

(3) High Speed Stochastic Agility in the Entire Tuning Range

This form is primarily used to resist active clutter, and reduce

detection and interception probability. As the above section accounts, because its agile frequency error is greater than the critical frequency error that can cause target backward-waves to interact, therefore it also can be used to increase target survey distance and reduce tracking error.

(4) Program-controlled Frequency Agility

Requirements are according to the program of specified regulations or preset arrangements for agility. For example gradient agility and grouped agility contain certain fixed frequency stochastic agility or do not contain certain fixed frequency stochastic agility. The latter two are to be able to use certain fixed frequency and responder contacts simultaneously with stochastic agility, or to camouflage into fixed frequency radar using detection aircraft that deceives the enemy, or to avoid certain narrow band jamming sources.

(5) Self Adapting Frequency Agility

In radar that is equipped with a jamming detection unit, the weak areas of the jamming frequency spectrum can be detected, and it automatically at high speed adapts the agility to this frequency.

Fully coherent frequency agility possesses fairly high agile adaptability, and can adapt to each different requirement, but generally fully coherent frequency agile radar can only operate on a limited number of dispersed frequency points. If there must be fairly satisfactory frequency coverage, it is necessary to have an ample amount of dispersed frequency.

Although noncoherent frequency agility can continuously change frequencies its tuning usually is mechanical tuning, therefore agile adaptability is fairly poor. In order to achieve each different agility form it is necessary to use some particular circuits. In the following section we will discuss some achievement methods of agile types of noncoherent frequency agile radar.

7.5.1 STOCHASTIC AGILITY ACHIEVEMENT METHOD

In each agile type the most commonly used and the most important agile type is stochastic agility. But in frequency agile magnetrons that use high speed motor drives (for example rotational tuning magnetrons, bent axis tuning magnetrons, and reverse tuning magnetrons), due to the mechanics of the rotating parts, inertia is fairly large. Therefore what achieves stochastic agility becomes a problem.

In this type of agile magnetron, the carrier frequency of the transmitting pulse is determined by the repeated frequency of motorized rotational speed and trigger pulse and the phase between the two. In multiple cavity type rotational tuning magnetrons, the amount of variation of the magnetron tuning frequency in the motorized rotational cycle also must multiply to the cavity amount. If the triggered repeated frequency is exactly equal to the tuning frequency, then the carrier frequency of the transmitting pulse will be a fixed frequency. If the repeated frequency of the pulse is onefold higher than the repeated frequency of tuning, it is related to its initial phase. When the initial phase is zero phase it still corresponds to the fixed frequency. When it initially is a 90° phase, it can obtain the two frequencies from the central frequency as the pulse frequency spectrums of $+\Delta f_A$ and $-\Delta f_A$. When repeated frequency of the pulse is four times the tuning frequency, it can obtain three frequency spectrums when zero phase: a frequency in the center, another in $+\Delta f_A$, and the third in $-\Delta f_A$, in its phase it still can obtain four frequency spectrums.

From this we can see that when using a fixed pulse repeated frequency and a fixed tuning frequency, the tuning spectrum number that is obtained is related to the ratio of the two frequencies, and also is related to the initial phase. When the frequency ratio of the two are simple whole numbers, the frequency spectrums that are obtained also are some fixed frequency spectrums separated by certain frequency differences. But if the frequency ratio of the two are not simple whole numbers, then the frequency spectrums at this time also are again not some fixed frequency spectrums. We can also assume that when the

initial phase is zero, after going through the least common multiple that is equal to the repeated cycle of the pulse and the repeated cycle of tuning, the entire frequency graph will then repeat. For example, when the repeated cycle of the pulse is 900 microseconds, and repeated cycle of the tuning is 1500 microseconds then the entire frequency graph will repeat after 4500 microseconds. In order to obtain the non-repeating frequency graph with the longest possible time, hopefully its least common multiple will be the maximum. By mathematical theory we can know that the least common multiple of these two prime numbers is the product of these two prime numbers. Therefore the desired selected frequency of the pulse and the repeated cycle of tuning are two prime numbers. This is also to say that the ratio of the two repeating frequencies that should be selected is an infinite decimal. There are many numbers that can be selected, but hopefully when the ratio of the two that is made by unstable frequencies generates variation, it still can obtain non-repeating frequency graph with a correspondingly long time. In the fifth chapter it was already explained that some people use electronic computers to compute that the ratio of the repeated frequency of tuning F_m and repeated frequency of the pulse F_p is 0.4388 under general conditions. Although the frequency graph that is obtained at this time still is not completely stochastically agile, we can consider that it is quasi-stochastically agile. In many applications (for example the previously referred to restraining of clutter from sea waves) it is already sufficient.

In order to achieve true stochastic agility it is necessary to use a stochastic signal to carry out modulation on the rotational speed of a motor or frequency of a trigger pulse. The first line of Fig. 7.60 draws a 10 frequency variation cycle within a 10 cavity magnetron tuner rotating one cycle (there also can be 10 frequency variation cycle types of agile magnetrons). The second line gives when the trigger pulse and tuning frequency are completely synchronous, that is they correspond to fixed frequency operational state. When a stochastic signal carries out modulation on the rotational speed of a motor, making the rotational speed of the motor change quickly or slowly, then it makes the repeating frequency of the trigger pulse

remain fixed and invariant, and also can obtain stochastic agility. This motor rotational speed modulation method also can have two achievement methods, one method is a digital coding method, this method is comparatively sensitive, but the design is comparatively complicated. The other method is directly using stochastic noise source after going through a band pass wave filter and a power amplifier, directly driving the tuning motor. It is said, using the latter method, within 20 minutes there will not be a repeating frequency graph.

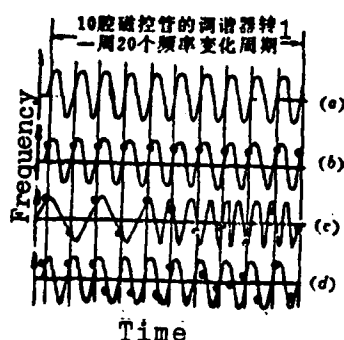


FIG. 7.60 USING A STOCHASTIC SIGNAL TO CARRY OUT MODULATION OF MOTOR ROTATIONAL SPEED OR PULSE REPEATED FREQUENCY TO OBTAIN STOCHASTIC AGILITY
KEY: (a) Variation of anode resonance frequency when rotational tuning; (b) When trigger pulse and tuning frequency are completely synchronous; (c) When tuner rotational speed is slightly slow or slightly fast; (d) When trigger pulse phase or repeating frequency vary; (1) Tuner of 10 cavity magnetron rotating a 20 frequency variation cycle

We can also obtain stochastic agility by using a stochastic signal to carry out modulation on repeated frequency of the pulse. The advantage of this method is not only because the carrier frequency of the transmitting pulse is stochastically agile, but also because its repeating frequency is stochastically agile within a certain range. This even more increases the difficulty of enemy detection and analysis. Its weakness is that there must be very great mobility on the original time system, if we cannot use a partial frequency fixed time system

of a transistor oscillator we must use main oscillator circuits or high frequency transistor oscillator selected partial frequencies. Aside from this, because its repeating frequency is not fixed, therefore we also cannot use signal process techniques that possess fixed delay time wires, for example video frequency accumulation, but this problem can be resolved by digital techniques.

When using stochastic signal to carry out modulation on the repeated cycles of the pulse, the range of its modulation must be limited. After modulation the minimum value of the repeated cycle should be greater than the time interval that corresponds to the maximum operational distance of the radar, to ensure the receiving of backward-wave signals. After modulation the difference between the maximum value and minimum value of the repeated cycle should correspond with half the tuning cycle.

7.5.2 ACHIEVEMENT METHOD OF PROGRAM-CONTROLLED FREQUENCY AGILITY

As the previous section recounts, under many conditions often the desired radar frequency is agile according to a regulated program. This is also to say, it requires that the carrier frequency of a transmitting pulse under radar is determined by the above given directives (voltage or number). This is very difficult to achieve in noncoherent frequency agile radar. This is because most radar of this type uses mechanical tuners, these runners all have very large inertia, therefore there is no way to tune to the assigned frequency in a very short time. Of course, in this type of radar we also can use the method of controlling the trigger pulse instant to achieve program-controlled agility. This is also to say that we are continuously measuring the tuning frequency of the magnetron, and when it is equal to the necessary frequency, we conduct triggering on the magnetron to make it produce the necessary frequency oscillation. Now we will discuss the operational principles of the program-controlled agile frequency system of noncoherent frequency frequency agile radar that is constructed according to this principle. Figure 7.61 draws out the program-controlled agility system of a rotational (or gyrating) tuning magnetron⁽²⁰⁾. In this sys-

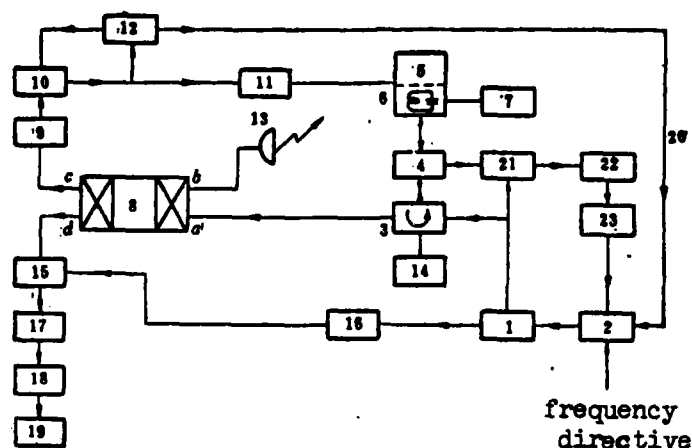


FIG. 7.61 FRAME DIAGRAM OF THE PROGRAM-CONTROLLED AGILE SYSTEM OF A ROTATIONAL (OR GYRATING) TUNING MAGNETRON
 KEY: (1) Voltage tunable oscillator; (2) Frequency controller; (3) Circulator; (4) Coupler; (5) Rotational tuning magnetron; (7) Motor; (8) Dual processor; (10) Trigger circuit; (11) Modulator; (12) Single steady-state trigger circuit; (13) Antenna; (14) Load; (15) Mixer; (16) Local oscillator; (18) Video frequency detector; (19) Display; (21) Mixer; (22) Central release; (23) Mixer

tem, the oscillator of the magnetron is not triggered by a fixed time pulse that comes from a common fixed timer, but is controlled by a frequency measured circuit. This frequency measured circuit uses voltage tunable oscillator 1 as a signal source, the frequency directive of the predetermined program uses the form of analogue voltage to go to frequency controller 2 of this voltage oscillator to cause this oscillator to produce an oscillation of predetermined frequency. This oscillation goes through circulator 3 and coupler 4 to the resonance cavity of the magnetron, when the tuning frequency of the resonance cavity of the magnetron is not equal to the predetermined frequency, most of the energy of this signal will be reflected and after going through circulator 3 goes to dual processor 8. This dual processor possesses this characteristic: the signal that is put in when the input signal power level is fairly low can only be according to the diagonal directional transmission in the figure, then from *a* to *c*, and from *b* to *d*; when the input signal is at a high power level (thus when the magnetron oscillates), it can only be according to the adjacent coming-forward

transmission, from *a* to *b* . Therefore, this low power level reflected signal is passed from *a* to *c* , and after being detected by detector 9 goes to a trigger circuit. When resonance cavity 6 of the agile frequency magnetron is driven by tuning motor 7 and tunes til it is equal to the predetermined frequency that is produced by voltage tuning oscillator 1, the output that is reflected then produces a minimum value. When this negative pulse goes to trigger circuit 10, a trigger pulse is produced, this pulse goes to a modulator 11 to make the magnetron produce oscillation, this in turn can make the magnetron oscillate to a predetermined frequency. Strictly speaking, when the magnetron oscillates, because the existence of the space charge makes its oscillator frequency not equal to the "cold" resonance frequency that is tuned by the resonance cavity, therefore there is also a difference value with predetermined frequency, this requires the frequency control directive that is added to be able to revise and correct in advance the difference of this "cold" and "hot" frequency, to make the frequency of magnetron oscillation accurately equal to the predetermined frequency. In order to prevent the magnetron triggering within the period of receiving the backward-wave, the same time that the trigger pulse that is produced in the trigger circuit 10 goes to a single steady-state trigger, the pulsewidth that is produced by this single steady-state is equal to the farthest backward-wave time interval. This pulse goes through guide line 20 to return to the frequency controller of the voltage tuning oscillator, causing it to not receive new frequency directives in the backward-wave time, the single steady-state does make trigger circuit 10 reduce after the backward-wave time, to await the minimum value of the new reflection. In order to make the receiver able to receive the backward-wave pulse in the backward-wave time, the output of the voltage tuning oscillator simultaneously goes to local oscillator 16, this local oscillator always has one intermediate frequency difference with the voltage tuning oscillator. Actually, if using the magnetron "cold" and "hot" frequency differences as intermediate frequency, this local oscillator is not necessary, we then can directly regard the output of the voltage tuning oscillator as the local oscillator signal. But as is recounted above, because the differences of the magnetron "cold" and "hot" frequency are not constant they can

vary with factors such as different tubes, ageing, and temperature. Moreover, we still hope the intermediate frequency can be equal to the usual chosen numeric value (for example 30MHz and 70MHz), but not equal to the difference of "cold" and "hot" frequency. At this moment we can, after the magnetron pulse transmission, again use an automatic frequency control system to precision tune the local oscillator frequency, and make the difference of it and the reflected frequency strictly equal to the predetermined intermediate frequency. This automatic frequency control system is formed by mixer 21, central release 22, and discriminator 23 in Fig. 7.61. Actually, this automatic control system also can use the various comparatively complicated frequency precision tuning system that is explained in the previous section, making the local oscillator able to even more accurately tune to the correct frequency, and reduce the bandwidth that the intermediate frequency signal occupies.

Actually, after the rotational tuning magnetron was discovered in the 1950's, because there directly was no way to resolve the problem of quick tracking of the local oscillator, there was no way to achieve stochastic frequency agile radar. The earliest thought out program was the program controlled agility method that is explained here. It does not cause the frequency of local oscillator tracking magnetron to vary, but makes frequency of the magnetron that is tuned according to the local oscillator to transmit. Of course, after the technological keys of local oscillator frequency tracking were resolved, applying this method to program-controlled agility still is perfectly useful.

Some shortcomings of the above system also exist. Because it uses the absorption that is produced when the magnetron resonance cavity scans local oscillator frequency as the trigger signals, this sunken wave form state is related to its position on the tuning curve (generally a sine wave). When it is located in the narrowest width of the negative pulse that is produced by the largest place of the tuning slope, the forward edge is steepest. Conversely, when it is located in a fairly small part of the slope of the tuning curve, this sunken forward edge varies slowly and the width widens. Under worst

conditions, when the local oscillator tunes to the edge of the magnetron tuning, this part of the slope of the tuning curve is zero, even so there is no method to produce a trigger pulse. In order to avoid producing this condition, we only can avoid the highest and lowest tuning frequencies, this way also narrows the range of practical, useful, jump frequency. Even though it is like this, because the slope of the tuning curve is not constant, therefore, the wave form of the negative trigger pulse that is formed by this still varies. This makes trigger delay time also unable to remain fixed and invariable. This trigger delay time can give rise to the carrier frequency of the actual transmitting pulse of the magnetron to be different from the frequency of local oscillator tuning. Therefore, the variations of trigger delay time can make this frequency difference produce variations, these variations cannot be eliminated by the method of predetermined compensation, because of this it finally can lead to the carrier frequency of the transmitting pulse to deviate from the predetermined frequency.

Another method of achieving program-controlled agility can resolve this problem. This method does not directly use this absorption wave form as the trigger signal but uses a comparative method of a sine wave that represents the magnetron tuning curve and a certain power level that is determined by the agility program to produce trigger pulse. The analogue voltage that represents the magnetron tuning curve can be obtained by two methods: one method is direct obtainment by the frequency readout device; in a system where no band has frequency readout we can use the second method, the method of tracking the magnetron cold resonance frequency that was introduced in the preceding section. Figure 7.62 is the block diagram of the principles of the program-controlled agility system of the latter method⁽²¹⁾. The local oscillator in the figure is controlled by a frequency tracking system, its operational principles are already explained. It makes the local oscillator search and track the magnetron tuning frequency in the backward-wave time and in a phase time interval before the trigger. When it catches up with the magnetron control frequency, it then can give the voltage that represents the magnetron tuning curve. If we compare this voltage

wave form and a power level determined by any agility program (generally we use a transmitting polar coupling dual steady-state circuit as the power level comparator), when the two power levels are equivalent, it produces a trigger pulse to trigger the modulator, and causes the magnetron to produce oscillation, this way, it can obtain the transmitting pulse of a predetermined frequency. But because the transmitting polar coupling dual steady-state upper trigger power level is generally not equal to the lower trigger power level, therefore there is a stagnation phenomenon. This can give rise to differences in the position of the trigger pulse that is produced when the tuning curve goes through predetermined power level from top to bottom and goes through predetermined power level from bottom to top, thereby causing the transmitting pulse carrier frequency that is produced under these two conditions to also have differences.

In order to eliminate this stagnant phenomenon, this program-controlled system uses a comparatively complicated trigger combination (see Fig. 7.62). The voltage wave form that represents the magnetron curve that comes from the frequency tracker goes to phase adder 13 and is mixed in phase adder 13 with the power level that is determined by the agility program, this power level can come to its own program controller and also can come to its own noise generator. The voltage that is put out by the phase adder is divided into two circuits: one circuit goes directly to transmitting polar coupling dual steady-state 15; the other circuit thus goes to phase adder 16, after going to a revision and correction voltage that is equal to the top and bottom trigger power level difference values of the transmitting polar coupling dual steady-state in phase adder 16, it again goes to transmitted polar coupling dual steady-state 18. Transmitting polar coupling steady-state 15 and transmitting coupling dual steady-state 18 possess completely identical circuits, and select transistors with identical parameters to make the two possess identical top and bottom trigger power level differences. The wave form that is put out by transmitting polar coupling steady-state 18 after going through differentiation goes to "OR" gate 22, the voltage wave form that is put out by transmitting polar dual steady-state 15 thus after first going through inversion in the inverter is again carried to the

differentiator for differentiation and to "OR" gate 22. This "OR" gate 22 is controlled by the frequency tracker, so that it closes within this searching time when the backward-wave time ends and goes to the local oscillator to begin tracking. It also causes the magnetron to be unlikely to erroneously trigger within this time. The trigger signal that is given by "OR" gate 22 goes to blockage oscillator 24 to produce the triggered pulse that is needed, this trigger pulse is respectively carried to the magnetron tuner and program controller to provide trigger use.

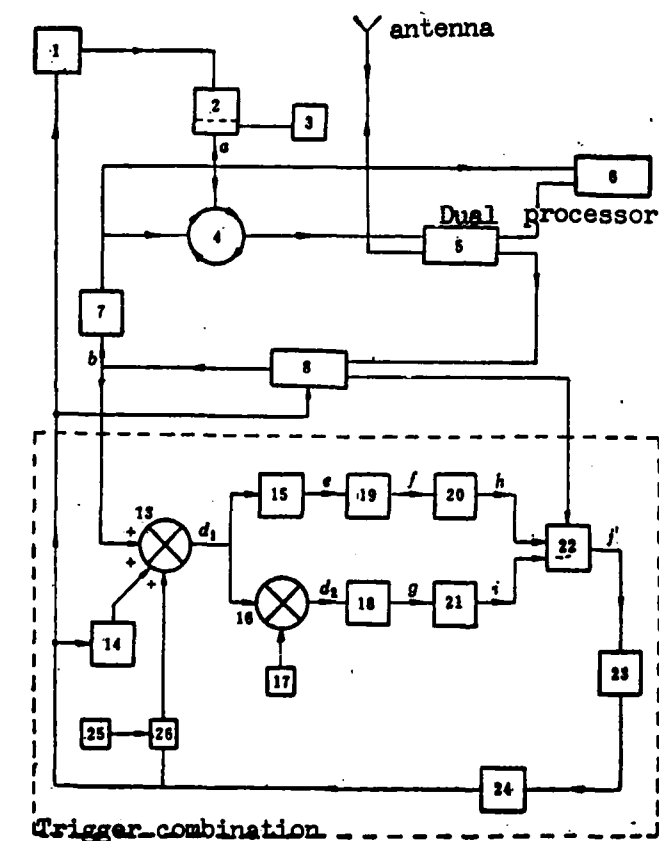


FIG. 7.62 BLOCK DIAGRAM OF THE PROGRAM-CONTROLLED JUMP FREQUENCY THAT USES THE METHOD OF POWER LEVEL COMPARISON TO PRODUCE TRIGGER PULSE

KEY: (1) Modulator; (2) Magnetron; (3) Tuning motor; (4) Circulator; (5) Dual processor; (6) Receiver; (7) Local oscillator; (8) Frequency tracker; (13) Phase adder; (14) Program controller; (15) Transmitting polar coupling dual steady-state; (16) Phase adder; (17) Revision and correction voltage source; (18) Transmitting polar coupling dual steady-state; (19) Inverter; (20) Differentiator; (21) Differentiator; (22) OR gate; (23) Amplifier; (24) Blockage oscillator; (25) Noise generator; (26) Voltage generating state

We will now take a look at the operational principles of the entire system. The relationship and wave form of the time of each part is as Fig. 7.63 shows. In the figure (a) represents the magnetron tuning curve, and f_1 , f_2 , and f_3 are the three predetermined frequencies that are determined by the agility program. In the figure (b) is the control voltage wave form that is given by the frequency tracker. This control voltage wave form realistically also represents the variation of local oscillator frequency. (c) in the figure is the program-controlled frequency directive voltage that is produced by the frequency program controller. In the figure (d) has two curves, in it the solid line d_1 represents the voltage wave form that goes to transmitting coupling dual steady-state 15 that is given by phase adder 13, while the dashed line d_2 represents the voltage wave form that goes to transmitting coupling dual steady-state 18 that is given by phase adder 16. (e) and (f) in the figure are the wave forms after the wave forming and inverting of the output of the transmitting coupling dual steady-state 15. In the figure (g) is the wave form of the output of two differentiators. (j) in the figure is the output of "OR" gate 22, and also is the wave form that goes to blockage oscillator 24 to form the trigger pulse. The positions of each wave form in the whole system are already marked in Fig. 7.62.

If we take t_0 as the time that the magnetron tuning curve center frequency f_0 corresponds to, the first trigger pulse that is determined by the frequency agile program is f_1 . The control voltage directive that this frequency corresponds to is V_{t1} (it is necessary to note that the specific numeric value of this control voltage not only should consider voltage value that the frequency tracker gives and the trigger power level value of the transmitting coupling dual steady-state, but also should correspond to revision according to the magnetron "cold" and "hot" frequency difference value). Voltage (b) that comes from the frequency tracker and directive (c) that comes from the program controller after phase adding in phase adder 13 are carried to two transmitting polar coupling dual steady-states. If the upper trigger power level of the transmitting coupling dual steady-state is V_{s1} , the power trigger power level is V_{s0} , its difference value is approximately 100 millivolts. After this difference value is produced by voltage source 17 it goes

through phase adder 16 and goes to input voltage d_1 . Therefore input voltage d_2 that goes to transmitting coupling dual steady-state 18 must be somewhat higher (100 millivolts higher) than the input voltage d_1 that goes to transmitting coupling dual steady-state 15.

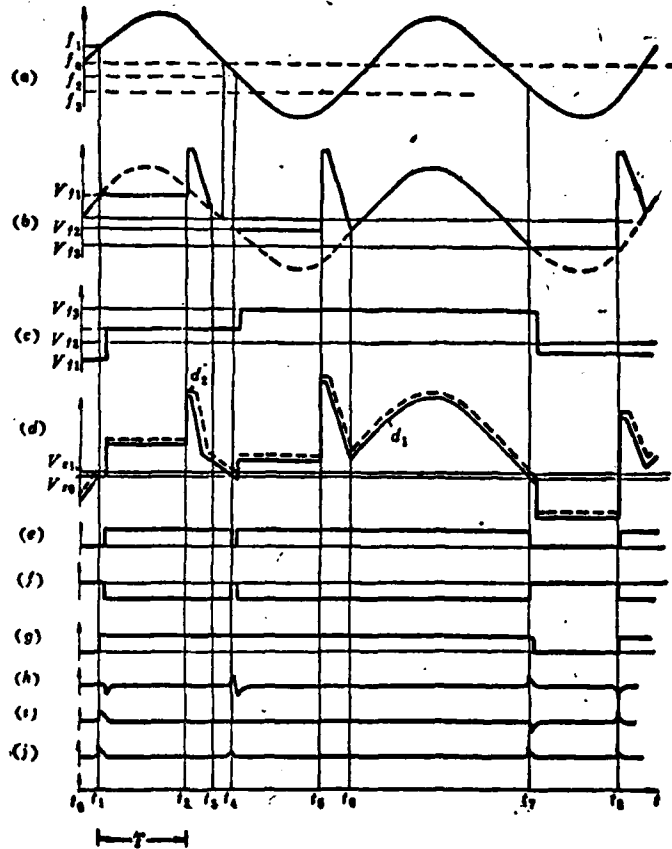


FIG. 7.63 CHART OF RELATIONSHIP AND WAVE FORM OF THE TIME OF EACH PART OF THE POWER LEVEL COMPARISON PROGRAM-CONTROLLED AGILITY SYSTEM

Therefore, transmitting polar coupling dual steady-state 18 will reach voltage V_{f1} that frequency directive f_1 corresponds to and is triggered before transmitting polar coupling dual steady-state 15. Presuming its trigger time is t_1 , the positive voltage jump change that it produces (see the first positive jump change in (g) of the figure) after going through differential circuit 21 produces a positive pulse (see the positive differential pulse in (i) of the figure). After this positive differential pulse goes through "OR" gate 22 it goes to the blockage

oscillator to form the trigger pulse. One circuit of the trigger pulse is carried to the modulator to make the magnetron produce oscillation with frequency as f_1 . Another circuit goes to the program controller to produce new frequency directives. These new frequency directives are f_2 , the corresponding voltage is V_{f2} . It is necessary to note that the wave form of this directive voltage is opposite of the expected frequency wave form phase. If the frequency drops from f_1 to f_2 it is a negative jump change, the voltage directive changing from V_{f1} to V_{f2} then is a positive jump change. This primarily is because the trigger power level of the transmitting coupling dual steady-state is fixed and invariable. When the voltage that represents the tuning curve drops, it must raise with its phase added frequency control directive voltage, then it can mutually compensate and make the transmitting coupling dual steady-state to trigger. After t_1 triggers, the control voltage that represents local oscillator frequency then locks on V_{f1} and is invariant. But after t_1 eliminates a little time, the program-controlled voltage jumps to V_{f2} , therefore, the output voltage after phase adder 13 also jumps up. At this time, transmitting coupling dual steady-state 15 is also triggered. But it causes its output wave form to go to the differential circuit after going through inversion. Therefore, after differentiation there is a negative pulse, and "OR" gate 22 can only go through a pulse of positive polarity, it cannot go through a pulse of negative polarity. Therefore the turning around of the transmitting coupling dual steady-state 15 cannot make blockage oscillator 24 trigger. After going through backward-wave time, the local oscillator of time t_2 jumps to the highest frequency (higher than the tuning frequency of the magnetron), it begins towards searching, time t_3 and the tuning frequency of the magnetron meet, and immediately begin to turn into the tracking state. Because the voltage that goes to transmitting coupling dual steady-state 15 must be 100 millivolts lower than the voltage that goes to transmitting coupling dual steady-state 18, therefore wave form d_1 first goes down to trigger power level V_{s0} and makes transmitting coupling dual steady-state 15 turn. The lower jump change of its output voltage after going through inversion changes into a positive jump change, the positive pulse after differentiation is carried to blockage oscillator 24 to form the trigger pulse after going through "OR" gate 22. This trigger pulse

is carried to the modulator to trigger the magnetron, the oscillator frequency that is produced by the magnetron is exactly equal to directive frequency f_2 . This trigger pulse at the same time is carried to the program controller, the program controller, after going through a very small delay time, immediately gives out three frequency directive voltage V_{f3} . Because this delay time is extremely small, therefore wave form d_2 still did not reach lower trigger power level V_{s0} and follows the upper jump, transmitting coupling dual steady-state 18 also does not have enough time to turn around and come back, but continuously stays at the 1 condition. Because these transmitting coupling dual steady-states have extremely small recovery times, therefore transmitting coupling dual steady-state 15 very quickly follows the upper jump, but, because after its inversion it is a negative pulse, therefore there is no trigger signal output. To the end of time t_5 backward-wave time, the local oscillator again begins to search, until t_6 turns into the tracking state. When going to time t_7 , d_1 reaches the lower trigger power level, the transmitting coupling dual steady-state firstly jumps down, after inversion the output produces a positive trigger signal. This causes the transmitting frequency of the magnetron to be the pulse of f_3 . After going through a little delay time, the program controller again gives out new frequency directives. The entire process continually goes on.

We can see that whenever the tuning curve meets from bottom to top with the frequency directive voltage, transmitting coupling dual steady-state 18 firstly triggers, because its input already goes up to a difference value of 100 millivolts, therefore it realistically is intersecting on the lower trigger power level; whenever the tuning curve meets from top to bottom with the frequency directive voltage, transmitting coupling dual steady-state 15 firstly triggers, and also is triggering on the lower trigger power level. Therefore, actually all frequency directive voltage takes the lower trigger power level as standard, this eliminates the influences that are produced by the top and bottom trigger stagnation.

The program controller is generally composed of a logical circuit,

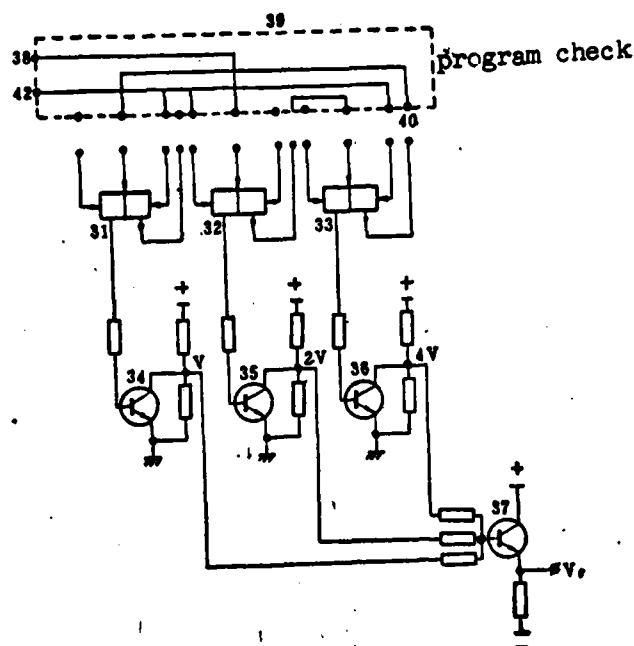


FIG. 7.64 A MOST SIMPLE ACHIEVEMENT PROGRAM OF A PROGRAM CONTROLLER

it can have many achievement programs. Figure 7.64 gives a most simple achievement program. In it 31, 32, and 33 are dual steady-state triggers, 34, 35, and 36 are voltage generators. 37 is the phase adder. The triggers have two states, the "0" state and the "1" state. When they are in the "0" state, the output is at a high electric potential, conducting from the voltage generator transistor; when they are in the "1" state it is opposite. When the transistor of the voltage generator conducts, its output is 0 voltage; conversely, when it stops, output is at a high electric potential. Its output voltage is determined by the voltage divider, in it 34 outputs are V volts, 35 outputs are 2V volts, 36 outputs are 4V volts. After going through the same phase adding resistance these voltages are 37 outputs from the transmission tracker. This way, the final output voltage V_r is determined by each trigger. In each trigger there are 33 output ends (unit "0" unit "1", and computer input), and an output end. These input and output ends are interlinked together through printed circuit board 39 that is called a program check. The program check has two inputs, one input is a trigger signal through 38 input, the other is a unit zero signal from 42 input, these two inout signals, after going through the printed circuit of the pro-

gram check, are linked through plug 40 and fixed contact 41. In the program check that is shown in the figure, the trigger signal goes to trigger 32, and trigger 32, 33 and 31 thus cascade, the output of trigger 32, after going through the program check, receives the computed input of trigger 33, and the output of trigger 33 receives the computed input of trigger 31. The linkage of the signal of unit "0" thus is to make trigger 31 unit "1", making triggers 32 and 33 unit "0".

The operational principles of the entire system are this way: when in the initial state, because only trigger 31 is located in "1" state, therefore the output voltage of transmission tracker 37 is V volts. When the voltage that represents the tuning curve intersects with it, it immediately produces a trigger pulse. On the one hand this trigger pulse is carried to the trigger magnetron, on the other hand it makes trigger 32 change from 38 into "1" state, therefore this voltage generator 35 puts out 2V volts voltage, and after the original V phase adding, obtains 3V voltage output. After this voltage and the tuning curve intersect, a trigger pulse is again produced. This trigger pulse makes trigger 32 change to "0" and 33 change to "1", thus output voltage changes into 5V; the next time one trigger pulse can obtain 7V voltage. The fourth trigger pulse makes trigger 32, 33, and 31 all change to "0" and obtain 0V output, and later can obtain an array of 2V, 4V, and 6V. This way, so long as the linkage form of the printed circuit that changes the program check can obtain the output voltage of a specially designated order, increasing the number of triggers can obtain even more operational frequency amounts. If we use an even more complicated logical circuit then we can obtain an even more complicated frequency form.

If we need to achieve stochastic agility, then we can use noise generator 25 (Fig. 7.62) and go to a voltage generating stage. This voltage generating stage in the trigger pulse instant carries out sampling on the noise voltage, and in the backward-wave time goes directly

down to a trigger pulse period to ensure that this sampling value is invariable. After this sampling value goes to a phase adder 13 and compare with the tuning curve voltage, it can then obtain stochastic agility.

A primary shortcoming of using this power level comparison method to achieve program-controlled agility is simply that its transmitting pulse carrier frequency is determined by using analogue voltage comparison, therefore if the voltage that the program controller produces generates drift, or when the trigger power level of the trigger follows the variations of temperature and power source voltage, there is a possibility to make the frequency of the transmitting pulse carrier frequency unable to stably remain a predetermined value, that is, a certain predetermined frequency of this transmission can have differences from the same predetermined frequency that is transmitted after going through a phase time. This frequency instability can become a primary problem in certain applications, for example when the responder or the identifier between the enemy and ourselves in the aircraft link, then it requires a fairly high frequency stability. Under this condition, we can use another program-controlled agile program that uses a cavity system to select frequency.

Figure 7.65 draws a block diagram of the program-controlled agile system of a cavity-selected frequency. Its operational principle is like this: the output of the voltage tuning local oscillator, after going through wave guide system 50, couples to cavity resonators 46, 47, 48, and 49. These resonance cavities tune on the necessary frequency, its specific number can be determined according to actual needs. These resonance cavities attach to each automatic detector 51, 52, 53, and 54. The output of these detectors link to gates 55, 56, 57, and 58. The switches of these gates are controlled by program controller 59. The output from these gates goes to "OR" gate circuit 60, the switch of this "OR" gate is controlled by local oscillator frequency tracker. When the local oscillator enters into the "cold" resonance frequency of the tracking magnetron, the frequency tracker gives a control signal to "OR" gate 50, to make this "OR" gate open. The program controller then selects certain cavity resonators according to the transmitting frequency that is

determined by the agile program, gives a gate control pulse, and the gate circuit of this circuit will open. When local oscillator frequency (also simply the "cold" resonance frequency of the resonance cavity of the magnetron) is equal to (actually is scanned) the frequency of this cavity resonator, the detector that is attached by this resonance cavity gives out a pulse, after going through its corresponding circuit and "OR" gate circuit 60 goes to amplifier 61 to carry out amplification, the pulse after amplification goes to a blockage oscillator to form a trigger pulse. One part of this trigger pulse is carried to the modulator to make the magnetron produce oscillation, another loop is taken to the program controller to provide new frequency directives to open the gate circuits that are related to it. Because this trigger pulse is formed according to the frequency of the voltage tuning local oscillator and mutual coinciding of the resonance frequency of the cavity resonator, and also is related to the trigger voltage, but only is determined by the geometric dimensions of the resonance cavity, therefore the transmitting pulse that is determined by this also has fairly high frequency stability. But it necessary to note that the frequency of actual oscillation of the magnetron is not completely equal to the cavity resonance frequency, and has difference of "cold" and "hot" frequency. Although this difference value can be revised and corrected in advance, as is previously recounted, due to various factors it can make the difference of the magnetron "cold" and "hot" frequency generates variation. This variation still can cause actual transmitting frequencies to deviate from the predetermined frequency. This factor also exists in the program-controlled agile system of the above-mentioned power level comparison method, therefore the method of using the cavity to select the frequency primarily can eliminate frequency instability that is brought about by power level instability in the power level comparison method.

Obviously using the program-controlled agile system of whole number form also can resolve the instability problem in analogue type program-controlled agile systems.

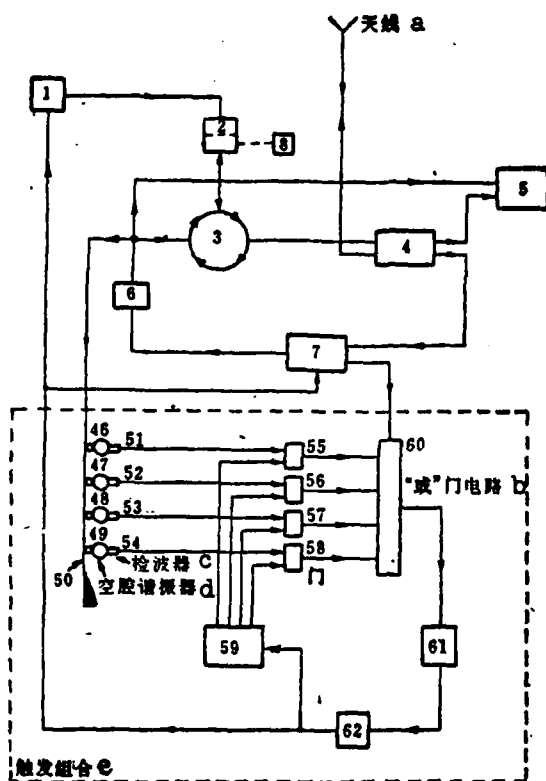


FIG. 7.65 BLOCK DIAGRAM OF PROGRAM-CONTROLLED AGILE SYSTEM OF CAVITY-SELECTED FREQUENCY
 KEY: (a) Antenna; (b) "OR" gate; (c) Detector; (d) Cavity resonator; (e) Trigger combination; (1) Modulator; (2) Magnetron; (3) Circulator; (4) Dual processor; (5) Receiver; (6) Voltage tunable local oscillator; (7) Frequency tracker; (8) Tuning motor; (59) Program controller; (61) Amplifier; (62) Blockage oscillator

7.5.3 STOCHASTIC AGILITY SYSTEM TO CONTROL FIXED FREQUENCY JAMMING

In frequency agile radar, although we can use high speed pulse stochastic agility, we still can receive the jamming of fixed frequency jamming. This is because stochastic agility has uniformly distributed emergence probability in the entire agile bandwidth, therefore as to fixed frequency stability we can say that stochastic agile radar tunes to exactly the probability on the jamming slope and is equal to the ratio of jamming bandwidth and agile bandwidth, for example if the rotational speed of this radar is 6 turns each minute, the repeating frequency of the pulse is 400Hz, if altogether 4000 pulses are trans-

mitted in the rotational cycle of the antenna, when the probability that jamming will occur is 0.05, on the plane position indicator, 200 root interval light lines can emerge. This can severely jam noise personnel discovering and tracking targets on the screen. Therefore it is necessary to make the agile transmitting pulse of the radar to avoid this jamming frequency. But in noncoherent stochastic agile radar, transmitting frequency of the radar has no method of control, the only method is to think of a way to control jamming on the receiver.

The block diagram of the entire system is shown in Fig. 7.66⁽²²⁾. For the purpose of simplification, its local oscillator automatic frequency control system is expressed as frequency tracker. This frequency tracker can cause the local oscillator to track the magnetron "cold" resonance frequency in a phase time before triggering, and after triggering then accurately tunes to one intermediate frequency higher than the oscillator frequency of the magnetron, and directly goes until backward-wave time ends. The video frequency signal that the receiver puts out goes to a video accumulator to carry out accumulation. The accumulator actually is an RC integrated circuit, others have fairly small discharge time constants, if it is smaller than the discharge time constant of the backward-wave time, it can go to a discharge before the trigger after the backward-wave ends. The output of this accumulator goes to a single steady-state trigger circuit, when jamming signals in the accumulator accumulate past a certain power level, then the trigger single steady-state causes it to turn around. Because the discharge time constant of the integrator is very short, therefore the backward-wave pulse is unlikely to make the output of the accumulator large enough to make single steady-state triggering. After single steady-state triggering it opens gate 18, and makes the local oscillator frequency control voltage that represents this cycle go through gate 18 into the memory circuit to be stored. Because local oscillator frequency has only one intermediate frequency difference from the transmitting frequency, therefore this voltage also can represent the transmitting frequency at this time, and also is the frequency of the jamming signal. This memory circuit has an extremely great discharge time constant, for example it has a discharge time constant that corresponds to 100 repeating cycles. Therefore, the voltage that represents jamming fre-

quency also can be stored this long of a time. This voltage that is stored goes to another comparing circuit and is compared with the voltage of the transmitting pulse carrier frequency after the representation of the automatic frequency controller, when the two are the same its output causes gate 21 to close. This comparing circuit is shown in Fig. 7.67. It is composed of two transmitting electrode transistors, its collecting electrode goes to a power level comparator after going through two diodes. When the basic voltage that goes to the two tubes is not equal, a tube with fairly high basic voltage will conduct, and the other tube will close due to the voltage decrease of the former on the shared transmitting polar resistance. At this moment, the voltage in the comparator will be determined by the tube with a comparatively high collecting electrode voltage, thus be determined by the collecting electrode voltage of the closed tube. When the basic voltage of the input that goes to the two tubes is equal, this is also when transmitting pulse carrier frequency is equal to jamming frequency, at this moment the two tubes simultaneously conduct, and output voltage is minimal. The voltage from the comparator output again goes to a control gate circuit 21 of the trigger that exerts density properties on the power level sensitivity, the video frequency signal that the receiver puts out goes through this gate circuit to the indicator. When the voltage of the comparing circuit output is minimum (this is also when the transmitting pulse carrier frequency is equal to the jamming frequency), gate 21 closes, causing the jamming signal that is received by the receiver to have no way to be carried to the indicator. This then completes the task of controlling jamming.

If the bandwidth of the jamming signal is wider than the bandwidth of the receiver, it can decrease the sensitivity of the comparator, and make it also able to move on the two input signals that are close to equal but not completely equal. At this time it can control the jamming signal that possesses a certain bandwidth. But if possessing a different jamming signal that does not stop a frequency within the frequency agile range, then a certain problem exists in the operations of this system. At this time, if what is stored in the memory circuit is the frequency of the first jamming stage, when the receiver tunes to the frequency of the second jamming stage, this jamming signal

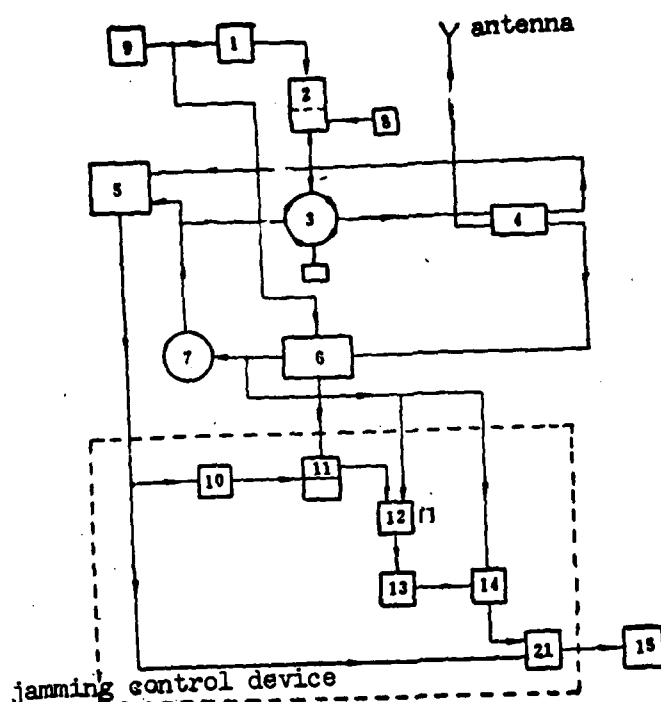


FIG. 7.66 JAMMING CONTROL DEVICE OF STOCHASTIC FREQUENCY AGILE RADAR

KEY: (1) Modulator; (2) Magnetron; (3) Circulator; (4) TR Switch; (5) Receiver; (6) Frequency tracker; (7) Voltage tuning local oscillator; (8) Tuning mechanism; (9) Trigger pulse source; (10) Accumulator; (11) Single steady-state; (12) Gate; (13) Memory circuit; (14) Comparator; (15) Display; (21) Gate

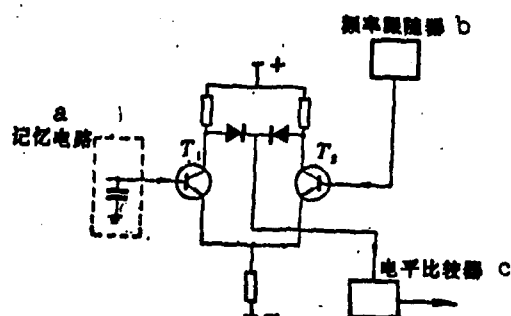


FIG. 7.67 DIAGRAM OF PRINCIPLES OF JAMMING FREQUENCY COMPARATOR
KEY: (a) Memory circuit; (b) Frequency tracker; (c) Power level comparator

then will go through gate 21 to the display. At the same time, the memory circuit will record the frequency of the second jamming stage. If the receiver still tunes to the frequency of the second jamming stage the next time, the jamming signal still can be restrained; conversely, if the receiver tunes to the frequency of the first jamming stage the next time, then this jamming signal still goes through gate 21 to the display. However, no matter what, after going to this jamming control circuit, when there are some different frequency jamming signals, it causes it to still have a certain jamming restraint effect. It only is the effect to eliminate the difference thereafter. As a matter of fact, using similar principles, so long as additionally using an appropriate logical control circuit, then it is completely possible to record several jamming stage frequencies, and we can restrain the jamming signals of these different frequencies.

Reference Material:

- (1) Local oscillators for frequency agile systems. P. Weinglas, and S. Svensson. Microwave J. 1977, Jan. p. 35.
- (2) Guidelines for using BWOs. J. Phillip. Microwave J. April, 1969. p. 77.
- (3) Choosing and Using BWO. A. T. Isaacs, B. F. Helms, Microwaves, March, 1966. pp. 28~34.
- (4) Think young with agile YIG and Varactor tuning. O. T. Robert, R. E. Brown. Microwaves, Dec. 1972.
- (5) GaAs FETs rival Gunn in YIG-tuned oscillators, T. Ruttan. Microwaves. July, 1977. pp. 42~48.
- (6) Microwave integrated oscillators for broadband high-performance receivers. IEEE Trans. Vol. MTT-20, No. 2. pp. 155~184.
- (7) Building an Oscillator Lump it, and like it. C. A. Bissegger. Microwaves. July, 1978.
- (8) VCO's in modern ECM Systems. R. N. Buswell. Microwave J. May, 1975. pp. 43~46.
- (9) Evaluating tuning response of VCO subsystems. K. R. Schoniger. MSN, July, 1977.
- (10) Let's clear up the confusion on PTD. A. Shipow. MSN April, 1977.
- (11) Single pulse AFC system. J. G. Isabeau, IRE Int. Conv. Rec. 1961 pt. 5 p. 278.
- (12) Radar sending installation. M. G. Disselen, U. S. Pat. № 3, 528, 071.
- (13) Device for regulating the frequency of an oscillator substantially in coincidence with variations in the natural frequency of a resonance circuit. B. O. As. U. S. Pat. № 3, 249, 937.
- (14) Means for correcting the local oscillator frequency in a radar system. U. S. Pat. № 3, 290, 678.
- (15) Device for frequency correction in a radar equipment. N. R. Carlsson. U. S. Pat. № 3, 611, 380.

- (16) Frequency agile local oscillator. J. B. Fuller. Microwave J. May, 1974, p. 31.
- (17) Subsystem approach to improvement in radar performance by frequency agility. J. B. Fuller. 73 Israel Conv. IEEE. 1/III~9/III.
- (18) Automatic frequency control circuit for frequency agile radar. E. J. Kolp, G. W. Harrington. U. S. Pat. № 4,023,169.
- (19) Automatic frequency control for frequency agility radar system. M. Selvin. U. S. Pat. № 3,413,634.
- (20) Radar transceiver device. U. S. Pat. № 3,168,736.
- (21) Device for generating high frequency pulses having a predetermined frequency by means of a continuously tunable magnetron. N. A. E. Wasterlid. U. S. Pat. № 3,358,282.
- (22) Device for disturbance suppression in a radar equipment. E. S. H. Borg. U. S. Pat. № 3,365,718.

CHAPTER VIII

THE STRUCTURE OF FULLY COHERENT FREQUENCY AGILE RADAR

8.1 GENERAL ACCOUNT

So-called fully coherent radar refers to the "coherence" of the transmitting pulse carrier wave and the local oscillator of the receiver when maintaining a strict phase relationship, this can make the backward-wave signal and the local oscillator signal after mixing still able to maintain their phase information. Therefore the transmitting carrier frequency signal of fully coherent radar and the local oscillator signal of the receiver must be produced by the same highly stable signal source (generally a transistor oscillator). This is also to say that the transmitter of fully coherent radar cannot use a high powered self-driving oscillator with very poor stability (such as a magnetron), and must use a master oscillator power amplification chain type (MOPA), using a high frequency signal of high stability and low power level that the transistor oscillator will produce, after going through multiple frequency amplification to a sufficiently high powered power level, again transmits.

In this fully coherent radar, because the wave form of the transmitting pulse is formed in the low power level, therefore it is possible to select each complicated wave form design (for example linear frequency modulation (FM) pulse, phase coding pulse, etc.) according to the technological requirements for military tactics, to obtain a fairly ideal signal vague plan function under certain conditions to improve the ability to identify radar distance and speed. Aside from this, because this radar can keep the Doppler information in the backward-wave signal (although receiving coherent or quasi-coherent radar can also keep it, its stability is much poorer than fully coherent), therefore it can achieve the pulse Doppler system for the purpose of accurately measuring the radial speed and restraining the strong surface features clutter. The main oscillator signal of fully coherent radar, after going through amplification and suitable power matching, can

go to the extreme power amplification stage of many parallel connections, and from this obtains many identical high power signals to drive the active phased array antenna. Therefore, the application of fully coherent radar systems extend to pulse compression, pulse Doppler, and phased array.

Like noncoherent radar, the greatest weakness of fixed frequency fully coherent radar is that jamming control is poor. Moreover, the main oscillator of early fully coherent radar was composed of a simple transistor oscillator and multiple frequency level, the carrier frequency of its transmitting pulse was completely fixed and untunable. Therefore its jamming control was even poorer than that of using a mechanical tuning magnetron. Later, although some different operational frequencies could be obtained by replacing with transistors or using fairly complicated frequency multiplication system, its jamming resistance still has not obtained basic improvement. Fully coherent radar will only obtain a very strong ability to resist jamming after true pulse jump frequency is achieved. Moreover, because the operational frequency of fully coherent frequency agile radar uses a digital technique for control, therefore it causes it to possess even greater agile sensitivity than noncoherent frequency agile radar, and can achieve even more complicated and exquisite program-controlled agility and self-adapting agility.

Figure 8.1 is a block diagram of early fully coherent frequency agile radar by the Emerson company of America⁽¹⁾. This radar uses several hundred transistor oscillators, these oscillators operate to close to 10MHz, but the frequencies are separated by very small intervals. Through a digital control logical circuit it can quickly select the output of an arbitrary oscillator in it. Therefore, using quasi-stochastic binary control we can obtain the linking wave signal of stochastic agility. Because these signals all are produced by transistor oscillators, therefore although using high speed agility of the repeated frequency of the pulse, the frequencies in each repeated cycle are all highly stable. The linking wave of this jump frequency goes through the appropriate solid frequency multiplier to the operational frequency of our radar. The output of the frequency multiplier has milliwatt magnitude, the signal of this low power level goes

to a traveling wave tube amplifier with a gain of 30dB to be amplified as a linking wave of watt magnitude. The output of this linking wave traveling wave is divided into two circuits: one circuit is carried down to a level traveling wave tube amplifier to be further amplified; the other circuit obtains the signal of the first local oscillator after going through a fixed directional coupler to take out a small part and mix with the first intermediate frequency transistor oscillator. The next traveling wave tube amplifier is a grid control pulse amplifier with a 30dB gain. After the grid of this traveling wave tube goes to the control pulse, it can obtain a pulse of kilowatt magnitude peak power in its output end. This medium-powered pulse then goes to the cross field power amplifier where the extreme gain is 20dB, after being amplified to 100kW it is carried through the circulator to the antenna and is transmitted out. The weak backward-wave signal that is received by the antenna is first amplified through a wideband tunnel diode low noise amplifier. Later it goes through a similar frequency control wave filter to the first mixer. The first mixer uses upper lateral band mixing, when transmitted frequency is f_s , and the first intermediate frequency is f_{01} , then the signal of the first local oscillator is $f_s + f_{01}$, after this local oscillator signal mixes in the first mixer with received f_s , it can obtain the first intermediate frequency signal with frequency as f_{01} , this first intermediate frequency signal is carried to the second mixer after going through amplification. The local oscillator signal of the second mixer is obtained after the second intermediate frequency transistor oscillator and the first intermediate frequency transistor oscillator mix in the upper lateral band, frequency is $f_{01} + f_{02}$, after the signal of this second local oscillator and first intermediate frequency signal mix, we can obtain the second intermediate frequency signal with frequency as f_{02} . After the second intermediate frequency goes through amplification, it is carried to the phase detector. The other circuit input of the phase detector is the output of the second intermediate frequency transistor oscillator. The output of the phase detector is carried to the lower signal processor and display.

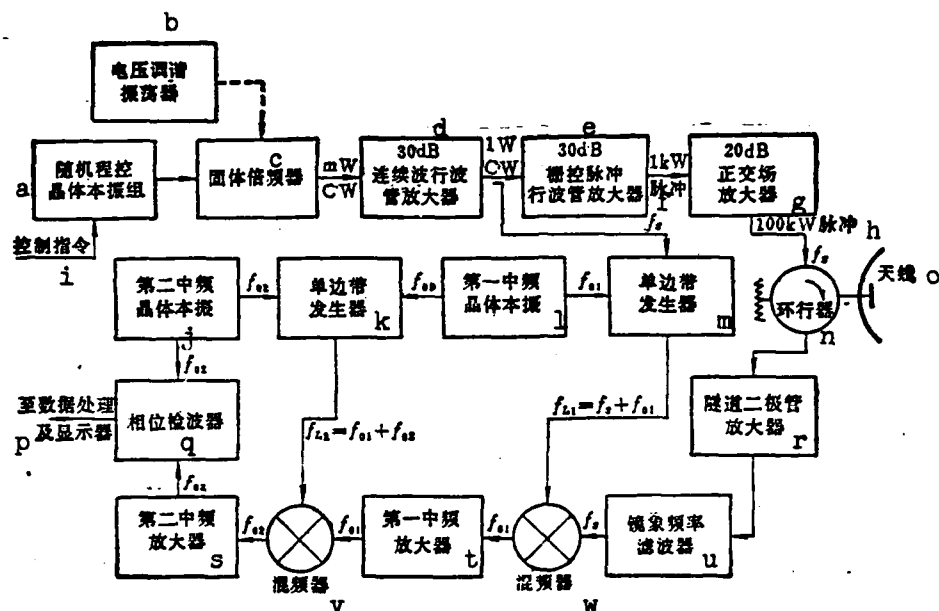


FIG. 8.1 BLOCK DIAGRAM OF FULLY COHERENT FREQUENCY AGILE RADAR

KEY: (a) Stochastic program-controlled transistor local oscillator group; (b) Voltage tuning oscillator; (c) Fixed frequency multiplier; (d) Linking wave traveling wave tube amplifier; (e) Grid control pulse traveling wave tube amplifier; (f) Pulse; (g) Cross field amplifier; (h) Pulse; (i) Control directive; (j) Second intermediate frequency transistor local oscillator; (k) Unilateral band generator; (l) First intermediate frequency transistor local oscillator; (m) Unilateral band generator; (n) Circulator; (o) Antenna; (p) to data processor and display; (q) Phase detector; (r) Tunnel diode amplifier; (s) Second intermediate frequency amplifier; (t) First intermediate frequency amplifier; (u) Tunnel frequency wave filter; (v) Mixer; (w) Mixer

Although fully coherent frequency agile radar generally can only be agile on a series of fixed frequencies, so long as the number of fixed frequencies is ample, that is, the frequency intervals are close enough, then as to its performance we can say that it corresponds to radar that can be continually tuned. What is even more important is that because its agility is completely achieved by using the electron form, and moreover still uses digital control, therefore its agile adaptability is much higher than noncoherent frequency agile radar that uses a magnetron. It can determine the selected arbitrary dispersed

frequency in the instant before the next trigger. Therefore it is possible to achieve even more complicated frequency agile radar, for example moving target indication radar, self-adapting frequency agile radar, etc.

Fully coherent frequency agile radar is much more complicated in design than non-coherent radar, therefore it is primarily used in radar with higher requirements. Table 8.1 lists the technological indexes of fully coherent frequency agile radar of several different uses and types⁽²⁾. From the table we can see that fully coherent frequency agile radar is extensively used in various different uses and types of radar from small scale to super long range, in military and civilian use, ground and airborne, fixed and moving. We can say that the newest designs of high performance military radar are almost all fully coherent frequency agile models.

8.2 MICROWAVE FREQUENCY SYNTHESIZER

The heart of fully coherent frequency agile radar is the microwave frequency synthesizer of a fully coherent digital control. This frequency synthesizer must be able to produce an ample number of highly stable dispersed spectrum lines on the frequency band that is operated by the radar. These spectrum lines must have both extremely high frequency spectrum purity and be able to use microsecond speed to quickly convert between them.

When in earlier times a frequency agile synthesizer that possessed high speed agile ability still had not been developed, a comb form spectrum line generator was extensively used, its operational principles are as Fig. 8.2 shows. After the highly stable signal that is produced by the transistor oscillator goes through powerful amplification, it goes to a step diode tuning generator, producing a series of comb form tuning waves. After going through the selected frequency of a yttrium iron garnet (YIG) magnetic tuning wave filter with this comb form tuning wave, it goes to the backward-wave tube oscillator and empties into phase lock. The frequency agile control directive is

TABLE 8.1 SOME DIFFERENT USES OF FULLY COHERENT FREQUENCY AGILE RADAR

Model #	ARSR-3	AN/TPS-43	AN/FPS-85	AN/APQ-140
Use	Air route lookout	Mobile 3 co-ordinate guide	Super long-range space lookout	Multiple function Aircraft carrier
System	Dual Beam, 2 coordinate	Multiple beam	Pulse compression, phased-array	Monopulse, phased-array
Affected Distance	>200 nautical miles (2M ²)	260 nautical miles (5M ²)	Satellite distance	
Wave Phase	1250-1350 MHz	2900-3100 MHz	442±5MHz	±5%
Agile Frequency number	39	16	51	
Moving Target Indication	Tripulse, cancelled out	Digital form, quadpulse, cancelled out	Digital form	
Polarization	Linear and Round	Perpendicular		Linear and Round (Right and left)
Antenna Gain	34.5dB, 33.5dB	38dB (lowest)		
Beam Form	Fan-shaped	6 beams	Pointed	C SC ² , fan shaped and pointed
Angle degree cover	60 kiloinch to 40°	10 kiloinch 20°	120° (bearing) 105° (angle of elevation)	+70° (bearing, angle of elevation)
Beam Width (level)	1.2°	1.1°	1.4° (transmitted) 0.8° (received)	
(perpendicular)			1.4° (transmitted) 0.8° (received)	
Scanning rate	5cycles/min.	6cyc/min.	20 frames/sec.	4500°/sec.
Peak Power	5MW	4MW	32MW	1.2kW
Average Power	3.3kW	6.7kW	160kW	160kW
Pulsewidth	2.0μs	6.5μs	1,5,10,16,25, 32,64,125,128, 250	
Repeated Frequency	310-364 8	250(average) 6		

firstly carried into a jump frequency control signal generator, this generator produces two control signals: a control signal going into a backward-wave power source to make the backward-wave tube oscillate to near the frequency that was assigned; and a control signal used to control the YIG magnetically tunes wave filter to select the necessary harmonic wave. This harmonic wave signal after going through a circulator goes to a backward-wave tube oscillator. The phase locked bandwidth of the backward-wave tube oscillator is related to the power electric level that empties into the phase lock signal, the power that empties in is exceedingly great, the phase lock bandwidth then is exceedingly wide. Figure 8.3 is the curve of the relationship between the phase lock bandwidth and the phase lock power of an X waveband backward-wave tube. The farther the preset frequency of the backward-wave tube is from the comb form harmonic wave frequency that is assigned, the greater the required phase lock power. In order to reduce as much as possible the phase lock power that is required, the required preset frequency of the backward-wave tube must be as standard as possible, at the same time the required electron beam power source voltage of the backward-wave tube should be as stable as possible. The total electron beam power source variation that is allowed is equal to the product of the reciprocal of the helical line modulation sensitivity of the phase lock bandwidth and the backward-wave tube.

Any common backward-wave tube can put the phase locked signal through a circulator to achieve emptying into the phase lock. But, this method, due to mismatching, wear and tear, and other factors, makes the phase locked signal produce noticeable attenuation. Therefore the required phase locked signal power level must be correspondingly high, this is also to say that its phase lock sensitivity is fairly low. Usually the phase lock power that this "output end method" requires is approximately 10dB lower than the backward-wave tube output power. This is also to say that the phase lock gain at this moment is approximately 10dB. But if the collecting electrode end of the helical line of the backward-wave tube adds a particular input end, then it can obtain even higher phase lock gain; at this time the necessary phase lock signal power can reduce 15-20dB or more.

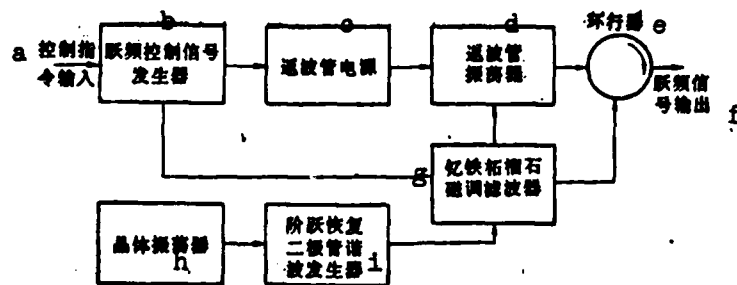


FIG. 8.2 COMB FORM HARMONIC WAVE GENERATOR
EMPTYING INTO A PHASE LOCKED FREQUENCY AGILE
SIGNAL SOURCE

KEY: (a) Control directive input; (b) Jump
frequency signal generator; (c) Backward-wave
power source; (d) Backward-wave tube oscillator;
(e) Circulator; (f) Jump frequency signal out-
put; (g) YIG magnetic harmonic wave filter;
(h) Transistor oscillator; (i) Step recovery
diode harmonic wave generator

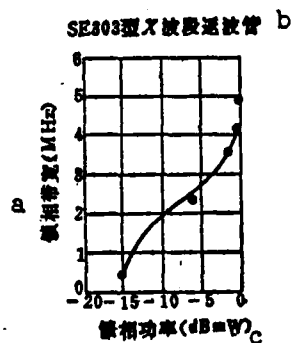


FIG. 8.3 RELATIONSHIP BETWEEN
PHASE LOCKED BANDWIDTH AND PHASE
LOCKED POWER OF AN X WAVEBAND
BACKWARD-WAVE TUBE

KEY: (a) Phase lock bandwidth;
(b) Model SE303 X waveband backward-
wave tube; (c) Phase lock power

The major shortcoming of this program is that using the harmonic wave generator it is very difficult to obtain a comb form frequency spectrum with concentrated intervals, moreover using the response of a magnetic harmonic wave filter takes a fairly long time, therefore it is not easy to achieve jump frequency between the pulses.

In order to obtain a comb form frequency spectrum with concentrated intervals, it is necessary to use frequency synthesis techniques. Frequency synthesis techniques earlier developed from low frequencies, now they have already been successfully applied to the realm of microwaves. In principle they can be divided into direct synthesis and indirect synthesis methods. In the following sections we will explain their operational principles in comparative detail.

8.2.1 DIRECT SYNTHESIS METHOD

All frequency synthesizers use one or several highly stable transistor oscillators as reference oscillators, the direct synthesis method uses a suitable radio frequency switch to carry out selection and combining on its high time harmonic wave, and obtains the necessary frequency in the microwave band after again going through mixing and frequency multiplication.

The direct synthesis method also can be divided into the three methods of direct switch selection method, decimel system switch selection method, and binary-decimal system switch selection method, according to its operational principles.

(1) Direct Switch Selection Method⁽³⁾

In fully coherent frequency agile radar, it often does not need to be able to operate on arbitrarily appointed frequencies, but only requires operating on a minor few dispersed frequency points, at this time it can use the relatively simple direct switch selection method. The diagram of its operational principle is as Fig. 8.4 shows.

Figure 8.4(a) gives the frequency synthesizer of 3 dispersed frequency points. Its operational principle is perfectly simple. Three highly stable transistor signal sources, after going through radio frequency switch selection, go to the bandwidth frequency multiplier and multiply to the operational frequency of the radar, and later are put out. This method is only suitable to conditions of smaller than

12 frequency points. When there is more than the required number of frequency points, we can use the program in Fig. 8.4(b). In the figure it uses four standard frequencies, after going through power distribution they go to select the switch; again after going through frequency multiplication and mixing, they can attain 64 dispersed frequencies, the multiple of frequency multiplier M is 4, the multiple of N is 16. Presuming f_1, f_2, f_3 and f_4 successively are 1, 2, 3, and 4 MHz and after going through M times of frequency multiplication we obtain 4, 8, 12, and 16 MHz; after going through N we obtain 16, 32, 48, and 64 MHz. All the mixers are the above frequency conversion models. At the final output we can obtain 64 dispersed frequencies that go from 21 to 84 MHz and have intervals of 1 MHz. Changing the standard frequency and the times of frequency multiplication we then can obtain its required equal interval dispersed frequency.

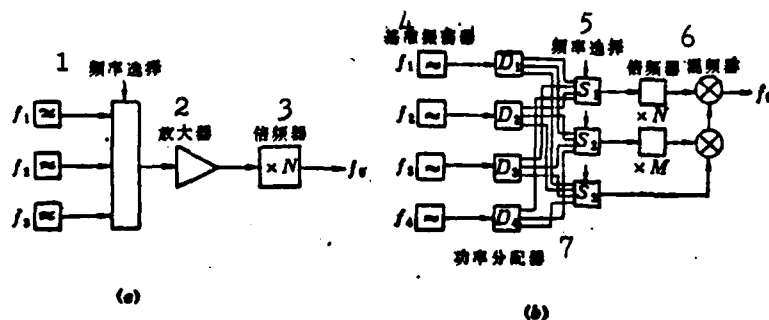


FIG. 8.4 DIRECT SWITCH SELECTION METHOD
KEY: (1) Frequency selection; (2) Amplifier;
(3) Frequency multiplier; (4) Standard oscillator;
(5) Standard selection; (6) Frequency multiplier, mixer;
(7) Power distributor

(2) Decimal System Switch Selection Method⁽⁴⁾

In order to be able to obtain output frequency according to decimal system variations, we can use the decimal system switch selection method that Fig. 8.5 shows. This method only uses one standard frequency source, after it goes to the harmonic wave generator, it uses 10 circuit band pass wave filters to separately select its 10 harmonic waves ($N=10$), after going through amplification in the amplifier it goes to a decimal switch matrix, this switch matrix has a total of ten circuit inputs and two circuit outputs, these two circuit outputs are

separately controlled by two digital directive signals, and can select an arbitrary circuit in the ten circuit inputs. After output frequency f_m goes to the mixer to be mixed with the second circuit output f_n , again after going through the band pass wave filter to filter out the parasitic signal it then can obtain final output $f_n + f_m/10$. Because f_m and f_n can be in the ten harmonic waves of the reference frequency at any time, therefore the final output can go from $1.1f_r$ directly to $11f_r$ altogether 100 frequencies.

Generally this method can only obtain high frequency signal output, in order to obtain the microwave signal it still must go through frequency multiplication or upper frequency conversion. Direct frequency multiplication generally is used in situations where the corresponding frequency band is fairly narrow. If it requires a frequency band with a fairly wide cover, then it can use its output to mix with a highly stable microwave source (upper frequency conversion). The direct frequency multiplication method can generally cause its short term stability to decrease.

(3) Binary-Decimal System Switch Control Method⁽⁵⁾

The binary-decimal system switch control method is particularly suitable to the frequency directive signal of the binary-decimal system. Its greatest advantage is that it reduces the ten comb frequencies that are required in the decimal system direct synthesis method to only two. Figure 8.6 is the frame diagram of the principles of 1248 binary-decimal system switch selection method. f_1 is input signal frequency, f_1 and f_2 are reference comb form frequencies. Their relationship is:

$$f_i = f_1 + 10^i \Delta f \quad (8.1)$$

Δf is its minimum frequency increment. K_1, K_2, K_3 , and K_4 are the frequency selection switches. All the mixers are lower frequency conversion form. All the switch positions that are drawn in the figure are positioned in the "0" position, if the position of K_1 changes from "0" to "1", namely, the output of the first mixer increases to $10\Delta f$,

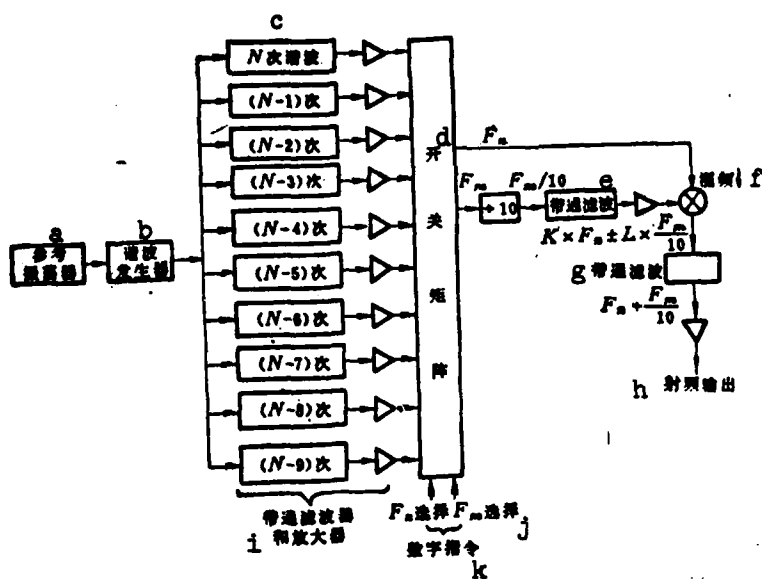


FIG. 8.5 DECIMAL SYSTEM SWITCH SELECTION FREQUENCY SYNTHESIZER

KEY: (a) Reference oscillator; (b) Harmonic wave generator; (c) Times harmonic wave; (d) Switch matrix; (e) Band pass filter; (f) Mixer; (g) Band pass wave filter; (h) Radio frequency output; (i) Band pass wave filter and amplifier; (j) Selection; (k) Digital directive

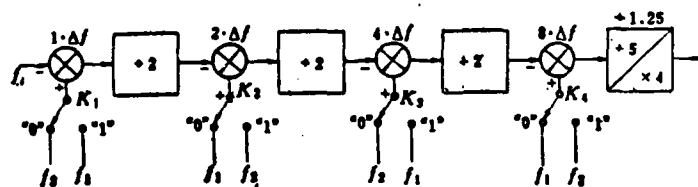


FIG. 8.6 1248 BINARY-DECIMAL SYSTEM SWITCH SELECTION METHOD

the output of the first mixer goes through $\div 2 \div 2 \div 2 \div 5 \times 4 = -10$, namely the final output frequency changes to $1 \cdot \Delta f$; but when K_2 changes from "0" to "1", output frequency changes to $2\Delta f$; when K_3 changes from "0" to "1", output frequency changes to $4\Delta f$; when K_4 changes from "0" to "1", output frequency changes to $8\Delta f$. Namely, its weighted averages respectively are 1, 2, 4 and 8. If the relationship between the selected reference frequency f_1 and input frequency f_i is:

$$f_i = 1.8f_1 + 10\Delta f \quad (8.2)$$

Then it can obtain output frequency equal to input frequency. Below we will give a digital example to explain: Assume $f_1=35\text{MHz}$, $\Delta f=0.1\text{MHz}$, from expression (8.2) we can obtain $f_1=1.8 \times 35 + 1 = 64\text{MHz}$, from expression (8.1) we can obtain $f_2=65\text{MHz}$. When all switches are positioned in position "0", the frequencies of the input signal frequency after going through each mixer and frequency divider successively are 30, 15, 49, 24.5, 40.5, 20.25, 43.75, and 8.75 and 35. Although its final signal frequency is equal to the input signal frequency, any variation of the input signal frequency to reflect in the output end reduce tenfold. Therefore, so long as we use several completely identical binary-decimal system contacts, we can construct a whole frequency synthesizer. For example, using three of this kind of stage of contacts, the first stage increment 0.1MHz in the final output end becomes an increment of 1kHz; the second stage is 10kHz, and the third stage is 100kHz. From this we can see that the basic structure of this frequency synthesizer is not a parallel selection type, but is a contact control type, it can be formed by completely identical binary-decimal system stage contacts, therefore its composition is simple, and it is convenient to make. So long as there are additional suitable frequency multipliers we can attain the necessary microwave frequency.

8.2.2 INDIRECT SYNTHESIS METHOD

The direct method uses comparatively many reference frequencies, matrix switches, frequency dividers, frequency multipliers, and mixers, thereby making its structure complicated, and cost increased.

In order to avoid the shortcomings of the direct synthesis method, we now extensively use the indirect synthesis method. In the indirect synthesis method, the output signal is directly taken from a voltage control oscillator, in order to make it able to possess frequency stability of a highly stable reference oscillator (generally a transistor oscillator), it uses phase lock techniques. In phase lock techniques phase discrimination is not directly carried out on the output frequency but is carried out on the reference signal intermediate frequency after going through appropriate mixing and dividing. This way, so long as

it changes its dividing ratio, it can change the output frequency. Figure 8.7 draws out a diagram of the principles of a typical indirect type frequency synthesizer⁽⁴⁾. From the figure we can see that this frequency synthesizer actually is a feedback control system that possesses a phase lock loop. Signal f_k of the reference oscillator, mixing with radio frequency output f_0 of the voltage control oscillator, after going through frequency multiplication M (lower frequency conversion), obtains $f_0 - Mf_R$, and again takes this signal to a program-controlled frequency divider to divide by N , the dividing ratio of this program-controlled frequency divider is program controllable. The frequency that is obtained discriminates with the reference frequency in the phase detector. The output of the discriminator is used to control the voltage control oscillator, making its oscillator frequency satisfy the relationship expression: $(f_0 - Mf_R)/N = f_R$, and the loop is locked because the size bandwidth of the locked circuit has limitations, therefore the frequency control directive must simultaneously go to the program-controlled frequency divider, the frequency multiplier, and the voltage control oscillator. It generally must preset the voltage control oscillator within a $(0.1-1)\%$ range of the assigned frequency, this requires the voltage control oscillator to have extremely good tuning linearity. The component that is the nucleus of the indirect type frequency synthesizer is the voltage control oscillator, generally they all use YIG tuned oscillators because they have extremely high spectrum purity, and extremely good tuning linearity; only their tuning speed is fairly low.

8.2.3 COMPARISON OF PROPERTIES OF FREQUENCY SYNTHESIZERS

The methods of direct synthesis and indirect synthesis that are explained in the preceding section both can achieve digital program-controlled frequency conversion, and also can possess the frequency stability of a reference oscillator. But, there are comparatively large differences on many other performance indexes. The following will emphasize the comparison of some important properties that are related to frequency agile radar applications.

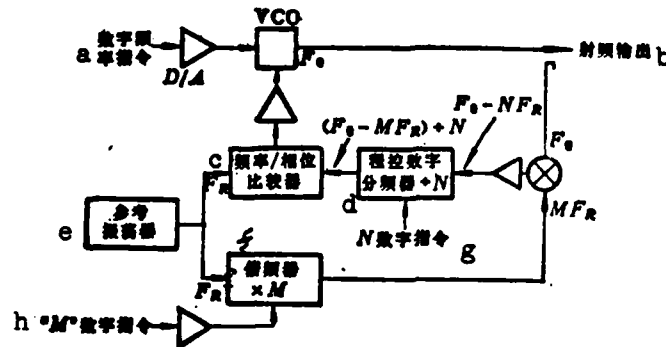


FIG. 8.7 INDIRECT FREQUENCY SYNTHESIZER
 KEY: (a) Digital frequency directive; (b) Radio frequency; (c) Frequency/phase comparator; (d) Program-controlled digital frequency divider; (e) Reference oscillator; (f) Frequency multiplier; (g) Digital directive; (h) Digital directive

(1) Frequency Agile Speed

Frequency agile radar generally requires the ability to be agile within an entire frequency band made in the pulse. The allowed frequency agility time generally is within some ten microseconds. The frequency agile time of the direct synthesis method primarily depends on the response time of the matrix switch, this time can be very short, generally around a few microseconds. The corresponding exchange time of the binary-decimal system switch control method is approximately 20 microseconds.

The frequency agile speed of the indirect synthesis method is fairly low, therefore it requires first to preset the voltage control oscillator on a new frequency and later it re-locks. Therefore its agility time is composed of two parts: one part is the frequency preset time, the other part is the lock time. The former is dependant on the voltage control oscillator that is chosen. As is recounted above, assuming that in order to obtain fairly high frequency spectrum purity we choose a YIG tuned oscillator, thus its preset time is correspondingly long. When the bandwidth is fairly narrow ($< 200\text{MHz}$), its tuning time is approximately some ten microseconds. The phase lock time of the circuit depends on the response time of the circuit, this is primarily

determined by the bandwidth and nonlinearity of the circuit. There is also a some ten microsecond increment. Therefore the agility time of the indirect synthesis method generally is greater than 100 microseconds. Although thus long of agility time also can be applied in frequency agile radar, it will be able to hold a fairly long purity time, reducing its effective operational time.

(2) Short Term Frequency Agility (Phase Noise)

In fully coherent frequency agile radar, because it is necessary to carry out coherent processing on received signals, therefore its short term frequency agility is a very important index. This short term frequency agility generally can be expressed by phase noise. Within the fairly narrow range of deviated carrier wave frequency, its phase noise is primarily determined by the reference oscillator in itself, therefore it decreases with the increase of frequency deviation (see Fig. 8.8). Within this scope, no matter if it is the direct synthesis method or indirect synthesis method, they both have the same phase noise. When the deviated frequency further increases, the hot noise that is produced by the amplifier and frequency multiplier will become a primary factor; this is primary is the direct synthesizer. Because its short term frequency agility is corresponding to a constant, therefore the phase noise will increase with the decrease of the frequency. Phase noise of the indirect synthesizer outside the phase lock bandwidth depends on the voltage control oscillator, although its phase noise is worse than that of the reference oscillator, outside a certain frequency deviation it is possible for it to be better than that of the direct synthesizer.

What is valuable to point out is that the binary-decimal system possesses extremely good phase noise. This is because in this frequency synthesizer, all the frequencies come from basic reference, therefore the frequency modulation (FM) of the output or phase noise possesses proportional value identical to the indirect synthesizer. Figure 8.9 gives the comparison of this frequency synthesizer with the indirect type frequency synthesizer. By the figure we can see that when deviated carrier frequency is within 100Hz, its phase noise must

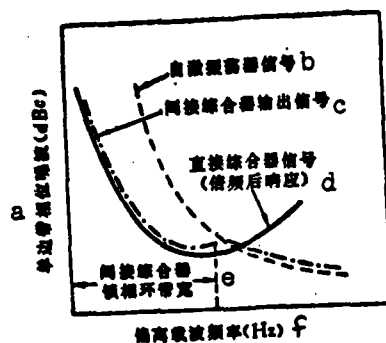


FIG. 8.8 PHASE NOISE OF FREQUENCY SYNTHESIZER
KEY: (a) Unilateral band noise; (b) Self-driving oscillator signal; (c) Output signal of indirect synthesizer; (d) Signal of direct synthesizer; (e) Indirect synthesizer phase locked circuit bandwidth; (f) Deviated carrier wave frequency.

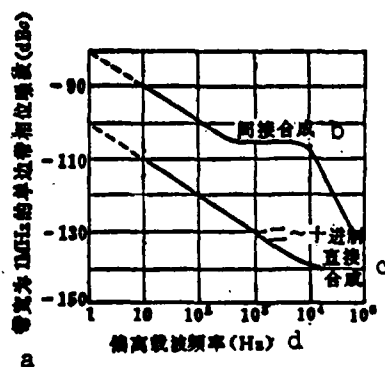


FIG. 8.9 PHASE NOISE OF BINARY-DECIMAL SYSTEM DIRECT SYNTHESIZER
KEY: (a) Unilateral band phase noise as 1MHz; (b) Indirect synthesis; (c) Binary-decimal system direct synthesis; (d) Deviated carrier wave frequency

be 20dB smaller than those of the indirect type frequency synthesizer. When deviation goes from 1KHz to 10KHz, it must be approximately 30dB higher.

(3) Stray Signals

Because numerous frequency multipliers, dividers, and mixers are used in the frequency synthesizer, therefore, naturally, various types of stray signals can exist. If reference frequency is not carefully selected, and various wave filters are not meticulously designed, it often can cause parasitic stray waves to reach a degree that is not allowable.

Obviously, because direct synthesis has numerous reference frequencies, frequency dividers, multipliers, and mixers, therefore the possibility of it producing stray signals can also increase, cross jamming of various signals in the matrix switch also can produce cross modulation. Contrarily, the stray signals of the indirect synthesis method are relatively easy to control. Because its output signal is directly conducted by the voltage control oscillator, therefore only those stray signals that are extremely close to the output frequency thereby falling within the phase lock bandwidth can be influential, and the phase lock bandwidth is only a few hundred kilohertz, sufficiently more narrow than the bandwidth of the total output signal. Therefore restraining the parasitic signal correspondingly must be somewhat easy.

So long as we carefully choose the frequency and meticulously design the wave filter circuit, and in addition add a fairly good shield and power source wave filter, the frequency synthesizers of these two types both can achieve stray signals that are lower than 60dB carrier frequency.

What is similarly worthy to mention is that the binary-decimal system direct synthesis method has extremely good properties in the area of restraining stray signals. In this frequency synthesizer, its stray signals are primarily from the clutter of the mixer and the cross coupling jamming in the two reference comb frequencies. Computations

clearly indicate that the various combined frequencies of 64 and 65MHz reference comb frequency selections and 35MHz input signal selection are fairly far from the output frequency, and relatively easy to filter out. Moreover the frequency divider after each mixing can reduce stray signal power level that is produced in the mixer to a quantity of $20\lg N$ (N is dividing ratio). Additionally, the $\frac{1}{10}$ of each decimal unit still can effectively reduce noise of the input signal and the stray signal lateral band to 20dB. All these factors in addition to the meticulously designed wave filter can cause this type of frequency synthesizer to obtain an outstanding stray signal power level of -100dB. Figure 8.10 is the comparison of the stray signal power level of this frequency synthesizer (decibel amount that is lower than the output carrier wave power level) and that of the indirect synthesizer. From the figure we can see that it must be 20-40dB lower than the stray signals of the indirect type frequency synthesizer.

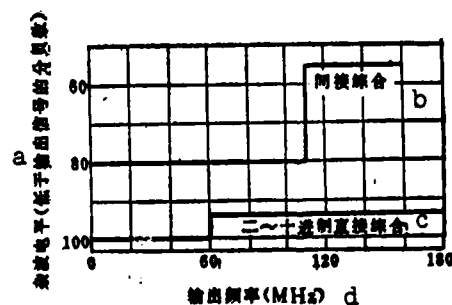


FIG.8.10 COMPARISON OF POWER LEVEL OF STRAY SIGNALS OF NON-HARMONIC WAVES
KEY: (a) Clutter power level (decibel amount that is lower than that of the output signal); (b) Indirect synthesizer; (c) Binary-decimal synthesizer; (d) Output frequency

The frequency synthesizer still has some other common technological indexes, for example long term frequency stability, frequency accuracy (precision), frequency readjustment (restability), etc. These indexes are not key for the frequency agile local oscillator, therefore we are not prepared to go into detail or cover everything.

From the above comparison we can know that in each type of frequency agile synthesizer, the method of using the binary-decimal system switch to control the direct synthesizer possesses the best properties, its switch time compares favorably with the general direct synthesis type, and its short term frequency stability (phase noise) and stray signal output are also better than those of the indirect synthesizer.

8.2.4 LOCAL OSCILLATOR OF FREQUENCY SYNTHESIZER OF FULLY COHERENT FREQUENCY AGILE RADAR

As a local oscillator of frequency agile radar it still must change the high frequency signal that is produced by the frequency synthesizer into the microwave frequency of radar operations. This conversion method can be divided into the three methods of direct frequency multiplication, upper frequency conversion, and phase lock loop. In the following sections we will respectively discuss these, and raise specific examples for explanation of their applications in frequency agile radar.

(1) Direct Frequency Multiplication Method

Figure 8.4(a) actually is the direct frequency multiplication method that is used. Using the radio frequency switch to directly select a highly stable transistor oscillator signal after going through the frequency multiplication chain directly multiplies to the necessary microwave waveband. The merits of this method are its simplicity and that there are no stray signals produced in the mixer; its shortcoming is that the corresponding bandwidth is fairly narrow, usually 10%, but it can already satisfy the requirements of frequency agile radar. Additionally, its frequency multiplication wear and tear is fairly great and it needs a powerful amplification stage, as a result its output power is fairly small; at the same time, the phase noise of the output signal also will increase with the frequency multiplication coefficient N according to $20\lg N$ (dB), causing the output phase noise to greatly worsen.

This direct frequency multiplication method generally is used in agile frequency magnetron moving target indication radar that possesses several fixed frequency points. Figure 8.11 is a block diagram of an X waveband workable order stable local oscillator with a VARIAN VSX-9600 arrangement that uses this program⁽³⁾.

A unilateral 8 throw PIN radio frequency switch can carry out selection on eight signal sources, in which six are highly stable transistor oscillators, one is a voltage control oscillator used for counter scanning and detection, and there is also an outer frequency basic. The transistor oscillator operates close to 100MHz, through a two-stage transistor double frequency multiplier it goes close to 400MHz, the advantages of the transistor frequency multiplier are that the necessary components are few and it possesses frequency multiplication gain. If the transistor is the operational frequency limit, it presents the best gain frequency. Thus the transistor frequency multiplier is more advantageous than the modified resistance frequency multiplier or the similar neglected basic diode frequency multiplier. Therefore it can play a certain isolator role thereby raising operational stability. Because in the frequency multiplication process, the bearing of the lateral band of the clutter corresponds to the carrier frequency and remains fixed, and the absolute value of the operational frequency forms a direct ratio increase with frequency multiplication coefficient N , therefore the input stage wave filter requirements are stringent. If it requires the frequency spectrum to be especially pure, then it is necessary to deploy a tubular distribution type limited wave filter in the first output end with the second transistor frequency multiplier. After going through further amplification, it takes the signal for frequency multiplication in a modified resistance four-fold frequency multiplier and goes to an L waveband. Again after going through powerful amplification to a 1 watt power level, it goes to be multiplied in another six-fold modified resistance frequency multiplier, to obtain the necessary 8.5-9.6GHz final output. This frequency synthesizer can give out 50 milliwatts power in the X waveband, its switch speed is less than 1 microsecond. Frequency stability in a temperature

range of -30°C to $+70^{\circ}\text{C}$ is 2.5×10^{-5} . Corresponding power varies less than 2dB. Amplitude modulation (AM) noise within any 1kHz bandwidth is as low as -125dBc, and its frequency modulation (FM) noise within 1Hz bandwidth of each 10kHz is as low as 0.1Hz. False signal output is as low as carrier frequency 70dB. These kinds of indexes can satisfy the requirements of high performance moving target indication systems.

(2) Upper Frequency Conversion Method

The upper frequency conversion method uses a highly stable microwave signal (actually also obtained after transistor frequency multiplication) and a fairly low frequency synthesis agile signal to carry out mixing (upper frequency conversion) to obtain the microwave frequency. This method will not worsen the phase noise of the output signal. But its output power level is fairly low, and clutter power level of nonharmonic waves increases. Therefore it is not often used in frequency agile local oscillators.

(3) Phase Lock Loop Method

The phase lock loop method directly puts out the signal from the microwave voltage control local oscillator. It also mixes with a microwave base (lower frequency conversion), and later carries out phase comparison with the agile source of a very high frequency, to make the voltage control oscillator track the agility of the frequency synthesizer. The output power electric level of this method is comparatively high, phase noise is close to the upper frequency conversion method, clutter primarily is microwave basic jamming going to the voltage control oscillator output end. So long as it carries out very good screening it also can obtain a fairly low power level. Therefore, this method presently is comparatively extensively used in microwave frequency synthesizers.

For frequency agile oscillators, the greatest shortcoming of the phase lock loop is that the lock time is fairly long, therefore the

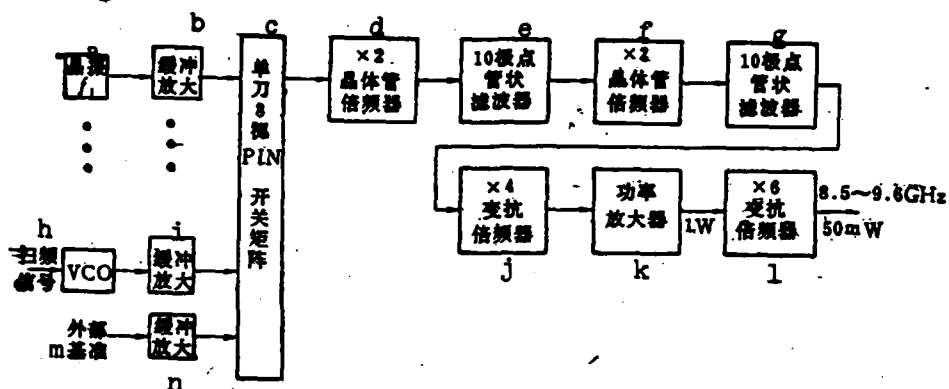


FIG. 8.11 VSX-9600 FREQUENCY AGILE LOCAL OSCILLATOR
 KEY: (a) Transistor oscillator; (b) Slow pulse amplification; (c) Unilateral 8 throw PIN switch matrix; (d) x2 transistor frequency multiplier; (e) 10 limited tubular wave filter; (f) x2 transistor frequency multiplier; (g) 10 limited tubular frequency wave filter; (h) Frequency scanning signal; (i) Slow pulse amplification; (j) x4 modified resistance frequency multiplier; (k) Power amplifier; (l) x6 modified resistance frequency multiplier; (m) Outer base; (n) Slow pulse amplification

transformation speed is fairly slow, the fastest must have a magnitude of several tens of microseconds. Aside from this, some problems of mistaken locking and damaged locking exist in this method, unlike in the direct synthesis method when the signal of any one middle unit disappears, the final output signal also disappears with it.

In the following section we will take a look at the model LOB-1 frequency agile local oscillator that uses this phase lock loop method, its principles are as Fig. 8.12 shows⁽⁶⁾. This local oscillator can use 100kHz precision and its interval can give out a signal of 1775.1 MHz to 2775.0MHz according to additional digital directives. In order to quicken the transformation speed, its low frequency synthesizer uses the multiple transistor direct synthesis method, each position is formed by ten transistor oscillator stages, its output passes through the digital gate control. What the 10MHz transistor oscillator stage actually produces is an $a \times 0.625\text{MHz}$ signal, after going through double frequency multiplication obtains $a \times 1.25\text{MHz}$, after the bandpass wave filter mixes with the second $b \times 0.125\text{MHz}$ signal, we obtain $a \times 1.25 + b \times 0.125\text{MHz}$, after again going through band pass amplification mixes with

$C \times 0.0125$, after four-fold frequency multiplying changes to the signal of $a \times 5 + b \times 0.5 + C \times 0.05 \text{ MHz}$, after again going through bandpass wave filter through two-fold frequency multiplication we obtain the final necessary signal, $a \times 10 + b \times 1.0 + C \times 0.1 \text{ MHz}$. The design of the mixing stage is extremely important. Analysis clearly shows that if the output frequency of this phase adding mixer is 1.29 times of the input frequency, then it can obtain minimum clutter output.

In order to take the frequency control of the backward-wave tube voltage control oscillator to 5 effective digits, we use the frequency preset signal to carry out presetting. Preset precision is 0.5% of the assigned frequency, in high frequency phase it is approximately 15 MHz. The latter 3 effective digits are achieved by using the phase lock circuit. To this end, we firstly reduce the previous 2 effective digits of the backward-wave tube oscillator frequency, this can be achieved through mixing with the output of a 100 MHz transistor oscillator harmonic wave frequency multiplier. The signal after mixing is $f_0 - A \times 100 \text{ MHz}$. Later we use output of this signal and the frequency synthesizer to carry out phase detection. But because after f_0 reduces to $A \times 100 \text{ MHz}$ from the latter 3 effective digits there still are several megahertz to several tens of megahertz errors, the frequency band of the phase detector is very narrow, therefore there is no way to compare. Therefore we simultaneously use the automatic frequency precision tuning system. At this time the signal that is actually given by the frequency synthesizer must be 60 MHz higher than the assigned signal. Then it is $(A+6) \times 10 + b \times 1.0 + C \times 0.1 \text{ MHz}$. After this signal mixes with $f_0 - A \times 100 \text{ MHz}$, the signal that is obtained is 60 MHz additional error frequency. This intermediate frequency message can be caught by a 60 MHz discriminator with a very wide frequency band, and later controls the backward-wave tube power source, causing it to be even more near the assigned frequency, then its frequency after mixing is even more close to 60 MHz. Later this intermediate frequency signal again carries out phase detection with the 60 MHz signal that is produced by the transistor oscillator, to completely accurately lock on the assigned frequency.

Its tuning and locking time are primarily determined by the response time of the phase lock system. The lock time of LOB-1 is approximately

30 microseconds. Output power can reach 100 milliwatts, power variations are smaller than 6dB, and clutter output is -60dB.

In frequency agile radar, it generally does not require precision to 5 effective digits, but only requires it for a number of limited dispersed frequency points, at this moment the phase lock loop method can be greatly simplified. The phase lock reference signal can use the comb form standard signal that possesses a corresponding interval, this standard signal can be formed by using the modulation method. Figure 8.13 is a Doppler radar low noise signal source that possesses frequency agile ability⁽⁷⁾. This radar operates to X waveband (10GHz), its standard frequency is provided by a 5MHz voltage control transistor oscillator (VCXO) (it can modulate $\pm 25\text{Hz}$). After going through x2 and x20 transistor frequency multipliers, again uses step diode x5 frequency multiplier to obtain 1GHz signal to go to the modulator, the 5MHz standard signal is regarded as the modulation signal and also goes to the modulator to produce the interval as a 5MHz highly stable comb form signal. The limiter causes the power electric level of each signal weight to be equal (approximately 1 milliwatt). Phase locking is directly carried out according to the L waveband (1GHz), the digital type frequency directive, after going through numeric model transformation, directly controls the frequency of the voltage control oscillator. Its precision should be higher than $\pm 0.25\%$, to ensure the correct locking of the phase lock loop. The output of the voltage control oscillator, after going through step tube 10-frequency multiplication, puts out the X waveband signal through 6 microband wave filters, each frequency interval is 50MHz, the modulation range is $\pm 50\text{kHz}$. So long as it changes the control voltage of the voltage control oscillator, it can be agile in each spectrum line. This is precisely the outstanding merit of the phase lock loop. However, directly detecting in the L waveband it is not easy to obtain highly stable signals. Therefore, in signal sources that require even higher stability, we generally do not use this method.

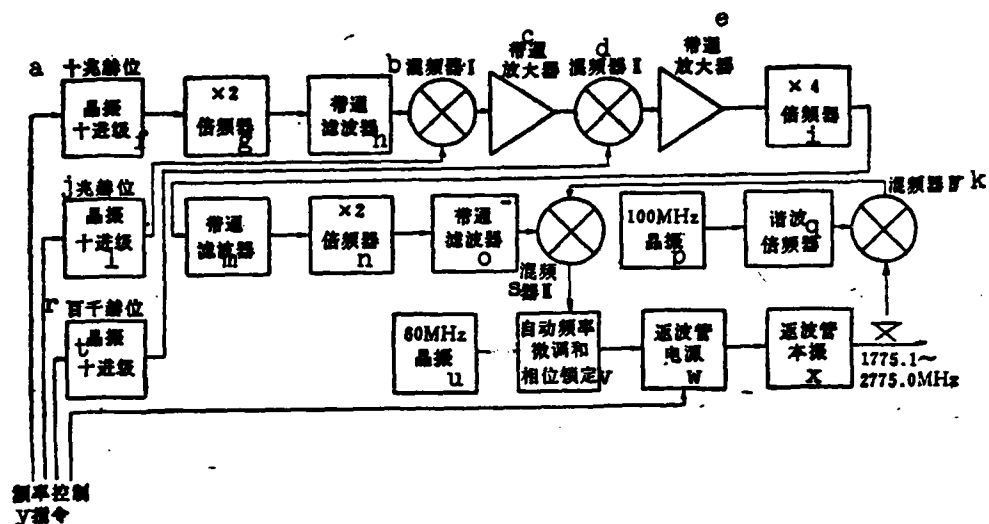


FIG. 8.12 MODEL LOB-1 FREQUENCY AGILE LOCAL OSCILLATOR

KEY: (a) 10MHz potential; (b) Mixer I; (c) Band pass amplifier; (d) Mixer II; (e) Band pass amplifier; (f) Transistor oscillator decimal stage; (g) x2 frequency multiplier; (h) Band pass mixer; (i) x4 multiplier; (j) MHz potential; (k) Mixer; (l) Transistor oscillator decimal stage; (m) Bandpass wave filter; (n) x2 frequency multiplier; (o) Band pass wave filter; (p) Transistor oscillator; (q) Harmonic wave frequency multiplier; (r) 100kHz potential; (s) Mixer; (t) Transistor oscillator decimal stage; (u) Transistor oscillator; (v) Automatic frequency precision tuning and phase locking; (w) Backward-wave to power source; (x) Backward-wave tube local oscillator; (y) Frequency control directive.

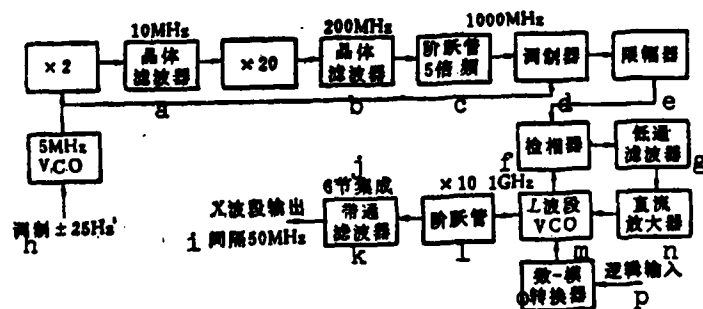


FIG. 8.13 DOPPLER RADAR AGILE SIGNAL SOURCE

KEY: (a) Transistor wave filter; (b) Transistor wave filter; (c) Step tube 5 frequency multiplier; (d) Modulator; (e) Limiter; (f) Phase detector; (g) Low pass wave filter; (h) Modulator; (i) 6 integrations; (j) 6 integrations; (k) Band pass wave filter; (l) Step tube; (m) L bandpass; (n) Continuous flow amplifier; (o) Number-model transformer; (p) Logical input.

The workable hour frequencies of modern current switch digital -- integrated circuits already reach as high as 100 mega even to gigahertz, thereby making the indirect synthesis method that Fig. 8.7 shows able to be very easily achieved. Figure 8.14 is this kind of highly stable radar agile frequency signal that is constructed by an indirect synthesis method⁽⁸⁾. This agility source can give a transmitted signal from 8800-9440MHz and a corresponding local oscillator message higher than 60MHz intermediate frequency. Within this 4% (640MHz) bandwidth, altogether there are 32 root spectrum lines spearated by 20MHz. By the 4MHz, 12MHz, and 60MHz produced by the standard signal of the transistor control, and the 2GHz standard signal, the former two signals act as reference signals of the phase lock loop, the intermediate frequency base is used in the receiver as a coherent oscillator, the 2GHz signal carries out lower frequency conversion with the L waveband signal of the voltage control oscillator, thereby producing a 100-228MHz signal, this signal can be used to carry out frequency division of the variable frequency divider that is composed of the integrated circuit of the transmitting polar coupling current switch. Its division ratio can be controlled by an additional program-controlled directive signal to vary within a 25-57 range. Because the digital discriminator operates on a 4MHz frequency, this causes the voltage control oscillator to operate on an arbitrary root spectrum line separated by 4MHz in a 1772-1900MHz range. This minimum frequency interval is determined by the loop bandwidth. The output value of the voltage control oscillator after going 5 frequency multiplication is regarded as the local oscillator signal output. In order to obtain a transmitting signal with frequency as low as 60MHz, we use another phase lock loop, the output power of this method must be much greater than that of the mixing method. This phase lock loop operates to 12MHz, after going through 5 frequency multiplication it can obtain 60MHz intervals.

All phase discriminators are digital, they can be used to identify the phase difference between the two methods, their output is a rectangular wave with the same frequency. The bandwidth of the rectangular wave represents the phase difference. After going through the low pass wave filter to filter out the signal standard and high amount of harmonic waves, it can obtain continuous flow voltage that forms a direct ratio

with the phase difference. This continuous flow voltage uses a low noise amplifier to carry out amplification. This ensures very low oscillator noise.

What is put out from the voltage control oscillator are continuous signals, these signals carry out modulation through a switch driver using a pulse signal. The above circuit then can obtain a narrow pulse signal that is used by the transmitter. The modulated pulse of the receiver is exactly opposite, also there is a local oscillator signal that can stop in the transmission period.

8.3 THE TRANSMITTER OF FULLY COHERENT FREQUENCY AGILE RADAR

Structurally, the transmitter of fully coherent frequency agile radar is no different than the transmitter of a common fully coherent master oscillator power amplification chain type. Only because the purpose of the primary design of frequency agile radar is raising radar jamming resistance, therefore it requires the transmitter to be able to have as wide as possible instantaneous bandwidth (not a tunable bandwidth), at the same time, because the radar operates on jump frequency form between the pulses, therefore it requires the output power of the transmitter in the operational frequency band to be as steady as possible. Generally it requires the output power fluctuation of the fully coherent frequency agile transmitter in the operational frequency band to be smaller than 1dB.

Although the instantaneous bandwidth of the entire radar not only depends on the transmitter but also is related to the antenna, transmission system, and rotational joints to a very high degree it primarily depends on the transmitter, and also is primarily determined by extreme power amplification stage. The preliminary stage and the excitement stage of the fully coherent frequency agile radar transmitter have no important differences from those of the common fully coherent radar transmitter, generally they all are composed of low power continuous wave traveling wave tubes (or only low power traveling wave tubes).

This section will carry out discussion on fully coherent frequency agile radar extreme power amplification stage. Its operational directives are basically determined by the corresponding partial directives of the entire radar.

The most key problem in extreme power amplification stage is the selection of the power amplification tube. Presently there are many types of power amplification tubes that can be selected, but they basically can be divided into two types. One type is a linear ray tube that is represented by a klystron and traveling wave tube (type O device); the other is a cross field device that is represented by a forward directional wave and backward-wave type cross field amplifier (CFA) (the so-called cross field amplifier simply refers to an electron device that is a cross of a magnetic field and an electronic field, also called a type M device). These two types of tubes both can be used in fully coherent frequency agile radar. The comparison of their primary performance indexes is shown in Table 8.2⁽⁹⁾.

It is common knowledge that linear ray tubes possess very high gain, but efficiency is fairly low, volume is fairly great; furthermore, because its necessary operational voltage is high, therefore its high voltage source volume is great, and it also needs X ray protection. Conversely, the efficiency of the CFA is high but gain is low; furthermore, because the necessary operational voltage is low, therefore volume is small and weight is light, and it is suitable in mobile radar stations such as automobile and airborne types.

8.3.1 APPLICATIONS OF LINEAR RAY POWER AMPLIFICATION TUBES IN FREQUENCY AGILE RADAR

Linear microwave tubes primarily refer to a microwave amplified tube that possesses rectilinear form electron rays. This type of tube primarily can be divided into the three types of traveling wave tube, klystron tube, and traveling wave-klystron mixed tube. Traveling wave tubes can also be divided into the two types of helical line traveling wave tubes and coupling cavity traveling wave tubes.

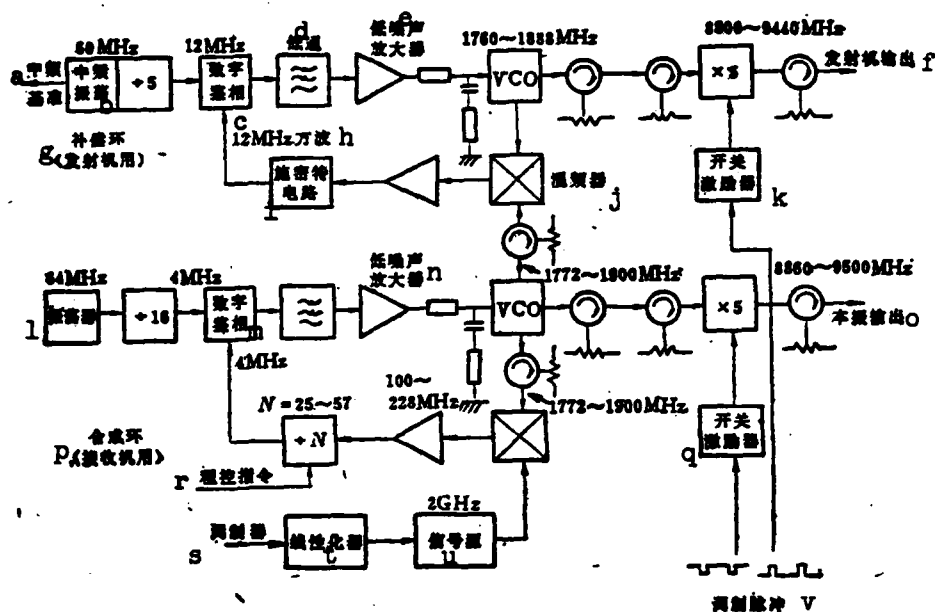


FIG.8.14 X WAVEBAND AGILE SIGNAL SOURCE OF INDIRECT SYNTHESIS METHOD

KEY: (a) Intermediate frequency base; (b) Intermediate frequency oscillator; (c) Digital phase discriminator; (d) Low pass; (e) Low noise amplifier; (f) Transmitter output; (g) Compensation loop(used by transmitter); (h) Block wave; (i)Exerting density circuit; (j) Mixer; (k) Switch driver; (l) Oscillator; (m) Digital discriminator; (n) Low noise amplifier; (o) Local oscillator output; (p) Synthesis loop(used by receiver); (q) Switch driver; (r) Program-controlled directive; (s) Modulator; (t) Linearizer; (u) Signal source; (v) Modulated pulse

The primary characteristic of traveling wave tubes is a broad bandwidth, the bandwidth of a helical line traveling wave tube can reach one frequency multiplication degree or higher, but power is fairly low, its peak power is lower than 10kW. The peak power of coupling cavity traveling wave tubes can reach 500kW, but bandwidth is slightly narrow, it still can reach 43%. The traveling wave tube is primarily used in airborne radar with a fairly low power level. Airborne radar mostly uses traveling wave tubes with cyclic field permanent magnetic focus, its average power limit is under several kilowatts. For the relation between average power and operational frequency of different types of tubes we can refer to Fig. 8.15⁽¹⁰⁾.

TABLE 8.2 COMPARISON OF SOME PRIMARY POWER AMPLIFICATION TUBES

	Linear Ray Tube			Cross Field Tube	
	Klystron	Traveling Wave	Mixer	Repeated Entry	No Repeated Entry
Bandwidth	(10-15)%	(10-18)%		(10-15)%	
Gain	30-70dB			6-28dB	
Effective-ness	(15-60)% Typical value is 30%(Static collecting electrode klystron typical value is 40%)			(30-75)% Typical value 45%	(20-50)% Typical value 30%
Clutter (1MHz bandwidth)	Typical value -90dB			Typical value -30 to -60dB	
Phase Modulation	Each 1% $\Delta E/E$ approximately 5° - 40°			Each 1% $\Delta I/I$ approximately 0.5° - 3°	
Sensitivity					
Useful Dynamic Range	40-80 dB			3-20 dB	
Dynamic/static impedance	0.8			0.05-0.2	
Voltage	High Voltage (1MW approximately needs 90 kilovolts)			Low Voltage (1 MX approximately needs 40 kilovolts)	
X Ray	Severe, must use lead covering protection			Generally not a problem	
Self Conducting	no			yes	yes
Self Stopping	no			yes (when bias placed electrode)	yes
Magnetic Field	Periodic permanent magnetism can reach 1MW (S waveband), other is electromagnetic iron, static collecting electrode klystron does not need			Needs permanent magnetism	
Ion Pump	Large tubes need			Self pumping	
Controlling Electrode	Model with or without anode, covered grid can use to 100kW peak value			With or without intercepting electrode	
Volume, weight	large, heavy			light, small	
Price	moderate	expensive		Low	moderate

Although the traveling wave tube has a fairly broad bandwidth, its bandwidth has a fairly strong relationship with peak value and efficiency. The greater the peak power of the tube, the narrower the bandwidth; the wider the bandwidth of the tube, the lower its efficiency (refer to Fig. 8.16)⁽¹⁰⁾. We can consider that on the traveling wave tube with peak power as several hundred kilowatts, its bandwidth is not wider than those of other types of tubes.

Large power traveling wave tubes generally use a triblade basic forward wave coupling cavity slow wave circuit. When peak power electric level surpasses 1MW, this forward basic wave circuit can reach a bandwidth of (10-15)%. But due to the chromatic dispersion of the triblade and centipetal form slow wave circuit, although it causes it to have fairly high power in the operational waveband, the gain on the edge of the frequency band drop very fiercely.

Figure 8.17 is the output power properties of model VA-112A traveling wave tube when there are different electron pouring voltage and current. From the figure we can see that when there is a low output power electric level (1MW), its bandwidth can reach 14.3%, but the variations of output power in its bandwidth surpass 3dB, when there is a high power electric level (>3MW), although power undulation reduces to 1dB or more its bandwidth is only 10.7%. From this we can see that when the high powered traveling wave tube must obtain a fairly steady output power, its bandwidth is not very wide.

In large-scale surface radar, its required peak power often reaches as high as several megawatts to several tens of megawatts, it is very difficult for high powered traveling waves to give this kind of high peak power, so we more often use klystrons.

Klystrons can give extremely great peak power. According to reports, they can give out 100MW in the S waveband. Although the waveband is relatively narrow, it is opposite from the traveling wave tube; the larger the output peak power of the tube, the easier it is to make the bandwidth wide. Only its efficiency sharply decreases with the bandwidth (refer to Fig. 8.16). When bandwidth is 1%, efficiency then

drops to only approximately 30%.

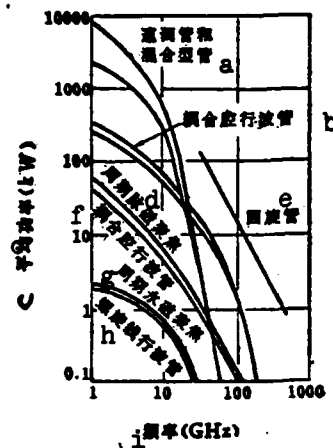


FIG. 8.15 RELATIONSHIP BETWEEN AVERAGE POWER AND FREQUENCY OF DIFFERENT TYPES OF LINEAR RAY TUBES
KEY: (a) Twystron; (b) Coupling cavity traveling wave tube; (c) Average power; (d) Cyclic pulse magnetic focus; (e) Cyclotron; (f) Coupling cavity traveling wave tube; (g) Cyclic permanent magnetic focus; (h) Helical line traveling wave tube; (i) Frequency

To sum up, the primary advantages of high powered klystrons are that gain is high (can reach 50dB and higher), phase linearity is good, and clutter output is low. But its major shortcoming is that the instantaneous bandwidth is narrow, and this is precisely the primary goal of frequency agile radar. Therefore researchers are using very great effort to resolve this problem.

To increase the klystron bandwidth there are primarily the following methods:

(1) Make the tuning distribution of the central cavity in a fairly wide frequency range.

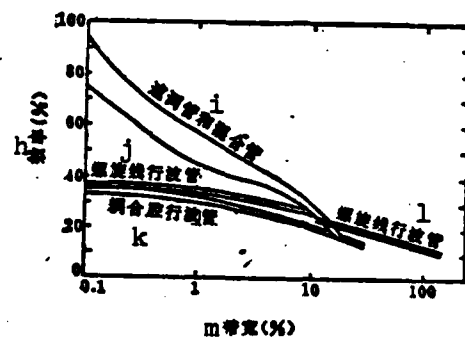
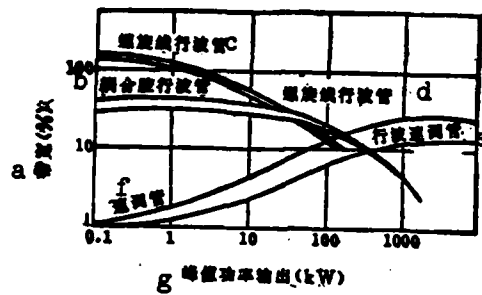


FIG. 8.16 RELATIONSHIP BETWEEN BANDWIDTH OF LINEAR RAY TUBE AND PEAK POWER AND EFFICIENCY
 (a) Bandwidth; (b) Coupling cavity traveling wave tube; (c) Helical line traveling wave tube; (d) Helical line traveling wave tube; (e) Traveling wave klystron; (f) Klystron; (g) Peak power output; (h) Frequency; (i) Twystron; (j) Helical line traveling wave tube; (k) Coupling cavity traveling wave tube; (l) Helical line traveling wave tube; (m) Bandwidth

(2) Use the method of cavity coupling to widen the resistance of the output cavity.

Although at this time we can increase the width of the frequency, the gain undulation in its operational frequency is fairly large. This also cannot satisfy the requirements for frequency agility between the pulses. To make its gain frequency properties steady, we can use the following methods:

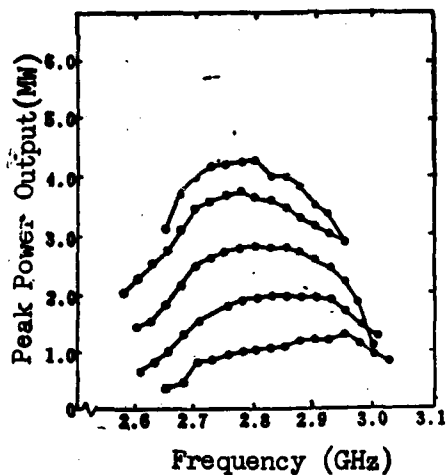


FIG. 8.17 OUTPUT POWER AND FREQUENCY PROPERTIES OF MODEL VA-125A HIGH POWER TRAVELING WAVE TUBE

(1) Make each cavity have different gap lengths and different loads.

(2) Use an electronic computer to carry out synthesis on the tuning frequency and Q value of the cavity, to make the limit of its response on a repeated frequency plane (thus the tuning frequency of the cavity) be positioned in an ellipse, to satisfy the requirements of a mutual corresponding response.

After adopting the above measures, we can make the klystron bandwidth with 1MW peak power electric level increase to approximately 5%. The klystron with 10MW level can reach approximately 10%.

Presently the klystron that has achieved the widest bandwidth is VA-812C, a P waveband klystron. Its operational frequency range is 400-450MHz, the electron bandwidth reaches 12%, peak power is 8MW, average power is 30kW, pulsewidth is 6 microseconds, peak voltage of the electron ray is 145 kilovolts, gain is 30dB, highest efficiency is 40%.

The efficiency of the wideband klystron must be inferior to the narrow band, its primary reason is that it uses a fairly high diversion system, to widen the frequency band and make the central cavity Q value decrease with the break that is made by the resistance of the output interval.

Recently, using the method of two harmonic waves together the transformation efficiency of the klystron can raise to 70-80%. But this is only suitable to narrow band klystrons, for wideband klystrons we can use a longer drift region to replace the two harmonic wave cavities to raise efficiency. Although efficiency can raise to approximately 58%, its corresponding bandwidth is still fairly narrow.

In the recent few years, frequency agile radar extensively uses a traveling wave twystron, it combines the advantages of the two tubes, from this it gets its name.

Regarding the klystrons we can say, the main advantage is that gain is high, the major part of its gain is obtained by its input cavity, therefore in this mixed type tube it uses the input cavity of the klystron as the primary measure to make it obtain high gain. But the primary weakness of the klystron is that the bandwidth is narrow, the primary method to increase its bandwidth is to decrease the Q value of its resonance cavity. Decreasing the Q value of its input cavity is comparatively easy to achieve, therefore driving power is fairly low, and after input cavity add loads it is not likely to bring about a high degree of wear and tear. But the power electric level of the output cavity is high, after add loading it can bring about a decrease in efficiency, because the output cavity is the major factor limiting the klystron bandwidth. In the mixed type diode it uses the triblade form output circuit of the traveling wave tube, this resolves the bandwidth problem of the output circuit, and using a short output wave (its gain is approximately 6-10dB) can ensure a high efficiency within the operational frequency, but this can give rise to dropping of gain on the frequency band edge (approximately 6-10dB). In order to resolve this problem we can join the frequency properties of different tuning klystron input cavities, make them mutually compensatory, and

finally can obtain the corresponding steadying properties.

This way, the mixed type tube has the same power electric level and operational frequency as the klystron, its bandwidth can increase approximately 50%, and its efficiency is almost the same as that of the klystron. Although gain is somewhat inferior to the gain of the klystron, it is higher than that of a traveling wave tube of the same length. Moreover, the undulation of its gain (when constant drive) within the frequency can reduce as low as 1dB. Unlike the traveling wave tube it reaches more than 6dB. Aside from this, the primary gain of the mixed type tube is obtained by part of the klystron, therefore the variation of its total gain on the electron beam voltage is unlike the kind of sensitivity of the traveling wave tube, when the electron beam voltage varies 10-20%, it still can keep the corresponding form of the gain and phase frequency properties invariant.

But, the mixed type of tube also has a certain weakness; its gain and phase properties do not have the kind of uniformity as those of the fairly low power forward directional basic wave coupling cavity traveling wave tube, this is due to the results of irregular tuning. Generally its phase properties deviate from a straight line when there is a 10% bandwidth approximately $\pm 25^\circ$, when there is a particular design it can reduce to $\pm 10^\circ$, this also can satisfy the requirements for pulse compression radar.

In the following section we will explain in detail some design methods and primary properties of model TV-2091 high powered twystron that was designed by France's Tang MuXun-CSF company that specialized in THD 1955 multiple beam fully coherent jump frequency radar⁽¹¹⁾. This is an S waveband, 20MW peak power tube.

Because the largest bandwidth that can be achieved by the antenna waveguide system of this multiple beam radar is approximately 10%, therefore it requires the bandwidth of the extreme power amplification tube to also at least be able to be 10%, so that it won't be likely to influence the bandwidth of the whole machine. Using a pure klystron, a band-

width of this width cannot be achieved, and the gain of a traveling wave tube is also too low. Therefore, it was decided to use a traveling wave twystron. Because part of the output circuit of the bandwidth of the tube is primarily determined by the klystron part, therefore this tube basically can be considered as a particular klystron. Because the klystron's electron beam production and formation section, electron beam and resonance cavity electromagnetic field energy conversion section, and output coupling section are correspondingly independent, therefore it is fairly easy to carry out a design to obtain the best parameters. The main contents of the design are deciding the electron beam resistance dimensions, drift tube length, drift length (adjacent cavity distance), resonance frequency of the resonance cavity, and Q value (it can add load). The design of the whole tube, aside from ensuring a certain output power and efficiency, primarily centers on the ability to have sufficient bandwidth, and when there is constant input power, the output power has as little undulation as possible in operational frequency, to suit the requirements for jump frequency between the pulses. In order to satisfy this requirement, we must adopt the following measures in the design of the tube: firstly we must use non-uniform cavity distribution intervals. Experiments prove that the gain undulation of 8 cavities that were evenly distributed reached 12dB, while the non-uniformly distributed cavities could be as small as 7dB; secondly its bandwidth output circuit uses three backward-wave filters, furthermore in its design method it does not use the mutual wave filter computation method that was often used in the past, but uses the best equivalent wave vein filter computation method. The undulation of the frequency properties that this method obtains is fairly small; the third measure is suitably selecting the resonance frequency and Q value of the resonance cavity, to mutually compensate with the undulation of the frequency properties of the output circuit and obtain the smoothest frequency properties.

After adopting the above measures, we can obtain as low as 1dB undulation in a 10% bandwidth. When maintaining a constant 100 watt input power, the output power properties in the pass band under two operational conditions are as Fig. 8.18 shows. From the figure we

can see that output power undulation when there is high-powered operation is only 0.85dB, its efficiency is also fairly high-it can reach 41%. The undulation when there is low-powered operation thus is fairly high, approximately 1.3dB. Efficiency also is fairly low, 39%.

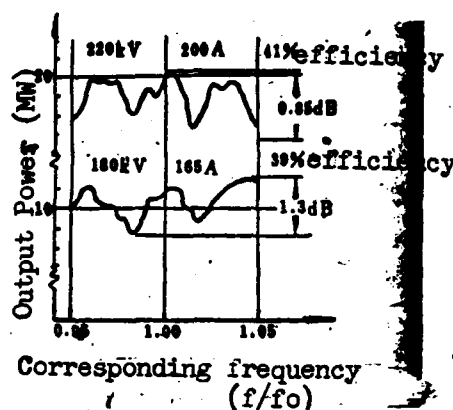


FIG. 8.18 PROPERTIES OF OUTPUT POWER AND FREQUENCY OF MODEL TV-2091 HIGH-POWERED TRAVELING WAVE KLYSTRON

Other parameter indexes of the TV-2091 six-cavity traveling wave klystron are as follows: gain as large as 50dB; efficiency as high as 30%; peak power 20MW; average power 30kW; pulsedwidth 10 microseconds. Using an oxidized beryllium moulded circular wideband output window, the standing wave ratio in operational frequency is lower than 1.1. Because output peak power is greater than the puncture power of the wave guide, therefore a high pressure atmosphere of 150 lbs/sq. inch is charged in the wave guide. The entire tube is water-cooled once, flow rate is 1.5 gal./minute, and again is evaporation-cooled.

At the same time another average-powered, even larger model TV-2092 tube was designed, it also operates in the S waveband, the bandwidth reaches 10%. Its peak power is 8MW, and average power reaches 200kW. Pulsedwidth is 500 microseconds. Its phase linearity is extremely good, thus it can be used in pulse compression radar systems of 500:1.

Table 8.3 gives the parameters of some typical traveling wave klystrons.

TABLE 8.3 PARAMETERS OF SOME TYPICAL TRAVELING WAVE KLYSTRONS

Model #	Frequency Range (gigahertz)	Corresponding Bandwidth(%) 1dB Undulation	Peak Power (MW)	Average Power (kW)	Gain (dB)	Efficiency (%)	Operation- al Ratio	Pulsewidth (Microseconds)
VA-145D	2.7-2.9	7.2	5	11	38	40	0.002	8
VA-145H	2.7-2.9	7.2	5	4	26	35	0.002	6
VA-145B	2.75-2.95	7.1	5	12	40	40	0.0025	10
VA-145E	2.9-3.1	6.9*	3	6.5	34	35	0.00175	7
VA-145J	3.015-3.215	6.5*	4.5	10	40	36	0.0025	10
VA-145F	3.1-3.6	7.5*	8	17	36	35	0.002	10
VA-145LV	3.1-3.5	12.1	1.0	1.0	30	30		50
VA-915A	3.1-3.6	14.9*	8	28	33	35	0.003	40
TV-2091	3.0	10.0	20.0	30.0	>50	>30		10
TV-2092	S	10	8.0	200				500
VA-146	5.4-5.9	8.9	3	10	35	40	0.002	20
VA-913A	5.4-5.9	8.9	5	10	40	38	0.002	20
VA-146M	5.4-5.9	8.9	5	10	36	35	0.002	10
VA-146C	5.4-5.9	8.9	5.5	10	36	40	0.002	12.5
Model #	Electron Beam Voltage (kV)	Electron Beam Current (amp)	Electron Beam Control	Weight (lbs)	Length (inches)			
VA-145D	117	84	Cathode	120	43			
VA-145H	117	90	Cathode	125	43			
VA-145B	125	92	Cathode	120	43			
VA-145E	117	80	Cathode	129	43			
VA-145J	117		Cathode	125	43			
VA-145F	155	125	Cathode	110	43			
VA-145LV	80	45						
VA-915A	180	151	Cathode	275	57			
TV-2091	220	225						
TV-2092								
VA-146	140	100	Cathode	100	35			
VA-913A	135	98	Cathode	128	35			
VA-146M	139	102	Cathode	100	35			
VA-146C	137	92	Cathode	100	35			

for 3dB instantaneous bandwidth

8.3.2 GENERAL PROPERTIES OF THE CROSS FIELD AMPLIFIER

In recent years, the cross field amplifier (CFA) has had extremely great development, especially after using a cathode driver, its gain increased to 28dB, overcoming its major drawback, and performance is even more ideal. Therefore it possesses even greater competitive ability than the linear ray tube.

The so-called CFA simply refers to the intersected state of its additional magnetic field direction and electronic field direction. The moving orbit of the electrons in it is an outer arranged line, its motion velocity is $v = E/B$ (E is electronic field strength, B is magnetic induction strength), and it is synchronous with the speed of the electromagnetic wave. In the process of energy exchange with the electromagnetic field, the kinetic energy of the electrons does not change, it only exchanges the potential energy into microwave energy, therefore its efficiency is very high. Also because its electron velocity v is much smaller than the electron velocity that is determined by the same voltage in the linear ray tube (approximately a 10 to 1 comparison), therefore the distance between the joints of its slow wave line is much smaller than the distance between the joints of the corresponding linear ray tube; when distance between the joints is the same, the operational voltage of the latter is much lower.

The CFA can be divided into two types, one type is the forward directional wave type, the other is the backward-wave type. In the forward directional type the direction of the radio frequency power flow in it and the direction of the radio frequency speed are alike, the backward-wave type then is opposite. In order to make the electron ray able to exchange energy with the high frequency electromagnetic field, the model and direction of its radio frequency speed must be consistent with the velocity and direction of the electron motion. Therefore the direction of the radio frequency power flow of the forward directional wave tube is the same as the direction of the electron motion. The backward-wave type then is opposite.

These two types of tubes can again each be divided into repeat entry and non-repeat entry types, the so-called repeat entry type simply refers to the electron newly entering the electromagnetic field to carry out energy exchange after exchanging energy with the radio frequency electromagnetic field. Therefore its gain receives the limitations of the feedback oscillator. It generally cannot be too high, only around some ten decibels. Usually the slow wave structure of the repeat entry type is circular. But the linear type of non-repeat entry also is circular. The repeat entry type usually uses distributed electron transmissions, its area is much larger than the area of the cathode transmission area in the corresponding linear ray tube electron gun, therefore it is a device with a high diversion coefficient. The distributed transmission can satisfy the requirements of the radar for high power and low voltage.

Although the cross field amplifier (CFA) has many types of tubes, presently the most commonly used is the repeat entry forward directional wave tube and the repeat entry backward-wave tube (usually called increased amplitude tube). These two tubes both are known for high efficiency and low volume. Recently, because they use a new structure of long circuit, cathode driver, cold cathode, high voltage cooling, etc., the performance of these tubes have had very great improvement.

High efficiency is regarded as the primary property of the model M device, the efficiency of the increased amplitude tube can reach as high as (40-80)%, the efficiency of the forward wave tube is slightly lower, but also is (30-60)%. Therefore conducting extreme power amplification can greatly economize on power source consumption. Using the CFA as an extreme transmitter, its overall efficiency is unusually close to extreme efficiency. For example, the overall efficiency of the two stage amplification chain is $\eta \approx 0.9\eta_{CFA}$. High efficiency must go through the power of cool dissipation to become low. It can simplify the cooling system and also further reduce the power that is necessary for cooling. The anode voltage of this tube is fairly low, on the one hand this can simplify the insulation problem, and therefore can increase the device density and be unlikely to produce a flickering phenomenon; on the other hand, again unlike X ray protection that is

required that way by the linear ray tube, this further reduces the volume of the device. Aside from this the installed height of the tube also is much lower than that of the linear ray tube, therefore it is convenient to use this device in highly limited trailers or in the engine room of aircraft.

Another merit of this type of tube is that it is very easy to make a wide frequency band, and this also is exactly what is necessary to raise the jamming resistance of frequency agile radar. Generally, the bandwidth of the forward wave tube can reach (10-15)%, the bandwidth of the increased amplitude tube of the backward-wave type is slightly more narrow, but also can reach (8-12)%. Moreover, in operational frequency it reaches a fairly high output power degree, its power level calibration is also very simple.

Another merit of the cross field amplifier (CFA) is that phase linearity is good, its deviated linearity is usually within $\pm 5^\circ$, and also its phase stability is fairly good, the phase variations that are caused by 1% current variations are $0.5^\circ - 3^\circ$. Therefore it is especially suitable for pulse compression radar.

The primary shortcoming of this kind of tube is that gain is fairly low, the gain of the increased amplitude tube is within the range of 6-18dB, and the gain of the forward directional wave tube is within the range of 10-16dB. This shortcoming makes the CFA suffer limitations in very long times. However, using cathode driver techniques this shortcoming has recently been overcome to a large extent. Much earlier some people assumed that if they used high frequency driving power from cathode input (cathode also makes slow wave lines), it would be convenient to set up a raised frequency field on the cathode surface; it takes the form of a derivative function to attenuate towards the direction of the anode, this way, the fairly small input power can make the cathode drive, thereby greatly raising the gain of the tube. At this moment the cathode plays a double role, both as input circuit and as an electron source. The radio frequency signal drives the electron transmission, and at the same time controls the size of

the electron current. A simplified diagram of its structure is as Fig. 8.19 shows⁽¹⁰⁾. According to reports, in 1975 Thunder Company manufactured a cathode driver platinum tube, the cathode uses a platinum manufactured cross structure, it operates in the L waveband, peak power is 1MW, gain surpasses 30dB, bandwidth is 8%, efficiency is 78%. In 1977 the cathode drive principle was again applied to a forward wave tube, and obtained a gain of higher than 28dB and a bandwidth of 14%. This kind of index makes the cross field device obtain even stronger competitive ability.

Another drawback of the cross field device is that its straight through plug-in loss is very small (for example the plug-in loss of the increased amplitude tube is only 0.5-2.0dB, the plug-in loss of the forward wave tube is only 1.5-3dB), therefore the standing wave ratio of the later stage can influence the former stage. For example if the standing wave ratio of the end stage load is 1.5:1, the power that is reflected by this standing wave ratio will be 14dB lower than the transmitting power. But after it goes through the tube, on certain frequencies it will group with the reflected power in the tube, when going to the input end of the tube it will only be 8dB lower than the transmitting power. If the gain of this end stage is 10dB, then this reflected power must be 2dB greater than the input power. This then can severely influence the operation of the former stage. Therefore in using the cross field device as the transmitter of the end stage power amplification, in the end stage and stage before the end it is necessary to add an iron oxygen isolator, to reduce the influence of the reflected power. As in the above example, even if adding an isolator that possesses a 16dB isolator ratio, it can only ensure the standing wave ratio seen from the stage before the end to be 1.5:1.

However, this shortcoming can also be utilized. When the end stage gain is fairly small, the output power absolute value of the stage before the end is fairly large, therefore it is possible to carry out "straight through" operations, when closing the end stage or when blockage occurs in the end stage, the power of the stage before the end will go through the end stage and go directly to the antenna.

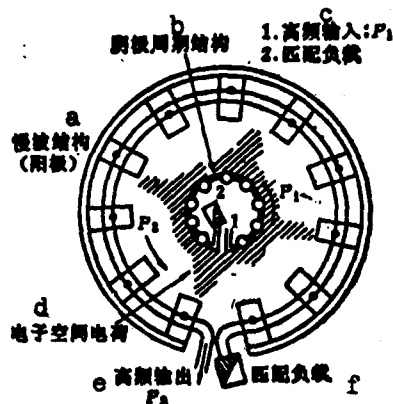


FIG. 8.19 SIMPLIFIED DIAGRAM OF THE STRUCTURE OF A CATHODE DRIVE CROSS FIELD DEVICE
KEY: (a) Slow wave structure (cathode); (b) Cathode cycle structure; (c) 1. High frequency input, 2. Matching load; (d) Electron space charge; (e) High frequency output; (f) Matching load

Another shortcoming of the cross field amplifier (CFA) is that output clutter signals are fairly great, within each megahertz bandwidth are approximately 30-60dB lower than carrier waves. Moreover, it is related to the driving power. The larger the input drive, the smaller the clutter. To put it differently, the clutter of the tube with high gain must be somewhat greater than that of the tube with low gain.

A very great property that the CFA has is that it can use a cold cathode. Because even if in a device that has a very high vacuum degree there are still enough gas elements (for example when the atmospheric pressure is 10^{-8} , there are approximately 3×10^8 elements/cubic centimeter). When adding high frequency energy, some certain gas elements in it will then be ionized, some certain free electrons will then be pulled back to the cathode surface. So long as the cathode is made from material that possesses a sufficient quadratic electron transmission system, then it can stimulate enough quadratic transmissions and cause its full cathode current to be quickly set up. Its setting

up time is very short, usually only five nanoseconds, therefore without needing any preheating or added heating time it can enter full peak power and full average power motion. Moreover, the variations of this cold cathode are not sensitive to the pulsewidth and operational ratio, and can be used in different operational forms. This cold cathode not only can economize on filament power, but also, due to the high voltage insulation, can save on filament transformer that has a very large volume. In certain tubes that have a high average power, because they generally have an approximately 5% input power dissipation on the cathode, therefore they even still must use liquid cooling to prevent the "cold" cathode from becoming too hot. In the past, because the quadratic transmission properties of the cathode material could not be controlled very well, therefore its length of operational life could not be ensured. Recently, after using the platinum metal quadratic transmission cathode, we can ensure its life will be as long as 10,000 hours or more.

As the previous section recounts, in applications of frequency agile radar, the end stage power amplification amplifier is required to have as wide as possible an instantaneous frequency band and have as smooth as possible output properties in operational frequency. Firstly, the bandwidth of the cross field amplifier (CFA) does not receive the limitations of gain drop, but primarily receives the limitations of the operational stability. The above two CFAs both belong to the repeat entry category, namely, their slow wave structures are approximately circular. This way, after the electrons that become beams by high frequency electromagnetic field accumulation go through the output system, they turn around to newly enter the input end of the slow wave system.

Because the newly-entered electrons become a beam, therefore when they enter into the input end of the slow wave structure they have the problem of being the same as or the opposite from the input radio frequency signal. When they are the same, it has a positive feedback effect and makes the gain of the entire tube increase. Opposite, it

will make the gain decrease. This phase relationship is related to the length of the slow wave structure and the frequency of the input signal. The shorter the length of the slow wave structure, the wider the frequency range that maintains the positive feedback. For example, regarding the increased amplitude tube that possesses a fairly short slow wave structure, it can maintain this positive feedback within a 10% bandwidth, although its slow wave structure is very short, it still can depend on the positive feedback to obtain equal gain and fairly high efficiency. Another advantage of tubes with this short slow wave structure is because its total phase length is fairly short (generally only 600°) therefore its "cold" and "hot" phase length variations are very small. Therefore, its phase stability is unusually good, typical value is when the anode current varies 1%, phase only varies 0.5 degrees.

In order to eliminate the limitations of the repeat entry electron beam assembly on its bandwidth, we can use an incontinuous slow wave structure, establishing a drift region between its input and output that does not have a high frequency field (see Fig. 8.20). This is to cause the repeat entry electron to be dispersed by the space charge before entering the input end. After using this method it can obtain an even wider bandwidth. But because there are no positive feedback effects of the repeat entry electrons, therefore in order to obtain the same gain it is necessary to have an even longer slow wave construction, generally its length reaches 14 wavelengths (approximately 5000° phase length). Precisely because of this reason, the frequency bandwidth of the forward directional wave must be wider than that of the backward-wave type increased amplitude tube, but because its phase length is relatively long, therefore its phase stability must be somewhat inferior to that of the increased amplitude tube. When its typical values each vary 1% of the anode current, the phase variation is approximately 2° . The long circuit also increases circuit wear and tear, thereby decreasing the efficiency of the tube, this is also one reason why the efficiency of the forward wave tube is lower than that of the increased amplitude tube.

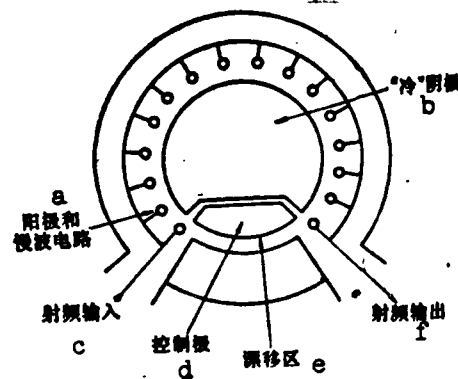


FIG. 8.20 USING THE DRIFT REGION AND CONTROLLING ELECTRODE TO SOLVE THE PROBLEM OF REPEAT ENTRY ELECTRON ACCUMULATION
KEY: (a) Anode and slow wave circuit; (b) "Cold" cathode; (c) Radio frequency input; (d) Controlling electrode (e) Drift region; (f) Radio frequency output.

However, after the slow wave structure lengthens it will cause the size of the anode to enlarge, this contributes to the stray heat factor of the anode and can increase the average power of the tube. In certain increased amplitude tubes that use long circuits, even though they do not use the drift region to eliminate accumulation of the electron beam, when they operate on a good several beneficial cycles with unbeneficial repeat entry in a 9% bandwidth, they also do not discover the undulation of gain in the bandwidth. The reason for this is still not too clear.

Next, although the forward wave tube and backward-wave tube have no particular striking differences in general parameters (such as bandwidth, gain, efficiency, etc.), when operating in a very wide frequency band, the anode voltage that is required is very different. The forward directional wave tube requires a comparatively constant anode voltage, while the backward-wave tube requires the anode voltage to vary with its operational frequency, to obtain relatively good operational properties. In fixed frequency radar, this is not an outstanding problem, but in variable frequency-especially frequency agile-radar, this problem is comparatively outstanding.

In order to understand this property it is first necessary to take a look at the differences between forward directional type and backward type cross field amplifiers (CFA) on frequency-phase shift properties. The so-called frequency-phase shift diagram (sometimes called a ω - β chart) also is the property of the phase shift of the slow wave structure following frequency variations. Figure 8.21 gives the frequency-phase shiftchart⁽⁹⁾ of the forward directional tube and the backward-wave type CFA. Because the direction of the radio frequency power of the backward-wave type CFA is opposite from the phase speed, therefore its frequency-phase shift chart is also opposite from that of the forward directional wave tube. In the figure the straight line that goes past the primary point represents the constant phase speed line. This phase speed corresponds to certain accelerated voltage of the anode. This way, if the tube is required to have an operational frequency band, the phase speed that it corresponds to also has a specific range. This specific range also determines the corresponding anode voltage variation range. If the frequency that changes the input signal does not correspondingly change the value of the anode voltage, then the speed of the electron beam cannot match the phase speed of the radio frequency electromagnetic field, and can cause the gain and the efficiency to simultaneously decrease. But, from the figure we can see that when the operational frequency varies, the anode variations that are required in the forward wave tube must be much smaller than those in the backward-wave type increased amplitude tube. This is also to say that the forward wave tube possesses fairly good "constant voltage" properties when the operational frequency varies, which is especially important in frequency agile radar. Because it can cause the radar to operate when there is high speed pulse jump frequency it still uses fixed anode voltage, this can cause a "continuous flow" type forward wave tube that does not need a modulator. For example, a forward wave CFA in a 10% frequency band only requires a 1% voltage variation when current is constant, because its dynamic-state resistance is only 10% of the static-state (continuous flow resistance); therefore when operating on a constant voltage source, the current pulled out by the tube will vary 10% in the entire operational frequency band.

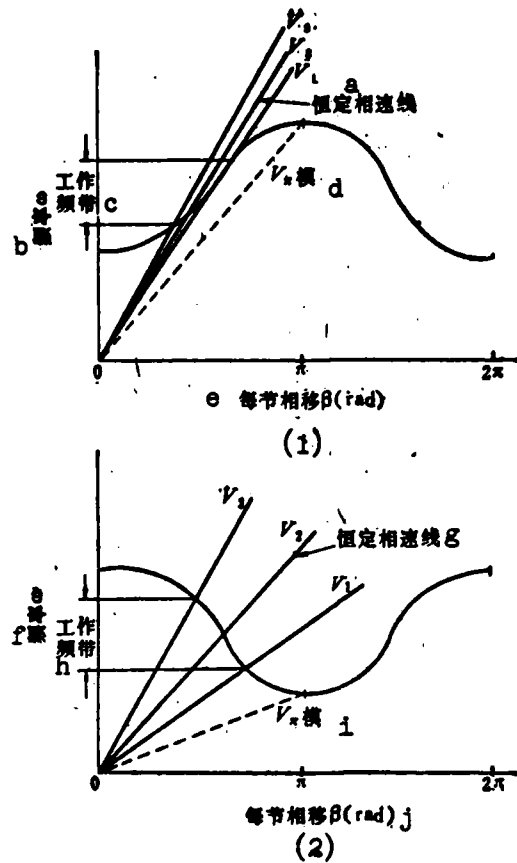


FIG. 8.21(1) FREQUENCY-PHASE SHIFT CHART OF FORWARD WAVE CFA (2) FREQUENCY-PHASE SHIFT CHART OF BACKWARD-WAVE CFA
KEY: (a) Constant speed line; (b) Frequency; (c) Operational frequency band; (d) Model; (e) Phase shift of each section; (f) Frequency; (g) Constant speed line; (h) Operational frequency band; (i) Model; (j) Phase shift of each section

The backward-wave type increased amplitude tube thus will not work. In order to make it able to operate in the best condition, when frequency varies 12%, it requires the anode voltage to vary 16% or more. If the anode voltage remains fixed and invariable, then its output power variations will not exceed 100%.

Although this weakness exists in the backward-wave type increased amplitude tube, this is not to say that this tube cannot be applied in frequency agile radar. This is because in the increased amplitude

tube with cathode pulse control, the voltage of the continuous flow high voltage source does not go directly to the microwave tube, but goes to the microwave tube after going through the modulation tube. Therefore, so long as we select the appropriate modulator circuit, causing its output resistance to match with the dynamic-state resistance of the tube, we can resolve this problem (we will discuss this problem later). But in the backward-wave type tube with continuous operation, conditions are not the same. At this time the continuous flow high voltage source goes directly to the microwave tube. Therefore this backward-wave type continuous flow operational tube can only operate on fixed frequency, so it actually is not useful. Only the forward directional wave type continuous flow operational tube is valuable for practical use.

In the CFA that uses a cold cathode, because its cold cathode depends on an additional radio frequency pulse to start, therefore an additional radio frequency pulse must not lead a certain time more than the cathode pulse high voltage, to make its cathode start fairly early. However, although a drift region exists in the tube it does not immediately stop after the radio frequency pulse is eliminated. This is because the repeat entry electrons still have sufficient energy, enough to make the quadratic electron transmission of the cathode be safeguarded (the hot electron transmission of the cathode also causes it to safeguard enough quadratic transmissions after the radio frequency input stops), this can cause the tube to produce oscillation at the frequency band edge or produce a wideband noise oscillator to go directly to the cathode pulse high voltage until it ends. In order to resolve this problem, in this type of CFA we often use a controlling electrode (see Fig. 8.20), sometimes called a closing electrode. In an instant before radio frequency ends, an anode is added on this collecting electrode to collect the electrons through the drift region. The rear edge of this positive pulse delays one time more than the rear edge of radio frequency input pulse, to ensure that the tube is not likely to start up again. Further research afterwards discovered that

using the controlling electrode often, we still can cause the tube to have "continuous flow operations", and also, so long as there is a constant high voltage on the anode and cathode of the tube, later depending on the radio frequency input making the tube start, we use a narrow pulse on the controlling electrode to make the tube close. Because the pulse voltage that is added on the controlling electrode only has $1/3$ of the pulse that was originally added on the cathode, and the current also only has $1/3$, therefore the requirements of the modulator can be greatly simplified. This can cause it to operate on exceedingly complicated modulated wave forms. For example, it can be used in pulse lumped modulation radar that simultaneously possesses very high distance identification and speed identification. But because the controlling electrode is an electrode with ground insulation, and heat dissipation is relatively difficult, therefore it has a certain limitation on the highest pulse repeated frequency. In continuous flow operational tubes, in order to avoid flickering between the anode and cathode, its continuous flow operational voltage also cannot be too high, therefore basic peak power also has certain limitations. Although this is the case, the power maximum that it can reach still can satisfy requirements for general applications. For example, in the band in a C waveband has an SFD-237 forward wave tube with a controlling electrode its continuous flow operational voltage is 27 kilovolts, peak output power reaches 1MW, and average power can reach 10kW.

Another method of continuous flow operations is using cathode extinguishing techniques. The cathode extinguished forward wave amplifier abolishes the controlling electrode, so long as the rear edge of the high frequency pulse and the corresponding anode that is added on the cathode is a positive pulse (extinguished pulse), it causes the tube to close. Actual test results show that the extinguished pulse that is added on the cathode can shorten the rear edge of the high frequency drive pulse. Although the modulated energy that it requires is greater than controlling electrode modulation, it eliminates the complicated controlling electrode structure, and therefore is worth using.

This continuous flow operational tube even can do self-closing. So-called self-closing is simply when the high frequency signal of the driver ends, the tube closes by itself, it is not necessary to add a narrow pulse control signal in the controlling electrode. This operational form also is called self-modulation. At this time, so long as there is a bias set voltage that is half of an equivalent anode voltage that is added on the controlling electrode, then that is fine. This controlling electrode is called a bias set electrode (or closing electrode), and this kind of tube is called a radio frequency key control continuous operational CFA. The bias set electrode will absorb 25% anode current when the tube conducts, therefore this tube can be considered as a partial reseat entry type. But it fully omits the pulse modulator, and also does not have the limitations of the repeating frequency of the pulse, but only must have a medium power bias voltage source.

In order to even better improve the properties of the self-modulating continuous flow operational tube, we conducted much research on the structure, form, and position of the bias set electrode. For example some people proposed that after the bias set electrode is not located in the drift region but is located in the input end, and furthermore makes it sink to beneath the surface of the cathode, the end also has a sudden break out. The cathode surface also has a slight slope. This then makes the bias set electrode able to even more effectively gather electrons after the high frequency pulse terminates, thereby causing the tube to close, when the high frequency pulse arrives it again can reduce its interception of the electrons, to form an amplification effect.

One shortcoming of this continuous flow operational CFA is that it is not suitable for wide pulse operations. Because dynamic-state resistance of the CFA is very low, therefore when its allowable output power at the pulse end varies 10%, the anode voltage is only allowed 1% variation. This requires the anode power source to have very great

capacitor. The wider the width of the transmitting pulse, the larger the capacity of the capacitor. Although this can enlarge the volume of the power source, no matter what it is much simpler than the complicated modulator.

One benefit of the tube operating in a "continuous flow state" is: because it is in full voltage from beginning to end, therefore so long as it is suitably designed, it cannot produce a π type oscillator. From Fig. 8.21 we can see that the π type oscillator of the forward wave tube is approximately 15% higher than its highest operational frequency; but the π type oscillator of the backward-wave type increased amplitude tube is 15% lower than its lowest operational frequency, further more the voltage producing a π type oscillator is lower than the normal operational voltage. In general cathode pulse modulation tubes, so long as the radio frequency input pulse already makes the cathode start, when the rising and falling of the pulse voltage goes through this voltage, it all can produce π type oscillation, this requires the cathode pulse to have an edge that raises and lowers faster than its setting up time. But in continuous flow operational tubes, the input radio frequency drive pulse is required to have fast enough rising time. Its reason is this: when the radio frequency drive reaches 1kW, it is enough to make the cathode start, but when it is necessary to reach the corresponding power (for example, in high powered tubes it is necessary to reach 50kW), it then can cause it to lock on the input frequency. Because the tube adds full continuous flow voltage, in the rising time of this input power it can produce full power clutter output. In order to reduce this clutter output, it requires the input drive pulse to have as short as possible a rising time.

8.3.3 SELECTION AND USE OF EACH TYPE OF CROSS FIELD AMPLIFIER⁽¹²⁾

To summarize the above discussion, the cross field amplifier (CFA) can be divided into three primary types according to their operational conditions: the cathode pulse control forward wave tube and backward-wave type increased amplitude tube, the continuous flow operational

band with controlling electrode forward wave tube, and the continuous flow operational self-modulating forward wave tube. When there are given technological requirements, exactly which tube to select is not only related to the properties of the tube itself, but is also related to such properties as the modulator that the tube uses, the high voltage power source, the pressure stabilizer, and the safeguard circuit.

In cathode pulse control CFA, it is necessary to possess the same full powered modulator with a magnetron. The modulator type that is used also can be divided into the two types of the simulation line soft tube modulator and hard tube modulator. The soft tube modulator generally uses a pulse transformer for coupling (see Fig. 8.22(a)), its output resistance is very high, therefore it is not only suitable for forward directional wave tubes, but also is suitable for increased amplitude tubes to operate in a frequency agile state. Although the voltage of the soft tube modulator is fairly low and efficiency is fairly high, its primary weakness is that it is not suitable for variable pulsewidth and wide pulse, and furthermore the pulse wave form that it forms is fairly poor, and can give rise to phase modulation in the pulse, therefore it is not suitable for pulse compression. Hard tube modulators can be divided again into the two types of common ground connection types and contact adjustment types. Because the capacitor of common ground connection type hard tube modulator for ground distribution is large and the requirements for the power source are high, therefore we often use the contact adjustment type. The diagram of its principles is shown in Fig. 8.22(b). To increase its output resistance to satisfy voltage variations when the increased amplitude tube has frequency agility, a feedback resistance of the cathode contact of the switch tube causes its output current to be constant. Therefore this hard tube modulator is also called a constant flow hard tube modulator. Because the adjustment effect of the switch tube can reduce the dropping of high voltage source in the pulse period, therefore this modulator can be allowed to use a fairly small high voltage capacitor. We will later discuss in detail the design and computations of this modulator.

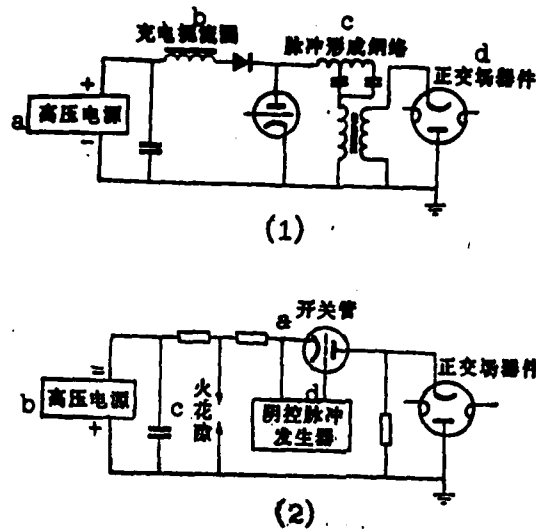


FIG. 8.22 PRINCIPLES OF POWER SOURCE
OF SOFT TUBE MODULATOR AND CONSTANT
FLOW HARD TUBE MODULATOR
KEY: 1. (a) High voltage power source;
(b) Choke; (c) Pulse forming mesh;
(d) Cross field device; 2. (a) Switch;
(b) High voltage power source; (c)
Spark interval; (d) Cathode control
pulse generator; (e) Cross field device

All the soft tube modulators and constant flow hard tube modulators can limit peak current when there is a microwave jump spark, therefore jump sparks in the tube of the CFA can bring about an individual leaking pulse.

Now we will take a look at the modulator and power source of the continuous operational controlling electrode forward directional wave tube. As is recounted above, because this tube can directly operate on the continuous flow power source, therefore a full powered pulse modulator is not necessary, but for causing the tube to close it needs a spark extinguishing pulse, this spark extinguishing pulse still needs to produce by using a low power modulator (see Fig. 8.23(a)). Because dynamic state resistance of the CFA is very low, it requires the dropping of output radio frequency pulse power to be as low as 10% (0.5dB), then it required the dropping of the high voltage power source to be

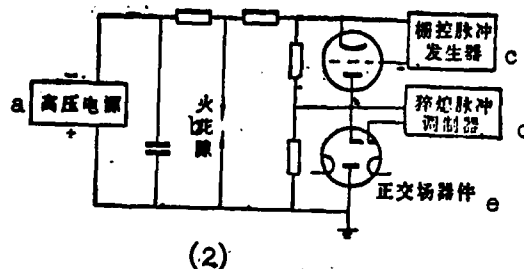
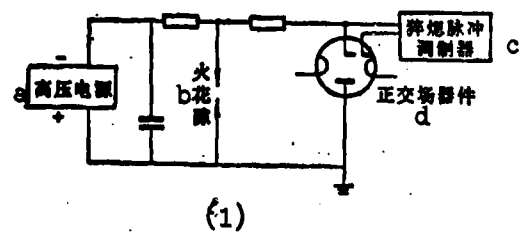


FIG. 8.23 DIAGRAM OF CIRCUIT LINKAGE OF CONTINUOUS FLOW OPERATIONAL FORWARD DIRECTIONAL WAVE TUBE WITH CONTROLLING ELECTRODE

KEY: 1. (a) High voltage power source; (b) Spark interval; (c) Sudden interval pulse modulator; (d) Cross field device. 2. (a) High voltage power source; (b) Spark interval; (c) Grid control pulse generator; (d) Sudden interval pulse modulator; (e) Cross field device

as low as 1%, this in turn requires an extremely large capacitor. In order to resolve this problem we can add a contact adjustment tube between the cross field device and the power source (Fig. 8.23(b)). This adjustment tube must endure the full peak voltage and power source of the microwave tube, therefore it will be as large as the hard tube modulator of a cathode pulse modulation cross field device, this loses the advantage of continuous flow operation. Therefore we generally use a contact voltage stabilizer in front of the high voltage capacitor, this makes the continuous flow operational cross field amplifier (CFA) to come into direct contact with the capacitor that stores energy. But doing this can produce another problem, that is that the jump sparks in the microwave tube can pull out extremely great current and cause damage to the tube. To limit this current, it is necessary to use a

limit and flow resistor in the output contact of the energy storage capacitor. With these we simultaneously should add a spark interval safeguard circuit (sometimes called a prize circuit). This spark interval triggers to disperse the jump spark circuit when the tube jump sparks. Although this can safeguard that the microwave tube is not likely to be damaged, when there is jump sparking in the tube it can cause the continuous flow operational forward wave tube to not only leak out a certain pulse, but also discontinues for a time of several milliseconds to several seconds, and goes directly to the power source until the energy storage capacitor fully charges. Recently a magnetron thyatron safeguard circuit has emerged, its volume is small, its cut-off time is short, and to a certain extent it resolves this problem. In brief, the application of the continuous flow operational forward wave tube primarily receives the limitations of the light problem, because the high voltage power source of the continuous flow operational tube is directly on the surface, therefore its jump spark probability is originally especially high, moreover, due to the effect of the safeguard circuit, the influence of the light on its operating is also especially great, therefore it can only decrease its peak power and average power as much as possible, in order to cause fairly low voltage.

Another problem of the continuous flow forward wave tube is that the cathode current follows the very fast rise of the radio frequency drive signal. Measurement test results show that its rising time can only be several nanoseconds. The current of this very fast rise can drive the oscillator on the power source leadwire, this oscillator can give rise to undesirable phase and amplitude modulation in the pulse period. In order to resolve this problem, we can use high voltage cable as the leadwire, and cause its resistance to match the limited low resistance of the light (see Fig. 8.24). At the same time, the inductance in itself of the energy storage capacitor is required to be as small as possible. The exceedingly fast rise of the cathode current can make the radio frequency pulse of its output rise exceedingly fast. This can make the spectrum of its radio frequency broaden. But

up till now there is still no effective method to control its rising time.

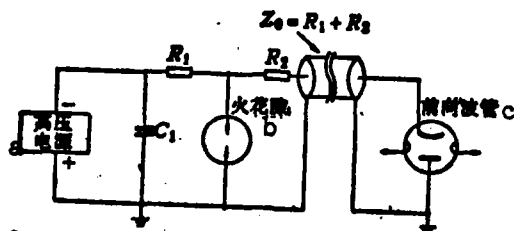


FIG. 8.24 FEEDBACK AND SAFEGAURD CIRCUIT OF THE CONTINUOUS FLOW OPERATIONAL FORWARD DIRECTIONAL WAVE TUBE

KEY: (a) High voltage power source;
(b) Spark interval; (c) Forward wave tube

On the basis of the above, we can list the properties of the modulators and high voltage sources that are used by the cross field amplifier (CFA). They are listed in Table 8.4.

In addition to the properties listed in Table 8.4, now we can also list a comparison of three primary types of CFA, listed in Table 8.5.

From the tables we can see that all these three types of tubes are suitable for jump frequency, moving target indication, and pulse compression.

When there is extremely high pulse repeating frequency (pulse interval < 20 microseconds) and a very narrow pulsewidth (several microseconds to point several microseconds), the cathode pulse control CFA is not very beneficial, because the energy of the modulator in the discharge on the parasitic capacitor is wasted. This can have a fairly striking influence on the overall efficiency, the forward wave tube with controlling electrode, so long as it has a relatively

low sudden extinguishing pulse, will be more suitable to high repeating frequency and short pulse than the former.

When there is a long pulse operation, the continuous flow operational cross field amplifier (CFA) is not very beneficial, because it needs a very large capacitor to limit the dropping of the output power in the pulse, if it requires the dropping of the power source capacitor to be less than 1-2%, it then signifies that the capacitor needs a pulse energy that is carried to the microwave tube that is 25-50 times the stored energy (because when the capacitor voltage drops 1% the stored energy will reduce 2%). As to using the constant flow hard tube modulator cathode pulse control CFA it can allow voltage on the capacitor to drop 5-10% in a long pulse period. This way, the capacitor, so long as the stored energy is carried to 5-10 times of the energy of the pulse of the microwave tube, this can greatly reduce the size of the capacitor. Although using a drop compensation net between the capacitor and the forward directional wave tube can reduce the capacitance that is needed by the continuous flow operations, this drop compensation net can make the forward edge of the pulse produce a small point when there are continuous flow operations. This is not very desirable.

The performance of continuous flow operations when there is high power is also very poor. This is primarily due to the jump spark that is caused in the tube. As is previously recounted, when there is high power the probability of jump sparking increases, each jump spark will make the whole system stop operating for several microseconds to several seconds, unless the jump spark rate of the tube reduces several levels, or circuit techniques can make its jump spark only leak a monopulse, at the present technological level this problem still cannot be resolved.

The so-called forward stage feed penetration (straight through) when radar decreases power application, with the end stage closed causes the power of the forward stage to penetrate the end stage tube and be carried to the antenna. Obviously there is no way to achieve

AD-A124 003

FREQUENCY AGILITY RADAR(U) FOREIGN TECHNOLOGY DIV
WRIGHT-PATTERSON AFB OH 45433-6101 06 DEC 82
FTD-ID(RS)T-0803-82

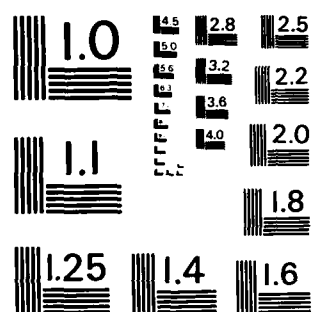
7/7

UNCLASSIFIED

P/G 17/8

NL

END
DATE
FILMED
3 83
DTIC



MICROCOPY RESOLUTION TEST CHART
NATIONAL BUREAU OF STANDARDS-1963-A

TABLE 8.4 SEVERAL DIFFERENT TYPES OF MODULATORS AND VOLTAGE POWER SOURCES THAT ARE USED BY CROSS FIELD AMPLIFIERS

Cross Field Amplifier Type	Modulator Type	Whether or not it is suitable for Jump Frequency Operation	Variable Pulsewidth Operation	Performance when high Repeated Frequency	Pulse Wave Form	Pressure Stabilizer Needed for Attenuating Wave Veins	Allowable high voltage Drop (when output power drop is 10%)
cathode pulse control increased amplitude tube and forward wave tube	simulated linear	yes	no	poor (efficiency drops)	has wave veins	continuous flow contact or resonant charge	
	constant flow hard tube	yes	yes	poor	good	not needed	>10%
Forward wave tube with controlling electrode and radio frequency key control	hard tube ground connect	no	yes	poor	good	contact pressure stabilizer	to 1%
	Continuous flow operation	yes	yes	good	good	contact pressure stabilizer	to 1%

Required Capacitor	Influence of Cross Field Device	
	Jump Spark	
	On Peak Current	On System Operations
small	Twice normal value	Barely a leak pulse
large	1-2 times normal value	Barely a leak pulse
large	High (transmitability limit from hard tube)	OR needs to use safeguard, later newly starts
large	Unusually high	Must use safeguard, later newly starts

TABLE 8.5 APPLICATION CHARACTERISTICS OF VARIOUS DIFFERENT TYPES OF CROSS FIELD AMPLIFIERS

Cross field amplifier type	Cathode pulse control forward wave tube and increased amplitude tube	Continuous flow operational	
		Controlling electrode forward wave tube	Radio frequency Control forward wave tube
Jump Frequency	good	good	good
Moving Target Indication	good	good	good
Pulse Compression	good*	good	good
Short pulse (<1 μ s)	poor	slightly poor	good
Long pulse	good	slightly poor	slightly poor
High powered	good	slightly poor	slightly poor
Forward stage feed Penetration	good	slightly poor	Not applied
Tube Efficiency	good	good	slightly poor
Modulator Efficiency	slightly poor**	good**	Extremely good
Total Efficiency	slightly poor	good	slightly poor

*Only can use hard tube modulator, soft tube modulator has wave vein problem in the pulse.

**When short pulse operations, performance worsens.

this operational pattern in the cold cathode radio frequency key control continuous flow operational tube. Although it can be achieved in the tube where the band has a controlling electrode, it is necessary to add a "safeguard close" pulse on the controlling electrode through the period of the entire pulse. The requirements of this pulse are completely different from those of the sudden extinguishing pulse, therefore we must have two different modulators, which complicates the design. But operating on the forward stage feed penetration in the cathode pulse control tube is not the slightest problem. The loss that it causes is only 1-2dB.

The efficiency of all these three tubes in themselves is almost the same, the radio frequency key control type tube is slightly different, but because the requirements of the modulators each are different, therefore the efficiency of the modulators has fairly great differences. The cathode pulse type requires a full powered modulator, its efficiency is correspondingly low; although the controlling electrode forward wave tube does not need a high-powered modulator to operate in continuous flow, its sudden extinguishing pulse still must have a medium-powered modulator; the radio frequency key control forward wave tube does not need any modulator, therefore its efficiency is the highest, corresponding to the efficiency of the continuous flow power source. This way, overall efficiency is slightly higher when the continuous flow operational forward wave tube is used.

To sum up the above explanation, although the continuous flow operational forward wave tube does not need a high-powered modulator, which really attracts people, in the end, because jump spark rate is fairly high, it can bring about the suspension of the system, which makes it useless. Only if we have a narrow pulse series with high repeated frequency in the required transmitting group will we then use a forward wave tube where the band has a controlling electrode (for example in MPS-36 radar a transmitting series of 5 pulsewidths 0.25-0.5 microseconds is required, interval is a 1 microsecond pulse, it uses the forward wave tube with controlling electrode). So the

cathode pulse control cross field amplifier (CFA) thus obtains extremely extensive use.

Table 8.6 gives the parameters of some CFAs.

From the table we can know that the efficiency of the increased amplitude tube is slightly high, but its bandwidth is slightly narrow. The backward-wave type increased amplitude tube that uses a long circuit can obtain fairly wide corresponding bandwidth simultaneously with high efficiency, moreover its average power maximum value also greatly increases. Model QR 1606 increased amplitude tube that is listed in the table is an example⁽¹³⁾. Its operational frequency reaches 12%, efficiency is as high as 60% or more, operational ratio reaches 0.054. This tube also uses a platinum quadratic transmitting cathode, its life is longer than 10,000 hours. The liquid cooling that is used on all surfaces on the structure is used to avoid a hot electron transmission of the cold cathode after starting the drive. The typical operational properties of this tube are shown in Fig. 8.25. From the figure we can see that in the operational frequency band an anode voltage variation reaching 16% or more is required. The largest pulsewidth of this tube reaches 200 microseconds or above, noise level is approximately as low as carrier frequency 55dB/MHz, it is especially suitable for pulse compression radar with high average power.

The biggest drawback of the increased amplitude tube is that anode voltage variations within a certain range are required in its operational frequency band. This is extremely unbeneficial for its jump frequency operational time. But, so long as we select the appropriate modulator circuit we can resolve this problem. In the following sections we will research some problems of the jump frequency transmitter of the increased amplitude tube.

TABLE 8.6 PARAMETERS OF SOME FORWARD WAVE TUBES AND INCREASED AMPLITUDE TUBES

Model #	Corresponding Bandwidth(%)	Peak Power (kW)	Average Power (W)	Frequency Range (gigahertz)	Gain (dB)	Effect- iveness (%)	Anode Voltage (kV)	Weight (lbs)	Note
QKS-1319	15	100	3000	1.2-1.4	15	50	10	35	
QKS-1396	10	40	200	3.135-3.465	13.5	50	11*	25	
QKS-1397	10	1000	5000	3.135-3.465	16	50	30*	70	
** SFD-237		1000	10000	C		35-45	27*		
SFD-257	8.9	1000	1000	5.4-5.9	13	50	30*	210	Band control electrode
L-5334	12	500	500	8.5-9.6	18	40	22	28	
QKS 1267	6.7	60	1800	2.9-3.1	20	55-63	25-29	50	
*** QKS 1110	6.7	1600	30000	2.9-3.1	9	60	50-54	120	
QR1606	12	1000	50000	3.1-3.5	10	55-68	28-33		
SFD-222	8.9	1000		5.4-5.9	17	45	38	60	

*Continuous Flow

**Forward Wave Tubes

***Increased Amplitude Tubes

8.3.4 APPLICATIONS OF INCREASED AMPLITUDE TUBES IN FREQUENCY AGILE RADAR (14)

As the previous section explains, because the reverse space harmonic waves of the backward-wave type increased amplitude tube follows the phase speed of the slow wave structure it increases with the frequency increase. Therefore in order to obtain suitable interaction, the speed of the electron beam must increase with the frequency increase. Its cathode voltage must also increase with the frequency. Figure 8.26 gives the volt-ampere characteristics of the increased amplitude tube. When there are different operational frequencies the increased amplitude tube has different volt-ampere characteristics. In the figure frequency f_2 is higher than frequency f_1 . The variations of peak current that are caused by the variations of this peak voltage are related to the load properties of the modulator that is used. Figure 8.23 also gives the load properties of soft tube (hydrogen thyrotron) modulator and hard tube modulator. From the figure we can see that if we use a soft tube modulator, then when the transmitting frequency changes in the operational frequency band, the variation of its current (ΔI_1) is in an allowable range, therefore the power going to the tube actually remains constant. Because the variations of efficiency following frequency are not marked (refer to Fig. 8.21), therefore the variations of the output power of the tube when frequency varies are also not great. Conversely, if using a hard tube modulator, from the figure we can see that when operational frequency varies, it will cause its peak current to have very large variations (ΔI_2), on one hand this will give rise to the variations of output power when there is jump frequency, on the other hand it even can cause the operational point of the increased amplitude tube to run outside of the stable area, therefore this cannot be allowed.

Although using a soft tube modulator can resolve the problem, because the pulse that is used by the soft tube modulator forms a mesh, it is interlinked with certain pulsewidths. If the radar is required to change the pulsewidth and repeated frequency of the pulse in operations, then there is no way to use the soft tube modulator.

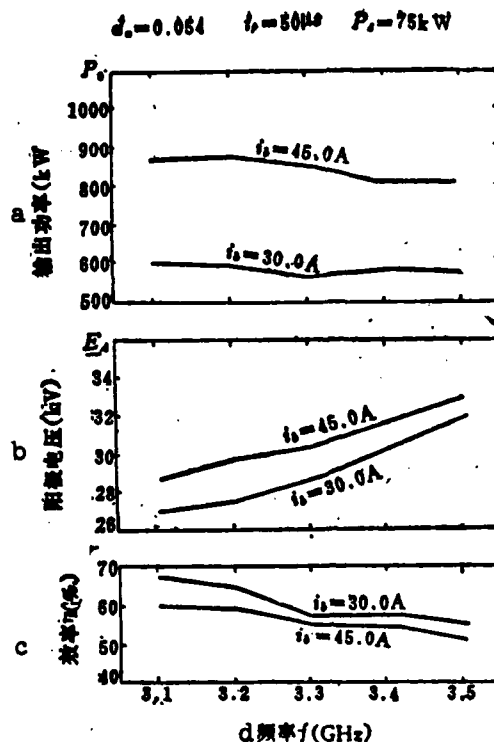


FIG. 8.25 OPERATIONAL PRINCIPLES
OF MODEL QR 1606 INCREASED AMPLITUDE
TUBE
KEY: (a) Output power; (b) Anode
voltage; (c) Efficiency; (d) Frequency

On top of that, the pulse wave form that is formed by the soft tube modulator is relatively poor, often its forward edge has peak ups and oscillation, this is very disadvantageous to the radar that uses pulse compression. Due to the above factors, many radars still require using hard tube modifiers. This way, if the radar operates in a jump frequency state it is necessary to carry out adjustment of its peak current. Because jump frequency is even carried out between the pulses, therefore it requires this adjustment to have extremely high speed. The simplest method is using the current negative feedback to stabilize its peak current, seen from another point of view it also is simply using the negative feedback to enlarge the output resistance of the modifier, causing the peak variation time of the modulator to bring about fairly small current variations.

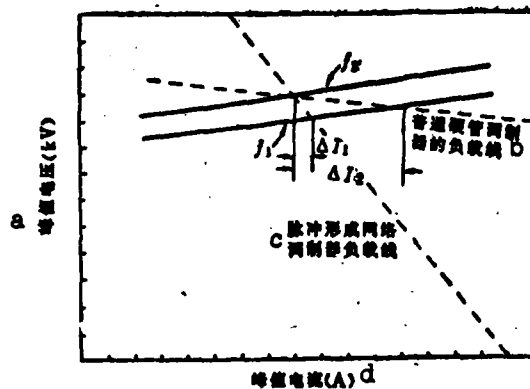


FIG. 8.26 VOLT-AMPERE PROPERTIES
OF THE INCREASED AMPLITUDE TUBE
KEY: (a) Peak voltage; (b) Load
line of ordinary hard tube modula-
tors; (c) Load line of pulse forming
mesh; (d) Peak current

In the following section we will take a look at specific modulator circuits that have feedback. The pulse modulator that is used by the cross field amplifier (CFA) is basically similar to the ordinary magnetron modulator. Simultaneously with the input radio frequency pulse, it needs a negative pulse high voltage added on the cathode (for the purpose of simplicity the cathode of the cooling unit is usually ground connected). The modulation tube of the ordinary hard tube modulator (switch tube) is connected between the energy storage capacitor and the high voltage power source, when the modulation tube conducts, it corresponds to ground connecting an end of the energy storage capacitor. The voltage that is charged by the stored energy uses the negative high voltage pattern to go to the microwave tube, causing the latter to enter into an operational state. But because the stored energy capacitor has very large geometric dimensions, the circuit where these two ends are not ground connected causes the distributed capacitance where the numeric value of the stored energy capacitor towards the ground is very large to load completely on the microwave tube. his specific numeric value of the distributed capacitance towards the ground depends on the volume of the capacitor, the

latter is determined by its capacity and its pressure endurance. To avoid the dropping of the pulse level, the energy that is stored in the capacitor is far greater than the energy that is transmitted by each pulse. For example, if the pulse is 50 microseconds, the power drop allowed in the pulse is 5%, peak power is 1MW, efficiency is 50%, thus the needed stored energy reaches 6,000 joules. Assume that operational voltage is 50 kilovolts. Then its distributed capacitance is approximately 150 picafarads. This large a distributed capacitance can give rise to many problems: firstly it can cause the forward edge of the pulse that goes to the cathode to worsen, and also can lead to producing a π type oscillation. Secondly it is necessary to provide a specific power on this distributed capacitance, this power is equal to the energy that is stored by it multiplied by the repeating frequency. This power also is provided by the modulation tube, this increases the power requirements for the modulation tube. Thirdly, this distributed capacitance must go through the appropriate channel to discharge when the pulse ends, its discharge time cannot be too long, otherwise it can influence the rear edge of the pulse. But the faster the discharge speed, the larger the necessary added power.

Another problem that is brought by the two ends of the energy storage capacitor not ground connecting is the safeguard problem of the light in the tube. Because when the energy exceeds 50 joules when light is in the tube it is possible to damage a microwave power tube, and the energy that is stored in the capacitor far exceeds this value (as in the above example where it reaches 6,000 joules), therefore it is necessary to use a trigger spark interval when there is light in the tube for the energy that is stored on it to discharge. If the two ends of the energy storage capacitor do not ground connect, then the two ends of the spark interval also cannot ground connect. A problem then exists in how the spark signal that is endured in the terrestrial electric potential circuit will turn to the trigger electrode that lies in the high electric potential spark interval.

In order to resolve the above problem it is best to use the modulation circuit where the stored energy capacitor ground connects, at this time the modulation tube has contacts between the energy storage capacitor and the microwave tube (as Fig. 8.27 shows). At the same time, in order to carry out peak current adjustment, there is a feedback resistor R_k that contacts in its cathode. But at this time, because the cathode and the grid of the modulation tube do not ground connect, therefore the problem exists of how will the modulation pulse signal go to the modulation tube that lies in negative high voltage. In order to resolve this problem, here we use an endurance high voltage pulse transformer (see Fig. 8.27). But due to the high voltage insulation level in the earlier stage, causing its leakage affect to enlarge and its driver inductance to reduce, this can bring about pulse rise time increase and pulse peak level drop. To improve its rise time we can appropriately reduce the ring amount, in order to resolve the problem of pulse peak drop, here we use the diode limiter method (see Fig. 8.27).

Although we ground connect one end of the energy storage capacitor in the modulation circuit, due to the capacitor of the increased amplitude tube cathode on the filament and the capacitor of the filament transformer on the ground, we still have the capacitor of the modulation tube cathode toward the ground equally making a distributed capacitance C_p of the increased amplitude tube cathode toward the ground. To make this distributed capacitance able to very quickly discharge after the pulse ends, in its two ends (then the increased amplitude tube cathode toward the ground) we use a discharge resistor R_c (see Fig. 8.27). The resistance value of this discharge resistor is determined by distributed capacitance capacity C_p and required discharge time T_f determining $(R_c = \frac{T_f}{1.65C_p})$. But because the discharge channel that is used is an ohm-resistor, it not only can deplete power when the pulse ends and discharges, but also can dissipate certain power in the pulse period: $(P_R = \frac{V^2}{R_c} \cdot \tau \cdot F)$.

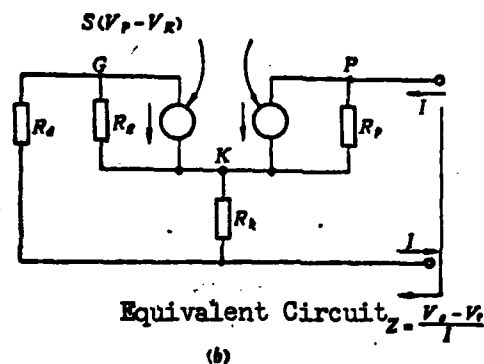
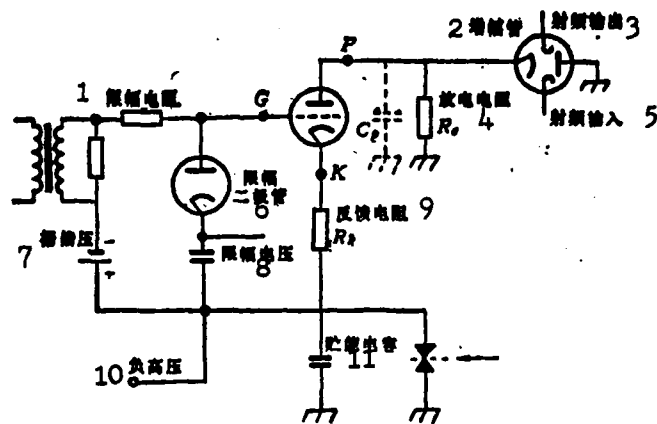


FIG. 8.27 DIAGRAM OF THE PRINCIPLES OF THE MODULATOR THAT USES CURRENT NEGATIVE FEEDBACK AND ITS EQUIVALENT CIRCUIT
 KEY: (1) Limiter resistor; (2) Increased amplitude tube; (3) Radio frequency output; (4) Discharge resistor; (5) Radio frequency input; (6) Limiter diode; (7) Grid bias voltage; (8) Limiter voltage; (9) Feedback distance; (10) Negative high voltage; (11) Energy storage capacitor

The key problem in this modulator is how to select the appropriate size cathode feedback resistor value, to cause it to be able to satisfy that the variations of peak current in the jump frequency period do not exceed the allowed range. If the variations of peak voltage of the increased amplitude tube in the jump frequency frequency band are ΔV_m , then allowable peak current variations are ΔI_m . This is output resistance R_m that is required by the microwave tube. It actually is the parallel connection between output resistance Z from the

modulator and discharge resistance R_c . Thus:

$$R_m = \frac{ZR_c}{Z + R_c} = \frac{\Delta V_m}{\Delta I_m} \quad (8.3)$$

Therefore, now the primary problem is finding the expression for modulator output resistance, however, based on given values ΔV_m and ΔI_m , the operational point of the modulator and computed cathode feedback resistance value of R_k is selected. Output resistance Z of the modulator with feedback resistance can be solved by the equivalent circuit in Fig. 8.24:

$$Z = \frac{r_p(R_g + R_s + R_k(1 - \mu_s)) + R_s(R_g(1 + \mu\mu_s) + R_k(1 + \mu))}{R_s(1 + \mu\mu_s) + R_g + R_k(1 + \mu\mu_s)} \quad (8.4)$$

In which:

- r_p — modulation tube feedback
- μ — modulation tube grid amplification coefficient
- R_g — grid resistance of the modulation tube
- μ_s — modulation tube grid amplification coefficient
- R_s — grid drive resistance

If we overlook the grid flow, then the above expression can be greatly simplified as:

$$Z = r_p + R_k(1 + \mu) \quad (8.5)$$

From given R_m and parameters of the tube we can compute the necessary R_k value:

$$R_k = \frac{1}{1 + \mu} \left[\frac{R_g R_m}{R_s - R_m} - r_p \right] \quad (8.6)$$

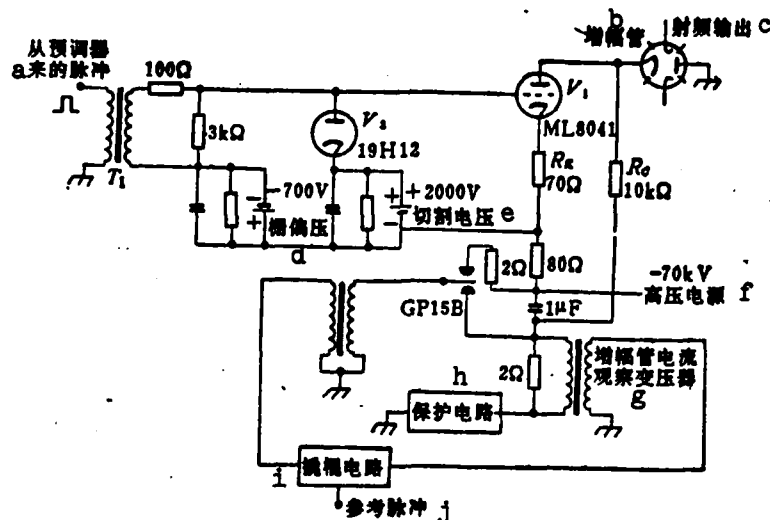


FIG. 8.28 DIAGRAM OF ACTUAL CIRCUIT THAT USES
A CURRENT NEGATIVE FEEDBACK MODULATOR
KEY: (a) Pulse coming from premodulator; (b)
Increased amplitude tube; (c) Radio frequency
output; (d) Grid bias voltage; (e) Separating
voltage; (f) High voltage power source; (g) In-
creased amplitude current detection transformer;
(h) Safegaurd circuit; (i) Prize circuit; (j)
Reference pulse

But because the modulation tube actually operates under grid flow conditions, therefore expression (8.5) can only be used as a rough estimate. A more precise value must find its differential parameters by the operational point of the modulation tube, and later a suitable R_k value will be selected and again its output resistance will be accurately computed by expression (8.4). If this value cannot satisfy the requirements then it must choose another R_k value to go directly to ΔI_m value and not exceed the allowed value. The R_k value can be determined by the graph method. The value of R_k becoming very small will cause the power dissipation of the modulation tube to become very large (causing its tube pressure drop to increase), while R_k becoming very large will require a very large grid drive. Therefore it is necessary to have a compromise.

Figure 8.28 gives the diagram of an actual circuit that uses a current negative feedback modulator.

The anode voltage in the entire jump frequency bandwidth of the increased amplitude tube that is used in it changes from 44 kilovolts to 56 kilovolts, peak current is 23 amps, furthermore when there is jump frequency only 3 amp variation is allowed. If using an ordinary hard tube modulator, its highest output resistance can only reach 1500 ohms, this will cause peak voltage to vary 8 amps and cannot be allowed. Now the cathode series uses 70 ohm feedback resistance, it can cause its output resistance to increase to 8 kilohms, the discharge resistance of the parasitic capacitor is 10 kilohms, after parallel connection is 4.45 kilohms. It can cause peak current to vary as little as 2.7 amps and thus can satisfy the requirements.

The parasitic capacitor that parallel connects with cathode resistance R_k (for example the parasitic capacitor of the modulation tube filament power source) can reduce feedback response speed. But if feedback response speed is exceedingly fast, when it possibly causes the cathode voltage of the increased amplitude tube to raise to π type voltage, it is worked with by the feedback circuit and sticks on the π type. Therefore it is necessary to limit the feedback response speed. In this circuit, when transmitted frequency very quickly varies, its peak current reaches stability approximately within 0.1 microsecond.

The capacity of the energy storage capacitor that is used is 1 microfarad, high voltage power source is -70 kilovolts. Therefore the stored energy is 2450 joules. Because the modulation tube is positioned on negative high voltage, to avoid possible external discharge, with the entire immersion of the tube in high voltage insulation oil we use forced oil circulation cooling. But its grid drive then becomes a problem, and it is necessary to use a high voltage pulse transformer that can endure 70 kilovolts in the first electrode, and a very good pulse response is also required. In order to avoid the influence of the dropping of the pulse peak on the feedback, in its second connection we use a low resistance limiter diode, and simultaneously design

the drive pulse amplifier to make it possess a very high inner resistance, to obtain fairly good limiter properties.

In order to prevent the inner tube spark current of the increased amplitude tube from being exceedingly large and causing damage to the tube, we use a spark interval in the two ends of the energy storage capacitor. The triggering electrode of this spark interval goes through a pulse transformer to link to an iron prize circuit, this circuit obtains a signal from a current detection transformer. When the discharge current of the energy storage capacitor exceeds a certain limit, then the triggered spark interval causes it to discharge. But because the spark interval can quickly ionize, therefore in the actual circuit in the two ends of the energy storage capacitor we also parallel connect a LC contact resonance return circuit (not drawn in the figure), the oscillator current of this return circuit can maintain the ionization of the spark interval, directly going to its sparking current in itself to be able to maintain its ionization.

This hard tube modulator that possesses current feedback that is actually manufactured can cause the increased amplitude tube to be successfully applied in jump frequency radar, it even can operate in a jump frequency state in the pulse. Actual tests show that when its operational frequency jumps at high speed from the lowest end to the highest end, the anode voltage variations of the increased amplitude tube reach 10 kilovolts, and peak current variations are as little as 2.5 amps.

Reference Material:

- (1) Frequency-agile radar jumps ahead. J. B. Brinton, Jr. *Microwaves*. Sept. 1968. pp. 11~14.
- (2) *Radar Technology*. Ed by E. Brookner, Artech House Books. 1977.
- (3) Compact multi-frequency stable sources in frequency agile systems. E. R. Scherer, *Microwave J.* Mar. 1976. pp. 41~44.
- (4) Two techniques for stable signal synthesis. *Microwaves*. Sept. 1976.

- (5) New technique yields superior frequency synthesis at lower cost. R. J. Papaieck, R. P. Coe. EDN. 1975. 10.20 pp. 73~79.
- (6) Voltage tunable local oscillator stabilized by frequency synthesizer. Microwaves. Jan. 1986. pp. 76~78.
- (7) Low noise microwave oscillator design. G. Ieranic, N. Gregory, and W. Murphy Proc. of the 29th Annual Symposium on Frequency Control Symp. pp. 248~263.
- (8) Electronic Warfare Jan-Feb. 1977. p. 38.
- (9) Radar Handbook. Ed. by M. I. Skolnik. chapt. 7 Mc Graw-Hill Book-

Co. Zhong Yi Ben "Lei Da Shou Ce", Di Si Fen Ce, Di Shi Wu Zhang, Guo Fang Gong Ye Chu Ban She, 1978 Nian Ban; "Chinese translation, "Radar Handbook", Book 4, Chapter 15, Defense Industry Press, published 1978".

- (10) Microwave Tube Technology review. DR. Stanley, F. Katsel. Microwave J. Vol. 20, No. 7 July, 1977. pp. 23~42.
- (11) Broadband klystrons for Multimegawatt radars. R. L. Mativier. Microwave J. April, 1971. p. 30.
- (12) Comparison of CFA for pulsed-radar transmitters. Microwave J. June, 1973. pp. 51~72.
- (13) A new backward-wave crossed field amplifier. J. Showron and F. Zawada. Microwave J. June, 1972. p. 54.
- (14) The use of amplitrons as microwave amplifiers in high power radar systems with frequency agility. G. Addario Chioce and G. Scerch. Int. J. Electronics, Vol. 20. No. 3 1969. pp. 237~252.

CHAPTER IX

SOME PARTICULAR FREQUENCY AGILE RADAR SYSTEMS

9.1 SELF-ADAPTING FREQUENCY AGILE RADAR

In overall design and parameter selection of radar, we often will meet with this condition: the requirements of several different kinds of tactical technology and requirements for the same technological parameters are contradictory, or different technological parameters are required under different application conditions and target conditions. At this time, it is not possible to simultaneously satisfy these contradictory requirements. In general radar design, we can only select the technological parameters that can satisfy the primary requirements based on the primary and secondary of the contradictions. But if this technological requirement is related to application conditions or target conditions, this is also to say that it unceasingly varies, thus the parameters that are chosen when beginning the design have much difficulty satisfying this requirement for variation.

In order to resolve this problem, radar that is presently designed often makes many technological parameters all variable. For example, frequency, power, frequency repetition, pulsewidth, receiver bandwidth, etc., in actual applications the specific parameter can be selected according to the specific conditions at the time. But by manually determining the environment and the variations of the conditions and again by artificially selecting technological parameters that are suitable to the environment and conditions, not only is reaction speed very slow, but also precision is very poor. Therefore we generally only can divide the corresponding parameters into a few rough grades, to provide observation personnel a selection when becoming aware of obvious needs.

With the development of environmental conditions monitoring technology and electronic computer and automatic control technology,

we now already can automatically conduct monitoring on the environment. The results of the monitoring compute the necessary best technological parameters. This radar system that can automatically adapt to the environment is called "self-adapting radar".

In the past there have been various different types of designs of self-adapting radar, the technological parameters that are primarily controlled by it are differentiated. The earliest design and also the simplest self-adapting radar is an angle measurement servo system with a variable bandwidth. This can be regarded as an example to explain the operational characteristics of self-adapting radar. In angle measurement automatic tracking radar, the bandwidth on the servo system often possesses contradictory requirements: in order to track a target that possesses a fairly large angle measurement, the bandwidth of the servo valve system is required to be enlarged, but in order to reduce the influence of the noise on angle tracking, we are also required to reduce the bandwidth of the servo system. Further research has found that these two contradictory requirements occur when there are different target conditions, when the target is fairly close to the radar station, its angle velocity that corresponds to the radar station is fairly large. At this time a fairly large servo bandwidth is required. When it is fairly far from the radar station, the corresponding angle velocity reduces, at the same time the backward-wave intensity, thus its signal-noise ratio, also decreases with it, at this time the contradiction of the noise in the servo system is outstanding, therefore it is desirable to select a fairly narrow servo system bandwidth. Consequently we design a variable bandwidth servo system, its bandwidth can automatically adjust according to target distance. This becomes a most simple "self-adapting" system.

Presently self-adapting radar is extremely complicated, among them some still use precision processing equipment to carry out real time control. The controlled parameters include various different parameters such as transmitting frequency, power, pulsewidth, frequency repetition, antenna beam form, scanning rate, receiver bandwidth,

and others. The most typical among them are: the automatically adapting antenna array on the quasi-jamming source with the antenna beam auxiliary zero point that is automatically based on the position of the jamming source; the automatically adapting moving target indication system that automatically detects the Doppler frequency shift of passive jamming and the concave mouth of the clutter control filter on the quasi-passive jamming frequency spectrum; and the automatically changing pulse frequency repetition (when angle of elevation is low, a low frequency repetition is used, with a high angle of elevation frequency repetition increases); and transmitting frequency (reducing transmitting power with the rise of angle of elevation) that is based on the direction of the antenna beam. As in the logical detection that is used in phased array radar, it can change its searching rate according to whether or not the target exists (in a region without a target, scanning is fast, a region with a target reduces scanning rate or stops the scanning), this also is a very important self-adapting radar system.

The transmitting frequency is an extremely important technological parameter of radar, many different application requirements can influence the selection of frequency, at the same time, as the above section recounts, when the transmitting frequency varies it also can give rise to many variations of target reflection properties (such as equivalent reflected area, angle noise, etc.). Therefore, how to automatically select the transmitting frequency of radar according to different application conditions and target conditions becomes the primary task of self-adapting frequency agile radar.

Because there are many different kinds of application requirements and target conditions are also everchanging, even if self-adapting frequency agile radar has no way to simultaneously satisfy these different conditions and requirements, then it can only respectively automatically adapt to variations of conditions according to different inertia requirements.

In the following section we will take a look at several different types of self-adapting frequency agile radar.

9.1.1 SELF-ADAPTING ANTI-JAMMING FREQUENCY AGILE RADAR

The frequency agile radar that is explained in the previous section is according to specified jump frequency or stochastic jump frequency, although we can already make its anti-jamming ability have very great improvement, because the frequency of the transmission is not selected according to jamming conditions, therefore it still has the possibility of receiving jamming. For example, if the jamming signal frequency spectrum only occupies $\frac{1}{p}$ of an angle bandwidth, then when we use probable stochastic agility it still will receive jamming within a $\frac{1}{p}$ duration.

In automatically adapting frequency agile radar, the carrier frequency of the transmitting pulse of the radar is not blindly stochastic disordered jumping, but has purposeful agility according to the frequency spectrum distribution of the jamming signal. This is also to say that the radar device has an analysis unit if jamming signal frequency spectrum detection, on the basis of the results of jamming signal analysis it will find the weakest region of its jamming force and later control the carrier frequency of the transmitting pulse and cause it to purposefully jump to the weakest frequency of the jamming signal.

This type of self-adapting frequency agile radar obviously possesses even better anti-jamming properties. This method presently is already generally recognized as one of the most effective means of anti-jamming⁽¹⁾.

The American company Varian produced a FAS-25 systematic that possesses self-adapting frequency agile ability. This systematic can be used to change the present radar (presently it is already used to

retrofit super bat spark control radar) systems. It uses a model VMX-1261A precision tuning coaxial magnetron. This magnetron can do high speed precision tuning in an 8600-9600MHz frequency range. Its output power is 200kW. It uses a VZW-1010C control system to carry out control, input control directive signal is ± 5 volts continuous current, its tuning sensitivity is 100MHz/amp. This control system has a 100kHz drive oscillator, the signal that is produced goes to the frequency readout resolver of the magnetron, the carrier wave amplitude of the resolver output receives the modulation of the rotational angle. This modulation signal goes to a synchronous detector (that is, a phase detector) to carry out resolving. The signal that is resolved is an analogue voltage that represents magnetron frequency. This voltage carries out comparison with an additional directive signal. After the error signal that is obtained goes through power amplification it goes to the servo motor of the magnetron tuning mechanism. After the servo motor turns, the tuning frequency of the magnetron then begins variation, until the frequency is equal to the directive frequency. The highest tuning frequency of this servo system can reach 40MHz/millisecond. When entering a 45Hz triangle wave, it can have frequency agility within 100MHz, that is it can scan 100MHz frequency range within 11.1 milliseconds, and its agile central frequency can be selected on ten fixed frequencies within a 1000MHz range, manually or through program control. When hand tuned, we can take the switch plate on the surface to a frequency increase or frequency decrease position, until the frequency readout display reaches the required frequency. The largest hand-tuned tuning frequency is 100MHz/second. Its operational frequency can also arbitrarily vary according to the wave forms of the input directive signals, so long as its variation rate is smaller than its largest tuning rate then it will work. Therefore, this precision tuning magnetron possesses a fairly large agile adaptability. In a sense we can regard it as an electronic tunable magnetron, only its tuning rate is fairly low. Exactly because of this, we can use it to form noncoherent self-adapting frequency agile radar.

In order to carry out self-adapting frequency agility, the FAS-25 possesses an interference avoidance processor (IAP). It causes the local oscillator to carry out linear frequency scanning in the radar recovery period. In the entire 1000MHz bandwidth of the radar operations, the period of frequency scanning is 100 microseconds, simultaneously with frequency scanning, the intermediate frequency output of the receiver is monitored, and the jamming signal amplitude when there are these different frequencies will be stored, accumulated, and compared, to find the frequency of a region without jamming or where jamming density is minimum. Later the frequency readjustment of the transmitter will go to these frequencies with no jamming or minimum jamming, thereby achieving self-adapting agility. The transmitting frequency revises once each interval of 250 milliseconds according to the program stipulations.

Aside from being used to control the frequency of the transmitter, the output signal of the IAP also goes to a jamming frequency spectrum display. It can display the jamming strength in the operational frequency range of the display radar (8600-9600MHz), the amplitude range of its display is 0-80dB higher than the noise power level (the range of the dynamic-state of the receiver is 80dB). This is even more convenient for noise personnel to observe jamming frequency distribution.

The primary weaknesses of this type of noncoherent frequency agile radar are that interception probability is low and reaction speed is low. Its reaction speed primarily receives the control of the tuning speed of the magnetron, moreover because this weakness exists it causes the shortcoming of the low interception probability not to become a problem.

The basic operational principles of fully coherent self-adapting frequency agile radar are completely the same as the above-discussed radar, but because it possesses extremely high tuning adaptability

therefore it can completely overcome the shortcoming of low response speed. If the equipment in this system uses a multiple channel jamming frequency spectrum that is formed by the surface noise filter to detect and analyze the receiver, then it can form corresponding ideal self-adapting frequency agile radar. Because the multiple channel detection receiver has 100% interception probability, it can carry out real time dependable analysis on the jamming signal multiple spectrum within a brief radar recovery period. In addition, the high speed tuning ability of the agile frequency synthesizer then has the possibility to achieve self-adapting agility between the pulses, and also each carrier frequency of the pulse is selected according to results of detection and analysis of the jamming frequency spectrum an instant before transmission. This then can cause the jamming source to be unable to jam, even if it is an aim type without inertial tracking.

9.1.2 LARGEST BACKWARD-WAVE AMPLITUDE SELF-ADAPTING FREQUENCY AGILE TRACKING RADAR

From the above analysis we can know that the backward-wave amplitude of the radar target (or its equivalent reflected area) is a transmitting pulse function, the transmitting frequency that changes the radar can obtain the largest possible backward-wave amplitude. But this functional relationship is not fixed and invariable but is a variable time function, when the radar that corresponds to the target has different angles of view, the frequency of the largest equivalent reflected area that it corresponds to is also different. Therefore, it is necessary to select the best operational frequency on the basis of different target angles of view. This is also self-adapting type frequency agile radar.

It is relatively easy to achieve this type of self-adapting frequency agility in tracking radar, because the radar only tracks single targets. The specific achievement program can be the same: the

radar first operates on gradient agility, then transmits a series of pulses with progressively increasing frequency, it later records the backward-wave amplitude of each pulse, thereby finding the frequency that its largest amplitude corresponds to, later the frequency is transmitted according to this, after a certain time passes, because the angle of view of the radar that the target corresponds to generates variations and causes the backward-wave amplitude to attenuate, after the backward-wave amplitude continues L times lower a certain predetermined gate limit, the radar once again switches to gradient agility, and again finds the best operational frequency when there are new conditions; it continues on in this way.

For example, if the frequency agility bandwidth of an X waveband tracking radar is 500MHz, pulse repeated frequency is 1000Hz (thus repeated cycle is 1000 microseconds). When it operates in gradient jump frequency, it can select its frequency interval close to critical frequency, for example 20MHz, and its number of grades reaches 25. Because its frequency repetition is fairly high, the necessary time for transmitting 25 grades is only approximately 25 milliseconds. The width of the frequency spectrum of the backward-wave amplitude undulation of the X waveband target is approximately 1-2.5Hz, thus we can know its related time is approximately zero point some seconds. This implies that after finding the largest frequency that corresponds to the backward-wave amplitude, it can continuously transmit several hundred pulses and still can maintain a large enough amplitude, later it again shifts to gradient jump frequency, in order to find the new frequency that corresponds to the largest backward-wave. Using this method to track targets, we can eliminate the slow undulation of backward-wave amplitude, thereby avoiding loss from undulation when the signal is detected, and increasing the affected distance (it can correspond with non-undulating target conditions). In addition to this, we also can eliminate errors of distance measurement and angle measurement that are brought about due to amplitude undulation. By what is explained above, the weakest backward-wave amplitude corresponds to the deflection center where view is the smallest, therefore this

method can also eliminate measurement errors that are caused by angle noise.

9.1.3 LARGEST BACKWARD-WAVE AMPLITUDE SELF-ADAPTING FREQUENCY AGILE SEARCHING RADAR

In the searching radar where the antenna does circular rotation, because the amount of backward-waves of each target is comparatively small, we must be able to find its best frequency. The problem is fairly complicated. Because at this time there is not enough time to transmit the gradient jump frequency signal to measure the best operational frequency, for example the number of pulses in a commonly-used beam is approximately 20, how to find its best operational frequency then becomes a comparatively difficult problem. Theoretical analysis shows that so long as we use a comparatively simple sequential logical circuit, we can have improvements of the detectability of the radar.

When the radar operates on frequency agility, the backward-wave that is received will have high speed undulation, its adjacent backward-wave amplitude can have very great differences. Figure 9.1 gives a graph of a typical backward-wave amplitude.

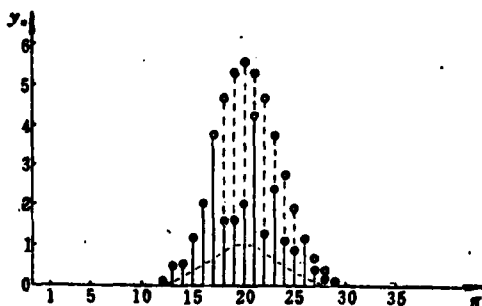


FIG. 9.1 GRAPH OF BACKWARD-WAVE OF FREQUENCY AGILE SEARCHING RADAR

The graph of backward-wave amplitude when radar operates on stochastic jump frequency in the pulse is expressed by black spots (in this

figure if the beam appearance is high the number of pulses of each target is 8). From the figure we can see that on some certain frequencies we can obtain very large backward-wave amplitude (for example the 17th and 21st backward-waves in the figure). If each instant uses the best frequency transmission then it is possible to obtain the backward-wave graph that is shown by the circles in the figure. But the problem primarily lies in how to find this best frequency. If using a gate limit device, after the backward-wave (for example the 17th) exceeds this gate limit, it immediately causes the transmitting carrier frequency to stop agility, and changes to the same frequency that was transmitted the last time (for example the frequency that was transmitted the 17th time) to use fixed frequency operations, it is then possible to obtain comparatively ideal results. But, if precisely the repetition that is due to the peak of the receiver noise causes it to exceed the gate limit, then later, if still using this frequency transmission, it is possible to cause the later backward-wave amplitude to decrease. Aside from this, the backward-wave undulation in itself that is caused by target movement can also possibly cause the original fairly useful frequency to become an unbeneficial frequency. In order to resolve this problem, we can add on a logical circuit. After it changes into a fixed frequency operation, if the continuous L times does not again exceed the predetermined gate limit, then the logical circuit causes it to change back to stochastic jump frequency. This then forms a sequential logic, it can be used to determine when it will change from stochastic jump frequency to fixed frequency, and when it will change from fixed frequency back to stochastic jump frequency. When $L=2$ (if continuing 2 times does not exceed gate limit) it changes back to stochastic jump frequency. The entire system and its flow chart are as Fig. 9.2 shows.

The backward-wave graph at this time is as Fig. 9.3 shows. The backward-wave amplitude of the stochastic jump frequency in the figure is expressed as spots, and the backward-wave amplitude of fixed frequency is expressed with circles (rings). After the 17th backward-wave exceeds predetermined gate limit V , the radar changes from

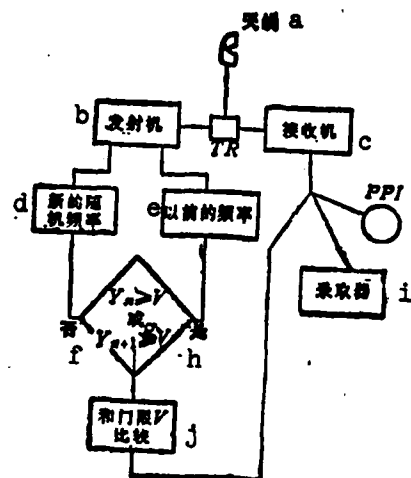


FIG.9.2 FLOW CHART OF SEQUENTIAL LOGIC OF FIXED TRANSMITTING FREQUENCY
KEY: (a) Antenna; (b) Transmitter; (c) Receiver; (d) New stochastic frequency; (e) Previous frequency; (f) Is not; (g) or; (h) is; (i) selector; (j) compared with gate limit V.

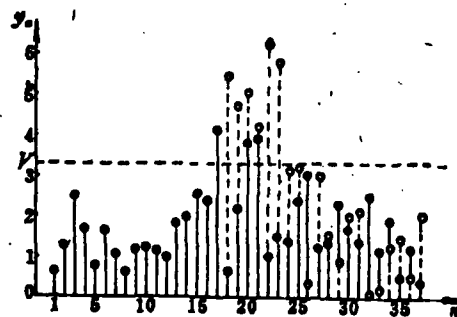


FIG.9.3 GRAPH OF BACKWARD-WAVE THAT USES SEQUENTIAL LOGIC (L=2)

stochastic jump frequency to fixed jump frequency, after the 24th and 25th continuous 2 times do not exceed the gate limit, then it already changes back to stochastic jump frequency.

After using this sequential logic, as to detectability of the radar, how much improvement is there all in all? This is an extremely complicated question. Because it not only is the same as the general problem of radar detection, but also is related to such factors as target undulation type, amount of accumulated pulse, required false alarm probability, and detection probability. Therefore it still is related to the numeric values of gate limit V and logic L in the sequential logic. When the pulse amount is 2, we still can use theoretical analysis to find its analysis value. But when pulse amount increases, the complexity of its analysis computations sharply increases.

In order to resolve this problem, we use an electronic computer and a Monte Carlo quantitative analysis program to carry out analogue computations. A preliminary few test results show that L is not an unusually critical parameter, therefore when finding the best gate limit V value, we use $L=2$. After gate limit V it is expressed by probability P that exceeds this gate limit when there is only noise, because it is a comparatively more useful parameter. Obviously, as to the two extreme conditions, when $V \rightarrow \infty$, i.e., $P=0$ it will always correspond to the interpulse jump frequency operating condition; but when $V \rightarrow 0$, i.e., $P=100\%$.

When conducting Monte Carlo analogue computations, we use a digital type smooth window detector, after the video frequency signal goes through gate limit T and becomes the two signals of 1 and 0, it enters a digital accumulation system, when the number of pulses that are accumulated in the same distance unit exceed the second gate limit N_1 , then it considers that the target begins. When the wave gate is in the sliding process, the number of accumulated pulses is smaller than N_2 , then it considers the target ended. For the purpose of simplification, generally we take $N_1 N_2 = N_0$.

Even if we use an electronic computer to carry out analogue computations, its computation process still is extremely complicated, it especially is not only required to find the detection probability when there are different pulse number M , signal-noise ratio, the first gate limit T , and the second gate limit N , but also must find the first gate limit T that can satisfy the required false alarm probab-

ity, thereby finding the best second gate limit value. In addition to this, the above computations also must be conducted when there are different P and L values. For the purpose of simplification we firstly only compute the results when L=2, and to find the best P value when L=2 again conducted analogue computations. The relationship between the first gate limit T and the required false alarm probability P_F can be found by the analysis method, this way when conducting analogue computations we can immediately adjust the position of the first gate limit T according to the required P_F value. As to the above-mentioned digital type smooth window accumulator, its false alarm probability can be solved by the following expression:

$$P_F = \binom{N}{M} P_n^M (1 - P_n)^{N-M+1} \quad (9.1)$$

In which N is the accumulated number of pulses, M is the second gate limit value, and P_n is the probability of the amount of the sampling of the restored narrow band gauss noise when the first gate limit is T becomes 1 (thus exceeding T):

$$P_n = \exp\left(-\frac{T^2}{2}\right) \quad (9.2)$$

If the required $P_F = 10^{-6}$, then we can solve the T value when N and M are different, listed in the following table:

TABLE 9.1 THE VALUE OF THE FIRST GATE LIMIT T WHEN CORRESPONDING TO $P_F = 10^{-6}$

M	N = 4	N = 8	N = 16
1	5.20		
2	3.86	3.97	
3	3.16	3.36	
4	2.62	2.93	3.20
5		2.61	
6		2.35	2.68
8			2.33
10			2.06
12			1.83

It is necessary to note that the value of false alarm probability P_F that this first gate limit T corresponds to is only the false alarm probability for single distance units. When there are R distance units in each scanning, and each scanning sweep (each cycle of rotation) of the antenna has five scans, then the average false alarm number FAS of each cycle of rotation of the antenna is:

$$FAS = P_f \times S \times R \quad (9.3)$$

If we use a wave gate tracking system that scans while tracking, then R in the formula can replace the distance element number in the wave gate (expressed by pulsewidth number), but still must multiply by wave gate number N_g .

When the three conditions of pulse number $M=4, 8$, and 16 , and P_F is approximately 10^{-6} , the results of the analogue computations that are conducted are as Fig. 9.4, 9.5, and 9.6 show. The logic that is used is $L=2$. The three figures that are listed all are the best graphs. Thus the value of P (thus the value of limit gate V) also is the best, and obtains the largest detection probability P in the range of $P_d=(40-90)\%$. As to when $M=4$, this best $P=0.001$; as to when $M=8$, $P=0.005$; as to when $M=16$, $P=0.05$. The value of the second gate limit N also is the best of the detection probability. As to when $M=4$, $N=2$; when $M=8$, $N=4$, when $M=16$, $N=6$.

For the purpose of simple comparison, the figure also lists when it does not have this sequential logic, it corresponds to the curve of fast attenuation and slow attenuation. It is necessary to note that their best second gate limit N value each is different. For the comparison of these curves, we can discover that the improvement that we have after using self-adapting jump frequency in the search radar can be better than stochastic jump frequency between the pulses. Furthermore, the larger the number of pulses in the beam, the more the

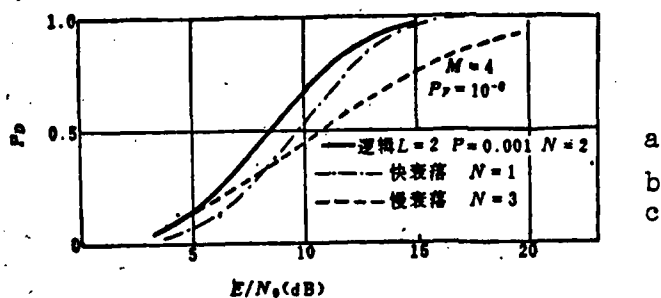


FIG. 9.4 ANALOGUE COMPUTATION RESULTS OF SEQUENTIAL LOGIC DETECTION PROPERTIES, $M=4$
KEY: (a) Logic; (b) Fast attenuation; (c) Slow attenuation

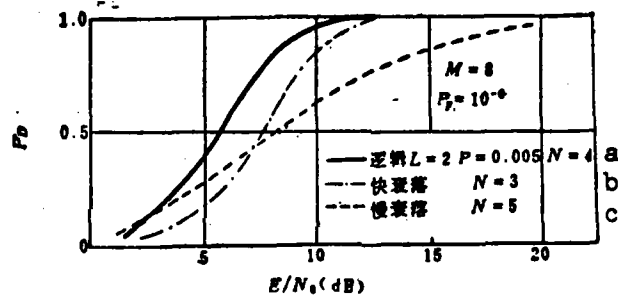


FIG. 9.5 ANALOGUE COMPUTATION RESULTS OF SEQUENTIAL LOGIC DETECTION PROPERTIES, $M=8$
KEY: (a) Logic; (b) Fast attenuation; (c) Slow attenuation

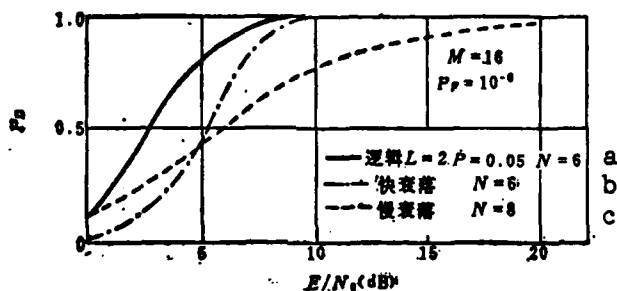


FIG. 9.6 ANALOGUE COMPUTATION RESULTS OF SEQUENTIAL LOGIC DETECTION PROPERTIES, $M=16$
KEY: (a) Logic; (b) Fast attenuation; (c) Slow attenuation

improvement, and the bigger the improvement, and the bigger the improvements in medium detection probability ($P_D=50\%$) range. From past analysis we also can know that when required detection probability is low, stochastic jump frequency will have almost the same properties as fixed frequency radar, it even will be somewhat worse, self-adapting jump frequency then is just not enough to supplement pure stochastic jump frequency.

Although these curves are the results of best P value, actually the P value (thus the gate limit V) also is not extremely critical. Figure 9.7 lists the different P value results when $M=8$. $P=0.005$ in it is best.

In the same way, parameter L that changes this logic also is not extremely clear, the analogue computation results on different L values when $M=8$ are shown in Fig. 9.8.

From the figures we can know that when $L=4$, we have improvements when there is a low signal-noise ratio, but when there is a high signal-noise ratio there is damage. When L value reduces it is exactly opposite. The results when there are different P values are not in this list, we can discover that the variations of parameter L value can use the corresponding variations of the P value to cancel out, when L value increases it can reduce P, and when L value is small, we can use a large P value. Generally speaking, the conclusion is this: parameter L value is not extremely critical, but when L value is fairly small it can obtain comparatively good results, and this is desirable when operating on multiple distance elements.

From the above results we still can obtain the E/N_0 value of the signal-noise ratio when corresponding probability P value (thus gate limit V value) are shown in the X point in Fig. 9.9. The figure gives the theoretical curve that is computed when there are only two pulses. From the figure we can see that although the theoretical

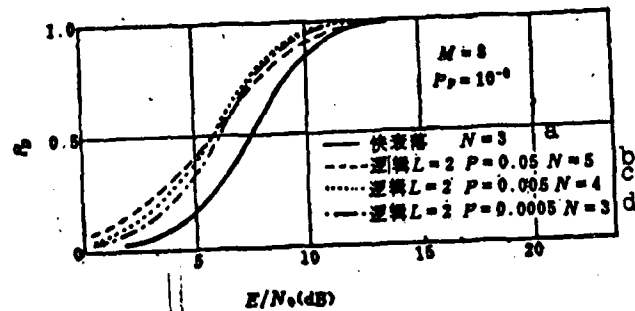


FIG.9.7 DETECTION PROPERTIES WHEN DIFFERENT P VALUES (Best P Value is 0.005)
KEY: (a) Fast attenuation; (b) Logic; (c) Logic; (d) Logic

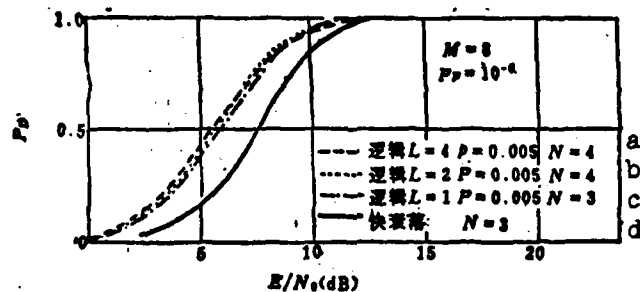


FIG.9.8 ANALOGUE COMPUTATION RESULTS WHEN DIFFERENT L VALUES
KEY: (a) Logic; (b) Logic; (c) Logic; (d) Fast attenuation

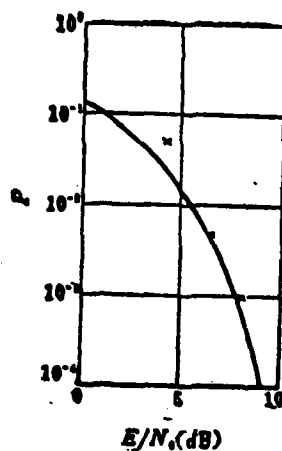


FIG. 9.9 SIGNAL-NOISE RATIO WITH LARGEST IMPROVEMENTS AND CORRESPONDING P VALUE

curve is computed according to when there are only two pulses, we also can extend it to general conditions. This curve can be regarded as when there is a given signal-noise ratio, to select a parameter of the best gate limit V .

After increasing the sequential logic, angle measurement precision on the radar is the same as when there is a general digital type sliding wave gate accumulator, the target bearing $\hat{\theta}$ that is estimated by it is the average value of the bearing when corresponding to the target beginning and end. This estimated bearing will deviate to a true target bearing, when there is a certain signal-noise ratio, we can solve the average value of its deviation $\hat{\theta}_e$ and its bearing-deviation difference value θ_e^2 . Then:

$$\hat{\theta}_e = \frac{1}{K} \sum_{i=1}^K \hat{\theta}_i \quad (9.4)$$

$$\theta_e^2 = \frac{1}{K-1} \sum_{i=1}^K (\hat{\theta}_i - \hat{\theta}_e)^2 \quad (9.5)$$

Currently we have made 300 tests on each signal-noise ratio, if $K=300$. The results that are obtained are shown in Fig. 9.10. The results that are obtained in the figure are expressed by the value that corresponds to a 3dB beam width. In order to carry out simple comparison, the figure also draws the angle measurement precision without this logic/ The X point represents the results when there is fast attenuation without this logic (its best third gate limit $N=3$), its average value is close to zero. The circles in the figure represent the results when $L=2$, $P=0.005$, and $N=4$, its average deviation is approximately 0.05 beamwidth. From this we can obtain the conclusion that the influence on angle measurement precision of the digital detection after adding sequential logic can be overlooked, if we can eliminate its average deviation, then we can even have improvement.

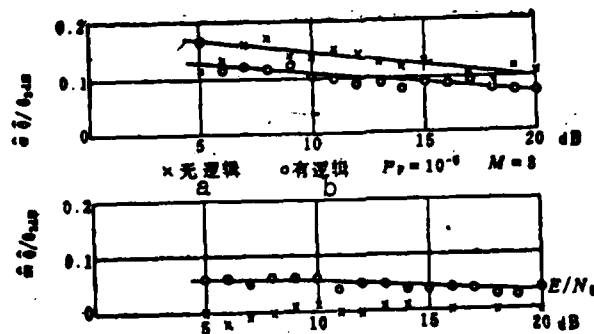


FIG. 9.10 INFLUENCE ON TARGET ANGLE MEASUREMENT PRECISION AFTER INCREASED SEQUENTIAL LOGIC
KEY: (a) Without logic; (b) With logic

All of the above discussion still is only limited to single distance element conditions, but when actually operating, generally all possess numerous distance elements. The operational principles of the logic at this moment are invariable, but due to the increase of the distance elements it causes the probability of this logic that is triggered by noise to increase, if the distance elements number is J , then the probability increase of this logic that is triggered by noise is:

$$P' = 1 - (1 - P)^J \approx JP \quad \text{when } P \leq 1 \quad (9.6)$$

Then it is the original J multiple. Therefore the radar transforms to the probability increase of fixed frequency operations, and will make the properties of the system worsen. The results of analogue computations that were conducted when there are multiple distance elements are shown in Fig. 9.11. The figure only lists results when $M=8$ and $P_F=10^{-6}$. From the figure we can see that even if it increases to 250 distance elements, its detection properties still must be better than the stochastic jump frequency radar of this logic.

In brief, to summarize the above discussion, we can obtain this conclusion: if in jump frequency radar where the antenna does circular scanning, so long as this radar can agilely volunteer to jump fre-

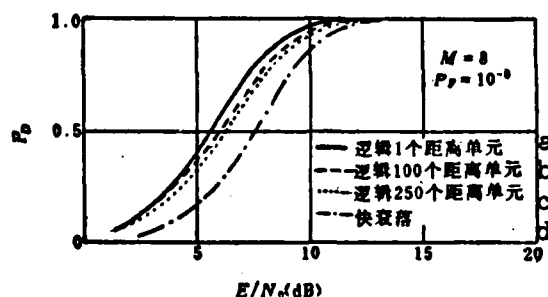


FIG. 9.11 DECREASE OF SYSTEM DETECTION PROPERTIES CAUSED BY MULTIPLE DISTANCE ELEMENTS

KEY: (a) Logic 1 distance element; (b) Logic 100 distance elements; (c) Logic 250 distance elements; (d) Fast attenuation

quency (generally the majority of fully coherent jump frequency radar is this way), then so long as it must increase to a comparatively simple sequential logic, it is caused to carry out self-adapting jump frequency according to the strength and weakness of the backward-wave and can possibly be even further improved to be better than the detection properties of general stochastic jump frequency radar. Furthermore, its degree of improvement increases with the pulse number, when pulse number is moderate ($M=8$) its improvement will be near 2.5dB. Furthermore, the improvement at medium level detection probability is comparatively marked. The angle measurement precision of the digital type sliding wave gate detector after using this logic is not influenced, it even can have great improvement.

If the radar antenna scans by electronic control then it can achieve step by step scanning. Thus this self-adapting jump frequency radar still can interact with sequential detection, causing it to have even greater improvement in the shortened searching time and on increased detectability.

9.2 THE SIGNAL PROCESSING SYSTEM OF GRADIENT JUMP FREQUENCY RADAR

From the conclusions of the fourth chapter regarding frequency agile radar angle measurement precision we can know that the minimum angle measurement error is generated when the backward-wave amplitude is the largest. Therefore we can design this kind of tracking radar, it transmits a series of frequencies as gradient jump frequency pulses, this series of different frequency pulses can transmit within a repeated cycle, and also can transmit on different repeated cycles (each repeated cycle only transmits a certain frequency pulse). Exactly what method to use is determined by the parameters that are required by video radar: specific distance, data rate, and the transmitter. Later the backward-wave pulse that is received achieves the "error selection division and collection method", that is, it selects its backward-wave amplitude as the largest angle error signal. This can make its tracking error minimal.

This gradient jump frequency radar can be applied to various different types of tracking radar such as triple dispatch monopulse, dual dispatch monopulse, or conical scanning. Although its transmitting signal is similar to the gradient jump frequency radar that is recounted in section 4.6 of chapter 4, the processing method for the backward-wave signal that it receives is different. It is not simply averaging various frequency backward-wave signals, but is selecting the largest one of its amplitudes to go to the angle servo system.

Figure 9.12 draws a block diagram of the "0 error selection division and collection" system of a triple dispatch monopulse tracking radar⁽⁴⁾.

This radar transmits four frequencies within one cycle repetition. The frequencies respectively are f_1 , f_2 , f_3 and f_4 , and each interval is δ pulses (see the wave form in the upper left corner in the figure). Because the tracking radar only needs to receive the backward-wave signal of one target, therefore the frequency of the local oscillator

of the receiver is controlled by the distance tracker, and successively tunes to f_1+f_0 , f_2+f_0 , f_3+f_0 , and f_4+f_0 (in which f_0 is the frequency of the intermediate frequency of the receiver). Like ordinary triple dispatch monopulse tracking radar, it also has 3 dispatch channels, one is used in distance tracking "sum" dispatch, the other two respectively correspond to the "difference" dispatches of bearing error and angle of elevation error. The video frequency that is put out by the "sum" dispatch channel goes to gates 22, 24, 26, and 28. These gates are controlled by the distance tracker, making it successively open according to the backward-wave deviation interval. The output signal from these gates is sent to two circuits; after one circuit it is carried to the video frequency delay time wire to carry out video frequency phase adding, then the backward-wave that corresponds to carrier frequency f_1 is carried to delay time wire 34 to be delayed 38, the backward-wave that corresponds to frequency f_2 is carried to delay time wire 32 to be delayed 28; the backward wave that corresponds to carrier frequency f_3 is carried to delay time wire 30 to be delayed 18; the backward-wave that corresponds to carrier frequency f_4 does not go through delay time but goes directly to video frequency phase adding. This way, the backward-wave signals of four different carrier frequencies that go to the video frequency phase adder coincide in time, then simultaneously emerge, therefore amplitude can instantaneously phase add. The video frequency signals after phase adding are carried to the distance tracker to carry out distance tracking. The other circuit signal that is put out from gate 22, 24, 26, and 28 goes to a comparator 38 to select the largest signal of its amplitude. The detailed block diagram of this comparator 38 is as Fig. 9.13 shows⁽⁴⁾. The return-wave signals that correspond to the four different frequencies that is sent to wave detectors and encoders 44, 46, 48 and 50. This detector come from gates 22, 24, 26, and 28, takes the return-waves amplitude through a storage circuit to be stored, and after going through a specific delay time changes to four standard pulses that are the same in time and are in direct ratios with the amplitudes and return-waves. To avoid mix ups, the forward side of these pulses all have a dual potential two dimensional coding signal; corresponding to f_1 is 11,

corresponding to f_2 is 00, corresponding to f_3 is 10, corresponding to f_4 is 01. Later these signals go to comparators and selectors 52, 54, and 56 to carry out comparison and selection. Later the largest one is selected (in the figure it is the backward-wave signal that corresponds to f_3 that has 10 coding) to be carried to a pulse selector 58, to select the gated wave gate pulse that comes from distance tracker 20. Later this gated pulse goes to bearing error selection gate 40 and angle of elevation error selection gate 42, to select the angle of elevation signal that corresponds to the largest backward-wave amplitude. Here it is necessary to point out that because the pulse delay time that is put out after going through the amplitude comparator must be greater than 3δ , therefore the wave gate pulse that is selected certainly cannot repeat this cycle, but only can repeat the next cycle. Therefore, this system actually is based on the largest backward-wave amplitude in this repeated cycle to select the error signal that is in the next repeated cycle. Therefore it is not a real time control system. Because frequency f_1 , f_2 , f_3 , and f_4 are fixed and invariant, therefore the variations of the backward-wave undulation and angle flash motion that correspond to these frequencies also are not very fast (then their interrelated time is fairly long), therefore using this method we also can select the angle error as minimum signal.

Another primary weakness of this method is that it only selects the strongest one in four backward-wave signals, the other three (including even if the amplitude is also a correspondingly strong backward-wave signal) are all cast aside. In order to overcome this drawback, in the following section we explain an improved selection method. After using this method, so long as its amplitude is larger than the backward-wave of a certain gate limit power level (this gate limit power level is determined by the average value of all the backward-wave amplitudes), all used as angle tracking signals, on the one hand resolves the problem of real time control, and on the other hand increases available signals, this then can cause tracking error to

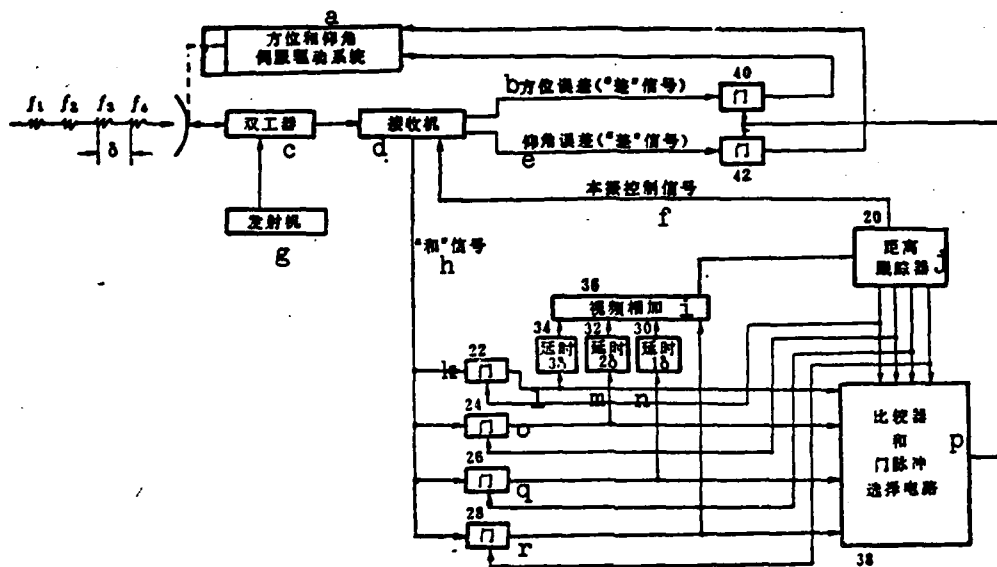


FIG. 9.12 BLOCK DIAGRAM OF "ERROR SELECTION DIVISION AND ACCUMULATION" SYSTEM OF A GRADIENT JUMP FREQUENCY TRIPLE DISPATCH MONOPULSE TRACKING RADAR

KEY: (a) Bearing and angle of elevation servo drive system; (b) Bearing error ("difference" signal); (c) Dual processor; (d) Receiver; (e) Angle of elevations error ("difference" signal); (f) Local oscillator control signal; (g) Transmitter; (h) "sum" signal; (i) Video frequency phase adder; (j) Distance tracker; (k) Gate; (l) Delay time; (m) Delay time; (n) Delay time; (o) Gate; (p) Comparator and gated pulse selection circuit; (q) Gate; (r) Gate

further decrease. The block diagram of this system is as Fig. 9.14 shows⁽⁵⁾.

The backward-wave signal that is put out by the "sum" dispatch of the receiver, after going through gates 22, 24, 26, and 28 are sent to two circuits, one circuit goes to a tap delay wire, four signals coincide in the output end of the delay wire, that is, the output end of the delay wire in a repeated cycle interval only has one pulse. Its amplitude is the total sum that goes through the signal of four gates. The output from this delay wire is divided into two

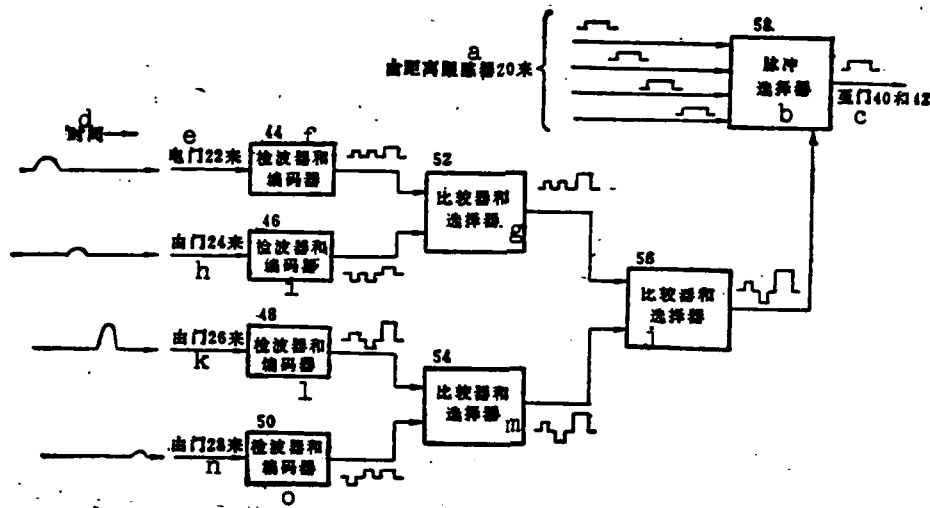


FIG. 9.13 DETAILED BLOCK DIAGRAM OF COMPARATOR 38
 KEY: (a) Coming from distance tracker 20; (b) Pulse selector; (c) To gate 40 and 42; (d) Time; (e) From gate 22; (f) Detector and Coder; (g) Comparator and selector; (h) From gate 24; (i) Detector and coder; (j) Comparator and selector; (k) From gate 26; (l) Detector and coder; (m) Comparator and selector; (n) From gate 28; (o) Detector and coder

cycles , one is sent to the distance tracker 20 to carry out distance tracking, the other goes to a sampling maintenance circuit to be stored and give a continuous flow reference power level that forms a direct ratio with the total sum of this backward-wave. The other circuit signal that is output from gates 22, 24, 26, and 28 also is sent to comparator 34 to carry out amplitude selection. The detailed block diagram of comparator 34 is as Fig. 9.15 shows⁽⁵⁾. The backward-wave signal that comes from gate 22, 24, 26, and 28 first goes to a sampling storage circuit to carry out storage, and later is compared with the gate limit power level in comparators 68, 70, 72, and 74. This gate limit power level is formed by continuous flow reference power level through gate limit adjustor 76 that comes from sampling storage 32. This gate limit adjustor actually is a voltage divider. The signal that exceeds the gate limit power level after comparing is used to control "AND" gates 78, 80, 82, and 84.

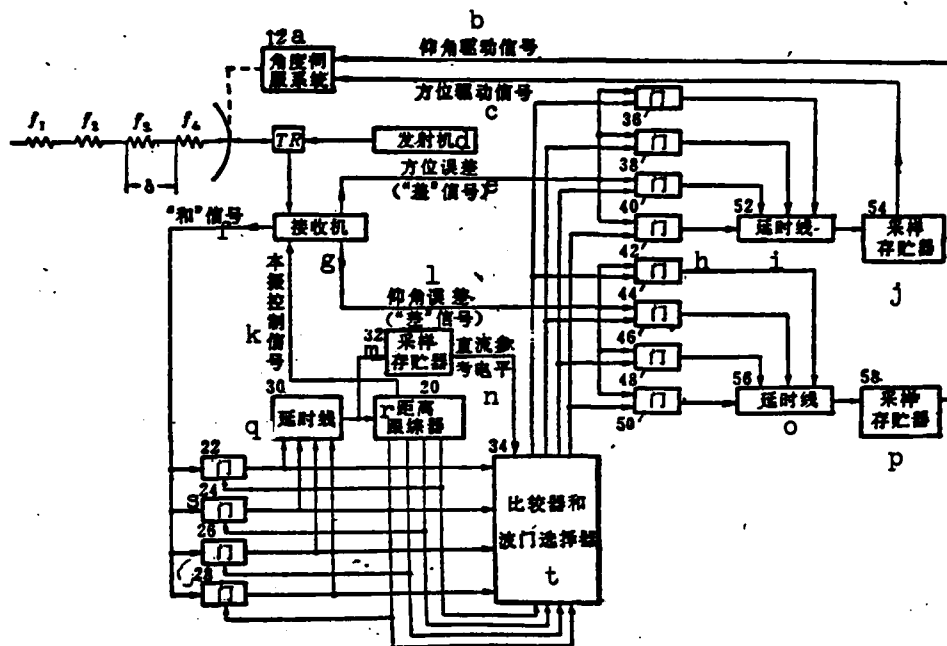


FIG. 9.14 BLOCK DIAGRAM OF FLUCTUATING GATE LIMIT POWER LEVEL BACKWARD-WAVE AMPLITUDE SELECTION METHOD

KEY: (a) Angle servo system; (b) Angle of elevation drive signal; (c) Bearing drive signal; (d) Transmitter; (e) Bearing error (difference signal); (f) "sum" signal; (g) Receiver; (h) Gate; (i) Delay time wire; (j) Sampling storage; (k) Local oscillator control signal; (l) Angle of elevation error ("difference" signal); (m) Sampling storage; (n) Continuous flow reference power level; (o) Delay time wire; (p) Sampling storage; (q) Delay time wire; (r) Distance tracker; (s) Gate; (t) Comparator and wave gate selector

These "AND" gates simultaneously control the signals that are selected from the distance tracker this way, only that circuit which exceeds the gate limit power level has selected wave gate output. What is drawn in the figures are the first circuit signal (it corresponds to the backward-wave with frequency as f_1), and the fourth circuit signal (it corresponds to the backward-wave with frequency as f_4) exceeding gate limit power level, therefore only these two circuits have selected wave gate output. The selected wave gates that are put out simultaneously go to gates 36, 38, 40, and 42 that control the bearing error signals and gates 44, 46, 48, and 50 that control angle of elevation error signal. In the example in the figure, only gates 36, 44, and

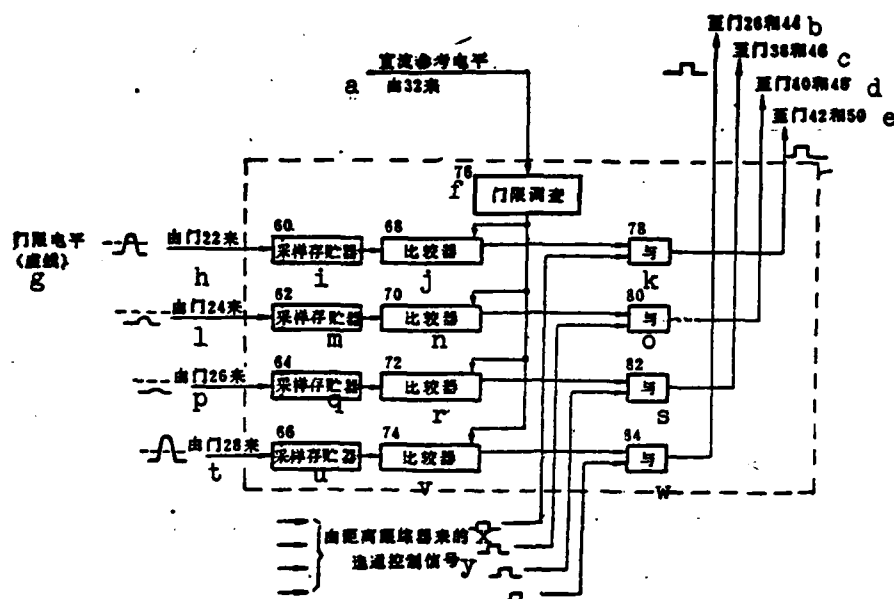


FIG. 9.15 DETAILED BLOCK DIAGRAM OF COMPARATOR AND WAVE GATE SELECTOR

KEY: (a) Continuous flow reference power level from 33; (b) to gates 26 and 44; (c) to gates 38 and 46; (d) to gates 40 and 48; (e) to gates 42 and 50; (f) Gate limit detector; (g) Gate limit power level(dashed line); (h) from gate 22; (i) Sampling storage; (j) Comparator; (k) And; (l) From gate 24; (m) Sampling storage; (n) comparator; (o) And; (p) From gate 26; (q) Sampling storage; (r) Comparator; (s) And; (t) From gate 28; (u) Sampling storage; (v) Comparator; (w) And; (x) From distance tracker; (y) Selection control signal

42 and 50 open, to select those angle of elevation error signals that correspond to the backward-wave amplitude exceeding the pre-determined gate limit power level. The bearing angle error signals that are put out by gates 36, 38, 40, and 42 go to tap delay wire 52, to obtain the time gate coinciding bearing error signal, and after going through sampling storage are sent to the servo system. In the same way, the angle of elevation error signals that are put out by gates 44, 46, 48, and 50 go to tap delay time wire 56, after going through coinciding phase adding, go to sampling storage 58 and alternate to the angle of elevation drive signal to drive the angle of elevation servo system.

In this system because after the backward-wave signal that need not equal the final one frequency again carries out amplitude comparison, and is directly compared with a gate limit power level, therefore causes it to possibly carry out real time control, that is, the backward-wave signal that exceeds gate limit power level in this repeated cycle immediately is carried with its corresponding angle error signal. This reduces delay and also can further reduce angle error. At the same time, because in delay wires 52 and 56 we can incessantly have angle error signal coinciding phase adding, we also raise the signal-noise ratio of angle error signal, and also we can raise its tracking precision. Because the time constant of sampling storage circuit 32 is fairly long, therefore the gate limit power level actually is determined by the mean value of the backward-wave amplitude of several repeated cycles. Its best value is determined by actual tests.

9.3 MOVING TARGET INDICATION SYSTEM THAT IS COMPATIBLE WITH FREQUENCY AGILITY

Strictly speaking, frequency agile radar and moving target indication systems are in principle mutually contradictory. In a typical moving target indication system, we use the "memory recall" of the coherent oscillator to transmit the phase of the pulse carrier wave, after highly stable local oscillator causes mixing it still can maintain the phase of the backward-wave. This way in the output end of the intermediate frequency amplifier, the phase of the successive backward-waves of surface features is invariable, and the phase of moving target backward-waves generates variations due to the Doppler effect. When the phase of the backward-wave and the phase of the coherent oscillator are discriminated in the phase detector, we then can obtain the phase of each backward-wave and its corresponding transmitting signal. The output after discrimination after storing a cycle in the delay time wire is compared with the backward-wave phase of the next pulse, we then can eliminate the fixed clutter of the surface features that possesses the same phase and only keep that of the

moving target, this way we can achieve the goal of only indicating moving targets. But in agile radar, because the carrier frequency of the adjacent pulse is different, and this causes the phase of the fixed target to also generate variations, therefore there is no way to use delay time to cancel out the system and eliminate it. Therefore the frequency agile radar system is mutually contradictory.

In noncoherent frequency agile radar, still another contradiction exists, the contradiction between agile adaptability of the frequency agile magnetron and frequency stability. It is very difficult to transmit a pulse that forms very high frequency stability and also can have high speed agility. Aside from this, in moving target indication radar, in order to ensure fairly high visibility, the local oscillator is required to have very high short term frequency stability. But in agile radar, because the local oscillator must be able to quickly catch up with the variations of the transmitting pulse carrier frequency, generally they are all voltage tuning and possess very high voltage tuning sensitivity, this oscillator generally is very difficult to achieve a very high short term frequency stability.

The earliest method that resolved this problem was causing these two systems to exist side by side but not be compatible, this is also to say that the two systems only can be independently used: when used in moving target indication systems, it only can operate in fixed frequency (in noncoherent frequency agile radar it can use jump frequency magnetron locking); and when the radar operates on frequency agility, then it gives up the moving target indication and uses a common indicator. But in a rotational tuning magnetron, because it uses a multiple cavity magnetron and rotational type tuning mechanism, its frequency stability is fairly poor, and even if locked in fixed frequency is also is very difficult to achieve relatively high visibility.

The precision tuning frequency agile magnetron thus overcomes this weakness to a certain degree. Because it is a coaxial type magnetron therefore it possesses fairly high frequency stability. At the same time, it also possesses fairly high speed agility, it generally can jump through the entire agile bandwidth within a 40 millisecond time. This way, it is possible to jump another frequency within the interval of a fairly short time simultaneously operating on moving target indication. It generally uses this agile magnetron moving target indication radar to operate on scanning to scanning jump frequency, that is, this cycle of antenna rotation uses a carrier frequency, the next cycle uses another carrier frequency. Therefore, it still cannot achieve high speed agility in an even shorter time.

In fully coherent frequency agile radar, because its transmitting signal is produced by a highly stable program-controlled frequency synthesizer, it both can have high speed agile jump frequency and possess fairly high frequency stability. Moreover, because the local oscillator signal and the transmitting pulse carrier frequency are produced by the same highly stable signal source (generally a transistor oscillator), therefore the problem of short term frequency stability of the local oscillator does not exist. But, the above mentioned basic contradiction still exists, it cannot achieve moving target indication simultaneously with jump frequency between the pulses.

9.3.1 MOVING TARGET INDICATION SYSTEM WITH GROUP AGILITY

If the radar does not operate on jump frequency between the pulses but operates on grouped jump frequency, then this contradiction can partially be resolved. The so-called group jump frequency is simply after transmitting a group (from two to several) of pulses with the same frequency, it jumps to a new frequency and transmits another group of pulses. Because the carrier frequencies of these groups of pulses are completely alike, therefore the backward-wave phase of the fixed target cannot vary, it can be cancelled out between

these groups of pulses. But between an adjacent group of pulses it cannot be cancelled out, thus so long as the output of the cancelled system goes to a selected circuit, the output when agility is eliminated can be fine. Obviously, this group agility system can only be achieved in fully coherent frequency agile radar.

Suitable compromise must be carried out to select the number of pulses in the group of group agility. Because there is no way to cancel out two adjacent pulses of frequency agility that have been carried out, therefore the output of the one that is cancelled out must be eliminated, this causes the number of pulses that are accumulated to suffer loss. When there is dual pulse cancellation, the ratio between the number of pulses that are lost and the accumulated pulses is $1/N_B$. In it N_B is the pulse in the group. When there is triple pulse cancellation, the ratio between the number of lost pulses and the number of accumulated pulses is $2/N_B$. Therefore in order to reduce loss, the bigger the desired N_B the better. But when N_B is exceedingly large, its anti-jamming properties also reduce. Therefore an exceedingly large N_B can increase the detected jamming interception and tracking probability. Therefore the number of pulses in its group is generally selected as 3-5.

When there is grouped agility, because the carrier frequencies of each group of pulses is different, therefore the blind speed that corresponds to them also is different. This is because blind speed can be expressed by the following expression:

$$v_b = \frac{150}{f_0 T_p} \text{ m/second} \quad (9.7)$$

In which f_0 is transmitting carrier frequency, expressed in gigahertz, T_p is repeated cycle of the pulse, expressed in milliseconds. By expression (9.7) we can know that the effect of carrier frequency f_0 and cycle T_p on blind speed is the same. In order to extend blind speed to the general method of using repeated cycle irregularities, this irregularity can use the pulse irregularity, and also can use

the method of group irregularity. From this we can infer that using the method of group agility we also can extend it to blind speed. Its effect should be the same as the group irregularity of the repeated cycle of the pulse. But in specific achievements there are certain difficulties, this is because we must extend the blind speed to outside the allowed value, requiring the range of its repeated cycle variations to be large enough, and if using the method of group agility to represent the group irregularity of the repeated cycle, its properties will receive the limits of the agile bandwidth. Therefore the same time as frequency group agility, we often use the group agility of the repeated cycle.

No matter if it is repeated cycle group agility or repeated cycle additional frequency group agility, the improvement factors on moving target indication systems possess obvious enhancement. In order to quantitatively research its performance, some people use an electronic computer to conduct analogue experimental research⁽⁶⁾. The assumed radar is 15cm phased array radar, its largest distinct distance is 30km (repeated cycle $T_p > 0.2$ milliseconds), and it requires detectability to threefold velocity moving target ($v > 1$ km/second), its moving target indication system is and I and Q cross channel triple pulse offset digital moving target system. We carried out research on 10 extended blind speed techniques. Research results showed that group irregularity or group irregularity with additional group agility possesses fairly high improvement factors, approximately 20dB higher than other technique averages. The group irregularity that is used is three pulses in one group, and three groups in one cycle, its repeated cycles respectively are 200, 225, and 250 microseconds. When using group agility, in each pulse 5% frequency agility is added, that is, carrier frequencies successively are 5.00, 5.25, and 5.50GHz. After using group agility, the factor of its improvement only reduces 1dB, but there is a fairly large influence on its frequency response. This can be seen from Fig. 9.16. The figure gives frequency performance when divided into group irregularities (expressed by the solid line). From the figure we can see that although using group agility can eliminate the original

blind speed, a zero point of 30dB emerges in the pass band. If we limit the required blind speed to two times the velocity, then its velocity response is somewhat better than group irregularity.

As the previous section recounts, although this group agility can be compatible with the moving target indication system, strictly speaking it is not a frequency agile system, because it does not carry out agility between the pulses but only agility between the groups. Therefore its anti-jamming properties must be poor, and also the number of accumulated pulses that can be supplied is reduced.

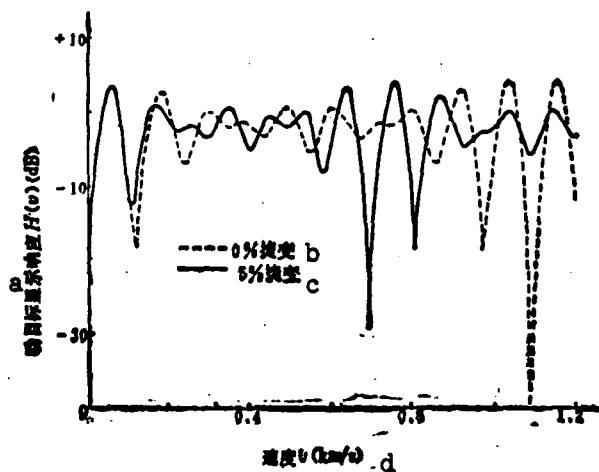


FIG. 9.16 FREQUENCY PROPERTIES OF MOVING TARGET INDICATION SYSTEM THAT USES GROUP IRREGULARITY AND GROUP AGILITY
KEY: (a) Moving target indication response; (b) Agility; (c) Agility; (d) Velocity

9.3.2 MOVING TARGET INDICATION SYSTEM WITH DUAL PULSE AGILITY⁽⁷⁾

In order to overcome these drawbacks, what is called a "dual pulse agility" moving target indication system was developed. This radar system also has paired agility, what is different lies in that this paired pulse is transmitted within the repeated cycle. This is also to say that within the same cycle two pulses of the same carrier frequency that are separated by a specified interval are successively transmitted. The interval of these two pulses usually

is far smaller than its repeated frequency, and is determined by the longest fixed target extended distance. Later it again jumps to a new carrier frequency to again successively transmit two pulses that have the same interval.

The operational principles of this paired pulse moving target indication system are also different than those of ordinary moving target indication systems. Firstly it does not use a coherent oscillator but directly uses the backward-wave tube difference method, where the first backward-wave pulse in the paired transmitting pulse carries out phase comparison with the second backward-wave pulse after delay time is equal to the interval of the time of the two pulses. As to the fixed clutter the phase of the two are completely alike, therefore the output of phase detection is zero; as to moving targets, although the interval of the two pulses is not large, the phase of its backward-wave already has differences, therefore the output of phase detection is not equal to zero. Therefore in this moving target indication system, we do not need an additional phase reduction circuit, and the phase detector in itself is also a destruction system. Moreover, because its fixed target does not separate the cycle and destruction but destructs in the cycle, therefore we also do not need to have the delay times equal to the long delay time wires of the repeated cycle, but only need to have the delay times equal to the correspondingly short delay time wires that are equal to the two pulse intervals when phase comparing.

This paired pulse moving target indication system possesses the following several advantages over the ordinary moving target indication system:

(1) Resolving the problem of exceedingly low blind speed. Because the moving target phase carries out comparison after only going through the time of the phase interval, and the interval of the two pulses is far smaller than the repeated cycle, therefore its

blind speed also is far higher than the blind speed that is determined by the repeating pulse. For example, if the interval of the two pulses is 150 microseconds, when the target uses a flight speed of v nautical miles/hour, then in the time of 150 microseconds, the distance of the target flight is:

$$\frac{v \times 185300}{3600} \times \frac{150}{10^6} = 7.71 v \times 10^{-3} \text{ cm}$$

If the radar operational frequency is 2830MHz (wavelength is 9.43cm), the corresponding speed when phase variation of the backward-wave is 2π is blind speed, then it is:

$$v_b = \frac{9430}{2 \times 7.71} = 610 \text{ nautical miles/hour}$$

or 1130 km/hour. This blind speed is far higher than that of ordinary moving target indication systems. For example, if the repeated cycle of the pulse is 3000 microseconds then when other corresponding conditions do not change, the blind speed of the ordinary moving target indication system is twenty times lower.

Although, when target speed is equal to half of the blind speed, when its phase difference is π , the output of the phase also is equal to zero, this point of half the blind speed can adapt a certain measure to be eliminated in the circuit (this problem will be discussed in detail in the following section).

(2) In ordinary moving target indication radar, the clutter-destruction ratio primarily receives the limits of the signal undulation that is caused by the antenna scanning control. In the paired pulse moving target indication system, because it carries out phase comparison in an even shorter time, therefore it can reduce the

effect of the widening of the antenna scanning frequency spectrum, that it, its limit-destruction ratio can be even higher.

(3) In paired pulse jump frequency, although it also carries out comparison after successively transmitting two pulses of the same frequency, because the interval of the two pulses is very short, and jump frequency actually still is carried out between the cycle, its effect corresponds to jump frequency between the pulses. Therefore its anti-jamming ability still corresponds to the anti-jamming ability of jump frequency radar between the pulses.

(4) The paired pulse moving target indication system does not need delay time duration to be equal to the long delay time wire of the repeated cycle, but only needs delay time duration to be equal to the short delay time wire of the interval of the two pulses, this correspondingly short ultrasonic delay time wire is much easier to manufacture than the long delay time wire.

Some shortcomings also exist in the paired pulse moving target indication system. The most primary among them is the so-called "phase contamination" problem. When the stray backward-waves of the first pulse are directly extended to exceed the interval of the two pulses, then clutter mixes with the second pulse. At this time the phase of the signal in the receiver is not significant, this will be able to cause the clutter of the repeated part have not way to be eliminated.

There are two methods to resolve this problem: one is appropriately increasing the interval between the two pulses (for example increasing it to 770 microseconds), but this can cause the blind speed to reduce (reduce to 119 nautical miles/hour), and at the same time can increase clutter restrained combtooth width. Therefore it is best if this interval does not increase too large. The general design is for a selector that uses several scanning interval. After

the radar is erect on a certain site, it then can select a suitable pulse interval based on the extension of the clutter of its cycle. Although this can eliminate mixing of clutter, the mixing of raindrop clutter and surface feature clutter and the mixing between raindrop clutter can still occur. The other method is improving the distance identification power, namely reducing the dimensions of the distance identification element, to make the clutter separate and also reduce the probability of mixing. The specific method is using pulse compression. If we use a 25:1 pulse compression system, we can take the original 5 microsecond pulsewidth compression to approximately 0.25 microseconds, that is, we can reduce the distance identification element 25 times.

When pulse compression combines with paired pulse moving target indication, it generally first takes the signal that is received and after going through mixing changes into the first intermediate frequency, and carries out hard limiting in the central release with its amplitude limited to the mean square root value of the noise to completely ruin its amplitude signal and only keep its phase signal, later it takes the signal after this limiting to the compression filter that is formed by the chromatic dispersion net, when its compression ratio is 25:1, its amplitude then increases $\sqrt{25}=5$ times, or 14dB. Its signal-noise ratio is 14dB. The signal that is put out by the compressed filter then goes to two delay time wires, the difference between their delay time duration is equal to the interval of the two pulses, the output after this delay time respectively goes to the amplitude detector and phase detector, after amplitude detection the output that goes through the "AND" gate is used to select the output after phase detection eliminates fixed clutter.

We will now discuss how to eliminate the half blind speed point in the phase detection destruction system. Assume the interval of the two pulses is 150 microseconds. The intermediate frequency pulse after going through pulse compression goes to the two delay time wires that have a delay time difference of 150 microseconds (see Fig.

9.17). The output after delay time first goes to one phase detector, the output from this phase detector is called "in phase" output, this output is one that has a half blind speed point (see curve A in Fig. 9.18). After delay time a circuit goes to a wide-band phase shifter to shift 90 degrees, this phase shifter can phase shift 90 degrees within a 5MHz bandwidth (thus input frequency band). The output that is still not phase shifted after phase shifting again goes to the second phase detector, the output from this phase detector is simply the so-called cross output (curve B in Fig. 9.18). Using phase adding after the "in phase" output signal carries out complete rectification and after the cross output carries out complete rectification, we then can obtain the speed response curve of curve C in Fig. 9.18. This speed response curve can eliminate the half blind speed point (still assuming blind speed in the figure is 610 nautical miles/hour, half blind speed point is 305 nautical miles/hour).

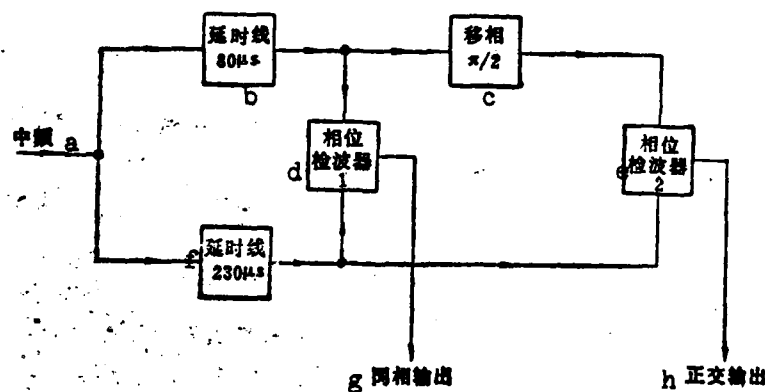


FIG. 9.17 METHOD TO ELIMINATE HALF BLIND SPEED POINT
KEY: (a) Intermediate frequency; (b) Delay time wire;
(c) Phase shift; (d) Phase detector; (e) Phase detector;
(f) Delay time wire; (g) "In phase" output;
(h) Cross output

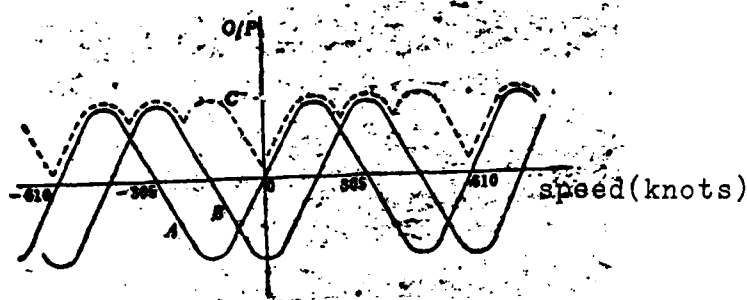


FIG. 9.18 SPEED RESPONSE OF "IN PHASE" OUTPUT AND "CROSS" OUTPUT AND AFTER THEY COMBINE

The block diagram of the phase destructor of the entire paired pulse moving target indication system is as Fig. 9.19 shows.

The intermediate frequency that comes from 80 microsecond delay time message channel, after going through pulse compression is divided into two circuits; one circuit goes to the amplitude detector, the other circuit goes to the phase detector after going through a variable phase shifter. The variable phase shifter is used to compensate the fixed phase difference of the two delay time message channels. The signal that comes from the 230 microsecond delay time circuit also respectively goes to the amplitude detector and the phase detector. The signal carries out comparison on the two circuits in the phase detector, the backward-wave of the fixed target with the same phase is eliminated and is not put out. In order to eliminate the half blind speed point of the speed response of this phase detector, these two circuits again go to a broadband 90 degree phase shifter, and after going through phase shifting 90 degrees, carry out phase detection. In order to obtain the single polarity output they are taken to the display, the output of these two phase detectors respectively go to the complete period rectifier and the half period rectifier, after their output goes through one "OR" gate mixing, it changes to one output, its speed response is as curve C in Fig. 9.18 shows. The signal of these two delay time circuits, after going through the amplitude detector, go to an "AND" gate circuit; only the coinciding signal can be put out through the "AND" gate. This

output in addition goes to a variable gate limit detector, only the power level surpassing the gate limit can form a rectangular pulse, the rectangular pulse is used to gate the output of the above mentioned "OR" gate, in order to compensate the delay time in the amplitude detector, after the output of the "OR" gate goes through a 0.2 microsecond delay time, it again goes to an "AND" gate. Although the gated pulse that is produced by the amplitude circuit can be formed by the fixed backward-wave, the output of the "OR" gate already eliminates the fixed backward-waves. Because the pulse that is formed after going through pulse compression is very narrow (only 0.25 microseconds), it is not easy to observe on the display, therefore the other circuit of the "AND" gate output goes through the pulse extender to make the pulsewidth widen to 6 microseconds, but this pulse extender will make the signal-noise ratio lose 3dB. The selection switch on the display can respectively select the unwidened and widened video frequency signal.

An actual radar system that uses the above paired pulse moving target indication, when operating in wideband pulse compression in addition to moving target indication, can obtain a 20dB destruction ratio. Because its pulsewidth is very narrow after pulse compression (only a few cycles intermediate frequency signal in the pulsewidth), therefore it causes the destruction properties of the phase detector to become poor. The destruction ratio of this system on raindrop clutter is approximately 10dB when without pulse compression, when with pulse compression it can make raindrop clutter reduce to the power level of the noise of the receiver (aside from the phase mixing that emerges). Visibility that is under clutter when it receives noise limits (SCV) is limited by the compression ratio that is used when compression ratio is 25:1, visibility under the best clutter is 14dB (realistically only 11dB), although raising limiter power level can raise visibility under clutter, when there is a large area of clutter, a stagnant appearance can emerge, therefore it still can operate the

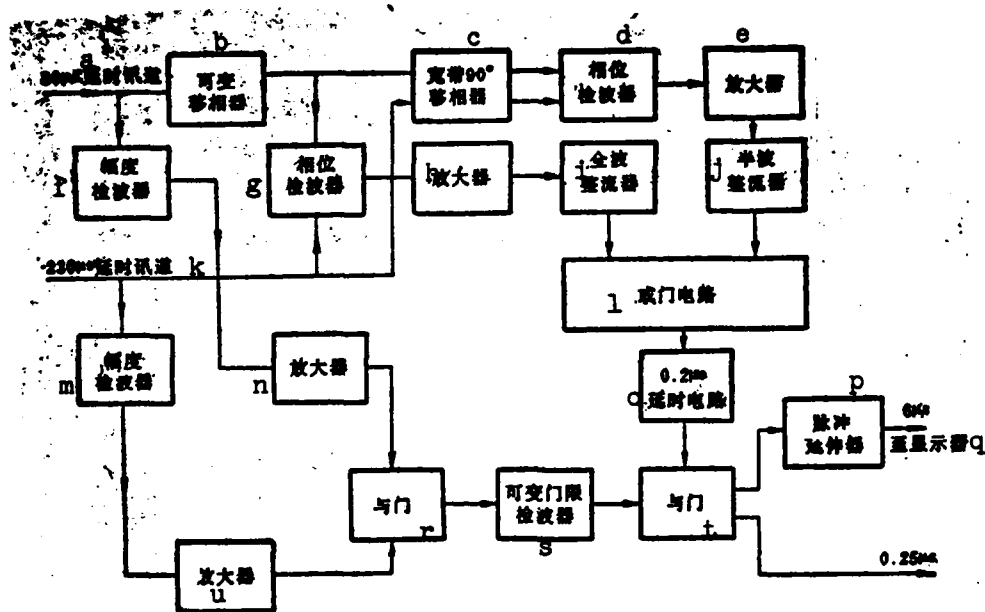


FIG. 9.19 BLOCK DIAGRAM OF PHASE DESTRUCTOR OF PAIRED PULSE MOVING TARGET INDICATION SYSTEM

KEY: (a) Delay time message channel; (b) Variable phase shifter; (c) Bandwidth 90° phase shifter; (d) Phase detector; (e) Amplifier; (f) Amplitude detector; (g) Phase detector; (h) Amplifier; (i) Complete period rectifier; (j) Half period rectifier; (k) Delay time message channel; (l) OR gate circuit; (m) Amplitude detector; (n) Amplifier; (o) Delay time circuit; (p) Pulse extender; (q) Display; (r) AND gate; (s) Variable gate limit detector; (t) AND gate; (u) Amplifier

noise limiter fairly well. From this we can see that the visibility under clutter that can be achieved by this paired pulse moving target indication system is still comparatively low.

9.3.3 MOVING TARGET INDICATION SYSTEM WITH FOUR-PULSE AGILITY⁽⁸⁾

Although the above-mentioned paired pulse moving target indication system also can overcome the contradiction of frequency agility and moving target indication to a large extent, some basic shortcomings still exist in it. Firstly, the paired pulse moving target indication system must use a fully coherent frequency agile system.

This causes the degree of complication of the equipment to greatly increase. Secondly, it has the problem of "phase contamination", enlarging the interval of the two pulses can cause blind speed to decrease, but using pulse compression can also cause the equipment to be further complicated.

In order to overcome these shortcomings, recently some people have proposed a four-pulse agility moving target indication system⁽⁸⁾. This system successively transmits a series of four pulses with the same interval within the repeated cycle of the pulse, and also, the four pulses can be produced by a noncoherent agile magnetron, because their intervals are very close (interval is 1.9 microseconds, pulsewidth 0.63 microseconds), therefore the frequency does not have time to be agile in the series. But its frequency between each series of pulses is agile. Because this series of pulses is produced by a magnetron, therefore its initial phases all are different and also it can be considered to have phase agility. In order to be able to carry out coherent processing on its backward-waves, it uses four coherent oscillators to separately record each initial phase. The block diagram of the entire system is as Fig. 9.20 shows. The oscillation that is produced by the magnetron in the figure, after going through -80dB power distribution, goes to the mixer and mixes with the stable local oscillator signal, on the one hand the intermediate frequency pulse that is obtained acts as a low automatic frequency precision tuning signal to revise and correct the local oscillator frequency; on the other hand it acts as a phase locking signal to lock the coherent oscillator. Because there are four coherent local oscillators that need to be locked, therefore it goes through a switch and respectively controls each corresponding coherent oscillator according to its transmitting order, and later after going through 90° phase drift obtains the in phase and cross coherent local oscillator signal.

After the signal of the receiver goes through the mixer and the central release, it goes to the intermediate frequency power

distributor, in order to be respectively carried to the phase sensitive detectors of the four circuits and the coherent oscillators to carry out phase detection.

If the magnetron that is used is a frequency agile magnetron, then its local oscillator still should possess corresponding high speed frequency tracking and frequency precision tuning device.

The characteristics of this four-pulse moving target indication system lie in:

(1) Increasing the pulse number in the group to four thereby increasing the pulses that can be processed, raises visibility under clutter, and even can possibly carry out Doppler frequency of the group (4) in the detector.

(2) Because it uses frequency agility between the series of pulses, not only can it improve the radar's anti-jamming, reduce loss from undulation of the backward-wave of the target, and increase angle measurement precision, but also can cause the clutter between the series to be interrelated. This especially is even more important for clutter produced by each pulse in the series to be interrelated. But mere frequency agility still has no way to resolve the problem of range secondary fragmentation. This range secondary fragmentation is caused by simultaneously processing the four pulses.

(3) This four-pulse moving target indication system uses a coherent magnetron transmitter, this not only simplifies the whole system, but also the phase agility between each pulse in the series contributes to eliminating the above-mentioned range secondary fragmentation, these all are already proven by computer analogue tests.

This four-pulse moving target indication system also can achieve Doppler signal processing in the Doppler detector, therefore it can

be considered as a radar system that possesses Doppler ability. In the following section we will discuss how to achieve this Doppler processing.

As the above section recounts, the output power from the intermediate frequency power distributor is sent to four phase detectors (see Fig. 9.21). Its output can obtain four in-phase and cross passages (the figure only draws one circuit). Later it goes to four modulation alternators. In order to carry out simultaneous processing on the four circuit signals, for each circuit signal respective delay times are 0, T, 2T, and 3T. It eliminates the initial delay time. Later it goes to the Doppler filter for formation. The composition that is formed in this Doppler filter is shown in Fig. 9.22. In it the first circuit corresponds to the fixed point of zero Doppler frequency, after the solid line section and the dashed line section of each circuit meet, the model value of the mean square root is obtained. It later is obtained after each pulse one by one goes through a 45° phase shift. It later obtains the final filter output according to the following expressions:

$$\begin{aligned} V_{0.5} &= |V_{45}| - |V_{315}| \\ V_1 &= |V_{90}| - |V_{270}| \\ V_{1.5} &= |V_{135}| - |V_{315}| \\ V_2 &= |V_{90}| - |V_{135}| \end{aligned} \quad (9.8)$$

The final speed response of the four circuit output is as shown in Fig. 9.23. That is, it can be equivalent to one group of Doppler filters, the speed response peak of each.

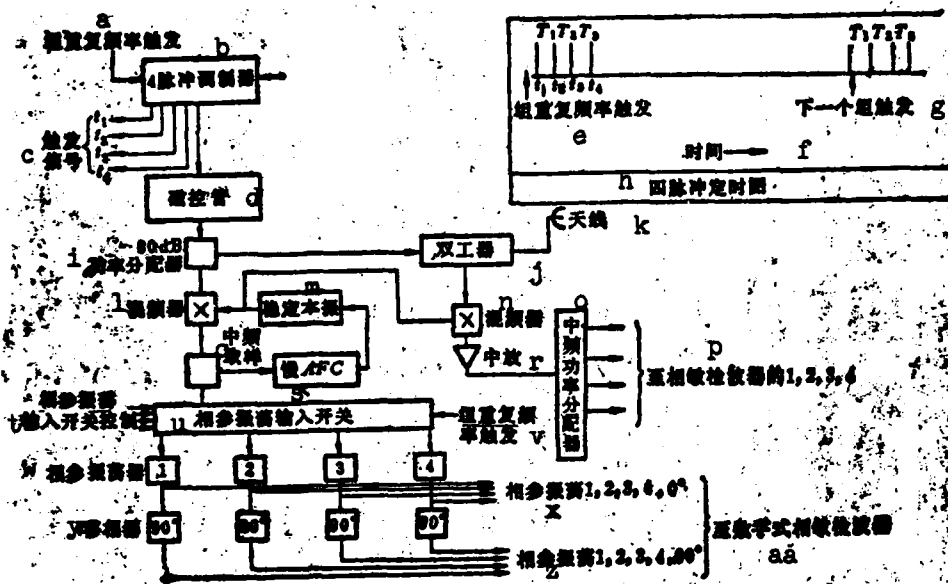
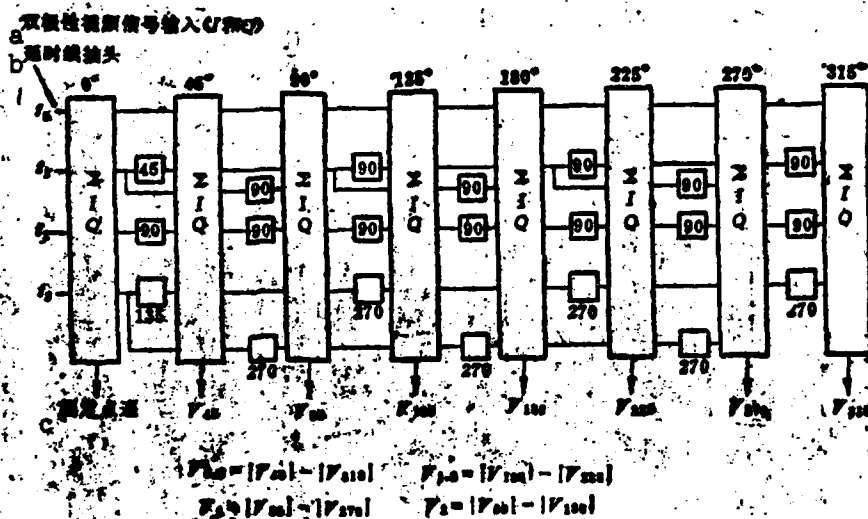
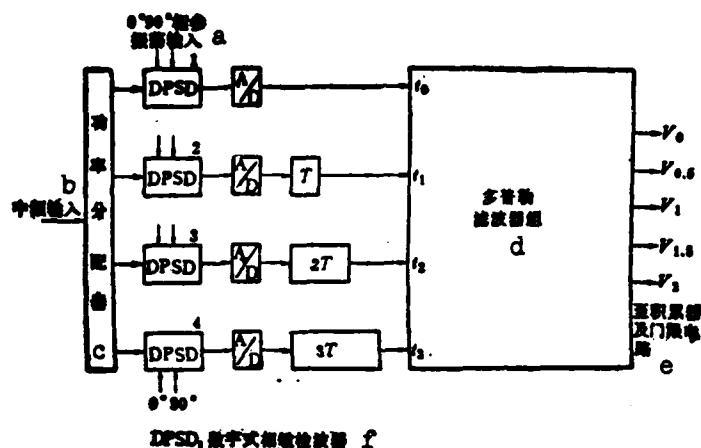


FIG. 9.20 BLOCK DIAGRAM OF FOUR PULSE MOVING TARGET INDICATION SYSTEM

KEY: (a) Group repeated frequency trigger; (b) 4 pulse modulator; (c) Trigger signal; (d) Magnetron; (e) Group repeated frequency trigger; (f) Time; (g) Next group trigger; (h) Four pulse fixed time; (i) Power distribution; (j) Dual processor; (k) Antenna; (l) Mixer; (m) Stable local oscillator; (n) Mixer; (o) Intermediate frequency power distributor; (p) To phase sensitive detectors 1,2,3, and 4; (q) Intermediate frequency sampling; (r) Central release; (s) Slow; (t) Coherent oscillator input switch control; (u) Coherent oscillator input switch; (v) Group repeated frequency trigger; (w) Coherent oscillator; (x) Coherent oscillator; (y) Phase shifter; (z) Coherent oscillators; (aa) To digital phase sensitive detectors

Because the interval of the pulse is very short, therefore the blind speed that it corresponds to is very high. We also can say that basically the blind speed problem does not exist. But the number of coherent accumulated pulses is very few, therefore it only can depend on the noncoherent accumulation of the pulses in each series, this accumulation still can restrain clutter after interrelation, thereby increasing its signal-clutter ratio.

But until now this system is only carried out in analogue experimental research, there still has been no concrete achievement.



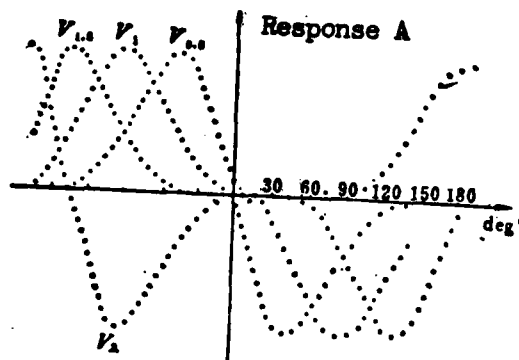


FIG. 9.23 SPEED RESONSE OF DOPPLER
FILTER GROUP

9.3.4 MOVING TARGET INDICATION SYSTEM THAT IS COMPATIBLE WITH SELF- ADAPTING FREQUENCY AGILITY

The method of transmitting several pulses in the repeating cycle of the pulse to carry out moving target indication invariably is not as good as processing between the cycles, especially for space lookout radar where repeating frequency is fairly high and affected distance is fairly low. Having to transmit relatively many pulses in the cycle to carry out moving target indication processing is fairly difficult, furthermore it is very difficult to obtain a relatively high index. The radar with this fairly high repeating frequency (approximately 1kHz to 5kHz) can use another moving target indication system with frequency agile compatibility⁽⁹⁾. The block diagram of the principles of this system is shown in Fig. 9.24. The radar that is suitable to it is fully coherent frequency agile radar that operates on several points of frequency, the radar can automatically adapt to the frequency agile type. The jamming prediction that comes from the jamming analysis device goes to a control logic, the transmitting frequency that controls the radar is located in the weakest region of the jamming. The signal that is received, after going through phase detection, goes to a model-number alternator, the output of the latter goes to a storage. This storage possesses a fairly low storage capacity, it can store the corresponding basic band video signals of many cycles, after these signals go through

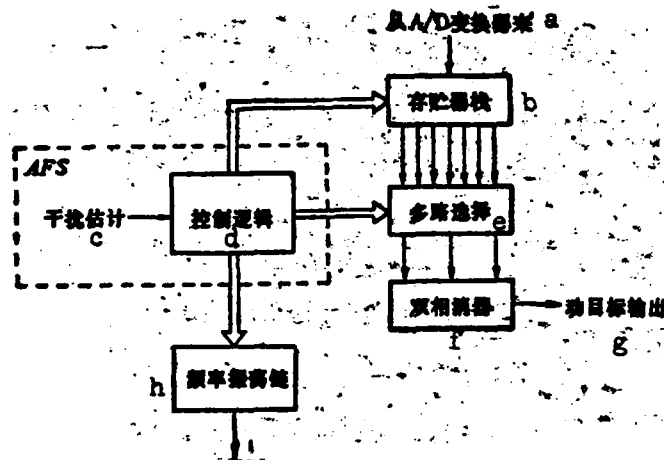


FIG. 9.24 BLOCK DIAGRAM OF PRINCIPLES OF MOVING TARGET INDICATION SYSTEM THAT IS COMPATIBLE WITH SELF-ADAPTING FREQUENCY AGILITY

KEY: (a) From A/D alternator; (b) Storage; (c) Jamming prediction; (d) Control logic; (e) Multiple circuit selector; (f) Dual destructor; (g) Moving target output; (h) Frequency oscillator chain; (i) To transmitter

multiple circuit selection they go to a dual destructor. Exactly selecting the signal of that circuit to go to the dual destructor is determined by the control logic. Figure 9.25 can explain its selection principle. If the storage altogether stores the signals of several repeating cycles, in it the signal that is scanned most recently (the n th time) goes to the input of the dual destructor (namely, three-pulse cancellation). If the radar altogether transmits 8 dispersed point frequencies (respectively f_1, f_2, \dots, f_8), the n -th transmission is f_2 , thus the carrier frequencies of the other two signals that carry out cancellation with it are also f_2 , and record in the control logic all the previous n transmitted frequencies, therefore we can select the signals that are taken from the storage to the destructor according to the transmitting pulse histories that are recorded. The examples in the figure are the $n-2$ time and the $n-8$ time, although these three times are not sequentially transmitted, because their carrier frequency is equally precise, therefore they can go to the destructor and offset the fixed backward-waves.

Clearly this system only can be suitable to the following two conditions: firstly, the backward-wave number that scans the target must be enough (that is the repeated frequency of the radar should be fairly high), otherwise, backward-waves with the same frequency that can provide destruction processing are very few, backward-waves that can have video frequency accumulation also will be very few; secondly, the number of frequency agile frequency channels cannot be too many, too many frequency channels also will cause the amount of backward-waves that have the same frequency to reduce.

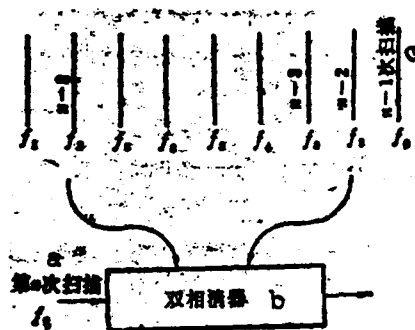


图9.25 双相消器信号的选择

FIG. 9.25 SIGNAL SELECTION OF DUAL DESTRUCTOR

KEY: (a) The n th scanning; (b) Dual destructor; (c) The n th scanning

Two questions naturally can be raised on this system: one question is exactly how large is the improvement factor of moving target indication that can be obtained by it; the other question is whether or not the method of ordinary moving target indication technology using repeated frequency reference differences to eliminate blind speed is efficient under these conditions.

The improvement factor IF of the dual destructor is defined as:

$$IF = CA + G_N \quad (9.9)$$

In which G_N is noise gain, and CA is clutter attenuation; the latter can be computed by the following expression:

$$CA = \frac{\int_{-\infty}^{\infty} S(f) df}{\int_{-\infty}^{\infty} |H(f)|^2 S(f) df} \quad (9.10)$$

In which $S(f)$ is clutter frequency spectrum, and $H(f)$ is delivery function.

$$H(f) = 1 - 2 \exp(-j2\pi f K_1 T) + \exp(-j2\pi f (K_1 + K_2) T) \quad (9.11)$$

In which K_1 and K_2 separately are the cycle numbers between the second and third pulse and the first and second that transmit the same frequencies.

Assuming the frequency spectrum of Gauss type clutter is

$$S(f) = S_0 \exp\left(-\frac{f^2}{2\sigma^2}\right) \quad (9.12)$$

In which σ is the standard difference of clutter frequency spectrum, thus substituting expression (9.10) we obtain:

$$CA = \frac{1}{1 - 4 \exp(1 - K_1^2) - 4 \exp(1 - K_2^2) + 2 \exp(-(K_1 + K_2)^2)} \quad (9.13)$$

In which

$$K_1 = \sqrt{2\pi} K_1 T \sigma$$

$$K_2 = \sqrt{2\pi} K_2 T \sigma$$

$G_N=6$ on the dual destructor, therefore we obtain:

$$IF = \frac{3}{3 - 2\exp(1-K_1^2) - 2\exp(1-K_2^2) + \exp(-(K_1+K_2)^2)} \quad (9.14)$$

So long as we know K_A and K_B values we can compute improvement factor IF , in the expression of K_A and K_B . T is the repeating cycle of the radar, approximately between 200 microseconds to 1 millisecond, σ can be assumed smaller than 1.5 m/second (corresponding to the forests and hills with wind velocity as 40km/hour) and additionally the frequency spectrum that is caused by antenna scanning widens. The problem primarily lies in that K_1 and K_2 when there is frequency agility is not fixed and invariant, but is a stochastic variable. Under this condition, the improvement factor of moving target indication also is not fixed. Therefore it only can be expressed by a statistic measure $P\{IF\}$, it represents the probability that reaches a certain IF . The value of K_1 and K_2 obviously are functions of the frequency channels that are used. Figure 9.26 gives the computed results of $P\{IF\}$ and IF when there are 3, 4, and 5 probable frequency. The more frequency that is used, the poorer its performance.

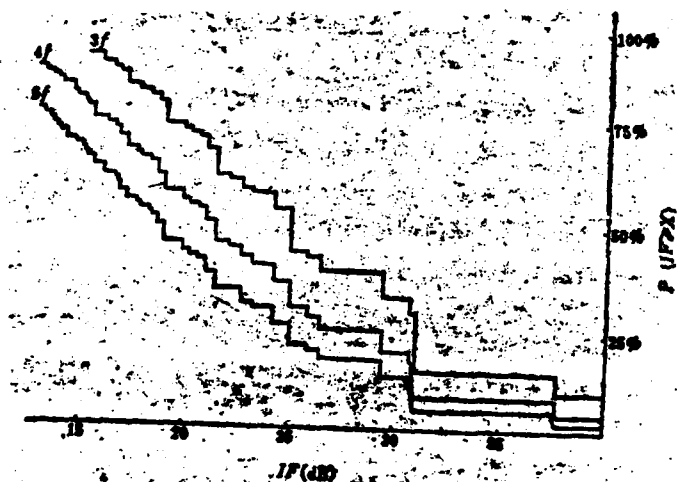


FIG. 9.26 MOVING TARGET IMPROVEMENT FACTOR WHEN THERE IS STOCHASTIC JUMP FREQUENCY

However, when there is self-adapting frequency agility, the probability of each frequency is equal. Under this condition, its probability is still related to such factors as frequency spectrum distribution of jamming clutter, multiple channel appearance, and antenna radiation graph. Therefore it is very difficult to use the analysis method for resolution, we can only use the analogue method for research.

If the number of frequency channels is exceedingly many, its improvement factor will drop; if the number of frequency channels is exceedingly few, then it is disadvantageous for anti-jamming. Analogue tests show that the best compromise between these two requires the ratio of the independent channel number that is used and the backward-wave of the scanned target to be $1/8$. When the number of frequency channels are more than this, its improvement factor can decrease. The other method to resolve this problem is the method of additionally forcing operation in a certain frequency simultaneously with self-adapting frequency agility. For example, the frequency that is in storage already has two certain frequencies, consequently it forces the transmitter to again transmit on a certain frequency to avoid its waiting period being too long.

In summary, after using self-adapting frequency agility, because the weakest region of jamming cannot be the same with each line of transmission, therefore the probability of operating on the same frequency is greater than with stochastic agility. For example, when randomly selecting three frequencies in the cycle when the target irradiates, we can obtain the average improvement factor as 28dB, and when carrying out self-adapting frequency agile radar on similar noise jamming we can obtain the average improvement factor of approximately 40dB. From this we can see that no matter if it is from an anti-jamming point of view or an anti-clutter point of view, self-adapting frequency agility is a better method of operation.

In ordinary moving target indication radar, the often-used variable repeating frequency method extends blind speed. For example, replaced with using six repeating frequencies can extend blind speed several fold. Can this method be used under conditions of self-adapting frequency agility? This also can only be investigated by using analogue tests. Tests show that when using the same frequency cycle order, the speed response that is obtained when operating on self-adapting frequency agility is extremely similar to when there is fixed frequency. Figure 9.27 draws the speed responses of fixed frequency and self-adapting frequency agility when there is a certain repeating cycle order.

From the above we can know that using this moving target indication system that is compatible with self-adapting frequency agility, it not only can self-adapt to obtain the best anti-jamming properties on the jamming frequency spectrum, but also has sufficiently satisfactory moving target indication improvement factor and speed response when with reference difference repeating frequency.

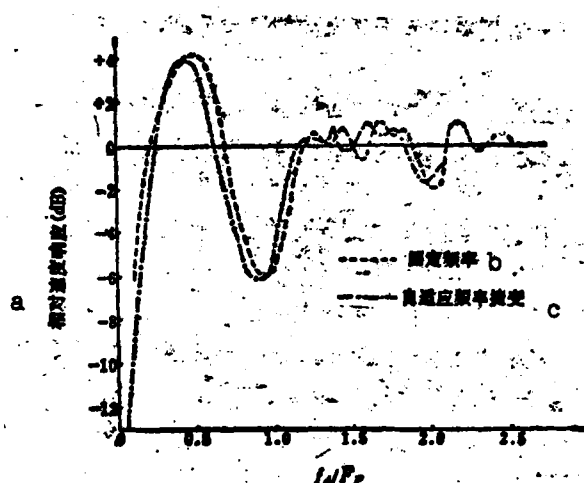


FIG. 9.27 SPEED RESPONSE WITH FIXED FREQUENCY AND SELF-ADAPTING FREQUENCY AGILITY
KEY: (a) Corresponding speed response; (b) Fixed frequency; (c) Self-adapting frequency agility

9.4 COHERENT PROCESSING OF FREQUENCY AGILE RADAR

In fixed frequency radar, so long as we maintain the strict phase relationship between the signal of the local oscillator and the transmitting frequency, we then can achieve coherent accumulation. As to the problem of unknown Doppler frequency of the target, it can be resolved by using the Doppler filter group. Presently this filter group is equivalent by Fast Fourier Transformation (FFT). But under conditions of frequency agility it is different. This is because the carrier frequency of each transmitting pulse is different. The corresponding Doppler frequency of the same radial speed also is different. The phase variations that arise from this also are different. There have been people attempting to compute the phase variations that are drawn into it in order to carry out revision and correction⁽¹⁰⁾, but because the preliminary phase of the reflected backward-wave of the target is unknown, it also is a fixed function of the frequency. Therefore, this phase variation has no method to estimate and revise and correct.

In radar where the frequency does gradient jump changing, the problem can be much simplified. At this time, because there is only one target that is tracked, there also is only one radial speed. Moreover the time of the irradiated target is comparatively long, the number of accumulated pulses is comparatively many. At this time, because the frequency makes patterned gradated jump changes we can regard it as being formed by the pulse where many different carrier frequency cycles are gradient cycles, as to each carrier frequency, they then correspond to fixed frequency radar, only its repeated frequency lowers k times (k is number of gradations). As to this frequency agile radar, it then can use the circuit coherent receiver to carry out accumulation. In tracking radar, coherent accumulation is achieved by Doppler frequency tracking; if we use an analogue

accumulation system we must have ~~R~~ frequency tracking loops. When using digital accumulation, we can use the method of phase compensations and time division, achieved with a digital coherent accumulation system. This digital accumulation system is extremely similar to a digital accumulation system that is used when there are several moving targets that possess different Doppler frequencies in the simultaneous tracking beam that uses monopulse Doppler tracking radar.

But in searching radar, conditions are very complicated. At this time, because it is possible to have several targets of different radial speeds at different distances in the same direction, under these conditions we carry out frequency agility, making the problem even more complicated. At this time, the same radial speed can produce different Doppler frequencies, if the carrier frequency can have an arbitrary frequency in the agile frequency band, the problem is complicated to where it is difficult to resolve.

As to the fully coherent frequency agile radar that only transmits a few fixed frequency points, we can use the multiple channel method to achieve coherent processing⁽¹¹⁾. Because many actual multiple frequency channel radars do not have coherence between each of its frequency channels, therefore between each of its frequency channels we only can use the method of noncoherent accumulation. But in each frequency channel, we also can use the method of the Doppler filter group to resolve the problem of the unknown radial speed. The block diagram of its specific system is shown in Fig. 9.28⁽¹²⁾. It is necessary to note that the figure only draws the Doppler filter group after one distance wave gate. As to the radar that has M distance wave gates, it must have M systems like this, we can see that this kind of system is extremely complicated.

As is previously explained, this Doppler filter group generally uses Fast Fourier Transformation (FFT) to be equivalent. Its number

of filters is equal to the processed count. To obtain enough Doppler frequency identification, the desired number of backward-waves of the same frequency that are obtained from the target will be more than enough. Because the total number of backward-waves that can be obtained when scanning the target is limited, to make the number of backward-waves of the same frequency enough, there are three methods that can be used. One is reducing the target of the number of frequency channels, the next is raising the repeated frequency, the third is using division and collection in the cycle. The first method, seen from an anti-jamming point of view, obviously is not desirable. Moreover too few frequency channels also can influence collection. Figure 9.29 gives the curve of the relationship between the number of frequency channels and the gains on the signal-clutter ratio after frequency division and collection when false alarm probability is 10^{-6} and detection probability respectively is 0.7 and 0.9. The reduction of frequency division and collection on loss from undulation increases with the number of frequency channels, but noncoherent accumulation loss also increases with the number of frequency channels, therefore, a best number of frequency channels exists. But, when detection probability is fairly high, the largest value is not obvious. From the viewpoint of reducing the amount of equipment the desired number of frequency channels should be as few as possible. From the figure we can see that using four frequency channels is fairly suitable. In order to improve its anti-jamming properties, the specific frequency value of these four frequency channels should be able to vary within a specified bandwidth.

Using high repeated frequency can increase the number of backward-waves, but can give rise to distance indistinction, we still must use the method of frequency repetition to eliminate it.

Using the Doppler filter group to carry out coherent processing can cause a certain loss, this loss is caused by the unknown Doppler frequency. Because even if there is a single frequency channel, no

matter in which filter the emerging output exceeds the gate limit they all will determine that the target exists. When there is a fixed gate limit, the false alarm probability will increase with the number of Doppler filters. But generally it is desirable to be able to maintain the false alarm probability as the assigned value, therefore its gate limit will follow the monotonic increase of the number of Doppler frequencies. This then brings about the loss on target detectability. Computations clearly show that when $P_D=0.9$ and $P_F=10^{-6}$, the loss of 8 filter groups is 0.6dB. In multiple frequency channels, because the radial speed of the target is unknown, and also the Doppler frequency shift that the same radial speed gives rise to in each frequency channel is different, additionally the existence of speed measurement indistinction makes it unable to find the Doppler filter that corresponds to the same radial speed in each frequency channel, so it is necessary to phase add the output of all the filters. This then gives rise to fairly large loss. Computations show that when there are 4 frequency channels and each channel has 8 filters, its loss reaches 2.05dB.

A simplified method is finding the largest one that is put out from the 8 filters, and later carry out noncoherent phase adding on the largest one that is put out from each frequency channel, and compare the results of the phase adding with the gate limit (see Fig. 9.28). When using this method in the same conditions, its loss is approximately 1.82dB, that is 1.22dB larger than single frequency channels. When there is a different number of filters, the comparison of the signal-clutter ratio SIR that is needed by the 4 frequency channels division and collection and when with the single frequency channel is shown in Fig. 9.30, the curve in the figure is according to the Swerling II model target, computed when $P_D=0.9$ and $P_F=10^{-6}$. One filter in the figure also corresponds to conditions when target speed is already known, its results are consistent with those in Fig. 9.28. Following the increase of Doppler filters, the loss of the four frequency channels increases more than the loss of the single

frequency channel increases, but when the number of filters is 8, its loss then increases very slowly.

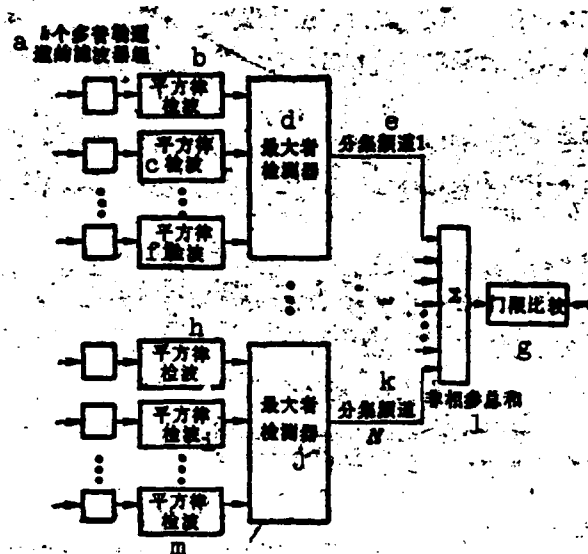


FIG. 9.28 BLOCK DIAGRAM OF COHERENT PROCESSING SYSTEM WITH MULTIPLE FREQUENCY CHANNEL

KEY: (a) Filter group of R multiple Doppler channels; (b) Square pattern detection; (c) Square pattern detection; (d) Largest detector; (e) Division and collection frequency channel; (f) Square pattern detection; (g) Gate limit comparison; (h) Square pattern detection; (i) Square pattern detection; (j) Largest detector; (k) Division and collection frequency channel; (l) Noncoherent sum; (m) Square pattern detection

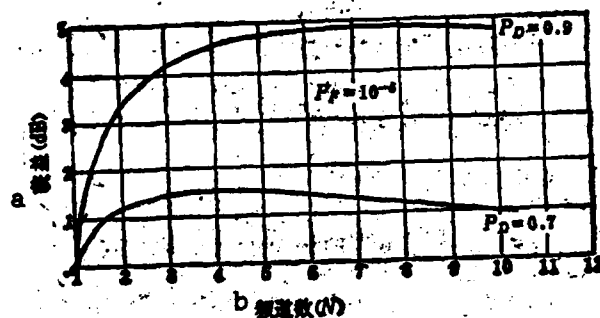


FIG. 9.29 CURVE OF RELATIONSHIP BETWEEN FREQUENCY DIVISION AND COLLECTION GAIN AND N. NUMBER OF FREQUENCY CHANNELS
KEY: (a) Gain; (b) Number of frequency channels

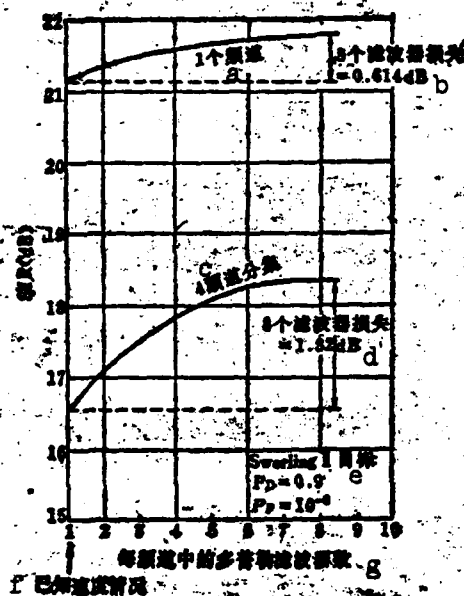


FIG. 9.30 COMPARISON OF SIGNAL-CLUTTER RATIO THAT IS NEEDED BY FOUR FREQUENCY CHANNELS AND SINGLE FREQUENCY CHANNEL WITH DIFFERENT NUMBER OF DOPPLER FILTERS
KEY: (a) Frequency channel; (b) Loss of 8 filters; (c) 4 frequency channels division and collection; (d) Loss of 8 filters; (e) Target; (f) Conditions of already-known speed; (g) Number of Doppler filters in each frequency channel

9.5 JUMP FREQUENCY TYPE FREQUENCY SCANNING RADAR

Frequency scanning type tricoordinate radar was a most efficient electronically-controlled scanning radar system that obtained widespread use before phased array radar, moreover, because its equipment is simple, it still until today obtains widespread use. The sortcoming of this radar is that its operational frequency is completely determined by the beam direction that is required, therefore there is no way to carry out selection according to other requirements (for example anti-jamming).

From a generalized point of view frequency scanning radar is also a type of frequency agile radar because the carrier frequency of its adjacent transmitting pulse can have very great differences, even though usually these frequency differences are not very great.

We will now take a look at the conditions when there are only two antenna radiating elements (see Fig. 9.31(1)). The distance between these two antenna elements is d , if the phase difference of the radio frequency signal of these two antennas is $(2\pi/\lambda)d \sin \theta$, its normal line in front of the wave then points in the direction of θ . In order to cause its feed-in radio frequency to have a phase difference, a feed wire with length as s connects between the two radiated elements (it generally is a wave guide in the radar), then so long as we input the wavelength of the radio frequency signal it can satisfy the following relationship:

$$\frac{2\pi s}{\lambda} - 2\pi n = \frac{2\pi}{\lambda} d \sin \theta \quad (9.15)$$

In which n is a positive whole number. This way we can make the beam direct towards θ .

Actually, the wave length of this wave guide is λ_g in which λ_g is the wavelength radio frequency signal in the wave guide when it makes the transmitting beam direction straight ahead (thus $\theta=0$).

From expression (9.15) we can obtain:

$$\theta = \arcsin \frac{s\lambda}{d} \left(\frac{1}{\lambda_g} - \frac{s}{s} \right) \quad (9.16)$$

From wave guide theory we can know that wavelength λ_g in the wave guide and wave length λ in free space have the following relational expression:

$$\lambda_g = \frac{\lambda}{\left[1 - \left(\frac{\lambda}{2a} \right)^2 \right]^{1/2}} = \frac{2ac}{(4f^2a^2 - c^2)^{1/2}} \quad (9.17)$$

In which a is long side of the wave guide
 c is speed of light in free space
 f is frequency of radio frequency signal

Replacing this expression with expression (9.16) we can obtain:

$$\sin \theta = \frac{s}{2a/d} \frac{2ac}{(4f^2a^2 - c^2)^{1/2}} \left(\frac{1}{\lambda_g} - \frac{s}{s} \right) \quad (9.18)$$

From this expression we can obtain the relationship of beam directional angle θ when there is a certain interval d and transmitting frequency. This relationship when $d=0.5\lambda$ is as Fig. 9.32 shows.

Corresponding frequency deflection in the figure is the frequency deflection when corresponding to the zero deflection angle, from the figure we can see that when there is the same corresponding frequency deflection, the longer the wavelength affecting the delay time wire (thus the larger λ), the bigger the deflection of the beam, and also

the bigger the angle that is limited by the two wave fragmentations. Therefore, in order to obtain a comparatively high deflection sensitivity (usually expressed by degree/MHz), we select a fairly large N value, at this time we use a wave guide bending into an S shape to increase its length. The contact feed when there are many antenna radiating elements is as Fig. 9.31(2) shows.

This way, so long as we change the transmitting frequency of the radar, we then can change the direction of the antenna beam. General frequency scanning radar is primarily used in tricoordinate radar of angle of elevation frequency scanning and bearing mechanical rotation. A simple block diagram of this radar is shown in Fig. 9.33. The directional command signal of the beam that is produced by the beam directional program controller on the one hand conducts a transmitting frequency command to the frequency synthesizer, on the other hand conducts the beam directional angle signal to the display. The frequency synthesizer produces a corresponding frequency according to the frequency command signal, one circuit is carried to the transmitter to conduct signal transmission; one intermediate frequency of the phase difference of the other circuit and the transmitting signal conduct the local oscillator signal to the receiver, after the transmitting signal goes through the power amplification chain it then goes to the frequency scanning antenna array. After the backward-wave signal that is received goes through mixing, central release, and detection, it goes to the display.

Roughly seen, the block diagram of this frequency scanning radar is completely the same as the block diagram of a fully coherent frequency agile radar. In that case, can frequency scanning radar be regarded as a particular type of frequency agile radar? For this question it is necessary to discuss several different types of actual frequency scanning radar systems.

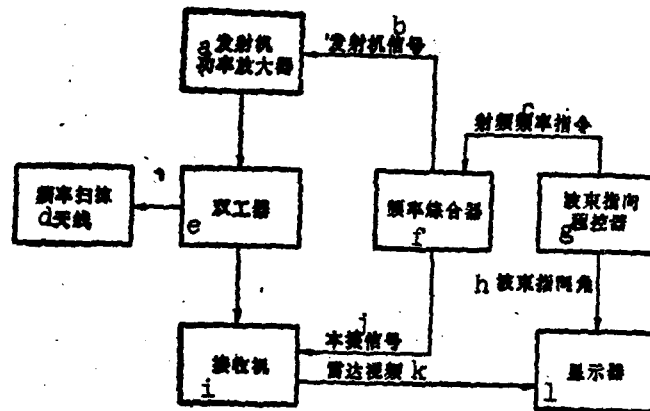


FIG. 9.33 SIMPLIFIED BLOCK DIAGRAM OF
FREQUENCY SCANNING RADAR
KEY: (a) Power amplification of the trans-
mitter; (b) Transmitter signal; (c) Radio
frequency frequency command; (d) Frequency
scanning antenna; (e) Dual processor;
(f) Frequency synthesizer; (g) Beam direc-
tion program controller; (h) Beam direc-
tional angle; (i) Receiver; (j) Local
oscillator signal; (k) Radar video fre-
quency; (l) Display

Although the carrier frequency of the transmitting pulse of frequency scanning radar must be determined by the required beam directional angle (generally the angle of elevation), there are still many designs of its transmitting wave form. Figure 9.34 draws four wave forms that can be selected. Assume that it requires transmitting carrier frequency to change from f_1 to f_n by the necessary beam scanning range. We then can have the four variation methods as in the figure (actually there are even more). The first is frequency scanning between the repeated cycle, variations of the frequency are produced between the repeating cycles of the pulse (also can be invariable, then the second repeating cycle still is f_1 ; also can jump change, then the second repeating cycle changes to f_n , but the interval of its adjacent pulse is then determined by the largest affected distance). The second wave form is frequency scanning in the repeated cycle,

transmitting a series of pulses with different frequencies from f_1 to f_n in one repeating cycle. The third wave form is frequency scanning in the pulse, cutting off the subpulses of different frequencies inside of one transmitting pulse. The fourth wave form is linear frequency scanning in the pulse, its carrier frequency linearly changes from f_1 to f_n inside of one transmitting pulse.

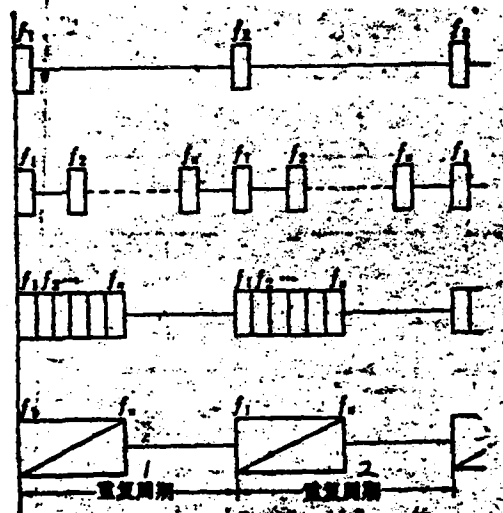


FIG. 9.34 FOUR WAVE FORMS OF FREQUENCY SCANNING RADAR THAT CAN BE SELECTED

KEY: (a) Repeating cycle; (b) Repeating cycle

From the above section we can see that seemingly these four wave forms are only very simple time coordinate compression. But further research can discover that the frequency scanning systems of these four different wave forms have many completely different qualities.

Firstly, the first wave form generally is called single beam frequency scanning. Its beam is a single brush form beam, its direction is determined by the frequency of the carrier frequency. The

block diagram of frequency scanning radar that Fig. 9.33 shows is the block diagram of this radar. Although this is the most simple frequency scanning radar, it has many special characteristics, firstly that it has a very high agility adaptability. The carrier frequency of its transmitting pulse can have various different alignments, for example it can have sequential jump frequency, but it can also carry out jump frequency not according to a specific sequence. Only at this time the directional of the antenna beam is also not scanning according to a specific sequence. But, at this time, if we must carry out stochastic jump frequency we have relatively great difficulty because the direction of the antenna between the pulses has very great variations, thus on certain directions it actually only transmits one pulse, this causes accumulation of pulses to become impossible, unless we use a moving target indication system that is similar to the one that is discussed above and is compatible with self-adapting frequency agility. The other important advantage of this frequency scanning system is that it can be used to achieve high speed searching of dual gate limit sequential detection. This sequential detection system possesses two gate limit power levels (see Fig. 9.35), when the video frequency voltage that is accumulated is as large as the second gate limit, the target exists. In single beam frequency scanning radar, the radar firstly in a certain beam position transmits the frequency that corresponds to this beam. After the backward-wave voltage that is received goes through accumulation, it is still as low as the power level of the first gate limit (in the figure, after successively transmitting two frequencies), thus it can be determined that there is no target in the beam direction, and the radar changes to another beam position (thus another frequency) to continue transmission. If the video frequency voltage that is accumulated is between the two gate limits, then it cannot determine whether or not there is a target and still continues to transmit pulses in this beam direction (thus using the original frequency); when the backward-wave signal voltage that is accumulated

exceeds the second gate limit, then it can be considered that there is a target. When using this method to carry out beam scanning, the speed of its scanning is not equal, it is fast in regions without a target, and slow in regions with a target. On the basis of theoretical computations, when there is a single distance element, if the required detection probability $P_D=0.9$ and $P_F=10^{-8}$, then the searching time in a region without a target is 1/10 that of ordinary radar, and the searching time in a region with a target is 1/2 that of ordinary radar.

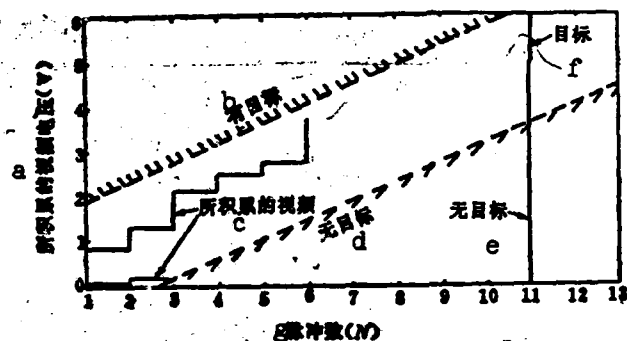


FIG. 9.35 DIAGRAM OF PULSE ALIGNMENTS OF SEQUENTIAL DETECTOR WITH SINGLE DISTANCE ELEMENT PROBABILITY RATIO
KEY: (a) Accumulated video frequency voltage; (b) With target; (c) Accumulated video frequencies; (d) Without a target; (e) Without a target; (f) Target; (g) Number of pulses (N)

This makes searching time greatly reduce and also corresponds to the increase of sensitivity. We can calculate when there are diverse distance elements, if required $P_D=0.86$, $P_F=3 \times 10^{-11}$, when the number of distance elements respectively are 30, 100, and 300, the sensitivity of the sequential detector with this probability ratio increases respectively 4.4dB, 3.6dB, and 3.2dB higher than the ordinary detector.

Secondly, this single beam frequency scanning system also can be not equal to the repeating cycle transmission, according to the height of the angle of elevation. Because the greatest altitude of the

target is specified, therefore, the higher the angle of elevation of the target, the shorter its slope, and the shorter the repeating cycle of the corresponding indistinct range finding. Therefore, single beam frequency scanning radar can follow the increase of the angle of elevation of the beam and the repeating cycle becomes shorter and shorter, this in turn can further reduce searching time and raise the data rate of the radar.

Secondly, the second transmitted wave form is seemingly only putting the time of the first wave form in axial compression, but it does bring out a new property, this is that the original single beam frequency scanning becomes a multiple beam scanning. Because it transmits a pulse that corresponds to n beam positions from $\theta_1 \sim \theta_n$ in a repeating cycle (its carrier frequency is $f_1 \sim f_n$), so long as it is divided into multiple dispatch channels in the receiver it then becomes a multiple beam radar. Figure 9.36 is the block diagram of this frequency scanning radar.

The multiple beam scanning radar, although the complication level of the equipment of the receiver and data processing system increases, its data rate of the backward-wave tubes also greatly improves. However, the transmitter of this radar requires a relatively high average power. Although the narrow band amplifier in the figure is drawn according to the frequency of f_1, f_2, \dots, f_n sequence, the transmission sequence of this multiple beam frequency scanning radar is not specifically according to this sequence. But at this time the backward-wave repeating cycle that is obtained by each beam message channel are not uniform.

The third wave form is basically the same as the second wave form. It only transmits f_1 to f_n n frequencies in a long pulse. This system requires the end stage high-powered transmission tube of the transmitter to possess the ability to transmit a long pulse.

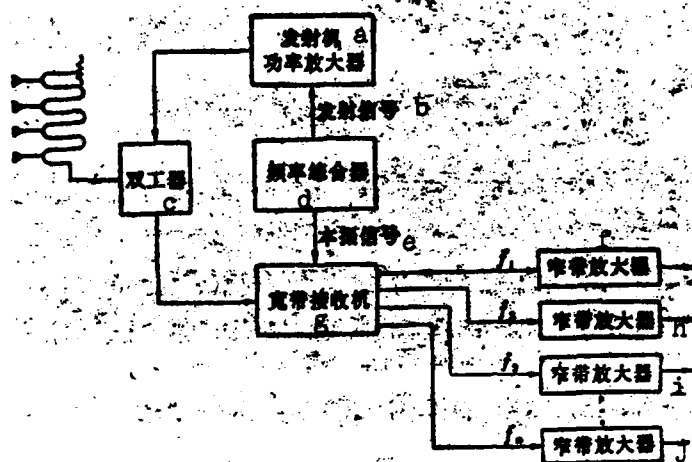


FIG. 9.36 BLOCK DIAGRAM OF MULTIPLE BEAM SCANNING RADAR

KEY: (a) Receiver power amplifier; (b) Transmitting signal; (c) Dual processor; (d) Frequency synthesizer; (e) Local oscillator signal; (f) Narrow band amplifier; (g) Wideband receiver; (h), (i), (j) Narrow band amplifier

We can say that the paired pulse system is a special case of this system. Only the two subpulses where the frequencies have slight differences are contained in a pulse that is transmitted by this radar, on the one hand this can increase the amount of impact in the pulse and increase angle measurement precision; on the other hand it can cause two beams to stagger, forming criss-cross scanning, used to catch the target.

The fourth wave form has intrinsic differences from the previous few forms. It forms a long pulse that makes linear frequency modulation in a pulse. Actually, this system combines frequency scanning and pulse compression, causing the scanning radar to possibly use pulse compression to improve its identification ability. Figure 9.37 draws the signal wave form of this frequency scanning radar. In the figure (a) is the linear frequency modulation signal that is transmitted, the relationship of its frequency and time is expressed

by the dashed line, and the relationship between the corresponding beam directional angle and time is expressed by the solid line. If a target exists in a certain angle position, then the backward-wave signal that it transmits also is a linear frequency modulation signal, only the frequency bandwidth of its scanning frequency must be very narrow, to correspond to the frequency range that the beam width corresponds to, the width of this signal in the time is thus determined by its scanning speed and antenna bandwidth, therefore amplitude A of the backward-wave is modulated by wave fragmentation graph of the antenna (as Fig. 37(b) shows). Unusually fortunate, this amplitude modulation is precisely what is needed by the pulse compression filter in order to restrain the weighted amplitude of distance lateral fragmentation. This backward-wave signal goes to a pulse compression filter to carry out compression that forms a linear relationship between a delay time period and frequency (see Fig. 9.37(c)). The signal after compression is as Fig. 9.37(d) shows. This way, so long as the scanning frequency speed of the earliest transmitted signal is high enough (thus total frequency band is narrow enough and transmitted pulsewidth is narrow enough), it can compress to the corresponding narrow degree. This scanning frequency speed thus is determined by the instantaneous bandwidth of the antenna. In this frequency scanning radar the determination of the target angle coordinates is obtained by using a frequency detector to carry out measurement on the average frequency of the backward-wave, therefore its angle measurement precision is not only related to the frequency angle measurement properties of the antenna but also is related to the frequency detection properties of the detector.

After understanding the basic operational properties of the above several types of frequency scanning radar, we can answer the question that was originally raised: exactly what are the common points and what are the differences between frequency scanning radar and frequency agile radar?

Looking at the transmitted wave forms, we at least can consider that the first and second frequency scanning radar systems coincide with the definition of frequency agile radar, the carrier frequencies of the adjacent pulses that they transmit are different. But in frequency scanning radar, because the carrier frequencies of the pulses that they transmit are completely determined by required beam directional angle, it not like that kind that can be arbitrarily chosen in ordinary frequency agile radar. Although the sequence of the beam directional angle can vary, to obtain continuity of information to increase angle measurement precision, the carrier frequency of the pulse in ordinary frequency scanning radar is transmitted according to the sequence, therefore its carrier frequency variations have specific patterns, this makes it fairly easy for the enemy detection receiver to obtain and analyze the operational properties of the whole frequency scanning radar that uses sequential detection, the variation of its transmitting carrier frequency must be even more patterned. Seen from the viewpoint of anti-jamming it is relatively advantageous.

Aside from this, in order to increase the anti-jamming properties of the radar, the wider the required jump frequency bandwidth of the radar the better. But in frequency scanning radar, in order to avoid receiving the limits of quadratic wave fragmentation, generally we select a fairly large N value (see Fig. 9.32), at this time the frequency bandwidth that is required is comparatively narrow, its anti-jamming properties receive influence. In frequency scanning radar of linear frequency modulation, its frequency bandwidth even more receives the limit of the scanning frequency speed that is allowed by the antenna.

Even more important, although the transmitting wave forms of frequency scanning radar are unusually similar to general frequency agile radar, because there is a strict relationship between the beam

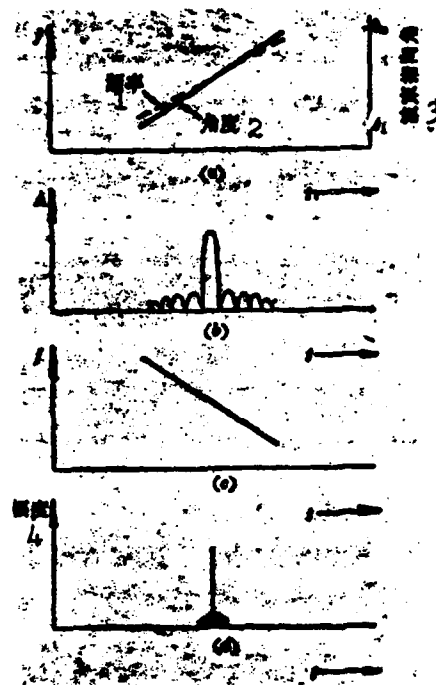


FIG. 9.37 DIAGRAM OF WAVE FORMS
OF PULSE COMPRESSION FREQUENCY
SCANNING RADAR
(a) Transmitting signal; (b) Re-
ceived signal; (c) Compression
filter delay time; (d) Pulse
after compression
KEY: (1) Frequency; (2) Angle meas-
urement; (3) Beam directional
angle; (4) Amplitude

directional angle and the transmitting frequency, therefore the target that is located in a certain angle of elevation only can be radiated by the signal with a frequency that this angle of elevation corresponds to, this completely loses the frequency division and collection characteristics of the backward-waves of the target of frequency agile radar, this is also to say, it cannot make the adjacent backward-waves related. This way, frequency scanning radar completely loses the improvements in the areas of range detection, angle measurement

precision, and amplitude identification that are made by frequency agile radar. This problem must be resolved. If we add an electronically tunable phase shifter in each s-shaped feed line to change the relationship of its frequency and directional angle in the pulse, this greatly increases the complexity of the equipment, causing it to change to a phased array radar.

In spite of this, frequency scanning radar (especially single beam frequency scanning radar) and frequency agile radar still have many similarities. Not only is much of the equipment extremely similar (for example the program-controlled frequency synthesizer and the power amplification transmitter), but also they fully have the possibility to further combine into an even newer radar system.

Reference Material:

- (1) ECCM from the radar designer's view point. M. A. Johnson and D. C. Stoner, *Electro/76 Rec. or Microwave J.* March, 1978, Vol. 21, №3.
- (2) Cost-effective radar retrofit adds frequency agility. J. Martin. *Microwave Systems News*, Oct. 1977. Vol. 7. №10. pp. 47~48.
- (3) A sequential logic for improving signal detectability in frequency-agile search radars. V. G. Hansen. *IEEE Trans. Vol. AES-4. №5. Sept. 1968*, pp. 763~773.
- (4) Signal Processor for Diversity Frequency Radar. D. D. Howard. U.S. Pat. №3, 487, 490. 1969.
- (5) Signal Processor for Diversity Frequency Radar. D. D. Howard. U.S. Pat. №3, 603, 995. 1971.
- (6) Velocity response characteristics of MTI radars using pulse or block stagger. R. C. Houts. *IEEE Int. Radar Conf.* Oct. 1977, pp. 177~181.
- (7) An experimental twin pulse MTI S-band radar with pulse compression.

Source: *IEEE Trans. AP-36, 1988, 15, 151-152*

- (10) Constant false alarm rate with adaptive sensitivity. O. J. Fox and M. Campbell. Proc. IEEE Conf., 1977, Oct. London, pp. 180-183.
- (11) Antenna for and BOLD radar system for a low cross-section radar. P. Petroski, S. Ramakrishna, C. K. Raghavan. Indian Radar Conf. Dec. 1978, Pune, pp. 114-117.
- (12) A proposed optimum detection scheme for non-frequency agile radar systems. P. N. Mariani, W. M. Waters. Proc. IEEE Southeastern Reg. Conf., 1978, Vol. 2, pp. 684-687.
- (13) Radar Design Principles. Fred E. Mithun. McGraw-Hill Book Co., 1968, p. 448.
- (14) Losses for frequency diversity waveform systems. E. Nitzberg. IEEE Trans. Vol. AP-24, No. May, 1976, pp. 474-482.
- (15) Radar Handbook. Ed. M. I. Skolnik, Chapt. 13. McGraw-Hill Book Co., 1978.

Zhong Yi Ben "Lei Da Shou Ce", Di Liu Fen
 Ce, Di Zi Zhang, Guo Fang Gong Ye Chu
 Ban She, 1978 Nain Ban; "Chinese translation,
 Radar Handbook, Book 6, Chapter 21, Defense
 Industry Press, Published 1978."

DATE
ILME